NOTE TO USERS

The original manuscript received by UMI contains pages with indistinct print. Pages were microfilmed as received.

This reproduction is the best copy available

UMI

GEOCHEMISTRY OF THE UCHI SUBPROVINCE, NORTHERN SUPERIOR PROVINCE: AN EVALUATION OF THE GEODYNAMIC EVOLUTION OF THE NORTHERN MARGIN OF THE SUPERIOR PROVINCE OCEAN BASIN

A thesis submitted to the College of

Graduate Studies and Research

in partial fulfilment of the requirements

for the degree of Doctor of Philosophy

in the Department of Geological Sciences

University of Saskatchewan

Saskatoon

By

Peter Nigel Hollings

Fall, 1998

© Copyright Peter Nigel Hollings, 1998. All rights reserved.

National Library of Canada
Acquisitions and Bibliographic Services
395 Wellington Street
Ottawa ON K1A 0N4
Canada

Bibliothèque nationale du Canada
Acquisitions et services bibliographiques
395, rue Wellington
Ottawa ON K1A 0N4
Canada

Your file Votre référence

Our file Notre référence

The author has granted a non-exclusive licence allowing the National Library of Canada to reproduce, loan, distribute or sell copies of this thesis in microform, paper or electronic formats.

L'auteur a accordé une licence non exclusive permettant à la Bibliothèque nationale du Canada de reproduire, prêter, distribuer ou vendre des copies de cette thèse sous la forme de microfiche/film, de reproduction sur papier ou sur format électronique.

The author retains ownership of the copyright in this thesis. Neither the thesis nor substantial extracts from it may be printed or otherwise reproduced without the author's permission.

L'auteur conserve la propriété du droit d'auteur qui protège cette thèse. Ni la thèse ni des extraits substantiels de celle-ci ne doivent être imprimés ou autrement reproduits sans son autorisation.

0-612-32786-8

Canada

UNIVERSITY OF SASKATCHEWAN

College of Graduate Studies and Research

SUMMARY OF DISSERTATION

Submitted in partial fulfilment

of the requirements for the

DEGREE OF DOCTOR OF PHILOSOPHY

by

Peter Hollings

Department of Geological Sciences
University of Saskatchewan

Fall 1998

Examining Committee:

Dr. G.J. Sofko	~~Dean/Associate Dean~~ Dean's Designate, Chair College of Graduate Studies and Research
Dr. J.F. Basinger	Chair of Advisory Committee, Department of Geological Sciences
Dr. R. Kerrich	Supervisor, Department of Geological Sciences
Dr. K. Ansdell	Department of Geological Sciences
Dr. C. Holmden	Department of Geological Sciences
Dr. J. Merriam	Department of Geological Sciences
Dr. S. Reid	Department of ~~Physics and Engineering Physics~~ Chemistry

External Examiner

Dr. D. Canil
School of Earth and Ocean Sciences
University of Victoria
P.O. Box 3055,
Victoria, BC V8W 3P6

Geochemistry of the Uchi subprovince, northern Superior Province: an evaluation of the geodynamic evolution of the northern margin of the Superior Province ocean basin

Older assemblages of the Uchi subprovince, northern Superior Province, Canada, ranging in age from 2.9 to 3.0 Ga, are dominated by an association of komatiite-tholeiite sequences intercalated with felsic volcanic rocks. Komatiites vary from weakly LREE enriched to strongly depleted. The majority of ultramafic rocks display the conjunction of negative Nb anomalies with trends of increasing SiO_2 and La/Sm_n, indicative of contamination by a felsic component. Many of the komatiites and komatiitic basalts are characterised by high V/Yb and Sc/Yb ratios which are unique amongst Archean komatiites. Tholeiitic flows intercalated with the komatiites typically display flat REE patterns with variable Nb anomalies, consistent with minor degrees of contamination. Two suites of felsic volcanic rocks are intercalated with the komatiite-tholeiite sequences of the older assemblages. Both types display pronounced LREE enrichment and negative Nb and Ti anomalies, but Type 1 has strongly fractionated HREE patterns, whereas Type 2 HREE are generally flat in conjunction with elevated compatible element contents. Collectively, the geochemical, geochronological and stratigraphic evidence from the northern Superior Province greenstone belts provide evidence for both a spatial and temporal association of mantle plumes and subduction zones during generation of the proto-continent nucleus to the Superior Province.

The 2.8-2.9 Ga assemblages of the Uchi subprovince comprise mafic tholeiites characterised by predominantly flat REE, along with volumetrically significant units of felsic to intermediate volcanic rocks, that display enriched LREE and moderately fractionated HREE in conjunction with pronounced negative Nb anomalies. The geochemistry and geochronology of these assemblages is consistent with the formation of ocean plateau fragments which were accreted to the Uchi paleo continental margin where they subsequently formed the basement for a subduction related arc complex.

Five distinct suites have been recognised in the ~2.7 Ga Confederation assemblage: (1) tholeiitic basalts with flat to smoothly depleted REE; (2) tholeiites with flat to weakly depleted LREE in conjunction with pronounced negative Nb anomalies; (3) Fe-rich basalts with elevated Ti and P contents, enriched LREE and fractionated HREE; (4) LREE enriched basalts and andesites with negative Nb anomalies; and (5) dacites and rhyolites with variably enriched LREE, moderately fractionated HREE and variable HFSE anomalies. The occurrence of this varied range of rocks in a single assemblage is comparable to modern back arc basins.

BIOGRAPHICAL

September, 1970	Born in London, England
June, 1992	B.Sc (Hons) Geology, Royal Holloway and Bedford New College, University of London

HONOURS

Graduate Student Scholarship, University of Saskatchewan, 1996-1998
Mineralogical Society Award, University of London, June 1991

Permission to Use

In presenting this thesis in partial fulfilment of the requirements for a Doctor of Philosophy degree from the University of Saskatchewan, I agree that the libraries of this university may make it freely available for inspection. I further agree that permission for copying of this thesis in any manner, in whole or in part, for scholarly purposes may be granted by my supervisor Dr. R. Kerrich or, in his absence, by the head of the Department of Geological Sciences or Dean of Arts and Science. It is understood that any copying of this thesis, or parts thereof, shall not be allowed without my written permission. It is also understood that due recognition shall be given to me and the University of Saskatchewan in any scholarly use which may be made of any material in this thesis.

Requests for permission to copy or make other use of material in this thesis, in whole or in part, should be addressed to:

Head of the Department of Geological Sciences
114 Science Place, University of Saskatchewan
Saskatoon, Saskatchewan, S7N 5E2.

Abstract

Older assemblages of the Uchi subprovince, northern Superior Province, Canada, ranging in age from 2.9 to 3.0 Ga, are dominated by an association of komatiite-tholeiite sequences intercalated with felsic volcanic rocks. Komatiites vary from weakly light rare earth element (LREE) enriched to strongly depleted (La/Sm_n = 0.36-1.6). The majority of ultramafic rocks display the conjunction of negative Nb anomalies with trends of increasing SiO_2, La, La/Sm_n and Th/Ce with decreasing Mg# and Ni, indicative of contamination by a felsic component. Many of the komatiites and komatiitic basalts are characterised by high V/Yb and Sc/Yb ratios (277-360 and 58-76 respectively) which are unique amongst Archean komatiites. Normalized V-Sc enrichments versus the heavy rare earth elements (HREE) are characteristic of mafic rocktypes derived from previously depleted mantle sources and occur, to some degree, in most mafic arc volcanic rocks. Tholeiitic flows intercalated with the komatiites typically display flat REE patterns with variable Nb anomalies and high Th/Ce ratios, consistent with minor degrees of contamination.

Two suites of felsic volcanic rocks are intercalated with the komatiite-tholeiite sequences of the older assemblages. Both types display pronounced LREE enrichment and negative Nb and Ti anomalies, but Type 1 has strongly fractionated HREE patterns, whereas Type 2 HREE are generally flat in conjunction with elevated compatible element contents. The predominant Type 1 rhyolite is directly comparable to southern Superior Province examples associated with oceanic arc sequences, and are comparable to Archean high Al, high La/Yb_n TTGs; they indicate a subduction-related origin for the northern examples. Type 2 rhyolite geochemical signatures may result from mixing of Type 1 rhyolites with tholeiitic magmas or variations in the mantle source.

Komatiite-tholeiite associations within Archean terranes are interpreted as the result of plume-related magmatism comparable to modern oceanic plateaux. In contrast intermediate and felsic rocks are typical of calc alkaline suites generally attributed to Archean subduction related environments. Collectively, the geochemical, geochronological and stratigraphic evidence from the northern Superior Province greenstone belts provide evidence for both a spatial and temporal association of mantle plumes and subduction zones during generation of the proto-continent nucleus to the Superior Province.

The 2.8-2.9 Ga assemblages of the Uchi subprovince comprise mafic tholeiites characterised by predominantly flat REE (La/Sm_n = 0.8-1.1). These are comparable to modern ocean plateau basalts, along with with volumetrically significant units of felsic to intermediate volcanic rocks, that display enriched LREE (La/Sm_n = 3.7-7.2) and moderately fractionated HREE in conjunction with pronounced negative Nb anomalies. The geochemistry and geochronology of these assemblages is consistent with the formation of ocean plateau fragments which were accreted to the Uchi paleo continental margin.They subsequently formed the basement for a subduction related arc complex, an environment comparable to regions of the southwest Pacific today.

Five distinct suites have been recognised in the ~2.7 Ga Confederation assemblage: (1) tholeiitic basalts with flat to smoothly depleted REE; (2) tholeiites with flat to weakly depleted LREE in conjunction with pronounced negative Nb anomalies; (3) Fe-rich basalts with elevated Ti and P contents, enriched LREE and fractionated HREE; (4) LREE enriched basalts and andesites with negative Nb anomalies; and (5) dacites and rhyolites with variably enriched LREE, moderately fractionated HREE and variable HFSE anomalies. The occurrence of this varied range of rocks in a single assemblage is comparable to modern back arc basins, where the complex interplay of mantle sources allows for the eruption of tholeiites, subduction modified tholeiites, OIB-like basalts and subduction related arc-type volcanic rocks.

Acknowledgements

Firstly I graciously acknowledge the financial and technical support of my advisor Rob Kerrich, who allowed me the intellectual freedom to explore new avenues of research. During the course of my studies, I received a University of Saskatchewan Postgraduate Scholarship. Funding for this study was also provided by CAMIRO-NSERC as part of a larger study, "Prospective Versus Barren Volcanic Belts for VMS Deposits: A New Exploration Strategy" that was conducted at the Department of Geological Sciences, University of Saskatchewan.

I am endebted to my external examinier Dr. Dante Canil and my advisory committee Drs. K. Ansdell, J. Basinger, C. Holmden, J. Merriam and S. Reid, for their inciteful comments and helpful advice.

I would like to thank Brian Kwan-Morgan and J. Jain for the invaluable assistance with ICP MS analyses and Kevin Ansdell for his help with obtaining isotope data. In addition drill core was obtained from a number of sources in order to sample areas with poor exposure or that were otherwise inaccessible. Steve McGibbon and Bob Chataway of Gold Corp. Inc., Red Lake; Brian Atkinson, Greg Stott and Glen Seim, OGS; Craig McDougall of Noranda Mining and Exploration Inc; and Paul Brown of Placer Dome Canada Ltd. all provided access to drill core.

I would particularly like to thank Derek Wyman whose patience and insights have greatly contributed to my understanding of Archean geochemical processes. I am also Other scientists who have enhanced my geological knowledge during my studies, through numerous discussions over they years, include: J. Fan, C. McCuaig, K. Durocher, G. Stott and A. Polat.

Finally I wish to thank my parents whose love, understanding and financial support during my sojourn in Canada has been invaluable. To Tootsie, our dachshund whose cold nose got me out of bed many mornings, I promise many long walks. Last, but definitely not least, my wife Jill, whose willingness to tolerate long hours in the lab and weekends in front of the computer has been without limits, and whose love has sustained me through the dark days when nothing seemed to be going right.

Table of Contents

Figure List

List of Tables

Abbreviations and acronyms

Rocktypes

MORB	Mid-Ocean Ridge Basalt
E-MORB	Enriched Mid-Ocean Ridge Basalt
N-MORB	"Normal" Mid-Ocean Ridge Basalt
OIB	Ocean Island Basalt
AUK	Aluminum-undepleted komatiites
ADK	Aluminum-depleted komatiites
TTG	Tonalite-trondjhemite-granodiorite
LOTI	Low Titanium tholeiites
BIF	Banded Iron Formation

Northern Superior

OMU	Opapimiskan-Markop unit, North Caribou greenstone belt
SRU	South Rim unit, North Caribou greenstone belt
NCGB	North Caribou greenstone belt
NCT	North Caribou Terrane
USG	Uchi-Sachigo-Goudalie superterrane

Analytical

ICP MS	Inductively coupled plasma mass spectrometer
XRF	X-ray Fluorescence

Geochemistry

PGE	Platinum Group Metals (Pd-Ir)
REE	Rare Earth Elements (La-Lu)
LREE	Light Rare Earth Elements (La-Sm)
HREE	Heavy Rare Earth Elements (Gd-Lu)
LILE	Large Ion Lithophile Elements (Sr, K, Rb, Ba, Th, Ta)
HFSE	High Field Strength Elements (Nb, Ta, Ce, P, Zr, Hf, Ti, Y)
La/Yb_n	Chondrite normalized ratio
Th/La_{pm}	Primitive mantle normalized ratio
Ti/Ti*	Normalized anomaly calculated with respect to adjacent elements on primitive mantle normalised diagram

CHAPTER 1

INTRODUCTION AND SCOPE

1.1 Background

The Superior Province of Canada is the world's largest Archean craton (Goodwin, 1991) and developed over 300 m.y., consequently it offers an excellent opportunity to investigate crustal growth mechanisms. However, the majority of volcanic terranes, particularly those outside the predominantly intra-oceanic 2.7 Ga Abitibi subprovince, remain poorly characterised. The Uchi subprovince, a series of east-west trending greenstone belts erupted on or near the North Caribou terrane (NCT) proto-continent to the north (Stott and Corfu, 1991), is thought to have formed one margin of the Late Archean ocean basin that closed during the convergence of the Minnesota River Valley terrane to the south and the NCT to the north (Hoffman, 1989; Williams et al., 1991; Jackson et al., 1994). Consequently it offers the opportunity to examine an environment that is likely substantively different from the more southerly belts of the Superior Province.

The nature of continental growth in the Archean, particularly the relative significance of mantle plume versus subduction related processes, has been a topic of debate in recent literature (Abbott, 1996; Stein and Goldstein, 1996). The fundamental observation of worldwide episodes of broadly coeval arc and plateau magmatism at ~2.7 Ga indicates the significance of plume processes in continental growth, although the details of these models are currently poorly constrained (Barley and Groves, 1992; Barley et al., 1995). Abbott (1996) and Condie (1997) have recently proposed that mantle plumes may be necessary to generate thick, buoyant oceanic crust that will tend to resist subduction.

Following the proposal by Campbell et al. (1989) and others that Archean komatiites were the product of mantle plumes, there has been an increasing interest in the topics of Archean analogues for modern plateaux or Large Igneous Provinces (Kent et al., 1996 and references therein). Evidence of interaction between plumes (or plateaux) and

subduction zones is increasingly recognized in the geologic record. Oceanic plateau obduction has been advocated for a number of Archean and Proterozoic terranes (Kimura et al., 1993; Stern et al., 1995; Stein and Goldstein, 1996) and for the Cretaceous Caribbean plateau (Saunders et al., 1996). In addition, plume influence on active subduction zones has been identified in the SW Pacific (Lau Basin; Pearce et al., 1995) and rapid recycling of sediments from subduction zones into nearby plumes is suggested by He isotopic evidence (Samoan plume; Farley, 1995). Direct plume impingement on subduction zones has been suggested in the case of the Yellowstone plume on the Farralon plate (Parsons et al., 1994), the mid-Cretaceous Marie Byrd Land plume on the Phoenix Plate subducting beneath Antarctica (Weaver et al., 1994) and an Abitibi plume acting upon a preexisting 2720 Ma arc (Dostal and Mueller, 1997; Wyman et al., 1997). Consequently determining the original geodynamic setting of these widespread tholeiite-komatiite sequences, and their relationship to convergent margin arc magmas, is of considerable significance for tectonic models of continental growth and greenstone belt formation.

Only a relatively small number of high precision trace element analyses have been published for the northern greenstone belts of the Superior Province, in comparison to the Abitibi greenstone belt which is perhaps the most comprehensively investigated Archean terrane (Capdevilla et al., 1982; Lafleche et al., 1992; Desrochers et al., 1993; Xie and Kerrich, 1994; Fan and Kerrich, 1997; Dostal and Mueller, 1997). The northern greenstone belts encompass rocks of a considerably greater age range than the Abitibi belt and consequently offer the potential for new insights into both the early stages in the development of the Superior Province and the nature of crustal growth processes.

1.2 Scope of the thesis

In an attempt to constrain the nature of crustal growth processes in the Superior Province, a comprehensive study of the geochemistry of the volcanic rocks of the 3.0-2.7 Ga Uchi subprovince was undertaken. The Uchi subprovince comprises an appropriate study area for a number of reasons, including: 1) the 300 m.y. of volcanic activity preserved in the subprovince provides a larger timespan over which to investigate the varying nature of crustal growth processes than is offered by more southerly greenstone belts; 2) the northern location of the subprovince provides a window into the proto-continental core of the Superior Province; 3) detailed mapping and extensive geochronological studies provide an excellent framework for interpretation of geochemical data; and 4) despite

encompassing a wide range of rock types over a range of ages the geochemistry of the Uchi subprovince remains relatively poorly constrained. The limited data available are typically incomplete, often lacking many key elements essential for the identification of magma associations and hence geodynamic settings.

This study utilises high precision low level trace element data derived by ICP-MS for ultramafic, mafic and felsic volcanic and intrusive rocks. By analogy with data from modern geodynamic environments, it is possible to evaluate the nature of the Archean terranes as well as make inferences as to the nature of the Archean mantle and potential mantle-crust interactions during petrogenesis of these rocks. In addition to distinguishing the geodynamic settings of distinct assemblages the dataset will be utilised to evaluate models that correlate these assemblages along the length of the subprovince.

1.3 Structure of the thesis

The thesis is organised as follows. The methodologies of field sampling and analysis are described in Chapter 2. Chapter 3 lays out the present understanding of the geological setting of the Uchi subprovince and the Superior Province as a whole, in order to establish a framework within which the geochemical data can be interpreted. In Chapter 4 a comprehensive geochemical database is presented for ultramafic to felsic rocks from the 2.9-3.0 Ga assemblages of the Red Lake, Rice Lake and Pickle Lake greenstone belts. This database is utilised to investigate the nature of the sub-Superior mantle at this time interval and evaluate the geodynamic environment in which the rocks were erupted.

The geochemistry of the 2.8-2.9 Ga Pickle Crow, Woman and Meen assemblages are evaluated in Chapter 5 and the data interpreted to establish the magma associations and the nature of the geodynamic environment. In Chapter 6 the nature of the ~2.7 Ga Confederation assemblage is evaluated. An extensive database from the Birch-Uchi greenstone belt is utilised to establish the geochemistry and geodynamic setting of the assemblage. This is then compared with data from the Confederation assemblage elsewhere within the Uchi subprovince, in order to investigate variations along this ~500 km paleo-continental margin.

Chapter 7 summarises the results of this study and integrates them to establish a model for the evolution of the proto-continental Superior Province. These results are then compared in terms of their significance to models for the evolution of Archean crustal growth

models.

CHAPTER 2

METHODOLOGY

2.1 Fieldwork

Sampling of the Uchi subprovince was begun by Derek Wyman during the 1994 field season as part of the CAMIRO-NSERC study, with a reconnaissance visit to the Pickle Lake greenstone belt. This resulted in the collection of 20 samples. More extensive field work by the author during the 1995 field season allowed for the collection of 350 samples from the majority of the greenstone belts in the western Uchi subprovince. An additional two hundred and thirty samples were collected during the 1996 field season. Where possible fieldwork was focussed on those greenstone belts where the geology and geochronology were well constrained; however, this was not always possible and some sampling was undertaken in order to correlate assemblages along the length of the subprovince. Sampling was generally conducted along highways, secondary bush roads and lakeshores, utilising published and preliminary Ontario Geological Survey (OGS) geological maps to ensure a representative range of rock types was sampled from each belt.

In addition, drill core was obtained from a number of sources in order to sample areas with poor exposure or that were otherwise inaccessible. In the Red Lake belt 12 drill core samples were provided by Steve McGibbon and Bob Chataway of Gold Corp. Inc., in order to compare the East Bay serpentinite with similar serpentinites adjacent to the mine site (Samples AB94 and GC95). In addition all samples from the Ball assemblage of the Red Lake belt were taken from drill core stored at the OGS Drill Core Library in Red Lake.

During the 1996 field season 111 samples of drill core from the Confederation assemblage of the Birch-Uchi greenstone belt, to the south west of the South Bay mine site, were collected from the OGS Drill Core Library at Red Lake, and from core made available by Craig McDougall of Noranda Mining and Exploration Inc. Drill holes were selected from

areas adjacent to the South Bay mine site as well as a number of localities to the south west of the mine site.

Samples from poorly exposed or inaccessible areas of the Pickle Lake and Lake St. Joseph belts were obtained from the OGS Drill Core Library at Sioux Lookout. All samples from the Meen-Dempster belt were provided by Greg Stott of the Ontario Geological Survey. Poor exposure on the Musslewhite Property, in the North Caribou belt of the Sachigo subprovince, meant that all data reported herein were acquired from drill core stored on the property, courtesy of Paul Brown of Placer Dome Canada Ltd.

2.2 Analytical techniques

Polished thin sections were prepared for all samples. Weathered surfaces were removed from all samples at the University of Saskatchewan prior to crushing in agate mills by X-ray Assay Laboratories (XRAL) Inc., Don Mills, Ontario. Agate mills were used so as to reduce risk of contamination of trace elements that occurs with tungsten carbide and some other materials (Jenner, 1996). Major elements were determined using X-ray fluorescence spectrometry (XRF) at XRAL, with relative standard deviations within 5%. Totals for major element oxide data were generally within 2% of 100% and have been recalculated to a 100% volatile free basis. Trace elements, including the rare earth (REE) and high field strength elements (HFSE), were analyzed using inductively coupled plasma mass spectrometry (ICP-MS; Perkin Elmer 5000) at the Department of Geological Sciences, University of Saskatchewan, following the protocol of Jenner et al. (1990) and Longerich et al. (1990). Forty trace elements including HFSE and REE were determined using an HF-HNO_3 dissolution, on 100 mg aliquots of powder. Thorium, Nb, Hf, Zr and REEs were also analyzed using the Na_2O_2 sinter technique of Longerich et al. (1990), on 200mg aliquots of powder, to circumvent potential problems associated with incomplete dissolution of refractory minerals hosting HFSE and REE, and/or their instability in analytes. The sinter data was then combined with acid dissolution data to form a composite data set, which tends to produce more reproducible data and smoother trace element patterns (Fan and Kerrich, 1997). Analysis of acids, distilled deionised water, and procedural blanks yielded levels of <10 ppb for Hf, Zr, Nb and REEs. Detection limits, defined as 3σ of the procedural blank, and referred to a rock, for some critical elements, in parts per million, are as follows: Th (0.01), Nb (0.006), Hf (0.008), Zr (0.004), La (0.01), Ce (0.009). Precision for most elements at the concentrations present

in the international reference material BIR-1, during the period of analysis, is between 2-8% relative standard deviations (Appendix A; Xie and Kerrich, 1994).

Ratios of HFSE/HFSE* are calculated following the logarithmic method of McCuaig et al. (1994), except that Gd is used in place of Eu for Zr/Zr* and Hf/Hf*. By convention REE ratios (e.g., La/Sm_n) are chondrite normalised to the values of Sun and McDonough (1989). Chondrite and primitive mantle normalised diagrams presented herein have been normalised using the values of Sun and McDonough (1989).

2.3 Alteration and metamorphism of Archean volcanic rocks

In the Superior Province, mafic and ultramafic flows have a history of seafloor hydrothermal alteration and greenschist to amphibolite facies metamorphism. The effects of these processes are variable with respect to different major and trace elements; however, there is a broad consensus that the elements least sensitive to disturbance are Al, Ti, the HFSE (Th, Nb, Ta, Zr, Hf), the REE (excepting Ce and Eu), Y, Sc, and V (Ludden et al., 1982; Arndt and Nesbitt, 1982; Lafleche et al., 1992; Jochum et al., 1991; Arndt, 1994). In contrast Ca, Na, K, Sr, Cs, Rb and Ba are widely recognised to be mobile under these conditions. Greenschist facies metamorphism will typically alter the mineral assemblage in mafic igneous rocks from clinopyroxene, plagioclase ± olivine to actinolite, albite, epidote and chlorite ± calcite and quartz, an approximately isochemical reaction that will typically not affect the REE and HFSE. Given that the majority of volcanic rocks within the study area have been metamorphosed to at least greenschist grade the term "meta" will be taken as implicit throughout this thesis.

In order to minimise the effect of alteration this thesis focusses on the generally immobile major elements (MgO, Al_2O_3, TiO_2), incompatible trace elements (Ni, Cr), high field strength elements (Nb, Th, Ti, Zr and Hf) and the rare earth elements (*c.f.*, Sun and Nesbitt, 1976; Nesbitt et al., 1979; Humphris, 1984; Jochum et al., 1991; Xie et al., 1993). In addition sampling of shear zones and areas of intense alteration was generally avoided, and further screening for carbonate alteration during thin section observation was undertaken.

Given the potential for alteration of major elements, particularly Na and K, which are typically used in the classification of tholeiitic and calc alkaline volcanic rocks, this thesis will principally utilise trace element data to subdivide the rock types. Generally calc

alkaline rocks are characterised by elevated La/Sm_n ratios (>2) in conjunction with negative HFSE anomalies whereas tholeiites display flat LREE and lack significant HFSE anaomalies. However, it is recognised that in some areas these subdivisions may be arbitrary given that the tholeiites may represent the primitive end member of the calc alkaline trend.

CHAPTER 3

GEOLOGICAL SETTING OF THE UCHI SUBPROVINCE

3.1 The Superior Province

The Superior Province, the world's largest Archean craton covering an area of 1,572,000 km^2, comprises a collage of plutonic, volcanic-plutonic, high grade gneissic, and metasedimentary dominated subprovinces ranging in age from 3.1 to 2.7 Ga (Fig. 3.1; Card and Ciesielski, 1986). Geophysical studies have demonstrated that the upper mantle below the Superior Province has the deepest anisotropic mantle root and fastest seismic velocities in North America (Grand, 1987; Silver and Chan, 1988). The Moho ranges from ~30 km below the English River subprovince to 36 km below the Berens River plutonic belt (Hall and Hajnal, 1969) Geochronological studies have demonstrated that accretion of greenstone belts was diachronous from north to south (Card and Ciesielski, 1986) in the south of the Province, whereas recent studies have suggested that in the north of the Province accretion was also occurring from the north (Stott, 1997).

In a recent synthesis Thurston et al. (1991) proposed the existence of the North Caribou Terrane (NCT), a collage of 2.9 - 3.0 Ga volcanic/plutonic sequences located dominantly within the Sachigo subprovince to the north of the Uchi subprovince. This is suggested to have comprised a proto-continent to which the remainder of the Superior Province was accreted from both the north and south (Fig. 3.1). Stott and Corfu (1991) further proposed that the Northern Pickle assemblage of the Pickle Lake greenstone belt, Uchi subprovince, could be correlated with the NCT.

More recently Stott (1997) proposed the existence of a composite Uchi-Sachigo-Goudalie terrane (USG), occupying the northern half of the Superior Province. This composite terrane contains a record of several orogenic episodes preserved in the greenstone belts ranging in age from 3.0-2.7 Ga. An important geological feature that sets some ~3 Ga Superior Province greenstone belts apart, is the eruption of komatiites and tholeiites over mature quartzite sequences, exemplified by the North Caribou and Steep Rock greenstone

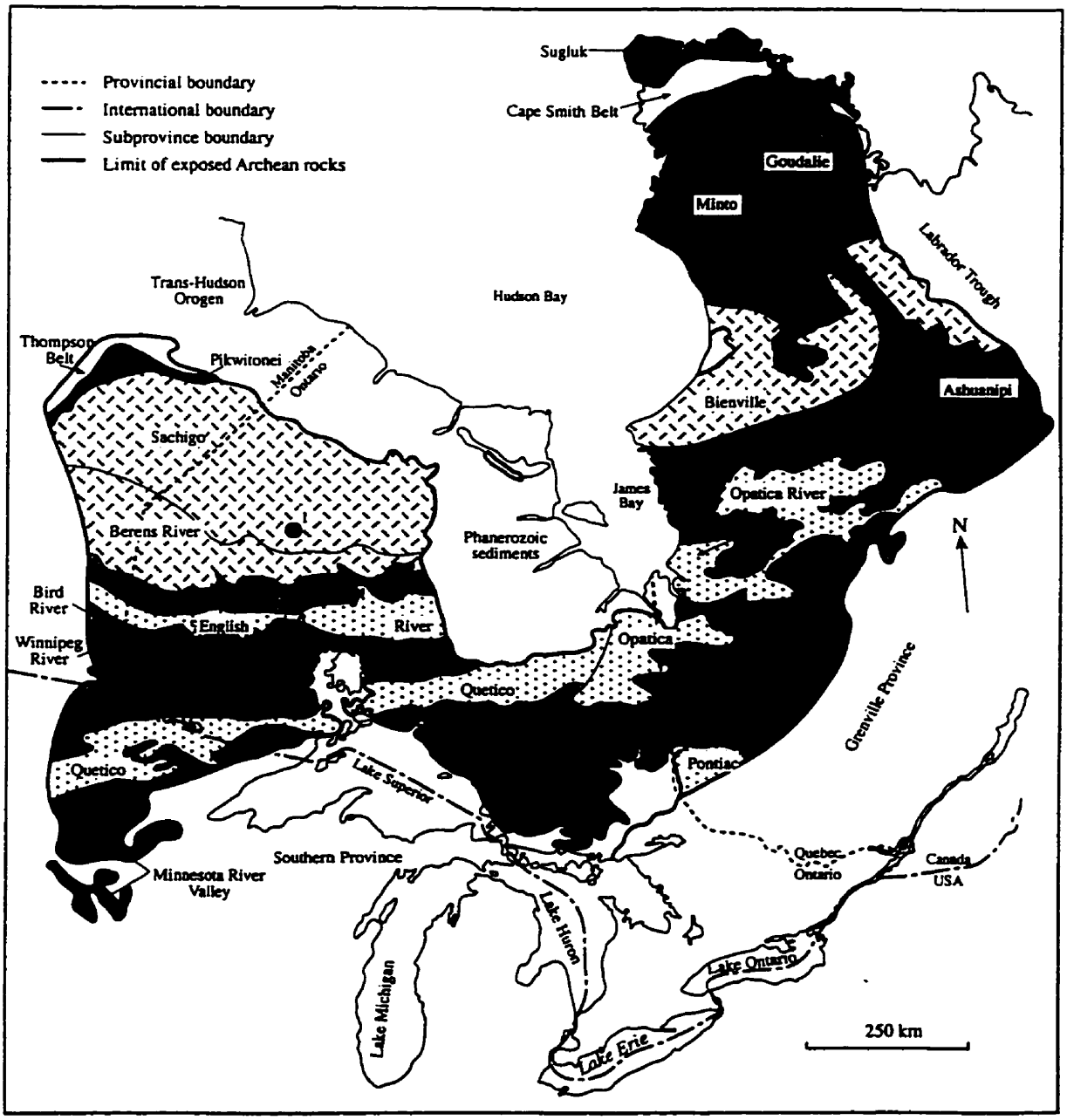

Figure 3.1. Map showing the location of greenstone belts sampled within the northern Superior Province (modified after Card and Ciesielski, 1986 and Stott, 1997). 1 = North Caribou, 2 = Rice Lake, 3 = Red Lake, 4 = Birch-Uchi, 5 = Meen-Dempster, 6 = Lake St. Joseph, 7 = Pickle Lake, 8 = Lumby Lake.

belts (Stott, 1997). Associations of quartzose wackes, conglomerates and other clastic and chemical sedimentary rocks with komatiites are a common but volumetrically minor component of older greenstone belts in the northern USG (Stott, 1997). Where exposed, the basal sequences unconformably overlie granitic basement and are interpreted as passive margin platformal sequences deposited during crustal rifting events (Thurston et al., 1987; Thurston and Chivers, 1990; Stott, 1997). Available U-Pb age dates indicate that USG basement sequences are ~3.0 to 2.9 Ga in age, with 2.95 – 2.93 Ga gneissic tonalites being dominant. The overlying platform sequences are >2850 Ma in age (Davis et al., 1988; Stott, 1997). Accordingly, basement underlying the platform sequences was not greatly older than the rift events themselves.

These older sequences have been interpreted as the result of rifting of passive margins of an older cratonic nucleus (c.f., Davis et al., 1988; Tomlinson et al., 1996), likely related to the impingement of a mantle plume on the continental lithosphere and are included within the NCT of Thurston et al. (1991). In contrast, the southern Superior Province belts, such as most of the Wawa and Abitibi are generally considered to be dominantly intraoceanic volcanic sequences (Desrochers et al., 1993; Xie et al., 1993; Fan and Kerrich, 1997; Polat et al., 1997).

The majority of the greenstone belts of the southern Superior Province were formed during widespread magmatism from 2770-2660 Ma (Corfu and Davis, 1992). From 2770-2710 predominantly oceanic sequences were created and amalgamated as exemplified by the Wabigoon and Abitibi subprovinces (e.g. Davis et al., 1988) and also by the creation of the ~2740 Confederation assemblage in the Uchi subprovince. Around 2710 Ma the Kenoran orogeny resulted in the southward younging accretion of oceanic crustal fragments. These events occurred around 2.71 Ga in the northern Superior, between 2.71 to 2.69 Ga in the centre of the Province and from 2.7-2.68 Ga in the south (Corfu and Davis, 1992).

3.2 The Uchi subprovince

The Uchi subprovince is a greenstone-granitoid type subprovince that extends some 600 km east-west from the Hudson Bay lowlands across the Ontario-Manitoba border. It is bounded to the north by the Sachigo subprovince and the metasedimentary English River subprovince to the south (Fig. 3.2). The subprovince is comprised of a number of greenstone belts which themselves contain sequences of supracrustal volcanic rocks that

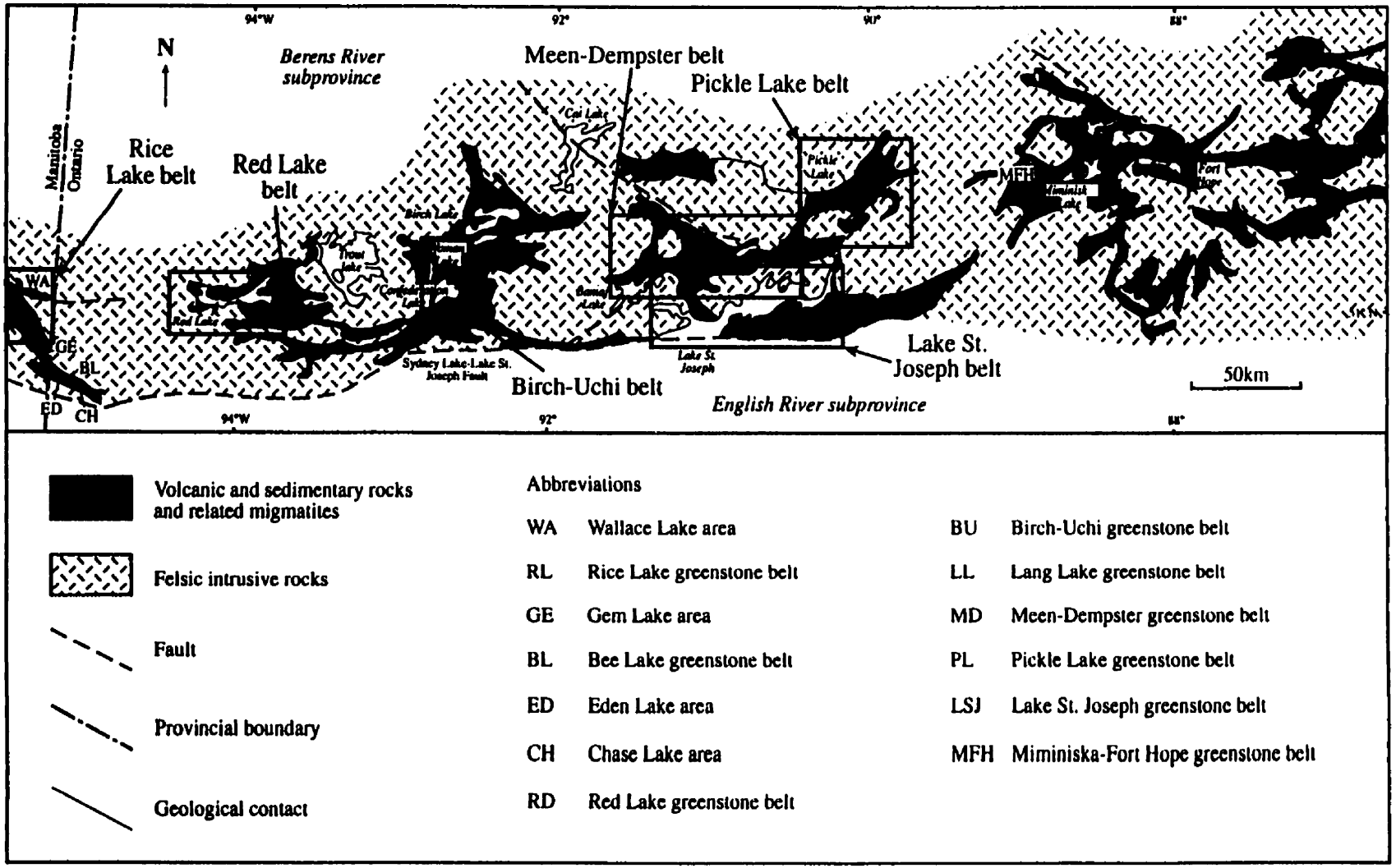

Figure 3.2. Generalized geological map of the greenstone belts and intrusive rocks of the Uchi Subprovince, showing the location of the greenstone belts investigated in this study. After Stott and Corfu (1991).

record some 280 million years of volcanism and erosion from 3.0 to 2.7 Ga. Stott (1997) interprets the La Grande River subprovince and the Goudalie domain, to be the easterly extension of the Uchi subprovince, based upon aeromagnetic trends beneath the Phanerozoic Moose River Basin (Fig. 3.1)

From west to east the principal belts are the Rice Lake, Red Lake, Birch-Uchi, Meen-Dempster, Pickle Lake and Lake St. Joseph greenstone belts (Fig. 3.2; Stott and Corfu, 1991). The greenstone belts are composed of a number of distinct assemblages, defined from mapping, lithological and geochronological relationships. Thurston et al. (1991) define an assemblage as "stratified volcanic and/or sedimentary rock units built during a discrete interval of time in a common depositional or volcanic setting". The pattern of ages of volcanic rocks across the Uchi subprovince (Stott and Corfu, 1991) suggest that the subprovince grew by southward incremental additions of crust onto an older paleocontinent in the north - the North Caribou terrane - which forms the core of the Sachigo subprovince (Thurston et al., 1991). According to Stott and Corfu (1991) the Uchi subprovince was an Andean-type margin of an Archean micro-continent that occupied most of the northern Superior Province from Manitoba to Quebec.

3.2.1 Pickle Lake Greenstone Belt

The Pickle Lake greenstone belt is located within the central Uchi subprovince; it is stratigraphically associated with the Meen-Dempster belt to the west and the Lake St. Joseph belt to the south (Fig. 3.2). Stott and Corfu (1991) divided the belt into four volcanic assemblages based on stratigraphic relationships, isotopic age data and aeromagnetic studies: in order of decreasing age these are the Northern Pickle (~2900 Ma), Pickle Crow (2870 Ma), Woman (2820 Ma) and Confederation (2750 Ma) assemblages (Fig. 3.3; *cf.* Sage and Breaks, 1982; Corfu and Stott, 1989).

Northern Pickle assemblage. The oldest, most northerly rocks in the belt have been termed the Northern Pickle assemblage by Stott (1996). Corfu and Stott (1991) proposed that this assemblage may be correlated with 2900-3000 Ma supracrustal rocks of the North Caribou Terrane to the north (Thurston et al., 1991). They base this correlation principally on similarities of stratigraphic sequences, as well as aeromagnetic anomalies that trend northeastwards towards the southern end of the North Caribou belt.

Mapping by Stott et al. (1989a, b) has shown that the Northern Pickle assemblage is dominated by massive and pillowed basalt flows, with minor sill-like mafic and ultramafic

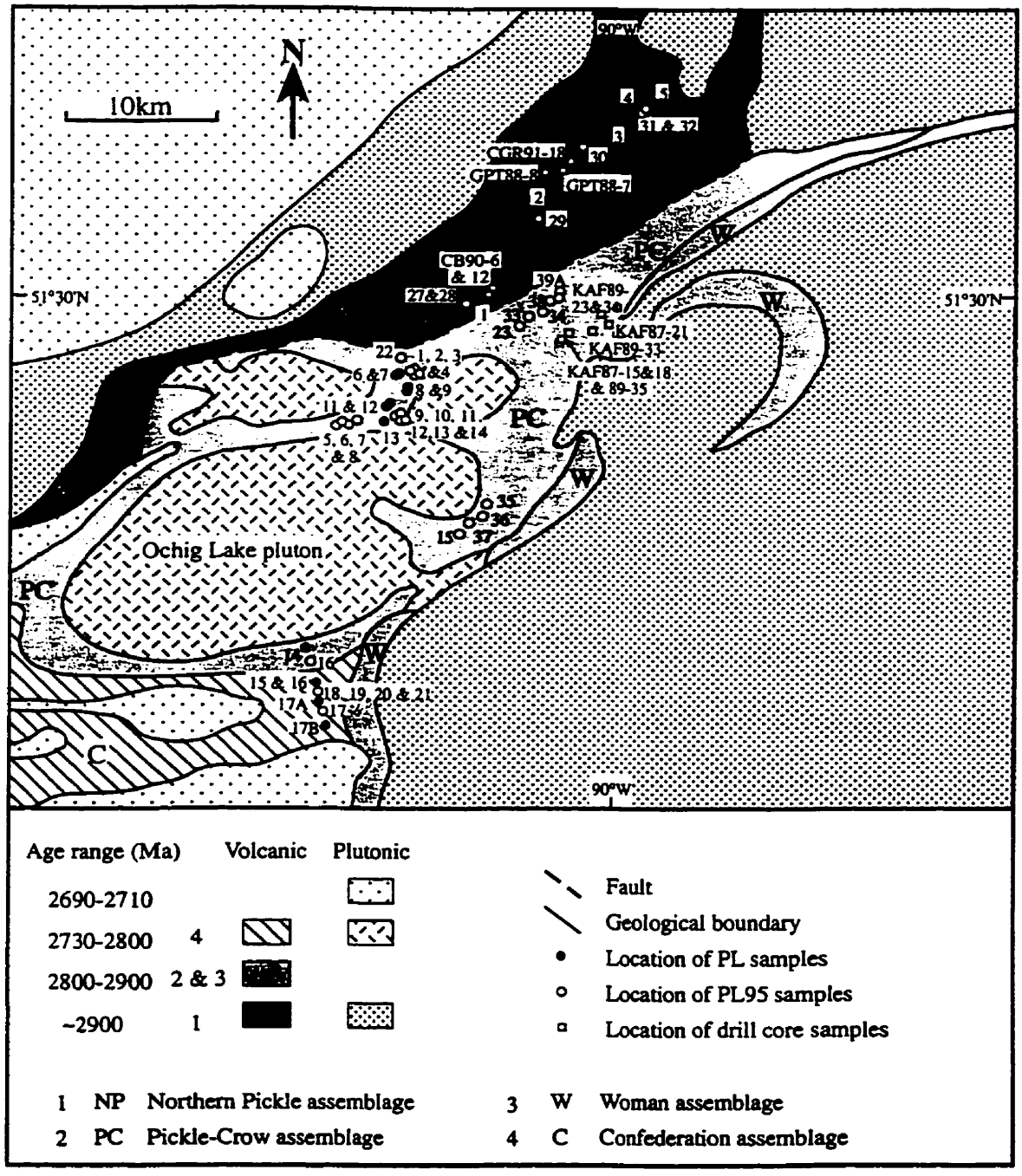

Figure 3.3 . Simplified geological map of the Pickle Lake greenstone belt. Modified after Stott and Corfu (1991). Sample locations for the Pickle Lake series rocks are illustrated (PL & PL95).

intrusives, and rare felsic tuffs. In addition, ultramafic rocks have been reported from the Thierry Cu-Ni deposit, located on the northwestern margin of the assemblage (Fig. 3.3; Sage and Breaks, 1982). Magnetite-quartz-banded iron formations are intercalated with the mafic volcanic rocks. The boundary of the Northern Pickle assemblage with the Pickle Crow assemblage to the south, has been defined on the basis of their distinct structural trends; northeast striking units in the former and an easterly strike in the latter (Stott and Corfu, 1991). The Northern Pickle assemblage is interpreted to young towards the south east based principally on correlations with stratigraphically similar rocks in the northern Keezik Lake area of the Miminiska Lake belt, where the tops are generally south-facing (Prest, 1939; Stott pers comm., 1998).

Pickle Crow assemblage. This assemblage comprises pillowed and massive basalt flows with intercalated banded iron formation (Fig. 3.3). This sequence is overlain by felsic tuffs and ashflows, in turn overlain by a second series of mafic volcanic rocks (Stott et al., 1989a, b). U-Pb dating of zircons from a porphyritic felsite within the Pickle Crow assemblage has yielded two zircon populations (Corfu and Stott, 1993a). The younger age of 2860±2 Ma is believed to be the formation age of the unit, whereas the older 2892±5 Ma age is interpreted as a xenocrystic component of an earlier volcanic episode (*op. cit.*).

Woman assemblage. Within the Pickle Lake belt, the Woman assemblage outcrops along the south east flank of the belt (Fig. 3.3), where a ~2000 m sequence of basaltic flows and minor dacitic to rhyolitic ash flows are recognised. A quartz phyric tuff has yielded a U-Pb age of 2836 Ma (Corfu, unpublished data referenced in Stott and Corfu, 1991).

Confederation assemblage. The youngest volcanic sequences in the Pickle Lake greenstone belt outcrop towards the south of the greenstone belt (Fig. 3.3). The assemblage consists of pillowed, vesicular and massive basalt flows which in places is capped by units of distal dacitic tuff (Stott and Corfu, 1991). No age has as yet been reported for the Confederation assemblage from within the Pickle Lake belt; however, the assemblage is stratigraphically similar to the Confederation assemblage in the Meen-Dempster belt.

Structure and metamorphism. According to Pye (1956) the greenstone belt as a whole is affected by a regional synformal structure with an axial plane trending northeast-southwest through the centre of the belt. In addition Pye (1956) identified the smaller

Pickle Crow syncline in the vicinity of the Pickle Crow gold mine. Recent work by Stott and Corfu (1991) has divided the belt into three structural domains:

- Domain 1 has the oldest tectonic fabric, comprising a steeply northwestward dipping schistosity
- Domain 2 consists of restricted contact strain aureoles around late intrusive complexes
- Domain 3 consists of a moderately northwest dipping schistosity also related to intrusive features.

Mineral deposits. The Pickle Lake greenstone belt is host to three gold deposits, the Pickle Crow, Central Patricia and Dona Lake mines, as well as the Thierry mine, a significant copper-nickel deposit. The Pickle Crow mine produced 44,982 kg of gold and 5,249 kg of silver before closing, whereas the Central Patricia produced 1,953 kg of gold and 1,814 kg of silver (Ferguson et al., 1971). The Thierry copper-nickel mine is a low-grade copper nickel deposit interpreted as being of magmatic origin, but remobilised during deformation (Patterson and Watkinson, 1984a, b).

3.2.2 Lake St. Joseph Greenstone Belt

The Lake St. Joseph greenstone belt is located within the Central Uchi subprovince, to the south of the Pickle Lake belt, with which it is stratigraphically associated (Fig. 3.2). Stott and Corfu (1991) subdivided the belt into three assemblages on the basis of stratigraphic and age relationships. The older Woman and Confederation assemblages form relatively minor units towards the west and north-east of the belt whereas the younger St. Joseph assemblage is areally the most extensive (Figs. 3.4 and 3.5).

Woman assemblage. This volcanic sequence outcrops towards the eastern end of the belt, and is believed to be equivalent to the Woman assemblage of the Meen-Dempster and Pickle Lake greenstone belts which have been dated at 2841-2805 Ma (Corfu, unpublished data referenced in Stott and Corfu, 1991). It is composed of tholeiitic basalts generally overlain by rhyolitic and dacitic tuffs. Stott and Corfu (1991) interpret these relationships as the result of island arc volcanism on a tholeiitic basaltic platform. Older 2.8-3.0 Ga assemblages of the Pickle Lake, Birch-Uchi and other greenstone belts are not represented in the Lake St. Joseph belt.

Confederation assemblage. According to Clifford (1969) the western portion of the Lake St. Joseph greenstone belt can be subdivided into three distinct units; the Upper and

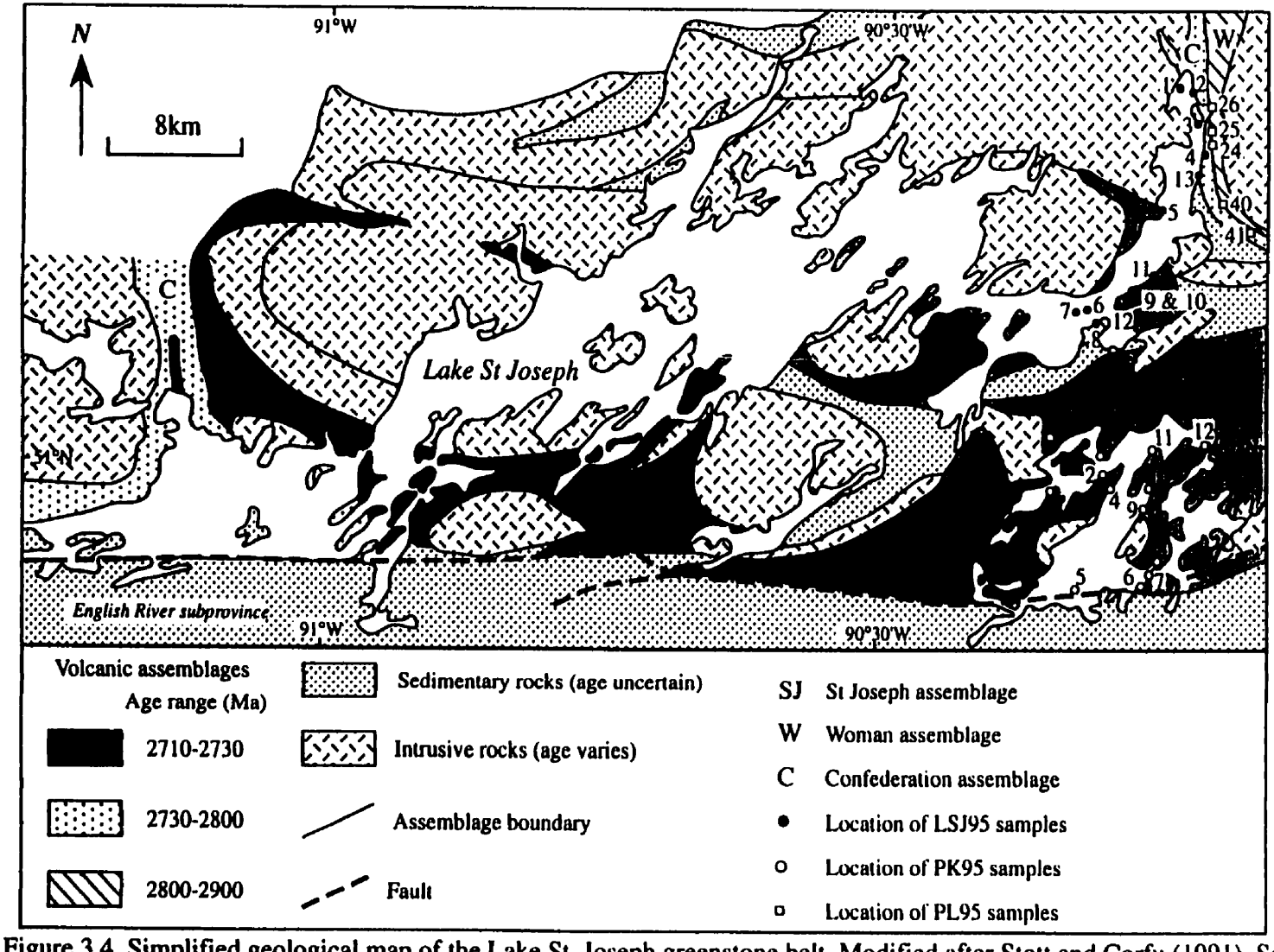

Figure 3.4. Simplified geological map of the Lake St. Joseph greenstone belt. Modified after Stott and Corfu (1991). Sample locations are identified for the Lake Pashkokogan (PK95), Lake St Joseph (LSJ95) and some Pickle Lake (PL95) series rocks.

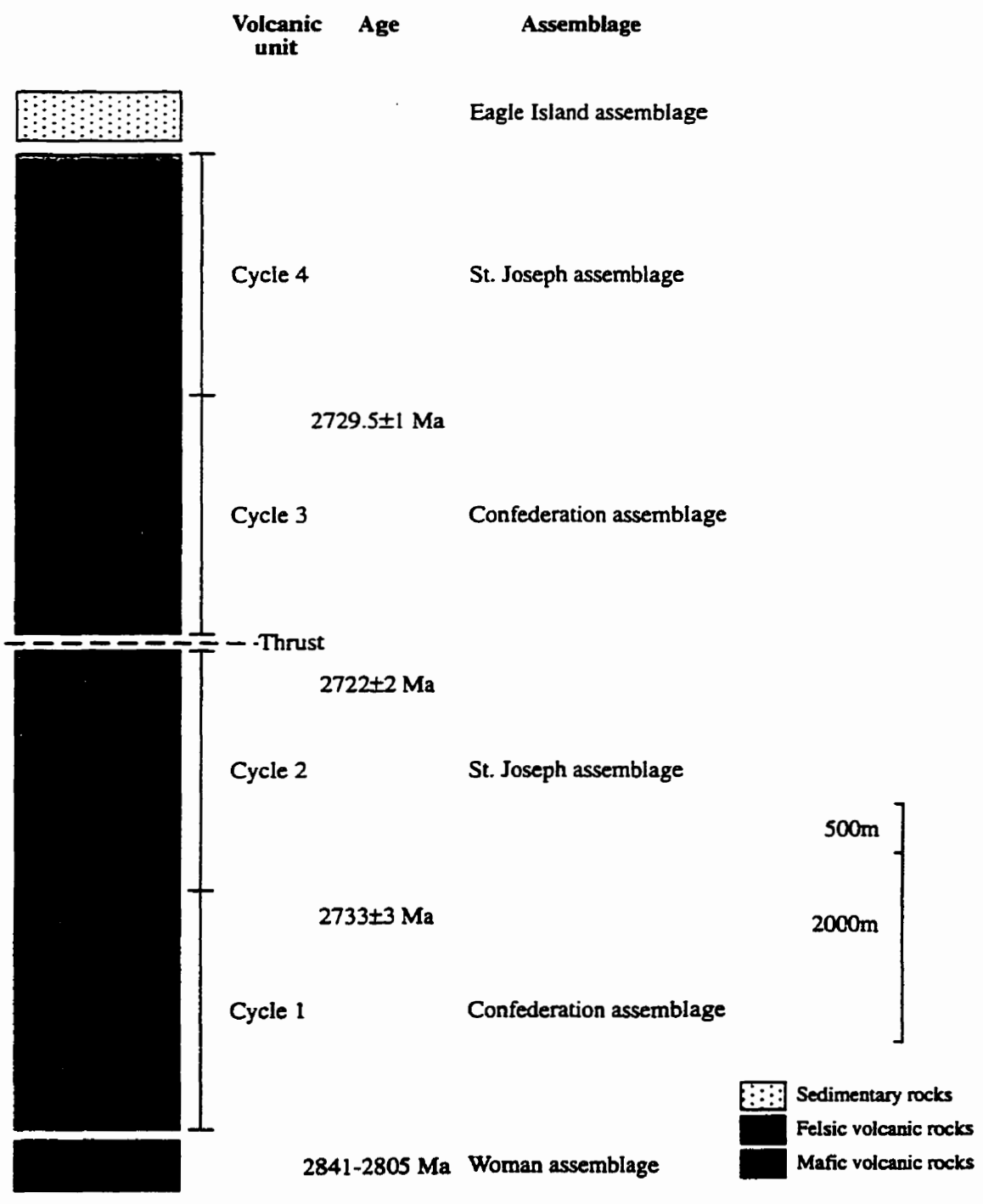

Figure 3.5. Representative tectono-stratigraphic columns through the western end of the Lake St. Joseph greenstone belt. The relative position of the Woman assemblage from the eastern margin of the belt is also shown. Approximate thicknesses are indicated where known. Age data from Stott and Corfu (1991).

Lower volcanic units, overlain by a sedimentary unit. Berger (1981) further subdivided the region by identifying a third volcanic unit. More recent work, including the dating of felsic units within the mafic volcanic sequences, has revealed a fourth, younger volcanic unit (Stott et al., 1987a, b; Corfu, unpublished data referenced in Stott and Corfu, 1991). The older units have been dated at 2733±3 Ma and 2729.5±1 Ma respectively (Cycles 1 and 3), and have been assigned to the Confederation assemblage, whereas the younger units (Cycles 2 and 4) have been assigned to the St. Joseph assemblage (2722±2 Ma; Stott and Corfu, 1991; Fig. 3.5). Cycle 2 outcrops between Cycles 1 and 3, indicating that the units have been tectonically interleaved (Stott et al., 1987a and b). Clifford and McNutt (1970) proposed that the rocks of the Confederation and St. Joseph assemblages, in the western part of the belt, are part of an Archean composite strato-volcano.

The Confederation assemblage is comprised of a lower tholeiitic unit dominated by pillowed and massive basalt flows approximately 2000 m thick, overlain by 500 m of dominantly dacitic to rhyolitic pyroclastic flows. This compositional transition is interpreted as the product of the geochemical evolution of the volcanic edifice with time (Clifford and McNutt, 1971).

St. Joseph assemblage. This is the youngest sequence of volcanic rocks within the Uchi subprovince, and is thought to reflect reactivation of the volcano after a hiatus of ~7 Ma. The assemblage comprises a lower unit of tholeiitic basalt, overlain by a thick sequence of pyroclastic deposits of dacitic to andesitic composition. The upper unit displays a compositional variation from dacitic, lithic tuff breccias, through highly vesicular tuff breccias, to an increasingly mafic dacitic to andesitic lapilli tuff; this trend in volcanic facies is consistent with eruption from a compositionally zoned magma chamber (Stott and Corfu, 1991). Stott (1996) has recently reported tentative evidence for the presence of komatiite flows within the St. Joseph assemblage.

Eagle Island assemblage. Sedimentary rocks of the Eagle Island assemblage unconformably overly the volcanic flows. It comprises siliciclastic sedimentary rocks with a St. Joseph assemblage provenance, as well as thick banded iron formation. Berger (1981) and Meyn and Palonen (1980) interpret the clastic iron formation association as the product of a submarine fan environment, in a late or post-tectonic basin.

The majority of published data on the Lake St. Joseph greenstone belt is derived from the western portion of the belt; however, Goodwin (1965) has shown that the eastern part of

the belt is lithologically and compositionally similar, with mafic volcanic rocks dominating the lower part of the stratigraphic sequence and felsic volcanic rocks predominating towards the top. In general the sequence youngs towards the south.

Structure and metamorphism. The Lake St. Joseph belt has been metamorphosed to amphibolite facies with garnet-hornblende and garnet-hornblende-biotite grade being abundant in the volcanic rocks (Goodwin, 1965). Structurally the belt is dominated by an east-west trending anticline (Stott and Corfu, 1991).

Mineral deposits. No economic mineral deposits have been recognised within the Lake St. Joseph belt; however, Stott and Corfu (1991) report the presence of massive sulfide clasts within the pyroclastic deposits of Cycle 1. In addition metasedimentary rocks adjacent to eastern Lake St. Joseph contain muscovite pegmatites with anomalous, but sub-economic, concentrations of rare lithophile elements.

3.2.3 Meen-Dempster Greenstone Belt

The Meen-Dempster greenstone belt is located towards the eastern part of the study area between the Birch-Uchi and Pickle Lake belts (Fig. 3.2). Stott and Corfu (1991) consider this belt to have been originally stratigraphically contiguous with the Pickle Lake belt to the east.

The Meen-Dempster belt comprises rocks of the Woman and younger Confederation assemblages (Fig. 3.6), which collectively are found along the length of the Uchi subprovince, as well as a recently proposed intervening Meen assemblage that has not yet been recognised from other greenstone belts of the Uchi paleo-continental margin (Stott, 1996). The Woman, Confederation and Meen assemblages strike east-west and have been shown to young towards the south (Fig. 3.6; Stott and Corfu, 1991). The following descriptions of the geology of assemblages within the belt are modified from Stott (1996) and Hollings et al. (1998).

Subdivision of the Woman and Meen assemblages. Stott and Corfu (1991) divided the Woman assemblage into two domains: the lower one is characterised by massive and pillowed mafic flows with rare thin felsic units and banded iron formation; the overlying domain includes a thick calc alkaline sequence, characterised by both proximal and distal pyroclastic deposits overlying a thin tholeiitic unit. The former is interpreted as the product of either a "back arc or basal platform", whereas the latter is

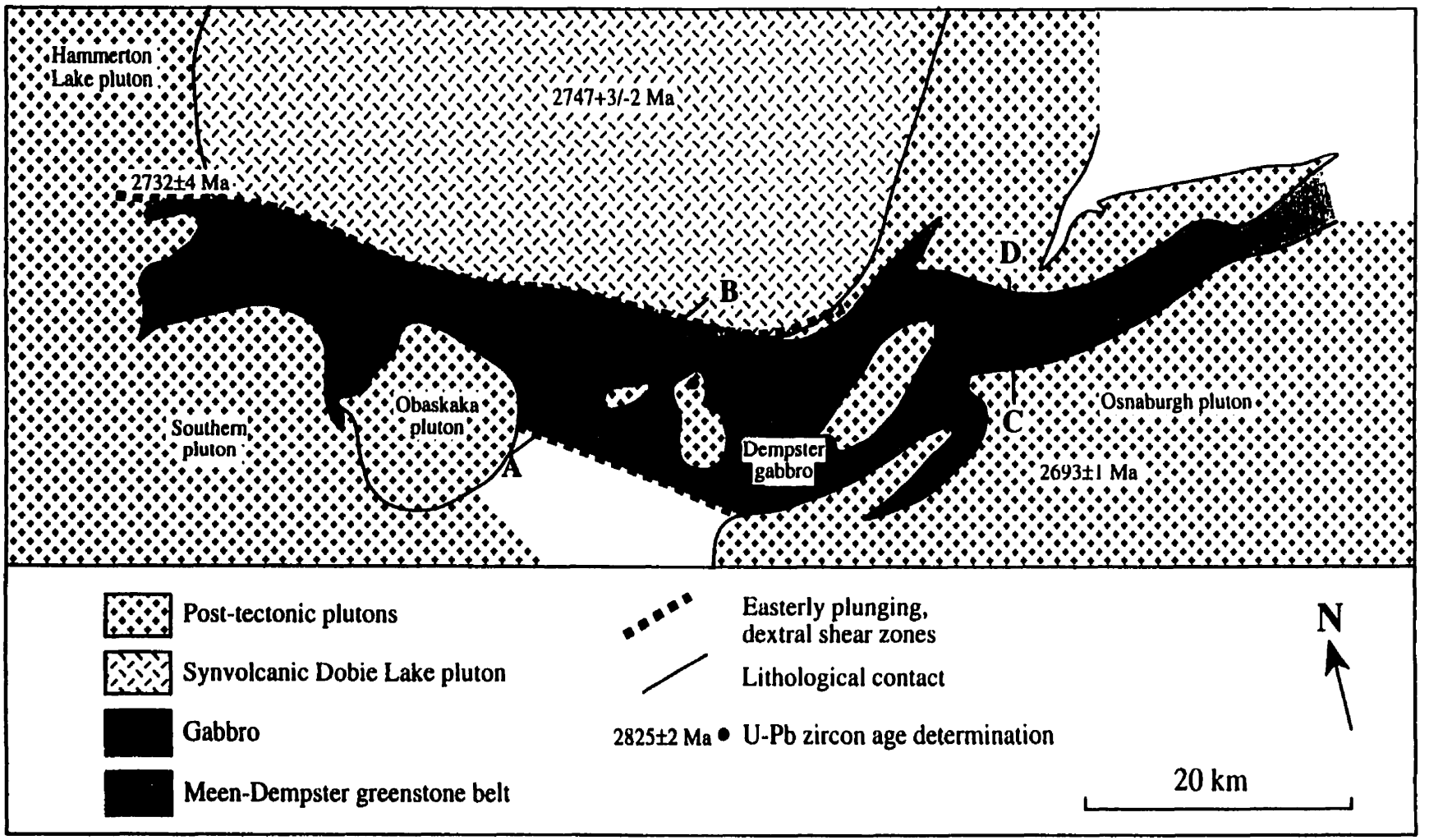

Figure 3.6. Simplified geological map of the Meen-Dempster greenstone belt. Modified after Stott and Corfu (1991). Lines A-B and C-D refer to sections on Figure 3.7.

considered to be of island arc affinity (Stott and Corfu, 1991). Recent work by Stott (1996) suggests that the Woman assemblage within the Meen-Dempster belt can be divided into two distinct assemblages: the Woman assemblage comprising rocks ~2840 Ma in age and a younger Meen assemblage consisting of rocks ~2825 Ma. This division broadly corresponds to the upper and lower portions of the Woman assemblage as defined in the Geology of Ontario (Stott and Corfu, 1991). A felsic tuff within the underlying tholeiites has been dated at 2842 +5/-2 Ma whereas the upper pyroclastic sequence has been dated at 2825±2 (F. Corfu, unpublished data, referenced in Stott and Corfu, 1991; Fig. 3.7). The top of the tholeiitic sequence is marked by Banded Iron Formation (BIF) which have been traced over 50 km and are interpreted to represent a significant hiatus in volcanic activity.

Scharer (1989) has dated a younger sequence of mafic and felsic volcanics towards the south of the belt, with two ages of 2816 and 2805 Ma. This sequence displays unusual geochemical characteristics and is thought to represent a distinct assemblage (Stott, pers comm., 1997). Thurston et al. (1991) have suggested that the termination of volcanism at ~2805 Ma is coincidental with the onset of the collision of the assemblage with the NCT.

The overall stratigraphic facing direction in the belt is southwards and the schistosity dips vertically to steeply northwards so that the strata are generally overturned across the belt, as is typical of much of the central Uchi subprovince. Some dacitic and iron formation units can be traced for several kilometres along strike.

Woman assemblage. The Woman assemblage lies along the northern margin of the belt and is composed dominantly of massive to pillowed basalt with at least two inter-flow units of banded magnetite iron formation, one of which can be traced geophysically for most of the length of the belt. Evidence of hydrothermal alteration of basaltic sequences is very limited. Thin units of dacitic to rhyolitic tuff and lapilli tuff occur locally interlayered between basalt flows. In contrast to the iron formation, these tuff units cannot be traced very far along strike. One of these tuff units has an U-Pb zircon age of 2842 +5/-2 Ma (Corfu and Stott, 1993b), demonstrating that the strata are comparable in age to the Woman assemblage in the Birch-Uchi belt further west (Fig. 3.2).

Meen assemblage. The Meen assemblage, dated at 2825±2 Ma (Corfu and Stott, 1993b), is a tabular sheet that can be traced for over 40 kilometres along strike, and is typically composed of dacitic pyroclastic deposits with minor rhyolitic units. There is

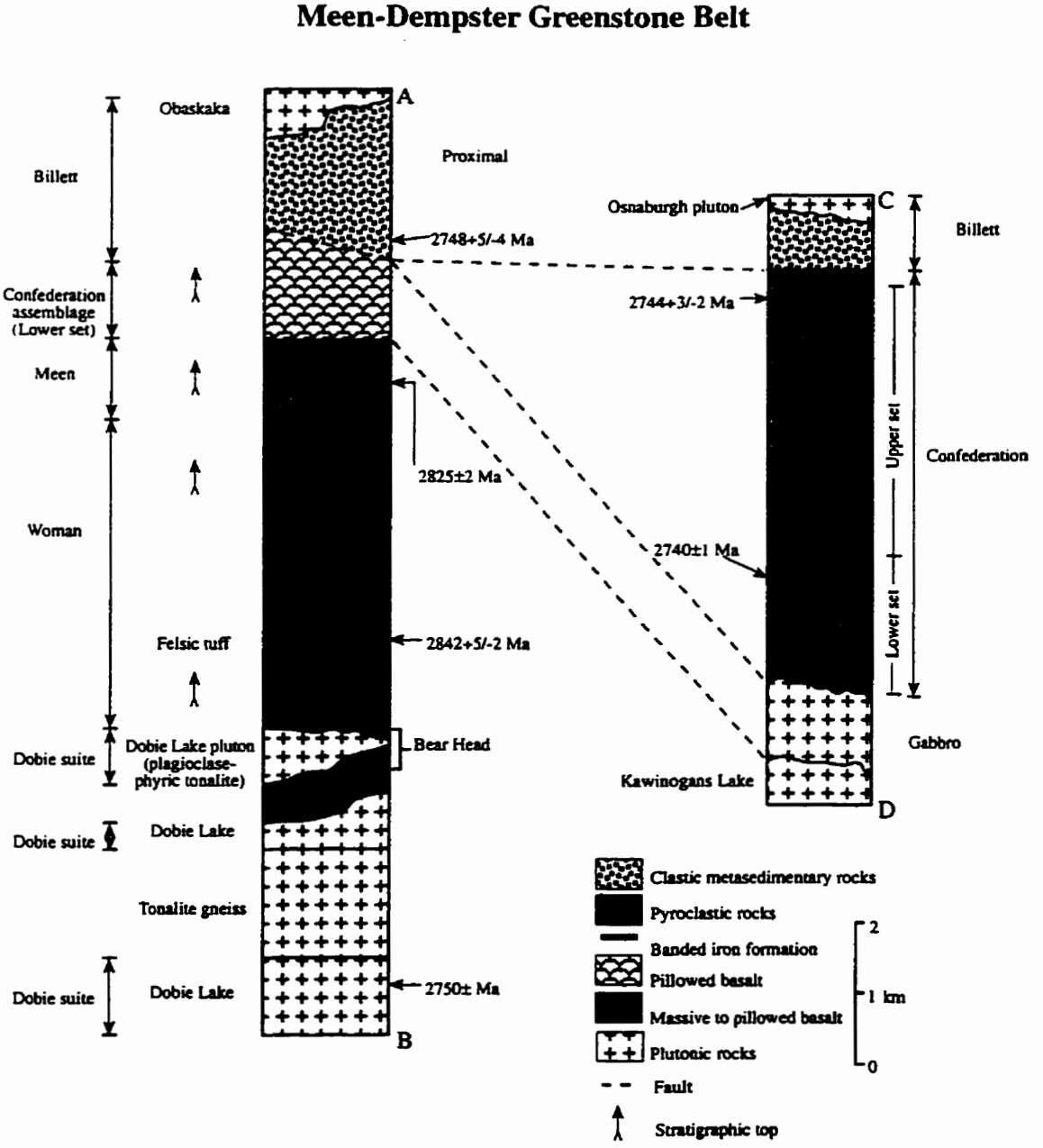

Figure 3.7. Tectono-stratigraphic sections displaying rock units and ages of the major assemblages in the Meen-Dempster greenstone belt. Modified after Stott and Corfu (1991). Locations of sections shown in Figure 3.6.

evidence for two volcanic centres in this sequence based on the presence of proximal pyroclastic facies comprising dacitic tuff breccia and pyroclastic breccia. One centre is at the western end of the belt on Meen Lake. The other, less prominent centre is west of the cross section AB in Figure 3.6. These two areas form the thickest sections of the pyroclastic sequence, which tapers along strike into finer grained, tuffaceous units that dominate much of the length of this sequence.

At the top of the sequence and particularly at the eastern end on Jacknife Lake, ferruginous chert, quartz-calcite-bearing marble, arenite and pyrite-graphite schist locally accompany the tuff and lapilli tuff beds. This sequence tapers at its eastern end on Jacknife Lake where shallowly dipping clastic and chemical metasedimentary beds overlie the pyroclastic rocks. Evidence for a coeval, and probably thin, basaltic cap on part of the pyroclastic sequence is seen 2.5 km southeast of Meen Lake where thin units of felsic to intermediate tuff and marble are interbedded with basaltic flows and basaltic tuff breccia. Exposed contacts between the pyroclastic rocks and the overlying basaltic pile are rare; no obvious shear zone or unconformity within the basalt or at the top of the pyroclastic sequence has been observed to separate the Meen and Confederation assemblages.

Confederation assemblage. The Confederation assemblage forms the southern half to two thirds of the belt. It contains two bimodal sequences of mafic to felsic volcanic rocks. Each set is composed of a basal platform of massive to pillowed basaltic flows with minor iron formation, overlain by a tabular sheet dominated by thickly bedded rhyolite to dacite tuff, representing distal ash-flows deposited in a subaqueous basin (Fig. 3.7). Fine-grained dacitic tuff of the lower set, on Dempster Lake, has a U-Pb zircon age of 2740±1 Ma, and this underlies the upper basalt-dacite set containing a dacitic lapilli tuff bed with a U-Pb zircon age of 2744 +3/-2 Ma (Fig. 3.6; Corfu and Stott, 1993a). The upper set is overlain by another basaltic sequence. There are no exposed contacts to reveal the primary or tectonic relationships between each of the basaltic and dacitic sequences in this assemblage. The evidence of slightly older volcanic units in the upper set overlying a younger sequence is consistent with either a tectonic stacking of different strata out of sequence or a duplication of one original bimodal sequence by thrust-stacking to form the two sets as described (Stott, 1996).

Billett assemblage. The Confederation assemblage is unconformably overlain by the clastic metasedimentary Billett assemblage. The Billett assemblage is dominated by feldspathic wacke-shale couplets, generally less than 40 cm thick, and includes a section

of interbedded polymictic conglomerate and wacke. All clasts appear to be derived from comparable proximal sources to the north. In particular, the trondjhemite clasts not only petrographically resemble the Dobie pluton but a U-Pb zircon age determination of 2748 +5/-4 Ma from one of the trondjhemite clasts compares closely with the age of the 2747 Ma Dobie pluton (Corfu and Stott, 1993b).

Structure and metamorphism. Stott and LaRocque (1983a, b) recognised two broad structural domains within the Meen-Dempster belt, both characterised by a steeply northward dipping schistosity that closely parallels the overturned volcanic bedding (Stott and Corfu, 1991). Locally this schistosity is overprinted by younger contact strain aureoles adjacent to late granitic plutons. Folding of strata is limited to local asymmetric rotation of strata so that the overall framework resembles a stacked set of steeply dipping, interlayered units dominated by basalt and dacite.

Mineral deposits. The Meen-Dempster belt is host to the Golden Patricia gold mine.

3.2.4 Birch-Uchi Greenstone Belt

The Birch-Uchi greenstone belt is located within the Central Uchi subprovince (Fig. 3.2). The presence of both gold deposits and the South Bay VMS camp within the belt has resulted in extensive volcanological and geochemical studies of the volcanic sequences that comprise the belt (e.g., Goodwin, 1967; Pryslak, 1971a, b; Thurston, 1985a; Thurston and Fryer, 1983; Lesher et al., 1986).

Mapping of the greenstone belt by Goodwin (1967) led to the identification of two cycles of volcanic activity, termed Cycles II and III by Nunes and Thurston (1980). Pryslak (1971a), mapping the western portion of the belt, later identified a lower stratigraphic unit (Cycle I). Each cycle is characterised by the progression from mafic to felsic rock types towards the top of the stratigraphic sequence (Figs. 3.8 and 3.9). Later work by Thurston (1985a, b) extended these subdivisions to encompass the entire greenstone belt. Geochronological studies of the Birch-Uchi belt by Wallace et al. (1986) and Nunes and Thurston (1980) demonstrated that these three volcanic sequences were not the product of progressive volcanism, but rather were the result of distinct magmatic events spanning some 220 million years.

It should be noted that in the early work by Thurston (1985a), the eastern portion of the

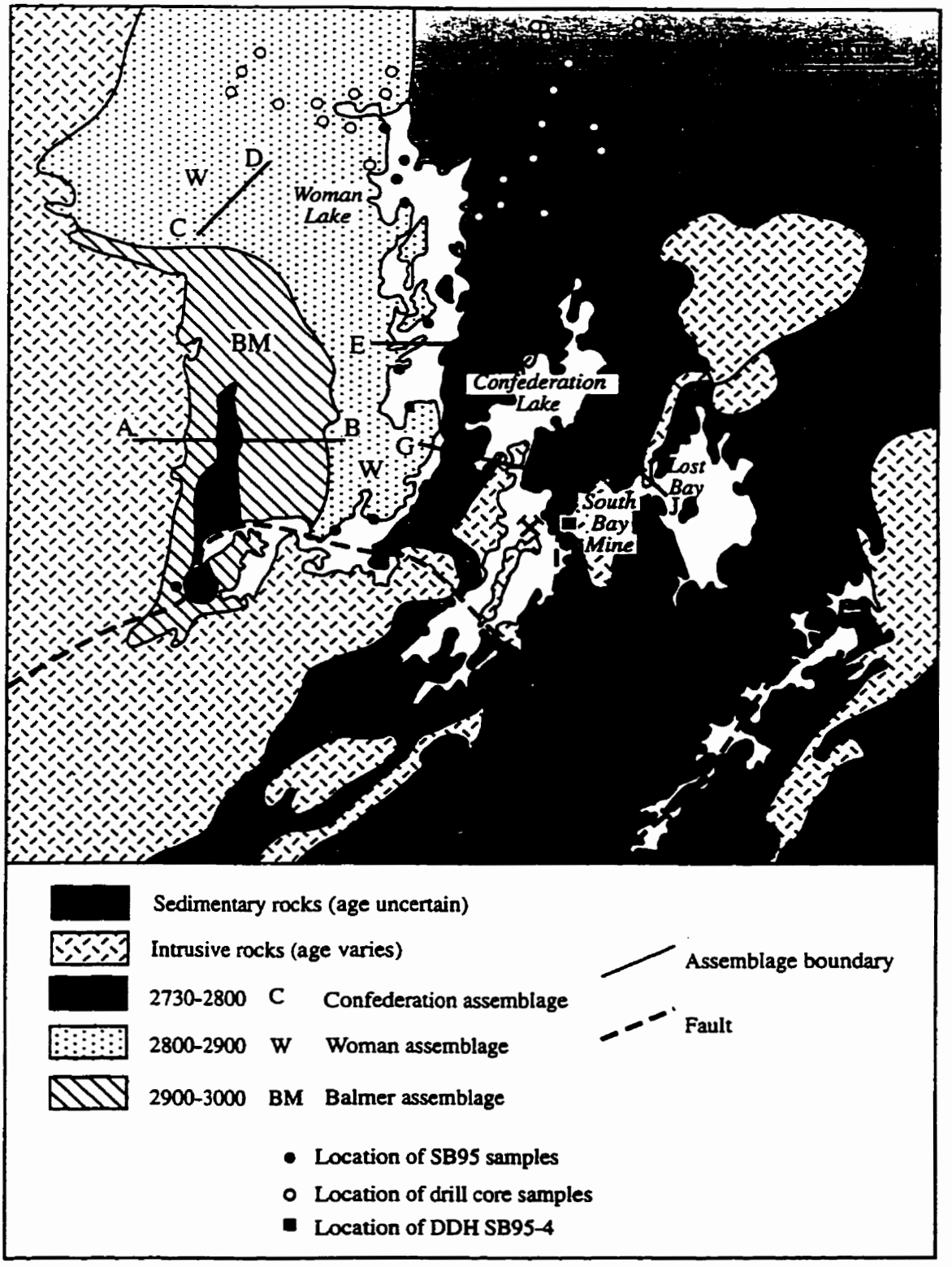

Figure 3.8. Simplified geological map of part of the Birch-Uchi greenstone belt, illustrating the locations of the South Bay mine site, DDH SB95-4 and South Bay surface samples (SB95). Letters A to J refer to tectono-stratigraphic sections on Figure 3.9. Modified after Stott and Corfu (1991).

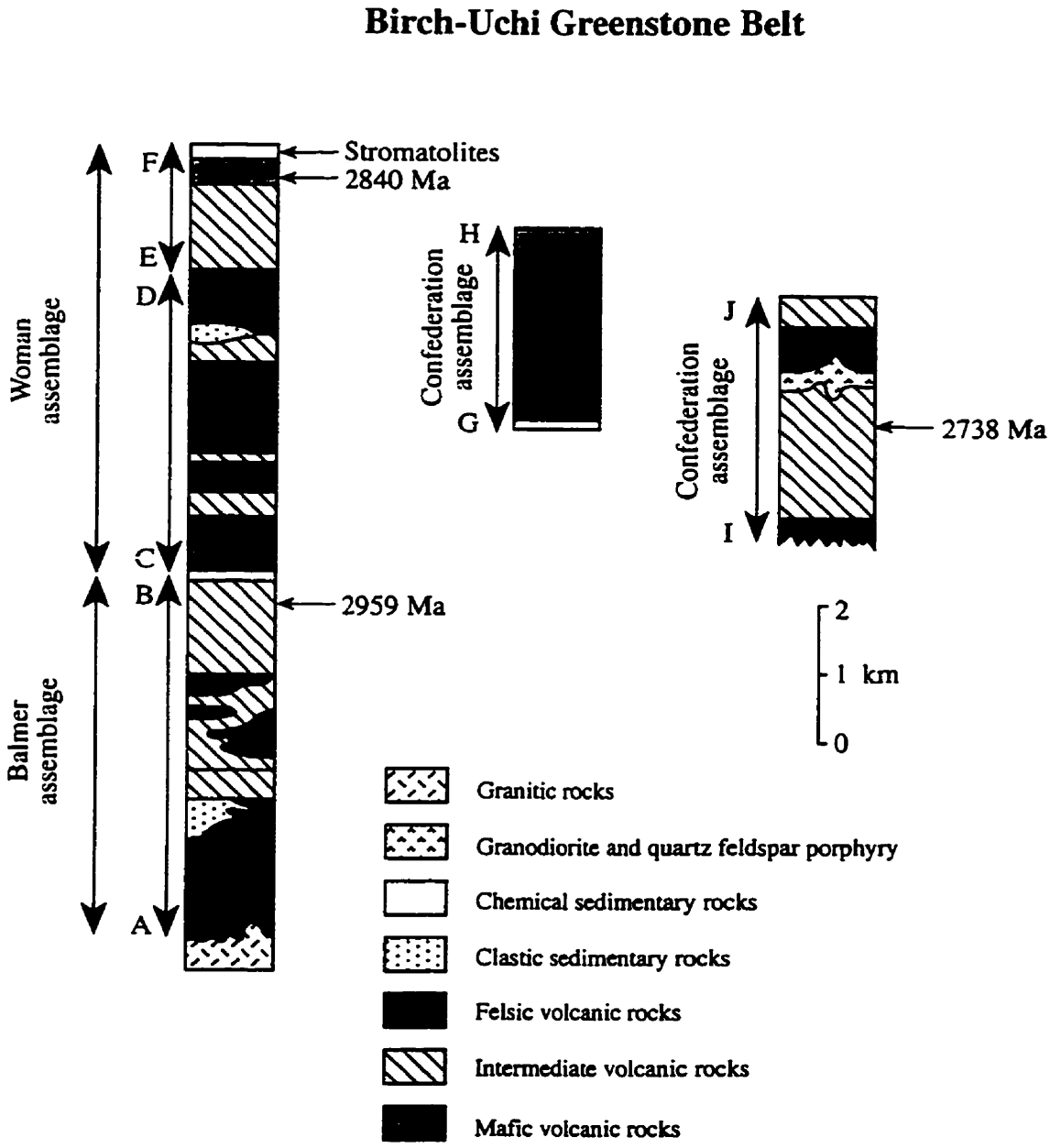

Figure 3.9. Composite tectono-stratigraphic section of the Birch-Uchi greenstone belt. Modified after Stott and Corfu (1991). Location of sections A to J is shown on Figure 3.8.

belt was classified in terms of the stratigraphic relationships defined in the western part of the belt, i.e., Cycles I, II and III. However, Noble (1989) has since shown that rock types to the east are in fact of comparable age to Thurston's Cycle III, and the stratigraphic similarities with Cycles I and II are coincidental. One result of this initial confusion over the stratigraphic relationships is that much of the early work on the area refers to other studies that utilise the terms Cycles I and II in the eastern portion of the belt, but these subdivisions are no longer valid (e.g., Wallace et al., 1986; Stix and Gorton, 1989). In the light of regional studies across the subprovince as a whole, Scott and Corfu (1991) have redefined the three volcanic sequences as distinct assemblages; the older Balmer assemblage (~2960 Ma), the Woman assemblage (~2840 Ma), and the younger Confederation assemblage (~2735 Ma; Figs. 3.8 & 3.9).

Balmer assemblage. This volcanic dominated assemblage occupies the lowest stratigraphic position within the greenstone belt, outcropping in the western portion of the belt (Fig 3.8). It is estimated to be ~4800 m thick, and has been subdivided into four formations (Thurston, 1985a). The lowermost Formation A comprises up to 2500 m of massive and pillowed mafic flows overlain by minor tuffs of intermediate composition; these in turn are overlain by the mixed wacke, argillite and intermediate to felsic tuffs of Formation B (~1500 m); Formation C consists of a thin unit of felsic tuffs up to 320 m thick, that interfingers with the top of Formation B; the sequence is capped by a thin unit (~60-70 m) of shallow water carbonate deposits, now metamorphosed to marble, and iron formation (Formation D). U-Pb dating of zircons in a rhyolite crystal lithic tuff from Formation C has yielded an age of 2959±2 Ma (Nunes and Thurston, 1980).

Woman assemblage. This assemblage is also a volcanic dominated sequence, located towards the centre of the Birch-Uchi greenstone belt (Fig. 3.8). Four distinct formations have been identified within the assemblage, termed E, G, H and J (Thurston, 1985a). As with the Balmer assemblage the lowest stratigraphic unit is comprised of ~3600 m of mafic and intermediate subaqueous flows overlain by minor intermediate to felsic tuff units and iron formation (Formation E). Formation G is characterised by up to 2800 m of proximal to distal massive flows of intermediate lapilli tuff; this is overlain by ~700 m of subaerial ignimbrite sheets and subaqueous ash flows interpreted to be the product of a Plinian eruption - Formation H (Thurston, 1980). The uppermost Formation J, is comprised of ~150 m of iron formation and shallow water carbonates, identified by Hofmann et al. (1985) as stromatolitic deposits. U-Pb dating of zircons within the felsic rocks of Formation H has yielded an age of 2840 Ma (Corfu, unpublished data referenced

in Wallace et al., 1986). The BIF of Formation J are likely correlative with BIF that cap the ~2840 Ma tholeiites of the Woman assemblage in the Meen-Dempster belt, ~50 km to the east.

Stott (1997) has interpreted the conformable contact between the Balmer and Woman assemblages in the western portion of the belt, in conjunction with ages of 2840 Ma for the Woman assemblage and the pluton intruding the base of the Balmer assemblage (Fig. 3.8), to imply that the Woman assemblage developed autochthonously or proximal to the Balmer assemblage.

Confederation assemblage. The youngest volcanic sequence dominates the eastern portion of the Birch-Uchi greenstone belt and is the most areally extensive of the three volcanic assemblages (Fig. 3.8). Extensive mapping of the Confederation assemblage has allowed the identification of numerous volcanic cycles (Thurston, 1985a and b, 1986; Good, 1988; Beakhouse, 1989; Stix and Gorton, 1989). Thurston (1986) proposed that one cycle, several thousand metres thick, represented felsic volcanism deposited on a submarine shield volcano that underwent Plinian eruptions and subsequent caldera collapse. Similarly Stix and Gorton (1989) have recognised the presence of numerous pyroclastic flow deposits, all less than three metres thick, within a pyroclastic unit near Lost Bay (Fig. 3.8).

Geochronological studies by Nunes and Thurston (1980) and Noble (1989) have yielded U-Pb ages of between 2735+4/-3 and 2739±2 Ma for felsic sequences within the Confederation assemblage. The eastern half of this assemblage can be shown to comprise a single sequence some 7000 m thick, whereas Noble et al. (1989) have shown that the western portion consists of a complex repetitive sequence of volcanic cycles. Radiometric dating of the belt is at present insufficient to distinguish whether this represents several rapidly deposited volcanic cycles, or alternatively tectonic interleaving of a single cycle (Stott and Corfu, 1991). Stott and Corfu (1991) advocate the tectonic interpretation, on the basis of stratigraphic patterns and folds observed in the eastern part of the belt.

On the eastern margin of the Birch-Uchi belt, Good (1988) and Bowen (1989) described a sequence of thick wackes and mudstones tectonically interleaved with basaltic flows. Stott and Corfu (1991) propose that this unnamed assemblage has been allochthonously or parautochonously transported northwards during the Kenoran orogeny.

Structure and metamorphism. Unlike the majority of greenstone belts in the Uchi subprovince, the Birch-Uchi belt is unique in that its tectono-stratigraphic units strike north-south. It has been suggested, but not yet convincingly demonstrated, that this is the result of northward transport of the Confederation assemblage during the Kenoran orogeny (Noble et al., 1989; Stott and Corfu, 1991). Evidence for this transport includes D1 deformation structures, characterised by a northward trending bedding parallel schistosity, as well as a D2 event which becomes more prominent towards the south of the belt. Stott and Corfu (1991) speculate that this north verging event may be the result of late stage orogenic shortening. The belt was originally interpreted to be centred on a north trending synclinorium, based both on opposing stratigraphic top directions, and the symmetry of the stratigraphy and the radiogenic ages of the units (Thurston, 1985a; Nunes and Thurston, 1980). However, it has been demonstrated that the radiogenic ages are not symmetrical across the fold structure and that stratigraphic relationships in the eastern portion of the belt are not in fact a repetition of the Woman and Balmer assemblages (Fig. 3.8; Noble, 1989; Noble et al., 1989).

Mineral deposits. The Birch-Uchi greenstone belt is host to the South Bay deposit, the only economically viable VMS deposit identified within the Uchi subprovince. During its ten years of activity some 1.6 million tons of ore with an average grade of 11% Zn, 2% Cu and 2.12 ounces Ag per ton were produced; the mine is now closed (Atkinson et al., 1990). The deposit is located above an endogenous rhyolite dome of quartz feldspar porphyry within what Thurston (1985a) described as Cycle III rhyolite (Confederation assemblage; Fig. 3.8). According to Thurston et al. (1978), the rhyolites which host the deposit are the product of a caldera-like structure. Campbell et al. (1981) state that the ore at the South Bay mine is associated with rhyolite flows and a high level quartz-feldspar prophyry intrusion. They proposed that the porphyries are the feeder connecting the rhyolites to an underlying subvolcanic magma chamber, the existence of which is supported by gravity studies (Thurston, pers comm., referenced in Campbell et al., 1981).

Recent exploration has focussed on a number of significant VMS hosting horizons located to the south west of the South Bay mine site (Fig. 3.10). These horizons are located within rocks of the Confederation assemblage but are not exposed on the surface (Stott, pers. comm., 1996).

In addition to the South Bay deposit the Birch-Uchi belt is also host to a number of small

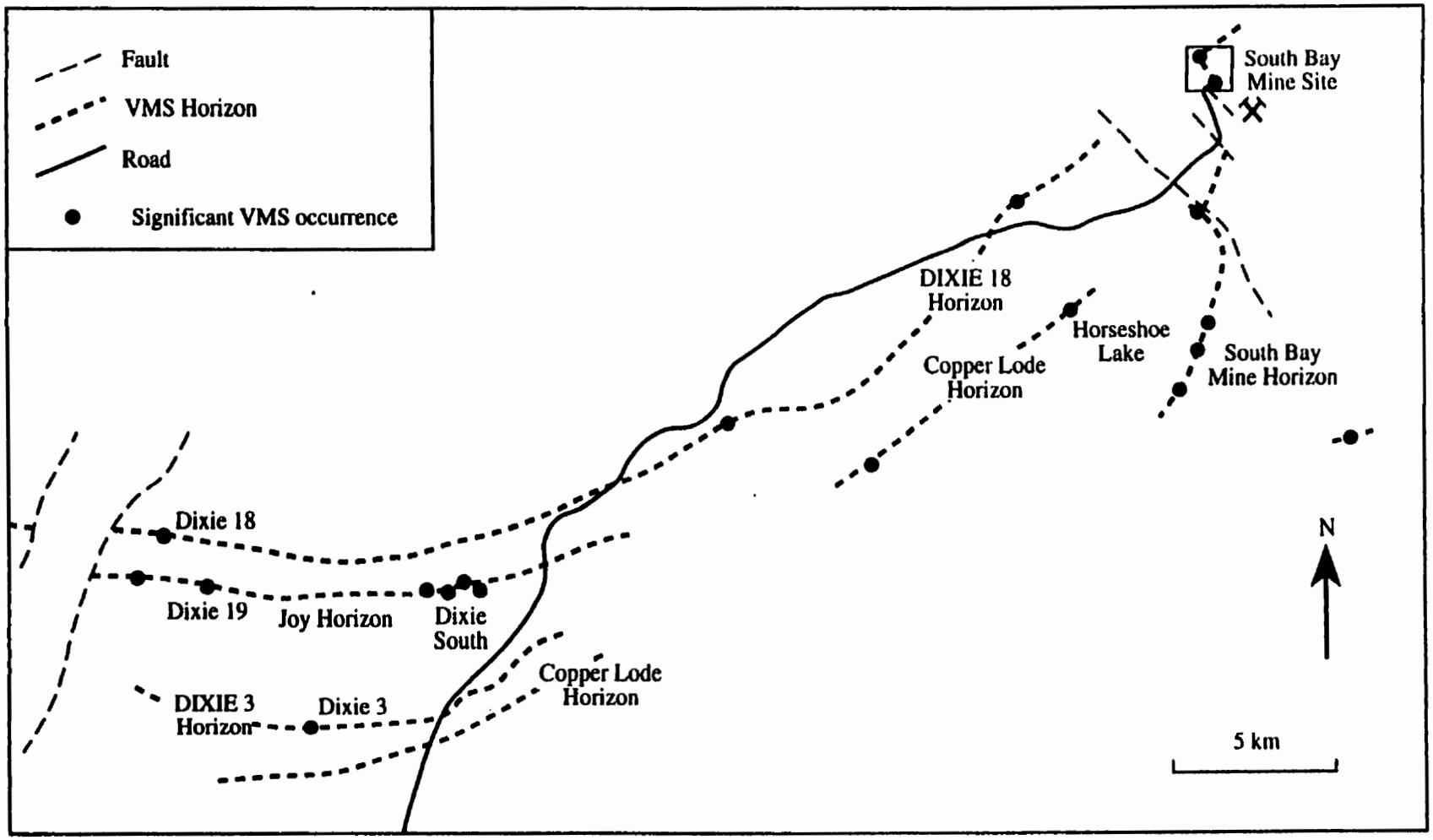

Figure 3.10. Location of drill holes sampled in 1996, in the Birch-Uchi greenstone belt. Absence of lithological subdivisions reflects limited exposure. Horizons are after a map prepared by Cumberland Resources Ltd.

gold deposits. Goodwin (1967) reports that the five mines in operation between 1933 and 1943 produced 245,582 ounces of gold and 42,612 ounces of silver. These deposits occur throughout the belt and are typically hosted in volcanic rocks of rhyolitic to andesitic composition (Goodwin, 1967).

3.2.5 Red Lake Greenstone Belt

The Red Lake greenstone belt is located towards the western end of the study area (Fig. 3.2) and comprises a number of distinct volcanic assemblages: from oldest to youngest these are the Balmer and Ball (2.9-3.0 Ga), the Woman (2.82 Ga) and the younger Confederation assemblage (2.7 Ga) The assemblages are those defined by Stott and Corfu (1991), based on the mapping of Pirie (1981) and Wallace et al. (1986). A geological map of the Red Lake belt is illustrated in Figure 3.11 and a reconstruction of the major tectono-stratigraphic units is given in Figure 3.12.

Balmer assemblage. This assemblage is the most areally extensive, constituting some 50% of the belt. It includes some of the oldest volcanic rocks of the Uchi subprovince dated at 2992 to 2958 Ma (Fig. 3.11; Corfu and Wallace, 1986; Corfu and Andrews, 1987). Tholeiitic basalt and komatiite lava flows dominate, with interflow banded iron formation (BIF). Distinctive chemical metasedimentary horizons can be traced for over 10 km, whereas thin rhyolitic units outcrop sporadically (Wallace et al., 1986). The Balmer assemblage is in tectonic contact with adjacent assemblages, faults having been identified along the boundary with the Confederation assemblage to the south and inferred along the submerged contact with the Bruce Channel assemblage to the east (Stott and Corfu, 1991). The Balmer assemblage has been correlated with the >2870 Ma Garner Lake assemblage of the Rice Lake greenstone belt to the west, and also outcrops along the eastern margin of the Birch-Uchi belt (Poulsen et al., 1996)

Ball assemblage. To the west of the belt the Ball assemblage is comprised of mafic flows interbedded with relatively large volumes of felsic and intermediate pyroclastic volcanic rocks and distinctive units of chemical sediments, including a carbonate horizon (Figs. 3.11 and 3.12). U-Pb zircon ages obtained from felsic units above and below the carbonate horizon have yielded ages of 2940±2 Ma and 2925±3 Ma respectively, indicating a significant hiatus in volcanic activity, during which BIF and carbonate units were deposited (Corfu and Wallace, 1986). The tuff units are located above and below one of the few occurrences of stromatolites identified in the Superior Province (Hofmann et al., 1986; Fig. 3.12).

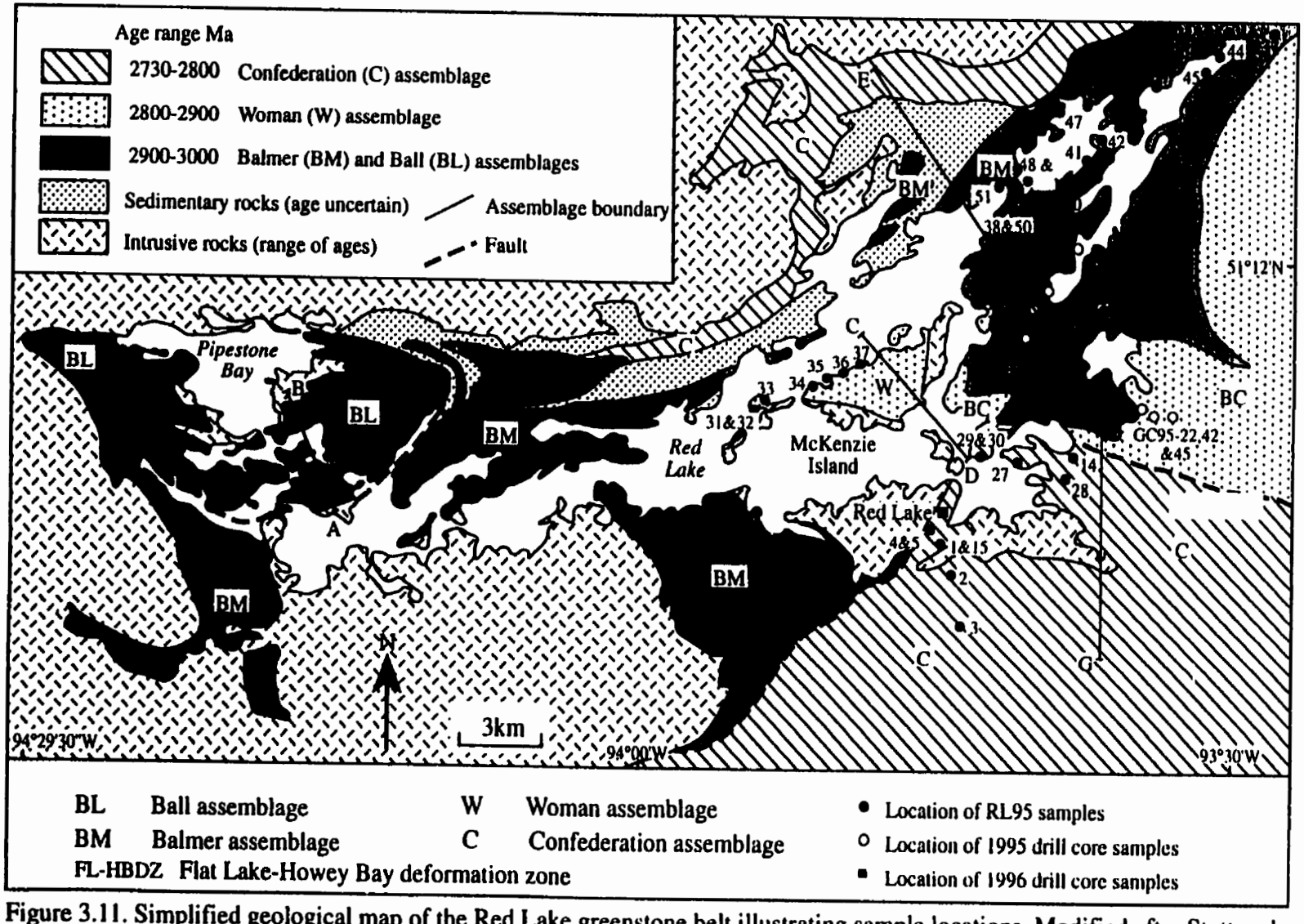

Figure 3.11. Simplified geological map of the Red Lake greenstone belt illustrating sample locations. Modified after Stott and Corfu (1991). The letters A-H refer to tectono-stratigraphic sections in Figure 3.12.

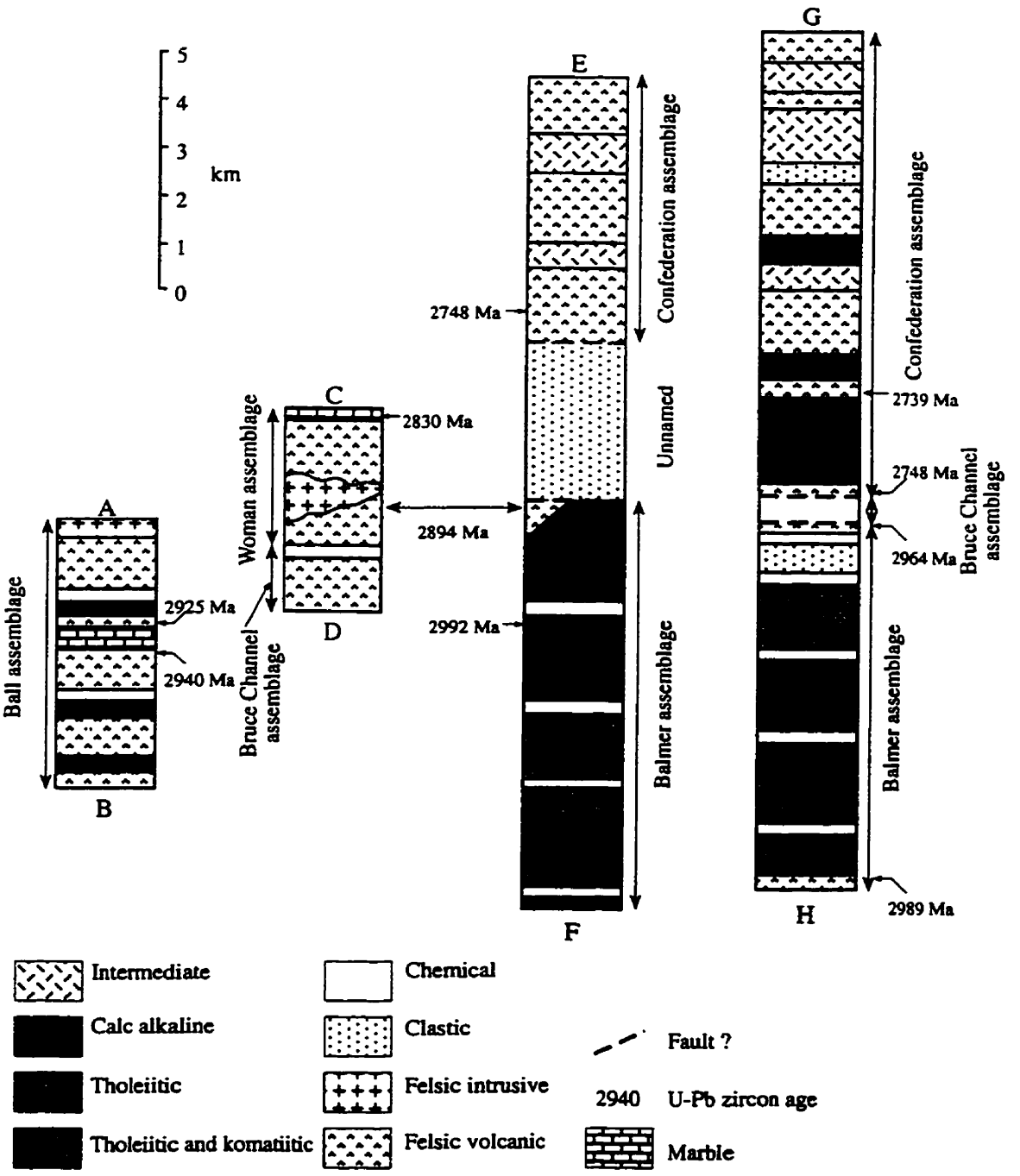

Figure 3.12. Tectono-stratigraphic sections showing typical rock units and ages of the major assemblages of the Red Lake greenstone belt. Modified after Wallace et al. (1986). Locations of sections are shown on Figure 3.11.

Woman assemblage. The single occurrence of the Woman assemblage within the Red Lake greenstone belt is on McKenzie Island, where it is represented by a sequence of felsic pyroclastic rocks, which have been dated at 2830 Ma (Fig. 3.11; Corfu and Wallace, 1986). The limited outcrop of this assemblage in the Red Lake area has made the determination of the nature of the contacts with surrounding assemblages difficult (Stott and Corfu, 1991). This 2830 Ma assemblage may be correlative with the Meen assemblage of the Meen-Dempster belt. However, recent dating of these felsic rocks has yielded zircons with ages as young as 2738 Ma (Corfu, pers. comm., 1996), casting doubt on the identification of these rocks as being part of the Woman assemblage

Confederation assemblage. This assemblage outcrops along the northern and southern margins of the greenstone belt (Fig. 3.11). It is characterised by repeated cycles of tholeiitic to calc alkaline volcanic rocks, commonly associated with voluminous pyroclastic deposits towards the top of the sequence (Fig 3.12). The latter have been stratigraphically correlated with the uppermost units of the Confederation assemblage within the Birch-Uchi belt to the east (Figs. 3.8 and 3.9; Stott and Corfu, 1991).

Structure and metamorphism. The Flat Lake-Howey Bay deformation zone is a major fault zone between the Balmer and Confederation assemblages, which is cut by the 2718 Ma Dome stock (Andrews et al., 1986; Corfu and Wallace, 1986). These structural and temporal relationships have been used by Stott and Corfu (1991), in conjunction with additional geological evidence, to infer that the various assemblages of the Red Lake greenstone belt were juxtaposed prior to 2718 Ma.

Volcanic rocks within the Red Lake belt have been variably metamorphosed, ranging from mid-greenschist to lower-amphibolite facies, the higher grades generally occurring along the margins of major plutonic complexes.

Mineral deposits. The Red Lake greenstone belt is host to some of Canada's larger gold deposits. The Campbell Mine, for example, has a production total of some 7 million ounces with known reserves of 3 million ounces in 1990 (Stott and Corfu, 1991). These deposits have been interpreted as the result of hydrothermal fluids associated with late stage ductile deformation and post peak metamorphism, approximately coeval with pluton emplacement (Fig. 3.13; Andrews et al., 1986).

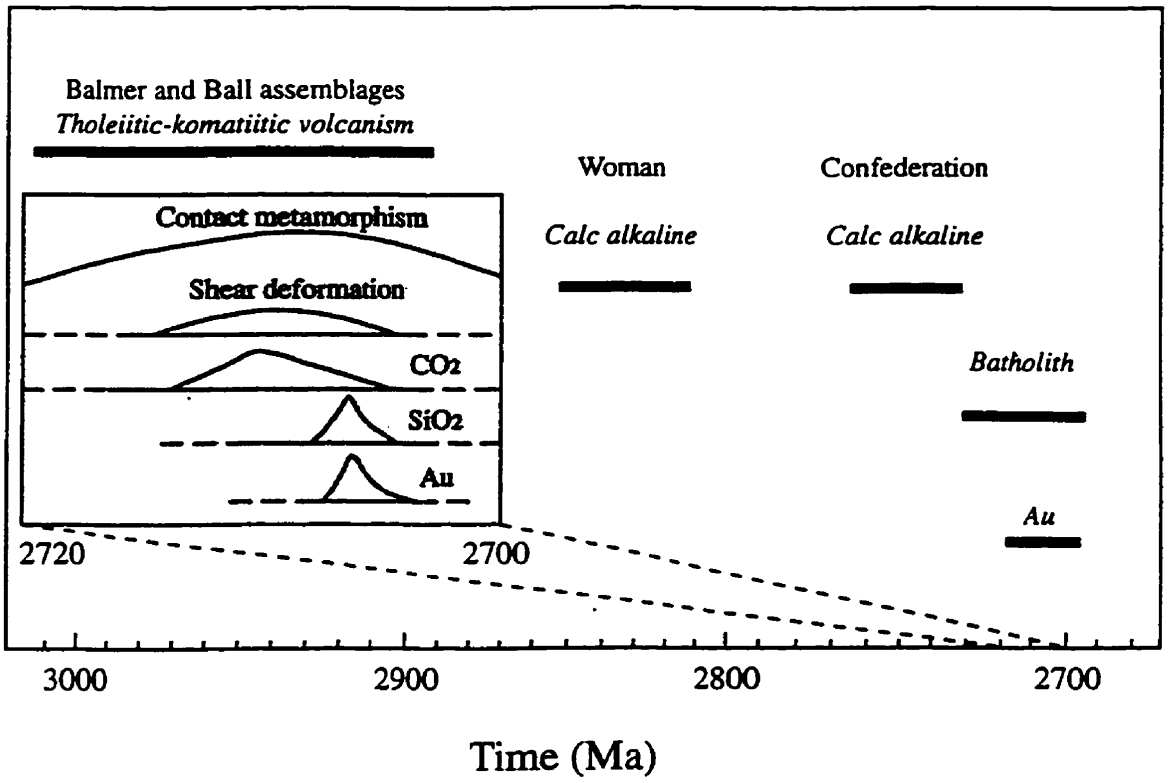

Figure 3.13. Summary of major events in the Red Lake greenstone belt, and their relative chronology. SiO_2 and CO_2 represent alteration associated with discrete shear zones. Au represents gold mineralisation. Modified after Andrews et al. (1986).

3.2.6 Rice Lake Greenstone Belt

The Rice Lake greenstone belt is located within Manitoba, at the western end of the Uchi subprovince (Fig. 3.2). The belt is bounded to the north by the Wanipigow River plutonic complex of the Berens River subprovince, whereas the southern boundary is transitional with the Manigotagan gneissic belt of the English River subprovince (Fig. 3.14; Weber, 1971a; McRitchie and Weber, 1971). Major faults demark the northern and southern margins of the belt, both displaying large apparent dextral offsets (Richardson and Ostry, 1996).

The Rice Lake belt has been subdivided into the dominantly volcanic Rice Lake group and the overlying metasedimentary rocks of the San Antonio Formation (Davies, 1963). According to mapping of Weber (1971a, b), the Rice Lake Group can be further subdivided into the Bidou Lake and Gem Lake subgroups, both of which are overlain by sedimentary rocks of the Edmunds Lake subgroup. Ritchie (1971) identified the volcanic and sedimentary rocks of the Wallace Lake area as the Wallace Lake subgroup. Recent remapping led to the recognition of the Garner Lake subgroup (Poulsen et al., 1996). Poulsen et al. (1996) proposed that the various formations, groups and subgroups listed above could be correlated with the assemblages of the Red Lake greenstone belt as defined by Stott and Corfu (1991). This correlation is illustrated in Table 3.1. In light of this correlation, and to allow for easier comparison with other sections of this chapter specifically and the thesis generally, the subgroups of the Rice Lake belt will henceforth be termed assemblages following the lithotectonic terminology of Thurston et al. (1991).

Table 3.1. Main supracrustal elements of the Rice Lake belt, modified after Poulsen et al. (1996). Uchi assemblages after Stott and Corfu (1991).

Assemblage	Former term	Age constraints	Uchi Equivalent assemblages
San Antonio	San Antonio Fm.	<2730 Ma	None
Edmunds Lake	Rice Lake Group	<2720 Ma, >2650 Ma	Billett assemblage, English River
Gem Lake		2722±2 Ma	St. Joseph assemblage
Bidou Lake		>2729 Ma	Confederation assemblage
Garner Lake		>2870 Ma	Balmer assemblage
Wallace Lake		<3000 Ma, >2920 Ma	Ball assemblage

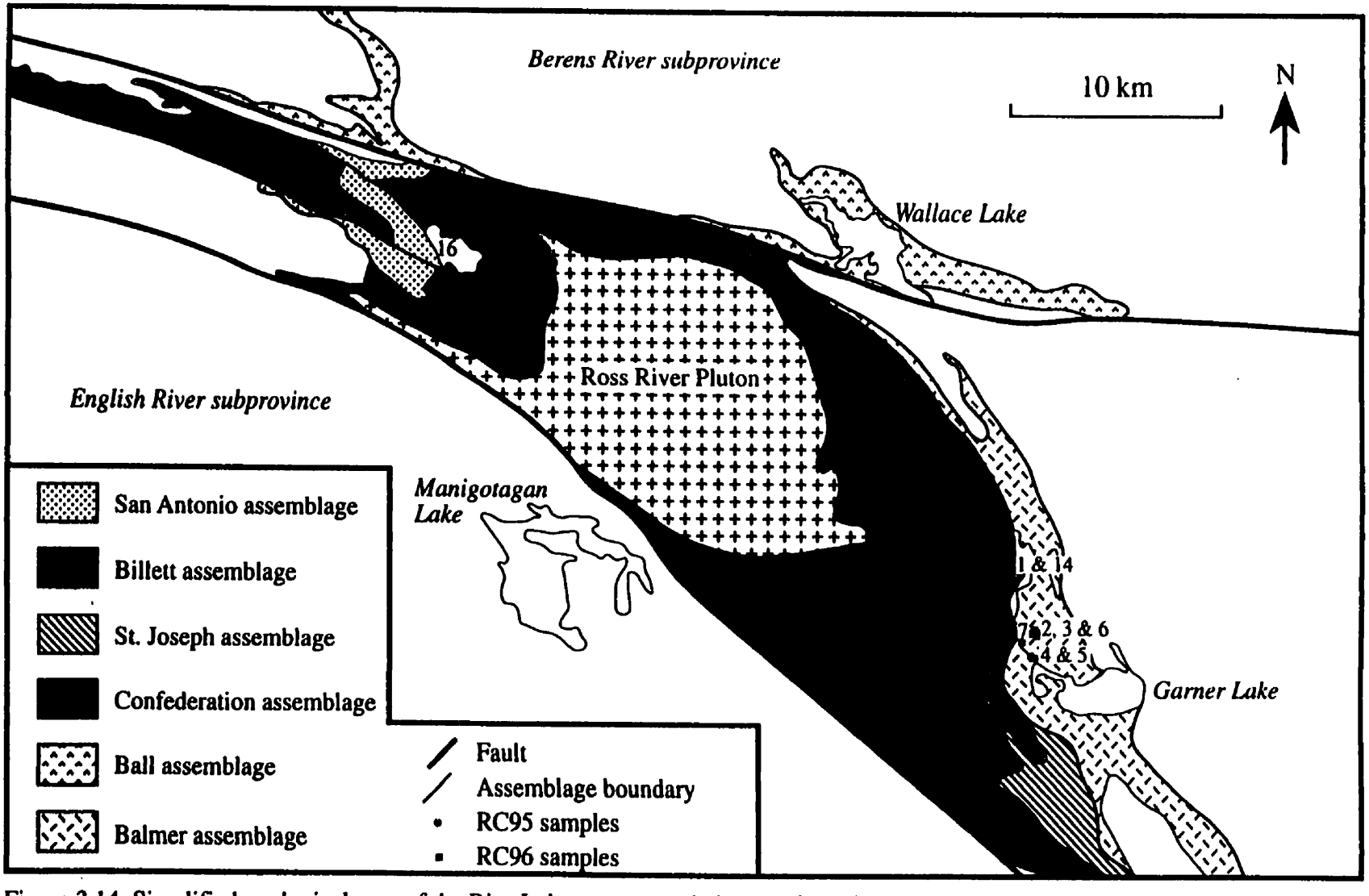

Figure 3.14. Simplified geological map of the Rice Lake greenstone belt, modified after Poulsen et al. (1996). Locations of samples from the 1995 (RC95) and 1996 (RC96) field seasons are illustrated.

Ball and Balmer assemblages. The Wallace Lake (Ball) assemblage was defined by McRitchie (1971) as comprising basal mafic volcanic rock types and volcanogenic sedimentary rocks of felsic to intermediate composition, overlain by a distinctive sedimentary sequence deposited in a shallow water environment. Theyer (1983) identified a spinifex textured ultramafic unit within these sediments. Detrital zircons within the sediments have been dated at ~3 Ga whereas a younger age limit is provided by a quartz feldspar porphyry dyke dated at 2.92 Ga (Poulsen et al., 1994).

The second circa 3 Ga assemblage is the Garner Lake (Balmer) assemblage, a coherent east-west trending stratigraphic sequence of supracrustal and intrusive rocks at least 5 km thick (Fig. 3.14; Poulsen et al., 1996). The base of the sequence is characterised by intercalated mafic and felsic units; however in the field an intense foliation makes it difficult to distinguish between volcanic or sedimentary protoliths (Poulsen et al., 1996). To the north are a sequence of mafic and ultramafic intrusions which have yielded zircons dated at ~2870 Ma (Poulsen et al., 1993). The 2870 Ma intrusive sequence, which implies an age of >2870 Ma for the assemblage as a whole, is overlain by units of felsic tuff and volcanic breccia, capped by a thin chemical sedimentary unit. Overlying this are a sequence of komatiites, komatiitic basalts, and basalts, in turn overlain by intercalated tholeiitic and calc-alkaline basalts (Poulsen et al., 1996). The >2.87 Ga age is close to that of the Pickle Crow assemblage, and may imply a correlation with that assemblage rather than the Balmer assemblage as proposed by Poulsen et al. (1996). Resolution of this question requires further geochronological studies.

Confederation assemblage. The majority of the Rice Lake belt is comprised of the Bidou Lake (Confederation) assemblage (Fig. 3.14; Table 3.1). Campbell (1971) divided this assemblage into a number of distinct formations; however, the assemblage as a whole includes a bimodal volcanic sequence of basalt and dacite-rhyolite (Weber, 1971b). The following description of the formations of the Confederation assemblage follows the classification scheme of Campbell (1971). The lowermost is the Stovel Lake Formation, a relatively uniform sequence of fine to medium grained feldspar greywackes that are in conformable contact with the overlying massive and pillowed basalts of the Tinney Formation. The Tinney Formation is overlain by the Dove Lake Formation; however the contact between the two is not exposed. The latter is represented by medium- to fine-grained greywackes with minor chert and volcanic agglomerates. Contacts between the formations are often obscured by deformation and intrusions; however, they generally tend to be conformable (Brommecker, 1996)

Rocks of the Gunnar Formation are composed almost entirely of pillow basalts with an approximate thickness of 875m; they overly the Dove Lake Formation with no apparent structural or depositional discontinuity (Brommecker, 1996). Overlying the Gunnar Formation, and in apparent stratigraphic contact, are basalts andesites and greywackes of the Stormy Lake Formation. The sedimentary rocks contain between 10 and 30% volcanic clasts and consequently have been termed volcaniclastic by Brommecker (1996). The contact at the base of the formation is sharp, and in some places volcanic breccia overlies pillow basalts of the Gunnar Formation. The Narrows Formation, consisting of volcanic breccias and tuffs, overlies the Stormy Lake Formation with no distinct structural or erosional disconformity. There are a number of thin intercalations of volcanogenic sandstone at the base of the Narrows Formation, which are similar to those of the Stormy Lake Formation. Brommecker (1996) has interpreted these observations to represent a gradational contact between the two. In general mafic volcanic rocks are less abundant towards the top of the stratigraphic sequence.

Seneshen and Owens (1985) proposed the existence of the new Manigotagan River Formation as the stratigraphic top of the Bidou assemblage, with the Edmunds Lake Formation reclassified as a distinct assemblage, a view supported by Brommecker (1996; Fig. 3.14). The lower part of the Manigotagan River Formation is gradational into the Narrows Formation, and has been interpreted to represent a transition into more extensively reworked porphyritic volcaniclastic rocks of similar composition to the Narrows Formation (Brommecker, 1996).

A U-Pb age of 2731 ±3.2 Ma has been obtained for a dacite from the Narrows Formation, and 2730 ±12.6 Ma for a dyke intruding the Gunnar Formation (Turek et al., 1989). In addition U-Pb dating of zircons in the Ross River pluton has yielded an age of 2731 Ma.

St. Joseph assemblage. The Gem Lake (St. Joseph) assemblage outcrops towards the south of the belt and is characterised by a basalt-andesite-rhyolite association with interlayered siliciclastic sedimentary rocks (Poulsen et al., 1996). Zircon from a rhyolite has yielded a U-Pb age of 2721.7 ±2 Ma (Davis, unpublished). However, Poulsen et al. (1996) speculate that it may still be comagmatic with the Confederation assemblage, as the youngest units of the that assemblage may have been eroded away. Poulsen et al. (1996) also postulate that the Manitotagan Formation, which Seneshen and Owens (1985) propose separates the Confederation and Edmunds Lake assemblages, may be part of the St. Joseph assemblage as it contains felsic clasts likely derived from rhyolites of the St.

Joseph assemblage (Seneshen, 1990).

Edmunds Lake assemblage. Turbiditic rocks of the uppermost Edmunds Lake Formation may be conformable with rocks of the underlying Gem Lake and Bidou Lake assemblages. However, Poulsen et al. (1996) suggest that this may not be the case based on the fact that U-Pb ages of detrital zircons and intrusions indicate an age of between 2720 and 2650 Ma for the assemblage (Table 3.1; Poulsen et al., 1996).

San Antonio assemblage. To the west, southwest and northwest, the rocks of the Rice Lake group, discussed above, are unconformably overlain by arkosic sandstones and conglomerates of the San Antonio Formation; there is no equivalent of these sedimentary rocks in the other Uchi greenstone belts to the east.

Structure and metamorphism. At least three phases of deformation have been recognised in the Rice Lake belt (Poulsen et al., 1996 and references therein), they are described as follows:

- D1 - isoclinal folding, with variable intensity of cleavage, resulting in north dipping structures
- D2 - tight folding and development of main penetrative foliation resulting in NW-SE folds
- D3 - open folding and development of ENE crenulation cleavage

Metamorphic grade is generally greenschist facies, but with an increase to amphibolite facies at the boundary with the Wanipigow plutonic rocks in the Wallace Lake area (Richardson and Ostry, 1996)

Mineral deposits. Over 200 gold occurrences have been reported from the Confederation assemblage of the Rice Lake greenstone belt, and there are 15 past producing deposits (Richardson and Ostry, 1996). In addition the San Antonio gold mine has recently been reopened. The three principal past producers are the San Antonio mine (42,000 kg Au), the Central Manitoba mine (4,287 kg Au) and the Gunnar mine (3,100 kg Au).

3.3 Summary

The age relationships of the various assemblages of the Uchi subprovince are summarised in Figure 3.15. Also included on this figure are the Lumby Lake and North Caribou greenstone belts from the Wabigoon and Sachigo subprovinces respectively (Fig. 3.1), which were sampled by the author but have been reported and discussed in Hollings et al. (1997), Hollings and Wyman (1998), Hollings and Kerrich (1998). It can be seen from Figure 3.15 that the older assemblages occur sporadically throughout the subprovince and are most common in the west, whereas the younger Woman and Confederation assemblages are present across the length of the Uchi subprovince.

The geology of the various assemblages is summarised in Table 3.2. In general, the older assemblages are dominantly comprised of mafic flows ± komatiites ± rare felsic flows, whereas the younger assemblages commonly lack komatiites and contain significant volumes of calc alkaline pyroclastic material commonly found stratigraphically above tholeiitic sequences.

The greenstone belts investigated in this study, record ~300 m.y. of the evolution of the Superior Province, including some of the earliest proto-continental events. Consequently by investigating the geochemistry, and hence the geodynamic setting, of the belts it will be possible to develop insights into the evolution of the Superior Province, as well as variations in the geodynamic setting along the length of the subprovince within a single assemblage

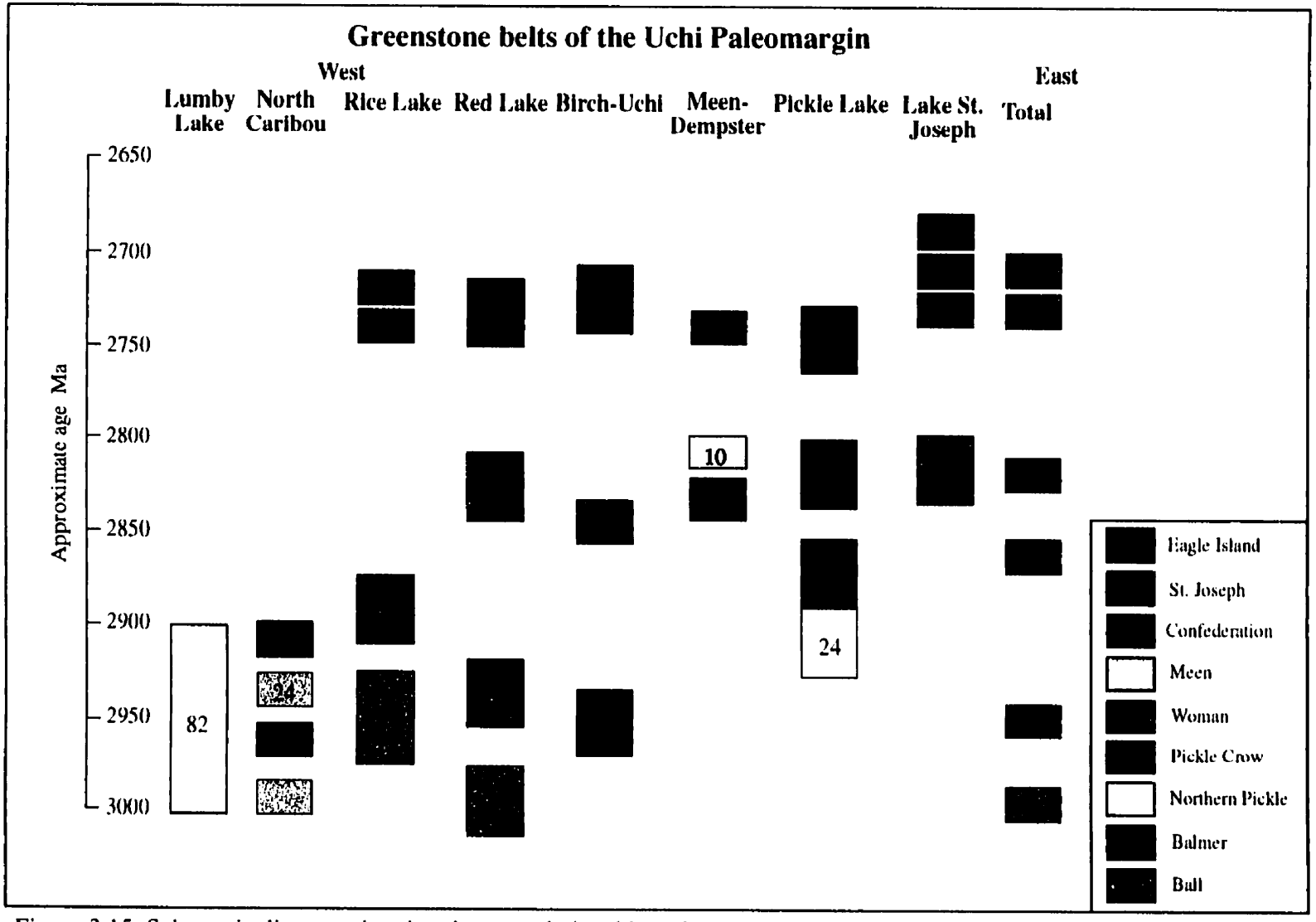

Figure 3.15. Schematic diagram showing the age relationships of assemblages within the Uchi subprovince. Numbers refer to the number of samples analysed.

Table 3.2. Summary of the age, geology and occurrence of the assemblages of the Uchi subprovince. X = present within belt.

Assemblage	Greenstone Belts						Age Ma	Characteristics
	Pickle Lake	Lake St. Jo.	Meen-Demp.	Birch-Uchi	Red Lake	Rice Lake		
Northern Pickle	X						>2900 ?	Dominantly massive and pillowed basalt flows with minor sill-like ultramafic intrusions. Rare intercalated BIF and felsic tuffs
Pickle Crow	X						2860±2	Basal massive and pillowed basalt flows with intercalated BIF, overlain by felsic tuffs and ashflows, in turn overlain by a second series of mafic flows
Balmer				X	X	X	2958-2992 2992+20/-9 2989±3 2964+5/-1	In the Birch-Uchi a lowermost formation of massive and pillowed mafic flows is overlain by minor intermediate tuffs, in turn overlain by mixed wacke, argillite and intermediate to felsic tuffs. This is overlain by a thin unit of felsic tuffs capped by shallow water limestones. At Red Lake the assemblage is dominantly basaltic tholeiite and komatiite with BIF and rare rhyolitic units. At Rice Lake the base of the sequence comprises intercalated mafic and felsic units overlain by a unit of tuffs and breccias, in turn overlain by komatiites and basalts overlain by tholeiitic and calc alkaline basalts.
Ball					X	X	2925±3-2940±2	At Red Lake mafic flows interbedded with relatively large volumes of felsic and intermediate pyroclastic volcanic rocks. At Rice Lake the assemblage comprises basal mafic volcanic rocks and felsic to intermediate volcanic derived sedimentary
Woman	X	X	X	X	X		2805-2841	Tholeiitic basalts commonly overlain by rhyolitic and dacitic tuffs in the Lake St. Joseph belt. In the Meen-Dempster belt it is characterised by massive and pillowed flows with rare thin felsic units. In the Birch-Uchi belt four formations are recognised, a thick basal unit of mafic and intermediate flows, overlain by minor intermediate to felsic tuff, superceded by thick proximal and distal subaqueous ash flows leading to subaerial ignimbrite sheets capped by shallow water limestones and stromatolites.
Meen			X				~2825	Proximal and distal calc alkaline flows
Confederation	X	X	X	X	X	X	2729±1-2733±3 2740±1-2744±2 2735±4-2739±2	At Pickle Lake a sequence of pillowed, massive and vesicular flows are capped by a distal dacitic tuff. In the Lake St. Joseph belt a lower tholeiitic unit is overlain by rhyolitic and dacitic flows. In the Meen-Dempster belt a series of cycles progressing from tholeiitic flows to calc alkaline pyroclastic rocks are found. In the Birch-Uchi belt numerous felsic pyroclastic cycles have been recognised. In the Red Lake and Rice Lake belts repeated cyles of tholeiitic to calc alkaline volcanism are recognised
Lake St. Joseph		X				X	2722±2	Lower unit comprising tholeiitic basalt overlain by thick dacitic to andesitic flows

CHAPTER 4

THE 2.9-3.0 Ga PROTO-CONTINENTAL SUPERIOR PROVINCE

4.1 Introduction

In this chapter the geochemistry of the ultramafic, mafic and felsic rocks of the older assemblages of the Uchi subprovince is reported. The geological relationships presented in Chapter 3 provide the framework within which the geochemical data will be interpreted. By examining the assemblages older than 2.9 Ga it is possible to investigate the early stages in the development of the Superior Province. These older components are preserved in the Rice Lake, Red Lake, Birch-Uchi and Pickle Lake greenstone belts. This chapter will discuss the rocks of the Balmer assemblage which Stott and Corfu (1991) and Poulsen et al. (1996) have suggested can be correlated across the length of the belt, and is also correlated with the North Caribou Terrane (NCT) in the Sachigo subprovince (Thurston et al., 1991). The geochemistry of the Ball assemblage will also be addressed as it is comparable in age to the Balmer assemblage but is only recognised in the Red Lake belt. As discussed in Chapter 3 the Northern Pickle assemblage has not yet been dated but is thought to be >2.9 Ga; this inferred age and geophysical correlations with the NCT are the principal reasons for discussing the assemblage within this investigation of the proto-continental Superior Province.

Archean greenstone belts from the northern Superior Province, ranging in age from 2.9 to 3.0 Ga, are distinct from their southern counterparts in at least four ways: (1) several of the komatiite sequences are characterised by a compositional signature of contamination; (2) there is evidence for older crustal basement to some of the greenstone belts; (3) several of the komatiites possess positive peaks of Sc and V relative to HREE, and (4) they are older than their southern counterparts. Consequently, comprehensively evaluating their geochemistry should allow for significant insights into crustal growth processes that are likely to be very different from those of the more southerly belts.

4.2 Ultramafic rocks of the Balmer and Ball assemblages

The geology of the Ball and Balmer assemblages is summarised in Table 3.2. In the following sections the geochemistry of the ultramafic to felsic rocks within the two assemblages will be presented, and discussed in terms of the geodynamic environments that can be interpreted from the data. Representative analyses of critical elements are presented within this chapter with the full data set displayed in Appendix B.

4.2.1 Introduction

Two basic types of komatiites have been recognised in Archean terranes. The Al-undepleted type (AUK) is characterised by higher Al_2O_3 contents, near chondritic Al_2O_3/TiO_2, Ti/Zr and Zr/Y ratios, depleted LREE but flat HREE, in conjunction with zero or weakly positive Zr and Hf anomalies. Al-depleted komatiites (ADK) have lower Al_2O_3 contents, Al_2O_3/TiO_2 and superchondritic Zr/Y ratios, fractionated REE and variably negative Zr and Hf anomalies (Nesbitt and Sun, 1976; Nesbitt et al., 1979; Arndt and Nesbitt, 1982; Xie et al., 1993). These are also referred to as Munro- and Barberton-types respectively (Arndt, 1994).

It is now generally accepted that the spinifex texture observed in many komatiites reflects eruption at anomalously high temperatures, best explained by invoking the presence of a superheated mantle plume (Arndt, 1994). Komatiites are widely held to be the product of thermally anomalous mantle plumes that formed oceanic plateaux, on the basis of thermodynamic models, experimental petrology, and by analogy with observations of modern hotspots and oceanic plateaux (Storey et al., 1991; Herzberg, 1992; Kerr et al., 1996).

4.2.2 Ball assemblage

Komatiites of the Ball assemblage at Red Lake possess MgO contents of 21-32 wt.% and display Al_2O_3/TiO_2 ratios typical of AUK (Table 4.1; Fig. 4.1). On plots of MgO versus other major elements (Fig. 4.2) the komatiites lie sub-parallel to olivine control lines for unaltered komatiites from Pyke Hill (Fan and Kerrich, 1997). Komatiitic basalts, however, generally plot perpendicular to these trends. When trace element concentrations are plotted against MgO, both komatiites and komatiitic basalts display trends close to olivine control lines for Ni, Cr and Co, as do komatiites for V, Zr and Ce, but komatiitic basalts show somewhat perpendicular trends, as for the major elements (Fig. 4.3).

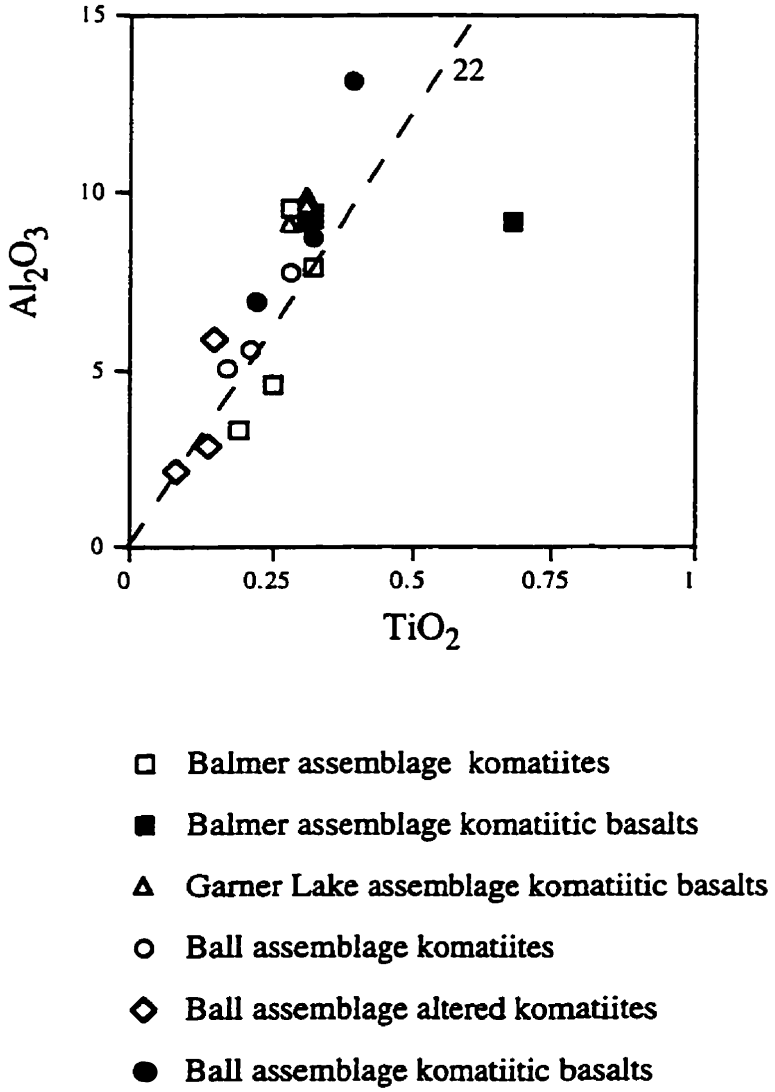

Figure 4.1. Al_2O_3 versus TiO_2 for ultramafic rocks from the 2.9-3.0 Ga assemblages of the Uchi subprovince. Dashed line represents the chondritic ratio.

Table 4.1. Representative analyses of key elements for ultramafic rocks of the Ball, Balmer and Garner Lake assemblages*

	Ball assemblage					
	Komatiites			Komatiitic basalts		
	NDCB7-09B	NDCB7-01C	NDCB7-09D	NDCB7-09C	NDCB7-12B	NDCB7-01C
SiO_2,	52.79	51.85	50.16	52.98	52.08	50.58
TiO_2,	0.17	0.21	0.28	0.22	0.32	0.39
Al_2O_3,	5.05	5.55	7.78	6.91	8.76	13.18
MgO	23.38	25.13	21.09	16.31	14.81	14.99
LOI	3.41	5.94	3.47	2.20	1.78	4.33
MgO	0.83	0.83	0.78	0.77	0.73	0.69
Ti	1184	1309	1783	1524	2006	2555
Cr	2551	2525	3222	1996	1205	2016
Co	99	94	93	73	55	79
Ni	1069	1079	652	311	251	435
(La/Yb),	1.40	1.75	1.28	2.88	2.15	10.18
(La/Sm),	1.19	1.55	1.46	2.64	1.70	5.07
(Gd/Yb),	1.04	1.04	1.05	1.09	1.23	1.28
Al_2O_3/TiO_2,	25	25	26	27	26	30
Th/Nb	0.23	0.42	0.28	0.64	0.32	0.56
Th/La	0.17	0.15	0.21	0.17	0.19	0.21
Zr/Y	4	3	3	4	5	16
Sc/La	320	296	337	601	141	498
Nb/Nb*	0.74	0.27	0.73	0.20	0.55	0.28
Zr/Zr*	1.13	0.72	1.42	1.12	1.40	1.09
Hf/Hf*	0.97	0.85	1.51	1.20	1.46	1.77
Ti/Ti*	0.83	0.71	0.92	0.86	0.83	1.21

	Balmer assemblage								Garner Lake assemblage			
	Komatiites				Komatiitic basalts				Komatiitic basalts			
	GCB94-43	AB94-140B	AB94-155B	RL95-51	RL95-40	RL95-50	AB94-147B	RL95-39	RCB96-3	RCB96-2	RCB96-5	RCB96-4
SiO_2,	43.95	50.82	45.71	46.06	49.84	51.32	46.86	53.59	52.93	53.44	52.76	52.86
TiO_2,	0.19	0.25	0.32	0.28	0.32	0.68	0.31	0.32	0.31	0.28	0.28	0.31
Al_2O_3,	3.34	4.64	7.91	9.55	9.29	9.21	9.22	9.38	9.09	9.14	9.12	9.60
MgO	37.55	26.82	28.13	21.69	16.61	16.04	15.87	12.62	13.94	12.41	13.58	12.72
LOI	10.33	13.12	13.24	5.16	5.04	4.99	6.50	6.28	3.84	3.63	2.72	3.95
MgO	0.86	0.81	0.81	0.76	0.74	0.72	0.71	0.68	0.73	0.69	0.69	0.68
Ti	1024	1406	1658	1680	1954	4311	1885	2367	2055	1838	1682	1957
Cr	3220	3657	3098	2064	2193	1821	1480	1101	1673	1499	1303	648
Co	110	112	92	75	90	76	74	84	63	59	78	45
Ni	1860	1992	954	454	524	351	326	216	402	347	216	113
(La/Yb),	0.62	1.24	0.68	0.26	0.56	1.28	0.67	0.78	0.67	0.54	0.56	0.29
(La/Sm),	0.54	1.10	0.80	0.36	0.64	1.01	0.87	0.94	0.81	0.66	0.56	0.36
(Gd/Yb),	1.17	1.10	0.85	0.79	0.97	1.19	0.84	0.88	0.91	1.03	0.86	0.88
Al_2O_3/TiO_2,	20	20	29	38	28	13	29	25	28	30	32	29
Th/Nb	0.11	0.16	0.29	0.17	0.22	0.20	0.20	0.30	0.14	0.15	0.29	0.19
Th/La	0.10	0.13	0.17	0.23	0.15	0.19	0.13	0.18	0.09	0.10	0.24	0.20
Zr/Y	2.04	2.27	1.74	1.49	1.63	3.20	1.78	1.95	1.54	1.32	1.79	1.78
Sc/La	322	392	303	991	362	198	401	440	418	464	405	509
Nb/Nb*	0.96	0.70	0.56	1.17	0.71	0.96	0.55	0.55	0.65	0.72	0.90	1.11
Zr/Zr*	0.77	0.94	0.96	1.11	0.98	0.99	1.01	0.99	0.81	0.90	0.99	1.01
Hf/Hf*	1.04	0.84	0.95	1.06	1.14	0.82	1.06	1.07	0.89	0.93	1.24	1.27
Ti/Ti*	0.79	0.77	0.86	0.98	1.00	0.84	1.00	1.21	0.99	0.92	1.01	1.15

* Complete data set in Appendix B

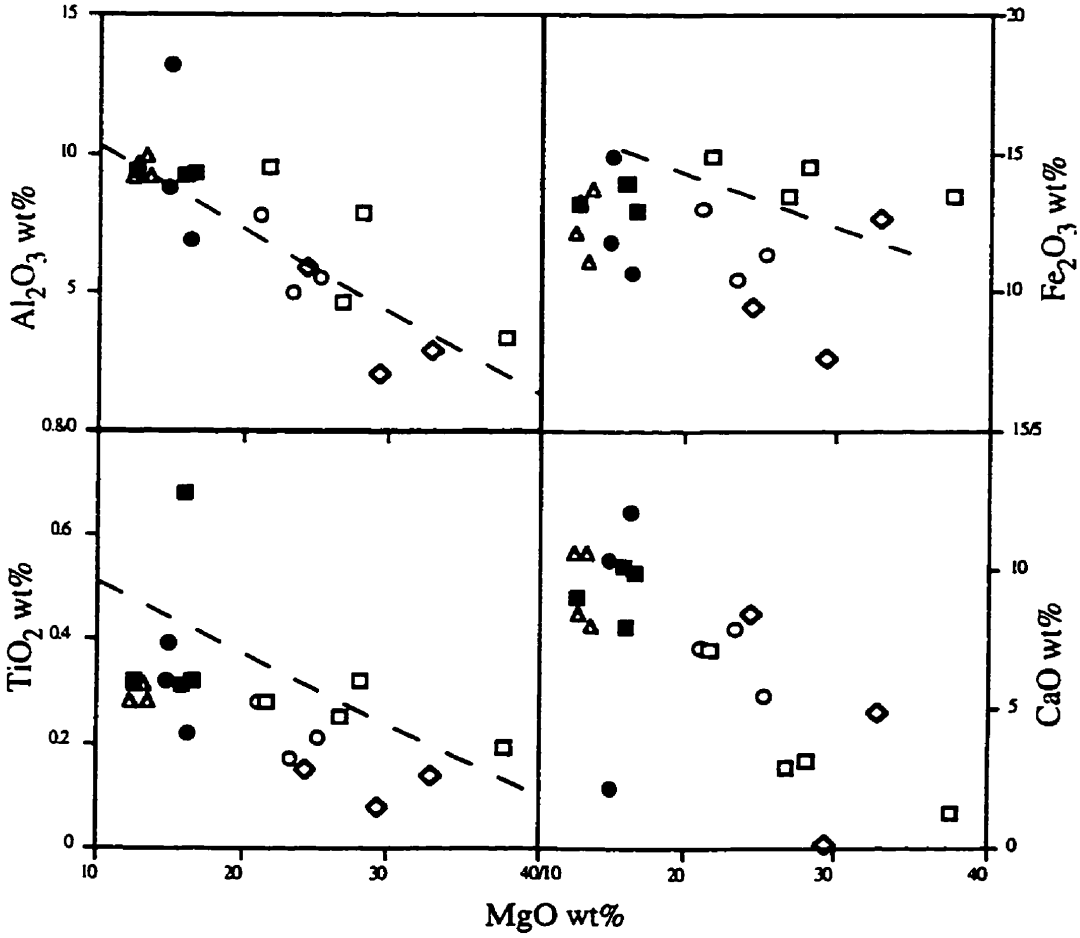

Figure 4.2. Major element variation diagrams for ultramafic samples from 2.9-3.0 Ga terranes. Legend as for Figure 4.1. The dashed lines represent olivine control line for least altered spinifex textured komatiites from Pyke Hill (Fan and Kerrich, 1997).

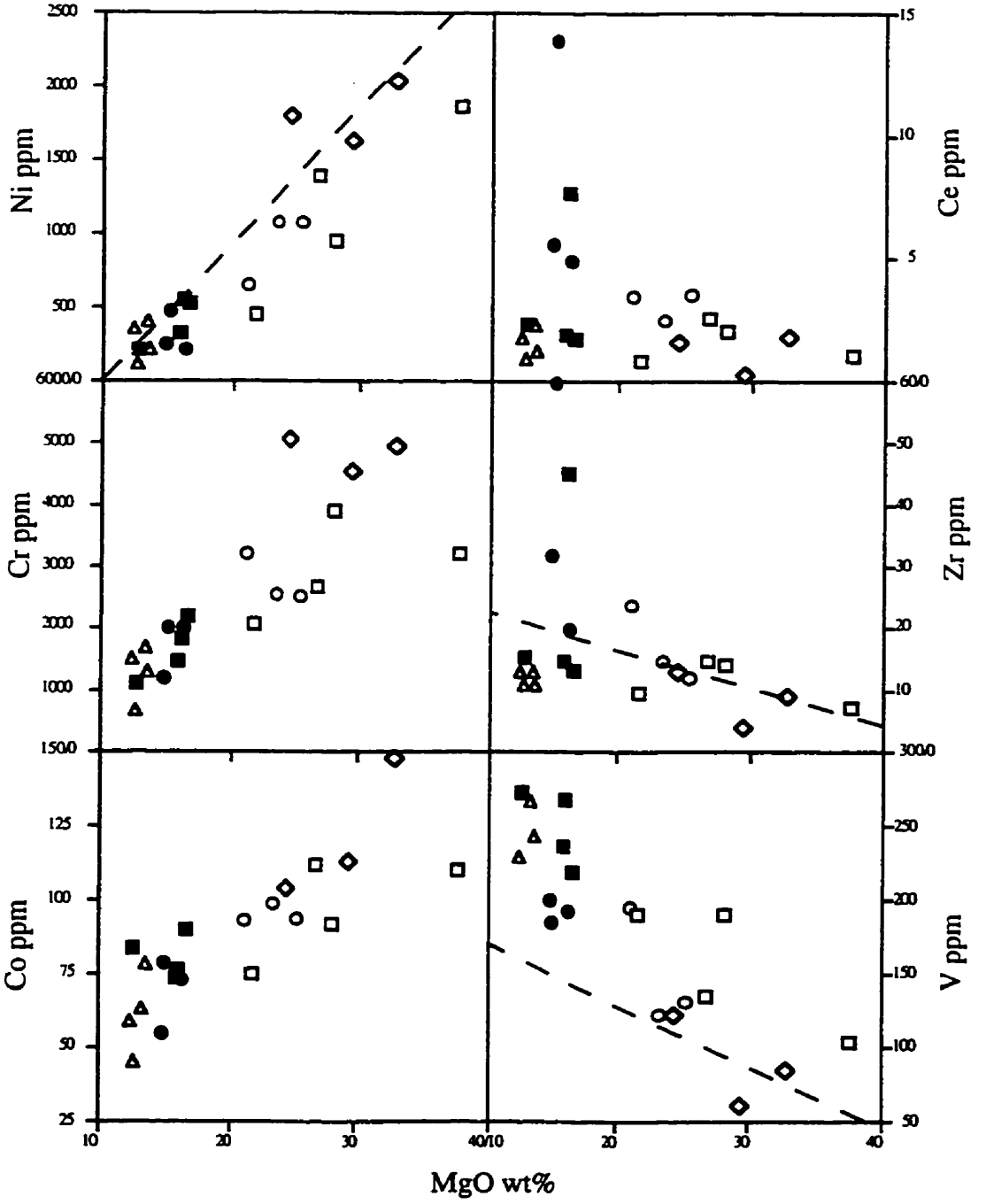

Figure 4.3. Trace element variation diagrams for ultramafic samples from 2.9-3.0 Ga terranes. Legend as for Figure 4.1. The dashed lines represent olivine control line for least altered spinifex textured komatiites from Pyke Hill (Fan and Kerrich, 1997).

Unfortunately the most primitive samples (NDC87-01B, NDC87-02A & NDC87-09A) characterised by the highest MgO and Ni contents, also have anomalously high LOI (4-20 wt.%) and erratic REE patterns typical of altered rocks, which makes the recognition of the primary characteristics difficult; consequently these three samples will not be considered further. The lack of correlation between LOI and REE loss indicates that LOI alone cannot be relied upon as a discriminant for alteration; for example the REE of NDC87-01B with LOI of 20 wt.% is not as disturbed as NDC87-09A which has an LOI of only 5 wt.%. Excluding the three altered samples MgO contents range from 21-25 wt.%, Al_2O_3 of 5-8 wt.% and Ni of 650-1080 ppm, with slightly elevated SiO_2 contents (50-53 wt.%; Table 4.1), relative to Munro spinifex zones where SiO_2 = 46-47 wt.% (Arndt, 1994).

The samples plot coherently from Ti to Sc on a primitive mantle normalised diagram, with flat HREE, but have variably fractionated LREE and Th/Ce, with consistently negative Nb anomalies (La/Sm_n = 1.2-1.6; Nb/Nb* = 0.3-0.6; Fig. 4.4). Both La and La/Sm_n increase with decreasing Mg# and Ni. Komatiitic basalts from the Ball assemblage have MgO contents of 15-16 wt.% in conjunction with Ni of 210-580 ppm and SiO_2 of 50-53 wt.%. They are moderately to strongly LREE enriched with flat HREE, and are characterised by negative Nb anomalies (Table 4.1; Fig. 4.4). Both the komatiites and komatiitic basalts display a positive upturn at V and Sc relative to the HREE (Fig. 4.4).

4.2.3 Balmer assemblage

Komatiites from the Balmer assemblage of the Red Lake belt have MgO contents of 22-37 wt.%, and Al_2O_3 of 3-10 wt.%, with elevated Ni (450-2060 ppm). Al_2O_3/TiO_2 ratios are close to the chondritic values of 22 (Fig. 4.1). On plots of both major and trace elements versus MgO, komatiites and komatiitic basalts show trends similar to the komatiites and komatiitic basalts of the Ball assemblage, with komatiites displaying sub-parallel trends but komatiitic basalts often showing perpendicular trends (Figs. 4.2 and 4.3).

The komatiites vary from weakly LREE enriched to strongly depleted (La/Sm_n = 0.36-1.10) in conjunction with variably fractionated HREE (Gd/Yb_n = 0.8-1.2; Fig. 4.5). There are minor to moderate Eu anomalies in all samples (Eu/Eu* = 0.55-0.86). The concave LREE of RL95-51 is thought to be the result of alteration given the coherence of the remaining REE and HFSE.

Ball assemblage

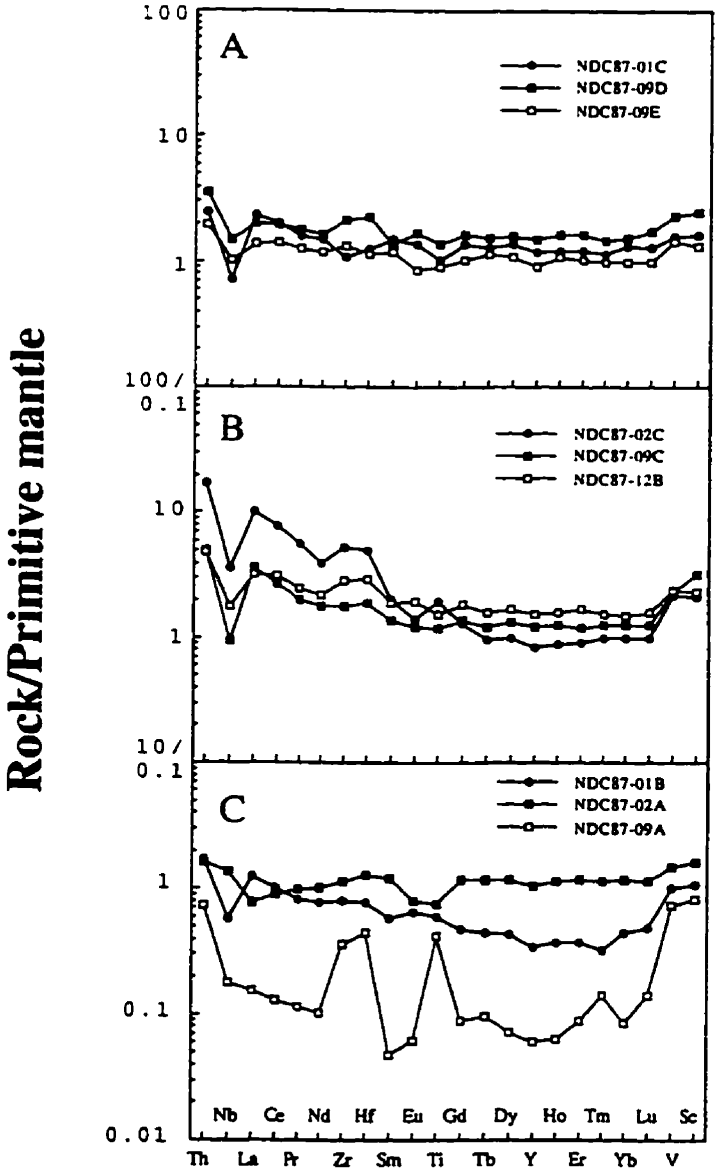

Figure 4.4. Primitive mantle normalised plots for A) komatiites, B) komatiitic basalts and C) altered komatiites of the Ball assemblage of the Red Lake belt.

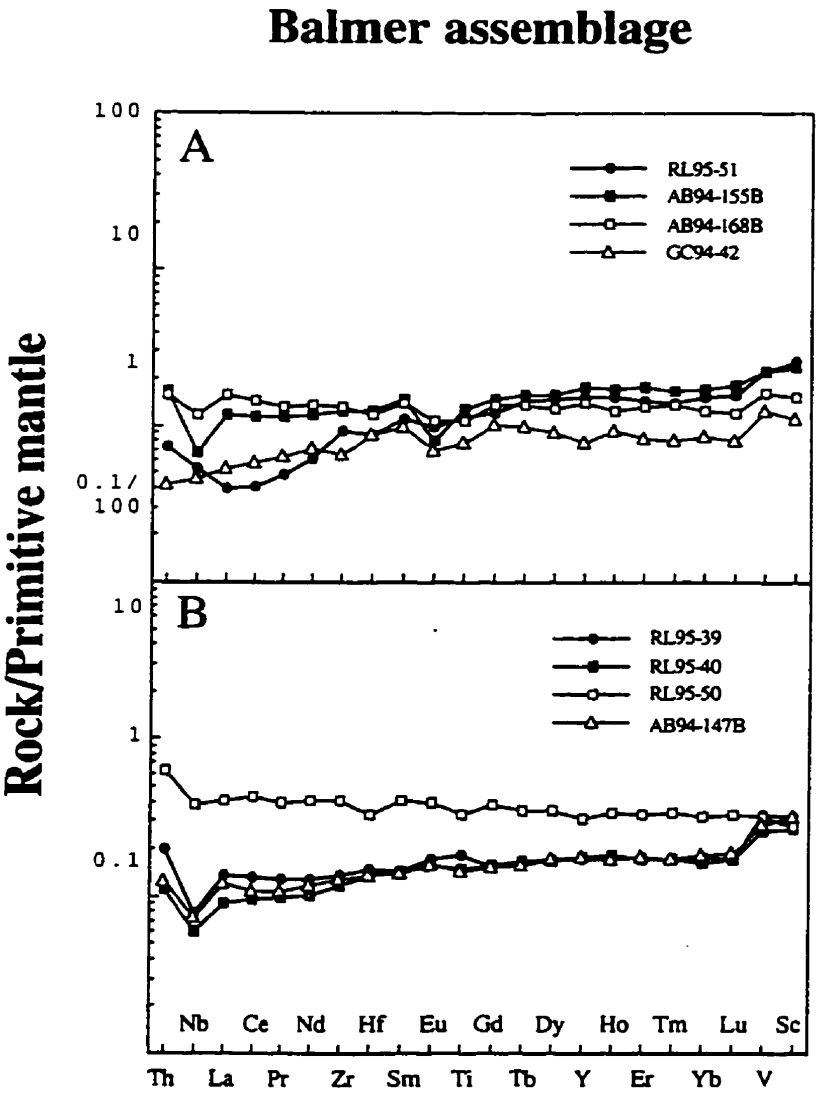

Figure 4.5. Primitive mantle normalised plots for A) komatiites and B) komatiitic basalts of the Balmer assemblage of the Red Lake belt.

Komatiitic basalts from the northern end of Red Lake display MgO contents ranging from 13-17 wt.%, Al_2O_3 of 9.2-9.4 wt.%, and Ni of 216-551 ppm. The three komatiitic basalts are characterised by a general decrease of MgO and Ni contents with increasing Th, Nb and LREE, also consistent with crustal contamination. Negative Nb anomalies are not accompanied by negative Ti anomalies. Sample RL95-39 is spinifex textured with pyroxene blades up to 2 cm long, partially overprinted by amphibole; no primary extrusive textures have been identified in any other samples. Eu anomalies are all zero to weakly positive (Eu/Eu* = 1.0-1.1).

The primitive mantle normalised diagrams are variable. Komatiite sample GC94-42 is the least disturbed: it has near chondritic Al_2O_3/TiO_2 and flat HREE (Gd/Yb_n = 1.2) with LREE depletion, and a smooth pattern through Th-Nb-La with no negative Nb anomaly (Fig. 4.5). In these respects it is comparable to Munro-type Al-undepleted komatiite. One komatiite has a near flat pattern with a negative Nb anomaly (AB94-168B). The remaining two feature positively fractionated HREE, variable LREE depletion and a smooth trend through Yb-V-Sc (Fig. 4.5). Komatiitic basalts possess weakly fractionated LREE and HREE, and all have negative Nb anomalies. Sample RL50 has a near flat primitive mantle normalised pattern (Fig. 4.5), the highest absolute abundances of the highly and moderately incompatible elements, and minor Nb and Ti anomalies (La/Yb_n = 1.3, Nb/Nb* = 0.96, Ti/Ti* = 0.84). It is possible that this reflects further contamination and/or fractionation of the komatiitic parental liquid. The majority of both the komatiites and komatiitic basalts are characterised by high V/Yb and Sc/Yb ratios (217-254 and 30-64 respectively) which are reflected in positive V and Sc relative to the HREE (Fig. 4.5).

Ultramafic flows of the Garner Lake assemblage in the Rice Lake belt comprise both spinifex textured flows and pillow basalts (Fig. 4.6). They are komatiitic basalts (MgO = 12-14 wt.%; Ni = 400-110 ppm; Table 4.1). They plot as a coherent group on diagrams of Al_2O_3 versus TiO_2, lying close to the chondritic value of 22, and form a coherent group

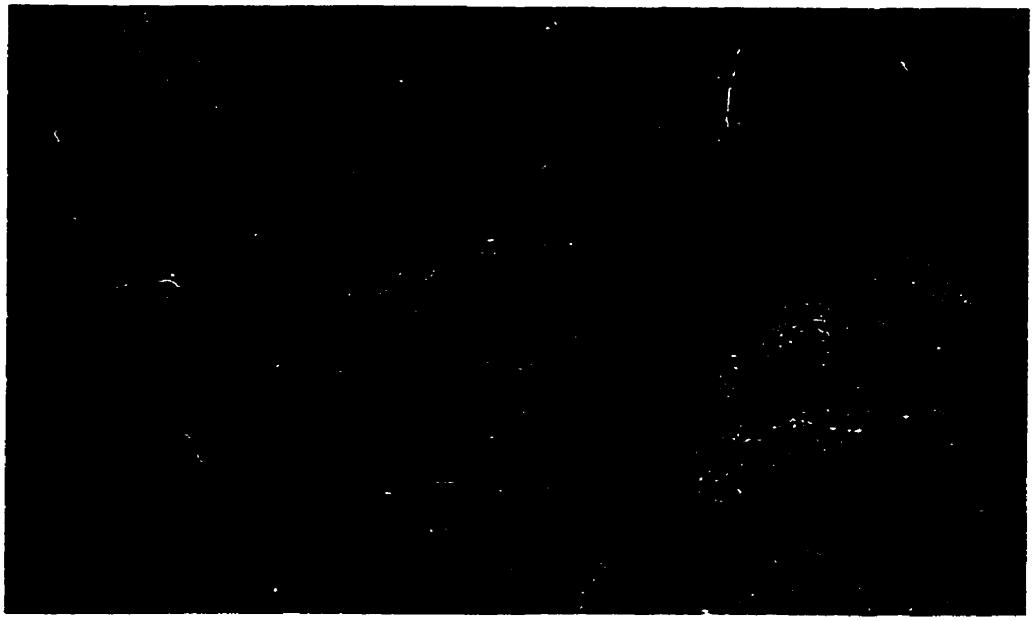

Figure 4.6. Photograph of spinifex textured pillow basalts from the Garner Lake assemblage of the Rice Lake belt. RC96-4 was sampled at this location.

on plots of MgO versus Al_2O_3 and TiO_2 but scatter somewhat against Fe_2O_3 and CaO (Fig. 4.2). On diagrams of MgO versus trace elements they plot as a tight cluster with no obvious trend excepting Co, V and Cr where they show trends comparable to komatiitic basalts from the Ball and Balmer assemblages (Fig. 4.3). Based on Al_2O_3 contents, Al_2O_3/TiO_2 ratios, Zr/Y <2.4, LREE depletion and near flat HREE, these are likely contaminated Al-undepleted komatiites (Figs. 4.1-4.3). They possess near flat HREE with variable LREE depletion (Fig. 4.7; La/Sm_n = 0.4-0.7; Gd/Yb_n = 0.9-1.0). The concave up pattern of RC96-4 likely stems from minor LREE loss. The komatiitic basalts display a positive upturn at V and Sc relative to the HREE, as for Balmer assemblage komatiites, in conjunction with high V/Yb and Sc/Yb ratios of 277-360 and 58-76 respectively (Fig. 4.7).

4.2.4 Additional ultramafic flows from the proto-continental Superior Province

In order to fully evaluate the nature of the proto-continental Superior Province this Chapter will also address data from the Lumby Lake and North Caribou greenstone belts presented in Hollings et al., (1996); Hollings and Wyman (1997), Hollings and Wyman (1998) and Hollings and Kerrich (1998). Hollings et al. (1996) reported the presence of both spinifex textured Al-undepleted komatiite flows and pyroclastic Al-depleted komatiites (ADK) from the Lumby Lake belt (Al_2O_3/TiO_2 of 18-21 and 4-5 respectively). The AUK have variably depleted LREE, with near flat HREE and lack HFSE anomalies in conjunction with near chondritic Al_2O_3/TiO_2, Ti/Zr and Zr/Y ratios (Table 4.2; Fig. 4.2). The ADK are LREE enriched with pronounced negative Zr and Hf anomalies but lack Nb and Ti anomalies (Fig. 4.8a).

The Al-undepleted komatiitic basalts (MgO = 10-11 wt.%) intimately associated with the komatiites in the Lumby Lake greenstone belt display much flatter REE characteristics, comparable to the Tisdale-type komatiites identified by Xie et al. (1993) in the Abitibi belt (Fig. 4.8a).

Komatiites from the Opapimiskan Markop Unit (OMU) of the North Caribou greenstone belt are characterised by elevated MgO and Ni contents (Table 4.2). On a primitive mantle normalised diagram there are a spectrum of patterns from relatively low to high LREE abundances accompanied by progressively larger La/Sm_n and Th/La ratios, and correspondingly deeper negative Nb anomalies (Hollings and Kerrich, 1998; Fig. 4.8b).

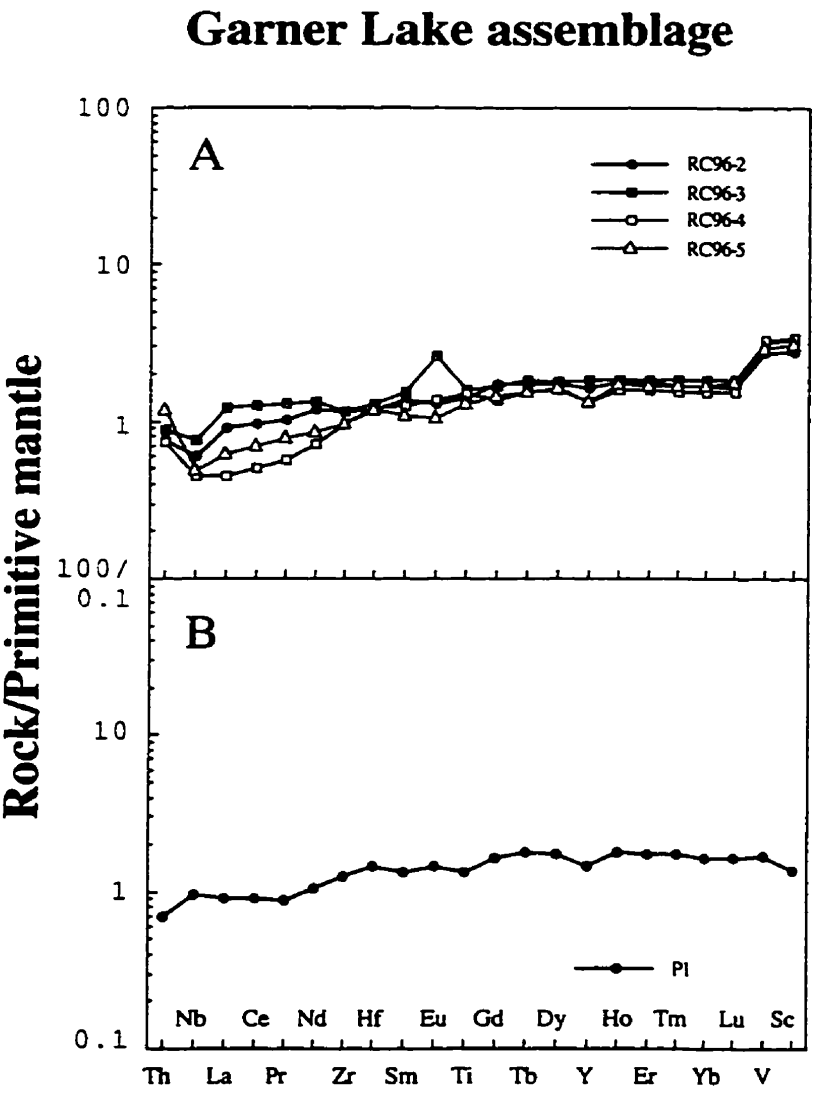

Figure 4.7. Primitive mantle normalised plots for A) komatiitic basalts of the Garner Lake assemblage of the Rice Lake belt and B) representative unaltered Al-undepleted komatiite from Pyke Hill (Fan and Kerrich, 1997).

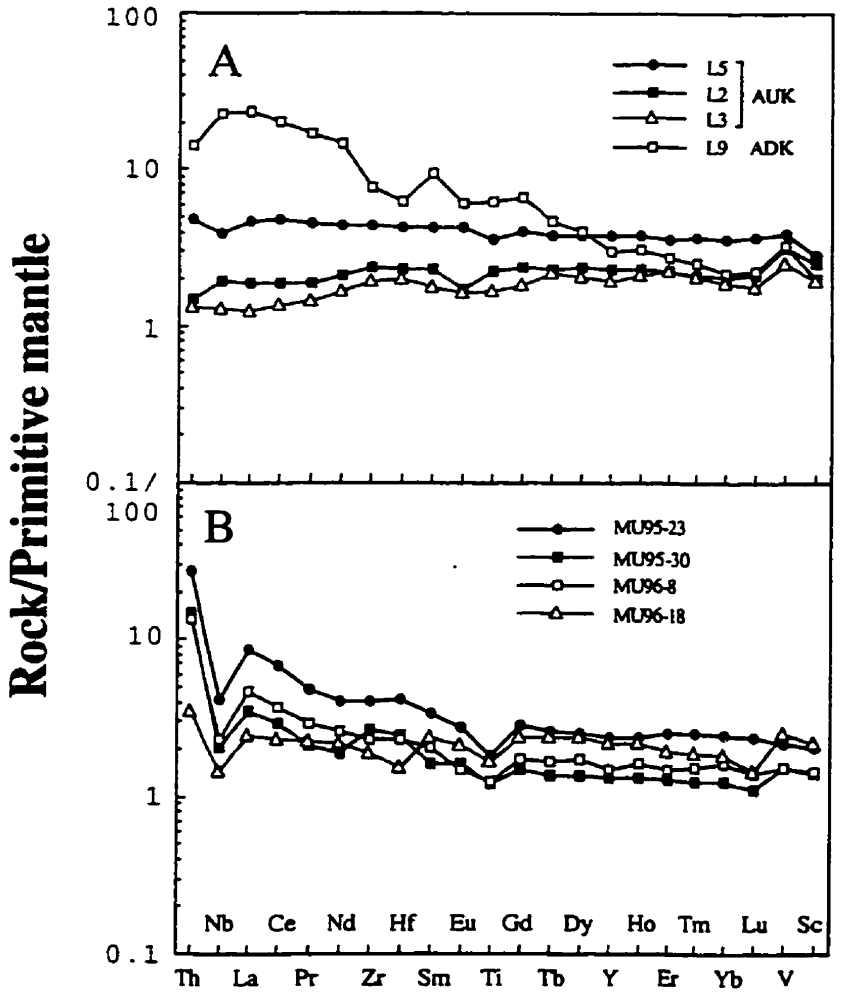

Figure 4.8. Representative primitive mantle normalised plots for komatiites from the Lumby Lake belt (A) and the Opapimiskan-Markop unit of the North Caribou greenstone belt. Data from Hollings and Kerrich (1998) and Hollings and Wyman (1998).

Table 4.2. Representative analyses of key elements for ultramafic rocks of the Lumby Lake and North Caribou greenstone belts. Data from Hollings et al. (1996), Hollings and Wyman (1997) and Hollings and Kerrich (1998).

	Lumby Lake				North Caribou belt - OMU			
	AUK		AUKB	ADK				
	L2	L3	L5	L9	MU96-8	MU95-30	MU96-18	MU95-23
SiO_2	47.78	50.20	51.30	48.47	47.38	52.24	47.60	49.67
TiO_2	0.49	0.37	0.78	1.38	0.28	0.27	0.37	0.41
Al_2O_3	8.92	7.39	12.90	5.53	6.24	5.65	5.63	8.68
MgO	22.05	18.53	10.44	23.50	23.99	23.10	22.12	20.30
CaO	7.42	9.50	9.41	1.78	7.03	6.87	9.43	7.31
LOI	4.99	1.73	1.63	3.04	14.36	3.84	7.24	3.15
Mg#	79	77	65	74	78	82	78	78
Ti	2958	2172	4667	8217	1322	1707	2393	2596
Cr	3033	2468	573	1803	2997	3274	2666	2304
Co	113	85	75	117	115	102	124	96
Ni	883	607	147	1179	988	701	1147	662
(La/Yb)n	0.91	0.67	1.29	10.54	2.89	2.76	1.35	3.54
(La/Sm)n	0.81	0.71	1.08	2.42	2.27	2.16	1.02	2.57
(Gd/Yb)n	1.16	0.98	1.11	3.00	1.08	1.17	1.31	1.18
AL_2O_3/TiO_2	18	20	16	4	27	19	14	20
Th/Nb	0.09	0.12	0.15	0.08	0.68	0.87	0.29	0.76
Th/La	0.10	0.13	0.13	0.08	0.36	0.53	0.18	0.39
Zr/Y	2.53	2.51	2.87	6.26	3.81	5.04	2.09	4.13
Sc/Lu	276	252	178	208	239	288	348	202
Nb/Nb*	1.05	1.11	0.87	0.85	0.40	0.49	0.57	0.39
Zr/Zr*	1.07	1.12	1.00	0.64	1.00	1.56	0.81	1.09
Hf/Hf*	1.04	1.15	0.97	0.53	0.99	1.40	0.68	1.14
Ti/Ti*	0.97	0.92	0.86	0.79	0.54	0.85	0.78	0.64

4.2.5 Eruption through oceanic or continental crust ?

Geological evidence from a number of the greenstone belts in this study indicate that there is potential for crustal contamination. In the North Caribou greenstone belt, for example, the tholeiites of the South Rim unit are underlain by crustally contaminated komatiites and basalts of the Opapimiskan-Markop unit as well as the metasedimentary Keeyask assemblage (Thurston et al., 1991). In addition negative epsilon Nd values for ultramafic rocks in the Balmer assemblage imply the presence of older continental crust underlying some of the Red Lake greenstone belt (Tomlinson et al., 1998). However, Tomlinson et al. (1998) interpret the lack of a contamination signature in the trace element geochemistry of the komatiites to indicate that the negative epsilon Nd values are the result of a prior melting event at ~3.1 Ga and not contamination. Further evidence for incorporation of older crust is provided by a summary of Sm-Nd isotope data for the western Superior Province provided by Henry et al. (1997a, b), which suggests that there is evidence for a 3.4 Ga recycled component in many areas.

The circa 100 m.y. age range preserved in the Lumby Lake belt allows for the possibility of contamination of later eruptions by preexisting crust, although epsilon Nd values of +2 to +4 for mafic to felsic volcanic rocks of the belt (Hollings et al., 1996; Hollings and Wyman, 1997), are typical of Archean mantle derived rocks (Blichert-Toft and Albarede, 1994) and preclude contamination by significantly older crust (>3.2 Ga). The presence of penecontemporaneous felsic volcanic rocks in each of the assemblages also represents a potential source of shallow level or post-eruptive contamination (e.g., Kidd Volcanic Centre of the Abitibi subprovince: Wyman et al., 1997; Barrie, 1997).

Komatiites and komatiitic basalts from the North Caribou greenstone belts all display the conjunction of negative Nb anomalies with trends of increasing SiO_2 and La/Sm_n, that is indicative of contamination by a felsic component (Hollings and Wyman, 1998). Similar trends are not obvious in the ultramafic rocks from the Red Lake and Rice Lake belts but this may simply be a reflection of the smaller sample set and the fact that individual samples may not be directly petrogenetically related given that thet are samples from different locations within assemblages. The presence of negative Nb anomalies in LREE enriched samples, but not LREE depleted ones, is consistent with crustal contamination (e.g. Fig. 4.5a). A crustal contamination model for siliceous high magnesium basalts (SHMB) at Kambalda, Australia, has been considered by Sun et al. (1989). Their study employed trace element data, along with Pb and Sm–Nd isotopic data, to show that the SHMB, which have SiO_2 contents of 51 to 55 wt. % and MgO contents of 10-16 wt.%,

were probably derived by contamination of komatiitic magmas by different types of felsic crust. This model is supported by the common field association of SHMB with uncontaminated komatiites (op cit).

Contamination of volcanic rocks by continental crustal material has been documented in a number of Archean terranes (cf. SHMB of Sun et al., 1989; Forrestania, Western Australia; Perring et al., 1996), where it has been shown to result in elevated SiO_2 contents and La/Sm_n ratios, often in conjunction with significant negative Nb anomalies. The majority of these studies have focussed on the contamination of high-MgO liquids (Arndt and Jenner, 1986; Barley, 1986; Sun et al., 1989; Perring et al., 1996). Sparks (1986) has demonstrated that the high heat of fusion of olivine and large crystallisation interval of komatiites means that they can assimilate three times as much material as basalts. In addition, deep crustal contamination results in up to 50% assimilation whereas surficial contamination of cold crust produces a maximum of 10%. Sun et al. (1989) showed that assimilation of ~15% felsic crust and 35% fractionation (AFC) would produce SHMB from the komatiitic magmas. This AFC results in LREE enrichment as well as pronounced negative Nb anomalies. Similar results have been demonstrated by Perring et al. (1996).

In order to evaluate the effects of crustal contamination, modelling was conducted using a contaminant with a composition similar to the felsic volcanic units found intercalated throughout the 2.9-3.0 Ga mafic-ultramafic sequences (see Section 4.4). These felsic volcanics possess similar trace element abundances to widespread Archean tonalite-trondjhemite-granodiorite (TTG) complexes (Martin, 1993). The LREE enrichment observed in ultramafic samples from the Ball and Balmer assemblages are associated with elevated SiO_2 contents in conjunction with negative Nb and Ti anomalies, comparable to those identified in crustally contaminated komatiites. The progressive LREE enrichment and increasing Nb anomalies seen in the komatiites from the Ball, Balmer and Garner Lake assemblages can best be explained by contamination.

Modelling of simple mixing between the least LREE enriched Ball komatiite and a representative felsic composition from that assemblage can account for the high Th contents, Th/Ce ratios and enriched LREE of the more evolved compositions, with as little as 5% felsic contaminant (Fig. 4.9a). Hollings and Kerrich (1998) modelled AFC processes with such a contaminant, assuming a Munro-type komatiitic precursor, a mixing

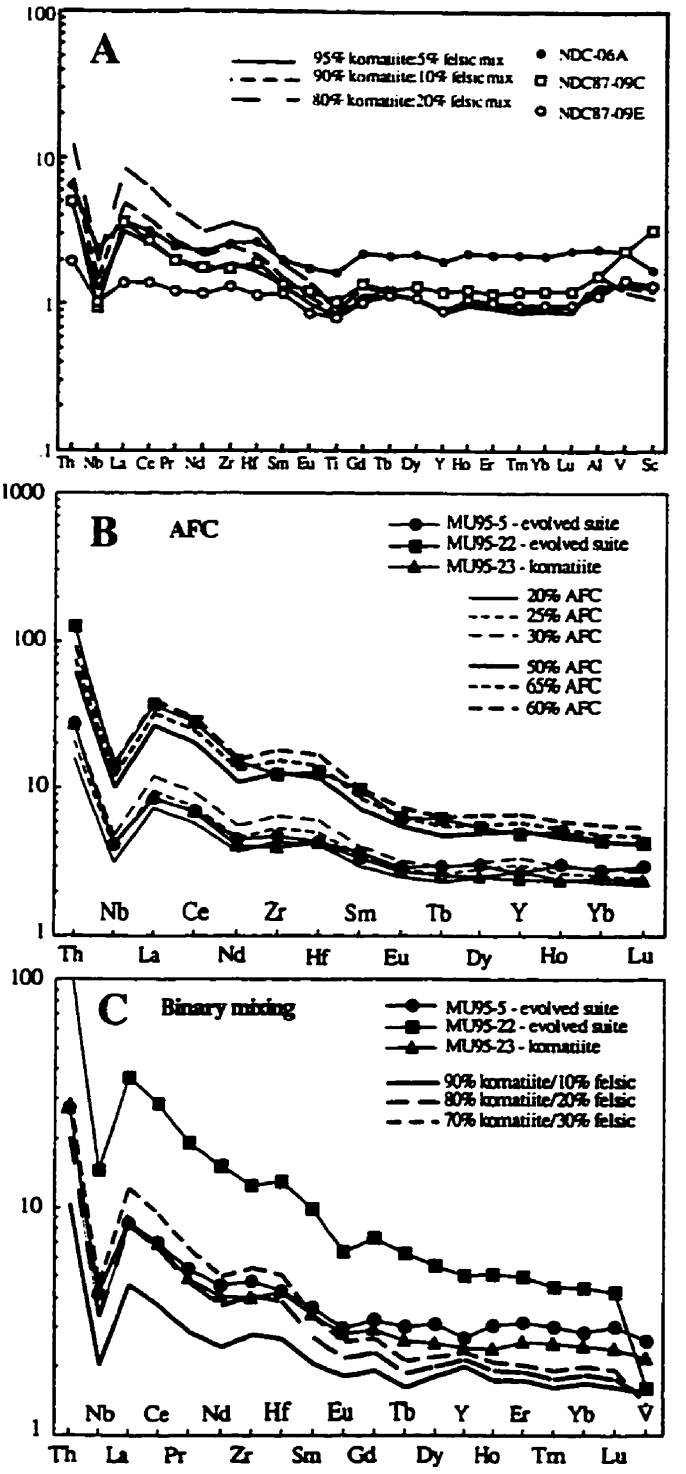

Figure 4.9. Results of numerical modelling of contamination of ultramafic rocks. A = simple binary mixing between Ball assemblage komatiite and felsic contaminant. B = Modelling of AFC for North Caribou greentsone belt (NCGB) komatiites with felsic contaminant. C = Simple binary mixing of NCGB komatiite and felsic contaminant. NCGB data from Hollings and Kerrich (1998).

ratio (r) of 0.5, and fractionation of 90% olivine and 10% spinel; and they demonstrated that it produced trace element patterns comparable to Opapimiskan-Markop unit komatiites at between 20 and 30% fractionation, and the high-Mg basaltic andesites at 50-60% fractionation (Fig. 4.9b), assuming contamination occurred at depth rather than as a post-eruptive process (c.f., Huppert and Sparks, 1985). Figure 4.9 shows the result of simple binary mixing between the same felsic material and Munro-type komatiites with no fractionation. It is clear that mixing between 20 and 30% felsic material will produce LREE abundances comparable to those of the komatiites, but at lower HREE abundances. In addition, binary mixing cannot account for the more evolved samples from the Opapimiskan-Markop unit. The high percentages of contaminant required by AFC-type processes require that contamination occurred at depth, given that surficial thermal erosion will introduce less than 10% contaminant (Huppert and Sparks, 1985).

Given the results of modelling, subsurface contamination of komatiitic liquids by crustal material of tonalitic composition via AFC-type processes is the simplest way to account for the trace element abundances of the komatiites. However, the elevated MgO contents of the Ball, Balmer and Opapimiskan-Markop unit komatiites is not consistent with 30 % fractionation of olivine nor 10-30% mixing of felsic crust, as both would tend to lower the MgO content, suggesting that the model presented above may not account for all features of the komatiites. The occurrence of the komatiites, their protolith and whether or not they are contaminated is summarised in Table 4.3

Table 4.3. Summary of ultramafic rock types in the 2.9-3.0 Ga terranes of the northern Superior Province. Lumby Lake data from Hollings et al. (1996) and Hollings and Wyman (1997), North Caribou greenstone belt data from Hollings and Kerrich (1998).

Greenstone belt	Rice Lake	Red Lake		Lumby Lake	Northern Caribou
Assemblage	Garner Lake	Ball	Balmer		
Ultramafic flows	AUKB*	AUK* AUKB*	AUK* AUKB*	ADK AUK AUKB	AUK* AUKB*

AUK = Al-undepleted komatiites, AUKB = Al-undepleted komatiitic basalts, ADK = Al-depleted komatiites, * = crustally contaminated.

4.2.6 Origin of the distinctive Yb-V-Sc systematics in the Red Lake and Rice Lake ultramafic rocks

The distinctive nature of the komatiites, particularly the variable HREE fractionation and

unusual Yb-V-Sc systematics (Fig. 4.4, 4.5 & 4.7), supports the suggestion of Poulsen et al. (1996) that the Garner Lake assemblage in Rice Lake is analogous to the Balmer assemblage at Red Lake. The high V/Yb and Sc/Yb ratios and associated positive anomalies at V and Sc on a primitive mantle normalised diagram have not, to the authors knowledge, previously been reported in komatiitic rocks. Pearce and Parkinson (1993) have proposed that high V/Yb and Sc/Yb ratios may be produced by melting a previously depleted or mantle source that is more depleted than the source of MORB; their modelling of melting trends within the spinel lherzolite facies showing strong depletions in Yb for small depletions in V and Sc.

There are at least three possible causes for this Yb-V-Sc signature of prior melting in the komatiites: (1) they have been contaminated by a felsic component, (2) dynamic melting within a mantle plume whereby mantle components are continually remelted, or (3) interaction with depleted sub-arc mantle possibly comparable to the source of boninitic rocks.

Whereas contamination by a felsic component can explain the Th-Nb-LREE systematics observed in ultramafic samples from the Balmer, Ball and Garner Lake assemblages (see section 4.2.5), it cannot account for the HREE-V-Sc characteristics. The positive Sc–V anomaly occurs in sample GC 94-42 (Fig. 4.5), which lacks an Nb anomaly or high La/Sm_n and is otherwise similar to Munro-type Al-undepleted komatiites, precludes crustal contamination as the cause of the V-Sc systematics. Accordingly, the relatively high abundances of V–Sc, relative to Munro-type AUK, appear to be characteristic of the Red Lake and Rice Lake komatiite source region, irrespective of possible contamination. Further, the Kambalda SHMB display normalized depletions of V and Sc, which Sun et al. (1989) attribute to the low abundance of these elements in local Archean felsic contaminants.

Dynamic melting in mantle plumes has recently been advocated for the Gorgona and Iceland plumes (Elliot et al., 1991; Arndt et al., 1997), where it has been invoked to explain the variation in FeO and incompatible element contents of picrites and tholeiites. It is suggested that melts produced during ascent are continuously extracted, so that more primitive picritic compositions represent melts of "least depleted" mantle entering the bottom of the melting column (Elliot et al., 1991). However, the absence of Yb-Sc-V anomalies, comparable to komatiites from this study, in high MgO picritic rocks associated with mantle plumes proposed to have undergone dynamic melting suggests that

this process cannot account for the distinctive characteristics of northern Superior Province ultramafic rocks (c.f., Kerr et al., 1996).

Boninitic rocks associated with island arcs feature variably fractionated MREE and HREE, high Al_2O_3/TiO_2 ratios and many have high Sc/Yb and V/Yb ratios (Table 4.4; Cameron et al., 1983; Cameron, 1989; Rogers et al., 1989; Brown and Jenner, 1989). Boninites are widely accepted to form by a two stage process. First stage melting causes depletion of compatible and moderately compatible elements as well as the REE, giving La/Sm_n and Gd/Yb_n <1. Then second stage enrichment by fluids and/or melts driven off the subducted slab, enriches the depleted, refractory mantle in LILE, LREE, and generally Zr and Hf relative to MREE. Further, normalized V-Sc enrichments versus HREE are characteristic of mafic rock types derived from previously depleted mantle sources and occur, to some degree, in most mafic arc rock types (Pearce and Peate, 1995).

It is suggested that a depleted source component may account for the distinctive HREE-V-Sc systematics of the komatiites. Consequently although the unusual HREE, Sc, V systematics of these AUK are not yet fully understood they would appear to be unique to the older northern greenstone belts of the Superior Province.

4.2.7 Summary

The spinifex texture observed in a number of the komatiites and komatiitic basalts from the Red Lake and Rice Lake belts implies that they were erupted at anomalously high temperatures (Arndt, 1994). This may be explained by invoking the presence of a mantle plume. However, Allegre (1982) has suggested that the high mantle temperatures could also be the result of melting wet mantle sources not associated with plumes. This model has recently been invoked by Grove et al. (1997) and Parman et al. (1997).Consequently the involvement of a plume in the petrogenesis of komatiites is still widely favoured especially given the association of plumes with Phanerozoic LIP (Large Igneous Provinces).

The geochemistry of the more primitive ultramafic rocks is comparable to Munro-type Al-undepleted komatiites. However, this primary signature has been overprinted by two distinct processes: the LREE enrichment and negative Nb anomalies are interpreted to be the result of crustal contamination by a felsic component, whereas the distinctive Yb-V-Sc systematics of the komatiites is thought to be a feature of the mantle source, best explained

Table 4.4. Comparison of Sc/Yb and V/Yb ratios for komatiites and komatiitic basalts of the older assemblages of the Superior Province and rocks from a variety of tectonic settings.

Location	Sc/Yb	V/Yb	La/Sm_n
Ball assemblage - komatiites	43-56	203-255	1.2-1.6
Ball assemblage - komatiitic basalts	53-90	273-378	1.7-5.1
Balmer assemblage - komatiites	42-60	217-254	0.4-1.1
Balmer assemblage - komatiitic basalts	30-64	168-313	0.7-1.0
Garner Lake assemblage - komatiitic basalts	58-77	277-360	0.4-0.8
Lumby Lake - komatiites[1]	25-42	160-265	0.5-1.3
Lumby Lake - komatiitic basalts[1]	27-29	186-190	0.9-1.1
Lumby Lake - Al-depleted komatiites[1]	31-55	240-253	1.9-2.4
North Caribou belt - komatiites[2]	29-44	130-248	0.8-2.9
Munro Township - komatiites[3]	21-31	-	0.3-0.9
Pechenga - picrites[4]	13-40	150-301	1.2-2.5
Lau Basin[5]	1-22	5-172	0.4-1.0
Selected boninites[6]	173-1125	85-350	0.8-2.8
Koh massif, New Caledonia - boninites[7]	60-84	296-347	0.8-1.2
Cyprus - boninites[8]	22-83	171-132	-
Kidd Creek - LOTI[9]	24-42	88-160	0.8-1.1

Data sources: 1) Hollings and Wyman (1997, 1998) and authors unpublished data; 2) Hollings and Kerrich (1998); 3) Xie et al. (1995); 4) Hanski and Smolkin (1995); 5) Pearce et al. (1995); 6) Cameron et al. (1983); 7) Cameron (1989); 8) Rogers et al. (1989); 9) Wyman et al. (1998), Wyman (in press)

by interaction of the plume with a highly depleted subduction related component. The lack of the distinctive Yb-V-Sc characteristics in tholeiites intercalated with the komatiites (see section 4.3) would appear to imply that this feature was inherited at depth before the plume interacted with the upper mantle that is widely accepted to be the source of the tholeiites (Campbell et al., 1989; Arndt, 1991).

4.3 Tholeiites of the Ball and Balmer assemblages

Tholeiites are present within all the older assemblages discussed herein, typically as the most areally extensive rocktype in each assemblage. Representative analyses are presented throughout the chapter with the full data set reported in Appendix B. In outcrop these tholeiites range from massive to pillowed flows (Fig. 4.10).

4.3.1 Ball Assemblage

The mafic to intermediate samples from the Ball assemblage range in composition from basaltic to andesitic where SiO_2 = 50-63 wt.%, with MgO from 7-13 wt.% and Fe_2O_3 of 7-13 wt.%. The tholeiites are characterised by moderate to pronounced LREE enrichment in conjunction with flat to weakly fractionated HREE (La/Sm_n = 1.8-3.4; Gd/Yb_n = 1.0-1.6), where REE fractionation and Nb anomalies increases (Nb/Nb* = 0.3-0.5) with decreasing Mg# (Fig. 4.11; Table 4.5). The enriched LREE of these mafic rocks is not typical of Mg- to Fe-tholeiites found in other ~3 Ga terranes (Hollings and Wyman, 1997), and are broadly comparable to calc alkaline basalts associated with island arcs. However the elevated MgO, Ni and Cr contents of these rocks (7-13 wt.%, 100-400 ppm and 300-1304 ppm respectively) suggests that they are related to the crustally contaminated komatiites of the Ball assemblage and not directly associated with a subduction zone influenced mantle.

4.3.2 Balmer Assemblage

Tholeiites from the Balmer assemblage of the Red Lake belt are Mg- to Fe-tholeiites with a relatively narrow range of silica contents (49-53 wt.%) and Mg# from 67-41 (Table 4.5). Total ranges of Ni and Cr are 570-50 ppm and 2620-20 ppm respectively. Both Cr and Ni decrease sympathetically with Mg#, whereas Fe_2O_3, Th, Nb, REE and Y increase. Ratios of Ti/Zr and Al_2O_3/TiO_2 tend to be subchondritic. The majority of more magnesian flows possess flat REE and primitive mantle normalised patterns (Fig. 4.12). The tholeiites display a spectrum of REE patterns from flat to weakly LREE enriched (Fig. 4.12A;

Figure 4.10. A) Photograph of pillow basalt from the Red Lake greenstone belt. Field note book for scale. RL95-26 sampled from this locality. B) Photograph of pillow basalt from the Rice Lake greenstone belt. Hammer for scale. RC96-1 sampled from this locality.

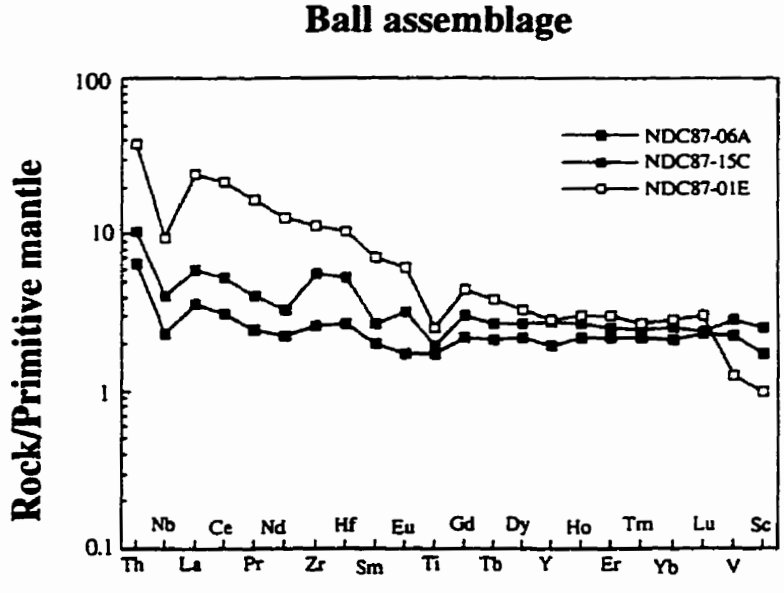

Figure 4.11. Primitive mantle normalised patterns for mafic volcanic rocks of the Ball assemblage, Red Lake greenstone belt.

Table 4.5. Representative analyses of selected elements for mafic volcanic rocks from the Balmer, Ball and Garner Lake assemblages*.

	Balmer assemblage													Ball assemblage		
	Red Lake belt										Birch-Uchi belt	Rice Lake belt		Red Lake belt		
	Tholeiites						L.REE enriched tholeiites					Tholeiite	Tholeiites			
	RL95-23	RL95-19	RL95-22	RL95-25	RL95-18A	RL95-18B	RL95-44	RL95-26	RL95-45	RL95-21	RL95-41	SH95-1	RCW6-6	RCW6-7	NIDC87-06A	NIDC87-01E	NIDC87-15C
SiO_2	48.94	54.34	50.46	51.33	50.11	52.04	50.45	50.23	51.02	51.41	50.56	50.18	52.50	49.65	50.82	52.87	50.27
TiO_2	1.03	1.97	1.12	1.66	1.70	1.69	0.60	0.93	0.62	0.71	1.05	1.24	0.75	0.66	0.35	0.48	0.40
Al_2O_3	15.01	14.07	16.27	13.61	14.65	14.33	13.08	14.50	13.62	14.75	12.73	14.25	16.53	14.88	10.49	13.65	12.71
Fe_2O_3	14.19	13.15	11.46	16.08	15.78	16.57	11.84	13.27	11.78	11.98	6.43	14.15	11.27	13.89	12.65	6.69	11.07
MgO	7.38	6.60	5.21	7.25	6.12	5.58	11.02	7.37	10.65	6.57	2.85	6.52	7.83	7.91	11.16	6.69	8.08
LOI	0.35	0.50	1.11	1.63	0.96	0.55	0.96	0.20	0.65	0.76	3.52	0.55	0.56	1.60	0.91	0.83	1.57
Mg#	53	52	50	50	46	43	67	55	67	55	49	50	43	56	69	69	62
Ti	6180	13820	6596	10737	9542	10733	3980	4110	3809	4025	5379	7245	5152	4331	2251	3262	2549
Cr	219	54	283	216	124	67	878	201	821	283	271	215	333	305	1904	556	502
Ni	127	54	143	35	52	56	247	90	243	108	139	88	155	131	345	151	93
Nb	3.48	8.34	3.99	7.01	6.56	5.52	2.16	3.09	2.47	3.17	2.07	3.86	1.87	1.72	1.04	0.87	2.06
Zr	63	143	65	124	112	102	47	52	44	47	78	82	41	36	29	17.5	62
Hf	1.78	3.35	1.88	3.45	2.65	2.88	1.46	1.45	1.04	1.12	2.11	2.30	1.20	0.99	0.83	1.25	1.62
Th	0.45	1.23	0.49	1.23	0.82	1.01	1.29	0.94	1.26	0.76	0.73	1.57	0.24	0.20	0.54	1.20	0.89
La	3.71	10.29	3.76	8.59	6.96	8.07	3.81	4.77	4.24	4.41	4.13	4.65	2.17	1.64	2.45	10.59	4.14
Sm	2.67	4.76	2.55	4.34	4.20	4.42	1.67	2.14	2.01	1.92	2.96	2.80	1.65	1.36	0.89	3.14	1.19
Gd	3.30	5.91	3.30	5.66	5.46	5.36	2.38	2.56	2.71	2.31	3.80	3.94	2.50	2.09	1.32	3.68	1.82
Yb	2.37	4.91	2.29	3.94	3.93	3.89	1.65	1.77	2.06	1.59	2.67	3.10	1.94	1.72	1.06	1.41	1.26
Lu	0.38	0.75	0.35	0.64	0.62	0.58	0.27	0.27	0.29	0.24	0.43	0.45	0.31	0.26	0.17	0.22	0.18
(La/Yb)n	1.12	1.50	1.18	1.56	1.27	1.49	1.66	1.93	1.47	1.99	1.11	1.11	0.80	0.69	1.66	8.49	2.36
(La/Sm)n	0.90	1.40	0.95	1.28	1.07	1.18	1.48	1.44	1.36	1.48	0.90	1.07	0.85	0.78	1.78	3.42	2.24
(Gd/Yb)n	1.15	0.99	1.19	1.19	1.15	1.14	1.20	1.19	1.09	1.20	1.18	1.19	1.07	1.01	1.03	1.58	1.20
Al_2O_3/TiO_2	14	8	15	7	9	8	19	21	21	22	20	12	19	21	27	25	30
Zr/Hf	35	43	34	36	42	35	32	36	42	35	37	36	34	36	35	39	38
La/Nb	1.07	1.23	0.94	1.23	1.06	1.46	1.76	1.55	1.72	1.39	2.00	1.21	1.16	0.96	1.46	2.42	1.45
Ta/Nb	0.13	0.15	0.12	0.18	0.12	0.18	0.60	0.30	0.51	0.24	0.35	0.41	0.13	0.12	0.33	0.47	0.31
Th/La	0.12	0.12	0.13	0.14	0.12	0.12	0.34	0.20	0.30	0.17	0.18	0.34	0.11	0.12	0.22	0.19	0.21
Zr/Y	2.84	3.62	2.70	3.54	3.13	3.23	2.76	3.04	2.68	3.09	3.08	2.96	2.32	2.22	3	10	5
Nb/Nb*	0.93	0.79	1.05	0.78	0.97	0.66	0.51	0.58	0.52	0.65	0.48	0.85	0.89	0.86	0.58	0.36	0.59
Zr/Zr*	0.96	1.08	1.01	1.04	1.03	0.88	1.12	0.89	0.84	0.89	1.11	1.16	0.98	1.09	1.22	1.19	1.04
Hf/Hf*	0.99	0.92	1.06	1.06	0.88	0.91	1.25	0.90	0.72	0.91	1.09	1.18	1.05	1.09	1.26	1.10	1.25
Th/Th*	0.81	1.03	0.90	0.86	0.79	0.87	0.79	0.69	0.65	0.76	0.63	0.88	1.01	1.02	0.82	0.45	0.66

* Full data set in Appendix B

La/Sm_n = 0.9-1.4 with one outlier). Niobium anomalies vary from zero to weakly negative and show a correlation with LREE enrichment (Table 4.5).

A distinct suite of mafic samples with SiO_2 = 50-59 wt.% and Mg# = 49-67 has also been recognised within the Balmer assemblage. They are characterised by mildly enriched LREE (La/Sm_n = 0.9-1.5; Table 4.5; Fig. 4.12B). In addition, all samples display pronounced negative Nb and Ti anomalies with Nb/Nb* and Ti/Ti* ranging from 0.48-0.65 and 0.63-0.79 respectively. In addition these samples display anomalously high Th contents reflected in Th/La ratios of 0.2-0.3. The elevated Ni and Cr contents of these rocks, particularly in the more Mg rich samples suggests that they may be petrogenetically related to the crustally contaminated komatiites. The elevated Th contents support this model as this feature is also present in the komatiites from the Balmer assemblage (Fig. 4.5).

Tholeiitic flows intercalated with komatiitic basalts of the Garner Lake assemblage are comparable to the more primitive tholeiites from the Balmer assemblage. The MgO ranges from 4 to 8 wt.%, and Al_2O_3 from 15 to 16 wt.%. They are characterised by weakly depleted LREE (La/Sm_n = 0.8, 0.9) and flat HREE (Gd/Yb_n = 1.0, 1.1; Fig. 4.12C), without any significant HFSE anomalies, and low Th/Ce ratios (Nb/Nb* = 0.9-1.2). The single sample from the Balmer assemblage of Birch-Uchi greenstone belt displays similar characteristics (Table 4.5).

4.3.3 Discussion

In order to fully evaluate the significance of the tholeiites from the older assemblages of the Uchi subprovince they will be compared with rocks of similar age from the Lumby Lake and North Caribou greenstone belts (Hollings et al., 1996; Hollings and Wyman, 1997; Hollings and Wyman, 1998; Hollings and Kerrich, 1998). The tholeiites can be divided into two types; those with uniformly flat primitive mantle normalised patterns such as Lumby Lake, Garner Lake and some Balmer assemblage samples and the South Rim Unit of the North Caribou greenstone belt (Fig. 4.12 and 4.13), and secondly those where the patterns vary from flat to weakly LREE enriched, often in conjunction with negative Nb and Ti anomalies (e.g., the Balmer and Ball assemblages, in the Red Lake greenstone belt; Fig. 4.12). This is similar to the komatiites where both contaminated and uncontaminated flows have been identified (Table 4.6).

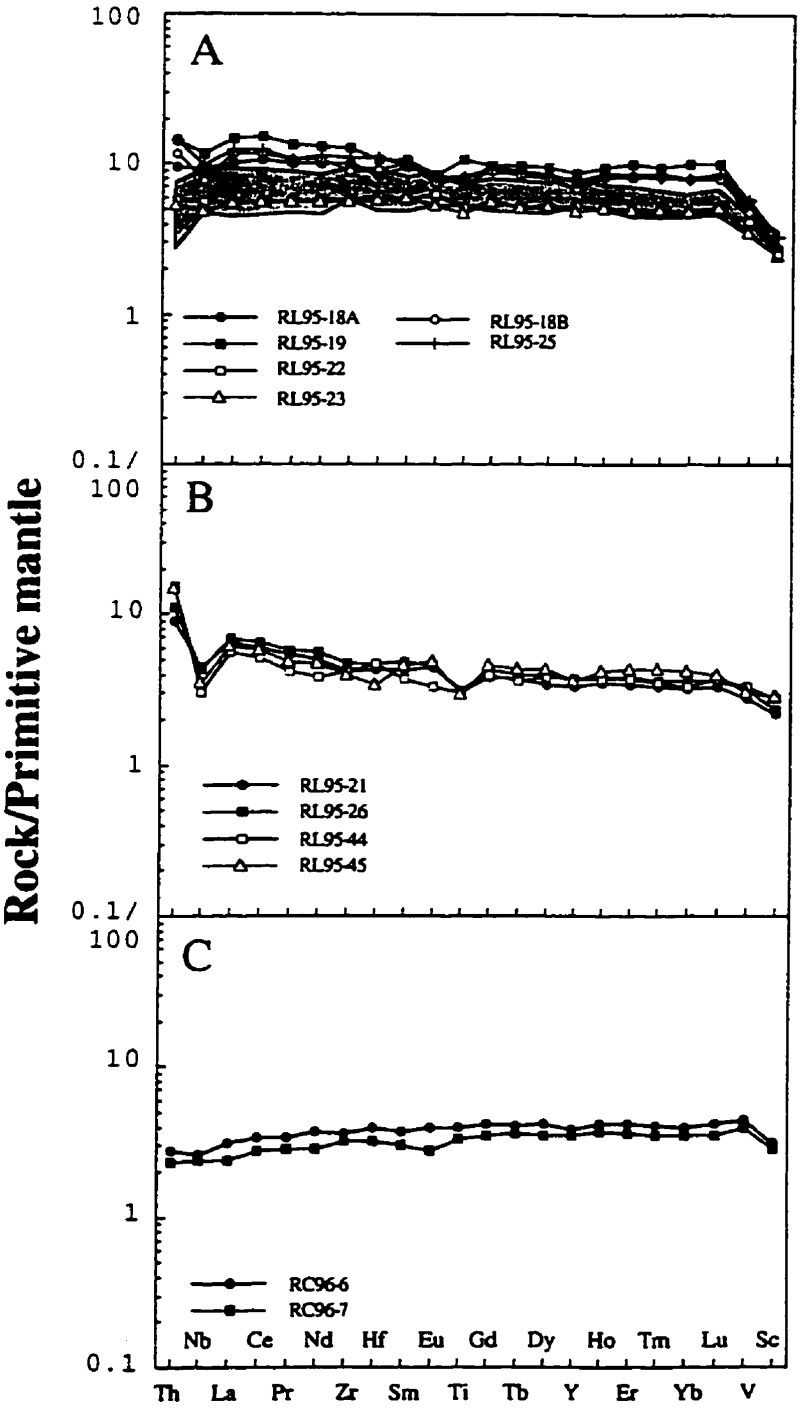

Figure 4.12. Representative primitive mantle normalised plots for A) tholeiites and B) LREE enriched tholeiites of the Balmer assemblage of the Red Lake belt and C) tholeiites of the Garner Lake assemblage of the Rice Lake belt. Shaded field is data for basalts from the Ontong Java ocean plateau (Mahoney et al., 1993).

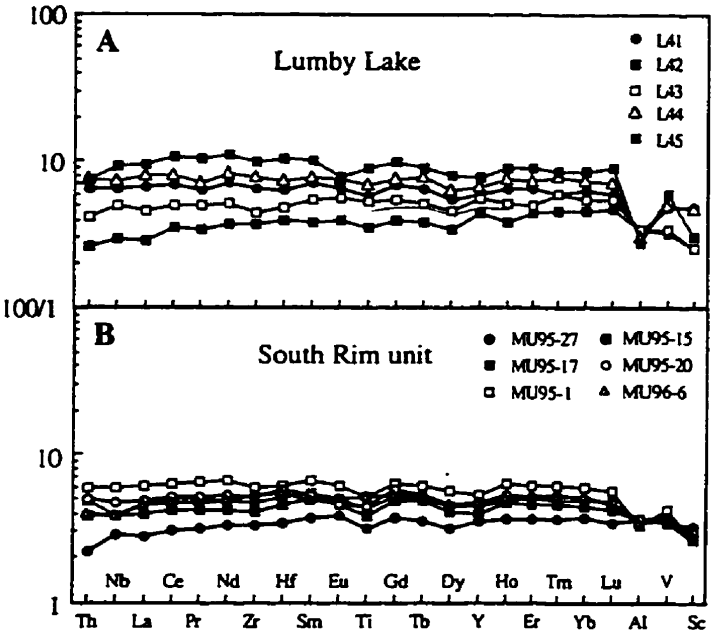

Figure 4.13. Representative primitive mantle normalised diagrams from A) the Lumby Lake belt and B) the South Rim unit of the North Caribou greenstone belts. Data from Hollings et al. (1998) and unpublished data of the author.

Collectively all five suites of basalts include Mg- to Fe-tholeiites, with basaltic andesites in the Ball assemblage and at Lumby Lake. Tholeiitic basalts from Lumby Lake plot close to primitive mantle lines for Zr versus Th, Nb, La, Sm, Zr and Yb (Fig. 4.14). The Garner Lake and South Rim tholeiites plot close to primitive mantle lines for all elements and do not extend to such high trace element contents. The Balmer tholeiites show similar trends, excepting Th enrichment relative to Zr, whereas the tholeiites of the Ball assemblage plot at Th and La enrichments, but Sm, Ti and Yb depletions relative to the other basalts (Fig. 4.14).

Table 4.6. Summary of ultramafic and mafic rock types in the 2.9-3.0 Ga terranes of the northern Superior Province. Lumby Lake data from Hollings et al. (1996) and Hollings and Wyman (1997). North Caribou greenstone belt data from Hollings and Kerrich (1998).

Greenstone belt	Rice Lake	Red Lake		Lumby Lake	Northern Caribou
Assemblage	Garner Lake	Ball	Balmer		
Ultramafic flows	AUKB*	AUK* AUKB*	AUK* AUKB*	ADK AUK AUKB	AUK* AUKB*
Mafic flows	MGT	MGT*	MGT*	MGT	MGT* MGT

AUK = Al-undepleted komatiites, AUKB = Al-undepleted komatiitic basalts, ADK = Al-depleted komatiites, MGT = Mg-tholeiites, * = crustally contaminated.

The most primitive Mg-tholeiites are distinctive in the conjunction of high Cr, Co and Ni with low Th and REE abundances, as well as flat to mildly depleted LREE. Magnesium tholeiites with similar compositional features are abundant in Archean greenstone belts of the Superior Province (Wyman et al., 1997; Ludden et al., 1982; Barrie et al., 1991).

Arndt (1991) has demonstrated that Mg-tholeiites with elevated Ni abundances cannot be fractionation products of komatiitic liquids. Rather, the high Mg and Ni character of Archean tholeiites reflects mixing of komatiites into upper mantle basaltic liquids, or contamination of komatiites by assimilation of crustal rocks. Mixing of komatiites and basalts is consistent with the plume model of Campbell et al. (1989), where komatiites are derived from the central core of the plume and tholeiites from melting of upper mantle entrained along the plume boundary. Such a model may well account for the elevated Ni and Cr contents of many of the plateau basalts reported herein.

The moderate LREE enrichment observed in the tholeiites in conjunction with the minor

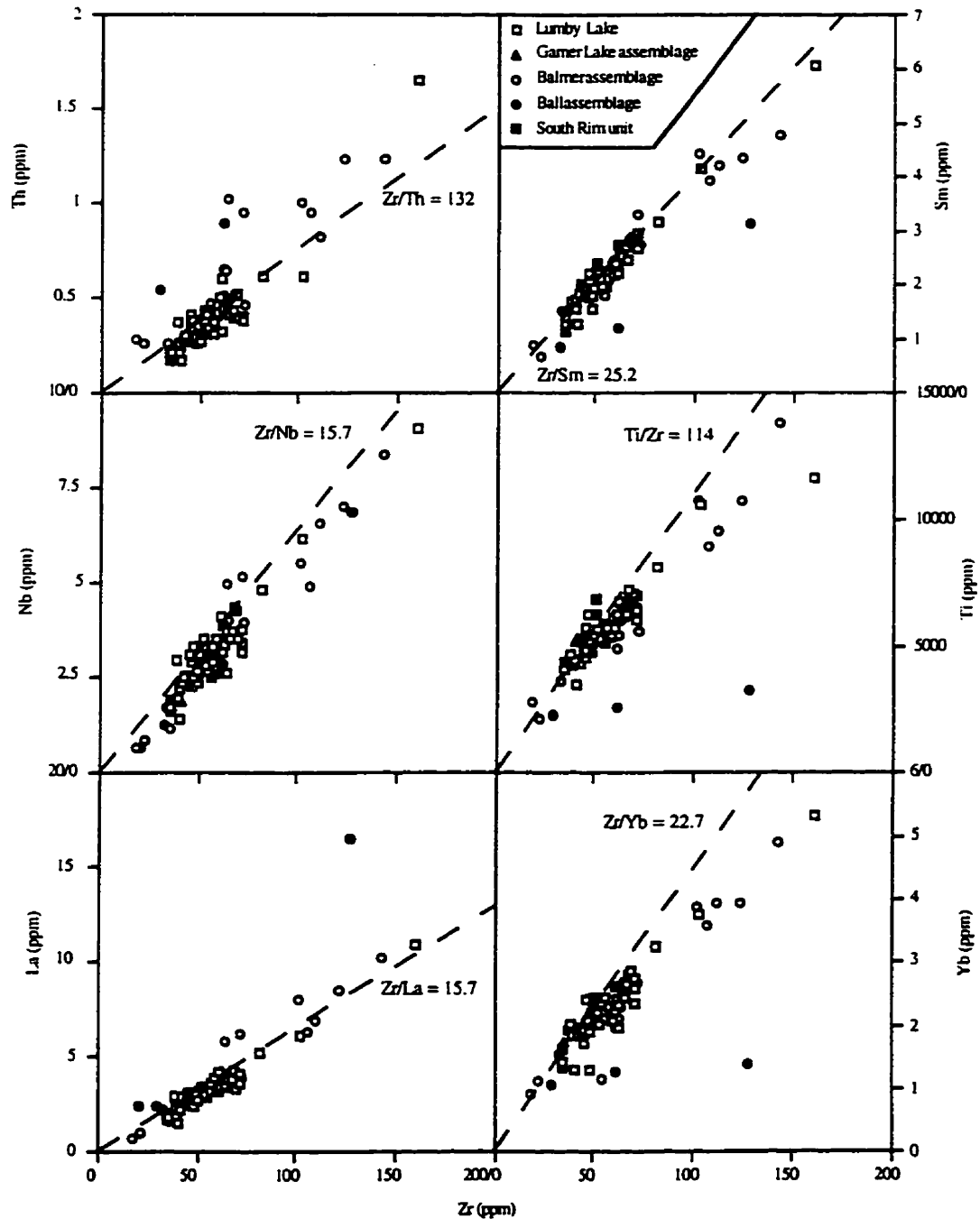

Figure 4.14. Trace element variation diagrams for mafic volcanic rocks of the 2.9-3.0 Ga assemblages of the Uchi subprovince. Dashed line represents chondritic ratios.

negative Nb anomalies is a feature reported from primitive arc tholeiites (e.g. Pearce et al., 1995). However, the association of these weakly LREE enriched tholeiites with both komatiites and tholeiites with flat trace element patterns is not observed in modern arcs. Consequently, given the association of crustally contaminated komatiites with the basalts that display LREE enrichment in the Balmer and Ball assemblages (Figs. 4.4 & 4.5), it seems likely that the characteristics of these rocks are also related to crustal contamination processes. Therefore, mafic rocks from the Balmer assemblage of Red Lake are interpreted as crustally contaminated plateau tholeiites.

These trace element characteristics may reflect crustal assimilation by a tholeiitic basalt liquid or alternatively more extensive crustal contamination of a komatiitic liquid. Given that the high heat of fusion of olivine and the large crystallisation interval of komatiites means that they have the potential to assimilate three times as much crust as basaltic magmas (Sparks, 1986), and that up to 50% contamination of komatiites might occur during the ascent of the magma (Huppert and Sparks, 1985), the latter explanation is the more likely.

Tholeiitic basalts from the Balmer and Ball assemblages of the Red Lake belt show evidence of contamination, however, basalts of the Rice Lake and North Caribou belts do not, despite the presence of crustally contaminated komatiites (Section 4.2.5). Figure 4.15, for example, plots Nb/Nb* values for the Superior Province tholeiites against La/Sm_n and compares the Archean rocks with data for Phanerozoic plateau basalts. Data for the Balmer and Ball assemblage tholeiites extend to high La/Sm_n ratios comparable to those observed in the Kerguelen and Broken Ridge plateaux tholeiites that are considered to have erupted through fragments of continental crust (Storey et al., 1992). In contrast, uncontaminated tholeiitic basalts from the Lumby Lake, Rice Lake and North Caribou belts plot close to the field of Ontong Java that erupted in an intra-oceanic environment.

Lesher and Arndt (1995) proposed that closely related contaminated and uncontaminated komatiites from Kambalda, Western Australia, were the result of later melts exploiting preexisting magma conduits without assimilating significant volumes of crustal material. Hollings and Kerrich (1998) invoked a similar mechanism to explain the presence of uncontaminated tholeiites overlying crustally contaminated komatiites in the North Caribou belt. This process may also explain the occurrence of uncontaminated tholeiites intercalated with the komatiites of the Garner Lake assemblage. Alternatively the lack of a contamination signature in the tholeiites may simply reflect the reduced ability of mafic

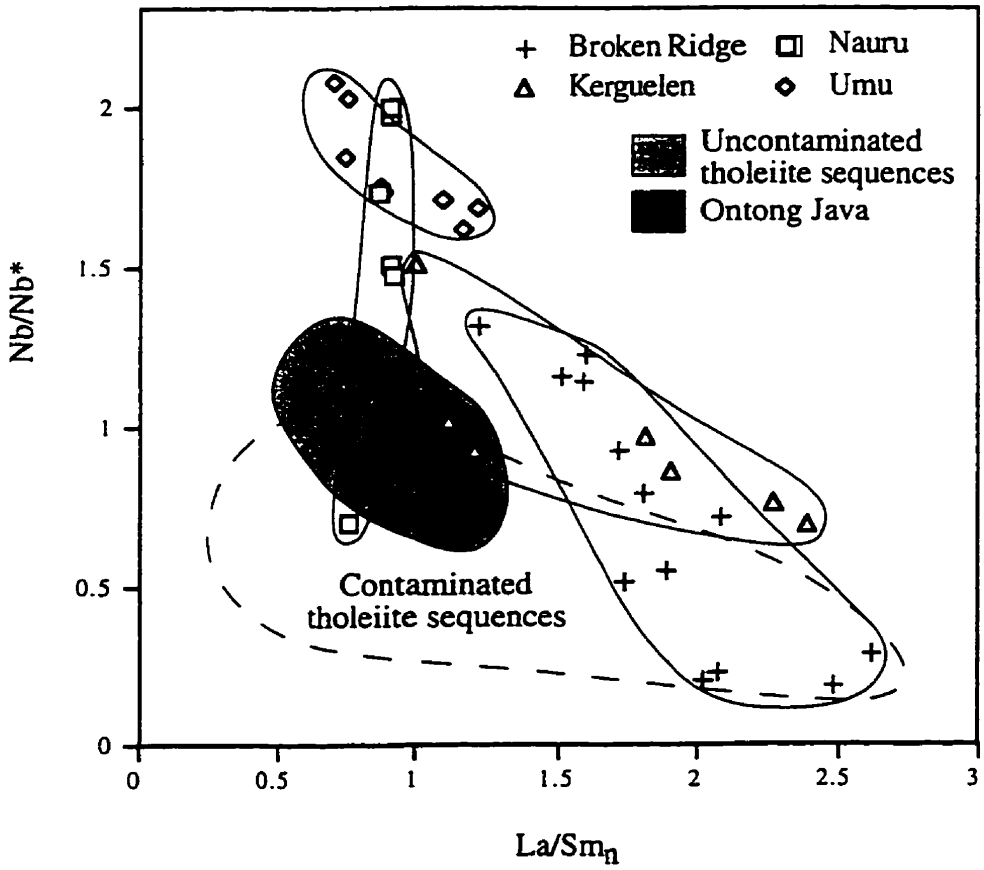

Figure 4.15. Comparison of La/Sm_n versus Nb/Nb* for modern oceanic plateaus and data from this study. Data from Floyd (1989), Mahoney et al. (1993, 1995) and Storey et al. (1992).

rocks to assimilate contaminants given their lower temperatures.

4.4 Felsic volcanic rocks of the Ball and Balmer assemblages

4.4.1 Introduction

The relative scarcity of the felsic rocks within the older assemblages of the Uchi subprovince necessitates comparison with the relatively well studied felsic rocks of the Lumby Lake and North Caribou belts (Hollings et al., 1996; Hollings and Wyman, 1997; Hollings et al., 1998; Hollings and Kerrich, 1998). Table 4.7 summarises the occurrence of felsic rock types within the ~3 Ga volcanic sequences. As with the ultramafic and mafic rocks representative analyses are provided throughout the section, with the full data set reported in Appendix B. The majority of felsic rock types from the ~3 Ga terranes are dacites or rhyolites (SiO_2 64-84 wt.%; Table 4.8) typically characterised by pronounced LREE fractionation in conjunction with pronounced negative Nb and Ti anomalies. HREE are more variable and may be either steeply fractionated (Type 1) or flat (Type 2; Fig. 4.16).

In all cases where either Type 1 or Type 2 rhyolites are found, they are intimately intercalated with the tholeiitic basalts. Given that many of them can be shown to be subaerial or subaqueous pyroclastic deposits this implies that they are coeval with the tholeiitic volcanism, and in the Lumby Lake belt, at least, they erupted contemporaneously over a period of at least 100 Ma (Hollings et al., 1996; Hollings and Wyman, 1997). The occurrence of Type 3 rhyolites within the Balmer assemblage of the Red Lake belt, characterised by flat REE patterns at 30-50 times primitive mantle values and comparable to FIII felsic volcanic rocks of Lesher et al. (1986), is unique amongst the older sequences.

4.4.2 Types 1 and 2 Felsic Volcanic Rocks

In a comprehensive study of felsic volcanics intercalated with 100 m.y. of ultramafic and mafic volcanism in the Lumby Lake belt, Hollings et al. (1996) and Hollings and Wyman (1997, 1998) identified two distinct suites of pyroclastic rocks. For the purpose of this study these will be utilised as a baseline against which other areas are compared and contrasted. The two suites are distinguished on the basis of Zr/Y and Al_2O_3/TiO_2 ratios, as well as the degree of HREE fractionation (Hollings and Wyman, 1997; Fig. 4.16). Type 1 are characterised by high Zr/Y ratios (>25) and Gd/Yb_n generally greater than two,

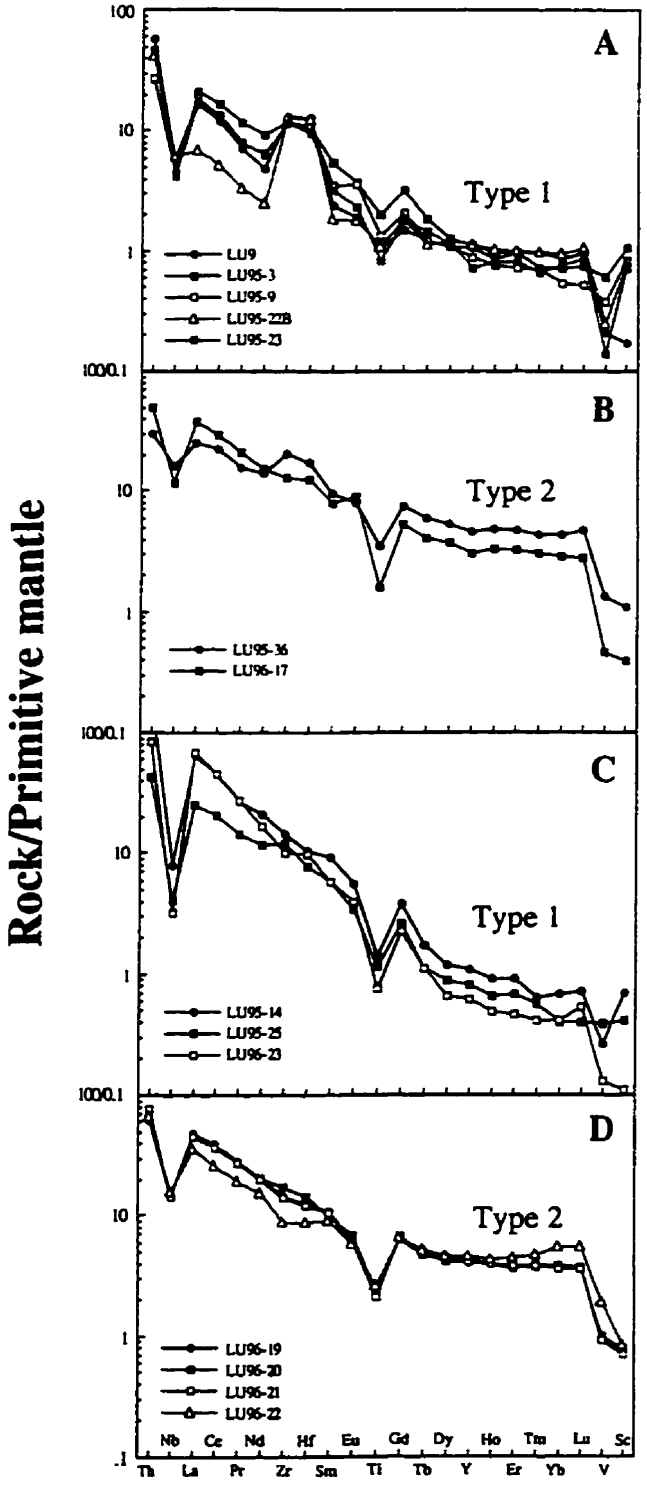

Figure 4.16. Primitive mantle normalised patterns for felsic rock types from the Lumby Lake belt. A = Type 1 extrusive rocks , B = Type 2 extrusive rocks, C = Type 1 intrusive rocks , D = Type 2 intrusive rocks. Data from Hollings and Wyman (1997) and unpublished data of the author.

whereas Type 2 display lower Zr/Y ratios (<15) and Gd/Yb_n less than two. Type 1 is broadly comparable to the FI-felsics of Lesher et al. (1986), whereas Type 2 is comparable to the FII series.

Table 4.7. Summary of ultramafic, mafic and felsic rock types in the 2.9-3.0 Ga terranes of the northern Superior Province. Lumby Lake data from Hollings et al. (1996) and Hollings and Wyman (1997), North Caribou greenstone belt data from Hollings and Kerrich (1998).

Greenstone belt	Rice Lake	Red Lake		Lumby Lake	Northern Caribou
Assemblage	Garner Lake	Ball	Balmer		
Ultramafic flows	AUKB*	AUK* AUKB*	AUK* AUKB*	ADK AUK AUKB	AUK* AUKB*
Mafic flows	MGT	MGT*	MGT*	MGT	MGT* MGT
Felsic rock types		T1	T2 T3	T1 T2	T2

AUK = Al-undepleted komatiites, AUKB = Al-undepleted komatiitic basalts, ADK = Al-depleted komatiites, MGT = Mg-tholeiites, T1 = Type 1 felsic, T2 = Type 2 felsic, T3 = Type 3 felsic, * = crustally contaminated.

Rhyolites from the Balmer assemblage have a narrow range of SiO_2 contents (74-76 wt.%), strongly fractionated LREE, but weakly fractionated HREE, and variable Nb and Ti anomalies, comparable to Type 2 felsic volcanic flows from the Lumby Lake area (Zr/Y = 5-14; Table 4.8; Fig. 4.17). They show complex compositional relationships in which increasing Ti and Fe are accompanied by an increase of Cr, Co, Ni, Sc, V and Cu to levels well above those typical of most rhyolites, as well as an increase of HREE abundances at decreasing Gd/Yb_n and Zr/Y ratios. In addition a third felsic subset (Type 3) has been recognised, characterised by generally flat REE (La/Sm_n = 1.4) at high absolute abundances. This is loosely comparable to the FIII rhyolites of Lesher et al. (1986).

Ball assemblage rhyolites (SiO_2 = 72-74 wt.%), are comparable to the Type 1 felsic suite of the Lumby Lake greenstone belt. They have Zr/Y ratios of 29-43 and are characterised by pronounced LREE enrichment and strongly fractionated HREE (La/Sm_n = 6.0-7.4; Gd/Yb_n = 3.3-6.0; Fig. 4.17; Table 4.8). There are systematic negative Nb and Ti anomalies, high Th contents and moderately to strongly positive Zr and Hf anomalies are present in all samples (Zr/Zr^* = 1.7-2.2).

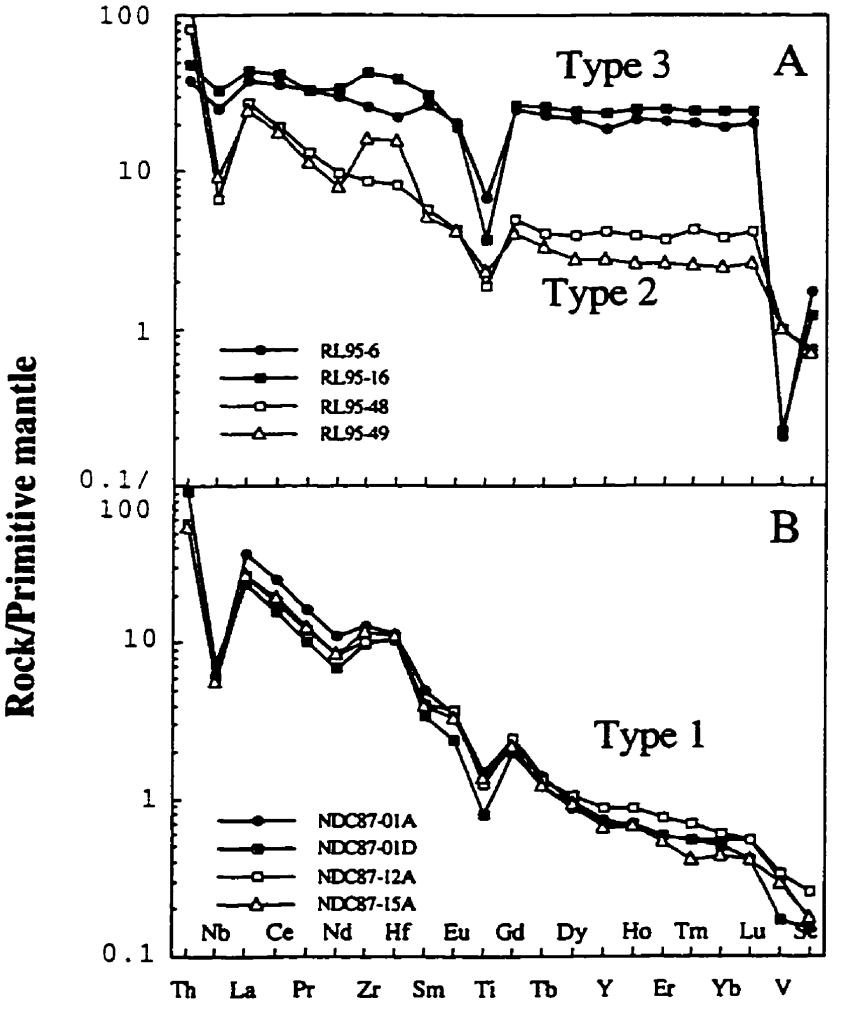

Figure 4.17. Representative primitive mantle normalised plots for felsic volcanic rocks from A) the Balmer assemblage and B) the Ball assemblage of the Red Lake greenstone belt.

Table 4.8. Representative analyses of selected elements from felsic volcanic rocks of the Ball and Balmer assemblages*.

	Ball assemblage				Balmer assemblage			
	Type 1				Type 2		Type 3	
	NDC87-01A	NDC87-01D	NDC87-12A	NDC87-15A	RL95-48	RL95-49	RL95-16	RL95-6
SiO_2	72.61	76.62	72.04	73.09	74.03	74.19	69.33	56.00
TiO_2	0.30	0.20	0.27	0.31	0.39	0.52	0.84	1.52
Al_2O_3	15.31	14.99	14.53	14.87	10.75	10.04	11.66	12.52
Fe_2O_3	2.47	1.54	2.77	2.17	4.52	7.06	8.25	17.31
MgO	1.26	1.25	1.57	1.65	2.39	2.60	0.95	1.84
LOI	1.27	2.25	2.04	1.89	3.20	1.42	0.96	0.15
Mg#	53	64	56	63	54	45	20	19
Ti	1917	1057	1640	1788	2478	3034	4893	8862
Cr	10	28	13	21	201	345	92	10
Co	12	5	8	7	20	33	9	23
Ni	4	16	6	11	63	82	6	1
Sc	3	3	4	3	13	12	21	30
V	25	14	28	24	82	83	19	17
Nb	4.24	5.15	4.37	4.05	4.75	6.62	23.17	17.87
Zr	142	110	114	129	98	179	480	286
Hf	3.54	3.34	3.18	3.38	2.54	4.84	11.90	6.81
Th	4.64	7.85	4.90	4.57	6.87	9.24	4.04	3.22
Y	3.31	3.13	4.00	3.01	19.20	12.73	106.89	84.86
La	25.20	16.17	18.39	18.13	18.70	16.56	30.24	25.76
Sm	2.19	1.52	1.79	1.77	2.59	2.25	13.52	11.88
Gd	1.47	1.19	1.48	1.31	2.95	2.39	16.06	15.08
Yb	0.27	0.25	0.30	0.21	1.89	1.23	12.02	9.55
Lu	0.04	0.03	0.04	0.03	0.31	0.19	1.81	1.50
(La/Yb)n	66.07	47.23	44.55	60.74	7.10	9.69	1.80	1.93
(La/Sm)n	7.44	6.85	6.65	6.60	4.66	4.75	1.44	1.40
(Gd/Yb)n	4.44	4.00	4.14	5.08	1.29	1.61	1.11	1.31
Al_2O_3/TiO_2	48	84	53	49	26	20	14	8
Zr/Hf	40	33	36	38	39	37	40	42
Zr/Y	43	35	29	43	5.10	14.09	4.49	3.37
Sc/La	72	85	108	100	42	62	12	20
Nb/Nb*	0.11	0.21	0.16	0.16	0.17	0.28	0.69	0.64
Zr/Zr*	1.72	2.04	1.74	1.99	1.15	2.51	1.33	0.90
Hf/Hf*	1.56	2.24	1.76	1.89	1.08	2.45	1.19	0.77
Ti/Ti*	0.42	0.31	0.40	0.46	0.35	0.52	0.13	0.26

*Full data set in Appendix B

Hollings and Kerrich (1998) reported the presence of felsic pyroclastic rocks intercalated throughout the mafic volcanics of the South Rim unit. The rhyolites are comparable to the Type 2 suite from Lumby Lake and are characterised by Zr/Y of 3-19, and LREE enrichment in conjunction with weakly fractionated HREE (La/Sm_n = 3.0-5.6; Gd/Yb_n = 1.1-2.3; Fig. 4.18). All samples have pronounced Nb and Ti anomalies combined with high Th contents and Th/Ce ratios, in conjunction with moderate positive Zr and Hf anomalies (Zr/Zr^* = 1.4-1.6).

4.4.3 Petrogenesis of felsic volcanic rocks

Felsic volcanic rocks characterised by strongly fractionated REE and lacking Eu anomalies (comparable to FI-type of Lesher et al., 1986) have been recognised in many of the older (~2.9-3.0 Ga) volcanic sequences investigated as part of this study, as well as greenstone belts of the Abitibi and Wawa subprovinces (Table 4.9). In the older belts of the Northern Superior Province, the volumetrically minor felsic volcanics occur intercalated with plateau tholeiites and komatiites, which are interpreted in this study to be the product of a mantle plume. In order to evaluate the petrogenesis of these felsic rocks data from the ~3 Ga Lumby Lake belt will be utilized, perhaps the most intensively characterised example of an old assemblage conducted by the author (Hollings et al., 1996; Hollings and Wyman, 1997, 1998).

The fractionated HREE of the FI type rocks are interpreted to be the result of melting at depth within the garnet stability field, which allowed for the fractionation of all REE and the retention of Y and HREE (Martin, 1986, 1994). Conventionally REE fractionation in Archean TTG is explained as the result of melting of subducted oceanic slab at depth. An alternative explanation for the origin of the FI patterns is that they were derived by the melting of mafic crust at the base of an over thickened oceanic plateau. However, the lack of negative Eu anomalies, generally considered characteristic of crustal melting (e.g., Taylor and McLennan, 1985), in conjunction with the presence of extensive plutonic complexes with identical trace element characteristics, suggests that this is the less likely alternative (such as the Marmion Lake Batholith, Lumby Lake greenstone belt; Fig. 4.16). The flatter HREE of FII rock types may be the product of shallower slab dehydration above the garnet stability field.

Type 1 felsic intrusive and related extrusive rocks display La/Yb_n ratios (7-165) which extend to the upper limits of the range documented for Archean granitoids (Martin, 1986, 1994) however, the majority of samples are typified by more moderate ratios (*e.g.*, 30).

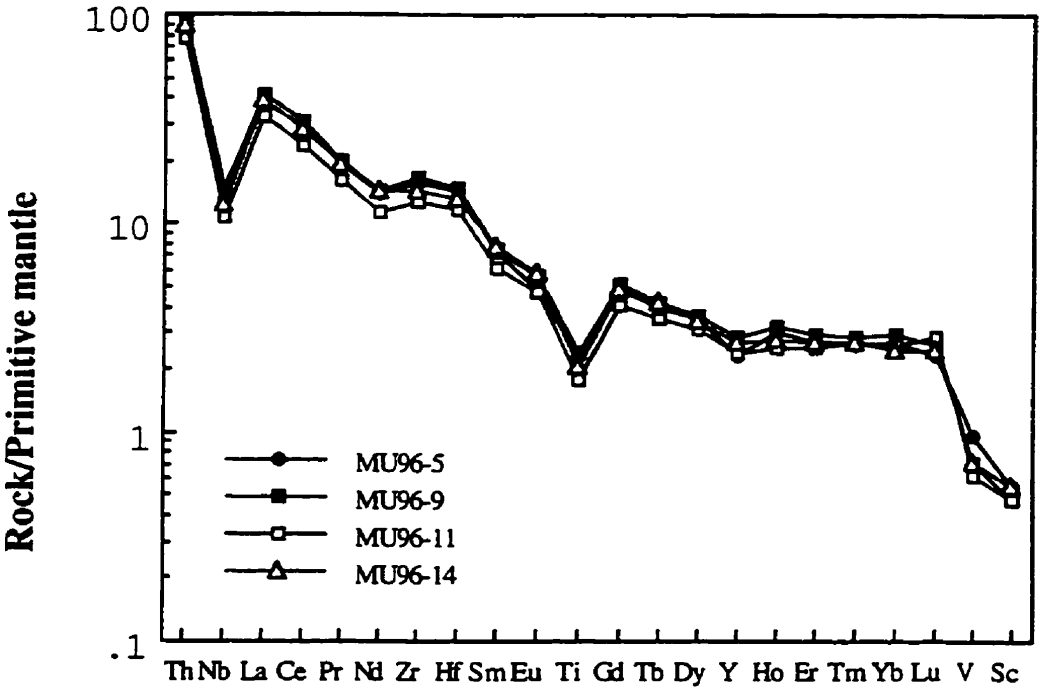

Figure 4.18. Representative primitive mantle normalised plots for Type 2 felsic volcanic rocks from the South Rim unit of the North Caribou greenstone belt. Data from Hollings et al. (1998) and authors unpublished data.

Table 4.9. Summary of occurrences of felsic rock types in the Superior Province

Subprovince	FI	FII	FI-FII	FIIIa	FIIIb	Associated rocks
Sachigo subprovince[1]						
North Caribou belt		•				MGT, AUK*, AUKB*
Uchi subprovince[2]						
Balmer assemblage, Red Lake	•	•		•		MGT, AUK*, AUKB*
Ball assemblage, Red Lake	•					MGT, AUK*
Northern Pickle assemblage, Pickle Lake		•				K†1
Pickle Crow assemblage	•					MGT, AUK, CAB
Meen assemblage	•					PAT?
Woman assemblage		•		•	•	MGT, CAB, PAT
Confederation assemblage	•	•		•	•	
Birch-Uchi belt	•	•	•	•	•	MGT, PAT, OIB, ICE
Red Lake and Pickle Lake belts						CAB
Meen-Dempster belt						MGT, OIB
Rice Lake belt						MGT, CAB
St Joseph assemblage		•				K†2, MGT, CAB
Wabigoon subprovince						
Lumby Lake belt[2]	•	•				AUK, AUKB, ADK, MGT, OIB
South Sturgeon Lake assemblage[3]		•		•		PAT, THO-CA
Northeast Arm assemblage[3]			•			MGT, PAT
North Sturgeon Lake assemblage[3]		•	•			MGT, PAT

Table 4.9 Continued. Summary of occurrences of felsic rock types in the Superior Province.

Subprovince	FI	FII	FI-FII	FIIIa	FIIIb	Associated rocks
Abitibi subprovince						
Blake River group[3]				•	•?	THO-CA, MGT, PAT
Kidd Creek[3]				•	•	AUKB, ICE, LOTI
Malartic Block - Val d'Or[3]	•	•		•	•	THO-CA, PAT
Krist[3]	•					MGT
Kamiskotia[3]				•	•?	THO-CA, ICE, PAT
Wawa subprovince						
Dayohessara[4]	•					MGT, AUK, ADK
White River[4]	•	•				MGT, CAB
Manitouwadge[4]	•			•		THO-CA
Heron Bay[4]	•					MGT, ADK, CAB
Schreiber-Hemlo[4]	•	•				MGT, AUK, AUKB
Winston-Big Duck Lake[4]	•	•		•		MGT, AUKB, CAB

AUK = Al-undepleted komatiiites, AUKB = Al-undepleted komatiitic basalts, ADK = Al-depleted komatiite, MGT = Mg-tholeiites, CAB = Calc alkaline basalt, PAT = Primitive arc tholeiite, ICE = Icelandites, LOTI = low-Ti tholeiite, THO-CA = transitional tholeiite-calc alkaline andesites, • = crustally contaminated, †= not sampled in this study, reported by (1) Sage and Breaks (1982) and (2) Stott (1996). Data sources: (1) Hollings and Kerrich (1998), unpublished data of the author; (2) this study; (3) D. Wyman, unpublished data, Wyman et al., 1997; (4) Polat, 1998.

Fractionation between the MREE and HREE are less variable in Type 1 rocks and Gd/Yb_n spans 5.6-6.5. The second (Type 2) felsic to intermediate suite is distinguished by less extreme MREE-HREE fractionation, producing flat HREE patterns on primitive mantle normalised diagrams, but are otherwise similar to Type 1. Martin (1986) interpreted HREE fractionation and low Yb contents to be characteristic of slab melting as the result of subduction of young hot crust that melts before it dehydrates. In contrast, samples with flat HREE and higher Yb contents likely underwent slab dehydration processes more typical of Phanerozoic subduction zones. Gromet and Silver (1987) invoked a similar mechanism to account for variations in REE abundances across the Peninsular Ranges batholith, the onset of HREE depletion being the result of a change from plagioclase-pyroxene to garnet-bearing eclogitic residual assemblages. The predominantly flat trace element patterns and relative scarcity of Type 3 rhyolites is consistent with them having fractionated from mafic tholeiitic parental compositions.

Rhyolites are a common minor component in post-Archean flood basalt provinces and may be generated by several mechanisms. Garland et al. (1995) describe two types of rhyolites from the Parana flood basalt province. The Chapecó rhyolites are characterized by elevated HFSE contents, particularly Ti, and are interpreted as the products of partial melts of underplated basalts. In contrast, the Palmas rhyolites are characterized by lower HFSE and Ti abundances, and are interpreted as the products of open system fractionation products of basalts. Neither class of rhyolites are comparable to the Type 1 or 2 rhyolites discussed here, although the volumetrically minor Type 3 rhyolites do resemble the products of Parana basalt fractionation (Fig. 4.16). However, the Palmas rhyolites are associated with a range of intermediate rock types generated by fractionation processes (op cit), whereas comparable intermediate rocks are not common in the northern Superior Province greenstone belts.

Irrespective of whether the Type 2 rhyolites reflect changes in the source regions or are the products of open system fractionation and/or mixing, the dominant Type 1 rhyolites are directly comparable to counterparts in the Abitibi belt of the southern Superior Province (Fig. 4.16). The Abitibi examples are associated with basalts and andesites that exhibit features characteristic of arc magmatism, such as LREE enrichment and fractionation, high Th/La ratios and normalised depletions of Nb and Ti (Capdevila et al., 1982; Feng and Kerrich, 1992), but the additional complexity of older crust is not a factor. Accordingly, a subduction origin for the Type 1 felsic rocks of the northern Superior Province is favoured.

4.4.4 Petrogenesis of Type 2 Felsic Rocks

A number of models have been proposed for the petrogenesis of the felsic volcanic rocks discussed above, including fractionation of mafic melts, partial melting and magma mixing. In the following section each of these models will be evaluated. In broad terms three models have been proposed for the petrogenesis of Archean TTG: (1) melting of pre-existing felsic crust; (2) melting at the base of thickened oceanic plateau; and (3) melting of downgoing slabs in a subduction zone. These will be evaluated below.

Conventional models for the petrogenesis of Type 1 and 2 felsic rocks invoke slab melting at depth with residual garnet to produce the steeply fractionated REE characteristics of the Type 1 felsics, whereas the Type 2 are thought to be derived at shallower depths as a result of slab dehydration which would not fractionate the HREE. Lesher et al. (1986) proposed that the geochemistry of Type 1 type rocks was consistent with low-degree partial melting of a mafic source region at high pressure, whereas Type 2 with flat HREE were consistent with high-degree partial melting of a crustal source or fractional crystallisation of an intermediate parent. Sutcliffe et al. (1993) advocated that the majority of plutonic rocks of the Southern Abitibi could have been derived from mantle sources, either by a two stage process involving a tholeiitic basalt precursor or by direct melting of metasomatised mantle.

An alternative class of mechanism for generation of the TTG batholith and felsic volcanic units would invoke their derivation directly from the plateau sequence. These types of models are commonly applied to the early Archean (>3.5 Ga) although most proponents envision plate tectonic processes, similar to those of the Phanerozoic, to have been active before 3.0 Ga (e.g., Kröner and Layer, 1992). Experimental studies demonstrate that melts comparable to Archean TTG can be generated by 20-40% melting of a mafic source at pressures greater than 18 kbar (Rapp et al., 1991), conditions which are compatible with both melting at the base of the plateau (e.g., Kröner, 1985) and melting of young and hot subducted lithosphere (e.g., Abbott and Hoffman, 1984). However the large volumes of felsic material preserved in the Marmion Lake batholith would seem to preclude derivation at the base of the plateau, given that no large batholiths have been identified in modern oceanic plateaux.

Arth et al. (1978) have shown that fractionation of a gabbroic liquid involving hornblende, plagioclase and biotite as the dominant phases could produce rhyolites with fractionated LREE but generally flat HREE (comparable to Type 2). Distribution

coefficients for hornblende in basic melts will result in LREE enrichment but no change in the slope of the HREE, whereas for more silicic compositions the distribution coefficients for the REE will result in fractionation of both LREE and HREE (Arth et al., 1978). These authors also noted that the distribution coefficients for hornblende and garnet during partial melting were probably very similar, and suggested that partial melting of amphibolite with a resultant hornblende rich residue could account for the steeply fractionated REE of many rhyolites and associated TTG suites. However, they suggested that the continuity of major and trace element variations of a suite of gabbros through trondjhemites in the 1.9 Ga Uusikaupunki-Kalanti TTG suite of southwest Finland was evidence that the suite was derived by fractional crystallisation leaving a hornblende-rich residue (or at least that this was the dominant process) rather than by partial melting of amphibolite or eclogite. However, Arth et al. (1978) acknowledged that this degree of preservation was unusual for Archean TTG suites, and consequently may represent a unique case, with partial melting being a more common petrogenetic process. Indeed few of the suites investigated in this study display a full compositional range suggesting that the Finland example may be atypical.

Rhyolites with the characteristics of Type 2 (FII) rocks have been identified in the Michipicoten belt of the Wawa subprovince (Sage et al., 1996) with an age range of 2.9-2.7 Ga. The older rocks are distinguished from the younger principally by the presence of negative Eu anomalies. Sage et al. (1996) propose that differences between these rhyolites and those of the Abitibi subprovince (higher La/Sm_n and Gd/Yb_n ratios) in conjunction with lower Zr/Th ratios indicates the rhyolites were derived from melting of a tonalitic source, likely preexisting Archean crust. However, they acknowledge that no xenocrystic zircons have been found to support this model. They further observe that these rhyolites are similar to those found in caldera complexes of the Chilean Andes, supporting their case for melting of preexisting crust. Sage et al. (1996) also suggest that the rhyolites are compositionally distinct from other felsic volcanic rocks of the Superior Province whereas, in fact they are transitional between FI and FII data of Lesher et al. (1986). The transitional nature of the rhyolites in conjunction with the lack of xenocrystic zircons suggests that they are more likely the result of melting and/or dehydration of downgoing slab.

More recently, Martin et al. (1997) working on Archean granites of South America, recognised two distinct suites; the "old grey gneisses" with strongly fractionated REE comparable to FI type felsic rocks and the "young grey gneisses" which are LREE

enriched but with flat HREE (comparable to FII-type). Martin et al. (1997) calculated that a parental dacitic magma could be derived by 5% melting of a mantle source leaving an olivine+orthopyroxene±garnet bearing residue; however this would not produce REE values comparable to those of their proposed parental liquid. Rather they propose that 30% melting of an enriched Archean tholeiite (EAT; Condie, 1981) with a hornblende+garnet+clinopyroxene+ilmenite±plagioclase assemblage would produce a melt with the appropriate characteristics. They also show that it is possible to fractionate the HREE by including as little as 1% zircon in the cumulate. The young grey gneisses (FII) are richer in LREE than the old grey gneisses, and have significantly higher K_2O contents but only slightly higher SiO_2. Consequently, Martin et al. (1997) conclude they cannot have been derived from a similar source to the old grey gneisses. Instead they propose that they were derived from the melting of an older crustal segment possibly the old grey gneisses, this is supported by negative epsilon Nd values for the young grey gneisses. High degrees of partial melting (>60%) with residual quartz, hornblende and plagioclase was modelled to produce results consistent with this petrogenetic scheme.

The high Cr, Co, Ni, Sc, V and Cu of the Type 2 felsic rocks identified in this study (Table 4.10) suggests another possible origin, namely by mixing of a Type 1 felsic rock with a tholeiitic magma. Data from the Lumby Lake belt indicates that the Type 1 felsic volcanics typically display higher silica contents than the Type 2 which is also consistent with contamination by tholeiitic melts. Derivation of the Type 2 felsic rocks by magma mixing (or contamination) and fractionation has been investigated as part of this study, given that the felsics are intimately intercalated with the tholeiites and therefore represent broadly coeval magmas. A typical Lumby Lake tholeiitic basalt was used as a parental magma and a 70% mafic/30% Type 1 felsic mix, followed by Raleigh fractionation of 60% plagioclase, 30% clinopyroxene and 10% spinel (distribution coefficients compiled by Rollinson, 1993). This model was found to generate trace element patterns consistent with the Type 2 felsic samples at 40 to 50% fractionation (Fig. 4.19; Hollings and Wyman, 1997, 1998).

Consequently it is suggested that in these ~3 Ga assemblages it is possible that the Type 2 felsic rocks, characterised by flatter HREE could be derived by mixing of the strongly fractionated felsics with plateau tholeiites, commensurate with field evidence for their coeval eruption. Lesher et al. (1986) indicated that FII's were typically characterised by a higher SiO_2 content than FI, which if true would require fractionation after mixing with a

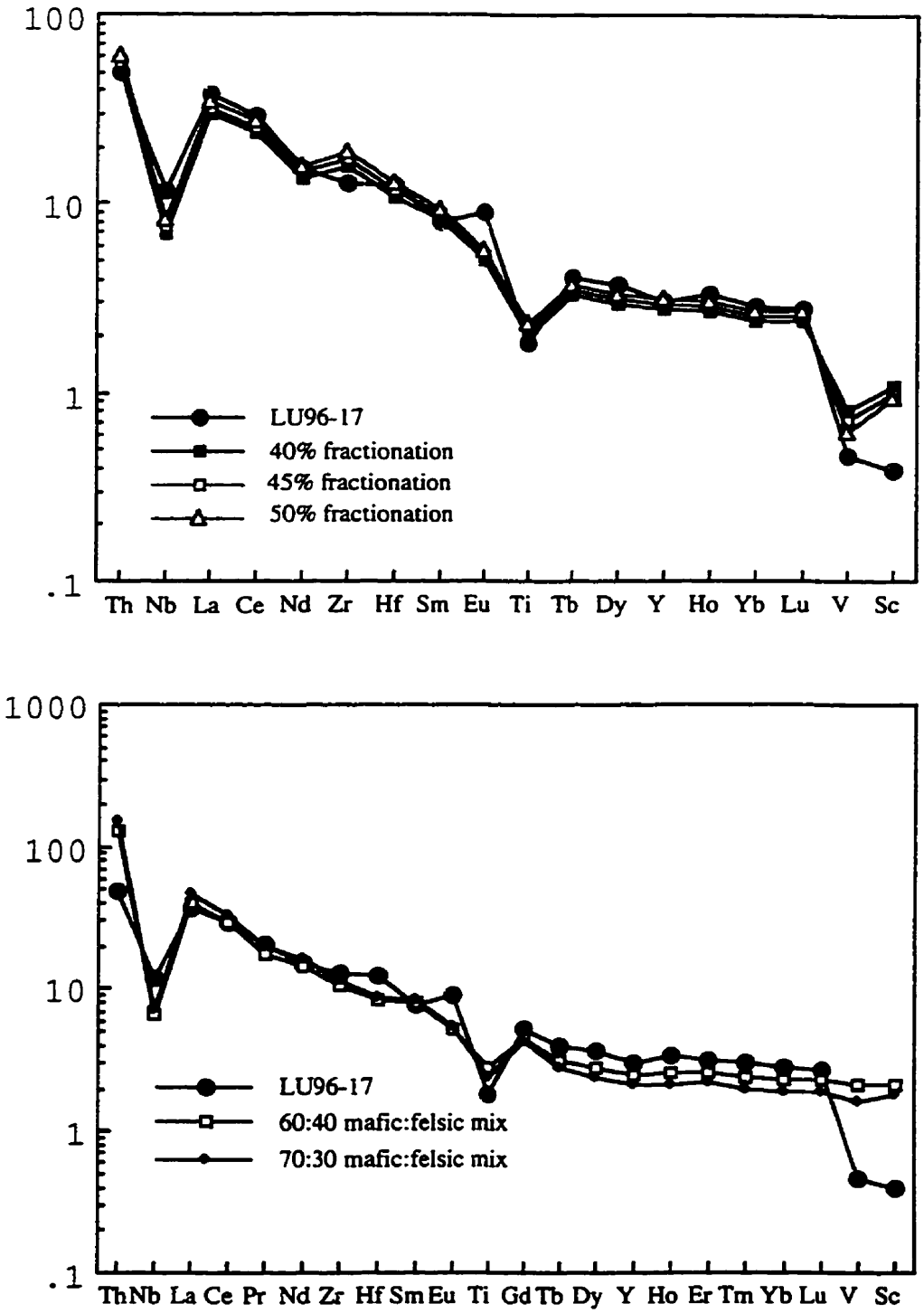

Figure 4.19. A) Primitive mantle normalised pattern illustrating the results of fractionating a Type 1 felsic volcanic rock. B) Primitive mantle normalised pattern illustrating the results of mixing a Type 1 felsic volcanic rock with a mafic tholeiite to produce a Type 2 composition.

mafic magma, as mixing would tend to result in lower SiO_2 contents. Data from the older assemblages indicates that the Type 1 felsics typically display higher silica contents than the Type 2 (Table 4.10). This is consistent with mixing of Type 1 felsic rocks and tholeiites and subsequent fractionation, with extensive fractionation producing the high SiO_2 contents observed by Lesher et al. (1986) but more moderate AFC resulting in the lower values of the Lumby Lake samples.

Table 4.10. Comparison of geochemical characteristics of Type 1 and 2 felsic volcanic rocks. Data for Meen and Confederation assemblages from Chapter 6.

	Lumby	Lumby	Ball	SRU	Balmer	Meen	Confed.
Type	Type 1	Type 2	Type 1	Type 2	Type 2	Type 2	Type 2
Age	~3 Ga	~3 Ga	~3 Ga	~3 Ga	~3 Ga	~2.7 Ga	~2.7 Ga
SiO_2	69-76	54-68	72-76	70-75	74-76	72-76	67-74
MgO	0.4-0.8	2.5-4.4	0.5-2.4	0.65-1.0	1-2.6	0.3-1.0	0.6-2
Gd/Yb_n	5.5-6.5	1.2-1.8	3.6-6.3	1.6-2.3	1.3-1.7	1.7-4	1.2-2.2
La/Yb_n	62-165	6-12	38-66	13-17	7-10	10-30	4-20
Ni	0-9	6-42	4-16	10-32	12-82	1-13	3-6
Cr	5-32	12-71	9-48	24-63	30-345	2-16	2-8
Co	3-6	17-26	6-13	11-23	3-33	2-10	3-34

In the ~3 Ga terranes examined as part of this study the Type 2 felsic intrusive and extrusive rocks have significantly higher Ni, Cr, Co and Ti contents than the HREE fractionated Type 1 counterparts with which they are associated. For example in the Lumby Lake belt Type 2 felsics with a range of SiO_2 contents from 54-68 wt.% have Ni contents of 6-42 ppm, Cr of 12-71 and Co from 17-26. In contrast the Type 1 volcanics display SiO_2 contents of 69-76 wt.%, Ni of 0-9 ppm, Cr of 5-32 ppm and Co of 3-6 ppm (Table 4.10). The differences in silica content between the two felsic rock types mean that the decreased Ni, Cr and Co contents could be the result of fractionation; however as illustrated in Figure 4.19 mixing with tholeiite melts can account for the HREE of the FII type and would also lower the silica content while increasing MgO, Ni, Cr and Co.

Further support for the mixing model is provided by Type 2 felsic volcanic rocks from the South Rim Unit of the North Caribou greenstone belt. Here the elevated SiO_2 contents of

the flows are comparable to the more evolved Type 1 rocks from the Lumby Lake area but Ni, Cr and Co contents are considerably higher (Table 4.10), supporting the model that mixing with tholeiite rich in Ni, Cr and Co could produce rocks with the characteristics of Type 2 type flows.

It is clear that there are differences in the trace element characteristics of Type 2 rocks from the younger assemblages (~2.7 Ga) investigated in this study compared to the older Type 2 rocks. For example felsic flows from the St. Joseph, Meen and Confederation assemblages of the Uchi subprovince (Chapter 6), with comparable La/Yb_n and Gd/Yb_n ratios to the older Type 2 from the SRU and the Lumby Lake area, display significantly lower Ni, Cr and Co contents at comparable levels of SiO_2 (Table 4.10).

4.4.5 Geodynamic Significance of the FI-komatiite/tholeiite Association

The intercalated nature of the felsic volcanics in the 3 Ga komatiite-tholeiite dominated terranes requires that they were erupted coevally. The close spatial association of inferred Archean plume-derived sequences and calc alkaline suites has been attributed to plateau-arc interaction (e.g., Desrochers et al., 1993; Stein and Goldstein, 1996). However, the stratigraphic evidence from the Lumby Lake belt indicates that the plateau accretion models of Desrochers et al. (1993) for the 2.7 Ga Abitibi belt, Boher et al. (1992) for the ~2.1 Ga Birimian terranes of West Africa and Stein and Goldstein (1996) for the Arabian-Nubian shield, where arcs develop on obducted oceanic plateau, cannot be directly applied in this case. Unlike the 2.7 Ga Malartic Block of the Abitibi belt, the coeval eruption of plume-related tholeiites and calc alkaline magmas in the Ball, Balmer and Lumby Lake stratigraphic sequence and particularly the late eruption of komatiites at Lumby Lake (Hollings and Wyman, 1998), implies the presence of both an active plume and subduction zone magmas. Moreover, TTG or calc alkaline magmatism is recorded from the beginning and, at least sporadically, throughout the 100 m.y. interval preserved in the Lumby Lake belt (Davis and Jackson, 1988; Hughes et al., 1997).

The presence of an active plume in conjunction with a subduction zone below these ancient terranes is conducive to the mixing of plateau tholeiites and Type 1 felsic volcanics as is envisaged for the petrogenesis of the Type 2 rocks with flat HREE. However in the Abitibi, and likely in the younger portions of the Uchi subprovince, the Type 2 felsic rocks may not have been derived by mixing with mafic melts but rather represent the result of slab dehydration processes as traditionally invoked. Desrochers et al. (1993) model for the Abitibi advocated the development of an arc complex on top of obducted

oceanic plateau that was choking a subduction zone, in this scenario the role of tholeiitic melts is reduced to that of a crustal contaminant, with lower degrees of assimilation and consequently reduced contributions to the melts. The trace element characteristics of the Type 1 felsic rocks are consistent with them having been derived at depth and then brought rapidly to the surface with no interval for shallow level fractionation that would produce Eu anomalies.

4.5 Northern Pickle Assemblage

4.5.1 Introduction

The geology of the Northern Pickle assemblage is summarised in Table 3.2. Geophysical correlations outlined in Chapter 3 suggest it may be correlated with the North Caribou Terrane (NCT) of the Sachigo subprovince. Representative analyses of key elements are presented within the chapter (Table 4.11) with the full data set displayed in Appendix B.

4.5.2 Geochemistry

Four tholeiitic basalts were analysed from the Northern Pickle assemblage of the Pickle Lake belt. MgO contents of the tholeiites range from 5-6 wt.%, Mg#'s from 43 to 49 and SiO_2 from 49 to 50 wt.%. Fe_2O_3 contents are uniform at 13-14 wt.%. There is a weak correlation between Ni and Cr and Mg#, with both Ni and Cr increasing as Mg# decreases. Primitive mantle normalised patterns are flat with only a slight downturn at Sc and V (La/Sm_n = 0.9-1.0; Fig. 4.20a).

In addition to the tholeiitic basalts a suite of alkali basalts has been identified within the Northern Pickle assemblage. Silica contents range from 47-54 wt.%, MgO from 3-9 wt.% and Fe_2O_3 from 13-20 wt.%, these latter values are generally higher than for the tholeiites (Table 4.11). Nickel and Cr contents are variable (32-196 ppm and 7-287 ppm respectively) with the majority of samples displaying a weak correlation between Ni and Fe contents. Both TiO_2 and P_2O_5 contents are generally higher than for the tholeiitic samples (TiO_2 = 1-2 wt.% versus ~1 wt.% for the tholeiites). The basalts are characterised by moderate to pronounced LREE enrichment and fractionated HREE (Fig. 4.20b-d; La/Sm_n = 1.3-3.0; Gd/Yb_n = 1.6-2.5). They display variable Nb, Zr and Hf anomalies ranging from zero to moderately negative (Nb/Nb* = 0.9-0.4; Zr/Zr* = 0.7-1.0; Table 4.11).

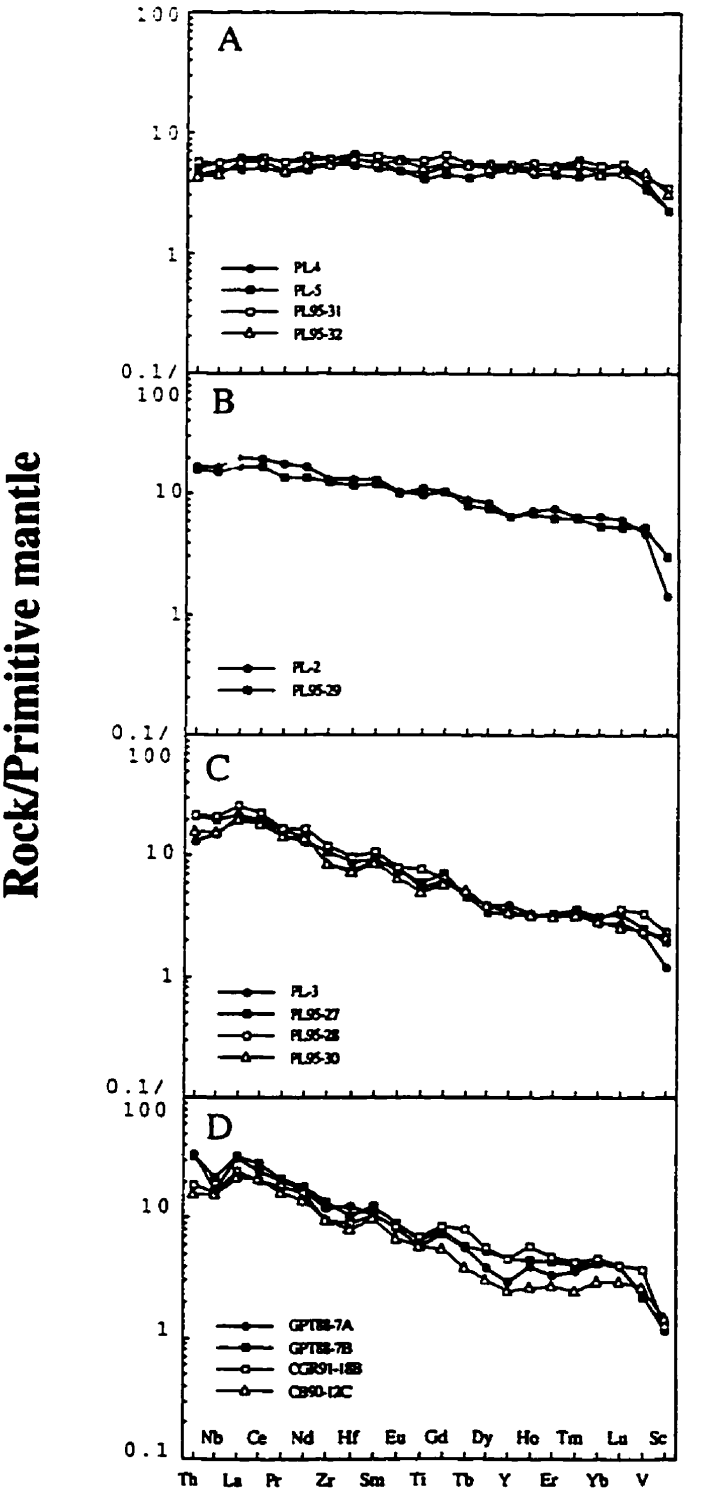

Figure 4.20. Primitive mantle normalised plots for A) tholeiites and B-D) alkali basalts of the Northern Pickle assemblage of the Pickle Lake greenstone belt.

Table 4.11. Representative analyses of selected elements for volcanic rocks of the Northern Pickle assemblage*.

	Tholeiites				Alkali basalts							Felsic
	PI.95-32	PI.4	PI.-5	PI.95-31	PI.95-29	PI.-2	PI.-3	PI.95-30	CGR91-18B	GPT88-7A	GPT88-7B	CB90-12C	PI.-1
SiO_2	49.26	49.47	49.61	48.80	48.48	48.57	50.64	50.28	47.40	51.94	50.61	50.81	61.53
TiO_2	0.99	1.04	0.99	1.49	2.02	2.03	1.98	1.86	1.50	1.36	1.50	1.35	0.78
Al_2O_3	15.31	14.88	14.95	15.58	12.71	12.67	15.43	16.22	14.03	14.46	13.50	16.03	15.78
Fe_2O_3	13.38	13.98	13.94	13.43	19.58	19.41	12.84	15.20	18.03	14.57	16.25	15.93	5.54
MgO	5.90	5.80	5.40	4.58	4.62	4.13	4.90	5.43	4.59	3.53	3.69	3.58	5.47
LOI	0.45	0.70	0.50	0.96	0.91	0.70	3.09	2.20	10.68	11.48	10.49	8.58	10.16
Mg#	49	48	46	43	34	33	46	44	36	35	31	33	0.68
Ti	6620	6809	5397	7652	14301	12589	7134	6527	8898	7520	8447	7428	2245
P	438	396	351	549	947	879	540	462	906	869	773	680	1154
Cr	379	385	360	421	198	51	206	174	69	26	42	8	429
Co	52	54	48	63	58	64	51	51	59	45	59	59	23
Ni	114	104	95	124	49	52	118	99	62	54	68	77	81
Sc	53	39	39	60	53	25	20	36	22	20	22	25	14.04
V	389	334	283	364	450	389	190	200	313	195	185	232	88.61
Nb	3.21	4.18	3.61	3.97	11.02	11.71	11.02	11.19	11.39	12.35	15.04	11.23	4.96
Zr	62	69	61	69	140	148	94	94	105	136	150	106	94.23
Hf	1.92	1.89	1.70	2.09	3.61	4.11	2.30	2.24	2.76	3.80	3.25	2.47	2.77
Th	0.37	0.44	0.37	0.49	1.34	1.43	1.11	1.34	1.57	2.88	2.78	1.32	5.39
V	23.44	24.44	23.58	25.54	29.73	29.25	17.77	15.67	20.49	13.29	20.48	11.33	11.18
La	3.94	4.05	3.39	4.35	11.45	13.71	14.57	13.67	16.95	21.80	22.27	15.05	20.70
Sm	2.47	2.54	2.31	2.88	5.31	5.78	3.98	3.88	4.56	4.69	5.47	4.32	3.15
Gd	3.31	3.12	2.68	4.02	6.16	6.27	3.65	3.48	5.08	4.30	4.67	3.20	2.63
Yb	2.23	2.57	2.32	2.70	2.72	3.18	1.35	1.41	2.25	2.06	2.04	1.41	0.95
Lu	0.34	0.41	0.35	0.42	0.39	0.45	0.21	0.19	0.30	0.29	0.30	0.22	0.14
(La/Yb)n	1.27	1.13	1.05	1.16	3.02	3.09	7.71	6.94	5.41	7.58	7.82	7.53	15.67
(La/Sm)n	1.03	1.03	0.95	0.97	1.39	1.53	2.36	2.27	2.40	3.00	2.63	2.25	4.24
(Gd/Yb)n	1.23	1.01	0.96	1.23	1.87	1.63	2.23	2.04	1.86	1.71	1.89	1.85	2.41
Al_2O_3/TiO_2	14	15	17	12	5	6	13	15	9	12	10	13	36.78
Zr/Hf	32	37	36	33	39	36	41	42	38	36	46	43	34.08
La/Nb	1.23	0.97	0.94	1.10	1.04	1.17	1.32	1.22	1.49	1.77	1.42	1.34	4.18
Th/Nb	0.11	0.11	0.10	0.12	0.12	0.12	0.10	0.12	0.14	0.23	0.18	0.12	1.09
Th/La	0.09	0.11	0.11	0.11	0.12	0.10	0.08	0.10	0.09	0.13	0.12	0.09	0.26
Zr/Y	2.63	2.83	2.59	2.71	4.69	5.08	5.31	6.03	5.14	10.21	7.35	9.36	
Nb/Nb*	0.80	1.04	1.08	0.87	0.91	0.80	0.68	0.71	0.54	0.42	0.59	0.68	0.18
Zr/Zr*	0.99	1.06	1.07	0.96	0.98	0.91	0.74	0.76	0.73	0.90	0.89	0.81	0.85
Hf/Hf*	1.12	1.05	1.07	1.05	0.91	0.91	0.65	0.66	0.69	0.91	0.70	0.68	0.90
Ti/Ti*	0.92	0.85	0.86	0.89	0.99	0.83	0.74	0.71	0.73	0.66	0.66	0.79	0.31

* Full data set presented in Appendix B

It is possible to subdivide the alkali basalts into three distinct suites based primarily on their Th-Nb-La systematics. The two samples with the highest Fe contents (PL95-29 and PL-2) display flat patterns through Th-Nb-La (Fig. 4.20b; Th/Nb = 0.12; Th/La = 0.10-0.12). A second suite is characterised by flat Th-Nb systematics (Th/Nb = 0.10-0.14) but both Th and Nb are depleted with respect to La (Fig. 4.20c). This is reflected in the high La/Nb ratios of 1.2-1.5 versus 1.0-1.2 for the first suite. The third suite, comprising samples GPT88-7A and GPT88-7B, is characterised by enriched Th and La but relative depletion in Nb, this is illustrated by the high Th/Nb ratios of 0.18-0.23 (Fig. 4.20d).

4.5.3 Discussion

Two distinct suites of mafic rocks have been identified in the Northern Pickle assemblage. The flat REE patterns and absence of pronounced HFSE anomalies in the first suite is similar to the Mg- to Fe-tholeiites found throughout both the Uchi subprovince and the Superior Province and have been interpreted as plume related plateau tholeiites (Desrochers et al., 1993; Xie et al., 1993; Hollings et al., 1996; Hollings and Wyman, 1997). The second suite is characterised by LREE enrichment generally unaccompanied by the pronounced HFSE anomalies typical of arc related rocks (e.g. Ti, Zr and Hf). The elevated Fe_2O_3 and TiO_2 contents of at least some of these rocks would appear to preclude them having fractionated from the plateau-type tholeiites given that the more evolved tholeiitic rocks, in terms of SiO_2 and Ni content, display low Fe_2O_3 contents (Table 4). The erratic HREE of a number of the samples (e.g. GPT88-7A and CB90-12A) is likely the result of alteration, given that the more alteration resistant elements (e.g., Zr and Hf) plot coherently with the least altered samples. This is supported by elevated LOI in many of the samples (up to 10 wt.%) and the presence of carbonate in thin section. The major and trace element characteristics of these basalts are similar in some respects to alkaline Ocean Island Basalts (OIB), generally accepted to be the result of asthenospheric upwelling and decompressional melting either because of elevated mantle temperatures associated with a plume or significant lithospheric thinning (Sun and McDonough, 1989; Hole et al., 1995).

The elevated Fe_2O_3 contents of a number of samples (>18 wt.%) are higher than is typical for OIB and may reflect fractionation of olivine which would result in Fe enrichment while depleting MgO, Ni and Cr; this is consistent with the data for the two Fe-enriched samples which display very low Ni and Cr (e.g., Cr ~20 ppm). OIB-like "Nb enriched basalts" have been identified in a number of modern arc environments including Mt. St.

Helens, Southwestern Japan, Northern Kamchatka and Costa Rica. (Defant et al., 1992). However, recent work by Defant et al. (1992) and Sajona et al. (1996) indicates they could be derived by melting of Nb-rich metasomatic phases such as amphibole and ilmenite in the deeper portions of a mantle wedge rather than being plume related as is generally accepted to be the case for true OIB. It has been argued that these Nb-enriched rocks have incorporated a plume (OIB) component (e.g., Reagan and Gill, 1989), however Defant et al. (1992) suggest that they are the result of mixing of hybridized slab-derived melt with the mantle, or alternatively that formation of slab-derived adakites may have left a MgO enriched residue.

OIB-like basalts have also been reported from a number of modern back-arc environments (e.g., Gill and Whelan, 1989; Stern et al., 1990; Pouclet et al., 1995), are associated with intra-arc extension in the Kamchatka arc system (Kepezhinkas, 1995), and may also be related to the subduction of a slab window and the melting of fertile mantle unmodified by subduction, as in the Late Cenozoic Antarctic Peninsular (Hole et al., 1995). Geodynamically, the source of these high Nb magmas is likely to be enriched domains, or low degree melts, in mantle unrelated to subduction processes, given that back arc opening is generally accompanied by a migration of fresh mantle material into the back arc region (Hawkins, 1994).

Wyman et al. (in prep.) have recognised OIB-like rocks in the Central Sturgeon Lake – Post Lake Cycle of the Sturgeon Lake assemblage of the Wabigoon subprovince. They describe the lower mafic rocks as being arc type, in terms of their high Zr/Y ratios (7-9) fractionated REE patterns (La/Yb_n = 4.5 - 7.5) and Nb depletions (Nb/Nb* = 0.56-0.77). Towards the middle of the sequence mafic rocks show features that are consistent with ocean island basalts (OIB's), whereas in the upper part of the mafic sequence there is an increased diversity of geochemical signatures from incompatible element depleted types to OIB's, to rocks with arc-type signatures. Wyman et al. (in prep.) suggest that this sequence is most plausibly related to a transition from arc rifting to back arc spreading, where the rifting induces low degree melts of asthenosphere represented by the OIB's. In the Sturgeon Lake belt the presence of overlying arc-like signatures in some of the uppermost mafic rocks is tentatively interpreted to indicate the continued influence of a subduction zone, or the influence of new subduction zones formed during plate reorganization.

The variable Nb-Th-La systematics of the Northern Pickle assemblage OIB-like rocks are

likely the result of some degree of interaction with subduction influenced mantle, where dehydration of subducting slabs results in pronounced Nb depletions. Consequently it is suggested that the OIB-like rocks have a source comparable to that of OIB-like basalts identified in back arc basins (e.g. Pouclet et al., 1995) and are generated when rifting results in low degree partial melting.

Access limitations in the poorly exposed Northern Pickle assemblage mean that sampling was confined to a strike-parallel transect. Consequently, the stratigraphic control is not sufficient to develop a model comparable to that of Wyman et al. (in prep.) for the Sturgeon Lake Assemblage where the geochemistry appears to record the opening of a back arc basin. The general facing direction in the Northern Pickle assemblage is interpreted to be to the south east (Stott, pers. comm., 1998). This places the more northerly plateau-type tholeiites towards the base of the sequence. The poor correlation between the Th-Nb-La anomalies and stratigraphy and the relative rarity of rocks typically associated with a volcanic arc also suggest that the assemblage may not represent a back arc basin. The observation that plateau-type rocks comparable to those found in the other older sequences of the Uchi subprovince suggests that the Northern Pickle assemblage may represent the rifting of an ocean plateau sequence comparable to that generated along the margins of the proto-continent.

4.6 Implications and geodynamic setting of the 2.9-3.0 Ga sequences

Numerical modelling demonstrates that crustal contamination is the simplest way to explain the LREE enrichment of the high SiO_2 komatiites from the North Caribou belt. This conclusion can be extended to include the LREE enriched komatiites from the Ball and Balmer assemblages of the Uchi subprovince, and consequently suggests a common geodynamic environment for the formation of these komatiites. This common environment is suggestive of a deep mantle plume erupting in part or in whole through continental lithosphere, as in the case of the SHMB of the Yilgarn craton, albeit in a submarine environment, Western Australia (Sun et al., 1989).

Clearly the exact nature of the contaminant has significant implications for the geodynamic environment. Modelling of komatiites from Opapimiskan-Markop unit used felsic pyroclastic flows found in an adjacent unit, which are also present in many of the ~3 Ga assemblages. In the Lumby Lake belt these flows have been shown by their stratigraphic relationships to be coeval with the mafic volcanics, and spanned an age range of ~100 Ma

(Hollings and Wyman, 1997, 1998) and are interpreted to be the result of interaction between mantle plumes and subduction zones. Given that felsic pyroclastic rocks are intercalated within the other 2.9-3.0 Ga sequences this genetic model may be applicable to them all.

There is substantial geochronological evidence for the contemporaneous existence of plume- and arc-related rock types within the older sequences of the USG. This includes the arc related volcanics of the 2980 Ma Agutua Arm assemblage, the presence of 2980 detrital zircons in the Keeyask assemblage of the North Caribou belt and tonalitic clasts dated at 2959 Ma in the Eyapamikama assemblage (Breaks et al., 1986; Thurston et al., 1991) and the 2990 to <2925 Ma age constraints on the plume-type North Caribou belt, and the Balmer, Rice Lake and Ball assemblages noted above. Although the U-Pb ages alone provide no indication of the proximity of arc and plume assemblages at the time of eruption, the presence of intercalated Type 1 rhyolites suggests the two tectonic processes were closely associated.

However, it must be recognised that trace element characteristics found in the felsic pyroclastic flows are common to TTG intrusions throughout the Archean, and consequently it is possible that preexisting crust formed principally of large intrusive complexes may have served as the basement on to which the komatiites were erupted. Indeed, as discussed in Section 4.2.3 there is significant geological evidence supporting the existence of older crust below those assemblages which display geochemistry indicative of contamination.

If it is assumed that the Balmer, Ball and Garner Lake assemblages of the Uchi subprovince formed part of the North Caribou Terrane, along with the North Caribou greenstone belt then there is evidence for some 75 Ma of plume activity. This age span is comparable to that documented in the Lumby Lake belt where some 100 Ma of volcanic activity is represented (Hollings et al., 1996; Hollings and Wyman, 1997). The unusual Yb-Sc-V systematics of the komatiites of the Balmer and Garner Lake assemblages and to a lesser extent the Ball assemblage, is strongly suggestive of a common mantle plume that would have existed for ~ 75 m.y., an age range comparable to that of modern plumes. For example, the > 70 m.y. Hawaiian hotspot track and the apparent association of modern hotspots such as Tristan da Cunha, Galapagos and Kerguelan/Heard Island with 80-130 Ma volcanism (Davies et al., 1989; Bercovici and Mahoney, 1994; Storey, 1995; Class et al., 1996) indicate it is possible that a single mantle plume was responsible for

the entire komatiite-tholeiite component of the Lumby Lake stratigraphy. However the absence of either the Yb-Sc-V upper mantle signature or a contamination signature in the Lumby Lake belts suggests either a distinct geodynamic environment or possibly distinct plumes.

The presence of uncontaminated geochemical signatures within the tholeiites of these older assemblages, may represent the development of mature magma conduits which served to isolate flows from contamination, as suggested by Hollings and Kerrich (1998) for the South Rim Unit of the North Caribou greenstone belt. Alternatively the generally cooler tholeiites may have been less able to assimilate material than the komatiites.

The consistent contamination signature in the Ball and Balmer assemblages, and the lack of such a signature in the Lumby Lake belt requires some explanation if the Lumby Lake belts is indeed a fragment rifted off the USG, as suggested by Davis and Jackson (1980) and Stott (1997). The contemporaneous mafic and felsic volcanism preserved in the USG and the Lumby Lake belts, as well as the occurrence of similar passive margin (rift type) sedimentary sequences in both areas, supports a common origin. One possible explanation is that the Lumby Lake belt was generated above a portion of the ascending mantle plume that was marginal to the Superior Province proto-continent and consequently free from the influence of pre-existing crust. Alternatively Wyman and Hollings (1998) have tentatively suggested that the Lumby Lake belt may have been formed as the result of subduction of a plume influenced ocean ridge (Fig. 4.21a). This would account for the longevity of the plume influence in a single greenstone belt as well as the intercalation of subduction influenced felsic flows with plume-influence ultramafic rocks. This model is consistent with the suggestion that the Lumby Lake belt developed marginal to a continental land mass. Given that the Iceland plume has been variously estimated to have a diameter of between 500 km and 2000 km (Taylor et al., 1997; Gill et

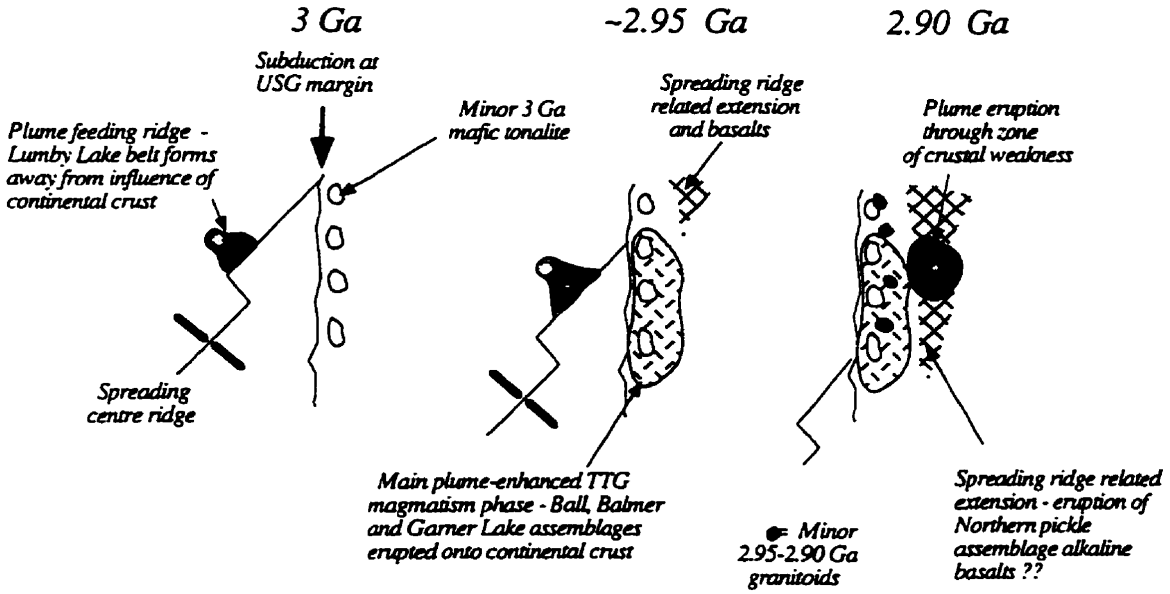

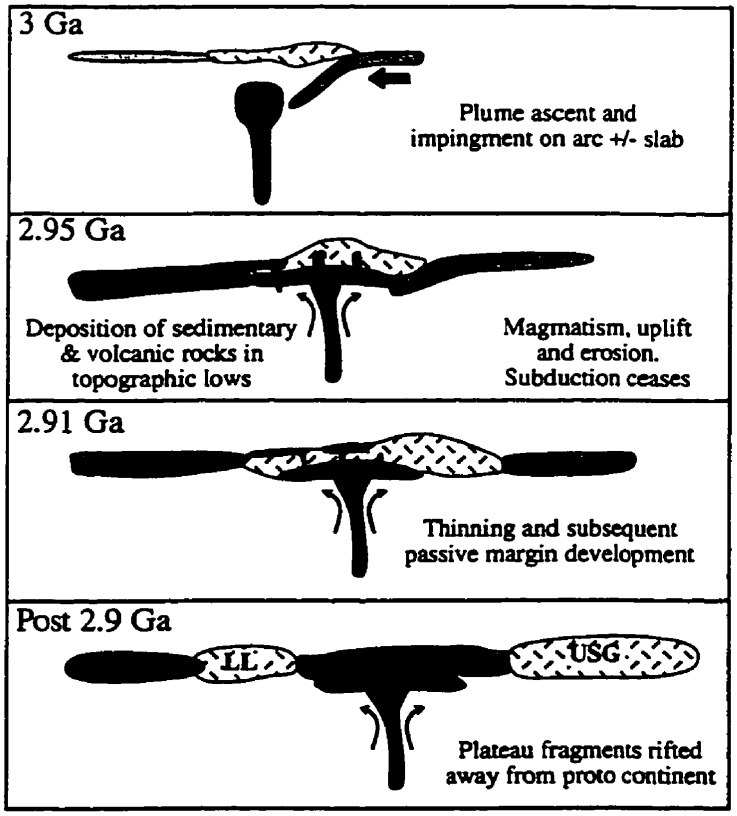

Figure 4.21. Schematic diagrams illustrating the interpreted geodynamic evolution of the proto-continental Superior Province

al., 1995) the potential for a single plume erupting through both oceanic and continental crust exists. However, the possibility that the two areas developed in isolation can not be eliminated.

The presence of pillow basalts in komatiite-tholeiite sequences throughout the older assemblages discussed in this chapter, provides convincing evidence that they were erupted in a submarine environment. The geochemical evidence on the other hand argues strongly for contamination by preexisting felsic crust. In a recent paper Puchtel et al. (1998) observed that many post 3.2 Ga volcanic sequences, including the Pilbara of Western Australia (Nelson et al., 1992), the Belingwe Belt of Zimbabwe (Bickle et al., 1994) and the Vetreny belt in the Baltic Shield (Puchtel et al., 1997) were erupted under water in basins within older continental crust. This is in contrast to most Phanerozoic continental flood basalts which have been erupted subaerially, with the possible exception of the Kerguelen oceanic plateau which nevertheless is thought to have erupted through continental crust (Operto and Charvis, 1995). Puchtel et al. (1998) further observed that plume impingement typically results in continental uplift which is not consistent with a submerged land mass. They suggest that the large volume of flooded continents that appear to have existed in the Precambrian, implies that either the volume of continental crust was large or that the depth of the ocean basins was lower than at present due either to the presence of more active Mid Ocean Ridges or because a large proportion was filled by oceanic plateau. Puchtel et al. (1998) favour the former model to explain the submarine basalts of the ~2.0 Ga Onega plateau given that extensive crustal growth is widely recognised to have occurred in the late Archean (~2.7 Ga), but acknowledge that evidence for extensive volumes of continental crust before 2.8 Ga is inconclusive. The presence of extensive submerged continental crust along the Uchi paleo-margin between 2.9 and 3.0 Ga may provide indirect evidence for extensive continental crust at that time, if the arguments above are valid. However, given that Archean oceanic plates are considered to have been smaller than modern counterparts and therefore the volume of ocean ridges was greater (Nelson and Forsythe, 1989), the possibility that submerged continents were the result of shallower oceans cannot be discounted .

The Northern Pickle assemblage would appear to record the rifting of the ocean plateau that is preserved along the length of the Uchi paleo-continental margin between 2.9 and 3.0 Ga. It is possible that this is the same event preserved at the top of the stratigraphy in Lumby Lake where both OIB-like basalts and aluminium-depleted komatiites are found (Hollings et al., 1996; Hollings and Wyman, 1997, 1998). Stratigraphic correlations

suggest that these likely rift-related rocks in Lumby Lake are <2.9 Ga; however, the evidence for multiple rifting events preserved in the sedimentary sequences of the USG and the lack of geochronological data for the Northern Pickle assemblage means that this correlation is at best a speculative one.

Collectively, the geochronologic and stratigraphic evidence from the northern Superior Province greenstone belts, and similarly-aged Lumby Lake belt, provide strong evidence for both a spatial and temporal association of mantle plumes and subduction zones during generation of the Uchi-Sachigo-Goudalie proto-continent nucleus of the Superior Province. It is therefore noteworthy that recent modelling suggests plume-ridge interactions adjacent to Archean subduction zones may have cause increased TTG magmatism and the development of long-term unsubductable arc lithosphere (Abbott, 1996). Further, Tarney and Jones (1994) note that the incompatible element systematics of Archean TTG are more consistent with melting of plume-type crust than MORB-type crust. Saunders et al. (1996) have argued that collision of a plateau with an active subduction zone will promote a reversal in the polarity of subduction, or a backstepping of the subduction zone, resulting in development of an arc complex on top of the plateau sequences. Arc magmatism along the margins of a plateau has also been advocated by Stein and Hofmann (1994) for the Arabian-Nubian shield where it is believed to have resulted in rapid crustal growth over a ~150 m.y. interval. The geological evidence for the contemporaneous eruption of plume- and arc-related volcanic rocks argues strongly for the interaction between plume-plateau and island arcs at the margins of the USG over a 100 m.y. interval. However, unlike many models applied to specific Archean or younger terranes, it is proposed that an active plume (or plumes) is required to account for the coeval eruption of komatiitic and TTG-like volcanic flows.

CHAPTER 5

EPISODIC CONTINENTAL GROWTH AT 2.9-2.8 Ga ALONG THE UCHI PALEO-CONTINENTAL MARGIN

5.1 Introduction

This chapter presents geochemical data for three assemblages of the Uchi subprovince: the Pickle Crow assemblage, found only in the Pickle Lake greenstone belt; the Woman assemblage, present throughout the study area, and the Meen assemblage, which to date has only been identified in the Meen-Dempster greenstone belt (Fig. 3.2). These assemblages represent the earliest phases of crustal growth along the margins of the newly formed proto-continental Superior Province (Chapter 4). Establishing how these assemblages developed and whether or not they formed autochthonously or allochthonously to the NCT, is of importance for models of the growth of the Superior Province. The geology of the three assemblages is discussed in Chapter 3 and summarised in Table 3.2. Full results for all samples analysed are presented in Appendix C, and representative analyses are given in this chapter.

5.2 The Pickle Crow assemblage

5.2.1 Introduction

The 2.86 Ga Pickle Crow assemblage is only found within the Pickle Lake greenstone belt at the eastern extent of the study area (Fig. 3.2). The geology of the assemblage is discussed in Chapter 3; it can be summarised as comprising massive and pillowed basalt flows overlain by felsic tuffs and ashflows, in turn overlain by a second series of mafic flows. The assemblage is host to the three gold deposits known within the Pickle Lake greenstone belt; one consequence of this is that the area has experienced extensive hydrothermal fluid activity associated with the formation of the gold deposits. Sage and Breaks (1982) identify an area of intensive carbonate alteration around the gold deposits. Field and petrographic observations confirm this. Notwithstanding this hydrothermal alteration it is surprising that only a small number of samples display trace element

patterns that can be seen to be significantly affected by alteration (Fig. 5.1). Throughout this study interpretation of geochemical data focusses on the relatively alteration insensitive elements (e.g. Ti, Al, HFSE and REE), however in Fig. 5.1 it can be seen that even these elements have been disturbed. Individual occurrences of alteration will be addressed throughout this chapter.

5.2.2 Ultramafic volcanic rocks

A single ultramafic sample has been identified from the eastern half of the Pickle Crow assemblage (KAF89-34B; Fig. 3.3). Prior to this study no ultramafic rocks had been recognised within the assemblage (Stott, 1996). In hand specimen KAF89-34B is a fine grained to aphanitic rock. Petrographic analysis shows it to be comprised of small blades of pyroxene with secondary intergrowths of amphibole, suggesting that it is an ultramafic flow rather than a cumulate. The MgO content of 23 wt.% and elevated Ni and Cr contents (respectively 1400 and 2660 ppm) are typical of ultramafic flows. The Al_2O_3/TiO_2 ratio of 7 is significantly lower than the chondritic value of 22 and comparable to values for Al-depleted komatiites (ADK) such as those of the Lumby Lake belt (Al_2O_3/TiO_2 = ~5; Hollings et al., 1996). An Fe_2O_3 content of 19 wt.% is higher than is typical for AUK (11-14 wt.%) but close to values for Lumby Lake ADK specifically, and ADK in general (~19 wt.%; Chapter 3; Hollings et al., 1996; Xie et al., 1993; Fan and Kerrich, 1997). The komatiite is characterised by flat LREE in conjunction with fractionated HREE, and Zr/Y greater than the primitive mantle value of 2.4 (La/Sm_n = 1.0; Gd/Yb_n = 1.7; Zr/Y = 4.3; Fig. 5.2).

The depleted HREE (Fig. 5.2) may be the result of alteration induced mobility especially given the high LOI value of ~10 wt.%. However, the smoothly coherent LREE and HFSE are consistent with a primary signature. This is supported by the fractionated HREE observed in some ADK (e.g. Lumby Lake, Gd/Yb_n = 2-3; Hollings et al., 1996) and suggests that this flow is petrogenetically similar to ADK. However, the incompatible element concentrations are lower than is typical for ADK (Zr = 39 ppm versus 80 ppm for Lumby Lake ADK). The Pickle Crow assemblage komatiite also lacks the pronounced LREE enrichment commonly observed in ADK (Lumby Lake ADK, La/Sm_n = 1.8-2.4). The HREE fractionation and minor negative Zr and Hf anomalies are consistent with melt segregation at depths greater than 400 km within the majorite garnet stability field (Xie et al., 1994).

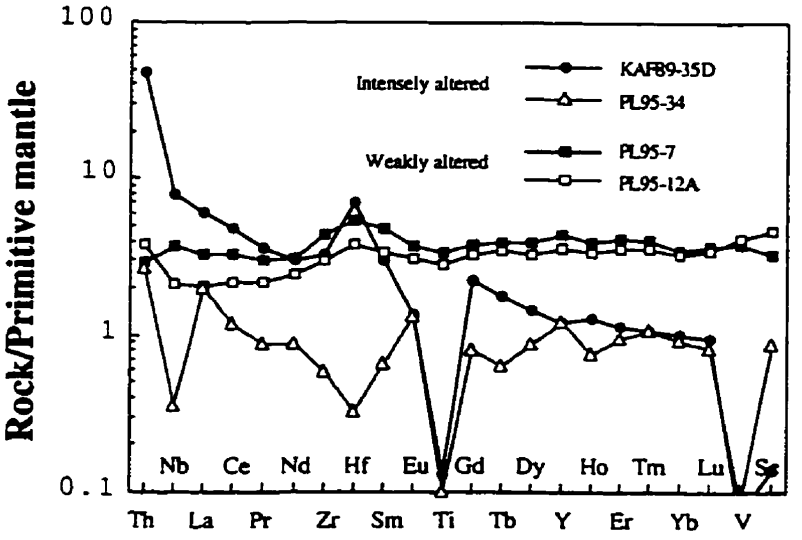

Figure 5.1. Primitive mantle normalised plots for altered mafic to felsic volcanic rocks of the Pickle Crow assemblage, Pickle Lake greenstone belt. Samples PL95-34 and KAF89-35D display extreme REE mobilty, whereas PL95-12A and PL95-7 illustrate only minor LREE loss.

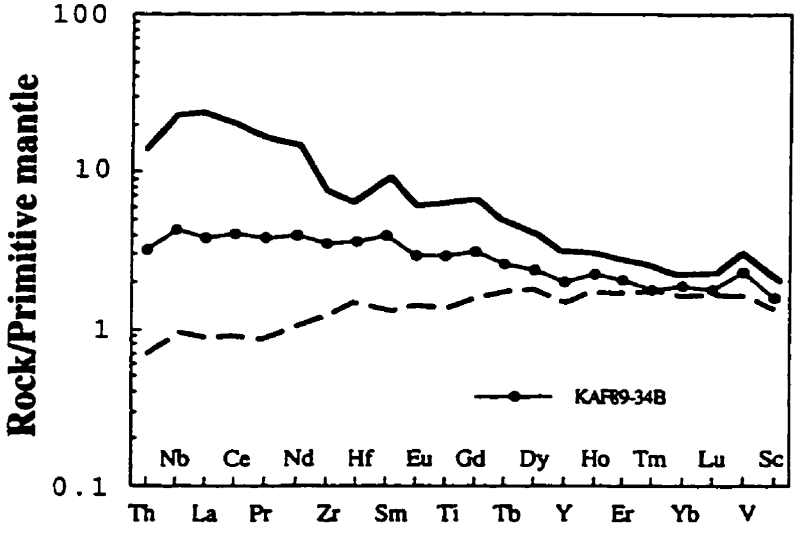

Figure 5.2. Primitive mantle normalised plots for the single komatiitic rock of the Pickle Crow assemblage, Pickle Lake greenstone belt. Dashed line is a representative unaltered Al-undepleted komatiite from Pyke Hill (Fan and Kerrich, 1997). Solid line is ADK from Lumby Lake (Hollings and Wyman, 1998).

Two distinct types of ADK have been recognised in the literature. One has smoothly fractionated REE patterns such as Boston Township, Abitibi greenstone belt, Barberton, S. Africa and the Yilgarn block of Australia (Jahn et al., 1980, 1982; Gruau et al., 1990; Jochum et al., 1991; Xie et al., 1993). The second type have convex up REE patterns such as those of Tisdale and Newton Townships, Canada (Cattell and Arndt, 1987; Fan and Kerrich, 1997). Cattell and Arndt (1987) advocated that the HREE depletion was the result of the presence of garnet during melting and the depleted LREE implied a depleted mantle source. Recently, Fan and Kerrich (1997) have proposed that the convex up REE patterns could reflect either mixing of two distinct komatiitic liquids, one with the characteristics of ADK and one with those of AUK, or alternatively contamination of the magmas while the melt passed through oceanic lithosphere. With only one ultramafic sample from the Pickle Crow assemblage it is difficult to draw any firm conclusions as to the cause of the somewhat atypical LREE and HFSE systematics of this ADK-like ultramafic flow. However, both models advocated by Fan and Kerrich (1997), to account for similar rocks in the Abitibi, are consistent with the data of this study.

5.2.3 Tholeiitic volcanic rocks

A range of mafic rock types can be identified within the Pickle Crow assemblage. The majority of samples are basalts and basaltic andesites with rare andesitic rocks (SiO_2 = 46-54 wt.%; Mg# = 56-65). Two samples fall outside this range, with SiO_2 contents of 60 and 61 wt.%. Magnesium contents range from 1-12 wt.% and generally decrease as SiO_2 content increases. Fe_2O_3 contents range from 7-17 wt.% (Table 5.1). Compatible element abundances are generally high (Ni = 35-210 ppm; Cr = 15-570 ppm, with the majority >200 ppm).

Primitive mantle normalised patterns of the tholeiites vary from flat to moderately LREE depleted, with the majority of samples clustering around an La/Sm_n value of 1 (Fig. 5.3a; La/Sm_n = 0.6-1.2). The HREE are flat to moderately fractionated with Gd/Yb_n ranging from 0.9-1.5, but the majority cluster around unity. HFSE anomalies are typically minor (e.g. Nb/Nb* = 0.7-1.3). Low LOI values of 0.5 to 3.3 wt.% in the more LREE depleted samples, in conjunction with petrographic studies of thin sections that confirm the presence of primary igneous textures, suggest that these samples have not been significantly affected by alteration. Accordingly the LREE depletion is interpreted as a primary feature.

Table 5.1. Representative analyses of selected elements for tholeiitic volcanic rocks from the Pickle Crow assemblage*.

	Tholeiites					Evolved tholeiite	Atypical tholeiites				Altered tholeiites		
	PI.95-23	KAF89-35B	PI.95-14	KAF89-33C	PI.95-16	PI.95-22	PI.95-33	KAF89-34A	PI.95-39	PI.95-41	PI.95-7	PI.95-12A	PI.95-4
SiO_2	49.29	51.01	47.72	50.88	48.45	52.21	59.15	50.31	49.03	47.14	48.15	47.35	61.20
TiO_2	0.61	1.09	0.99	1.11	0.92	1.02	1.71	0.46	1.22	1.72	0.89	0.62	1.01
Al_2O_3	14.92	14.16	15.84	16.79	16.25	15.55	19.45	11.91	14.25	15.13	15.33	15.50	19.12
Fe_2O_3	12.19	12.62	14.20	11.36	13.49	11.97	7.17	13.01	13.65	16.26	14.72	11.84	5.82
MgO	10.51	8.58	8.18	6.20	7.12	7.95	1.79	12.45	8.75	6.31	9.22	6.33	2.34
LOI	3.09	0.60	1.11	0.40	0.65	4.60	1.63	0.86	0.40	1.06	1.42	3.25	2.86
Mg#	65	60	56	55	54	59	30	71	59	46	58	54	47
Ti	3845	6380	5263	7592	5620	6187	10162	2641	7359	10928	4489	3729	6251
Cr	565	419	343	314	434	397	243	385	304	221	253	481	277
Ni	209	97	167	115	131	143	118	89	107	47	102	147	1--
Nb	1.48	2.90	2.44	3.84	1.93	7.29	5.75	1.03	4.64	7.81	2.66	1.51	2.95
Zr	32	58	48	65	53	129	107	23	79	115	50	34	59
Hf	1.01	1.64	1.61	1.84	1.81	3.61	2.64	0.70	2.17	3.29	1.67	1.18	1.75
Th	0.18	0.33	0.26	0.55	0.36	0.98	0.70	0.13	0.55	1.10	0.25	0.12	0.70
La	1.50	2.94	2.60	4.04	3.11	7.54	7.06	1.38	5.10	8.51	2.29	1.41	3.71
Sm	1.33	2.63	1.97	2.38	2.11	4.31	4.15	1.11	3.18	4.84	2.13	1.49	1.95
Gd	1.95	3.45	2.83	3.03	2.92	5.47	5.38	1.49	4.09	5.80	2.31	1.97	1.97
Yb	1.80	2.56	2.05	2.18	2.30	4.14	3.03	1.30	2.44	3.19	1.73	1.63	0.93
Lu	0.26	0.35	0.31	0.31	0.34	0.63	0.33	0.19	0.40	0.46	0.27	0.26	0.13
(La/Yb)n	0.59	0.82	0.91	1.33	0.97	1.30	1.67	0.76	1.50	1.91	0.95	0.62	2.88
(La/Sm)n	0.73	0.72	0.85	1.10	0.95	1.13	1.10	0.80	1.04	1.14	0.69	0.61	1.24
(Gd/Yb)n	0.89	1.12	1.14	1.15	1.05	1.09	1.47	0.95	1.38	1.50	1.11	1.00	1.75
Al_2O_3/TiO_2	23	13	18	15	17	15	11	27	12	8	20	25	18
Zr/Hf	32	35	30	35	29	36	40	32	37	35	30	29	30
La/Nb	1.01	1.01	1.06	1.05	1.61	1.03	1.23	1.34	1.10	1.09	0.86	0.93	1.26
Th/Nb	0.12	0.11	0.11	0.14	0.19	0.13	0.12	0.13	0.12	0.14	0.10	0.21	0.24
Th/La	0.12	0.11	0.10	0.14	0.12	0.13	0.10	0.09	0.11	0.13	0.11	0.23	0.19
Zr/Y	1.97	2.67	2.57	3.40	2.65	3.56	4.30	1.95	3.14	3.36	2.47	2.02	7.65
Nb/Nb*	1.04	1.06	1.03	0.95	0.61	0.95	0.82	0.75	0.88	0.87	1.10	1.10	0.77
Zr/Zr*	1.02	0.92	0.98	1.05	1.02	1.14	0.96	0.86	0.98	0.90	1.16	1.05	1.01
Hf/Hf*	1.16	0.95	1.19	1.08	1.28	1.15	0.86	0.96	0.97	0.93	1.41	1.13	1.21
Ti/Ti*	0.94	0.84	0.88	1.12	0.89	0.90	0.85	0.81	0.81	0.82	0.80	0.86	1.26

* Full data set in Appendix C

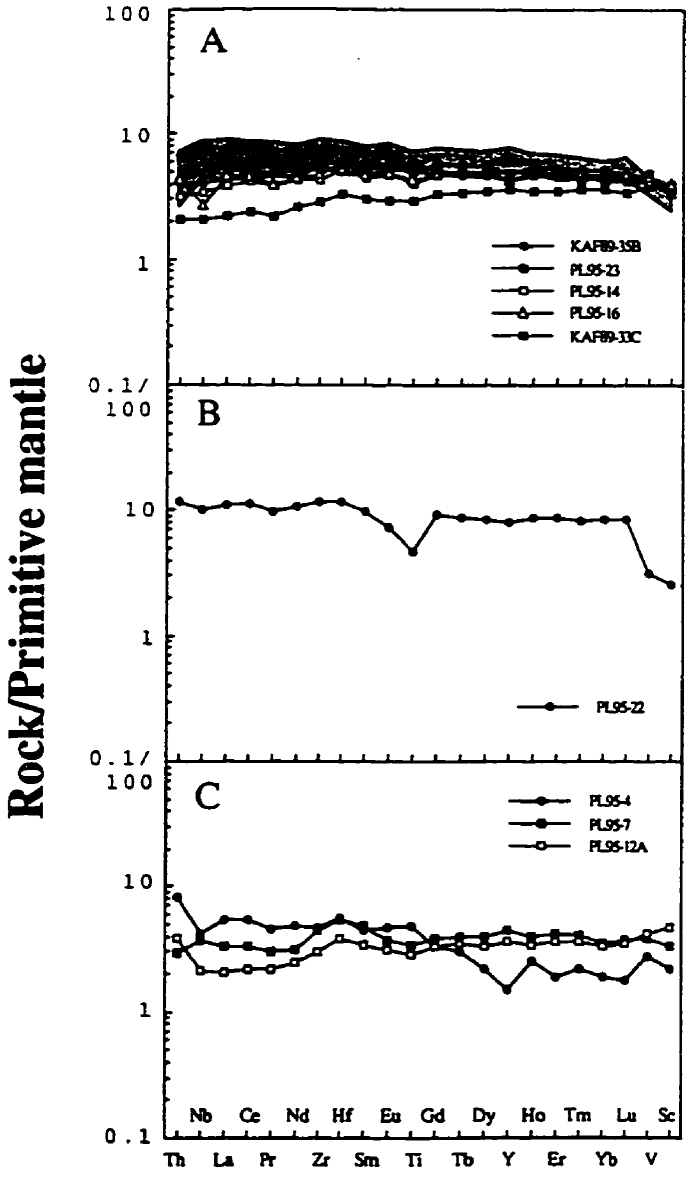

Figure 5.3. Representative primitive mantle normalised plots for A) tholeiites, B) evolved tholeiite, and C) altered tholeiites of the Pickle Crow assemblage of the Pickle Lake greenstone belt. Shaded field is data for basalts from the Ontong Java ocean plateau (Mahoney et al., 1993).

A single tholeiite is characterised by a flat trace element pattern at ~10 times primitive mantle abundances, which is significantly higher than for the main population of the tholeiites (Fig. 5.3b). An SiO_2 content of 52 wt.% and MgO of 8 wt.%, in conjunction with Ni and Cr values of 143 ppm and 400 ppm respectively, are comparable to the majority of the tholeiitic suite. This sample likely represents the product of closed system fractionation of the same primitive melts that produced the flat patterned tholeiites.

In addition three samples display erratic trace element patterns interpreted to be the result of alteration (Fig. 5.3c). The convex up LREE systematics of basalts PL95-7 and PL95-12A are interpreted to be the result of minor LREE loss. The erratic HREE of PL95-4 is not typical of tholeiites examined in this study and is also interpreted as an alteration feature.

5.2.4 Intermediate volcanic rocks

Calc alkaline basalts to andesites of the Pickle Crow assemblage are characterised by SiO_2 contents of 50-56 wt.%, MgO of 3-10 wt.% and Fe of 9-16 wt.%. Chromium and Ni contents display a bimodal distribution ranging from 8-70 and 110-180 ppm Ni, and 5-50 and 540-730 ppm Cr respectively. These subsets display distinct trends on plots of major and trace elements versus MgO, suggesting that they have distinct shallow level fractionation histories (Fig. 5.4; Table 5.2).

Based on the REE and HFSE abundances it is possible to divide the calc alkaline rocks into two distinct suites. The majority of samples are characterised by moderate LREE enrichment, negative Nb, variable Ti and weakly positive Zr and Hf anomalies (Fig. 5.5a, b; La/Sm_n = 2.2-3.3; Nb/Nb* = 0.2-0.4; Zr/Zr* = 0.9-1.3). Two samples display more pronounced LREE enrichment in conjunction with larger negative Nb and strongly negative Zr and Hf anomalies (Fig. 5.5c; La/Sm_n = 4.3; Nb/Nb* = 0.1; Zr/Zr* = 0.5). Thorium is strongly enriched over La (Th/La = 0.22-0.28), in contrast to the tholeiitic basalts of the Pickle Crow assemblage where Th/La = ~0.1 .

5.2.5 Felsic volcanic rocks

Two examples of high silica rock types were collected in the Pickle Crow assemblage. As discussed in Section 5.2.1, these two samples appear to have undergone moderate to extensive alteration. The nature of this alteration will be addressed here. Sample PL95-34 shows signs of having undergone silicification, whereas KAF89-35D has been identified

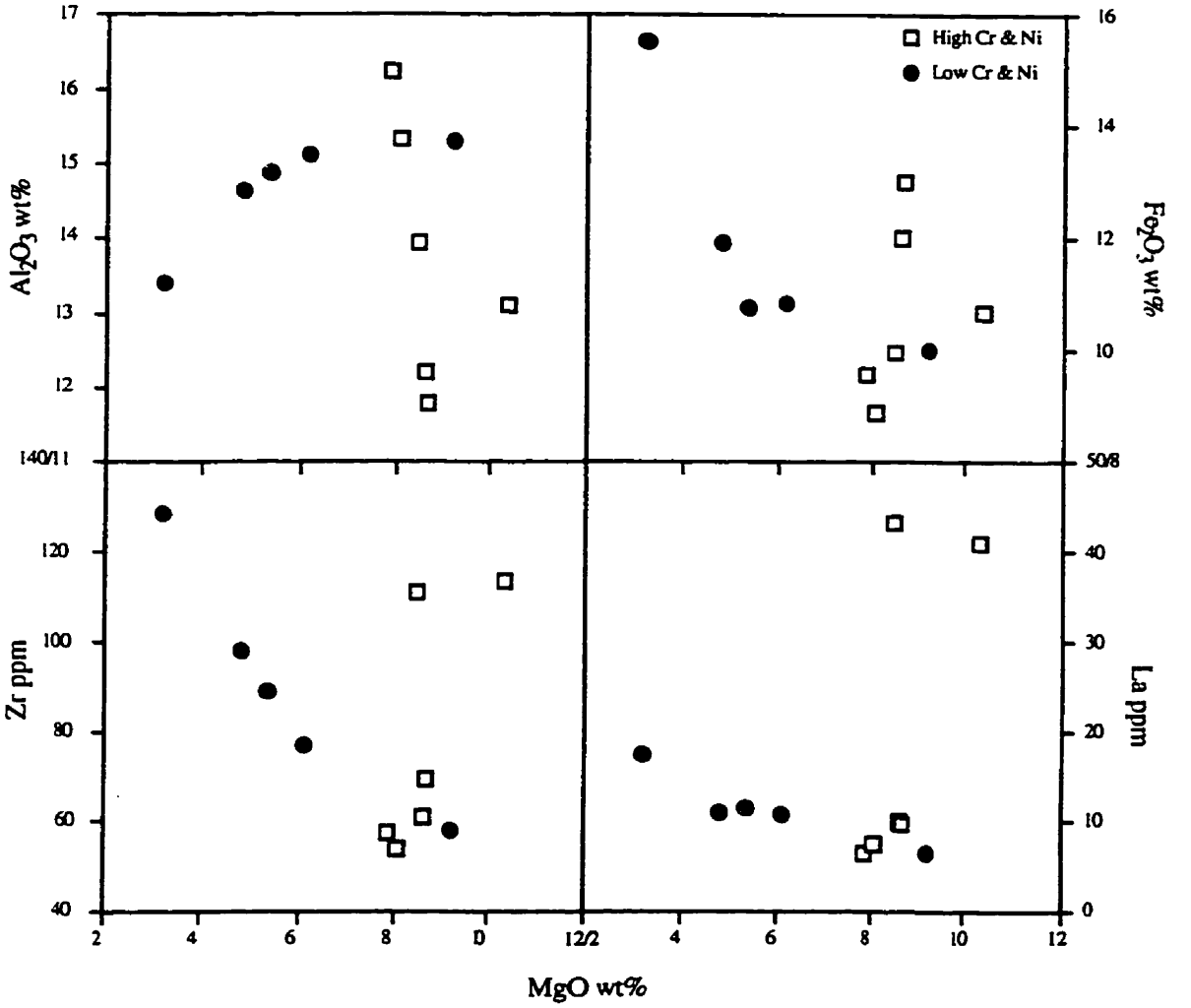

Figure 5.4. Major and trace element variation diagrams for calc alkaline volcanic rocks from the Pickle Crow assemblage of the Pickle Lake greenstone belt. Open symbols have high Ni and Cr contents, closed symbols have low Ni and Cr contents.

Table 5.2. Representative analyses of selected elements for calc alkaline mafic to felsic rocks from the Pickle Crow assemblage *.

	Calc alkaline - mafic to intermediate											Felsic	
	PL95-9	KAF87-18B	KAF89-35C	PL-12	KAF87-21C	PL95-10	PL-11	KAF87-21B	KAF87-23A	KAF89-35A	KAF87-21A	KAF89-35D	PL95-34
SiO_2	50.83	53.10	53.44	52.45	52.69	53.19	53.21	54.89	55.81	56.06	55.85	78.34	64.20
TiO_2	0.85	0.56	0.52	0.85	0.58	0.72	0.73	0.65	0.64	0.90	1.16	0.04	0.03
Al_2O_3	13.10	15.29	15.33	13.95	16.23	12.21	11.80	15.13	14.88	14.63	13.40	13.89	0.35
Fe_2O_3	10.71	10.03	8.90	9.96	9.59	12.01	13.02	10.84	10.77	11.95	15.55	0.75	31.11
MgO	10.38	9.19	8.07	8.45	7.84	8.62	8.64	6.13	5.36	4.79	3.22	0.20	2.53
LOI	1.83	1.47	1.99	1.06	0.65	0.60	1.21	0.30	0.45	1.01	0.50	1.11	0.00
Mg#	68	67	67	65	64	61	59	55	52	47	31	38	15
Ti	5184	6661	3037	4981	3349	4690	4079	4009	3317	6126	6640	174	136
Cr	711	24	544	554	583	716	733	47	38	13	5	8	312
Ni	176	54	109	116	121	147	135	74	59	39	8	2	8
Nb	7.52	3.38	2.66	7.86	2.58	4.55	4.08	3.84	4.08	4.42	5.99	5.71	0.25
Zr	114	58	54	111	58	61	70	77	89	98	129	37	6
Hf	3.23	1.50	1.32	2.89	1.75	1.68	1.77	1.93	2.25	2.84	3.63	2.19	0.10
Th	8.90	1.89	1.77	9.69	1.90	2.67	2.60	2.96	3.03	2.93	4.01	4.10	0.23
La	41.20	6.64	7.55	43.46	6.66	10.05	9.90	10.96	11.64	11.24	17.52	4.26	1.37
Sm	6.18	1.92	1.69	6.48	1.82	2.50	2.66	2.30	2.29	2.79	3.53	1.37	0.29
Gd	5.34	2.14	1.90	5.13	2.31	3.17	3.10	2.59	2.83	3.45	4.26	1.34	0.48
Yb	1.55	1.44	1.31	1.76	1.73	1.60	1.72	1.75	1.67	2.10	3.35	0.50	0.46
Lu	0.22	0.21	0.18	0.25	0.23	0.25	0.25	0.25	0.22	0.31	0.45	0.07	0.06
(La/Yb)n	19.01	3.30	4.15	17.72	2.76	4.52	4.12	4.50	5.01	3.84	3.75	6.16	2.12
(La/Sm)n	4.31	2.24	2.88	4.33	2.36	2.59	2.40	3.08	3.28	2.61	3.21	2.01	3.04
(Gd/Yb)n	2.84	1.23	1.20	2.41	1.10	1.64	1.49	1.23	1.40	1.36	1.05	2.24	0.87
AL_2O_3/TiO_2	15	14	29	17	28	16	17	22	26	14	12	474	15
Zr/Hf	35	39	41	38	33	37	39	40	40	35	35	17	65
La/Nb	5.48	1.96	2.84	5.53	2.59	2.21	2.43	2.85	2.85	2.55	2.92	0.75	5.50
Th/Nb	1.18	0.56	0.66	1.23	0.74	0.59	0.64	0.77	0.74	0.66	0.67	0.72	0.91
Th/La	0.22	0.28	0.23	0.22	0.29	0.27	0.26	0.27	0.26	0.26	0.23	0.96	0.17
Zr/Y	6.51	4.38	4.86	6.54	4.92	3.34	4.25	4.54	5.06	4.85	5.56	6.81	1.18
Nb/Nb*	0.14	0.43	0.27	0.14	0.28	0.34	0.31	0.27	0.27	0.31	0.24	1.00	0.10
Zr/Zr*	0.53	1.05	1.08	0.49	1.12	0.85	0.94	1.12	1.26	1.20	1.18	1.10	0.76
Hf/Hf*	0.55	0.99	0.95	0.47	1.23	0.84	0.87	1.01	1.15	1.26	1.20	2.13	0.43
Ti/Ti*	0.36	1.30	0.67	0.34	0.65	0.66	0.56	0.65	0.52	0.78	0.68	0.05	0.14

* Complete data set in Appendix C

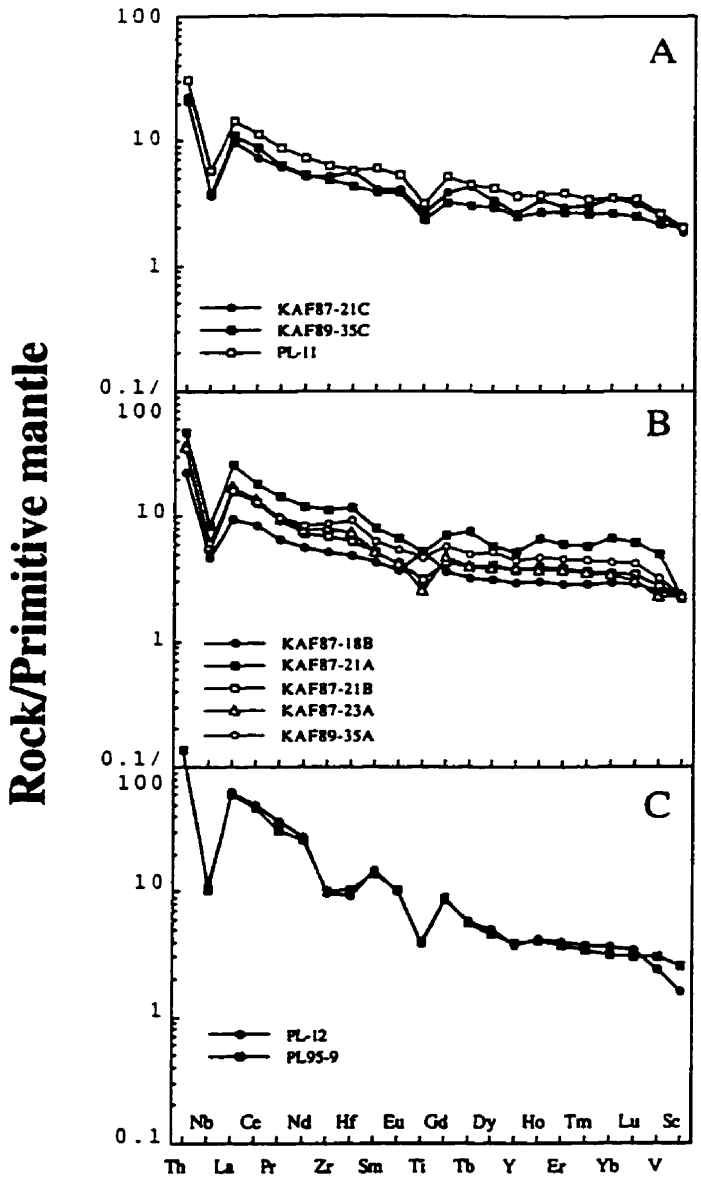

Figure 5.5. Representative primitive mantle normalised plots for calc alkaline volcanic rocks from the Pickle Crow assemblage of the Pickle Lake greenstone belt. A) high Ni and Cr, B) low Ni and Cr and C) high Ni and Cr.

as a quartz-feldspar porphyry dike, indicating the SiO_2 content is likely primary. These samples display extremely erratic trace element patterns, with significant depletions of the compatible elements (Co and Ni less than 10 ppm; Table 5.2). In addition, mobility of Nb, Zr and Hf as well as REE is reflected in erratic Th/Nb, Th/La, Zr(Hf)/MREE, and fractionated Zr/Hf ratios (Zr/Hf = 17 and 65 respectively, versus 36 for primitive mantle; Table 5.2; Fig. 5.6). Petrographic examination of these samples shows them to have undergone extensive carbonate alteration. The extensive alteration of these samples and consequent REE mobility makes them unsuitable for geochemical studies and hence determining the geodynamic setting in which they were erupted.

5.2.6 Discussion

Tholeiites with flat trace element patterns comparable to those of the Pickle Crow assemblage have been recognised in a number of Archean greenstone belts, where they are interpreted as the eruptive products of a mantle plume in an oceanic plateau or hotspot setting (Thurston, 1990; Desrochers et al., 1993; Kent et al., 1996; Kerrich et al., 1998). Similarities between the flat REE patterns of the tholeiites of the Pickle Crow assemblage and those reported by Mahoney et al. (1993) for the Ontong Java plateau (OJP) support this contention (Fig. 5.3a).

Unlike the tholeiites of the older assemblages discussed in Chapter 4 the Pickle Crow assemblage tholeiites extend to more LREE depleted values than the OJP (e.g., Figs. 4.12 and 5.3a). Those samples with slightly depleted LREE may reflect the influence of a relatively more depleted mantle source similar to, but less depleted than, N-MORB. The intercalation of these rocks with the plateau type tholeiites may be the result of a heterogeneous source region. Kerr et al. (1996) have suggested that the presence of mafic and ultramafic rocks with variably depleted REE on Gorgona island may reflect the heterogeneous nature of the mantle plume. Alternatively, dynamic melting, as suggested by Arndt et al. (1997) for the Gorgona plume and Elliot et al. (1991) for the Iceland plume, could also account for the range of LREE depletion. Arndt et al. (1997) propose that low degree partial melts would separate from the source region as the plume crossed the mantle peridotite solidus. These high pressure melts would be characterised by high MgO and incompatible element abundances, perhaps somewhat similar to the single Pickle Crow assemblage ultramafic sample, and would consequently leave the residue depleted in incompatible elements. Melting of this residue would produce progressively more depleted magmas. Elliot et al. (1991) showed that dynamic melting in the Iceland plume would produce Fe-rich magmas towards the base of the plume. These melts would

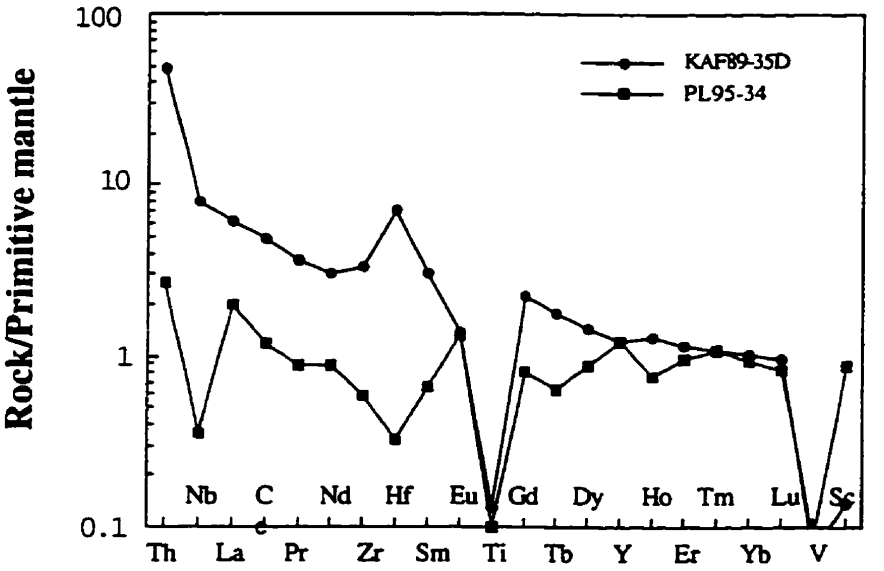

Figure 5.6. Primitive mantle normalised plots for felsic volcanic rocks of the Pickle Crow assemblage of the Pickle Lake greenstone belt. Both samples display erratic REE patterns resulting from alteration.

have higher incompatible element abundances than MgO-rich/Fe-poor magmas derived from the top of the plume, which would tend to be depleted in the incompatible elements. This is consistent with data from this study, whereby the most LREE depleted tholeiite displays the highest MgO content (Fig. 5.3; Table 5.1).

A small subset of samples within the tholeiitic suite display minor variations that may be of petrogenetic significance. Basalt KAF89-34A is characterised by a positive up turn at V and Sc on a primitive mantle normalised diagram, reflected in elevated Sc/Yb and V/Yb ratios (55 and 215 respectively; Fig 5.7a). This geochemical feature is comparable to values for the Ball assemblage komatiites (Sc/Yb = 43-56 and V/Yb = 203-255; Table 4.4; Figs. 4.5 and 4.7). Given that this sample has the highest MgO content (12.5 wt.%) of any of the tholeiitic suite it may have been derived in a similar manner to the komatiites and komatiitic basalts of the Balmer and Ball assemblages, which are interpreted as the result of melting of a depleted source region in a subduction zone setting (Chapter 4).

Three samples display weak LREE enrichment with minor variable Nb anomalies (PL95-33, PL95-11 and PL95-39) which are comparable to the trace element signature of the single komatiitic sample (Fig. 5.7b). A common magma source is supported by the elevated Fe_2O_3 content of PL95-11 which is comparable to that of the komatiite. However, other tholeiites, which lack an LREE enriched signature, display higher Fe_2O_3 contents and preclude the use of this feature alone as a diagnostic feature.

Depletion of HFSE (Nb, Ta, Zr, Hf) relative to LILE and LREE is a dominant characteristic that distinguishes subduction related rocks from MORB and OIB (Hawkesworth et al., 1993; Pearce and Peate, 1995 and references therein). The HFSE depletions of the calc alkaline rocks of the Pickle Crow assemblage are consistent with a supra-subduction zone environment.

On Figures 5.4 and 5.5 it can be seen that there are three distinct subtypes of calc alkaline rocks. The first suite has high Ni and Cr and moderately enriched REE, while the second has comparable levels of REE enrichment but low Ni and Cr abundances. The third suite has high Ni and Cr in conjunction with strongly enriched LREE. The distinct trends displayed by the high and low Ni samples on Figure 5.4 are likely the result of distinct fractionation trends, whereas the fact that the two trends appear to merge at higher MgO contents suggests a common source. It is suggested that these distinct trends are the result of variations in the nature of the fractionation process. Open system fractionation,

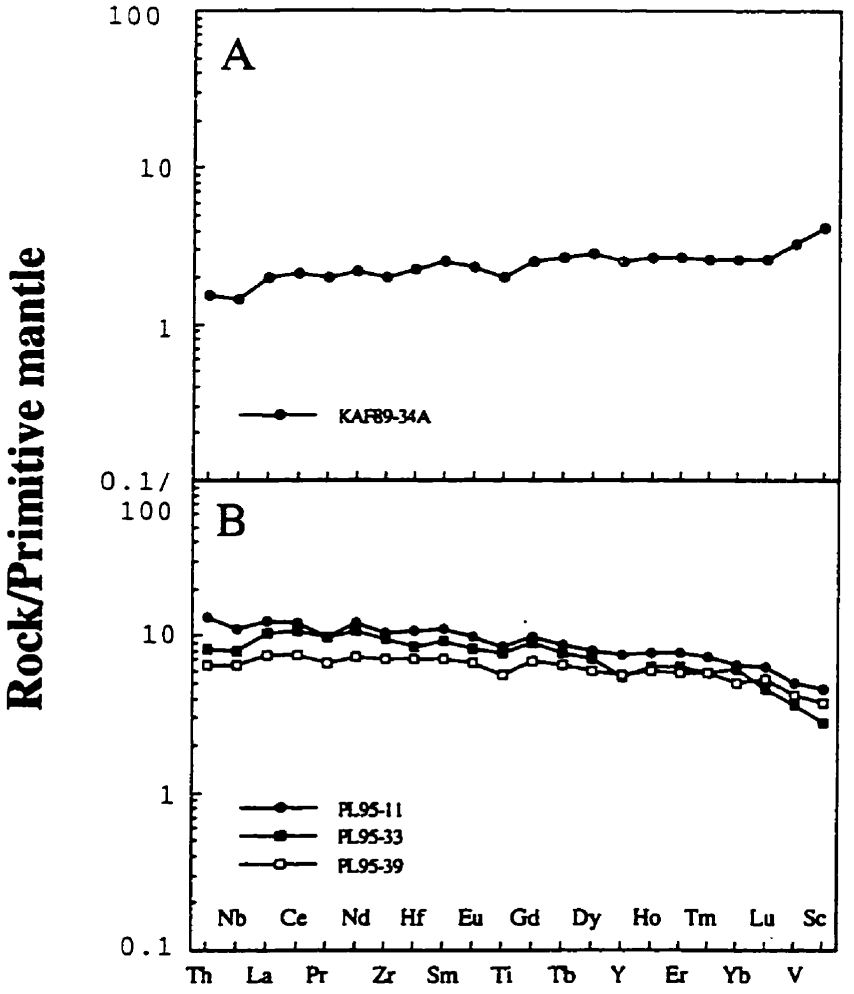

Figure 5.7. Primitive mantle normalised plots for atypical mafic volcanic rocks of the Pickle Crow assemblage of the Pickle Lake greenstone belt.

where the magma chamber is periodically replenished by more primitive melts which mix with the fractionated liquids, will tend to buffer the more compatible elements (MgO, Ni, Cr) while enriching the incompatible elements (O'Hara, 1977; Taylor and Nesbitt, 1995). This process likely accounts for the similar Ni and Cr abundances but variable LREE of the high Ni suites. In contrast, closed system fractionation will deplete the compatible elements without greatly affecting the incompatible elements, and would account for the fact that the low Ni suite has LREE abundances comparable to the less LREE enriched members of the high Ni suite. In summary, the fact that trends for both suites merge at higher MgO values suggests a similar mantle source. The magmas must either have undergone shallow fractionation in distinct magma chambers, or the nature of the fractionation varied between open-system and closed system with time.

5.2.7 Geodynamic setting

Stott and Corfu (1991) recognised the presence of two tholeiitic sequences, separated by a series of dacitic volcanic flows in the Pickle Crow assemblage. The geochemical analyses reported here demonstrate the presence of both arc related calc alkaline volcanic rocks and tholeiitic rocks with a geochemical signature comparable to that of the Ontong Java Plateau (Mahoney et al., 1993).

There is little evidence to establish the magmatic relationship between the two distinctive volcanic suites. It is possible that they represent the coeval eruption of arc and plateau rock types as advocated for the 2.9-3.0 Ga assemblages discussed in Chapter 4. The geology of the Pickle Crow assemblage is somewhat different from that of the older assemblages in that it does not contain significant volumes of ultramafic rocks. In addition the intermediate to felsic rocks are volumetrically significant, comprising a 2.5 km unit of dacite and rhyodacite (Stott, 1996). This is in contrast to the 2.9-3.0 Ga sequences, where the felsic to intermediate volcanic rocks comprise thin flows intercalated throughout the predominantly mafic stratigraphy. The presence of this extensive calc alkaline unit suggests that the calc alkaline volcanic sequence was not coeval with the tholeiitic plateau basalts. Rather it seems likely that the calc alkaline rocks were erupted over the plateau sequence after plume-related magmatism ceased.

Recent studies have suggested that thickened plateau lithosphere will tend to resist subduction and accrete to continental margins (Saunders et al., 1996). The accretion of plateaux fragments would tend to choke the subduction zone which will then back-step allowing for the development of a calc alkaline arc complex on top of the plateau.

Desrochers et al. (1993) have proposed that the Malarctic block of the Abitibi greenstone belt represents a 2705 Ma arc complex which developed on accreted and deformed 2720 Ma - 2715 Ma plateau fragments. Similarly, Stein and Goldstein (1996) have proposed that the late Proterozoic Arabian-Nubian shield is a fragment of an oceanic plateau that resisted subduction, and was subsequently overprinted by calc alkaline magmatism at its margins as the subduction zone stepped back. A similar model is envisaged for the Pickle Crow assemblage.

Stott (1996) has correlated the Pickle Crow assemblage with a possible extension in the Miminiska-Fort Hope belt to the east (Fig. 3.2), implying that the 2.89 Ga inherited zircons within the assemblage may be correlated with the 2.89 Ga Bruce Channel assemblage in the Red Lake belt. He proposes the latter tectonically underlies the Pickle Crow assemblage and suggests that these sequences may have been part of a ~2.89-2.84 Ga terrane, termed the Pickle terrane, which was accreted to the North Caribou Terrane (op cit.). The timing of accretion is not known but must precede the ~2.84 Ga juxtaposition of the Woman assemblage.

It is important to establish whether the arc volcanics were erupted onto the plateau sequence before or after it accreted to the NCT. This question is highlighted by the fact that no ages have yet been reported for the calc alkaline sequence. The ~2.84 Ga age comes from the base of the mafic sequence. Comprehensive geological mapping in conjunction with detailed geochronological studies would likely help resolve this question. In the absence of such a study, preliminary conclusions can be drawn from the geochemical data. In a comprehensive evaluation of modern arcs, Pearce and Peate (1995) observed that continental arcs can be distinguished from oceanic arcs by, amongst other things, the Nb/Yb ratios. Calc alkaline rocks from the Pickle Crow assemblage have Nb/Yb of 1.5-4.0 which lie well within the continental arc field of Pearce and Peate (1995). This observation suggests that the arc rocks were erupted after the Pickle Crow plateau accreted to the NCT, endorsing the model whereby the arc volcanics were erupted after accretion to the continental margin (Fig. 5.8).

5.3 Woman and Meen assemblages

5.3.1 Introduction

The Woman assemblage occurs in all greenstone belts examined as part of this study, with the exception of the Rice Lake greenstone belt. In contrast, the Meen assemblage has

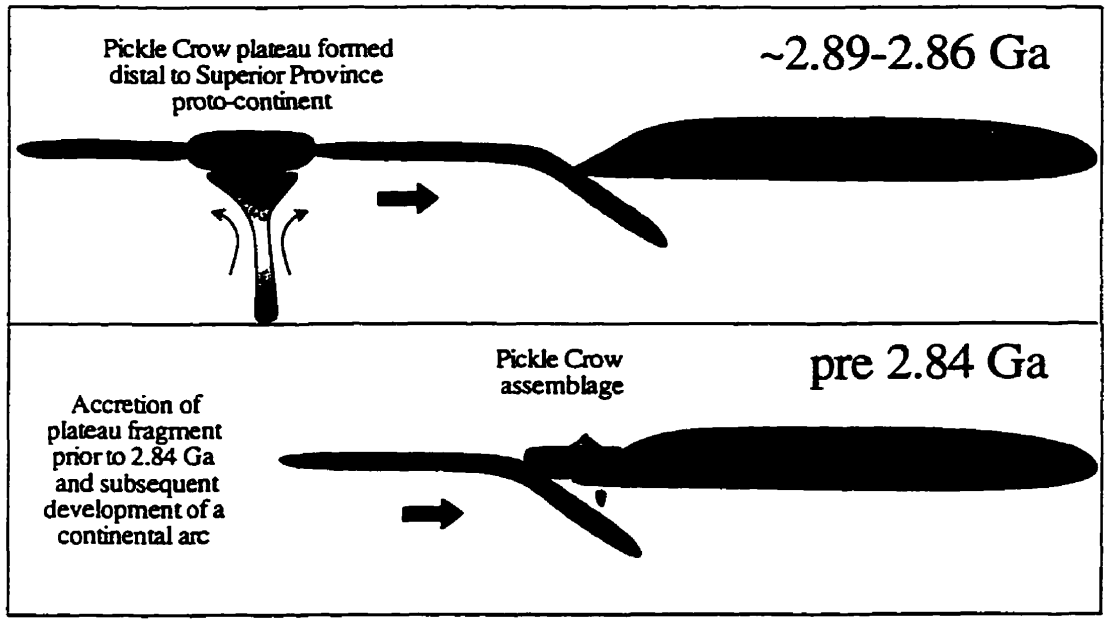

Figure 5.8. Schematic diagram illustrating the proposed geodynamic setting for the Pickle Crow assemblage. Plume related plateau magmatism at ~ 2.89-2.86 Ga is followed by accretion of plateau fragments prior to 2.84 Ga. Continued subduction results in the development of a continental arc complex on the obducted plateau tholeiites.

to date only been recognised within the Meen-Dempster belt. As discussed in Chapter 3, the Woman and Meen assemblages of the Meen-Dempster belt comprise a series of tholeiitic basalts dated at 2842 Ma at the base, overlain by distal and proximal calc alkaline pyroclastic deposits dated at 2825 Ma (Stott and Corfu, 1991; Scharer, 1989; Figs. 3.6 and 3.7). The limited radiometric data for the Woman assemblage in the remainder of the Uchi subprovince precludes definitive recognition of the Meen assemblage across the subprovince.

The geology of the Woman and Meen assemblages is discussed in Chapter 3 and summarised in Table 3.2. Comprehensive analytical results are presented in Appendix C and representative values in the chapter. This section evaluates the geochemistry of the two assemblages and utilises the trace element data to investigate the geodynamic setting.

5.3.2 Woman assemblage of the Meen-Dempster belt

A suite of mafic to intermediate tholeiites are the dominant rock type of the Woman assemblage in the Meen-Dempster belt. They display SiO_2 contents of 47-56 wt.%, MgO of 5-10 wt.% and Fe_2O_3 of 2-13 wt.% (Table 5.3). Petrographically the samples are pillowed or massive flows with the exception of 82GRS-0139, which is a mafic fragmental. However, the range of Fe values does not appear to be a continuous spectrum, but is a bimodal population of high and low Fe-contents. The Ti/Zr ratios of the more primitive Mg-tholeiites are generally close to the chondritic value, whereas two of the three Fe-rich samples scatter away from this value (Fig. 5.9a). The poor correlation with the chondritic Al_2O_3/TiO_2 value on Figure 5.9b is likely the result of shallow level fractionation. Incompatible elements appear to vary coherently with Zr, defining a series of tight linear trends, with no marked scatter of the Fe-tholeiites away from chondritic values (Fig. 5.10).

The majority of samples are characterised by flat or weakly depleted LREE and mildly fractionated HREE (La/Sm_n = 0.8-1.1; Gd/Yb_n = 0.1-1.2; Fig. 5.11a; Table 5.3). Thorium/La ratios are close to the primitive mantle value of 0.11 (0.10-0.14). In addition these tholeiites are characterised by negligible Nb, Ti, Zr and Hf anomalies relative to neighbouring elements on a primitive mantle normalised plot (Nb/Nb* = 0.7-1.0; Zr/Zr* = 0.9-1.1; Fig. 5.11a).

Three samples do not fall within the general trends described above. Samples

Table 5.3 Representative analyses of selected elements for volcanic rocks from the Woman assemblage of the Meen-Dempster greenstone belt*

	Tholeiites								Felsic	
	82GRS-0035	82GRS-1582	82GRS-0139	84GRS-1366	84GRS-0047	84GRS-1235	84GRS-0075	84GRS-1036	84GRS-0822	84GRS-1038
SiO_2	47.51	49.94	52.84	53.64	55.12	55.31	55.59	56.00	73.96	62.12
TiO_2	0.74	0.64	1.08	0.68	0.88	0.92	1.26	1.93	0.43	1.71
Al_2O_3	16.01	15.06	15.38	17.21	16.63	17.18	18.18	16.49	16.24	16.57
Fe_2O_3	11.62	11.93	12.97	2.47	2.39	3.51	2.43	4.15	0.37	2.78
MgO	8.48	6.80	5.02	10.31	9.44	6.36	8.45	7.55	0.99	0.10
LOI	0.40	0.50	0.81	1.21	1.01	2.78	1.42	2.04	1.32	2.46
MgO	0.62	0.56	0.46	0.90	0.90	0.80	0.88	0.80	0.85	0.07
Cr	358	194	240	410	289	268	197	227	11	59.44
Ni	133	135	106	189	162	157	112	87	11	29
Nb	2.57	1.65	6.45	2.16	1.76	2.43	3.05	5.44	5.22	21.52
Zr	36	31	119	34	32	48	58	93	111	395
Hf	1.00	0.85	3.06	0.94	0.87	1.40	1.56	2.51	2.93	
Th	0.46	0.23	0.88	0.25	0.26	0.28	0.42	0.75	5.82	
La	3.75	1.91	7.62	2.00	1.83	2.69	3.46	6.68	8.65	101.46
Sm	1.81	1.43	3.94	1.39	1.47	1.88	2.16	4.12	1.50	12.30
Gd	2.28	1.87	5.06	1.81	1.97	2.60	2.84	4.95	1.24	7.17
Yb	1.71	1.46	3.83	1.53	1.65	2.06	2.25	3.17	0.61	1.95
Lu	0.26	0.21	0.55	0.20	0.23	0.32	0.33	0.50	0.08	0.31
La/Yb_n	1.57	0.94	1.43	0.94	0.80	0.94	1.10	1.42	10.21	37.36
La/Sm_n	1.34	0.86	1.25	0.93	0.80	0.92	1.03	1.05	3.73	5.33
Gd/Yb_n	1.10	1.06	1.09	0.98	0.99	1.05	1.04	1.22	1.68	3.05
Al_2O_3/TiO_2	22	22	14	23	22	18	13	7	51	9.68
Zr/Hf	36	36	39	36	37	34	37	37	38	-
Th/Nb	0.18	0.14	0.14	0.12	0.15	0.11	0.14	0.14	1.11	-
Th/La	0.12	0.12	0.12	0.13	0.14	0.10	0.12	0.11	0.67	-
Zr/Y	2.11	2.17	3.43	2.28	2.13	2.39	2.66	2.78	20.44	12.83
Nb/Nb*	0.66	0.84	0.85	1.03	0.86	0.95	0.86	0.83	0.25	-
Zr/Zr*	0.75	0.89	1.14	0.99	0.92	1.02	1.05	0.88	2.34	0.85
Hf/Hf*	0.75	0.90	1.06	1.00	0.90	1.09	1.03	0.86	2.24	0.00
Ti/Ti*	0.83	0.97	0.57	1.04	0.95	0.94	1.13	1.00	0.55	0.40

* Full data set in Appendix C

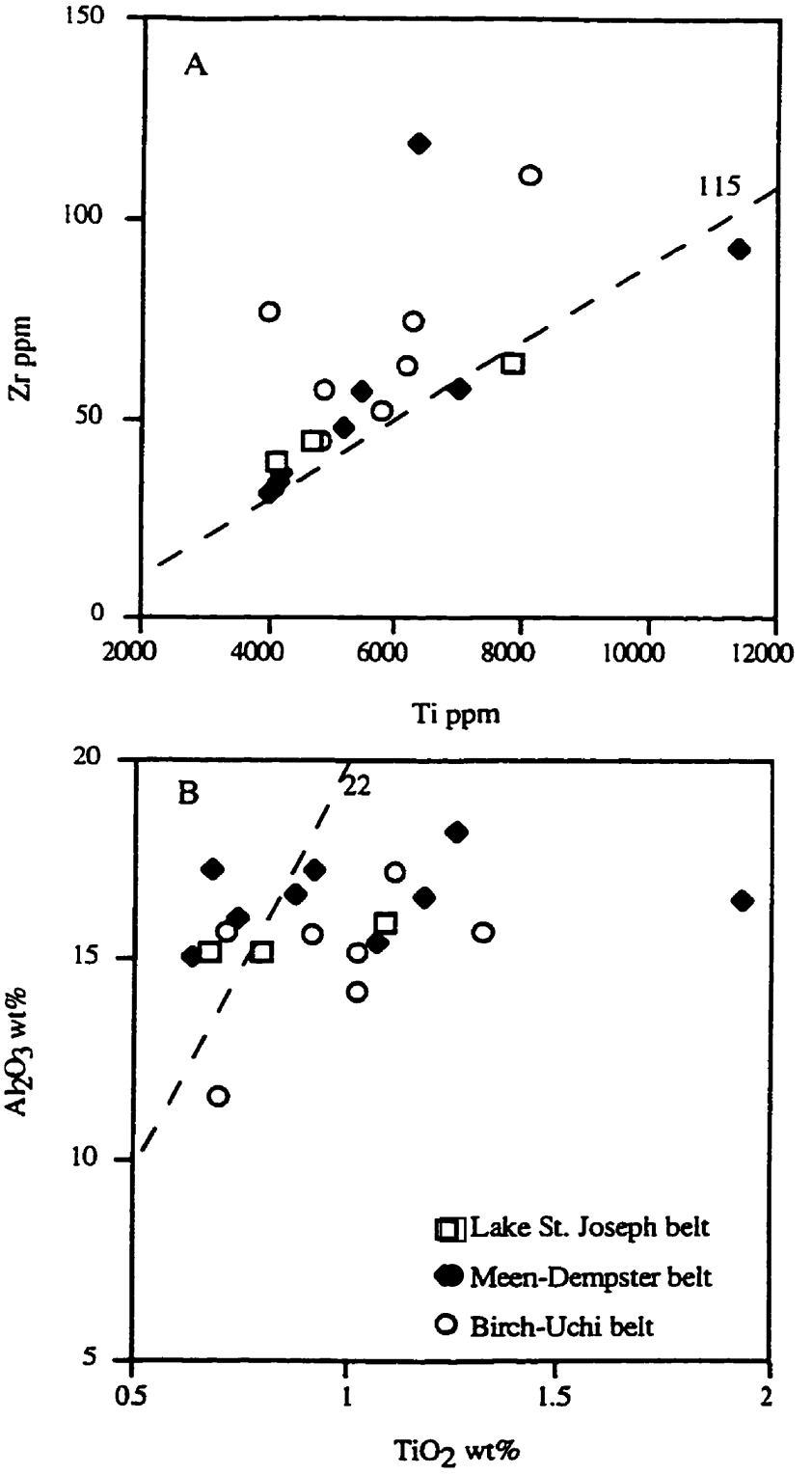

Figure 5.9. Interelement plots for tholeiites from the Woman assemblage of the Uchi subprovince. Dashed lines represent chondritic ratios.

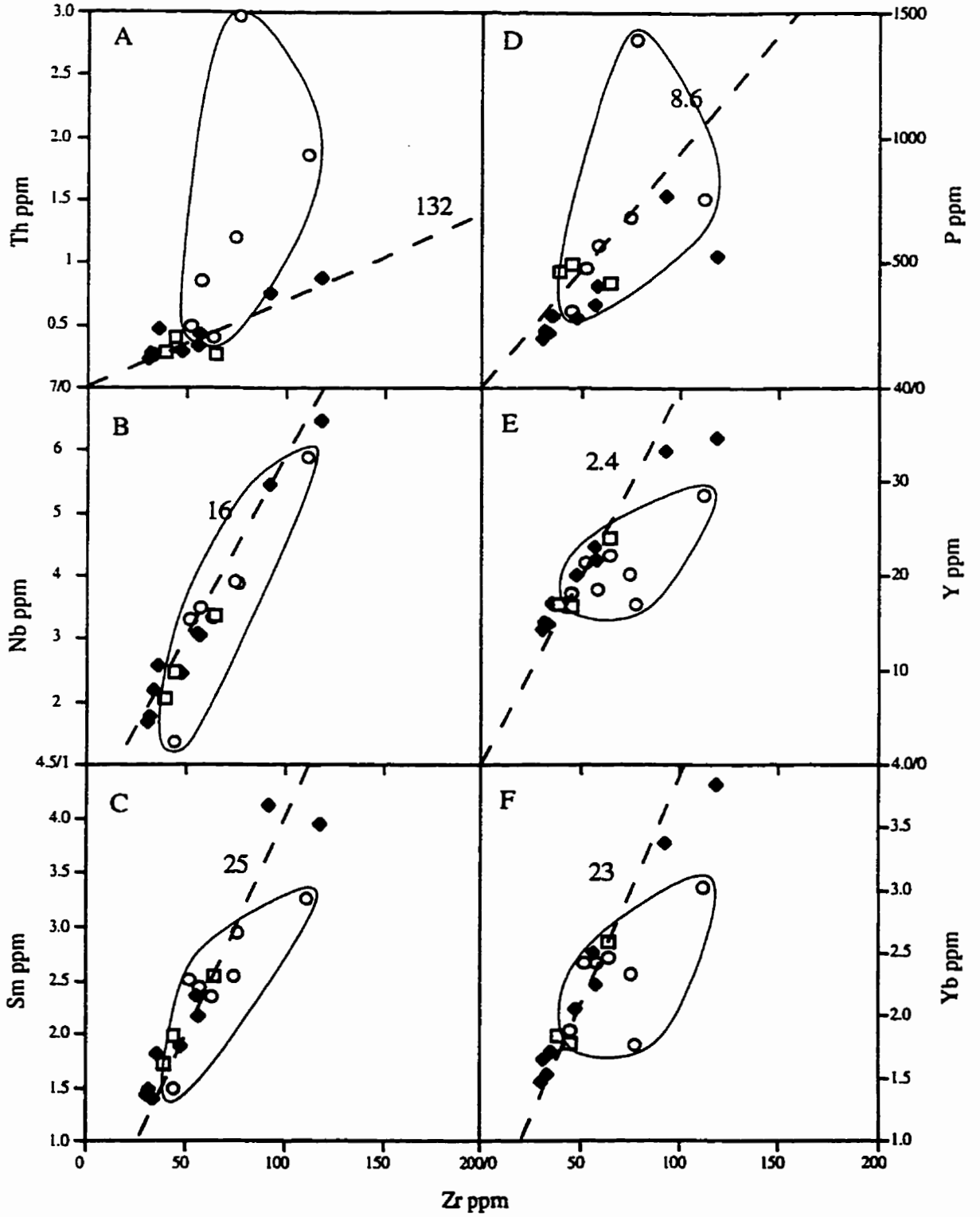

Figure 5.10. Interelement plots for tholeiites from the Woman assemblage of the Uchi subprovince. Legend as for Figure 5.9. Dashed lines represent chondritic ratios. Solid field encompasses samples from the Birch-Uchi assemblage.

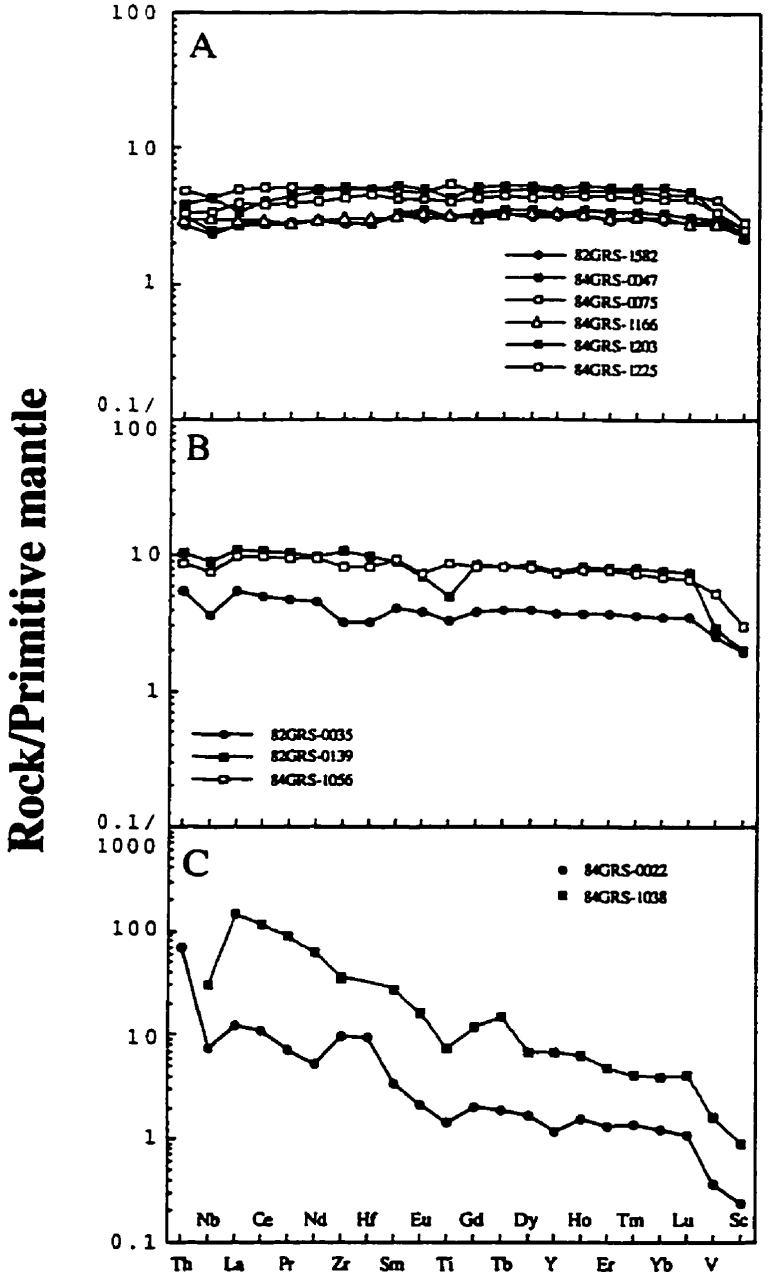

Figure 5.11. Representative primitive mantle normalised plots for A) tholeiites, B) evolved tholeiites and C) felsic volcanic rocks of the Woman assemblage of the Meen-Dempster greenstone belt.

82GRS-0139 and 84GRS-1056, are characterised by generally flat patterns but at significantly higher absolute abundances, ~10 times primitive mantle versus 2-6 times for the typical tholeiites (Fig. 5.11b). The third anomalous sample is characterised by moderate LREE enrichment and flat HREE (82GRS-0035; La/Sm_n = 1.3; Gd/Yb_n = 1.1; Fig. 5.11b), in conjunction with pronounced negative Nb, Ti, Zr and Hf anomalies (Nb/Nb* = 0.6; Zr/Zr* =0.8).

Volumetrically minor felsic units were also sampled in the Woman assemblage (SiO_2 = 62 and 74 wt.%; Table 5.3; Fig. 5.11c). They are characterised by Al_2O_3/TiO_2 ratios of 10-51 and Zr/Y of 13-20, in conjunction with pronounced LREE enrichment and fractionated HREE (Fig. 5.11; La/Sm_n = 3.7-5.3; Gd/Yb_n = 1.7-3.1). Pronounced negative Nb and Ti anomalies are observed in both samples (Nb/Nb* = 0.3; Ti/Ti* = 0.4-0.6), whereas Zr and Hf anomalies vary from weakly negative to strongly positive (Zr/Zr* = 0.9-2.3).

5.3.3 Woman assemblage of the Birch-Uchi Belt

Mafic samples from the Woman assemblage of the Birch-Uchi greenstone belt are a compositionally uniform suite with SiO_2 of 48-52 wt.%, Fe_2O_3 of 12-15 wt.% and MgO of 7-13 wt.% (Table 5.4). Titanium/Zr ratios are consistently subchondritic and scatter widely (Fig. 5.9). On plots versus Zr samples define linear trends versus Nb and Sm. They scatter widely versus P, Y and Yb, and define a distinct trend versus Th compared to the Meen-Dempster and Lake St. Joseph suites (Fig. 5.10).

This suite is characterised by weakly depleted to strongly enriched LREE and flat to weakly fractionated HREE (La/Sm_n = 0.9-1.7; Gd/Yb_n = 1.0-1.4; Fig 5.12a, b; Table 5.4). They also display high La/Nb, Zr/Y and Th/La ratios (La/Nb = 0.8-2.0; Zr/Y = 2.5-4.5; Th/La = 0.1-0.4). The variable Th/La ratios, at higher values than the primitive mantle value of 0.1, imply that the source for these samples was variably enriched in Th relative to La. The weak to moderate Nb and Ti anomalies seen in the majority of samples is consistent with a subduction zone signature (Nb/Nb* = 0.4-0.8; Ti/Ti* = 0.5-1.0; Fig. 5.12a, b).

Intermediate rock types range in composition from basaltic andesites to andesites (SiO_2 = 54-62 wt.%). The majority of the suite is characterised by strongly enriched LREE and moderately fractionated HREE (La/Sm_n = 3.0-4.4; Gd/Yb_n = 1.4-2.4; Fig. 5.12c-e; Table

Table 5.4. Representative analyses of selected elements for volcanic rocks from the Woman assemblage of the Birch-Uchi greenstone belt*.

	Mafic							Intermediate									Felsic
	MI.88-11	MI.88-10	MI.88-05	SB95-38	SB95-42	SB95-32	MI.88-07	SB95-39	SB95-41	MI.88-06	SB95-36	SB95-33	MI.88-15	SB95-37	SB95-40	MI.88-16	MI.87-02
SiO_2	50.36	48.00	49.57	49.21	51.99	47.53	49.29	57.10	57.62	60.67	55.51	59.15	58.10	61.99	54.89	51.62	74.82
TiO_2	0.69	1.11	0.92	1.03	0.71	1.33	1.02	0.96	0.62	0.60	0.87	0.84	0.65	0.89	0.87	2.11	0.31
Al_2O_3	11.59	17.19	15.61	15.18	15.70	15.74	14.18	17.80	17.45	15.22	16.78	17.81	15.64	17.11	18.31	12.19	11.72
Fe_2O_3	12.45	14.38	14.03	14.84	12.31	15.23	15.40	10.66	9.76	6.62	10.87	5.77	8.78	8.38	11.05	18.71	2.71
MgO	13.43	8.05	7.67	8.09	6.67	7.21	7.01	7.78	6.23	4.20	5.70	2.79	3.71	3.18	4.01	3.21	1.42
LOI	6.16	6.73	3.47	11.85	5.06	0.40	11.11	5.77	4.77	10.86	2.72	5.49	5.49	4.77	3.58	8.10	4.77
Mg#	70	55	55	55	54	51	50	62	58	58	54	52	50	46	44	27	54
Ti	3979	6316	4872	6205	4824	8114	5828	4567	3949	3387	3811	4488	3838	4403	4950	12815	1622
Cr	1183	204	264	258	452	176	275	272	122	26	244	29	40	128	143	6	3
Ni	372	193	131	134	159	207	74	85	96	30	235	52	23	95	117	8	5
Nb	3.89	3.92	3.49	3.34	1.37	5.09	3.31	8.08	8.42	9.22	9.30	8.40	6.94	9.60	7.71	10.24	15.71
Zr	77	74	58	64	44	112	52	161	164	190	177	171	131	201	131	201	115
Hf	2.24	2.07	1.71	1.72	1.26	2.59	1.57	3.21	3.75	5.19	4.23	4.27	3.28	5.06	3.35	5.75	8.47
Th	2.98	1.21	0.85	0.40	0.33	1.85	0.49	3.64	7.15	10.18	6.64	7.56	7.44	10.17	3.82	1.77	16.20
La	7.93	6.18	5.04	4.01	2.00	4.97	4.10	17.96	15.57	31.60	30.90	31.50	27.42	25.81	17.96	15.24	50.99
Sm	2.95	2.54	2.44	2.35	1.50	3.26	2.51	3.80	3.11	4.69	5.05	5.38	4.25	4.82	3.48	7.62	7.61
Gd	3.01	3.32	3.23	3.13	2.41	4.34	3.11	3.14	3.19	4.19	4.16	4.48	3.64	3.82	3.21	9.58	6.15
Yb	1.76	2.34	2.42	2.47	1.89	3.02	2.42	1.79	1.84	2.33	1.62	2.07	1.27	2.07	1.28	6.36	3.40
Lu	0.24	0.35	0.36	0.36	0.27	0.43	0.38	0.28	0.26	0.37	0.26	0.32	0.20	0.32	0.19	0.94	0.56
(La/Yb)n	3.22	1.90	1.49	1.16	0.76	1.18	1.21	7.20	6.05	9.74	13.65	10.92	15.52	8.92	10.02	1.72	10.77
(La/Sm)n	1.73	1.57	1.33	1.10	0.86	0.98	1.05	3.05	3.23	4.36	3.95	3.78	4.16	3.46	3.33	1.29	4.33
(Gd/Yb)n	1.41	1.17	1.10	1.05	1.05	1.19	1.06	1.45	1.43	1.56	2.12	1.79	2.38	1.52	2.07	1.25	1.50
Al_2O_3/TiO_2	17	16	19	15	19	11	15	22	26	27	26	24	24	23	22	6	50
Zr/Nb	34	36	34	37	35	43	33	50	44	37	42	40	40	40	39	35	37
La/Nb	2.04	1.58	1.45	1.20	1.46	0.84	1.24	2.22	1.85	3.43	3.32	3.89	4.54	2.69	2.33	1.49	3.24
Th/Nb	0.77	0.31	0.24	0.12	0.24	0.31	0.15	0.45	0.85	1.13	0.71	0.93	1.23	1.06	0.50	0.17	1.03
Th/La	0.38	0.20	0.17	0.10	0.16	0.37	0.12	0.20	0.46	0.33	0.25	0.24	0.27	0.39	0.21	0.12	0.32
Zr/Y	4.53	3.70	3.09	2.86	2.45	3.89	2.44	9.70	9.01	7.74	9.95	8.92	9.08	9.98	10.89	3.79	9.11
Nb/Nb*	0.40	0.52	0.63	0.84	0.69	1.26	0.72	0.40	0.47	0.20	0.23	0.20	0.16	0.31	0.36	0.58	0.22
Zr/Zr*	0.92	1.04	0.90	1.03	1.23	1.35	0.82	1.27	1.63	1.21	1.03	0.97	0.94	1.27	1.15	0.99	1.21
Hf/Hf*	0.97	1.05	0.96	1.01	1.26	1.14	0.90	0.92	1.35	1.20	0.90	0.87	0.86	1.15	1.06	1.02	1.18
Ti/Ti*	0.53	0.86	0.69	0.91	1.00	0.85	0.83	0.52	0.50	0.30	0.33	0.36	0.39	0.41	0.59	0.99	0.89

* Full data set in Appendix C

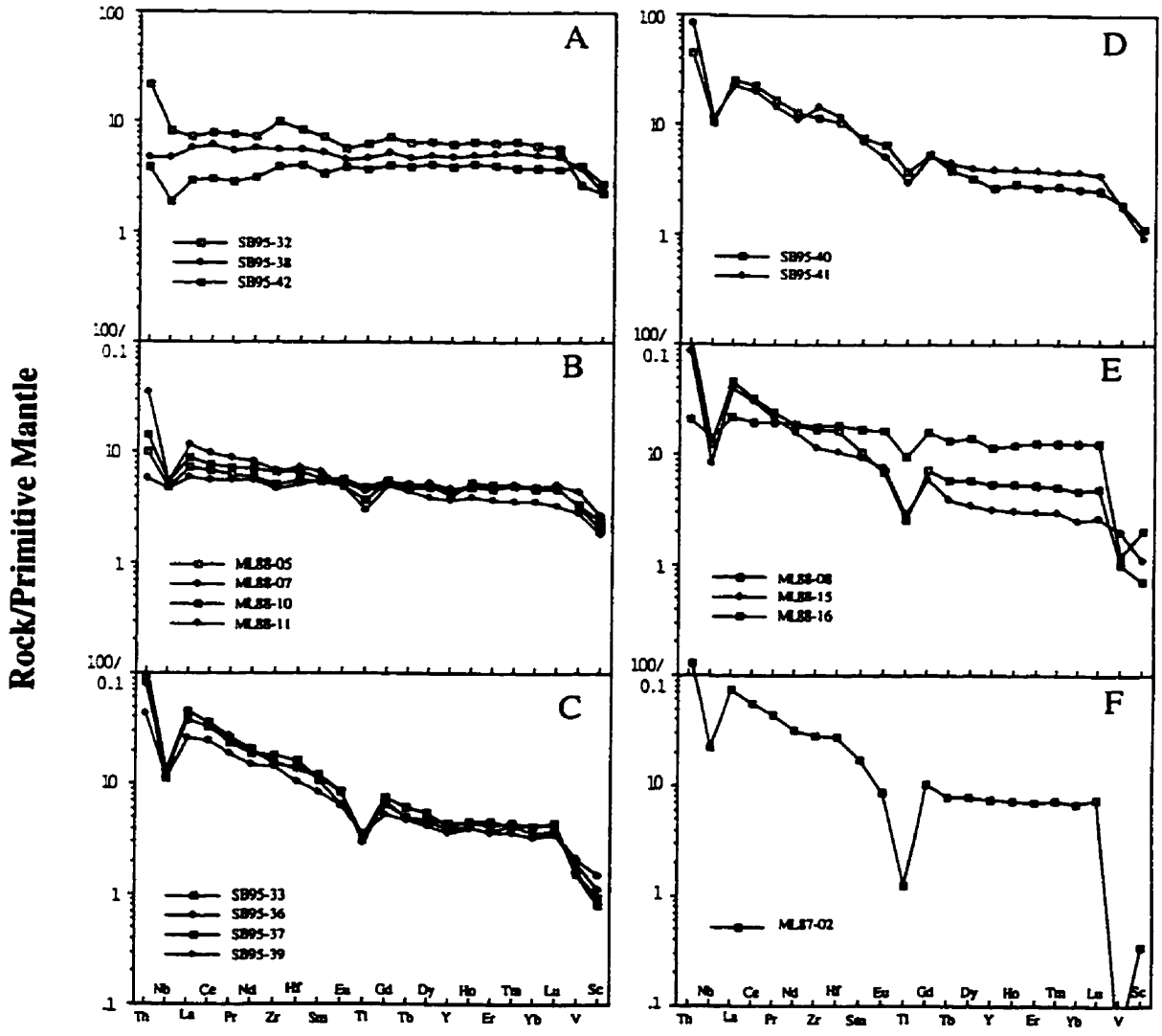

Figure 5.12. Representative primitive mantle normalised diagrams for samples from the Woman assemblage of the Birch-Uchi greenstone belt. A and B = mafic rocktypes; C, D and E = intermediate rocktypes; F = felsic rocktype.

5.4). An exception to this is ML88-16 which displays only weak LREE enrichment and weakly fractionated HREE (La/Sm_n = 1.3; Gd/Yb_n = 1.3; Fig 5.12). The negative Nb and Ti anomalies seen in these samples are characteristic of calc alkaline andesites erupted in an island arc environment (Gill, 1987; Pearce and Peate, 1995). A number of samples display weak Eu anomalies indicative of plagioclase fractionation (*e.g.*, SB95-37 and ML88-08; Eu/Eu* = 0.74 and 0.79 respectively; Fig. 5.12c, e). The negative Nb and Ti anomalies seen in these samples are characteristic of calc alkaline andesites erupted in an island arc environment. Zirconium and Hf anomalies are variable from zero to weakly positive.

LOI values for all samples are relatively high, implying moderate degrees of alteration. This finding is consistent with petrographic studies which reveal that the majority of samples have undergone extensive chlorite and weak to moderate carbonate alteration (carbonate alteration is particularly pronounced in ML88-08; LOI = 10.9 wt.%). However, the generally smooth and coherent patterns displayed in Figure 5.12 suggests that the trace element abundances have not been significantly disturbed.

The single rhyolitic sample from the Woman assemblage displays the marked LREE enrichment and weak HREE fractionation characteristic of arc related volcanic rocks (SiO_2 = 75 wt.%; La/Sm_n = 4.3; Gd/Yb_n = 1.5; Fig. 5.12f). These are features typical of Type 2 felsic volcanic rocks (Chapter 4). The pronounced Nb and extreme Ti anomaly is also consistent with an arc-like tectonic setting (Nb/Nb* = 0.2; Ti/Ti* = 0.1).

5.3.4 Woman assemblage of the Red Lake Belt

Four samples were collected from the Woman assemblage where it outcrops along the north-western shore of McKenzie Island (Fig. 3.11). They range in composition from dacites to rhyolites with 62 to 71 wt.% SiO_2 and Mg#'s of 48-38. Field and textural evidence indicates that these volcanic rocks are pyroclastic deposits. Low LOI values in conjunction with petrographic observations indicate that these samples have undergone only minor chlorite alteration. The volcanic flows are characterised by strong LREE enrichment, with weakly to moderately fractionated HREE (Fig. 5.13; La/Sm_n = 3.7-5.6; Gd/Yb_n = 1.4-2.5; Table 5.5). Pronounced negative Nb and Ti anomalies are present in all four samples (Nb/Nb* = 0.1-0.2; Ti/Ti* = 0.3-0.5). Zirconium and Hf display mildly positive anomalies (Zr/Zr* = 1.2-1.4).

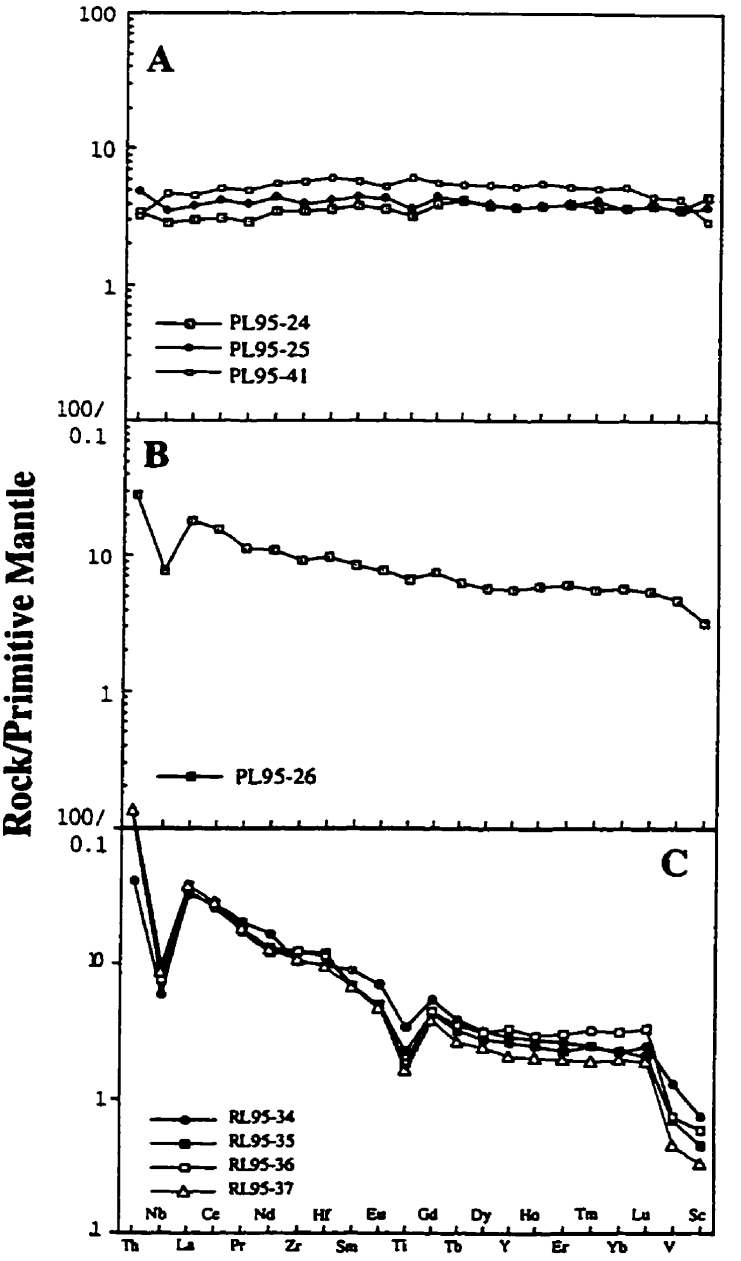

Figure 5.13. Primitive mantle normalised plots for volcanic rocks from the Woman assemblage of the Lake St. Joseph (A, B) and Red Lake belts (C).

Table 5.5. Representative analyses of selected elements for volcanic rocks from the Woman assemblage of the Red Lake and Lake St. Joseph greenstone belts*.

	Red Lake belt				Lake St. Joseph belt			
	RL95-34	RL95-36	RL95-35	RL95-37	PL95-24	PL95-25	PL95-41	PL95-26
SiO_2	61.75	68.40	70.71	70.84	48.89	49.29	51.40	53.68
TiO_2	0.71	0.37	0.44	0.41	0.67	0.79	1.09	1.44
Al_2O_3	17.38	14.99	14.89	15.30	15.17	15.16	15.90	12.04
Fe_2O_3	6.25	3.70	3.78	3.40	12.51	12.60	11.46	14.49
MgO	2.62	1.46	1.00	0.80	8.12	7.70	4.68	3.14
LOI	0.91	2.30	0.96	0.86	0.86	0.45	2.09	1.73
Mg#	48	46	37	34	59	57	47	32
Tl	4425	2368	2905	2125	4115	4681	7888	8576
Cr	22	110	56	41	486	428	344	105
Ni	20	41	27	19	112	139	192	16
Nb	4.30	5.43	7.06	6.21	2.05	2.47	3.36	5.54
Zr	118	138	137	120	39	45	64	103
Hf	3.06	3.46	3.68	2.93	1.13	1.30	1.91	3.02
Th	3.53	8.90	10.79	10.57	0.29	0.41	0.28	2.43
La	22.62	23.77	26.02	25.99	2.08	2.67	3.15	12.45
Sm	3.96	3.03	3.09	2.99	1.72	1.98	2.54	3.77
Gd	3.26	2.67	2.58	2.30	2.37	2.63	3.30	4.44
Yb	1.08	1.56	1.11	0.97	1.84	1.78	2.58	2.85
Lu	0.18	0.25	0.15	0.14	0.28	0.30	0.33	0.41
(La/Yb)n	15.02	10.96	16.80	19.25	0.81	1.08	0.87	3.13
(La/Sm)n	3.69	5.07	5.44	5.62	0.78	0.87	0.80	2.13
(Gd/Yb)n	2.50	1.42	1.92	1.96	1.07	1.22	1.06	1.29
Al_2O_3/TiO_2	23	37	31	42	22	19	12	8
Zr/Hf	39	40	37	41	35	34	33	34
La/Nb	5.26	4.37	3.69	4.18	1.01	1.08	0.94	2.25
Th/Nb	0.82	1.64	1.53	1.70	0.14	0.16	0.08	0.44
Th/La	0.16	0.37	0.41	0.41	0.14	0.15	0.09	0.20
Zr/Y	9.01	9.22	11.55	12.63	2.30	2.64	2.66	4.03
Nb/Nb*	0.15	0.17	0.20	0.17	0.99	0.95	1.16	0.37
Zr/Zr*	0.87	1.35	1.28	1.16	0.94	0.90	1.00	0.95
Hf/Hf*	0.82	1.23	1.24	1.02	0.99	0.95	1.09	1.01
Ti/Ti*	0.49	0.33	0.41	0.32	0.81	0.81	1.08	0.83

*Full data set in Appendix C

5.3.5 Woman assemblage of the Lake St. Joseph Belt

Three tholeiitic samples collected from the Woman assemblage of the Lake St. Joseph greenstone belt comprise a uniform suite of relatively primitive Mg-tholeiites (Mg# = 59-47; Fe_2O_3 = 12-13 wt.%). Titanium/Zr ratios lie close to the chondritic value of 116 (Fig. 5.9), whereas Al_2O_3/TiO_2 ratios scatter widely (12-22). The three samples define broadly chondritic trends on plots versus Zr for the generally immobile elements Nb, Sm, Y and Yb, but scatter versus Th and P (Fig. 5.10).

The three samples are characterised by flat or weakly depleted LREE and flat HREE (La/Sm_n = 0.8-0.9; Gd/Yb_n = 1.1-1.2; Table 5.5; Fig 5.13). However, the higher LOI of sample PL95-41, in conjunction with pervasive carbonate alteration observed in thin section may account for the LREE depletion seen in the sample (LOI = 2.1 wt % versus 0.5-0.9 wt.% for PL95-4 & 25; Fig 5.13). Small or zero Nb anomalies in conjunction with weak Ti anomalies indicates the absence of crustal contamination in these samples (Nb/Nb* = 1.0-1.2; Ti/Ti* = 0.8-1.1; Fig. 5.13). The absence of significant Eu anomalies rules out plagioclase fractionation or accumulation (Eu/Eu* = 0.93-0.97). Thorium/La ratios of 0.14 to 0.15 (PL95-41 excepted) are relatively close to the primitive mantle value of 0.10.

The remaining sample collected from the Woman assemblage is a basaltic andesite with an SiO_2 content of 54 wt % and an Mg# of 32. PL95-26 is characterised by strongly enriched LREE and variably fractionated HREE (La/Sm_n = 2.1; Gd/Yb_n = 1.3; Table 5.5; Fig. 5.13). The andesite has high La/Nb and Zr/Y ratios (La/Nb = 2.3; Zr/Y = 4.0) and displays a negative Nb anomaly and weakly negative Ti anomaly (Nb/Nb* = 0.4: Ti/Ti* = 0.8; Fig. 5.13).

5.3.6 Meen Assemblage of the Meen-Dempster belt

Volcanic flows from the Meen assemblage range from andesitic to rhyolitic in composition with SiO_2 contents varying from 56-76 wt.%, MgO from 0.3-8.0 wt.% and Al_2O_3 of 14-17 wt.% (Table 5.6). The andesite is characterized by moderate LREE enrichment and weakly fractionated HREE (La/Sm_n = 2.2; Gd/Yb_n = 1.1; Fig. 5.14). A pronounced negative Nb anomaly is consistent with a subduction modified sub-arc mantle source (Nb/Nb* = 0.3).

The rhyolites are characterised by pronounced LREE enrichment and moderately to

Table 5.6. Representative analyses of selected elements for volcanic rocks from the Meen assemblage, Meen-Dempster greenstone belt*.

	84GRS-1206	82GRS-0120	84GRS-0022	82GRS-0224	82GRS-1022
SiO_2	57.60	72.54	73.96	74.79	75.77
TiO_2	0.77	0.48	0.43	0.46	0.12
Al_2O_3	15.91	16.40	16.24	16.75	14.35
Fe_2O_3	2.12	2.35	0.37	0.19	0.97
MgO	8.08	0.69	0.99	0.34	0.50
LOI	1.21	1.32	1.32	1.21	0.70
Mg#	89	39	85	80	53
Ti	4360	2688	1877	3181	517
Cr	372	12	11	17	3
Ni	105	13	11	11	2
Nb	3.06	5.71	5.22	5.83	5.17
Zr	57	97	111	100	89
Hf	1.44	2.49	2.93	2.40	2.70
Th	1.54	5.11	5.82	4.84	6.57
La	6.47	18.13	8.65	13.68	16.85
Sm	1.87	2.22	1.50	2.41	1.51
Gd	2.30	1.69	1.24	1.57	1.14
Yb	1.66	0.55	0.61	0.32	0.47
Lu	0.24	0.09	0.08	0.05	0.07
(La/Yb)n	2.79	23.75	10.21	30.27	25.52
(La/Sm)n	2.23	5.28	3.73	3.67	7.21
(Gd/Yb)n	1.14	2.56	1.68	4.01	1.99
AL_2O_3/TiO_2	20	36	51	32	166
Zr/Hf	40	39	38	42	33
La/Nb	2.12	3.18	1.66	2.35	3.26
Th/Nb	0.50	0.90	1.11	0.83	1.27
Th/La	0.24	0.28	0.67	0.35	0.39
Zr/Y	3.36	17.91	20.44	22.90	17.74
Nb/Nb*	0.36	0.24	0.50	0.35	0.21
Zr/Zr*	1.08	1.22	2.34	1.27	1.61
Hf/Hf*	0.99	1.14	2.24	1.11	1.76
Ti/Ti*	0.83	0.55	0.55	0.65	0.16

* Full data set in Appendix C

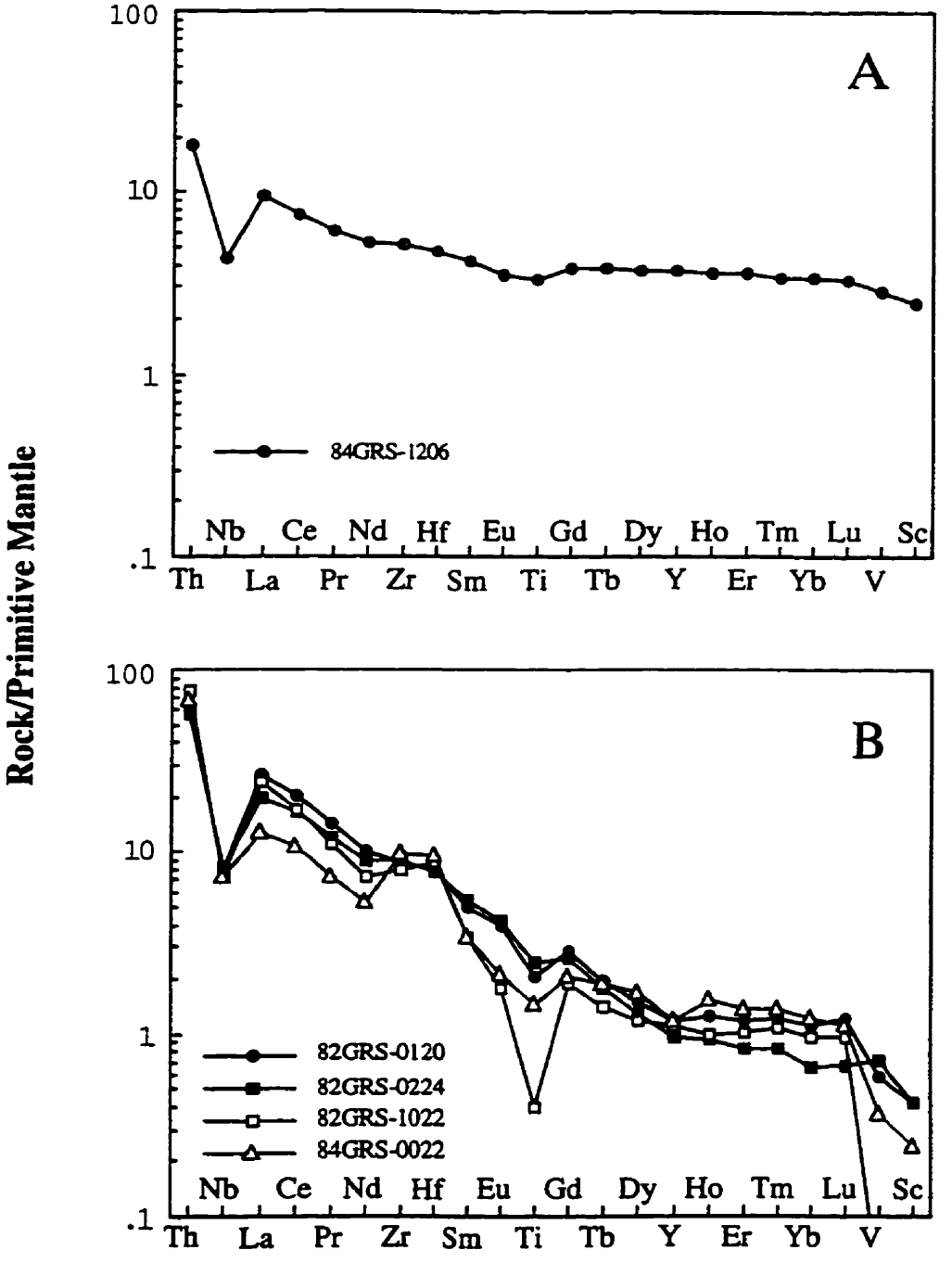

Figure 5.14. Primitive mantle normalised plots from the Meen assemblage of the Meen-Dempster greenstone belt.

strongly fractionated HREE (La/Sm_n = 3.7-7.2; Gd/Yb_n = 1.7-4.0; Fig. 5.14). These REE systematics occur in conjunction with pronounced negative Nb and Ti anomalies (Fig. 5.14). Thorium/La ratios of 0.3-0.7, and Zr/Y of 18-23 are consistent with a subduction related source. Zr and Hf anomalies are weakly to moderately positive (Zr/Zr* = 1.1-2.4; Hf/Hf* = 1.0-2.2).

5.3.7 Discussion

In the Meen-Dempster greenstone belt Stott (1997) has subdivided the Woman assemblage into the ~2.82 Ga Meen and the ~2.84 Ga Woman assemblages. This study demonstrates that these two assemblages have distinct geochemical characteristics.

Silica contents for the Woman assemblage tholeiites extend to higher values than reported for the Ontong Java plateau (58 wt% versus 50 wt% for OJP). However, similarities between the flat REE patterns of the tholeiites of the Woman assemblage and those reported by Mahoney et al. (1993) for the OJP are consistent with a plateau origin, as noted above for the Pickle Crow assemblage. The presence of an extensive BIF deposit within the Woman assemblage of the Meen-Dempster belt may indicate there was a significant hiatus in the eruption of the basalts. However, tholeiites to the north of the BIF are geochemically indistinguishable from those to the south. Barley et al. (1997) have suggested that the emplacement of a Large Igneous Province may be responsible for the rapid deposition of extensive Paleoproterozoic BIF, as a result of increased sub-oxic iron- and silica-rich water associated with magmatism. This is consistent with the well developed BIF horizons within the Woman assemblage.

There is a relative paucity of felsic volcanic flows within the Woman assemblage, as only two outcrops were sampled for this study. The trace element characteristics of these flows are comparable to the range documented for Archean granitoids (Martin, 1986, 1994). The pronounced positive Zr-Hf anomaly observed in 84GRS-0022 is not thought to be the result of LREE loss associated with alteration, given the low LOI and lack of petrographic evidence for any alteration. Rather, it is likely the result of fractional crystallisation of hornblende in a dacitic magma will result in positive Zr (Hf) anomalies (cf., compilation of distribution coefficients in Rollinson, 1993).

All samples from the Meen assemblage are calc alkaline in character, displaying pronounced LREE enrichment and strong negative Nb and Ti anomalies (Fig. 5.14). The trace element characteristics are typical of Archean arc-related felsic rock types and recur

in younger convergent margin settings (Drummond and Defant, 1990; Tarney and Jones, 1994). Andesite (84GRS-1206) lacks the variable Ti anomaly observed in the more evolved rhyolites, but displays a pronounced negative Nb anomaly consistent with a subduction zone signature. The elevated compatible element abundances and lower absolute REE abundances are consistent with the andesite representing the source for the rhyolites. Hawkesworth et al. (1997) have shown that arc related basalts and andesites with higher Th contents receive a greater contribution from subducted sediments, and further that high Th/Ce ratios are a feature of sediments with a substantial continental component. The Th/Ce value of 0.1 for the Meen assemblage andesite is comparable to the lower end of the range of values for modern day continental arcs (Hawkesworth et al., 1997), and distinctly higher than values for assemblages of the Abitibi Subprovince that were generated in an oceanic environment (e.g., Lafleche et al., 1992; Wyman, unpublished data) implying that the arcs were close to a continental margin. Niobium/Yb ratios of 2-18 are also consistent with a continental arc (c.f., Pearce and Peate, 1995).

The largest data base on the Woman assemblage has been collected from within the Birch-Uchi belt. Consequently identification of the Meen assemblage within the belt may be possible. The single age known for this belt is one of 2840 Ma from a felsic tuff towards the top of the assemblage. The composite stratigraphic column of Stott and Corfu (1991; Fig. 3.9) indicates that intermediate volcanic rocks are intercalated with the mafic volcanic rocks towards the centre of the assemblage (section C-D on Figs. 3.8 and 3.9). The repetition of mafic and intermediate rocks within this relatively small portion of the assemblage may represent tectonic stacking. Consequently it is not possible to rule out structural repetition, but if the stratigraphy is intact, the younger Meen assemblage cannot be present within the Birch-Uchi belt. In conclusion, further geochronological studies are necessary in order to determine if the calc alkaline rocks of the Woman assemblage in the Birch-Uchi belt can be correlated with the Meen assemblage of the Meen-Dempster belt.

The samples taken from the southern portion of the Woman assemblage of the Birch-Uchi belt, which are stratigraphically lower in the sequence, display the flattest trace element patterns (Figs. 3.8 and 5.12a). Mafic samples collected from towards the top of the stratigraphy display a positive correlation between the degree of LREE enrichment and the magnitude of the negative Nb anomaly (Fig. 5.12b). The majority of mafic volcanic samples from the Woman assemblage of the Birch-Uchi belt are comparable to rock types typically found in an oceanic arc geodynamic setting today (e.g. Gill, 1987, Pearce and Peate, 1995). Weak LREE enrichment seen in the samples suggests that they may in fact

be primitive arc tholeiites developed in the early stages of arc formation. The progression from flatter patterns towards the base of the sequence to more arc like patterns towards the top is consistent with the initiation of arc volcanism.

The limited sample set from the Woman assemblage of the Lake St. Joseph and Red Lake belts make it difficult to adequately interpret the geochemistry. Samples from the Woman assemblage in the Red Lake greenstone belt are all calc alkaline in character. However, in the Lake St. Joseph belt the presence of both tholeiitic and calc alkaline rock types is consistent with the model that the assemblage represents an island arc sequence developed upon a tholeiitic platform (Stott and Corfu, 1991). The similar trace element normalised patterns of PL95-26 of the Lake St. Joseph Woman assemblage and 84GRS-1206 of the Meen assemblage is tentatively interpreted to imply a correlation and consequently the presence of the Meen assemblage within the Lake St. Joseph belt (Figs. 5.13 and 5.14). The absence of tholeiitic samples in the Red Lake belt is likely a reflection of the limited outcrop in the area as opposed to significant variations in the makeup of the assemblage as a whole.

5.3.8 Implications and geodynamic setting

Recent modelling indicates that oceanic plateaux with crustal thicknesses greater than ~25 km will tend to be too buoyant to subduct (Saunders et al., 1996). As a consequence, plateaux may have contributed substantially to crustal growth via accretion at continental margins (Abbott, 1996; Kent et al., 1996; Saunders et al., 1996). It is suggested that this is the case for the plateau-like Woman assemblage of the Meen-Dempster greenstone belt which would have been accreted to the proto continental North Caribou Terrane. A modern analogue for this scenario is the coast of Central and South America where high Mg-lavas, likely associated with either the Galapagos or Easter Island plumes, have been accreted at a continental margin (Aitken and Echeverria, 1984; Storey et al., 1991; Alvarado et al., 1997; MacDonald et al., 1997). Corfu and Stott (1996) noted mixed isotope characteristics of zircons from a felsic tuff in the Woman assemblage and suggested that it was the result of interaction between tholeiitic magma and preexisting continental crust, a model that is consistent with a tectonic setting such as that described above.

The younger, and dominantly calc alkaline, Meen assemblage in the Meen-Dempster belt most plausibly represents an arc related sequence developed on top of the accreted plateau fragments 15 m.y. after plume volcanism. As discussed in Section 5.2.6, Desrochers et

al. (1993) have proposed a similar model for the Malarctic block of the Abitibi greenstone belt, where a 2705 Ma arc complex developed on accreted and deformed 2720 Ma - 2715 Ma plateau fragments. Recently, Tejada et al. (1996) have proposed that the islands of Malaita and Santa Isabel in the Solomon Islands represent a modern example of an arc sequence developed on an accreted plateau fragment, in this case a fragment of the Ontong Java plateau. Similarly, Stein and Goldstein (1996) have proposed that the late Proterozoic Arabian-Nubian shield is a fragment of an oceanic plateau that resisted subduction and was subsequently overprinted by calc alkaline magmatism at its margins as the subduction zone stepped back.

The geochemistry of the Woman assemblage in the Lake St. Joseph and Red Lake belts is consistent with the plateau accretion model. However, the Woman assemblage of the Birch-Uchi belt does not really fit this model. Assuming the ~2.84 Ga age from the top of the sequence is not the result of tectonic stacking, then the assemblage records extensive arc volcanism at the same time as dominantly tholeiitic plateau-type volcanism in the Meen-Dempster belt. Given the potential for tectonic stacking in greenstone belts, for example the Confederation assemblage of the Lake St. Joseph belt (Stott et al., 1987a, b), it seems likely that a younger age has simply not been identified and that the Woman assemblage of the Birch-Uchi belt does contain the Meen assemblage. Alternatively the arc volcanics in the Birch-Uchi belt Woman assemblage may simply represent an earlier phase of arc volcanism at ~2.84 Ga, and consequently may constrain the time of accretion.

Stott (1996) has proposed that the Woman assemblage developed marginal to the proto-continental Superior province. The apparent structural conformity between the Woman and Pickle Crow assemblages of the Pickle Lake belt supports this interpretation. The fact that the Trout Lake batholith, which is spatially associated with the Woman assemblage, has intruded rocks of the Balmer assemblage in the Birch-Uchi belt also endorses this scenario (Noble et al., 1985; Stott, 1996). The presence of an older 2857 Ma tonalite in the Lake St. Joseph batholith to the south of the Woman assemblage is interpreted to have separated from the Pickle terrane when the Woman arc complex formed. This also implies a continental setting for the arc (Stott, 1996). Geochemical data from this study is broadly consistent with Stott's (1996) model, but rather than the Meen arc complex developing directly on the margins of the continent, the recognition of the older Woman assemblage plateau sequence in the Meen-Dempster belt suggests it developed on accreted and obducted plateau fragment that formed away from the continental margin (Fig. 5.15).

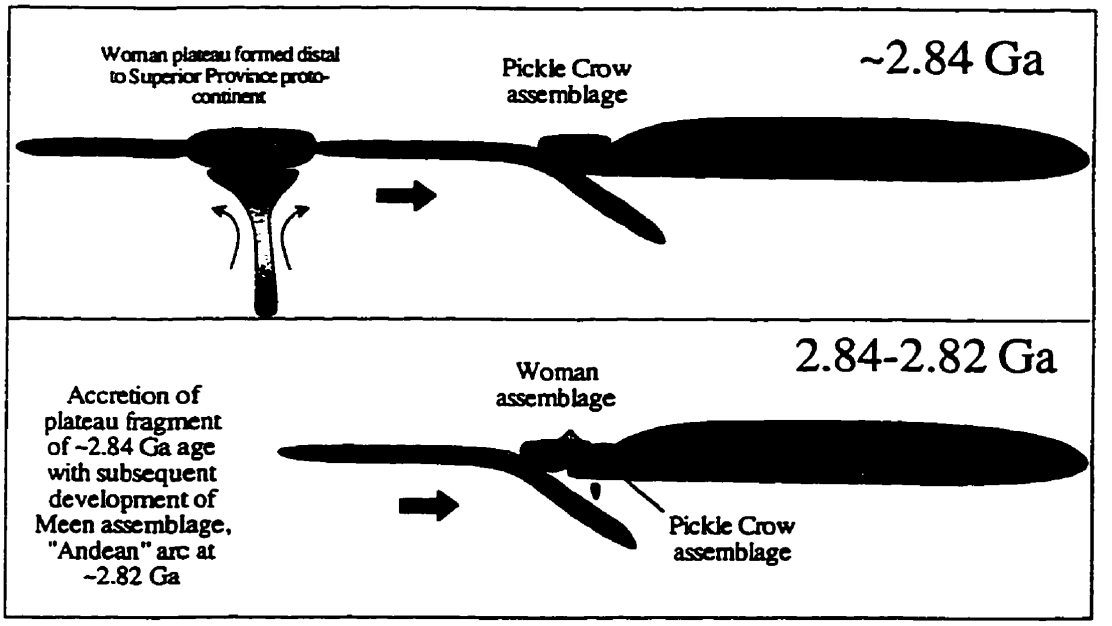

Figure 5.15. Schematic diagram illustrating the proposed geodynamic setting for the Woman and Meen assemblages. Plume related plateau magmatism at ~ 2.84 Ga is followed by accretion of plateau fragments ~2.82 Ga. Continued subduction results in the development of a continental arc complex (Meen assemblage) on the plateau tholeiites.

5.4 Conclusions

The large scale plume activity recorded in the ~3 Ga terranes discussed in Chapter 4 appears to have terminated at around 2.9 Ga, leaving a substantial continental land mass (the NCT) to which the remainder of the Superior Province accreted from both the north and south. The Pickle Crow assemblage of the Pickle Lake belt likely represents the next stage of continental development and displays distinctive geochemistry to the older terranes. This assemblage comprises dominantly plateau type rocks that are interpreted to have been accreted to the Superior Province proto-continent. Subsequent subduction led to the development of an arc complex on the accreted plateau fragments (Fig. 5.8).

Following the formation of the Pickle Crow assemblage, the ~2.84 Ga Woman assemblage developed; this is the oldest assemblage to be present along the length of the subprovince. Stott (1996) has suggested that the spatial association with coeval plutons, intruded into older rocks to the north, requires that the Woman-Meen assemblage formed as an arc marginal complex on the edge of the NCT, rather than as an intra oceanic arc that was later accreted to the NCT. The geochemical data presented here suggests that the arc volcanics were indeed from a continental arc, but that they were erupted onto accreted fragments of a ~2.84 Ga plateau rather than the 2.9-3.0 Ga proto-continent itself (Fig. 5.15).

The southwest Pacific region provides an excellent analogue for the Uchi paleo-continental margin, as it preserves accreted fragments of diverse lithologies and geodynamic settings. The Solomon Islands in particular have been shown to comprise rocks of clear oceanic plateau affinity but also a significantly younger component interpreted to represent a back arc basin (Tejada et al., 1996). The Meen-Dempster belt appears to record a very similar geological history, albeit over a longer timescale. Numerous authors have suggested that plateau accretion may have been an important crustal growth mechanism from the Archean onwards (Abbott, 1996; Stein and Goldstein, 1996). Development of an arc complex on an accreted oceanic plateau, as recorded in the Woman and Meen assemblages, supports this model.

Continental growth in the period 2.8-2.9 Ga occurred by processes distinct from those in the interval 2.9-3.0 Ga. Instead of coeval plume-arc magmatism, as identified in the older assemblages, the Pickle Crow, Woman and Meen assemblages appear to record plateau accretion and subsequent arc development, comparable to recent magmatism in the south

west Pacific region.

CHAPTER 6

THE CONFEDERATION ASSEMBLAGE, A ~2.7 Ga ARC COMPLEX ALONG THE UCHI PALEO-CONTINENTAL MARGIN

6.1 Introduction

This chapter presents geochemical analyses from the Confederation assemblage of the Uchi subprovince. The Confederation assemblage is present in all greenstone belts investigated in this study with an age range of ~15 m.y. (Table 3.2). Consequently it offers the opportunity to investigate variations in the geochemistry of an Archean arc complex over both space and time. The Confederation assemblage is one of the youngest assemblages developed along the Uchi paleo-continental margin. Its geological characteristics are briefly summarised in Table 3.2. Comprehensive analyses of all samples collected in this study are presented in Appendix D with representative samples discussed in the chapter.

Data from the Rice Lake, Red Lake, Birch-Uchi, Meen-Dempster, Pickle Lake and Lake St. Joseph greenstone belts will be presented in this Chapter (Fig. 3.2). The samples range in composition from basalt to dacite in the Red Lake and Pickle Lake belts, and from basalt to rhyolite in the Birch-Uchi, Rice Lake, Meen-Dempster and Lake St. Joseph belts. However, it should be noted that the more limited compositional range occurs in the belts with the smallest sample sets, and consequently may reflect a sampling bias.

6.2 Tholeiitic basalts

Tholeiitic volcanic rocks are found within the Confederation assemblage of four of the six greenstone belts sampled in this study.

6.2.1 Birch-Uchi greenstone belt

Tholeiites from the Birch-Uchi belt display a wide compositional variation from Mg- to Fe-tholeiites over a broad range of Mg#'s from 59-26 (SiO_2 = 45-52 wt.%; Fe_2O_3 = 10-

20 wt.%; MgO = 3-10 wt.%; Table 6.1). Data scatter widely about the chondritic Ti/Zr and TiO_2/Al_2O_3 values (Fig. 6.1). When trace elements are plotted against Zr the data define tight linear trends with Nb, Sm, Y and Yb (Fig. 6.2). LREE are variably depleted to enriched within the suite, whereas HREE are weakly to moderately fractionated (Fig. 6.3a; La/Sm_n = 0.8-1.3; Gd/Yb_n = 1.2-1.8). Niobium anomalies are consistently negative in all samples (Nb/Nb* = 0.7-1.0).

A second suite of tholeiitic samples have been recognised from a drill hole on the South Bay Mine site (Fig. 6.3b; Table 6.1). They extend to a higher range of SiO_2 contents (SiO_2= 50-59 wt.%; MgO = 2-5 wt.%; Fe_2O_3 = 13-20). These evolved tholeiites display moderate LREE enrichment (La/Sm_n = 1.3-1.6) and moderately negative Nb anomalies (Nb/Nb* = 0.4-0.7). The magnitude of the Nb anomalies is correlated with silica content and increased LREE enrichment.

6.2.2 Meen-Dempster greenstone belt

Two tholeiitic suites have been recognised in the Confederation assemblage of the Meen-Dempster belt. The first suite is comprised of basaltic and andesitic volcanic rocks (SiO_2 = 47-58 wt.%). More evolved examples are characterised by significantly lower Fe_2O_3 contents (2-4 wt.% versus 13-15 wt.%) at comparable MgO contents. The drop in Fe_2O_3 is not accompanied by significant fractionation of other compatible elements which have relatively uniform abundances within the suite (e.g. Ni, Cr and Ti). These tholeiites are characterised by flat to LREE depleted patterns (La/Sm_n = 0.7-1.0; Gd/Yb_n = 1.0-1.3; Fig. 6.4a; Table 6.2), and lack significant Nb, Ti, Zr and Hf anomalies (Nb/Nb* = 0.9-1.2; Zr/Zr* = 0.8-1.2). Thorium/La ratios in the more primitive basaltic samples are close to the primitive mantle value of 0.1 (Th/La = 0.10-0.14), whereas the more evolved samples are characterised by slightly elevated Th/La values (0.15-0.18). Zirconium/Hf ratios for all samples are close to the chondritic value of 36 (35-39), whereas Zr/Y vary from 2.1-3.7.

The second suite comprise a compositionally uniform group of basalts with SiO_2 contents varying between 50-51 wt.%, MgO from 7-8 wt.% and Fe_2O_3 from 12-13 wt.%. They are characterised by flat to weakly depleted LREE in conjunction with flat HREE comparable to the suite described above (La/Sm_n = 0.8-1.0; Gd/Yb_n = 0.9-1.0; Fig. 6.4b; Table 4). This second suite differs from the tholeiites described above in that they

Table 6.1. Representative analyses of selected elements for tholeiitic volcanic rocks from the Confederation assemblage of the Birch-Uchi greenstone belt*.

	South Bay mine site Tholeiites						South Bay mine site DDH Evolved tholeiites			
	SL87-03	SL88-15	SL88-06	SH87-05	SB95-22	SL87-04	SB95-4M	SB95-4N	SB95-4O	SB95-4P
SiO_2	45.02	49.65	50.38	48.04	51.65	50.73	52.32	49.68	59.45	55.50
TiO_2	0.74	0.94	1.31	0.93	2.07	2.26	1.76	1.88	1.40	1.48
Al_2O_3	15.73	14.71	16.97	15.03	12.02	12.74	13.57	12.19	12.26	12.69
Fe_2O_3	14.59	10.93	16.54	13.76	18.71	19.63	17.47	19.62	13.09	16.61
MgO	9.71	5.35	7.51	5.75	3.87	3.10	4.08	5.31	2.24	3.45
LOI	14.54	6.00	6.39	4.50	4.33	6.49	2.56	2.51	2.51	2.15
Mg#	59	52	50	48	31	26	34	37	27	31
Ti	4404	5209	8809	6610	9254	13390	9008	9818	7626	7581
Cr	379	112	247	395	24	3	12	42	5	3
Ni	228	116	214	191	30	2	27	71	5	9
Nb	1.72	4.36	3.54	3.03	9.61	11.47	9.01	7.13	13.23	9.66
Zr	35	59	63	54	168	197	156	129	257	178
Hf	1.05	1.64	1.89	1.67	4.46	5.85	4.61	3.91	6.56	4.97
Th	0.21	0.38	0.57	0.47	1.68	1.76	1.65	1.36	2.28	2.18
La	2.01	5.11	4.64	4.24	12.66	14.72	12.62	11.02	18.68	19.20
Sm	1.68	2.47	2.79	2.58	6.41	7.52	5.89	5.01	8.97	7.66
Gd	2.32	3.19	3.40	3.31	8.05	9.70	7.21	6.20	11.50	9.44
Yb	1.06	1.47	1.89	2.30	5.22	5.63	4.94	4.27	7.68	6.30
Lu	0.16	0.23	0.32	0.33	0.79	0.92	0.72	0.62	1.14	0.90
(La/Yb)n	1.36	2.49	1.76	1.32	1.74	1.87	1.83	1.85	1.74	2.18
(La/Sm)n	0.77	1.34	1.08	1.06	1.27	1.27	1.38	1.42	1.35	1.62
(Gd/Yb)n	1.81	1.79	1.48	1.19	1.28	1.42	1.21	1.20	1.24	1.24
AL_2O_3/TiO_2	22	17	11	13	8	6	9	7	10	10
Zr/Hf	34	36	33	32	38	34	34	33	39	36
La/Nb	1.17	1.17	1.31	1.40	1.32	1.28	1.40	1.55	1.41	1.99
Th/Nb	0.12	0.09	0.16	0.16	0.17	0.15	0.18	0.19	0.17	0.23
Th/La	0.10	0.07	0.12	0.11	0.13	0.12	0.13	0.12	0.12	0.11
Zr/Y	3.00	3.61	2.97	2.25	3.64	3.29	3.58	3.40	3.48	3.10
Nb/Nb*	0.94	0.80	0.69	0.70	0.73	0.68	0.67	0.59	0.66	0.44
Zr/Zr*	0.86	0.87	0.86	0.82	0.99	0.99	0.99	0.95	1.06	0.85
Hf/Hf*	0.92	0.87	0.94	0.92	0.95	1.06	1.06	1.04	0.99	0.86
Ti/Ti*	0.88	0.73	1.13	0.89	0.51	0.62	0.55	0.70	0.30	0.35

* Full data set in Appendix D

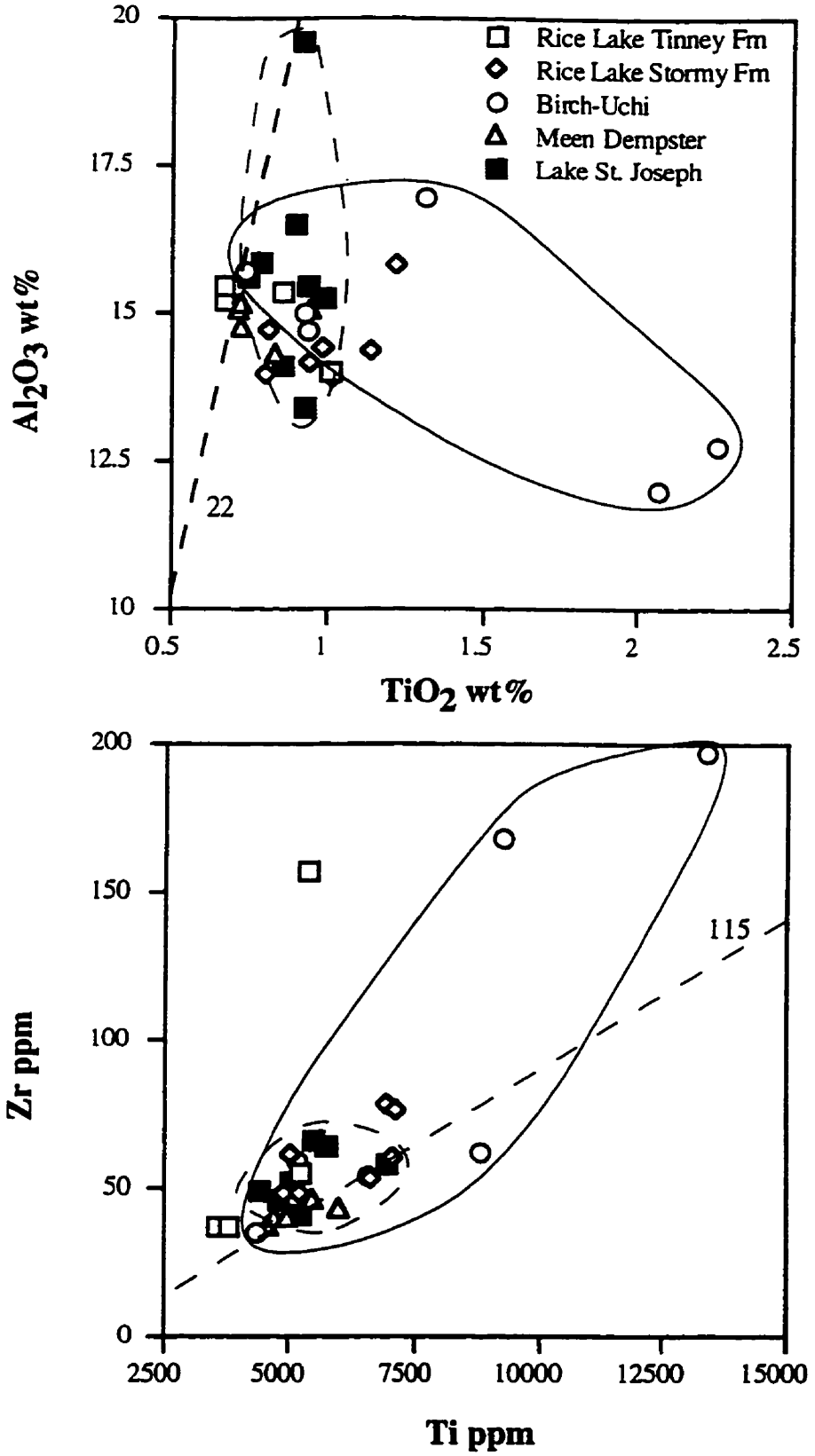

Figure 6.1. Interelement plots for tholeiitic rocks from the Confederation assemblage of the Uchi subprovince. Dashed lines represent chondritic ratios.

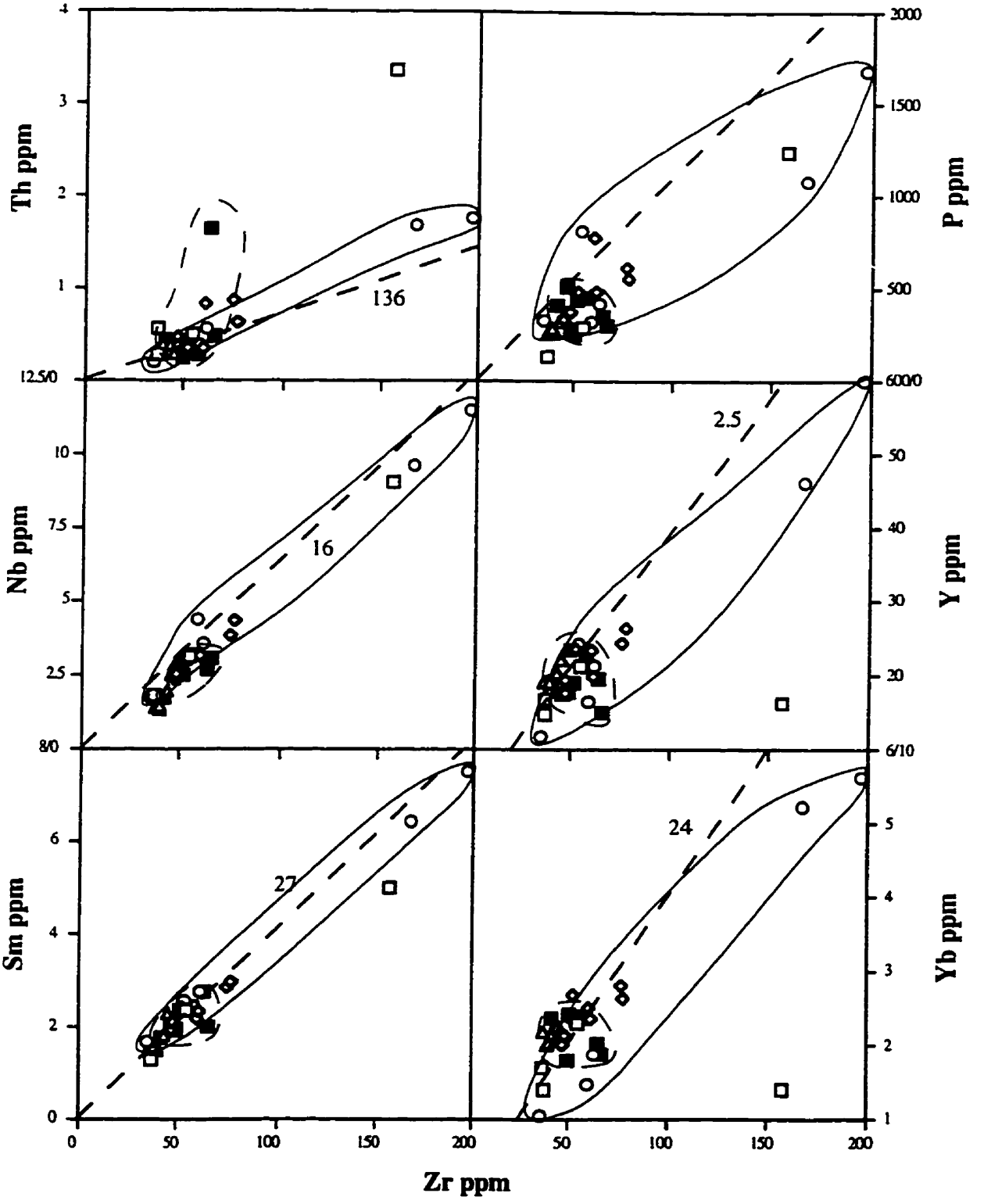

Figure 6.2. Interelement plots for tholeiitic rocks from the Confederation assemblage of the Uchi subprovince. Legend as for Figure 6.1. Dashed lines represent chondritic ratios.

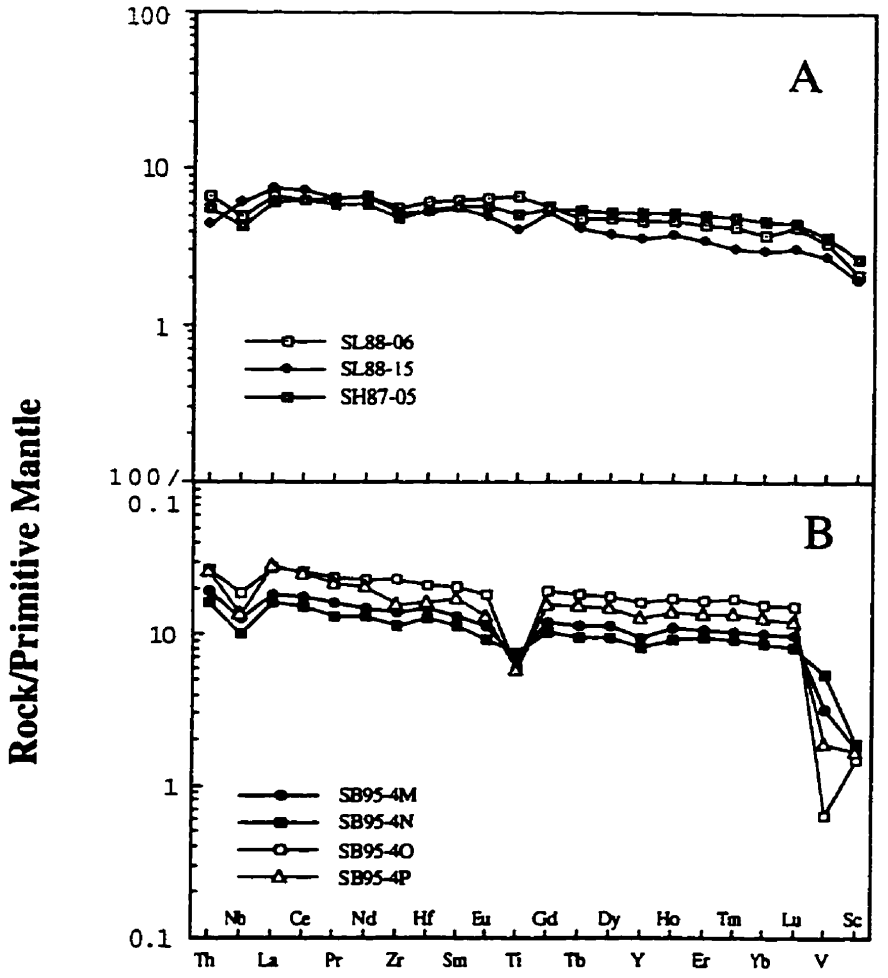

Figure 6.3. Primitive mantle normalised trace element diagrams for tholeiitic samples from the South Bay mine site, Birch-Uchi greenstone belt.

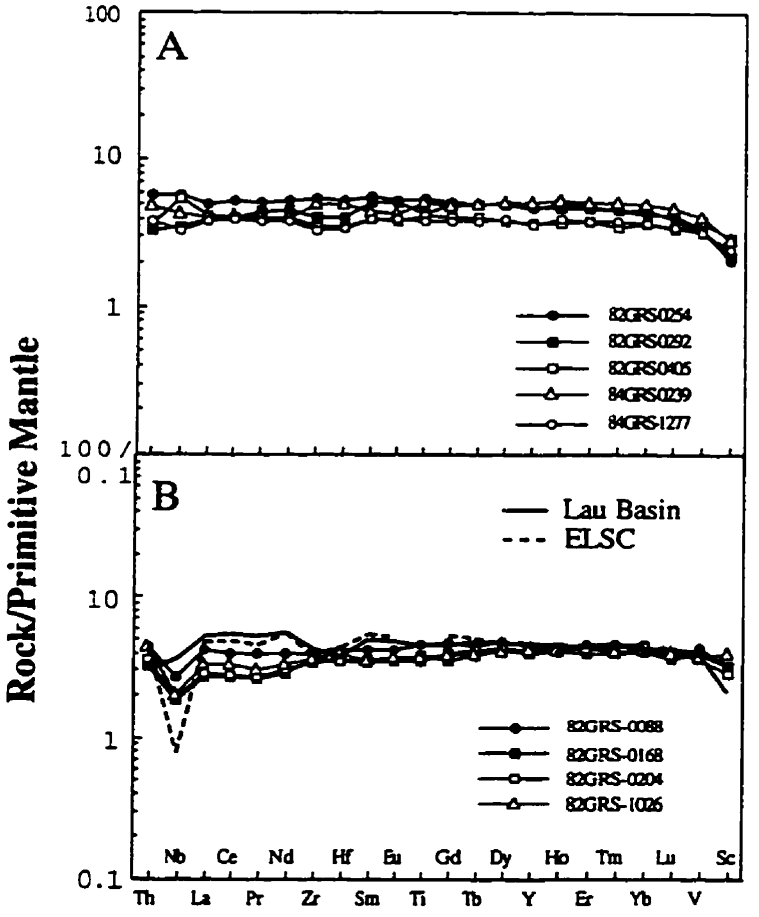

Figure 6.4. Primitive mantle normalised trace element diagrams for tholeiitic samples from the Confederation assemblage of the Meen-Dempster greenstone belt. Lau Basin data from Pearce et al. (1995), East Lau Spreading Centre (ELSC) data from Ewart et al. (1994).

Table 6.2. Representative analyses of selected elements for tholeiitic volcanic rocks from the Confederation assemblage of the . Meen-Dempster greenstone belt*

	Tholeiites					Subduction influenced tholeiites			
	82GRS-0254	82GRS-0292	82GRS-0405	84GRS-1277	84GRS-0239	82GRS-1026	82GRS-0168	82GRS-0088	82GRS-0204
SiO_2	46.56	48.27	48.41	54.77	57.65	49.88	50.12	50.81	51.43
TiO_2	1.14	0.95	0.69	0.94	1.18	0.73	0.72	0.84	0.73
Al_2O_3	16.43	15.07	14.06	16.82	17.33	15.16	15.07	14.30	14.78
Fe_2O_3	14.91	13.24	13.04	2.84	2.31	12.29	12.40	12.78	12.52
MgO	7.25	8.44	6.85	7.83	6.55	8.04	7.28	6.98	7.54
LOI	0.70	0.60	0.71	0.50	0.50	0.50	2.15	0.40	1.11
Mg#	0.52	0.58	0.54	0.86	0.86	0.59	0.56	0.55	0.57
Ti	7093	5535	5443	5007	6618	4769	5012	5997	4617
Cr	186	307	493	273	243	378	437	364	374
Ni	105	137	165	157	105	134	146	117	127
Nb	4.13	2.52	3.86	2.32	3.08	1.45	1.32	1.91	1.36
Zr	61	46	40	37	55	41	40	44	38
Hf	1.62	1.26	1.09	1.06	1.56	1.24	1.09	1.29	1.09
Th	0.49	0.28	0.31	0.32	0.41	0.38	0.28	0.38	0.30
La	3.43	2.71	2.90	2.66	2.76	2.30	1.87	2.83	1.95
Sm	2.49	2.31	1.75	1.74	1.98	1.58	1.50	1.83	1.61
Gd	3.08	2.97	2.40	2.28	2.85	2.31	2.11	2.80	2.38
Yb	2.13	2.25	1.84	1.81	2.49	2.04	2.00	2.23	2.17
Lu	0.31	0.29	0.25	0.26	0.35	0.29	0.27	0.27	0.30
(La/Yb)n	1.16	0.86	1.13	1.06	0.80	0.81	0.67	0.91	0.64
(La/Sm)n	0.89	0.76	1.07	0.99	0.90	0.94	0.80	1.00	0.78
(Gd/Yb)n	1.20	1.09	1.08	1.04	0.95	0.94	0.87	1.04	0.90
Al_2O_3/TiO_2	14	16	15	18	14	19	18	14	19
Zr/Hf	37	37	36	35	36	33	37	34	35
La/Nb	0.83	1.08	0.75	1.15	0.90	1.59	1.42	1.48	1.44
Th/Nb	0.12	0.11	0.08	0.14	0.13	0.26	0.21	0.20	0.22
Th/La	0.14	0.10	0.11	0.12	0.15	0.17	0.15	0.13	0.16
Zr/Y	2.83	2.10	2.35	2.25	2.40	2.16	2.27	2.19	1.99
Nb/Nb*	1.07	0.98	1.37	0.85	0.98	0.52	0.62	0.62	0.60
Zr/Zr*	1.00	0.84	0.88	0.85	1.16	1.06	1.16	0.98	1.01
Hf/Hf*	0.97	0.83	0.88	0.88	1.18	1.17	1.14	1.04	1.06
Ti/Ti*	1.01	0.84	1.05	0.99	1.10	0.99	1.11	1.05	0.93

* Full data set in Appendix D

systematically display pronounced negative Nb anomalies and lack the downturn at V on a primitive mantle normalised diagram (Nb/Nb* = 0.6-0.7; Fig. 6.4b). Zr/Y ratios are less variable than for the first mafic suite, ranging from 2.0-2.3.

6.2.3 Rice Lake greenstone belt

Both the Tinney and Stormy Lake formations of the Rice Lake greenstone belt comprise tholeiitic rocks. Of the two formations, the Tinney formation is compositionally the more varied as reflected in the greater range of Mg#'s, Fe and Mg contents (Table 6.3). This is evident in Figure 6.2 where samples define a much greater range than for the Stormy Lake Formation which tend to cluster around 50 ppm Zr. Silica contents of Tinney formation samples range from 49-51 wt.%, Fe_2O_3 = 10-15 wt.% and MgO = 6-9 wt.%, whereas, Stormy Lake samples display ranges of 49-51 wt.%, 13-16 wt.% and 6-8 wt.% respectively. As with samples from the Birch-Uchi belt, LREE abundances range from weakly depleted to enriched (La/Sm_n = 0.9-1.2). Negative Nb anomalies are present in the majority of samples (Nb/Nb* = 0.6-1.2).

6.2.4 Lake St. Joseph greenstone belt

The samples from the Lake St. Joseph belt are basalts and basaltic andesites ranging in composition from Mg- to Fe-tholeiites over a range of Mg# from 61-43 (SiO_2 = 49-52 wt.%; Fe_2O_3 = 10-13 wt.%; MgO = 4-10 wt.%; Table 6.4). For the majority of samples Ti/Zr ratios are near chondritic, whereas Al_2O_3/TiO_2 ratios scatter below the chondritic line (Fig. 6.1). In plots of trace elements versus Zr most samples cluster around primitive mantle values; zirconium is correlated with Sm and Nb. Zirconium/Th ratios vary from near to greater than chondritic, whereas Zr-Y and Zr-Yb cluster at generally subchondritic values (Fig. 6.2).

Light REE are variably enriched or depleted, whereas the HREE are generally flat (La/Sm_n = 0.8-1.3; Fig. 6.6). The majority of samples display zero to weakly negative Nb anomalies in conjunction with zero to slightly positive Zr and Hf anomalies (Nb/Nb* = 0.6-1.2; Fig. 6.6).

6.2.5 Discussion

Tholeiites of the Confederation assemblage can be divided into two suites: those with flat patterns and those with weakly depleted to enriched LREE in conjunction with negative

Table 6.3. Representative analyses of selected elements for tholeiitic volcanic rocks from the Confederation assemblage of the Rice Lake greenstone belt*.

	Tinney Formation				Stormy Lake Formation						
	RC95-11	RC95-9	RC95-12	RC95-10	RC95-8	RC96-1	RC95-6	RC95-5	RC95-7	RC96-16	RC96-14
SiO_2	51.52	49.22	61.11	49.85	50.63	49.92	51.15	49.83	49.08	50.82	51.04
TiO_2	0.67	0.67	0.86	1.01	0.81	0.82	0.95	1.14	1.22	0.99	1.02
Al_2O_3	15.20	15.46	15.38	14.03	13.96	14.72	14.18	14.36	15.83	14.43	13.89
Fe_2O_3	10.83	12.41	7.90	14.56	13.54	13.69	13.34	15.61	14.34	14.43	14.61
MgO	9.16	8.36	5.03	5.65	8.32	7.20	6.77	7.69	6.82	6.41	6.08
LOI	2.15	3.63	2.09	3.09	2.46	1.73	3.15	3.04	4.82	2.09	2.04
Mg#	65	60	58	46	57	54	53	52	51	49	48
Ti	3812	3558	5416	5238	4960	5288	5107	7118	6971	7100	6647
Cr	361	337	109	244	97	336	119	72	234	300	218
Ni	145	141	74	73	73	110	58	59	92	155	110
Nb	1.81	1.84	9.08	3.15	2.50	2.50	3.07	3.83	4.33	3.11	3.03
Zr	37	37	158	55	48	49	62	77	78	61	53
Hf	1.11	1.14	3.83	1.57	1.44	1.40	1.72	2.18	2.17	1.75	1.56
Th	0.29	0.56	3.36	0.50	0.46	0.36	0.83	0.86	0.62	0.34	0.34
La	1.55	1.92	24.06	3.58	2.73	3.14	4.45	5.27	4.74	3.58	3.65
Sm	1.29	1.47	5.02	2.37	1.94	2.10	2.35	2.84	2.97	2.19	2.42
Gd	1.75	2.18	4.08	3.16	2.52	2.70	3.14	3.90	3.92	3.32	3.21
Yb	1.41	1.70	1.40	2.31	2.01	2.12	2.35	2.80	2.62	2.50	2.67
Lu	0.20	0.26	0.21	0.34	0.28	0.31	0.36	0.43	0.39	0.39	0.41
(La/Yb)n	0.79	0.81	12.33	1.11	0.97	1.06	1.36	1.35	1.30	1.03	0.98
(La/Sm)n	0.78	0.84	3.09	0.97	0.91	0.97	1.22	1.20	1.03	1.06	0.98
(Gd/Yb)n	1.02	1.06	2.41	1.13	1.04	1.05	1.10	1.15	1.24	1.10	0.99
Al_2O_3/TiO_2	23	26	17	16	17	16	16	12	13	12	12
Zr/Hf	34	32	41	35	33	35	36	35	36	35	34
La/Nb	0.86	1.05	2.65	1.14	1.09	1.26	1.45	1.37	1.09	1.15	1.21
Th/Nb	0.16	0.31	0.37	0.16	0.18	0.14	0.27	0.22	0.14	0.11	0.11
Th/La	0.18	0.29	0.14	0.14	0.17	0.11	0.19	0.16	0.13	0.09	0.09
Zr/Y	2.55	2.23	9.74	2.62	2.75	2.54	3.16	3.16	2.98	2.62	2.27
Nb/Nb*	1.18	1.00	0.33	0.88	0.91	0.79	0.64	0.70	0.91	0.88	0.83
Zr/Zr*	1.17	1.02	0.93	0.92	1.02	0.92	1.04	1.04	1.05	1.08	0.90
Hf/Hf*	1.26	1.14	0.82	0.94	1.10	0.96	1.04	1.07	1.06	1.12	0.96
Ti/Ti*	1.01	0.79	0.47	0.76	0.89	0.88	0.74	0.85	0.81	1.04	0.94

* Full data set in Appendix D

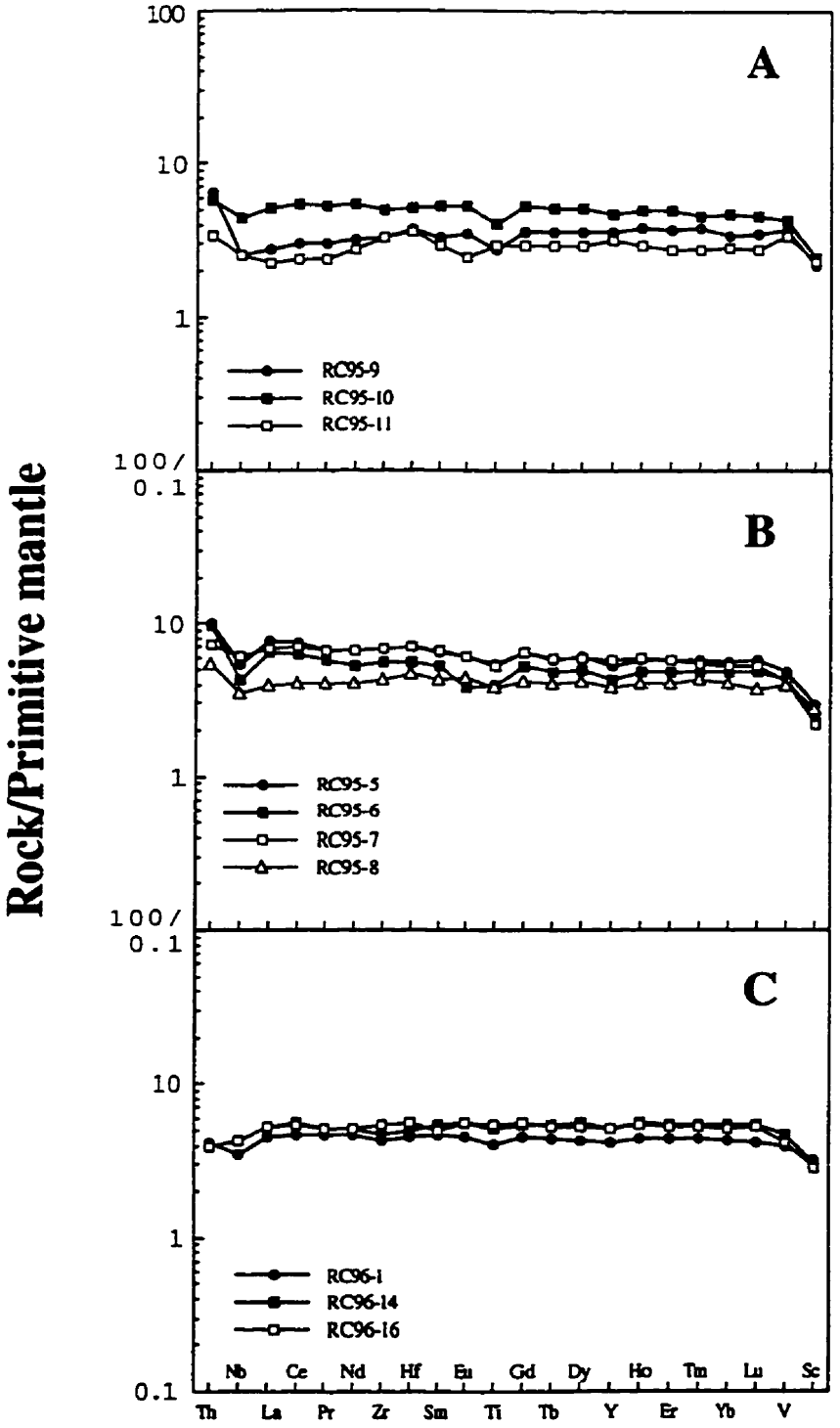

Figure 6.5. Primitive mantle normalised diagrams for tholeiitic basalts from the Confederation assemblage of the Rice Lake greenstone belt. A) Tinney formation, B) and C) Stormy Lake formation.

Table 6.4. Representative analyses of selected elements for tholeiitic volcanic rocks from the Confederation assemblage of the Lake St. Joseph greenstone belt*.

	Tholeiites							
	DL87-8B	DL87-9B	DL87-15A	LSJ95-3	DL87-11B	DL87-15C	DL87-9A	WL87-10A
SiO_2	49.22	50.59	52.20	48.26	49.64	50.82	53.79	52.14
TiO_2	0.79	0.75	0.86	0.94	0.99	0.93	0.92	0.90
Al_2O_3	15.86	15.61	14.09	15.47	15.28	13.41	19.62	16.49
Fe_2O_3	12.05	11.14	12.95	14.25	13.13	14.15	9.67	13.73
MgO	8.63	6.70	7.19	7.83	7.21	6.51	3.87	4.65
LOI	1.21	2.93	1.73	0.40	0.91	3.41	1.32	0.71
Mg#	61	57	55	55	55	50	47	43
Ti	4451	5244	4827	5774	6935	5097	5487	5122
Cr	290	334	369	250	365	88	358	259
Ni	124	145	60	102	168	46	133	92
Nb	2.68	1.75	2.37	2.67	3.20	2.52	3.09	2.75
Zr	49	42	47	65	59	52	67	51
Hf	1.50	1.26	1.43	1.96	1.62	1.56	1.78	1.45
Th	0.37	0.44	0.38	1.64	0.28	0.33	0.49	0.24
La	3.40	2.56	2.82	4.40	2.90	2.85	3.87	2.95
Sm	1.93	1.76	2.05	2.76	2.45	2.37	2.01	1.96
Gd	2.53	2.64	2.69	3.21	3.29	2.86	2.44	2.83
Yb	1.80	2.39	2.08	2.02	2.38	2.40	1.88	2.43
Lu	0.27	0.36	0.32	0.32	0.32	0.35	0.26	0.34
(La/Yb)n	1.35	0.77	0.97	1.56	0.87	0.85	1.47	0.87
(La/Sm)n	1.14	0.94	0.89	1.03	0.76	0.78	1.25	0.97
(Gd/Yb)n	1.16	0.91	1.07	1.32	1.14	0.98	1.07	0.96
AL_2O_3/TiO_2	21.00	17.7	17.19	15.8	13.0	15.58	21.0	19.0
Zr/Hf	32.94	33.3	32.61	33.0	36.1	33.58	37.4	35.0
La/Nb	1.27	1.46	1.19	1.64	0.91	1.13	1.25	1.07
Th/Nb	0.14	0.25	0.16	0.61	0.09	0.13	0.16	0.09
Th/La	0.11	0.17	0.13	0.37	0.10	0.12	0.13	0.08
Zr/Y	2.79	2.18	2.68	3.34	2.60	2.79	4.45	2.16
Nb/Nb*	0.78	0.63	0.78	0.62	1.18	0.83	0.76	0.94
Zr/Zr*	0.99	0.98	0.92	0.92	0.97	0.94	1.25	1.02
Hf/Hf*	1.09	1.07	1.02	1.01	0.98	1.01	1.22	1.06
Ti/Ti*	0.80	0.96	0.81	0.77	0.97	0.78	0.98	0.86

* Full data set in Appendix D

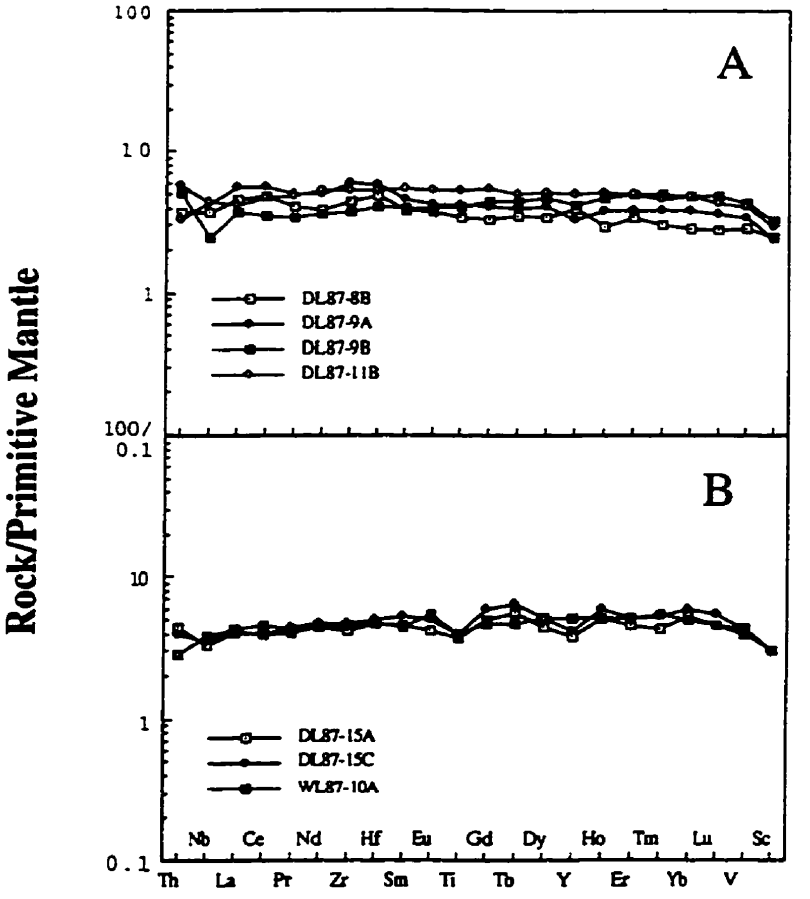

Figure 6.6. Primitive mantle normalised trace element diagrams for tholeiitic samples from the Confederation assemblage of the Lake St. Joseph greenstone belt.

Nb anomalies. In general both suites are present in all sampled greenstone belts (Figs. 6.3-6.6). The flat REE and absence of pronounced HFSE anomalies of the first suite of tholeiites, particularly in the Meen-Dempster belt, is similar to the Mg- to Fe-tholeiites found throughout the Superior Province and have been interpreted as plume related plateau tholeiites (Desrochers et al., 1993; Hollings and Wyman, 1997; Kerrich et al., 1998; Chapter 4).

The second suite is characterised by variable LREE in conjunction with moderate negative Nb anomalies. The LREE depleted character of the tholeiites in the Meen-Dempster belt suggests they are not crustally contaminated plateau tholeiites given that crustal contamination typically produces pronounced LREE enrichment (e.g. Sun et al., 1989). Rather it is suggested that the negative Nb anomalies reflects a subduction zone influence on a depleted MORB-like mantle source. Pearce et al. (1995) and Ewart et al. (1994) present data for LREE depleted basalts from the Lau basin where a range of Nb anomalies are interpreted to be the result of a variable subduction zone influence on the back arc mantle (Fig. 6.4). Gribble et al. (1996) have also documented interaction between MORB mantle and a subduction zone component in the Mariana trough back arc, resulting in primitive mantle normalized trace element patterns comparable to these Archean examples. Although the LREE enrichment observed in the other tholeiites that display weak Nb anomalies, precludes the elimination of crustal contamination as the source of the geochemical characteristics, they are interpreted to have a similar origin to the Meen-Dempster tholeiites. No xenocrystic zircons have been reported from the Confederation assemblage (Stott and Corfu, 1991), despite the presence of the North Caribou terrane along the Uchi paleo-continental margin. This argues strongly in favour of a subduction related origin for the Nb depletions, rather than contamination.

6.3 Calc alkaline volcanic rocks

Calc alkaline volcanic rocks are present in all the occurrences of the Confederation assemblage sampled in this study, and may comprise the dominant rock type of the assemblage. SiO_2 contents are typically higher than for tholeiites ranging from 46-68 wt.%.

6.3.1 Birch-Uchi greenstone belt

The calc alkaline samples from the Birch-Uchi belt are characterised by a limited range of SiO_2 contents, with only one sample greater than 55 wt.% (SiO_2 = 46-62 wt.%). This

range, in conjunction with higher than normal MgO contents, is more typical of tholeiitic suites; however, the suite as a whole displays variable LREE enrichment in conjunction with moderate negative Nb anomalies (La/Sm_n = 0.9-4.0; Nb/Nb* = 0.2-0.9; Fig. 6.7a). Samples scatter widely on the majority of element-ratio plots with the exception of Th/La_{pm} where clear trends are defined distinct from those of the other greenstone belts (Fig. 6.8; Table 6.5). The elevated Th contents of these rocks is unique within the Confederation assemblage and is reflected in high Th/La ratios (0.2-0.4).

Three mafic samples (SiO_2 = 48-52 wt.%; MgO = 3-7 wt.%; Fe_2O_3 = 13-18 wt.%) from the Dixie 19 diamond drill hole (DDH), located to the south west of the South Bay mine (Fig. 3.10), display somewhat atypical characteristics. They are progressively more depleted in Th, Nb and La relative to Ce on a primitive mantle normalised plot (Th/Nb = 0.04-0.09; Fig. 6.7b). The samples are LREE enriched with fractionated HREE (La/Sm_n = 1.4-1.6; Gd/Yb_n = 1.5-2.5; Table 6.5). The Th-Nb-La systematics of SJV91-1M, which has the most primitive Ni abundances (146 ppm) suggests that the two samples with lower Ni and Cr contents (Ni = 2-14 ppm), but higher absolute REE abundances and more extreme HFSE anomalies, may represent closed system fractionation products from this more primitive protolith. The two more evolved samples, are characterised by anomalously high phosphorous contents (0.9-1.7 wt.%). This suggests the accumulation of a P-rich minor phase such as apatite, and an unusual fractionation history, which may also account for the Zr-Hf anomalies.

Two mafic samples analysed from the bottom of the Dixie 3 DDH are characterised by SiO_2 contents of 50-52 wt.% and Fe_2O_3 = 14-15 wt.% in conjunction with moderate LREE enrichment and negative Ti and Nb anomalies (La/Sm_n = 2.3-2.4; Gd/Yb_n = 2; Nb/Nb* = 0.6-0.7; Fig. 6.7c; Table 6.5). They are similar to those at the top of the Dixie South area DDH (Fig. 6.7d). The two samples from the Dixie 3 area DDH are characterised by high MgO contents of 11-16 wt.%, whereas samples from the Dixie South area DDH have lower MgO contents of 4-5 wt.%. The broadly similar patterns but differing MgO contents suggest that the Dixie 3 samples may be the more primitive protolith for the Dixie South samples. Trace element characteristics of these rocks are broadly similar to rocks from the Northern Pickle assemblage of the Pickle Lake greenstone belt and basalts from the top of the stratigraphic sequence in the Lumby Lake belt (Chapter 4; Hollings and Wyman, 1998).

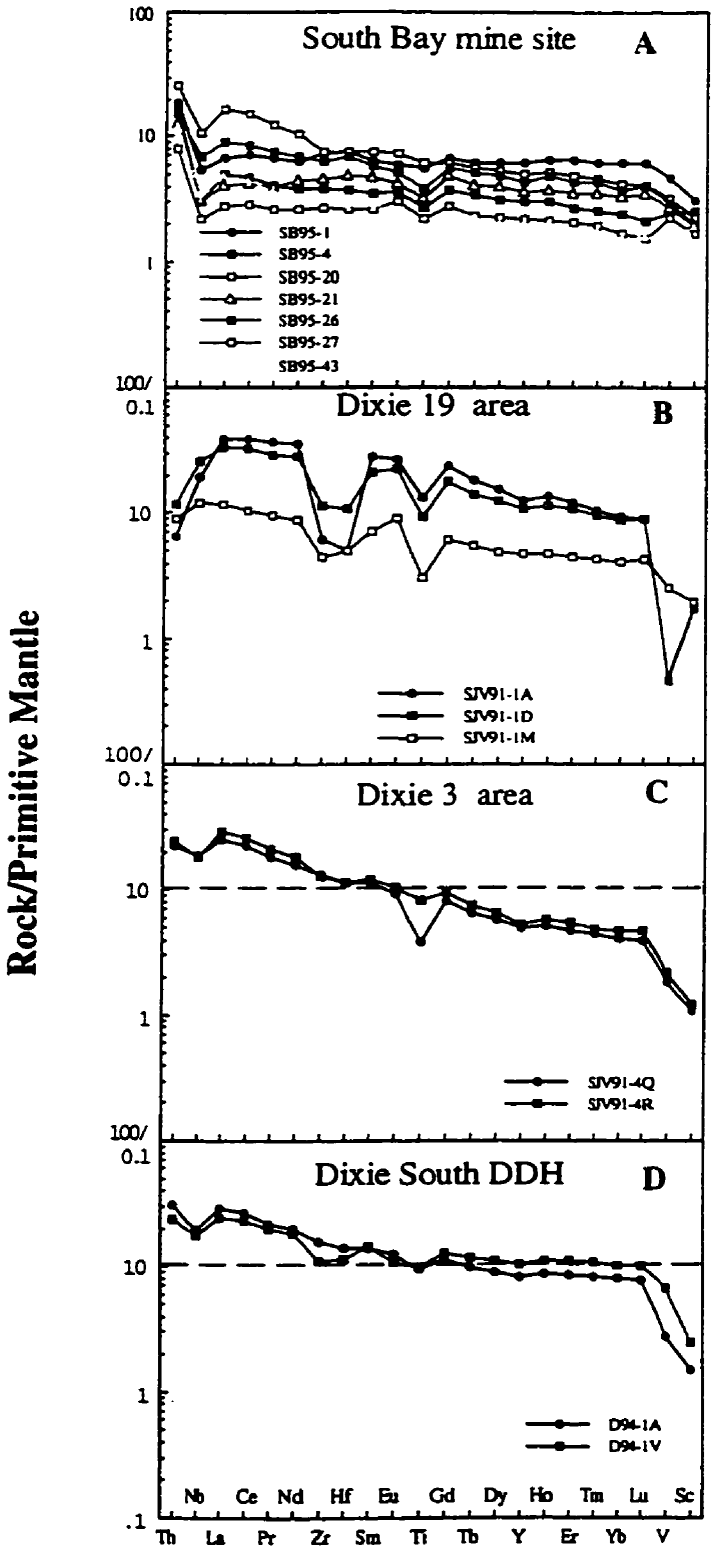

Figure 6.7. Primitive mantle normalised trace element diagrams for calc alkaline and OIB-like volcanic rocks from the Confederation assemblage of the Birch-Uchi belt. A) South Bay mine site, B) Dixie 19 area, C) Dixie 3 area and D) Dixie South DDH

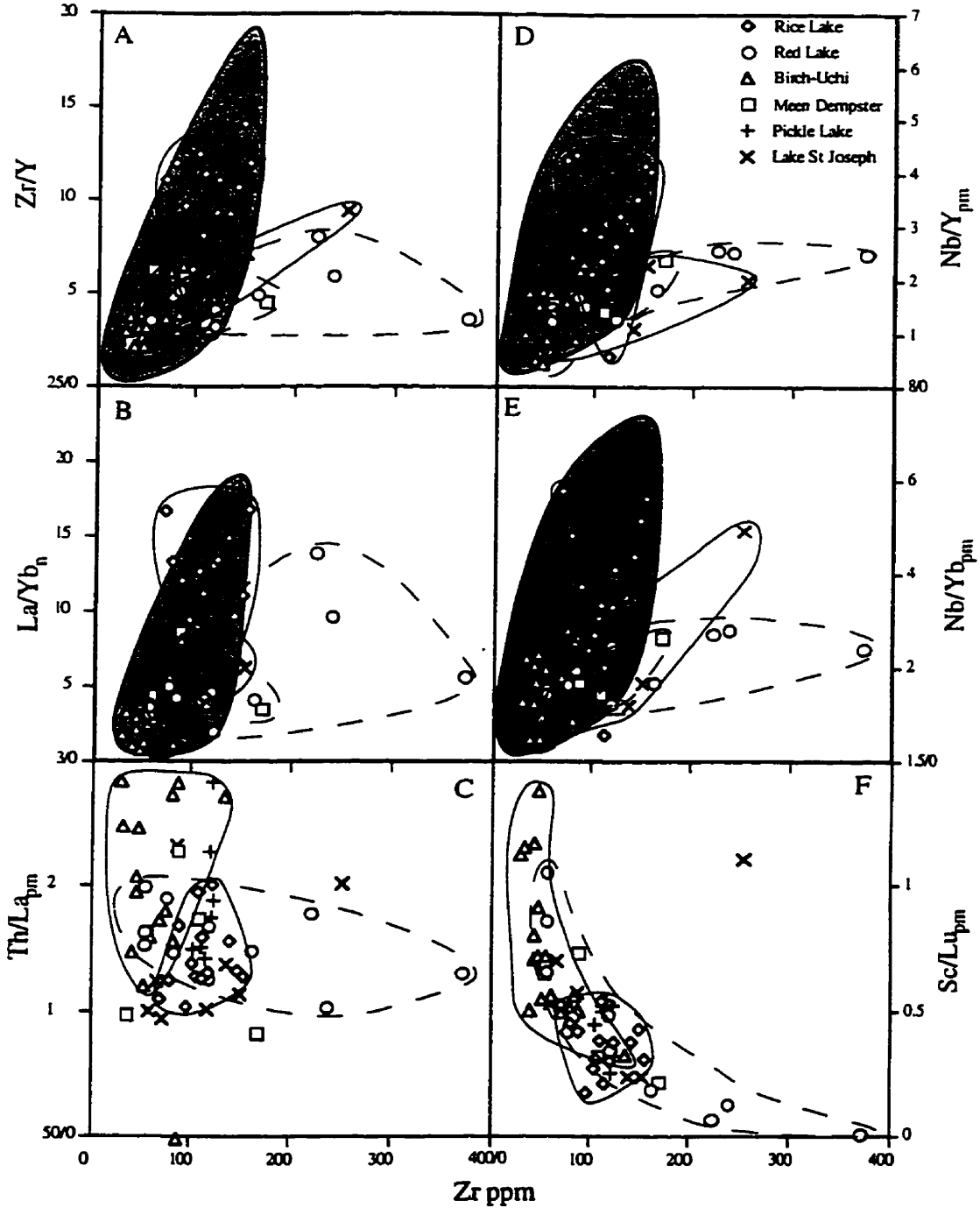

Figure 6.8. Plots of primitive mantle normalised ratios versus Zr for calc alkaline rocks from the Confederation assemblage of the Uchi subprovince. Shaded field is data from Sturgeon Lake greenstone belt, Wabigoon subprovince (Wyman et al., in prep).

Table 6.5. Representative analyses of selected elements for calc alkaline and alkaline volcanic rocks from the Confederation assemblage of the Birch-Uchi greenstone belt*.

	Calc alkaline							Transitional alkali basalts						
								Dixie 3 DDH		Dixie South DDH		Dixie 19 DDH		
	SB95-4	SB95-20	SB95-21	SB95-23	SB95-26	SB95-27	SB95-43	SJV91-4Q	SJV91-4R	D94-1A	D94-1V	SJV91-1A	SJV91-1D	SJV91-1M
SiO_2	48.66	46.58	47.99	47.67	48.35	47.52	51.98	50.34	51.63	52.12	51.65	48.02	51.06	51.99
TiO_2	0.59	1.43	0.82	0.92	0.89	0.61	0.45	1.92	1.90	2.24	2.11	2.97	2.02	0.64
Al_2O_3	16.29	17.76	15.48	15.44	16.43	16.02	17.75	17.47	17.35	13.21	12.76	13.40	14.08	15.84
Fe_2O_3	11.53	14.21	13.50	15.23	12.48	11.48	9.82	14.00	15.09	16.73	17.72	18.07	17.91	12.59
MgO	9.60	6.97	8.26	8.95	7.67	10.28	4.41	15.62	10.99	4.56	4.04	3.84	3.09	7.27
LOI	3.95	3.09	2.46	2.88	2.30	3.79	5.54	7.82	6.28	0.25	0.15	0.00	0.91	0.60
Mg#	65	52	57	56	58	66	50	71	62	37	33	32	28	56
Ti	3506	8040	4133	4996	4948	2848	2325	4919	10815	12534	12591	17103	11915	3952
Cr	398	337	282	268	242	389	371	36	50	1	6	4	18	46
Ni	171	235	177	211	191	248	91	63	70	1	20	2	14	146
Nb	2.16	7.67	2.25	3.93	4.85	1.56	2.45	13.22	12.95	13.80	12.77	13.69	18.42	8.57
Zr	43	85	51	55	71	30	34	146	143	177	122	68	128	50
Hf	1.14	2.32	1.50	1.60	2.14	0.82	0.86	3.53	3.52	4.34	3.56	1.56	3.15	1.54
Th	1.44	2.21	1.08	0.64	1.30	0.67	1.02	1.90	2.10	2.59	2.03	0.55	0.99	0.75
La	3.46	11.50	2.81	4.33	6.12	1.91	3.34	17.44	19.80	20.10	16.84	27.05	23.42	8.07
Sm	1.55	3.34	2.10	2.42	2.53	1.17	1.26	4.97	5.32	6.29	6.42	12.56	9.24	3.17
Gd	2.19	3.63	2.88	2.83	3.30	1.63	1.45	4.88	5.63	6.75	7.67	14.03	10.41	3.62
Yb	1.18	2.06	1.62	1.36	1.85	0.83	0.76	2.02	2.34	3.90	5.01	4.59	4.36	2.01
Lu	0.16	0.30	0.26	0.21	0.30	0.11	0.12	0.29	0.35	0.57	0.74	0.66	0.67	0.32
(La/Yb)n	2.11	4.00	1.24	2.29	2.37	1.65	3.15	6.20	6.07	3.70	2.41	4.23	3.85	2.88
(La/Sm)n	1.44	2.22	0.86	1.16	1.56	1.05	1.72	2.27	2.41	2.07	1.69	1.39	1.64	1.64
(Gd/Yb)n	1.54	1.46	1.47	1.72	1.47	1.62	1.57	2.00	1.99	1.43	1.27	2.53	1.97	1.49
Al_2O_3/TiO_2	27	13	22	18	20	33	45	21	9	6	6	5	7	24
Zr/Hf	38	37	34	35	33	37	39	41	40	41	34	44	38	33
La/Nb	1.60	1.50	1.25	1.10	1.26	1.23	1.36	1.32	1.53	1.46	1.32	1.98	1.27	0.94
Th/Nb	0.66	0.29	0.48	0.16	0.27	0.43	0.42	0.14	0.16	0.19	0.16	0.04	0.05	0.09
Th/La	0.41	0.19	0.38	0.15	0.21	0.35	0.31	0.11	0.11	0.13	0.12	0.02	0.04	0.09
Zr/Y	3.16	3.78	3.13	3.83	3.59	2.97	3.74	6.43	5.93	4.68	2.60	1.20	2.62	2.38
Nb/Nb*	0.57	0.59	0.80	0.88	0.73	0.80	0.66	0.65	0.57	0.60	0.68	0.49	0.73	0.91
Zr/Zr*	1.06	0.86	0.99	0.87	1.01	1.02	0.99	0.99	0.86	0.95	0.67	0.19	0.47	0.57
Hf/Hf*	1.02	0.85	1.05	0.91	1.11	1.01	0.91	0.86	0.77	0.84	0.71	0.16	0.45	0.63
Ti/Ti*	0.75	0.91	0.66	0.76	0.68	0.81	0.68	0.40	0.78	0.76	0.71	0.51	0.48	0.46

* Full data set in Appendix D

Four basaltic andesites and andesites from the Dixie 18 DDH comprise a third distinct suite of samples (SiO_2 = 52-60 wt.%; Fe_2O_3 = 15-17; MgO = 2.5-7.3; Fig. 6.9; Table 6.6). The high P_2O_5 contents (0.2-0.4 wt.%) are comparable to icelandites which are defined by Jackson and Fyon (1991) as a rock of intermediate composition with P_2O_5 >0.3 wt.%. Jackson and Fyon (1991) state that two types of icelandite have been recognised in the Abitibi subprovince, with the two groups having either more or less than 2 wt.% TiO_2. Samples from this study have TiO_2 of 1.3 to 2.1 wt.% and would appear to be transitional between the two types. The LREE are moderately enriched and the HREE are weakly fractionated (La/Sm_n = 1.2-1.5; Gd/Yb_n = 1.0-1.3). High absolute REE abundances, La/Nb ratios greater than unity (1.11-1.35) and low Th/Nb ratios (0.15-0.21), in conjunction with the elevated total REE content, are consistent with the derivation of the icelandites by fractionation of tholeiites without significant crustal assimilation.

6.3.2 Meen-Dempster greenstone belt

Two distinct suites of calc alkaline rocks have been recognised within the Confederation assemblage of the Meen-Dempster belt. The first suite comprises two samples where SiO_2 contents are 48 and 55 wt.%, Fe_2O_3 = 9 and 11 wt.% and MgO = 4 and 12 wt.%. They are characterised by strongly enriched LREE and flat to moderately fractionated HREE (La/Sm_n =3.0-3.1; Gd/Yb_n = 1.0-1.9; Fig. 6.10a). Sample 82GRS-0056 is a high Mg basalt (SiO_2 = 48 wt.%; MgO = 12 wt.%; Table 6.6) and consequently likely represents a fairly primitive sample given the high Ni and Cr contents (565 and 880 ppm respectively). In contrast, 82GRS-0297 is an andesite with an SiO_2 content of 56 wt.% and MgO of 5 wt.%. Thorium/La ratios are relatively high at 0.2-0.3, as are Zr/Y ratios (5.8 and 6.4). These two samples display pronounced negative Nb and Ti anomalies in conjunction with negative to positive Zr and Hf anomalies (Nb/Nb^* = 0.2-0.3; Zr/Zr^* = 0.7-1.4; Fig 6.10a).

Two basalts and one basaltic andesite comprise the second suite (SiO_2 = 47-56 wt.%). The basalts display significantly higher Fe_2O_3 contents (19-20 wt.%) than other mafic suites, in conjunction with the lowest MgO (4-5 wt.%), whereas the basaltic andesite has lower Fe_2O_3 (4 wt.%) but higher MgO (7 wt.%). Titanium and P_2O_5 contents are higher than in the other mafic suite (~2 wt.% versus <1.1 wt % for TiO_2) whereas Ni and Cr are low (Table 6.6). These samples are characterised by moderately enriched LREE and

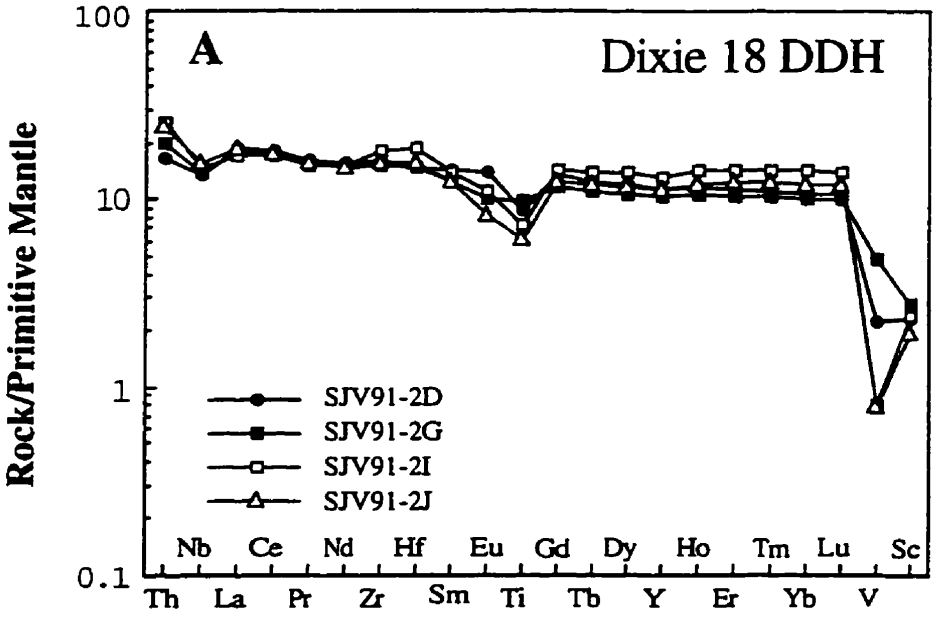

Figure 6.9. Primitive mantle normalised diagram for icelandites from the DIXIE 18 DDH, Birch-Uchi greenstone belt.

Table 6.6. Representative analyses of selected elements for calc alkaline volcanic rocks from the Confederation assemblage of the Birch-Uchi and Meen-Dempster greenstone belts*.

	Birch-Uchi belt				Meen-Dempster belt				
	Dixie 18 DDH Icelandites				Intermediate calc alkaline		OIB-like		
	SJV91-2D	SJV91-2G	SJV91-2I	SJV91-2J	82GRS-0056	82GRS-0297	82GRS-1187	82GRS-0106	84GRS-0032
SiO_2	54.27	52.58	56.48	59.98	47.93	55.69	47.68	48.57	56.33
TiO_2	1.92	2.11	1.57	1.33	0.31	0.71	2.22	1.90	2.01
Al_2O_3	12.48	13.43	12.27	10.61	11.49	13.77	13.14	12.52	16.67
Fe_2O_3	15.72	14.75	16.43	17.02	10.96	9.38	19.87	19.09	4.37
MgO	3.49	4.39	2.52	7.30	12.32	4.48	4.38	5.36	7.14
LOI	0.20	0.15	0.00	0.25	3.41	1.52	0.10	0.00	0.10
Mg#	*33*	*40*	*25*	*49*	*0.71*	*0.51*	*0.33*	*0.38*	*0.78*
Ti	11276	12734	9383	8011	2038	5227	14937	11747	6282
Cr	20	6	5	3	880	505	5	43	58
Ni	21	20	2	2	566	88	23	65	46
Nb	9.53	10.09	10.48	11.04	2.28	3.65	14.23	11.51	6.03
Zr	183	169	202	176	57	88	172	127	103
Hf	4.58	4.59	5.75	4.91	1.41	2.19	4.05	3.35	2.66
Th	1.43	1.67	2.20	2.10	1.36	5.05	1.79	1.27	0.93
La	12.84	12.59	11.61	12.70	6.71	17.92	17.55	6.61	5.74
Sm	6.46	5.47	6.21	5.48	1.46	3.69	7.02	4.80	3.95
Gd	8.12	7.06	8.45	7.43	1.39	3.39	7.10	5.01	4.36
Yb	5.32	4.95	7.01	5.96	1.11	1.49	3.69	2.60	2.76
Lu	0.78	0.74	1.04	0.89	0.17	0.20	0.52	0.34	0.39
(La/Yb)n	1.73	1.82	1.19	1.53	4.35	8.61	3.41	1.82	1.49
(La/Sm)n	1.28	1.49	1.21	1.50	2.97	3.14	1.62	0.89	0.94
(Gd/Yb)n	1.26	1.18	1.00	1.03	1.04	1.88	1.59	1.59	1.31
Al_2O_3/TiO_2	7	6	8	8	33	16	5	6	8
Zr/Hf	40	37	35	36	41	40	42	38	39
La/Nb	1.35	1.25	1.11	1.15	2.95	4.92	1.23	0.57	0.95
Th/Nb	0.15	0.17	0.21	0.19	0.60	1.38	0.13	0.11	0.15
Th/La	0.11	0.13	0.19	0.16	0.20	0.28	0.10	0.19	0.16
Zr/Y	3.50	3.62	3.36	3.43	6.24	5.79	4.48	4.69	3.73
Nb/Nb*	0.69	0.73	0.87	0.79	0.26	0.13	0.86	1.35	0.88
Zr/Zr*	1.08	1.12	1.23	1.16	1.36	0.74	0.88	1.02	1.04
Hf/Hf*	0.98	1.10	1.27	1.17	1.21	0.67	0.75	0.98	0.97
Ti/Ti*	0.62	0.81	0.51	0.50	0.57	0.58	0.84	0.95	1.03

* Full data set in Appendix D

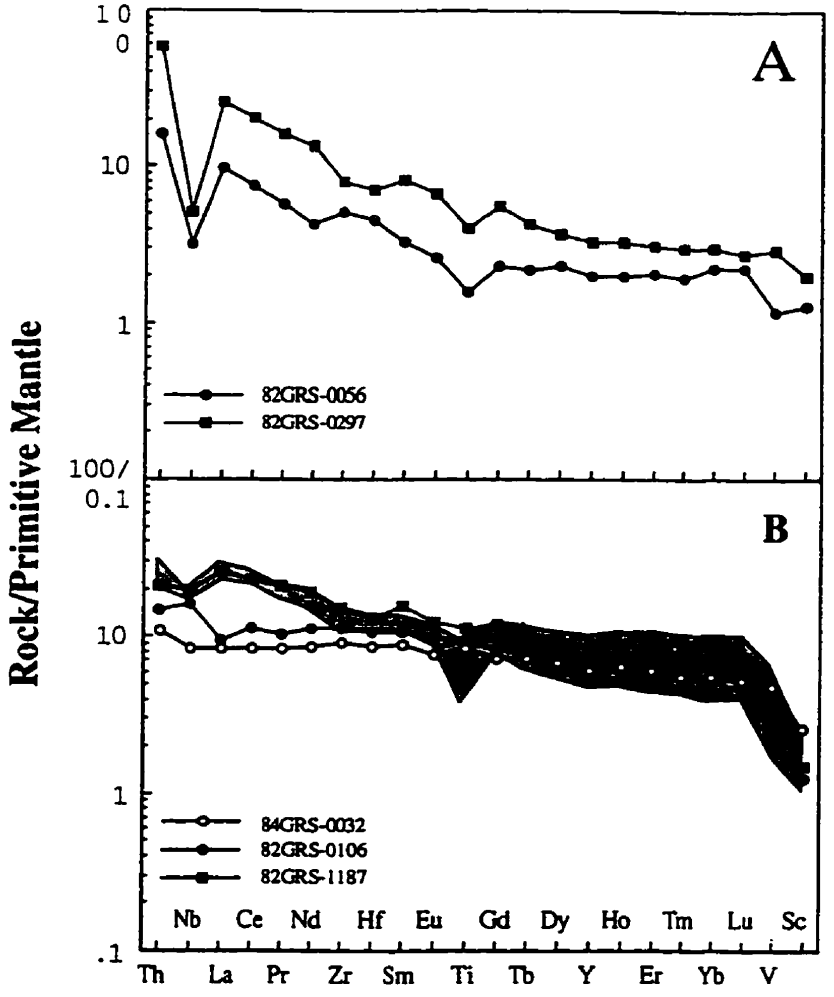

Figure 6.10. Representative primitive mantle normalised diagrams for calc alkaline (A) and alkaline (B) samples from the Confederation assemblage of the Meen-Dempster greenstone belt. Shaded field represents OIB-like rocks from the Dixie 3 and Dixie South areas of the Birch-Uchi belt.

fractionated HREE (La/Sm_n = 0.9-1.6; Gd/Yb_n = 1.6-1.6; Fig. 6.10b; Table 6.6). They display weak but variable Nb, Zr and Hf anomalies but lack significant Ti anomalies (Fig. 6.10b). One of the two Fe-rich basalts has lower REE abundances and less fractionated REE, with a maximum at Ce and a downturn at La, in conjunction with a positive Nb anomaly and a Th/Ce ratio of 0.06. The other has greater REE abundance and smoothly fractionated REE with a negative Nb anomaly and Th/Ce of 0.04. These rocks are comparable to the OIB-like rocks of the Birch-Uchi greenstone belt (Fig. 6.7c and d).

6.3.3 Rice Lake greenstone belt

Mafic to intermediate rocks from the Rice Lake belt display SiO_2 of 50-68 wt.%, Fe_2O_3 from 4-15 wt.%, and MgO from 1-5 wt.%. The trace element patterns are similar to the more typical calc alkaline rocks described above from the Meen-Dempster belt. They display pronounced LREE enrichment in conjunction with strongly negative Nb and variable negative Ti anomalies (La/Sm_n = 2.3-4.6; Nb/Nb* = 0.1-0.4; Fig. 6.11). However, a number of samples are distinctive in that they are characterised by weakly positive Zr and Hf anomalies, not seen in the samples from other areas (Table 6.7). The basalts and andesites of the Rice Lake belt fall in fields distinct from the majority of samples on Figure 6.8, and typically lie on vertical trends.

6.3.4 Lake St. Joseph greenstone belt

Mafic to intermediate rocks from the Lake St. Joseph belt display SiO_2 of 45-60 wt.%, Fe_2O_3 from 6-16 wt.%, and MgO from 3-10 wt.%. The majority are LREE enriched with weakly fractionated HREE and pronounced negative Nb anomalies (La/Sm_n = 1.3-2.7; Gd/Yb_n = 1.1-2.3; Nb/Nb* = 0.1-0.3; Fig. 6.12; Table 6.8). Sample PL95-40 is an outlier to the suite and is characterised by greater LREE enrichment and more fractionated HREE (La/Sm_n = 3.8; Gd/Yb_n = 10; Fig. 6.12). The low SiO_2 content of the basalt and high Ni and Cr contents preclude it having fractionated from the remainder of the suite (Table 6.8).

6.3.5 Pickle Lake greenstone belt

The nine calc alkaline samples from the Pickle Lake belt are predominantly basaltic andesites to andesites (SiO_2 = 54-60 wt.%; Fe_2O_3 = 10-15 wt.%; Table 6.8). They are characterised by moderate to strong LREE enrichment in conjunction with weakly fractionated HREE (La/Sm_n = 2.0-2.5; Gd/Yb_n = 1.2-1.4; Fig. 6.13a & b). Pronounced

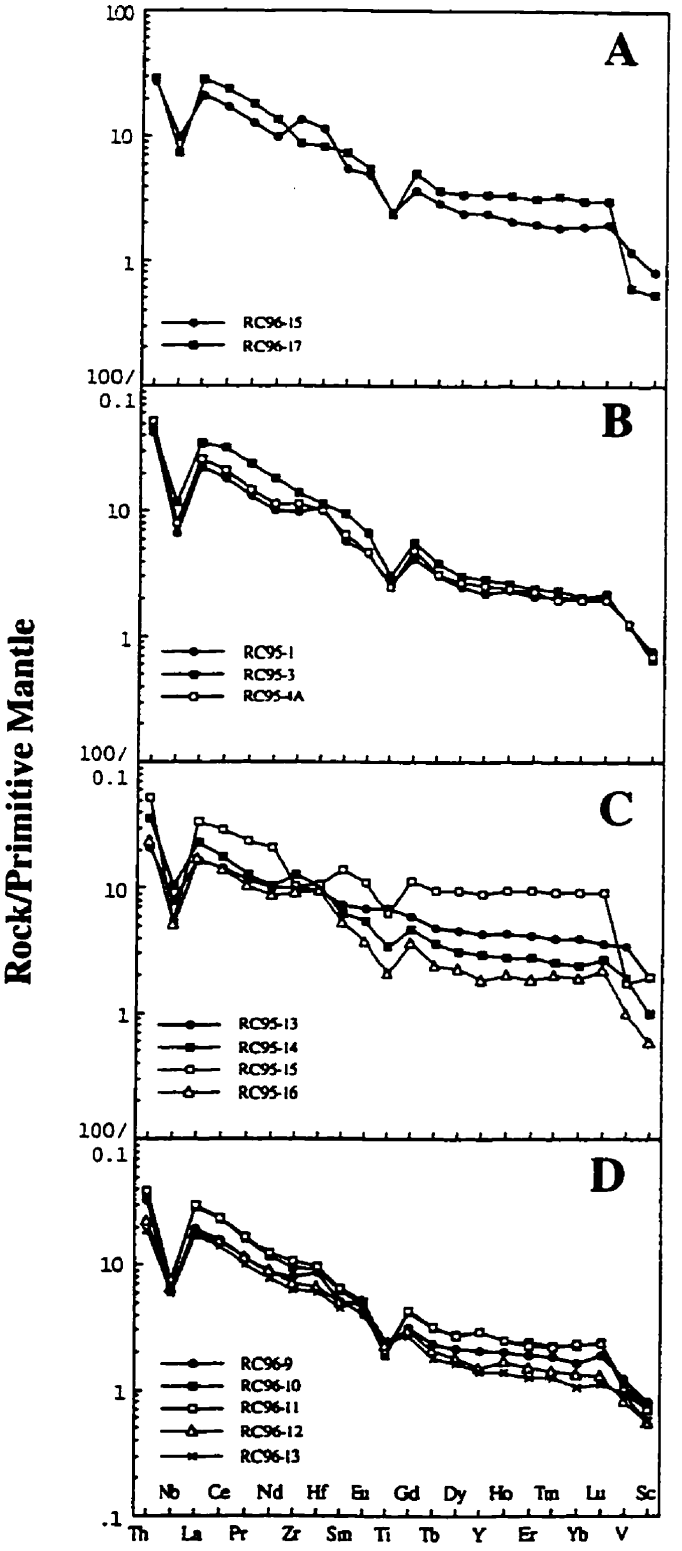

Figure 6.11. Primitive mantle normalized diagrams for calc alkaline samples from the Confederation assemblage of the Rice Lake belt. A = Gunnar formation, B-D = Narrows Formation

Table 6.7. Representative analyses of selected elements for calc alkaline volcanic rocks from the Confederation assemblage of the Rice Lake greenstone belt*.

	Gunnar Fm		Narrows Formation											
	RC96-15	RC96-17	RC95-14	RC96-9	RC95-1	RC95-3	RC95-4A	RC96-13	RC96-12	RC95-13	RC95-16	RC96-11	RC96-8	RC96-10	RC95-15
SiO_2	65.92	68.13	61.09	64.99	64.26	65.51	65.28	60.82	62.99	50.08	62.18	67.82	72.22	67.90	57.79
TiO_2	0.45	0.46	0.67	0.50	0.55	0.67	0.53	0.52	0.53	1.39	0.54	0.44	0.35	0.41	1.30
Al_2O_3	16.95	16.03	17.17	17.10	16.54	15.30	16.14	19.44	17.17	17.16	16.68	15.57	12.64	14.59	13.76
Fe_2O_3	5.08	4.86	7.72	5.42	5.42	5.65	5.09	5.72	5.08	13.19	5.49	4.66	5.82	4.24	14.50
MgO	2.68	1.18	4.15	2.75	2.72	2.62	2.33	2.53	2.09	5.19	2.12	1.76	1.59	1.01	2.58
LOI	3.25	2.88	3.90	3.09	2.72	1.68	1.78	2.78	5.48	6.44	7.13	1.78	0.96	4.33	4.93
Mg#	54	35	54	53	52	51	50	49	47	46	46	45	38	34	28
Ti	3110	3023	4474	2911	3390	3974	3166	3155	2930	8948	2657	2670	2005	2487	8134
Cr	19	7	59	31	38	30	31	42	31	76	33	14	21	40	8
Ni	24	5	60	36	38	24	35	38	30	93	23	14	2	88	7
Nb	7.00	5.16	7.44	4.31	4.71	8.31	5.67	4.26	4.61	5.61	3.68	5.41	26.84	4.98	3.77
Zr	151	98	144	90	111	157	125	71	80	114	105	122	308	108	115
Hf	3.49	2.53	3.19	2.71	3.30	3.49	3.13	1.89	2.07	2.96	2.90	3.04	8.11	2.84	3.11
Th	2.33	2.45	3.01	2.77	3.64	3.74	4.42	1.61	1.89	1.77	2.00	3.33	6.86	3.10	4.49
La	14.33	19.30	15.62	13.37	15.17	23.73	17.78	11.91	12.28	11.34	11.69	20.64	45.94	19.82	22.91
Sm	2.39	3.27	2.82	2.30	2.59	4.22	2.91	2.05	2.25	3.22	2.36	2.88	9.53	2.80	6.17
Gd	2.18	2.98	2.80	1.85	2.46	3.34	2.85	1.62	1.76	3.59	2.12	2.55	9.01	2.50	6.84
Yb	0.94	1.49	1.17	0.80	0.98	1.02	0.96	0.51	0.66	1.92	0.94	1.14	5.47	1.13	4.55
Lu	0.14	0.23	0.20	0.14	0.15	0.16	0.14	0.08	0.09	0.27	0.16	0.17	0.88	0.18	0.68
(La/Yb)n	10.93	9.28	9.54	11.96	11.14	16.73	13.32	16.62	13.25	4.24	8.89	12.95	6.02	12.60	3.61
(La/Sm)n	3.88	3.81	3.58	3.75	3.78	3.63	3.94	3.76	3.53	2.28	3.20	4.63	3.11	4.57	2.40
(Gd/Yb)n	1.92	1.65	1.97	1.91	2.08	2.71	2.46	2.61	2.19	1.55	1.86	1.84	1.36	1.83	1.24
Al_2O_3/TiO_2	33	32	23	35	29	23	30	37	35	11	37	35	38	35	10
Zr/Hf	43	39	45	33	34	45	40	37	39	38	36	40	38	38	35
La/Nb	2.05	3.74	2.10	3.11	3.22	2.86	3.13	2.80	2.66	2.02	3.18	3.81	1.71	1.98	6.08
Th/Nb	0.33	0.47	0.41	0.64	0.77	0.45	0.78	0.38	0.41	0.31	0.54	0.61	0.26	0.62	1.19
Th/La	0.16	0.13	0.19	0.21	0.24	0.16	0.25	0.14	0.15	0.16	0.17	0.16	0.15	0.16	0.20
Zr/Y	14.02	6.26	10.62	9.65	11.29	11.97	11.00	11.02	11.92	5.85	12.47	9.20	5.82	8.04	2.78
Nb/Nb*	0.38	0.22	0.36	0.25	0.25	0.31	0.25	0.28	0.30	0.42	0.25	0.20	0.48	0.19	0.14
Zr/Zr*	1.86	0.88	1.58	1.19	1.29	1.07	1.29	1.06	1.06	1.19	1.37	1.21	1.00	1.12	0.60
Hf/Hf*	1.56	0.82	1.27	1.30	1.39	0.86	1.17	1.02	0.99	1.13	1.37	1.10	0.95	1.07	0.62
Ti/Ti*	0.54	0.38	0.63	0.56	0.53	0.42	0.43	0.69	0.58	1.04	0.47	0.39	0.09	0.37	0.50

* Full data set in Appendix D

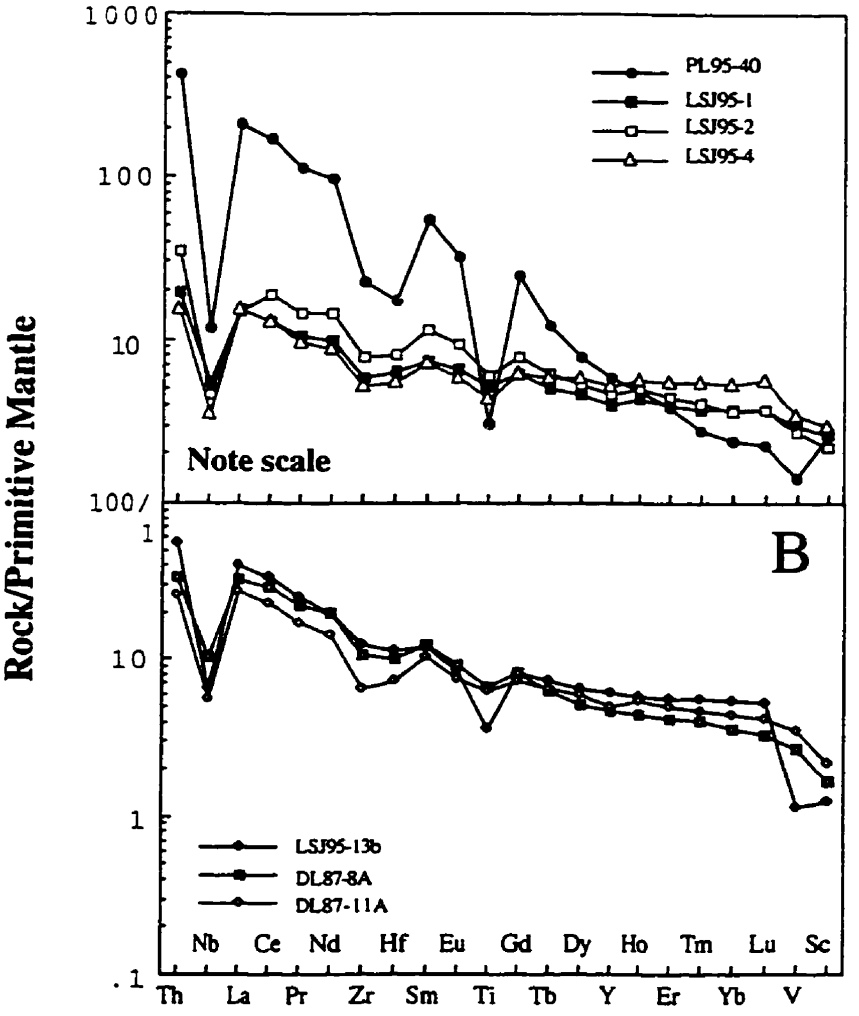

Figure 6.12. Representative primitive mantle normalised diagrams for calc alkaline samples from the Confederation assemblage of the Lake St. Joseph greenstone belt.

Table 6.8. Representative analyses of selected elements for calc alkaline volcanic rocks from the Confederation assemblage of the Lake St. Joseph, Red Lake and Pickle Lake greenstone belts*.

	Lake St. Joseph belt					Red Lake belt							Pickle Lake belt				
	P1.95-40	LSJ95-2	LSJ95-4	DH87-8A	DH87-11A	R1.95-30	R1.95-14	R1.95-28	R1.95-29	R1.95-15	R1.95-3	R1.95-2	P1.-17A	P1.95-21A	P1.95-21B	P1.-17B	P1.95-17
SiO_2	54.58	55.22	44.89	52.04	49.53	51.77	47.77	52.12	49.73	58.14	59.20	60.98	62.33	54.60	54.80	52.83	54.91
TiO_2	0.64	1.22	0.90	1.28	1.15	0.58	0.59	1.17	0.65	1.59	0.87	1.13	0.63	1.36	1.44	1.47	1.71
Al_2O_3	13.80	16.71	16.50	14.65	16.58	17.78	17.59	15.89	16.88	13.04	14.60	14.58	16.71	12.15	12.67	11.26	13.11
Fe_2O_3	6.43	9.58	14.86	11.88	15.56	7.36	12.70	12.45	10.44	14.82	9.67	10.40	8.41	16.33	15.79	16.77	17.91
MgO	9.63	4.01	8.63	7.77	4.11	2.84	4.25	3.71	2.43	2.23	1.44	1.78	2.49	1.90	1.76	1.82	2.79
LOI	0.55	0.40	0.86	0.81	0.55	11.35	8.69	11.23	12.74	4.88	0.45	0.30	0.70	1.21	0.20	0.15	0.20
Mg#	77	48	56	59	37	46	42	40	34	25	44	27	39	34	34	33	26
Ti	3991	7710	5663	8778	8151	3421	3319	6935	3977	9501	4683	6963	3277	8140	9093	8423	10110
Cr	448	190	294	290	380	116	176	185	103	144	52	4	184	100	101	195	191
Ni	316	122	127	201	263	162	222	110	151	3	45	5	50	25	27	22	3
Nb	8.42	3.27	2.50	7.32	4.00	3.05	3.18	4.33	4.26	9.83	9.47	16.00	7.08	5.34	6.15	6.21	7.71
Zr	253	86	59	118	73	55	55	84	76	120	164	239	122	113	114	122	123
Hf	5.39	2.48	1.70	3.10	2.24	1.44	1.54	1.98	1.99	3.19	3.82	5.24	3.34	3.22	2.88	3.65	3.48
Th	36.51	2.95	1.30	2.84	2.17	1.45	1.46	1.64	2.92	3.54	4.01	6.74	9.04	2.72	3.05	3.21	3.44
La	146.00	10.24	10.50	22.56	18.67	7.20	5.92	9.03	12.59	17.08	21.92	52.70	32.17	14.57	14.47	14.84	9.80
Sm	24.39	5.03	3.17	5.49	4.56	1.99	1.85	2.88	2.75	4.51	5.16	10.58	4.72	3.76	3.84	4.01	3.16
Gd	14.76	4.73	3.66	4.85	4.40	2.32	2.12	3.27	3.01	5.44	5.71	9.88	4.08	4.34	4.57	4.55	4.22
Yb	1.18	1.80	2.62	1.76	2.15	1.44	1.37	1.52	1.78	2.70	3.82	3.94	1.74	2.57	2.79	3.16	2.84
Lu	0.17	0.28	0.41	0.24	0.31	0.21	0.19	0.23	0.25	0.40	0.58	0.59	0.26	0.38	0.42	0.47	0.43
(La/Yb)n	88.91	4.08	2.87	9.17	6.22	3.60	3.10	4.25	4.99	4.54	4.12	9.59	13.24	4.07	3.72	3.36	2.48
(La/Sm)n	3.87	1.31	2.14	2.65	2.65	2.33	2.07	2.03	2.91	2.44	2.74	3.22	4.40	2.50	2.44	2.39	2.01
(Gd/Yb)n	10.36	2.17	1.15	2.27	1.69	1.33	1.28	1.77	1.40	1.67	1.24	2.07	1.94	1.40	1.36	1.19	1.21
Al_2O_3/TiO_2	20.5	12.6	17.2	9.8	12.0	31	32	14	30	8	19	12	30.58	8.87	8.32	9.41	7.63
Zr/Hf	47.0	34.9	34.4	38.3	32.5	38	35	42	38	38	43	46	36.35	35.16	39.60	33.44	35.38
La/Nb	17.35	3.13	4.21	3.08	4.67	2.36	1.86	2.09	2.91	1.74	2.31	3.29	4.54	2.73	2.35	2.39	1.27
Th/Nb	4.34	0.90	0.52	0.39	0.54	0.48	0.46	0.38	0.69	0.36	0.42	0.42	1.28	0.51	0.50	0.52	0.45
Th/La	0.25	0.29	0.12	0.13	0.12	0.20	0.25	0.18	0.24	0.21	0.18	0.13	0.28	0.19	0.21	0.22	0.35
Zr/Y	9.46	4.16	2.45	5.58	3.22	3.49	3.97	5.11	4.86	4.17	4.97	5.91	6.34	4.99	4.46	4.08	4.78
Nb/Nb*	0.04	0.38	0.20	0.28	0.17	0.35	0.45	0.39	0.29	0.46	0.37	0.24	0.16	0.29	0.35	0.33	0.54
Zr/Zr*	0.31	0.60	0.66	0.68	0.54	0.97	1.04	1.03	0.89	0.88	1.02	0.69	0.75	0.99	1.02	1.05	1.50
Hf/Hf*	0.24	0.62	0.70	0.64	0.60	0.91	1.07	0.88	0.84	0.85	0.86	0.55	0.74	1.02	0.93	1.14	1.53
Ti/Ti*	0.08	0.62	0.66	0.67	0.72	0.63	0.66	0.89	0.46	0.76	0.34	0.27	0.30	0.80	0.86	0.78	1.12

* Full data set in Appendix D

negative Nb anomalies are present in all samples, however only PL-17A displays a pronounced Ti anomaly (Nb/Nb* = 0.16-0.54; Fig. 6.13). PL-17A is also characterised by a greater LREE enrichment and more fractionated HREE (La/Sm_n = 4.4; Gd/Yb_n = 1.4).

6.3.6 Red Lake greenstone belt

The Confederation assemblage samples from the Red Lake belt are all calc alkaline in character, with no tholeiitic samples among the representative suite collected. They are generally intermediate and display moderately to strongly enriched LREE, in conjunction with variably fractionated HREE (La/Sm_n = 1.5-4.0; Gd/Yb_n = 1.2-2.1; Fig. 6.13c & d). Typically the more evolved samples are characterised by higher REE abundances in conjunction with more pronounced V and Sc troughs likely the result of clinopyroxene and o/or oxide fractionation. Deep negative Nb anomalies are observed in all samples, while Ti anomalies generally increase with the degree of LREE fractionation (Nb/Nb* = 0.2-0.6; La/Sm_n = 1.6-3.4).

6.3.7 Discussion of calc alkaline volcanic rocks

Many calc alkaline samples of the Confederation assemblage display the pronounced LREE enrichment and relatively high Zr/Y ratios, in conjunction with strong negative Nb and Ti anomalies, characteristic of a subduction related arc source. Thorium/Ce values of 0.10-0.14 are comparable to the lower end of the range of values for modern day continental arcs (Hawkesworth et al., 1997), possibly implying that some continentally derived sediments were incorporated in the subduction zone.

The distinctive nature of the Birch-Uchi belt samples, which are characterised by low SiO_2 contents and only moderate LREE enrichment is reflected in Figure 6.8. The Birch-Uchi belt samples can be readily distinguished on a Th/La_{pm} versus Zr plot where they form a discrete field falling to higher Th/La_{pm} values than is typical for the other calc alkaline suites. Similarly on a plot of and Sc/Lu_{pm} versus Zr the Birch-Uchi data extends to the highest values of all the calc alkaline suites. The elevated Th/La_{pm} ratios of the Birch-Uchi primitive arc rocks, illustrated by the positive Th peaks on Fig 6.7a, are not found elsewhere within the Confederation assemblage. Thorium/Ce ratios for these rocks range from 0.03-0.22. The lower values are within the range of MORB and OIB (0.016-0.052), but the higher values require the input of sediments with a substantial continental component (Hawkesworth et al., 1997). Consequently the Th-Nb-La systematics of these

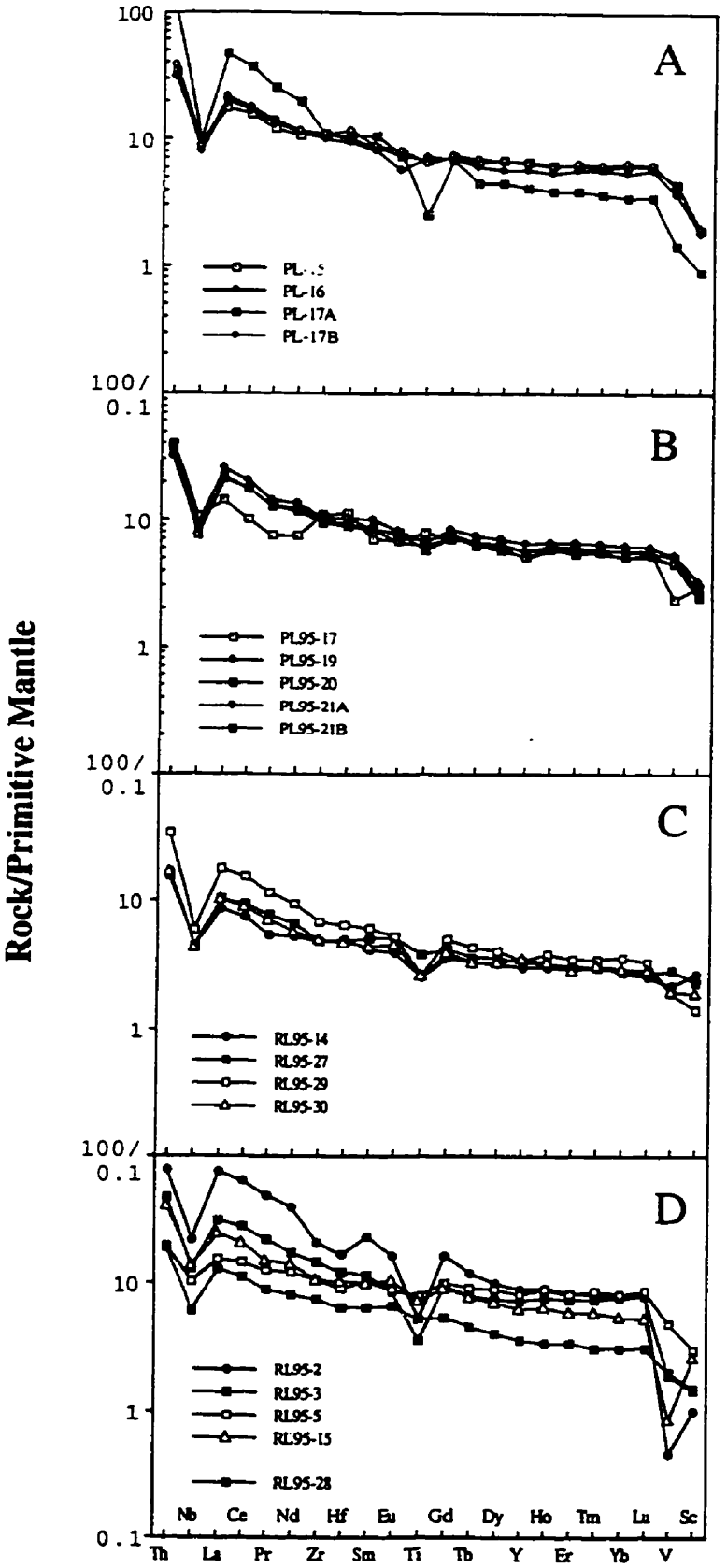

Figure 6.13. Representative primitive mantle normalised trace element diagrams for calc alkaline rocks from the Confederation assemblages of the Pickle Lake and Red Lake greenstone belts. A, B = Pickle Lake belt; C, D = Red Lake belt (C = mafic, D = intermediate).

rocks are interpreted to be the result of subducted sediments in the mantle below the arc. The lower end of the field for the calc alkaline rocks overlaps with the Nb depleted tholeiites from the Birch-Uchi belt (Figs. 6.3a and 6.7a), suggesting the tholeiites are more primitive end members of the same petrogenetic series.

The Rice Lake belt samples display nearly vertical trends in Zr/Y, La/Yb_n, Nb/Y_{pm} and Nb/Yb_{pm} vs Zr coordinates (Fig. 6.8). This trend is not seen in the calc alkaline volcanics from any other greenstone belt. These rocks are also unique in that they are the only suite to display consistently positive Zr and Hf anomalies. Numerical modelling of fractionation, using the distribution coefficients of Rollinson (1993), indicates that positive Zr and Hf anomalies can be accounted for by hornblende fractional crystallisation between dacitic and rhyolitic composition. It is possible that a similar mechanism has generated the anomalies in these basaltic andesites to andesites. The positive Zr and Hf anomalies are also present in a suite of calc alkaline rocks from the Sturgeon Lake belt of the Wabigoon subprovince (Wyman et al., in prep.). These rocks display similar vertical trends to the Rice Lake rocks possibly suggesting a common petrogenetic origin.

In addition to the more typical calc alkaline rocks, a distinct mafic suite characterised by LREE enrichment, but lacking the HFSE anomalies typical of arc related rocks, has been recognised in a number of greenstone belts (Figs. 6.7b-d and 6.10b). The elevated Fe_2O_3 of some samples and high TiO_2 contents in all samples of this suite would appear to preclude them having fractionated from the plateau-type tholeiites given that the more evolved tholeiitic rocks, in terms of SiO_2 and Ni content, display low Fe_2O_3 contents (Table 6.5 & 6.6). The major and trace element characteristics of these basalts are comparable to alkaline Ocean Island Basalts (OIB), which are generally accepted to be the result of low degrees of partial melting associated with asthenospheric upwelling related to either a plume or significant lithospheric thinning (Hole et al., 1995). Brommecker (1996) has reported a Fe-tholeiite in the Manigotagan River formation of the Rice Lake belt with an extremely high TiO_2 content. This tholeiite may be similar to the rocks of the Meen-Dempster and Birch-Uchi belt but no trace element data is available, making this correlation speculative.

The high Fe_2O_3 contents of 19-20 wt.% in two of the samples are significantly higher than is typical for OIB. One potential source of the high Fe content is contamination with the extensive BIF horizons found within the belt; however, this would not account for the

relative Ti enrichment nor the distinctive REE fractionations. An alternative explanation is fractionation of olivine which would result in Fe enrichment while depleting MgO, Ni and Cr; this is consistent with the data for the two Fe-enriched samples which display very low Ni and Cr (e.g., Cr = 5-43 ppm). Hanski and Smolkin (1989) have reported early Proterozoic ferropicrites from Pechenga, Kola Peninsular with up to 20 wt.% Fe. Hanski and Smolkin (1995) have proposed that the ferropicrites were derived from a peridotitic source that was inherently richer in iron than is typically observed in mantle xenoliths, possibly derived from an Fe-rich lower mantle (Hanski, 1992). Small volumes of iron-rich basalts have also been noted at Pechenga with Fe contents of 18-24 wt.% (Skufin, 1980). Basaltic portions of a differentiated komatiitic flow, in Boston Township, Abitibi Subprovince have major and trace element compositions comparable to the Confederation assemblage samples (Xie et al., 1993; Stone et al., 1995) although Stone describes his locality as a thick differentiated flow. Alternatively Stone et al. (1995) have proposed that metasomatic enrichment of Fe, Ti, Nb and REE in depleted mantle could account for the characteristics of the ferropicrites. The metasomatising agent is suggested to be small volume melts formed at garnet present depths in a mantle plume, that were entrained by the plume and enriched the depleted upper mantle. This model is similar to that proposed by Eggins (1992) for OIB petrogenesis.

OIB-like "Nb enriched basalts" have been recognised in a number of modern arc environments including Mt. St. Helens, Southwestern Japan, Northern Kamchatka and Costa Rica (Defant et al., 1992). In every case these rocks are found in conjunction with adakites and are associated with the subduction of young, hot oceanic crust. Adakites themselves are relatively rare in modern subduction zones and are interpreted to be the product of melting of young, hot crust (Defant et al., 1992; Sajona et al., 1993, 1996; Yogodzinski et al., 1995). This is similar to the conditions thought to have been prevalent in the Archean where it resulted in the generation of TTG-type melts. It has been argued that these Nb-enriched rocks have incorporated a plume (OIB) component (e.g. Reagan and Gill, 1989), however Defant et al. (1992) suggest that they are formed by mixing of hybridized slab-derived melt with the mantle, or alternatively that formation of slab-derived adakites may have left a MgO enriched residue. OIB-like basalts have also been reported from a number of modern back arc environments (e.g. Gill and Whelan, 1989; Stern et al., 1990; Pouclet et al., 1995). It is suggested that mantle upwelling, as a result of lithospheric extension associated with the opening of a back arc basin, may have entrained "blebs" of enriched lower mantle, unaffected by subduction zone processes. This may account for the high Fe basalts observed in the Confederation assemblage. The

variable Th-Nb-La systematics of the three OIB-like rocks is likely the result of some degree of interaction with subduction influenced mantle.

Rocks similar to these OIB-like basalts have been recognised in the 2.9-3.0 Ga Northern Pickle assemblage of the Pickle Lake greenstone belt (Chapter 4). As discussed for the Northern Pickle assemblage, OIB-like rocks are found towards the base of the stratigraphic sequence in the Sturgeon Lake belt of the Wabigoon subprovince. They are thought to represent an early stage in the development of a back arc rift, where low degree partial melts are erupted through the rifted crust (Wyman et al., in prep). Such a model is consistent with the data from the Confederation assemblage where the 'OIB-like' rocks are found in the older Meen-Dempster and Birch-Uchi portions of the assemblage.

6.4 Felsic volcanic rocks

6.4.1 Introduction

The most diverse range of felsic rocks within the Confederation assemblage has been identified within the Birch-Uchi greenstone belt. Felsic volcanic rocks have not been sampled from the Pickle Lake occurrences of the Confederation assemblage, whereas the Red Lake, Lake St. Joseph, Rice Lake and Meen-Dempster belts have yielded only a small number of felsic rocks (Table 6.9).

Table 6.9. Summary of occurrences of felsic volcanic rocks in the Confederation assemblage

Distribution Association	**FI**	**FII**	**FI-FII**	**FIIIa**	**FIIIb**
Birch-Uchi belt MGT, PAT, CAB, ICE, OIB	●	●	●	●	●
Red Lake belt CAB		●			
Lake St. Joseph belt MGT, CAB	●	●	●		
Meen-Dempster belt MGT, CAB, OIB	●	●	●		
Rice Lake belt MGT, PAT, CAB		●			

MGT = Mg-tholeiites, PAT = Primitive arc tholeiites, CAB = calc alkaline basalts, ICE = Icelandites, OIB = OIB-like basalts

In a review of felsic volcanic rocks of the Superior Province, Lesher et al. (1986)

Table 6.10. Data for FI, FII and FIII felsics from Lesher et al. (1986)

	n	SiO2	TiO2	Rb	Sr	Y	Zr	La	Yb	Th	Hf	Sc	(La/Yb)n	Eu/Eu*	Zr/Y
								FI							
Abitibi Belt															
Bowman	1	67	0.55	24	257	12	110	7.20	0.81	0.60	2.70	0.90	5.80	1.30	9.20
Skead															
Otto—Buston	3	64 - 68	0.31 - 0.34	57 - 89	320 - 514	6 - 7	119 - 142	9.2 - 14	0.46 - 0.56	1.7 - 2.0	3.1 - 3.5	2.4 - 5.6	10 - 20	1.4 - 2.0	17 - 24
St. Anthony	4	65 - 69	0.35 - 0.50	8 - 56	147 - 333	8 - 9	110 - 127	9.7 - 12	0.56 - 0.87	1.4 - 1.6	2.4 - 2.8	8.4 - 12	9.0 - 14	1.0 - 1.1	14 - 18
Wabigoon Belt															
Kakagi Lake	4	64 - 69	0.43 - 0.51	37 - 72	250 - 616	6 - 12	102 - 149	10 - 26	0.61 - 1.2	1.4 - 1.9	2.4 - 3.3	6.9 - 14	5.8 - 16	1.1 - 1.5	11 - 19
L. of the Woods	10	67 - 72	0.23 - 0.52	36 - 64	289 - 537	3 - 10	90 - 140	12 - 46	0.47 - 1.2	2.1 - 8.6	2.4 - 3.6	5.0 - 13	11 - 36	0.92 - 1.4	14 - 31
Shoal Lake															
Upper	3	65 - 69	0.30 - 0.65	54 - 70	125 - 476	12 - 31	169 - 273	27 - 36	1.4 - 3.8	4.4 - 6.6	3.5 - 6.0	2.5 - 12	6.1 - 13	0.87 - 1.1	8.8 - 11
Lower	4	69 - 74	0.16 - 0.42	12 - 61	376 - 475	4 - 6	90 - 107	12 - 19	0.53 - 0.88	2.0 - 5.0	2.3 - 2.9	1.6 - 8.5	14.0 - 22.0	1.3 - 1.5	17 - 27
Sturgeon Lake															
Cycle 3	2	72	0.33 - 0.48	12.0 - 27.0	182 - 298	5 - 10	142 - 145	14 - 19	0.43 - 0.78	3.0 - 3.3	2.8 - 3.2	7.6 - 21	30 Dec	0.89 - 1.2	15 - 29
Uchi Belt															
Confederation Lake cycle III															
Hy Lake, U	1	77	0.26	51	81	9	86	38	0.75	18	2.20	1.70	34	70	9.80
								FII							
Abitibi Belt															
Miscma															
Bernhardt	1	66	0.79	5	175	17	96	9.30	1.70	1.90	2.90	25	3.60	1.40	5.6
S. Magini—Dasserat	4	68 - 73	0.39 - 0.49	45 - 60	43 - 109	38 - 48			3.9 - 5.8	2.8 - 4.3	5.4 - 8.3	7.8 - 12	2.3 - 2.7	0.57 - 82	6.2 - 7.0
Wabigoon Belt															
Wabigoon Lake	7	64 - 76	0.37 - 0.89	20 - 67	58 - 264	29 - 46	225 - 404	21 - 42	3.4 - 6.0	4.7 - 9.5	5.5 - 11	4.4 - 16	2.5 - 5.4	0.56 - 0.91	7.4 - 11
Sturgeon Lake															
Cycle2	1	81	0.20	62	46	46	406	42	4.60	7.90	8.70	6.60	6.80	0.54	8.80
Cycle 1b	2	77 - 81	0.20 - 0.31	55 - 56	57 - 58	37 - 43	305 - 431	39 - 42	4.2 - 4.7	7.6 - 7.9	7.0 - 9.0	4.4 - 7.0	5.4 - 6.6	0.53 - 0.57	8.2 - 10
Cycle 1a	8	73 - 78	0.16 - 0.73	12 - 76	36 - 200	33 - 55	294 - 412	27 - 43	3.6 - 5.5	5.5 - 9.3	6.6 - 9.0	5.1 - 12	5.3 - 6.1	0.35 - 0.73	6.4 - 10
								FIIIa							
Abitibi Belt															
Noranda district															
Misc. II—IV	9	67 - 76	0.26 - 0.99	10 - 62	26 - 101	25 - 70	170 - 362	9.8 - 37	3.4 - 8.7	1.5 - 7.1	3.9 - 8.6	7.9 - 20	1.8 - 2.8	0.44 - 0.91	4.7 - 6.8
Dun	4	73 - 76	0.22 - 0.37	12 - 24	44 - 61	38 - 53	191 - 251	14 - 22	5.1 - 6.7	2.0 - 3.1	4.7 - 6.0	7.0 - 13	1.8 - 2.2	0.65 - 0.94	4.2 - 5.4
Waite	2	73 - 77	0.21 - 0.33	21 - 24	17 - 26	46 - 52	285 - 299	15 - 21	5.4 - 6.3	2.6 - 2.8	6.5 - 7.0	10 - 15	1.5 - 2.6	0.61 - 0.74	5.5 - 6.5
Amulet	6	72 - 78	0.25 - 0.58	<1 - 47	4.8 - 35	44 - 65	275 - 370	19 - 28	5.4 - 7.1	2.7 - 3.4	6.8 - 8.3	11 - 17	2.0 - 2.6	0.37 - 0.72	3.9 - 6.6
Deschenes	2	70 - 72	0.47	27 - 33	40 - 45	50 - 56	294 - 297	14 - 21	9.30	2.3 - 2.4	5.6 - 5.9	14 - 15	1.5 - 2.2	0.60 - 0.69	5.3 - 5.9
								FIIIb							
Abitibi Belt															
Kamiskotia															
Normal	11	71 - 79	0.17 - 0.46	30 - 128	0.7 - 43	108 - 149	304 - 410	39 - 61	12 - 18	6.3 - 11	8.0 - 12	1.7 - 3.9	2.1 - 2.9	0.31 - 0.41	2.5 - 2.9
Fractionated	4	77 - 79	0.12 - 0.27	48 - 90	16 - 55	72 - 90	215 - 341	53 - 67	7.1 - 11	7.2 - 8.8	5.8 - 8.7	1.9 - 3.0	3.6 - 4.9	0.34 - 0.44	2.4 - 3.1
Kidd Creek	6	77 - 84	0.09 - 0.14	87 - 157	23 - 73	78 - 128	194 - 318	28 - 63	9.5 - 15	7.3 - 12	6.7 - 10	1.4 - 3.2	1.9 - 2.9	0.29 - 0.40	2.0 - 2.9
Garrison	2	72 - 76	0.27 - 0.33	<1	43 - 64	142 - 188	526 - 543	32 - 38	19 - 22	3.1 - 3.3	14 - 16	2.0 - 3.9	1.30	0.46 0.49	2.9 3.7
Noranda district															
NW rhyolite	2	67 - 70	0.45 - 0.47	17 - 24	8.8 - 28	97 - 116	372 - 442	26 - 28	12 - 14	3.2 - 4.2	8.5 - 11	11	1.1 - 1.4	0.41 - 0.46	3.80
Uchi Belt															
Confederation Lake Cycle III															
South Bay	10	70 - 80	0.26 - 0.73	11 - 50	35 - 210	106 - 199	450 - 732	36 - 79	9.0 - 24	9.1 - 12	12 - 20	2.8 - 11	1.9 - 3.6	0.41 - 0.61	3.0 - 5.8
QFP (all)	5	76 - 81	0.29 - 0.40	3.0 - 32	50 (1)	133 - 149	470 - 520	55 - 62	11 - 17	7.0 - 8.1	14 - 15	1.3 - 4.1	2.2 - 3.2	0.50 - 0.59	3.3 - 3.9
Hy Lake, L.	6	68 - 79	0.18 - 0.53	23 - 119	11 - 88	82 - 238	233 - 708	57 - 161	9.6 - 32	9.5 - 16	7.9 - 24	1.5 - 2.7	1.9 - 3.9	0.20 - 0.35	2.4 - 3.0

proposed four broad subdivisions (Table 6.10). FI felsic volcanic rocks are described as dacites and rhyodacites with steeply fractionated REE (La/Yb_n = 6-34) and high Zr/Y ratios (9-31). FII felsics are rhyodacites to rhyolites with gently sloping REE (La/Yb_n = 2-6) and moderate Zr/Y (6-11). FIII felsics are rhyolites to high Si rhyolites characterised by relatively flat REE (La/Yb_n = 1-4); these were further subdivided into FIIIa with moderate negative Eu anomalies, low Zr/Y (4-7) and high Sc abundances and FIIIb with pronounced negative Eu anomalies, low Zr/Y (2-6) and low Sc abundances (Table 6.9). The FI felsics are typically interpreted as being derived from slab melting within the garnet stability field, FII are interpreted to be the result of dehydration of the subducting slab and metasomatism of the mantle wedge, whereas FIII represent shallow level fractionation of magmas of tholeiitic composition (e.g. Lesher et al., 1986). In Chapter 4 the terms Types 1, 2 and 3 were introduced and correlated with FI, FII and FIII of Lesher et al. (1986); however, this classification scheme has not yet been expanded to encompass the variety in FIII (Type 3) rocks revealed in this study. Consequently the terminology of Lesher et al. (1986) will be utilised in the following sections.

6.4.2 Minor occurrences of felsic volcanic rocks

A dacite and a rhyolite were sampled from the Confederation assemblage of the Red Lake belt (SiO_2 = 65-73; Table 6.11). They are both characterised by pronounced LREE enrichment but generally flat HREE (La/Sm_n = 3.4-4.1; Gd/Yb_n = 1.3-2.1) and pronounced negative Nb anomalies (Nb/Nb* = 0.2-0.4; Fig. 6.14a). These are comparable to FII's of Lesher et al. (1986).

The felsic rocks of the Meen-Dempster belt Confederation assemblage range in composition from dacites to rhyolites with SiO_2 contents varying from 67-75 wt.% and Mg#'s from 0.43-0.17 (Table 6.11). The trace element systematics of the felsic rocktypes suggest that they can be subdivided into two distinct sub groups (Fig. 6.14b). A single sample displays pronounced LREE enrichment and generally flat HREE (La/Sm_n = 2.4; Gd/Yb_n = 1.3; Fig. 6.14b), consistent with FII felsics. The second subgroup comprises the two most evolved samples, both rhyolites, with SiO_2 contents of 73-75 wt.%. They are characterised by strongly enriched LREE and moderately to strongly fractionated HREE (La/Sm_n = 5.6-5.8; Gd/Yb_n = 2.2-7.1; Fig. 6.14b). Both samples display pronounced Nb and Ti anomalies but positive to negative Zr and Hf anomalies (Nb/Nb* = 0.1-0.2; Zr/Zr* = 0.9-2.1; Fig. 6.14b). These are comparable to the FI group of Lesher et

Table 6.11. Representative analyses of selected elements for felsic volcanic rocks from the Confederation assemblage of the Red Lake, Meen-Dempster, Lake St. Joseph and Rice Lake greenstone belts*.

	Red Lake		Meen-Dempster			Lake St. Joseph					Rice Lake
	FII		FI			FI		FII			FII
	RL95-1	RL95-4	84GRS-0205	82GRS-0412	84GRS-1244	LSJ95-13a	DL87-15B	DL87-12A	DL87-12B	WL87-10B	RC96-8
SiO_2	64.95	72.74	72.84	74.93	67.08	72.87	71.84	76.84	60.77	83.31	72.22
TiO_2	0.18	0.37	0.49	0.21	1.31	0.29	0.25	0.08	1.39	0.13	0.35
Al_2O_3	12.76	13.87	16.42	14.52	13.65	15.89	15.53	13.35	16.98	9.61	12.64
Fe_2O_3	9.40	2.86	1.18	1.66	4.93	0.65	1.93	3.16	12.17	2.15	5.82
MgO	0.38	0.77	0.71	0.56	2.05	0.31	0.81	1.45	2.73	0.51	1.59
LOI	5.93	2.04	1.63	0.40	0.40	1.42	1.47	1.68	0.50	1.01	0.96
Mg#	8	37	57	43	48	51	48	50	33	35	38
Ti	1037	2148	1772	1097	5788	1403	1330	446	8064	756	2005
Cr	3	8	8	8	2	18	39	4	3	7	21
Ni	2	5	6.4	3.7	5.9	7	2	8	3	2	2
Nb	40.19	11.14	3.35	6.15	6.93	2.70	3.18	7.45	7.67	15.96	26.84
Zr	372	223	101	131	110	93	105	86	153	183	[illegible]
Hf	10.39	5.42	2.49	3.70	2.85	2.39	3.03	3.46	4.28	4.71	8.11
Th	14.43	11.98	5.77	15.94	3.87	4.14	3.29	7.59	3.82	7.14	6.86
La	89.15	54.28	24.72	16.79	18.02	17.77	14.24	30.19	27.31	37.05	45.94
Sm	16.95	8.60	2.86	1.89	4.79	2.16	1.96	4.21	5.99	5.41	9.53
Gd	17.81	7.07	1.71	1.53	5.01	1.50	1.52	3.61	5.99	4.19	9.01
Yb	11.53	2.82	0.18	0.58	3.26	0.24	0.44	1.66	3.14	2.32	5.47
Lu	1.75	0.47	0.03	0.09	0.46	0.03	0.06	0.23	0.42	0.34	0.88
(La/Yb)n	5.54	13.82	96.87	20.67	3.96	52.34	23.10	13.06	6.24	11.43	6.02
(La/Sm)n	3.40	4.08	5.59	5.75	2.43	5.31	4.69	4.63	2.94	4.42	3.11
(Gd/Yb)n	1.28	2.08	7.72	2.17	1.27	5.10	2.85	1.80	1.58	1.49	1.36
Al_2O_3/TiO_2	74	38	54	79	12	67.2	68.6	177.8	12.4	76.3	38
Zr/Hf	36	41	40	35	39	39	35	25	36	39	38
La/Nb	2.22	4.87	7.37	2.73	2.60	6.59	4.48	4.05	3.56	2.32	1.71
Th/Nb	0.36	1.07	1.72	2.59	0.56	1.53	1.04	1.02	0.50	0.45	0.26
Th/La	0.16	0.22	0.23	0.95	0.21	0.23	0.23	0.25	0.14	0.19	0.15
Zr/Y	3.61	8.04	28.04	20.33	3.47	23.59	18.15	5.63	7.17	9.27	5.82
Nb/Nb*	0.35	0.17	0.10	0.23	0.29	0.11	0.16	0.19	0.22	0.34	0.48
Zr/Zr*	0.70	0.73	0.92	2.08	0.79	1.19	1.57	0.59	0.79	0.95	1.00
Hf/Hf*	0.71	0.64	0.83	2.13	0.74	1.11	1.64	0.86	0.80	0.89	0.95
Ti/Ti*	0.02	0.11	0.32	0.26	0.47	0.31	0.30	0.05	0.53	0.06	0.09

* Full data set in Appendix D

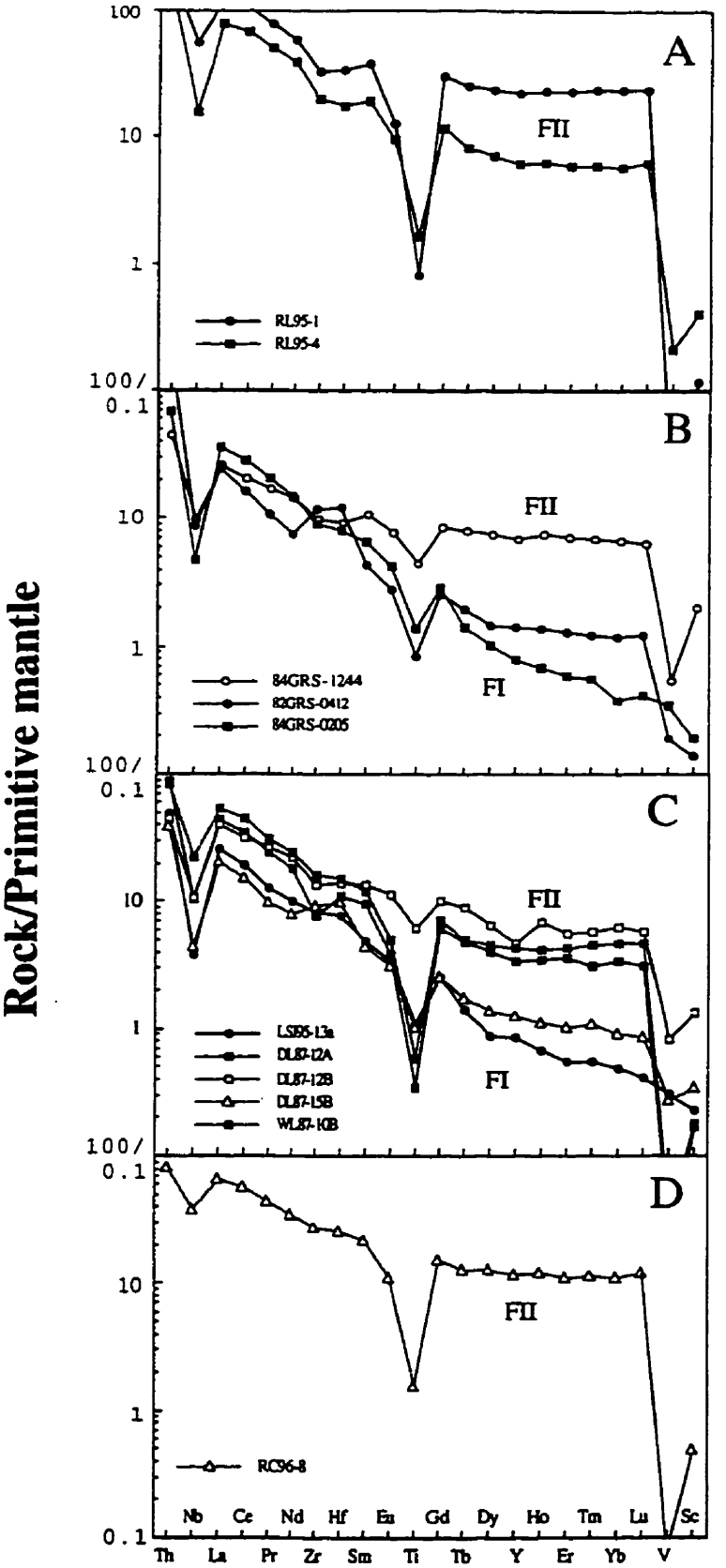

Figure 6.14. Primitive mantle normalised diagrams for felsic rocks from the Confederation assemblage of the Red Lake (A), Meen-Dempster (B) Lake St. Joseph (C) and Rice Lake (D) greenstone belts.

al. (1986).

A similar range of rock types has been identified in the Lake St. Joseph belt. Two rhyolites with silica contents of 72-73 wt.% are characterised by steeply fractionated REE typical of FI felsics (La/Sm_n = 4.7-5.3; Gd/Yb_n = 2.9-5.1; Fig. 6.14c). The remaining three samples range from dacite to high silica rhyolite (61-83 wt.%; Table 6.11) and are characterised by enriched LREE but flatter HREE typical of FII felsics (La/Sm_n = 2.9-4.6; Gd/Yb_n = 1.5-1.8; Fig. 6.14c).

A single rhyolite collected from the Rice Lake belt (SiO_2 = 72 wt.%) displays enriched LREE and flat HREE typical of FII felsics (La/Sm_n = 3.1; Gd/Yb_n = 1.4; Fig. 6.14d).

6.4.3 The Birch-Uchi greenstone belt

As discussed above a diverse range of felsic volcanic rocks have been sampled from the Confederation assemblage of the Birch-Uchi belt. The majority of outcrop samples from the vicinity of the South Bay mine site are spherulitic rhyolites comparable to FIII volcanics of Lesher et al. (1986). They are characterised by pronounced negative Eu anomalies, high abundances of the HFSE, low Zr/Y and low absolute Sc abundances (Fig. 6.15a). In addition, a second suite has been identified within the assemblage, characterised by steep trace element patterns and fractionated HREE characteristic of rocks derived from within the garnet stability zone as suggested for the FI type of Lesher et al. (1986; Fig. 6.15c). FII-like rhyolites with pronounced LREE enrichment and flat HREE have also been recognised (Fig. 6.15b). Rhyolites from a diamond drill hole (DDH) at the South Bay mine site are comparable to the FIII type rhyolites of Lesher et al. (1986), and identical to spherulitic rhyolites reported from the South Bay mine area. Low La/Sm_n ratios (<2) and high absolute Sc abundances (>7 ppm), in conjunction with positive Zr and Hf anomalies (Fig. 6.16a; Table 6.12) suggests these rhyolites are similar to the FIIIa type of Lesher et al. (1986). The rhyolites display extremely consistent trace element geochemistry over a vertical interval of 240m.

Samples taken from above a mineralised zone in the Horseshoe Lake area DDH (HL96-1) are similar to those from the South Bay mine site (Fig. 3.10), albeit with slightly greater degrees of LREE enrichment and a wider range of absolute REE abundances (Fig. 6.16b; Table 6.12). Flat REE and pronounced Eu, Ti and V anomalies are typical of FIIIa rhyolites of Lesher et al. (1986). Samples taken from below the mineralised zones display

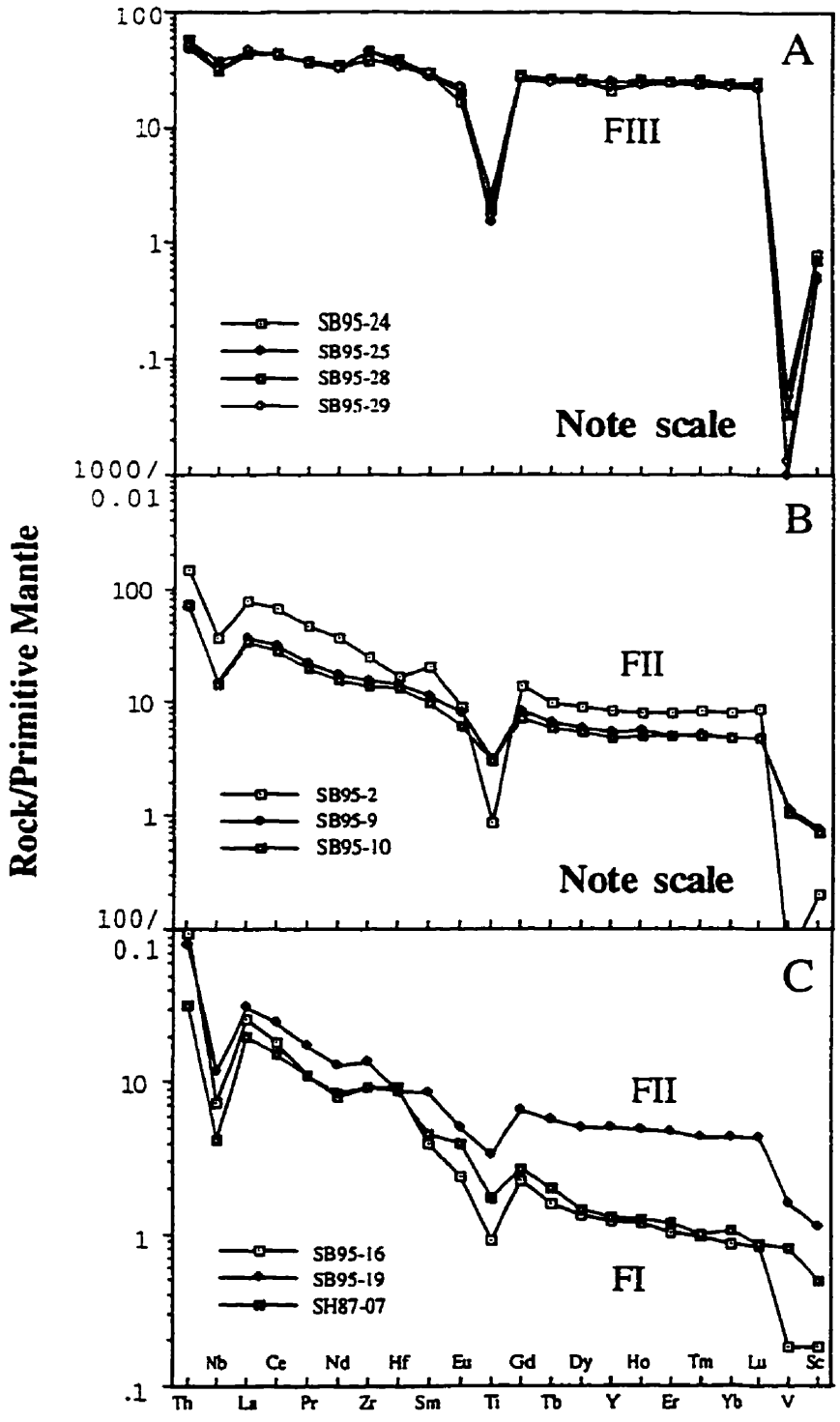

Figure 6.15. Representative primitive mantle normalised diagrams for felsic samples collected from outcrop adjacent to the South Bay mine site. A = FIII felsic rocktypes; B = FII felsic rocktypes; C = FI and FII felsic rocktypes.

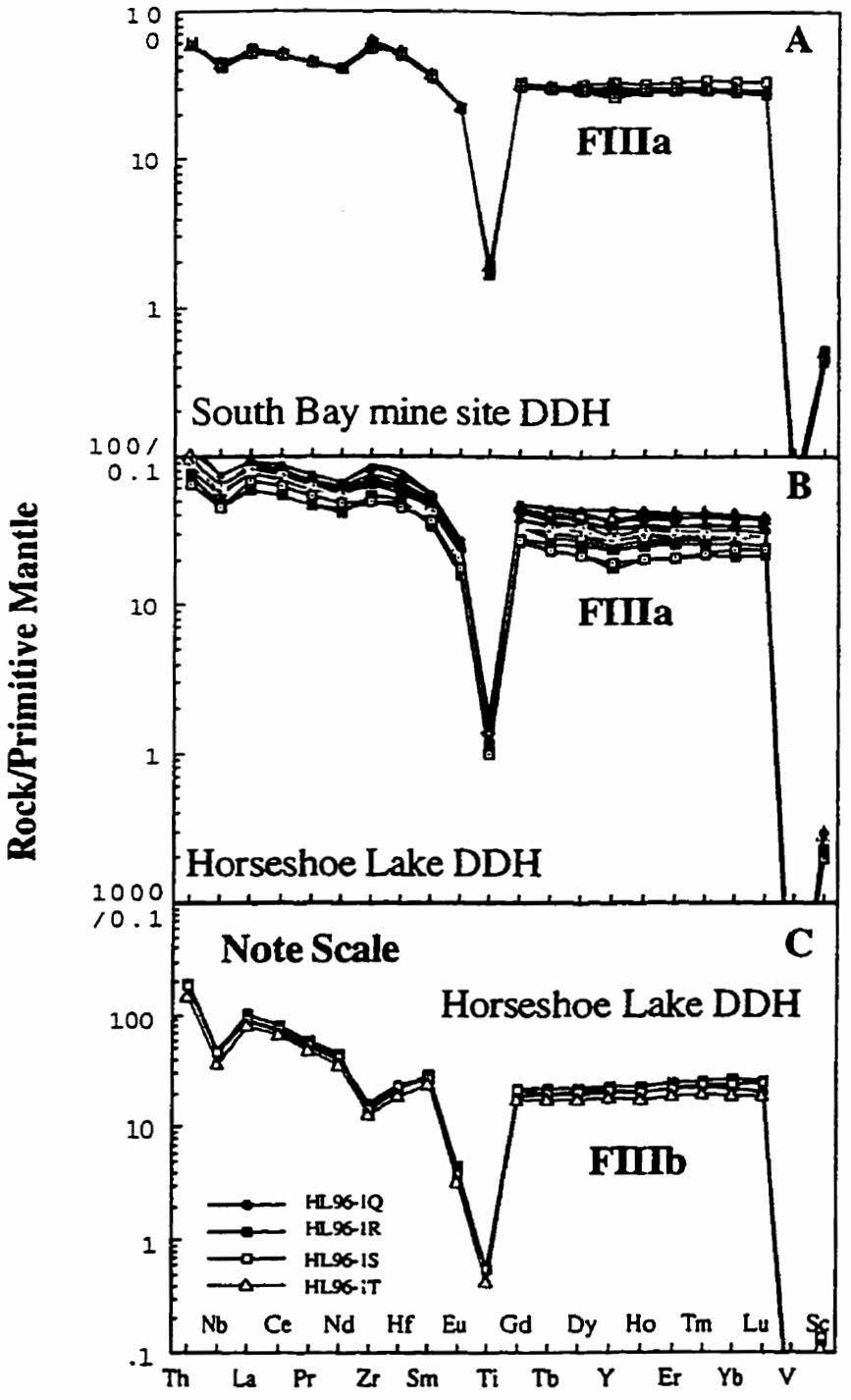

Figure 6.16. Primitive mantle normalised diagrams for representative samples from the VMS hosting Confederation assemblage, Birch-Uchi greenstone belt. A = FIIIa, South Bay mine site DDH; B = FIIIa, Horseshoe Lake DDH; C = FIIIb, Horseshoe Lake DDH.

Table 6.12. Representative analyses of selected elements for felsic volcanic rocks from the Confederation assemblage of the Birch-Uchi greenstone belt*.

	South Bay mine site								Horseshoe Lake DDH			
	FI		FII			FIIIa			FIIIa		FIIIb	
	SH87-07	SB95-16	SB95-10	SH87-02	SH87-09	SB95-25	SB95-29	SB95-4F	HL96-1A	HL96-1I	HL96-1S	HL96-1T
SiO_2	69.89	74.81	63.65	68.18	69.75	70.14	70.21	73.01	74.29	83.75	78.10	81.94
TiO_2	0.42	0.22	0.64	0.78	0.69	0.42	0.40	0.44	0.34	0.30	0.13	0.10
Al_2O_3	14.06	13.95	15.52	11.47	10.67	12.35	12.33	11.64	10.71	8.91	11.94	10.28
Fe_2O_3	3.52	1.75	5.83	9.93	9.67	8.05	7.93	6.11	7.62	1.57	1.26	0.69
MgO	1.73	0.46	2.35	1.16	1.34	0.82	0.28	0.62	0.50	0.13	0.26	0.08
LOI	4.28	1.94	2.67	5.49	3.84	2.83	0.60	1.11	1.16	0.81	0.65	0.45
Mg#	52	37	47	20	23	18	7	18	13	15	31	20
Ti	2263	1180	3952	4599	4624	1932	2236	2547	1708	1424	723	560
Cr	77	7	40	2	2	4	14	8	5	4	5	14
Ni	47	3	42	1	1	1	2	2	1	1	2	2
Nb	2.97	5.28	10.38	31.62	29.31	22.11	22.83	30.33	42.42	34.67	33.39	26.91
Zr	103	103	159	507	468	515	439	633	756	609	164	114
Hf	2.71	2.87	4.15	13.95	13.40	10.94	10.13	16.04	19.38	15.49	7.16	6.08
Th	2.70	7.94	6.13	5.72	5.55	4.02	4.34	5.28	8.23	6.16	15.47	12.46
La	13.49	17.72	23.33	41.29	38.99	29.99	32.94	34.94	58.53	39.92	62.71	55.52
Sm	2.04	1.73	4.34	16.47	17.24	12.02	13.01	15.19	22.12	14.76	12.23	10.71
Gd	1.59	1.36	4.27	19.50	18.95	15.50	16.04	18.28	25.20	16.63	12.67	10.70
Yb	0.51	0.42	2.40	14.95	13.02	11.01	11.29	14.04	19.35	12.70	12.06	9.54
Lu	0.06	0.06	0.36	2.29	1.97	1.68	1.74	2.04	2.82	1.88	1.86	1.40
(La/Yb)n	18.92	30.39	6.96	1.98	2.15	1.95	2.09	1.78	2.17	2.25	3.73	4.17
(La/Sm)n	4.26	6.60	3.47	1.62	1.46	1.61	1.64	1.49	1.71	1.75	3.31	3.35
(Gd/Yb)n	2.57	2.68	1.47	1.08	1.20	1.16	1.17	1.08	1.08	1.08	0.87	0.93
AL_2O_3/TiO_2	37	70	23	15	14	38	33	27	37	38	98	111
Zr/Hf	38	36	38	36	35	47	43	39	39	39	23	24
La/Nb	4.54	3.36	2.25	1.31	1.33	1.36	1.41	1.15	1.38	1.15	1.88	2.06
Th/Nb	0.91	1.50	0.59	0.18	0.19	0.18	0.19	0.17	0.19	0.18	0.46	0.46
Th/La	0.20	0.45	0.26	0.14	0.14	0.13	0.13	0.15	0.14	0.15	0.25	0.22
Zr/Y	17.43	18.47	7.07	3.93	3.89	4.41	4.33	5.16	4.37	5.67	1.67	1.72
Nb/Nb*	0.17	0.20	0.35	0.71	0.70	0.69	0.60	0.81	0.64	0.77	0.42	0.38
Zr/Zr*	1.46	1.66	1.14	1.12	1.01	1.55	1.27	1.52	1.23	1.46	0.44	0.43
Hf/Hf*	1.40	1.67	1.08	1.11	1.05	1.19	1.07	1.40	1.14	1.35	0.69	0.66
Ti/Ti*	0.50	0.30	0.36	0.10	0.10	0.06	0.06	0.06	0.03	0.04	0.02	0.02

* Full data set in Appendix D

Table 6.12. Continued *

	Dixie 19 DDH					Dixie South DDH				Dixie 3 DDH		
	FI		FIII			FIIIb		FIIIa		FIII		
	SJV91-1B	SJV91-1Q	SJV91-1L	SJV91-1N	SJV91-1O	D94-1B	D94-1L	D94-1U	D94-1W	SJV91-4E	SJV91-4F	SJV91-4G
SiO_2	77.21	58.54	59.19	78.04	58.66	78.13	74.46	74.31	72.72	76.96	70.34	79.08
TiO_2	0.18	0.72	0.93	0.22	1.40	0.17	0.20	0.60	0.62	0.26	0.24	0.21
Al_2O_3	12.90	14.28	15.92	12.11	12.50	11.57	12.33	10.79	11.27	13.84	12.19	10.65
Fe_2O_3	1.75	7.44	12.80	4.27	14.72	2.22	3.30	5.83	5.75	1.55	6.81	2.33
MgO	0.33	6.98	9.35	3.55	5.45	1.18	2.94	1.00	1.21	0.85	1.97	1.50
LOI	0.76	0.50	3.68	0.96	0.00	1.06	1.32	0.60	1.42	1.47	0.70	0.70
Mg#	29	67	62	65	45	54	66	27	32	55	39	59
Ti	1130	4056	5276	978	8206	1017	1055	3745	3962	1616	1438	1273
Cr	6	499	3	6	8	5	3	4	8	4	5	4
Ni	1	146	1	1	4	1	0	1	2	1	4	3
Nb	11.70	9.73	54.14	21.87	17.51	35.11	56.80	30.15	29.59	37.39	29.82	28.04
Zr	168	132	675	245	219	233	538	464	452	349	272	253
Hf	4.41	4.22	16.98	8.29	6.22	8.71	18.37	12.61	13.32	11.09	9.35	8.51
Th	5.57	3.81	11.62	14.01	2.27	13.51	11.54	5.86	5.99	14.83	12.79	10.85
La	25.17	26.59	83.18	69.84	22.84	60.36	78.81	37.43	40.14	63.11	57.40	49.15
Sm	3.66	5.86	26.38	11.33	8.62	13.78	29.30	14.55	16.14	14.13	12.65	11.38
Gd	3.32	5.15	32.41	11.15	10.74	14.08	31.04	16.90	18.82	13.77	13.82	11.33
Yb	1.82	1.79	23.69	7.59	8.73	13.39	23.13	11.87	13.11	10.72	10.69	8.18
Lu	0.30	0.25	3.61	1.09	1.39	1.87	3.03	1.82	1.87	1.62	1.71	1.23
(La/Yb)n	9.90	10.66	2.52	6.60	1.88	3.23	2.44	2.26	2.19	4.22	3.85	4.31
(La/Sm)n	4.45	2.93	2.04	3.98	1.71	2.83	1.74	1.66	1.61	2.88	2.93	2.79
(Gd/Yb)n	1.50	2.38	1.13	1.21	1.02	0.87	1.11	1.18	1.19	1.06	1.07	1.15
Al_2O_3/TiO_2	67	21	18	74	9	68	69	17	17	52	51	50
Zr/Hf	38	31	40	30	35	27	29	37	34	31	29	30
La/Nb	2.15	2.73	1.54	3.19	1.30	1.72	1.39	1.24	1.36	1.69	1.93	1.75
Th/Nb	0.48	0.39	0.21	0.64	0.13	0.38	0.20	0.19	0.20	0.40	0.43	0.39
Th/La	0.22	0.14	0.14	0.20	0.10	0.22	0.15	0.16	0.15	0.24	0.22	0.22
Zr/Y	9.40	6.59	11.33	3.60	2.88	2.26	2.61	4.19	4.07	3.75	2.86	3.71
Nb/Nb*	0.33	0.30	0.59	0.24	0.67	0.48	0.63	0.73	0.68	0.49	0.42	0.47
Zr/Zr*	1.40	0.70	0.85	0.65	0.91	0.56	0.66	1.15	1.01	0.81	0.70	0.73
Hf/Hf*	1.33	0.82	0.77	0.80	0.93	0.75	0.82	1.13	1.08	0.93	0.87	0.89
Ti/Ti*	0.13	0.29	0.07	0.03	0.34	0.03	0.01	0.09	0.09	0.05	0.04	0.04

* Full data set in Appendix D

broadly similar REE patterns to those above the zone, but with more LREE enriched patterns (Fig. 6.16a; La/Sm_n >3.7 versus La/Sm_n <2). The footwall samples also display more pronounced Eu anomalies in conjunction with negative Zr and Hf anomalies, whereas samples above the zone of mineralisation are characterised by weak to moderate positive Zr and Hf anomalies. Variations in the degree of LREE enrichment and Zr and Hf are consistent with the samples above the mineralised horizon being of type FIIIa whereas those below are FIIIb.

Rhyolites from the Dixie 19 DDH are consistent with the FIII type of Lesher et al. (1986). However, the trace element characteristics are somewhat transitional between type FIIIa and FIIIb (Fig. 6.17a; Table 6.12). Scandium contents, for example range from 3 to 17 ppm with the reported range for FIIIa typically 10-15 and for FIIIb 1.5-4.0 (Table 6.12). Similarly La/Yb_n ratios, while predominantly close to 2.5, also encompass the range of FIIIa and FIIIb subgroups. On plots of Zr versus Y, and Zr/Y versus Sm/Y, these samples lie within the fields occupied by FIIIb rhyolites (Fig. 6.18).

Two samples from the Dixie 19 DDH comprise a distinct suite of felsic volcanics; both are characterised by pronounced LREE enrichment, generally flat HREE and negative Nb and Ti anomalies (Fig. 6.18; Table 6.12). However, it is unlikely that the two are cogenetic as the more primitive sample (SJV91-Q) displays higher REE abundances than the rhyolite, and consequently cannot have fractionated to produce the more evolved sample. The rhyolite itself falls within the FI classification of Lesher et al. (1986), having an La/Yb_n ratio of 10, towards the lower end of the typical range. However, the flat HREE are more typical of FII rock types, suggesting that this sample may be transitional between the two subgroups.

The majority of rhyolites from the Dixie South area DDH are of the FIIIb subgroup, and display low Sc contents and negative Zr and Hf anomalies (Fig. 6.17b; Table 6.12). These FIIIb samples plot as a coherent suite on Figure 6.18b, but fall into two distinct fields on Figure 6.18a which plots absolute HFSE abundances. The high and low-HFSE rhyolites occur in cycles within the drill hole suggesting recurring fractionation, eruption and recharge of a magma chamber, probably at shallow crustal levels. Significantly, similar cycles are not observed in the Dixie 19 area further west along the "Joy Horizon" (Fig. 3.10) and a single continuous field is defined for the Dixie 19 samples on Fig. 6.18a. This finding implies multiple vents and source chambers, with slightly different

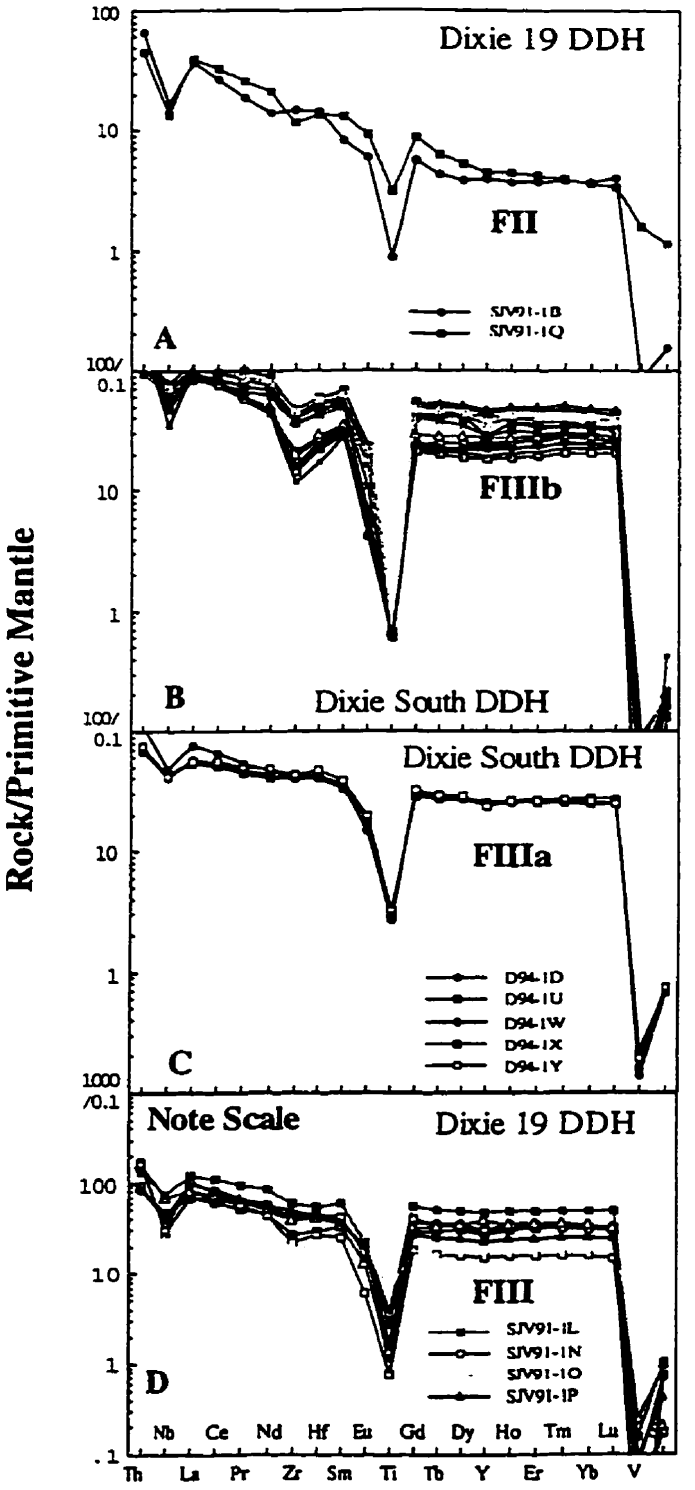

Figure 6.17. Primitive mantle normalised diagrams for representative samples from the Confederation assemblage of the Birch-Uchi belt, A = FI, Dixie 19 DDH, B = FIIIb, Dixie South DDH; C = FIIIa, Dixie South DDH; D = FIII, Dixie 19 DDH.

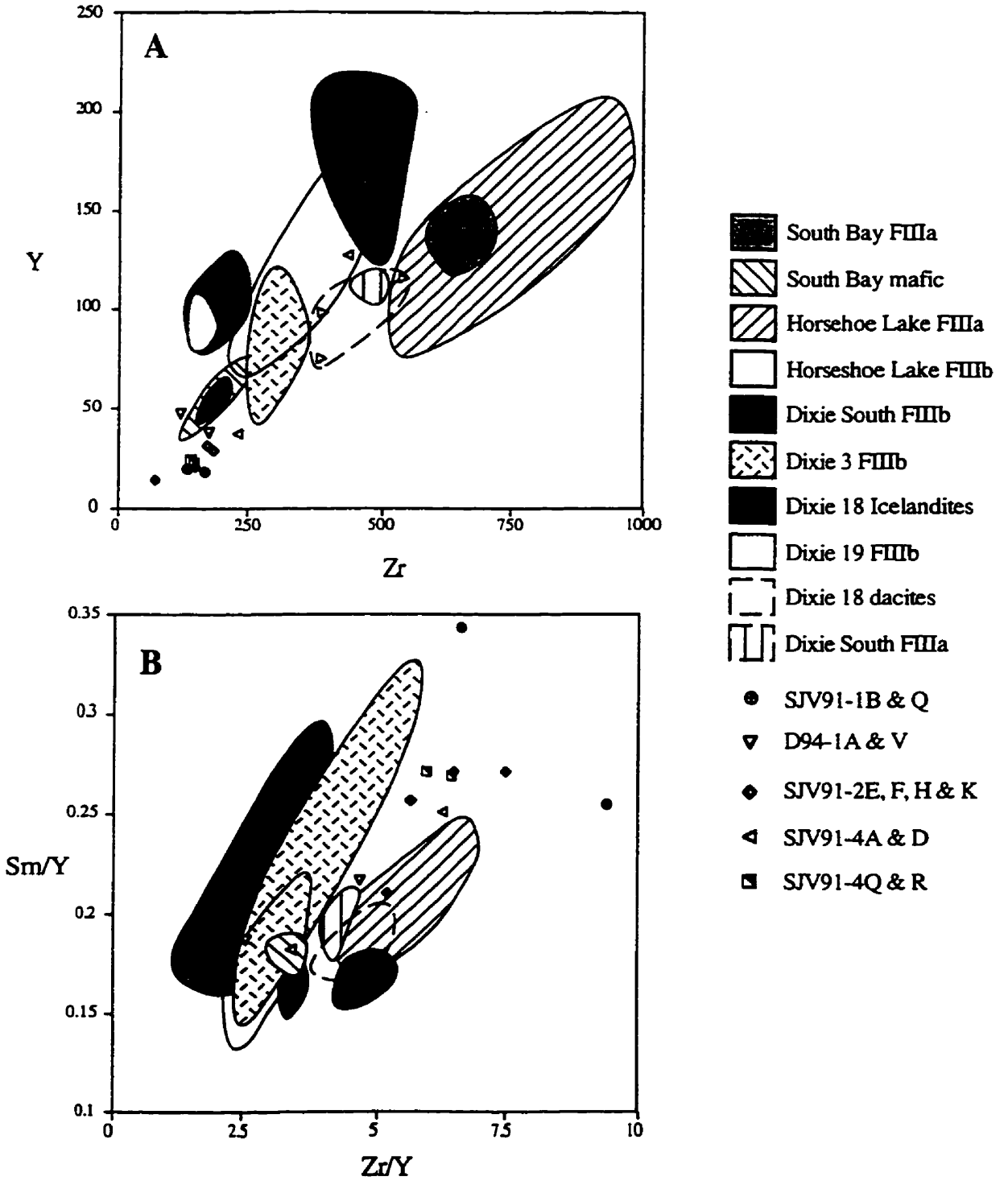

Figure 6.18. Zr versus Y (A) and Sm/Y versus Zr/Y (B) for felsic rocktypes from the Birch-Uchi greenstone belt.

fractionation and eruption patterns, were active penecontemporaneously and had a spacing on the order of a few (1-3) kilometres. The remaining rhyolites are more typical of FIIIa and display positive Zr and Hf anomalies in conjunction with higher Sc abundances (Figs. 6.17c).

Three felsic samples collected from the top of the Dixie 18 DDH are characterised by trace element patterns similar to those of FIIIa rhyolites, with low La/Yb_n ratios and high Sc abundances (Fig. 6.19a; Table 6.12). The similarity between the dacites and the intermediate icelandites found stratigraphically below them (Fig. 6.19) is consistent with the dacites being the product of more extreme fractionation of the andesites. Figure 6.18 displays Zr versus Y for these samples; the linear relationship between the icelandites and the dacites supports the model that the rhyolites fractionated from the icelandites. However, the trend is sufficiently broad to preclude ruling out the low-P basaltic andesites as a potential precursor. A second suite with FII-like characteristics is intercalated with the icelandites (Fig. 6.19b).

The majority of samples from the Dixie 3 DDH (SJV91-4) are rhyolites or high silica rhyolites with trace element characteristics of FIII type felsic rocks (Fig. 6.19c; Table 6.12). La/Yb_n ratios for these samples vary from 4-8 which is higher than the range reported for FIII felsics and is closer to those of FI; however La/Yb_n ratios are typically higher in type FIIIb than in FIIIa (Lesher et al., 1986). Scandium contents are consistent with these rocks being FIIIb felsics, as Sc values are generally lower than the range for FIIIa. A third line of evidence comes from the negative Zr and Hf anomalies which are associated with FIIIb type felsics at Horseshoe Lake (Fig. 6.19c). However, it is recognised that the degree of LREE enrichment seen in these samples is more typically associated with FI or FII felsics, although both these groups are generally characterised by lower SiO_2 contents than those found in the Dixie 3 samples (with the exception of FII felsics from Sturgeon Lake where SiO_2 contents up to 81 wt.% were reported by Lesher et al., 1986; Table 6.10).

6.4.4 Discussion of felsic volcanic rocks

The extensive database obtained from the Confederation assemblage of the Birch-Uchi greenstone belt allows for a number of observations and conclusions to be drawn concerning the petrogenesis of these rocks.

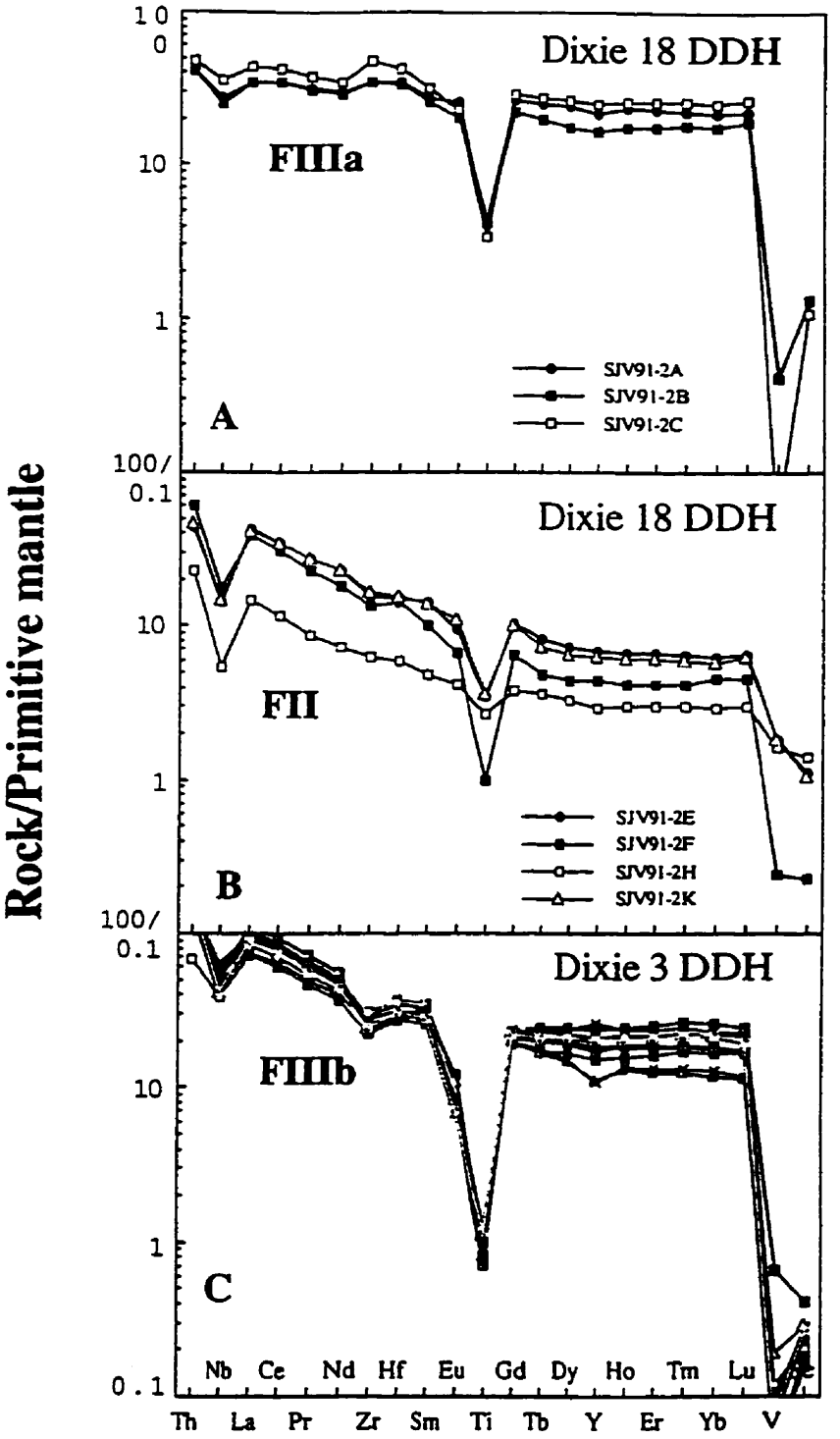

Figure 6.19. Primitive mantle normalised diagrams for felsic volcanic samples from the Dixie 18 and Dixie 3 DDH, of the Birch-Uchi greenstone belt.

The data presented above illustrates a number of limitations with the classification scheme of Lesher et al. (1986), as is to be expected as the Archean felsic database is expanded. Many of the felsic rocks discussed above display trace element patterns characteristic of various subtypes of the Lesher et al. (1986) classification, yet SiO_2 contents place them outside the range for those groups (e.g. the FIIIa dacites of the Dixie 18 DDH). This implies that SiO_2 contents are a poor tool for discriminating the various felsic subtypes. Also many of the samples analysed in this study are transitional between Leshers subtypes (e.g. the Dixie 3 DDH samples). This compositional overlap suggests that the felsic rock types of the Birch-Uchi belt have been formed by a combination of petrogenetic processes, rather than the distinct mechanisms proposed by Lesher et al. (1986). Consequently these classifications cannot be universally applied; for example FIIIa samples from the Birch-Uchi belt have Sc abundances consistently higher than the range reported by Lesher et al. (1986), whereas the FIIIb from this study display Zr/Y and Eu/Eu* ratios lower than typical values for FIIIb. Therefore, precise trace element data presented above provides a powerful means of distinguishing several subtypes of "FIII" felsic rocks in the area of the South Bay Mine.

Trace element analyses have revealed high and low-HFSE rhyolites indicative of recurring fractionation and recharge of a shallow level magma chamber, adjacent to suites of samples which do not display these characteristics. This implies multiple penecontemporaneous vents and magma chambers. Significant mineralised zones present in a number of drill holes, such as the South Bay mine site, Horseshoe Lake and Dixie South are associated with variations in the trace element characteristics of the volcanic host rocks. This observation is consistent with VMS deposition during periods of quiescence which permitted evolution of distinct magma batches in stable, periodically recharged magma chambers. Thin mineralized zones in the Dixie 18 hole do not appear to be associated with significant variations in geochemistry, which may reflect VMS deposition over comparatively shorter intervals between eruptions from a more open or "steady state" magma plumbing system.

In Figure 16.20 the relationship between the various felsic rocks of the Birch Uchi belt is evaluated by examining the HFSE anomalies. This plot can be used to distinguish between the FIIIa and FIIIb sub types of felsic volcanic rocks, with FIIIa rhyolites from the South Bay mine site DDH and the Horseshoe Lake DDH plotting with higher Zr/Zr* anomalies but also with a steeper trend than the FIIIb rhyolites. This plot would also seem to indicate that while many characteristics of the Dixie 19 suite are transitional between

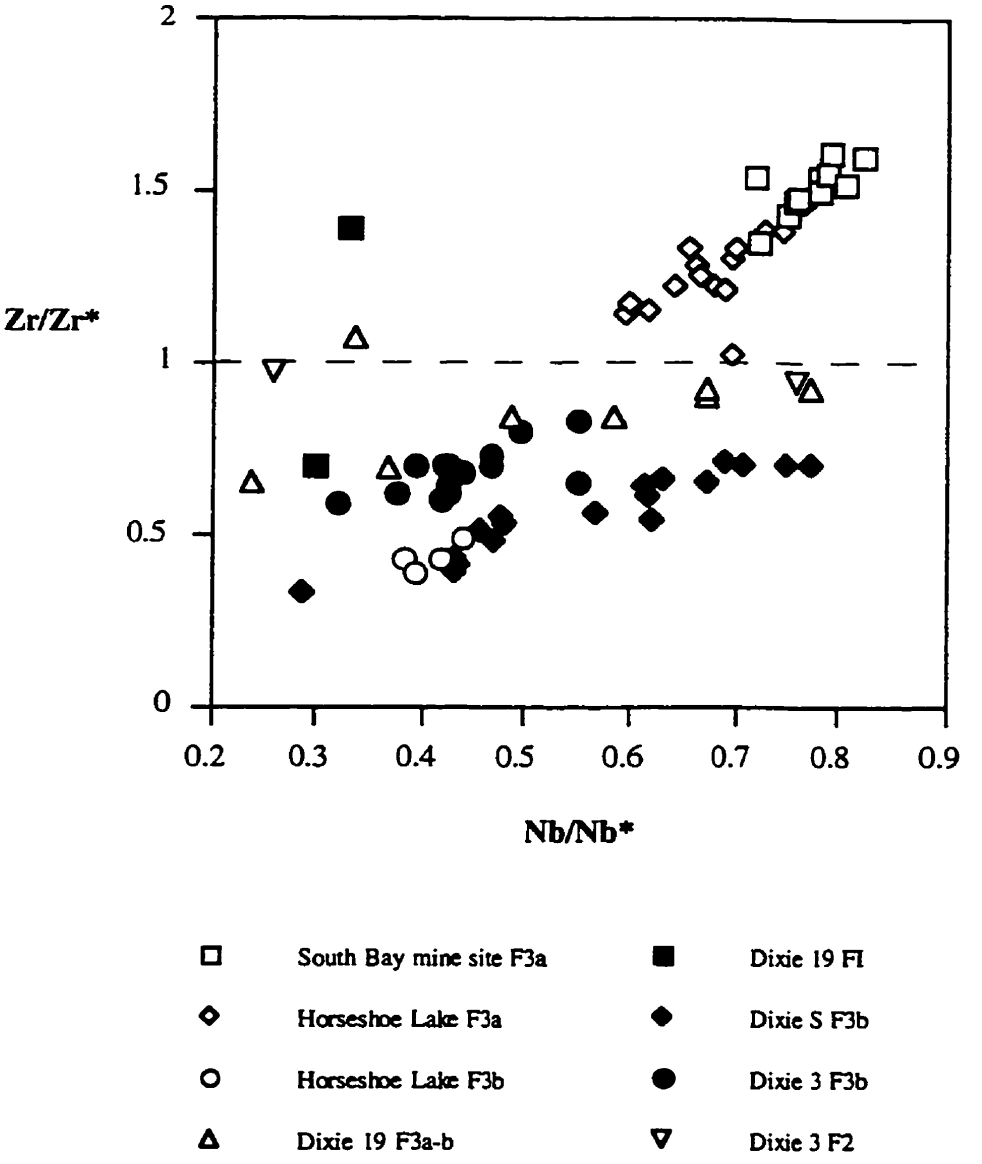

Figure 6.20. Nb/Nb* versus Zr/Zr* for felsic samples from the Confederation assemblage of the Birch-Uchi greenstone belt. Illustrating possible petrogenetic relationships between distinct suites.

FIIIa and FIIIb they are more closely related to FIIIb's. Figure 6.20 may also allow for correlation between different DDH from distinct areas, the overlap between the FIIIa rhyolites from the South Bay mine site and Horseshoe Lake DDHs suggest a petrogenetic link. Similarly the overlap between the Horseshoe Lake FIIIb and Dixie South FIIIb rhyolites indicates that these too may be petrogenetically linked.

6.5 Implications and geodynamic setting

6.5.1 Stratigraphy of the Rice Lake greenstone belt

Detailed mapping of the Confederation assemblage of the Rice Lake greenstone belt, in conjunction with the geochemical results discussed above, make it an excellent area for examining the relationship between the tholeiitic and calc alkaline volcanic rocks. The geochemistry of the Confederation assemblage in the Rice Lake belt is set in its stratigraphic context in Figure 6.21.

Brommecker (1996) conducted a comprehensive review of the Confederation assemblage stratigraphy in the Rice Lake greenstone belt. He observed that the Stormy Lake formation was comprised of both sedimentary rocks and intermediate tuffs, with all analyses from this formation plotting on the calc alkaline trend. Data from this study contradicts this finding as only tholeiitic rocks with flat trace element patterns have been identified, although this may well be a reflection of the limited sample set (Fig. 6.21). The Narrows formation was described as comprising dacites to rhyolites that also plot in the calc alkaline field (Brommecker, 1996). The sedimentary units in the Narrows formation are compositionally similar to those of the Stormy Lake formation, which Brommecker (1996) interpreted to indicate that the contact was gradational on a large scale. Data from this study indicates that the rocks from the Narrows formation are indeed calc alkaline in character (Fig. 6.21). Brommecker (1996) reports that the lower part of the Manigotagan River formation is clearly gradational into the Narrows formation, with the lower part of the Manigotagan River formation representing a transition upwards into more extensively reworked volcaniclastic rocks of similar composition to the Narrows formation. To summarise, the work of Brommecker (1996) is consistent with the formations of the Confederation assemblage in the Rice Lake belt having been deposited as a stratigraphically coherent package, and is not the result of tectonic stacking. This interpretation is supported by the work of Campbell (1971) who proposed that the rocks of the Gunnar and Stormy Lake formations are also in stratigraphic contact.

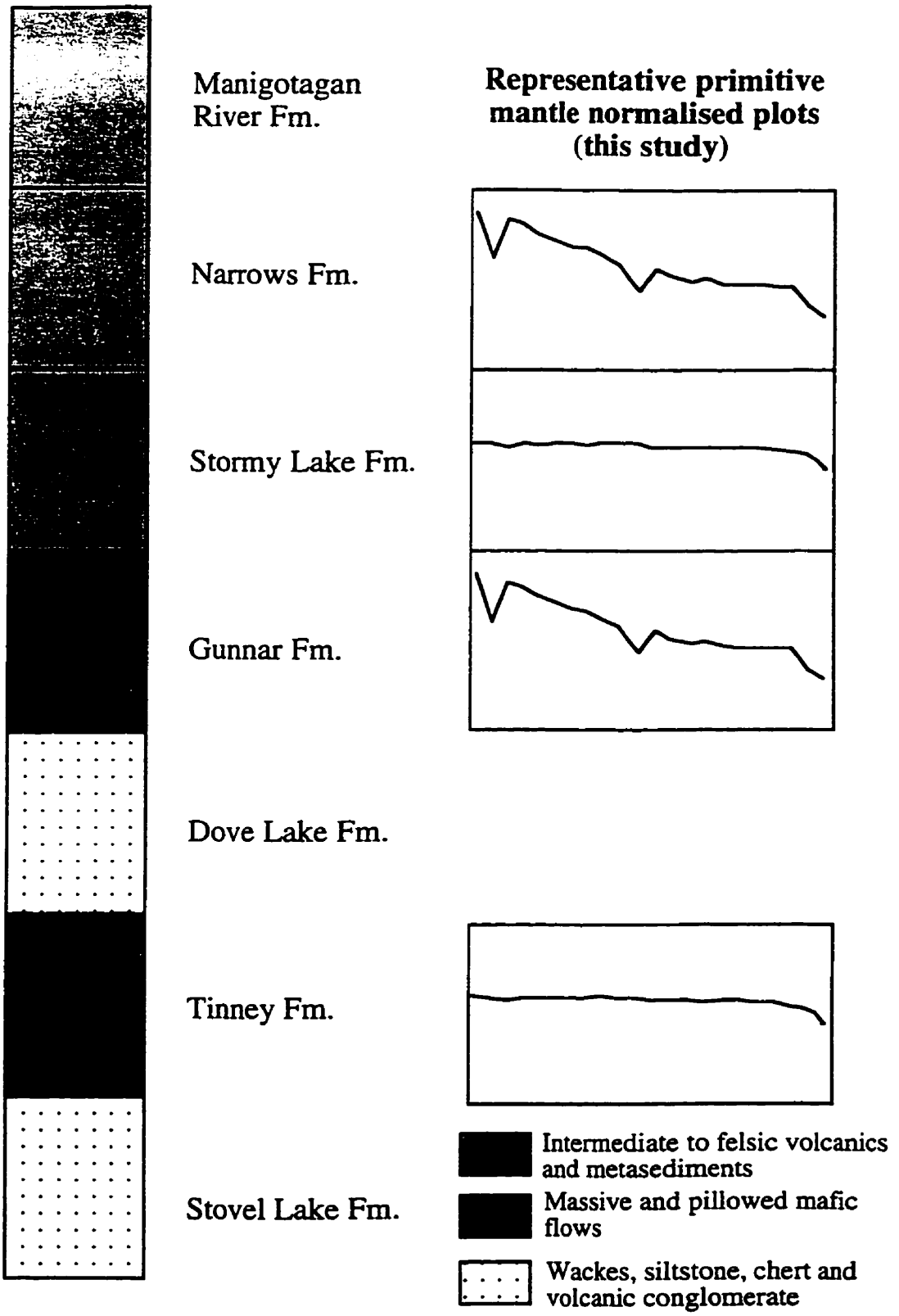

Figure 6.21. Schematic stratigraphic column for the Rice Lake greenstone belt and associated primitive mantle normalised patterns for data from this study, illustrating the intercalation of tholeiitic and calc alkaline volcanic rocks in an apparently continuous stratigraphic sequence.

Mapping in the Rice Lake belt indicates that Mg-Fe tholeiitic basalts are intercalated with calc-alkaline, arc related basalts in a stratigraphic relationship, without the presence of major faults (Brommecker, 1996). This stratigraphic relationship is significant because it implies that two distinct mantle components must have co-existed under the Uchi paleo-continental margin at ~2.7 Ga: one producing tholeiitic basalts and the other mature arc-related calc alkaline flows. One possible explanation for this is the conjunction of an arc with an active mantle plume similar to that envisaged for Kidd Creek complex (Wyman et al., 1997), or the older terranes of the Superior province (Chapter 4). However, the Confederation assemblage of the Rice Lake belt lacks the komatiites and low Ti tholeiites found at Kidd Creek (Wyman et al., in press) and incorporates significantly larger volumes of calc alkaline rocks than are present in the 3.0-2.9 Ga sequences. Consequently it is suggested that the Rice Lake greenstone belt may have been erupted in a back arc setting. Calc alkaline volcanics from a mature arc, deposited as volcaniclastic turbidity flows and subaqueous pyroclastic flows, were intercalated with tholeiites from the back arc rift.

6.5.2 Summary of results

A diverse range of rock types have been recognised in the Confederation assemblage. They can be summarised as follows:

1) Tholeiitic rocks with flat REE patterns and no HFSE anomalies. These are broadly comparable to the flat patterned tholeiites identified in all the older assemblages discussed in Chapters 4 and 5, which have been interpreted as plume-related ocean plateau tholeiites based on similarities with modern oceanic plateau (Mahoney et al., 1993). However, the association with the volcanic rocks discussed in points 2-5 below suggests that they formed in a back arc setting unrelated to a mantle plume. The absence of plume related komatiites in the Confederation assemblage supports this assumption.
2) Tholeiites with variably depleted to enriched LREE in conjunction with negative Nb anomalies. These are interpreted to be subduction influenced tholeiites likely erupted in either a primitive arc or back arc setting.
3) Calc alkaline mafic and intermediate volcanic rocks with enriched LREE and negative HFSE anomalies, consistent with an island arc setting. The degree of LREE enrichment in the Birch-Uchi greenstone belt is consistent with evolution from primitive arc tholeiites to more mature calc alkaline compositions.
4) OIB-like mafic flows characterised by LREE enrichment but lacking the HFSE anomalies of the island arc calc alkaline rocks. Rocks similar to these are reported

from a variety of modern arc settings.

5) A diverse range of felsic rocks including FI's derived from the melting of subducted oceanic slab, mantle wedge related FII's, as well as FIII's and associated icelandites, interpreted to be derived from the fractionation of tholeiitic magmas (c.f. Lesher et al., 1986).

6.5.3 Geodynamic setting

There is limited evidence for an older phase of volcanism in the Confederation assemblage, namely the 2747 +4/-3 Ma felsic volcanic rocks of the Lang Lake belt and the coeval 2750±3 Ma Dobie Lake pluton (Corfu and Stott, 1993b). The 2744±3 Ma and 2740 ±1 Ma ages from the Meen Dempster belt have been correlated with the intrusion of the Ochig Lake pluton and the Pickle Lake stock in the Pickle Lake belts (2741±2 Ma and 2740±2 Ma; Corfu and Stott, 1993a, b). A younger phase of volcanism has also been recognised, as recorded by the 2733 and 2730 Ma ages of the volcanic rocks in the Lake St. Joseph belt, the 2730 Ma ages from the Rice Lake belt and the 2733-2729 Ma plutonic age from the Red Lake belt (Corfu and Wallace, 1986; Stott and Corfu, 1991; Corfu and Stott, 1993a, b). In summary geochronological data for the Confederation assemblage spans a range of some 15-20 m.y. from the oldest occurrence in the Meen-Dempster belt to the youngest in the Lake St. Joseph belt.

Numerous researchers have interpreted the Confederation assemblage of the Birch-Uchi belt as a back arc sequence (Lesher et al., 1986; Noble, 1989; Corfu and Stott, 1993a). Corfu and Stott (1993a) recognised three suites in the Confederation assemblage of the central Uchi subprovince (Birch-Uchi, Meen-Dempster and Pickle Lake belts). The first comprises post tectonic TTG plutons in the Pickle Lake belt with epsilon Hf of 6.1 which suggest melting of juvenile crust along shallow dipping subduction zones (Corfu and Stott, 1993a). A second member of the arc suite, comprising an arc sequence of tholeiitic basalts overlying calc alkaline rocks with epsilon Hf of 3.2-4.0, either melted from metasomatised mantle or was contaminated by interaction with older basement. Corfu and Stott (1993a) identified a third suite of bimodal rhyolites and basalts based on the epsilon Hf values of 6.1 from the Found Lake porphyry in Birch-Uchi belt, which is associated with the FIII rhyolites common throughout the belt. They suggest that the epsilon Hf value is consistent with melting of tholeiites derived from a depleted mantle source, likely in a back arc regime. The occurrence of icelandites and the apparent fractionation of these to more felsic FIIIb compositions suggests the presence of longlived shallow magma chambers. It also supports the suggestion that the tholeiites melted to generate FIII's, as

although the origins and significance of icelandites remain poorly constrained, isotopic evidence suggests that associated rhyolites in Iceland represent melts of mafic crust (Sigmarsson et al., 1991). Noble (1989) determined epsilon Nd of five FIII tuffs and sills from the Birch-Uchi belt with values ranging from 1.7 to -1.2, which he interprets to be the result of variable degrees of contamination by significantly older crust. An alternative explanation is recycling of older (~3 Ga) sediments derived from the NCT. Stevenson (1995) has suggested that this process may account for the spectrum of epsilon Nd values in mafic to intermediate volcanic rocks of the North Spirit Lake greenstone belt. Distinguishing between these two processes is not possible, but the latter process is favoured given the other evidence for a back arc geodynamic setting.

Corfu and Stott (1993a) summarised their study by suggesting that the Birch-Uchi Confederation assemblage was erupted into a back arc basin, a view shared by Noble (1989) and Lesher et al., (1986). They also suggested that the Meen-Dempster belt was erupted in an arc setting. Further, structural evidence indicates that the ~2740 Ma plutons of the Pickle Lake belt were intruded into an already deformed and consolidated terrane, suggesting a continental arc setting.

The complex nature of the geochemistry in the Birch-Uchi belt and specifically the presence of primitive arc tholeiites and OIB-like rocks, is consistent with the model that the Birch-Uchi Confederation assemblage formed in a back arc basin. Hawkins and Allan (1994) have shown that there is no one specific back arc magma type; both MORB-like and arc-like magmas may be produced along with the transitional magma types commonly ascribed to back arc settings. Moreover, the various magma types can erupt simultaneously within the back arc environment. A diverse range of rock types have been recognised in modern back arc basins, like the Lau basin, including N-MORB, subduction influenced MORB, arc and OIB-like basalts (Gill, 1987; Saunders and Tarney, 1991; Pearce et al., 1995).

This study has demonstrated that similar volcanic rocks, including OIB-like and subduction influenced tholeiites, are present in the Meen-Demspter belt. This suggests that the Confederation assemblage of the Meen-Dempster belt is a back arc sequence and not an arc, as suggested by Corfu and Stott (1993a). The lack of significant volumes of the felsic volcanic rocks associated with rifting (e.g. FIII rhyolites and icelandites) and the presence of VMS deposits, as found in the Birch-Uchi belt, may be accounted for by the older age of the Meen-Dempster Confederation assemblage (2744 Ma versus 2735-2739

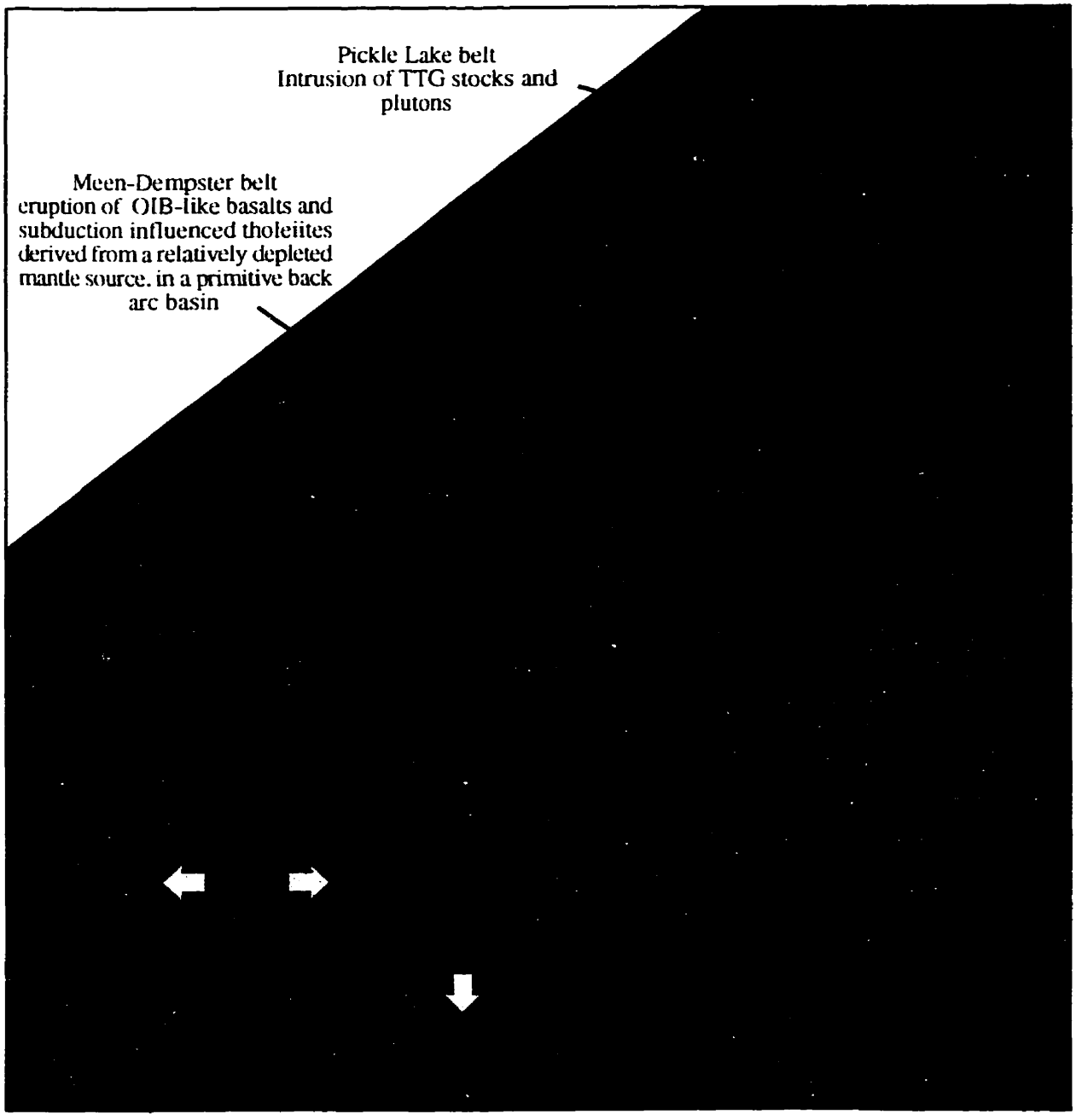

Figure 6.22. Schematic diagram depicting the geodynamic setting of the Confederation assemblage at ~ 2.74 Ga

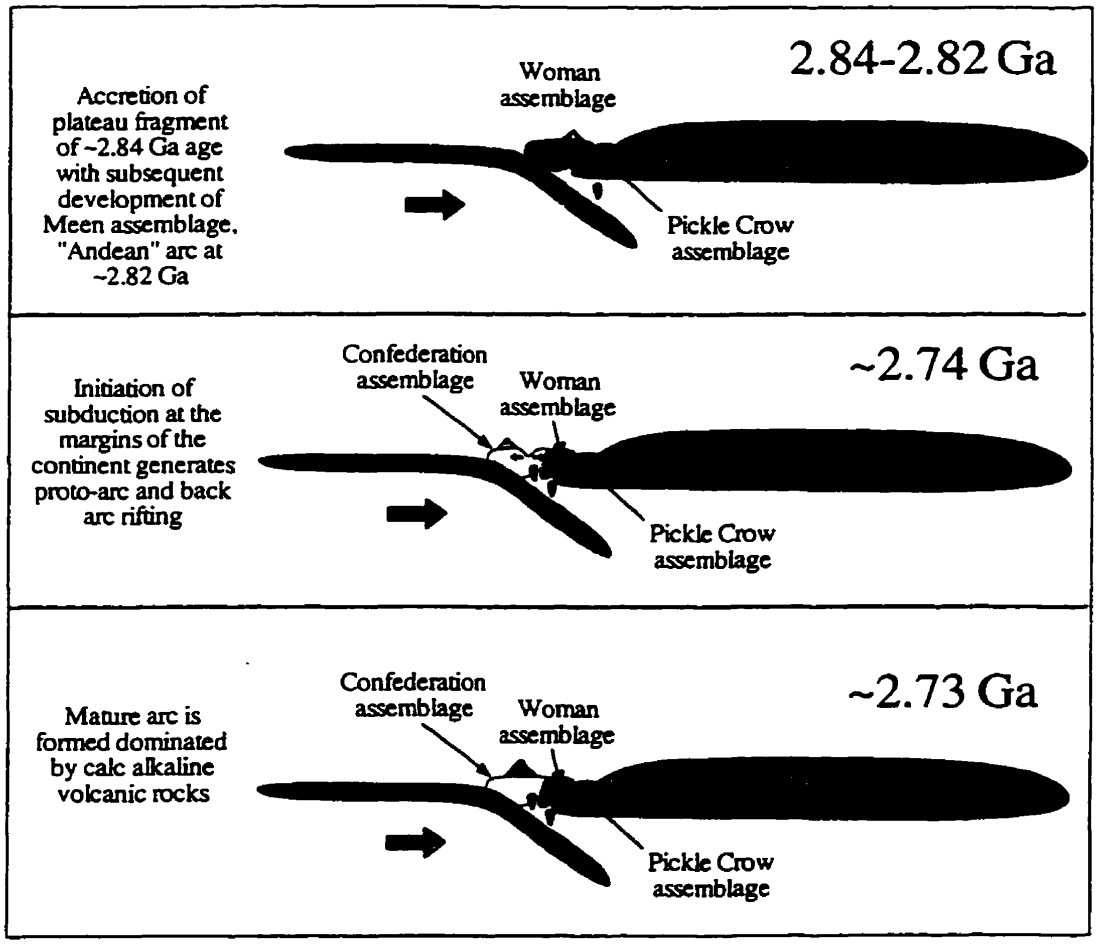

Figure 6.23. Schematic diagram illustrating the proposed geodynamic setting for the Confederation assemblage. The initiataion of subduction at ~2.74 Ga results in development of a back arc basin (Meen-Dempster and Birch-Uchi belts). With time the arc matures and calc alkaline rocks are erupted at ~2.73 Ga.

Ma). It is suggested that the Meen-Dempster belt represents an earlier phase in the rifting of the arc,whereas the Birch-Uchi belt represents a more mature back arc basin (Figs. 6.22 and 6.23). The intrusion of slab derived TTG's in the Pickle Lake belt may simply reflect the absence of a back arc rift in that area at that time.

Corfu and Stott (1993a) suggest that extension behind arcs requires steep subduction, but that this conflicts with the idea of shallow angle subduction of young, warm oceanic lithosphere that they propose is required to generate the TTG suite that was intruded into Pickle Lake belt at that time (~2740 Ma). Consequently they suggest that the back arc basin may be the result of a plate boundary irregularity that created local extension in an otherwise dominantly shallow angle subduction regime. They conclude that the older 2744-2740 Ma suite developed by arc volcanism but that the expression of the magmatism varied along the length of the arc. Bédard et al. (1998), in a study of the Betts Cove ophiolite, Newfoundland, suggested that attempted subduction of the continental margin on promontories would have slowed convergence, allowing for trench rollback and extension of the overriding plate within reentrants (Harris, 1992; Cawood and Suhr, 1992). This concept is consistent with Corfu and Stotts (1993a) proposal that irregularities in the Uchi margin were responsible for the coeval eruption of TTG in the Pickle Lake belt and back arc rocks in the Birch-Uchi belt. However, recent studies have suggested that back arc basin development can be related to the initiation of subduction and not necessarily to the angle of descent of the subducting slab (e.g. Bédard et al., 1998).

Wharton et al. (1995) have summarised the relationship between arc volcanism, rifting and back arc spreading as follows:

1) Establishment of a proto-arc, following the initiation of subduction, with eruption of depleted tholeiitic and ultradepleted boninitic magmas

2) Rifting of the proto arc to form a trenchward frontal arc, a remnant arc and an intervening back arc basin where tholeiitic magmas are erupted during back arc spreading

3) Establishment of a second phase of arc volcanism between the rifted margin of the frontal arc and the back arc basin; initially volcanism will be both tholeiitic and calc alkaline in character, but as the arc stabilises and matures calc alkaline volcanism will dominate.

The ~25 m.y. time span that Wharton et al. (1995) propose for this sequence is comparable to that of the Confederation assemblage. It is suggested that the geology and

geochemistry of the central Uchi Confederation assemblage is consistent with this model. The TTG intrusions were emplaced into the arc at Pickle Lake and the OIB-like rocks erupted into the back arc basin that developed behind the arc front (Stage 2 of Wharton et al., 1995). The predominance of calc alkaline rocks in the younger occurrences of the Confederation assemblage is consistent with Stage 3 of the Wharton et al. (1995) model reflecting the development of a more mature arc complex.

Similarly diverse assemblages have also been documented in Precambrian back arc settings. Sharkov and Smolkin (1997) have suggested that the association of tholeiites with flat REE patterns, alkaline OIB like rocks and calc alkaline andesites in the Proterozoic Pechenga-Varzuga belt is best interpreted as a back arc sequence. The stratigraphy of the ~2.2 Ga Pechenga-Varzuga indicates that opening of the back arc was characterised by the eruption of alkaline basalts and iron-rich titaniferous picrites, broadly comparable to the OIB-like rocks of the Birch-Uchi and Meen-Dempster belts.

6.6 Conclusions

The wide range of geochemical compositions preserved in the Confederation assemblage provides strong evidence for its origin as a back arc basin. Field evidence and the new geochemical data presented above indicate that a general stratigraphic pattern in the assemblage may consist of lower OIB-like rocks overlain by subduction influenced tholeiites that are in turn overlain by an association of plateau-type tholeiites and upper intermediate to felsic calc alkaline rock types. Consequently, it is suggested that the OIB-like rocks represent the earliest phase in the opening of the basin, where the OIB-like basalts most plausibly represent melts derived from relatively enriched components introduced by mantle upwelling as a result of lithospheric thinning. In the older Meen-Dempster belt these OIB-like rocks are associated with subduction influenced tholeiites, derived from a relatively depleted mantle source. In the Birch-Uchi belt the OIB-like rocks are associated with Nb depleted tholeiites with less depleted LREE indicative of a less depleted source. This may reflect the influx of relatively less depleted mantle as the back arc basin opens and matures. The youngest phase of the Confederation assemblage comprises calc alkaline rocks consistent with a mature island arc.

At present, the significance of the "plateau-type" basalts with no Nb anomalies closely associated with the calc alkaline volcanic rocks is uncertain. However, the ~ 2740 Ma period corresponds with the onset of plume-related volcanism elsewhere in the Superior

Province (e.g., Abitibi belt: Dostal and Mueller, 1997). The intimate association of the contrasting rock types in the Confederation assemblage may reflect an example of arc-plume interaction now recognized in the southern part of the Province (op cit.; Wyman et al., 1997). Alternatively allochthonous stacking of the plateau basalts onto the subduction related sequence, prior to continued arc volcanism, may account for the stratigraphic relationships. To date, no indication of a discontinuity between the sequences has been recognised, but this does not preclude the possibility of the presence of a cryptic thrust fault.

CHAPTER 7

SUMMARY AND CONCLUSIONS

7.1 Summary of findings

The comprehensive database presented in this thesis allows for a number of conclusions to be drawn about the ~300 m.y. of volcanic activity preserved within the Uchi subprovince. The principal conclusions of this thesis are as follows:

(1) The 2.9-3.0 Ga greenstone belts discussed in Chapter 4 include suites of ultramafic rocks, which are generally accepted to be related to mantle plumes. Komatiites within the Lumby Lake belt, interpreted to be a fragment rifted off the North Caribou Terrane (NCT), as well as within the Balmer and Ball assemblages provide compelling evidence for over 100 m.y. of plume related activity in the early stages of the development of the Uchi paleo continental margin. Several plumes, ascending over different time intervals during a period of enhanced plume activity, could account for the extended period of plateau-type volcanism recorded in these older assemblages. However, the > 70 m.y. Hawaiian hotspot track, and the apparent association of modern hotspots such as Tristan da Cunha, Galapagos and Kerguelan/Heard Island with 80-130 Ma volcanism (Davies et al., 1989; Bercovici and Mahoney, 1994; Storey, 1995; Class et al., 1996) indicate that it is possible for a single mantle plume to be responsible for the entire komatiite-tholeiite component of the assemblages.

(2) A number of komatiites from the Ball and Balmer assemblages, and in the North Caribou greenstone belt (Hollings and Kerrich, 1998), display evidence for interaction with continental crust. This is indicated by the correlation between progressive LREE enrichment and negative Nb anomalies.

(3) The distinctive HREE-V-Sc systematics of the komatiites from the Balmer and Garner Lake assemblages supports the correlation of the two assemblages as

suggested by Poulsen et al. (1996). The HREE-V-Sc systematics of the ultramafic rocks from the Ball, Balmer and Garner Lake assemblages cannot be accounted for by crustal contamination models. Rather they are interpreted to be the result of interaction with previously depleted mantle, possibly similar to the mantle source for boninites, and are tentatively suggested to record interaction between a mantle plume and subduction influenced mantle. These systematics would appear to be unique to the older northern greenstone belts of the Superior Province, given that they have not been recognised from southern Superior belts.

(4) Further evidence for a strong spatial association of arc and plume magmatism is provided by the sporadic felsic volcanic units intercalated throughout the stratigraphy of the older assemblages. Two felsic rock subtypes recognised within the older assemblages both display geochemical characteristics consistent with melting of basaltic ocean crust in a subduction zone. The predominant Type 1 rhyolite is directly comparable to southern Superior Province examples associated with oceanic arc sequences, and are comparable to Archean high Al, high La/Yb_n TTGs. Intercalated tholeiite-komatiite and calc alkaline volcanic sequences of the Lumby Lake belt span the 3.0 to 2.9 Ga period and, along with numerous granitoids intruded throughout this period, provide direct evidence that plume and arc type geodynamic processes operated simultaneously or intermittently in close association (Hollings and Wyman, 1998). This model can be extended to encompass the Ball and Balmer assemblages of the Uchi subprovince.

(6) Collectively, the geochemical, geochronological and stratigraphic evidence from the northern Superior Province greenstone belts, as well as the similarly-aged Lumby Lake belt provide strong evidence for both a spatial and temporal association of mantle plumes and subduction zones during generation of the Uchi-Sachigo-Goudalie (USG) proto-continent nucleus of the Superior Province. It is therefore noteworthy that recent modelling suggests plume-ridge interactions adjacent to Archean subduction zones may have caused increased TTG magmatism and the development of long-term unsubductable arc lithosphere (Abbott, 1996). If as Davis and Jackson (1988) and Stott (1997) suggest, on the basis of contemporaneous pulses of mafic and felsic magmatism preserved in both areas, the Lumby Lake belt is a fragment rifted off the nascent USG, then it must have formed marginal to the proto-continent through which the Ball and Balmer assemblages were erupted in order to have inherited their crustal contamination signature. This interpretation is

supported by the lack of any isotopic evidence for contamination of Lumby Lake komatiites and tholeiites by continental crust (Hollings et al., 1996).

(7) The Northern Pickle assemblage of the Pickle Lake greenstone belt is tentatively interpreted to record the rifting apart of the NCT. OIB-like basalts identified in the assemblage, are similar to samples from the top of the tectono-stratigraphic sequence in the Lumby Lake belt, where the REE enrichment is interpreted to be the result of small degree partial melts thought to be associated with the early stages of rifting. Poor stratigraphic control in the Northern Pickle assemblage prevents the development of a detailed model to account for the occurrence of both plateau type and OIB-like basalts.

(8) The Pickle Crow assemblage of the Pickle Lake belt is interpreted to preserve the first phase of continental growth along the newly formed proto-continental Superior Province. Tholeiitic basalts with flat REE patterns are interpreted to be ocean plateau tholeiites that were accreted to the Uchi paleo continental margin prior to the formation of the Woman assemblage at ~2840 Ma. Intermediate to felsic volcanic rocks stratigraphically above the tholeiites are compositionally similar to modern rocks found in continental island arcs. This result is consistent with the generation of an island arc complex following choking of the subduction zone by the newly accreted plateau fragment. Subsequent back stepping of the subduction zone led to development of a volcanic arc complex (c.f., Saunders et al., 1996).

(9) The Woman-Meen assemblage developed subsequent to formation of the Pickle Crow assemblage. This study has demonstrated that the ~2825 Ma Meen assemblage of the Meen-Dempster belt is comprised of calc alkaline arc volcanics. The older ~2840 Ma Woman assemblage consists predominantly of plateau-like tholeiites. These relationships are consistent with the Woman assemblage forming as an ocean plateau and accreting to the Uchi paleo-continental margin some 15 m.y. later, at which point the Meen assemblage arc complex was generated in a similar manner to that suggested for the calc alkaline rocks of the Pickle Crow assemblage.

(10) In order to identify the presence of the Meen assemblage within other occurrences of the Woman assemblage along the length of the subprovince, detailed geochronological studies would be necessary. However data from this study reveals the presence of both tholeiitic and calc alkaline rocks in many occurrences of the

Woman assemblage. Consequently the plateau accretion model suggested for the Meen-Dempster belt is tentatively extended to encompass the Woman-Meen assemblages in the subprovince as a whole.

(11) The final stage in the evolution of the Uchi subprovince is preserved in the Confederation assemblage and related Lake St. Joseph assemblage. The data presented in this study is consistent with previous models for the Confederation assemblage of the Birch-Uchi belt, which has been interpreted as having formed in a back arc basin (Lesher et al., 1986; Noble, 1989). This study has demonstrated that the volcanic rocks of the Confederation assemblage of the Meen-Dempster belt also display a geochemical signature of a back arc basin. Geochemical and geochronological data are consistent with a model whereby the back arc basin grew progressively wider, from east to west (Fig. 6.22). Within the Confederation assemblage it is possible to establish a progression with time. Formation of a simple island arc system, preserved in the Red Lake and Pickle Lake calc alkaline volcanics, was followed by a more complex rifted back arc association represented by the complex geochemistry of the VMS hosting rocks of the Birch-Uchi belt. The progression culminates in the intercalation of tholeiites and arc rocks seen in the Rice Lake greenstone belt, which is interpreted to represent a mature phase of the back-arc rift.

7.2 Implications for models of Archean continental growth

Although it is widely recognised that plate tectonic processes comparable to those acting today are likely to have occurred in the Archean (e.g. Desrochers et al., 1986; Abbott, 1996; Saunders et al., 1996), recent work has revived the concept of non-plate tectonic models. For example Hamilton (1998) advocates a fixist model for Archean greenstone belts, arguing strongly against the presence of plate tectonics in the Archean. This study provides strong evidence for the presence of subduction zones over a period of some 300 m.y. from ~3 Ga supporting models that invoke plate tectonics in the Archean.

Various models have been advocated for the nature of continental growth (Armstrong, 1991; McCulloch and Bennett, 1994; Taylor and McLennan, 1995) and, although the rate of growth is not yet fully constrained, it is now widely accepted that continental crust has grown by accretionary processes at convergent margins since the early Archean (Taylor and McLennan, 1995; Condie, 1997). Models for the mechanism of continental growth

have included accretion of oceanic plateau, accretion of island arcs, obduction of normal oceanic crust, and Andean-style arc magmatism.

Oceanic plateau tend to be thicker and more buoyant than normal oceanic crust and consequently are relatively unsubductable (Saunders et al., 1996). Numerous examples of plateau obduction and subsequent arc development are recognised in the literature (e.g., Desrochers et al., 1986; Stein and Goldstein; 1996; Tejada et al., 1996). Data for the Woman-Meen and Pickle Crow assemblages of this study is consistent with a plateau accretion model, particularly given the ~15 m.y. interval between the formation of the plateau-type Woman assemblage and the arc related Meen assemblage. The Confederation assemblage does not provide such compelling evidence for plateau obduction but does record the development of an arc - back arc complex along the margins of the Uchi subprovince.

The stratigraphic evidence from the older assemblages investigated in this study indicates that the plateau accretion models of Desrochers et al. (1993) for the 2.7 Ga Abitibi belt, Boher et al. (1992) for the ~2.1 Ga Birimian terranes of West Africa and Stein and Goldstein (1996) for the Arabian-Nubian shield, where arcs develop on obducted oceanic plateau, cannot be directly applied. Unlike the plateau accretion model, the coeval eruption of tholeiites and calc alkaline magmas implies the presence of an active plume or plumes for 100 m.y. The geochemistry and geochronology of these assemblages is consistent with ~100 m.y. of plume-arc interaction, as indicated by intercalation of sparse TTG-like felsic volcanic rocks within the predominantly plateau-like stratigraphy. Wyman and Hollings (1998) have tentatively identified this association in the Lumby Lake greenstone belt to be the product of plume-modified ridge subduction, in a model similar to that of Abbott (1996) for the Taitao ophiolite complex. Condie (1997) has suggested that the first continents in the Archean would have formed by collision of ocean ridge/plateau blocks with each other, which is consistent with the above models. The data for the subprovince as a whole requires interaction between a plume and a subduction zone along the margins of a continent in order to account for the variable contamination signature in the komatiites.

Evidence of interaction between plumes or plateaus and subduction zones is increasingly recognized in the geologic record (Kimura et al., 1993; Stern et al., 1995; Stein and Goldstein, 1996; Saunders et al., 1996). In addition, plume influence on active subduction zones has been identified in the SW Pacific (Lau Basin; Pearce et al., 1995)

and direct plume impingement on subduction zones has been suggested in the case of the Yellowstone plume on the Farralon plate (Parsons et al., 1994), the mid-Cretaceous Marie Byrd Land plume on the Pheonix Plate subducting beneath Antarctica (Weaver et al., 1994). Plume-arc interaction has recently been advocated for the Kidd Creek volcanic complex of the Abitibi greenstone belt (Wyman et al., 1998).

The observations and results from the Uchi subprovince presented in this study bear not only on models for the development of the Superior Province itself, but also the crust-mantle evolution of the Archean in general. A number of models have been suggested for the evolution of the Earths crust-mantle system, these include:

(1) McCulloch (1993) proposed that subducted Archean slabs were largely disaggregated and consequently unable to penetrate into the deep mantle, limiting recycling to the upper mantle. As a result a low viscosity upper mantle lid formed isolating the upper and lower mantle into distinct convection cells. In the post-Archean the subduction of older, colder oceanic crust resulted in slab dehydration rather than slab melting allowing slabs to penetrate into the lower mantle, promoting recycling of lithosphere that was returned as OIBs. He argued that the depleted upper mantle 'stepped down' as continental crust was progressively created.

(2) Campbell and Griffiths (1992) advocate that since ~4 Ga, the upper mantle has been depleted and underlain by a 'geochemically neutral' lower mantle, in turn underlain by a geochemically depleted lower mantle that was the source of LREE depleted Al-undepleted komatiites. They suggest that the absence of OIB-type rocks in Archean plumes, but their widespread occurrence in post-Archean plumes, is the result of tapping of modified oceanic lithosphere at the core mantle boundary. They interpret this to indicate that subduction processes were active at ~3.8-4.0 Ga, implying that whole mantle convection has occurred throughout much of the Earths history.

(3) An alternative to these models is that of Stein and Hofmann (1994) who proposed that episodic crustal growth and major orogenic events may have been associated with discrete episodes of major plume activity. They defined this relationship as mantle overturn and major orogenesis (MOMO). During these MOMO episodes whole mantle convection would dominate, whereas in the intervening periods the upper and lower mantle would have comprised discrete convection cells.

The recognition of LREE enriched Al-depleted komatiites and associated OIB-like basalts in the older assemblages of this study and in the Lumby Lake greenstone belt (Hollings and Wyman, 1998), contradicts the first model presented above. The presence of LREE depleted Al-undepleted komatiites is in accord with the second model. Evidence for an extensive episode of plume related crustal growth between 2.9-3.0 Ga is broadly consistent with the MOMO model of Stein and Hofmann (1994).

7.3 Future work

Although this study has recognised a diverse range of geochemically distinct volcanic rocks, which have been utilised to generate the geodynamic models presented above, a number of questions remain to be resolved and should be addressed in future studies:

- The isotopic (Sm-Nd, Lu-Hf, Re-Os) compositions of the distinctive komatiites from the Ball and Balmer assemblages.

- The role of sediment subduction in Archean arc magma compositions, particularly the strongly Th-enriched basalts of the Birch-Uchi greenstone belt.

- Geochronological studies of the Meen assemblage within the Woman assemblage of the Uchi subprovince outside the Meen-Dempster belt.

- Geochronological studies of the calc alkaline rocks of the Pickle Crow assemblage in order to constrain the timing of arc development and plateau fragment accretion.

- Evaluation of models presented in this study in light of the Western Superior Lithoprobe transect that is currently underway.

References

Abbott. D.H., 1996. Plumes and hotspots as sources of greenstone belts. Lithos 37, 113-127.

Abbott D. H. and Hoffman S. E., 1984. Archean plate tectonics revisited 1. Heat flow, spreading rate, and the age of subducting oceanic lithosphere and their effects on the origin and evolution of continents. Tectonics, 3, 429-448.

Aitken, B.G. and Echeverria, L.M., 1984. Petrology and geochemistry of komatiites and tholeiites from Gorgona Island, Colombia. Contributions to Mineralogy and Petrology, 86, 94-105.

Allegre, C. J., 1982. Genesis of Archaean komatiites in a wet ultramafic subducted plate. *In* Arndt, N.T. and Nisbet, E.G., eds., Komatiites: Allen and Unwin, London, 495-500.

Alvarado, G., Denyer, P. and Sinton, C.W., 1997. The 89 Ma Tortugal komatiitic suite, Costa Rica: Implications for a common geological origin of the Caribbean and Eastern Pacific region from a mantle plume. Geology, 25, 439-442.

Andrews, A.J., Hugon, H., Durocher, M., Corfu, R. and Lavigne, M.J., 1986. The anatomy of a gold bearing greenstone belt: Red Lake, northwestern Ontario, Canada, *in* Proceedings of Gold '86, an International Symposium on the Geology of Gold Deposits, Konsult International Inc., Toronto, 3-22.

Armstrong, R. L., 1991. The persistent myth of crustal growth. Australian Journal of Earth. Sciences, 38, 613-630.

Arndt, N. T., 1991. High Ni in Archean tholeiites. Tectonophysics, 187, 411-419.

Arndt, N.T., 1994. Archean komatiites. *In*; Condie, K.C. (ed.), Archean crustal evolution, Elsevier, 11-44.

Arndt, N.T. and Jenner, G.A., 1986, Crustally contaminated komatiites and basalts from Kambalda, Western Australia, Chemical Geology, 56, 229-255.

Arndt, N.T. and Nesbitt, R.W., 1982, Geochemistry of Munro Township basalts, *in* Arndt, N.T. and Nisbet, E.G., eds., Komatiites: Allen and Unwin, London, p. 309-329.

Arndt, N.T., Kerr, A.C. and Tarney, J., 1997. Dynamic melting in plume heads: the formation of Gorgona komatiites and basalts. Earth and Planetary Science Letters, 146. 289-301.

Arth, J.G., Barker, F., Peterman, Z.E. and Friedman, I., 1978. Geochemistry of the gabbro-diorite-tonalite-trondhjemite suite of southwest Finland and its implications for the origin of tonalitic and trondhjemitic magmas, Journal of Petrology, 19, 289-

316.

Atkinson, B.T., Parker, J.R. and Storey, C.C., 1990, Red Lake Resident Geologist's District-1990; *In* Report of Activities 1990, Resident Geologists, Ontario Geological Survey, Miscellaneous Paper 152, 31-66.

Barley, M.E., 1986, Incompatible element enrichment in Archean basalts: a consequence of contamination of older sialic crust rather than mantle heterogeneity, Geology, 14, 947-950.

Barley, M.E. and Groves, D.I., 1992. Supercontinent cycles and the distribution of metal deposits through time. Geology, 20, 291-294.

Barley, M.E., Pickard, A.L. and Sylvester, P.J., 1997. Emplacement of a large igneous province as a possible cause of banded iron formation 2.45 billion years ago. Nature, 385, 55-58.

Barley, M.E., Groves, D.I., Krapez, B. and Kerrich, R., 1995. The late Archean: A major anomaly in global metallogeny, Precambrian '95, Montreal, Canada, 314 p.

Barrie, C.T., 1997. Komatiite flows of the Kidd Creek Footwall, Abitibi Subprovince, Canada. Economic Geology Monograph 10 The Giant Kidd Creek Volcanogenic Massive Sulfide Deposit, Western Abitibi Subprovince, Canada: In Press.

Barrie, C.T. and Shirey, S.B., 1991. Nd and Sr isotope systematics for the Kamiskotia-Montcalm area: implications for the formation of Late Archean crust in the western Abitibi subprovince, Canada: Canadian Journal of Earth Science, 28, 58-76.

Barrie, C. T., Gorton, M. P., Naldrett, A. J. and Hart. T. R., 1991. Geochemical constraints on the petrogenesis of the Kamiskotia gabbroic complex and related basalts, western Abitibi Subprovince, Ontario, Canada: Precambrian Research, 50, 173-199.

Beakhouse, G.P., 1989. Geology of the Western Birch Lake area, Kenora District, Patricia Portion, Ontario Geological Survey, Open File Report 5700, 106p.

Bédard, J.H., Lauziere, K., Tremblay, A. and Sangster, A., 1998. Evidence for forearc seafloor-spreading from the Betts Cove ophiolite, Newfoundland: oceanic crust of boninitic affinity. Tectonophysics, 284, 233-245.

Bercovici, D., and Mahoney, J., 1994. Double flood basalts and plume head separation at the 660 kilometre discontinuity. Science, 266, 1367-1369.

Berger, B.R., 1981. Stratigraphy of the western Lake St. Joseph greenstone terrain. Unpublished Msc thesis, Lakehead University, Thunder Bay, 117p.

Beswick, A.E., 1983. Primary fractionation and secondary alteration within an Archean ultramafic lava flow. Contributions to Mineralogy and Petrology, 82, 221-231.

Bickle, M. J., Nisbet, E. G., and Martin, A., 1994. Archean greenstone belts are not

oceanic crust. Journal of Geology, 102, 121-138.

Blackburn, C.E., Johns, G.W., Ayer, J.A. and Davis, D.W., 1991. Wabigoon Subprovince, *In*: Geology of Ontario, Ontario Geological Survey, Special Volume 4, Part 1, 303-382.

Blichert-Toft, J. and Albarede, F., 1994. Short-lived chemical heterogeneities in the Archean mantle with implications for mantle convection. Science, 263, 1593-1596.

Boher, M., Abouchami, W., Michard, A., Albarede, F. and Arndt, N.T., 1992. Crustal growth in West Africa at 2.1 Ga. Journal of Geophysical Research, 97, 345-369.

Bowen, R.P., 1989. Geology of the Slate Lake area, District of Kenora (Patricia Portion), Ontario Geological Survey, Report 256, 82p.

Breaks, F.W., Osmani, L.A. and deKemp, E.A., 1986. Opapimiskan Lake project: Precambrian geology of the Opapimiskan-Forester Lakes area, District of Kenora, Patricia Portion, *in* Summary of Fieldwork and other Activities, 1986, Ontario Geological Survey, Miscellaneous Paper 132, 368-378.

Brommecker, R., 1996. Geology of the Beresford Lake area, south eastern Manitoba (52L/14), Manitoba Energy and Mines, Open File Report 3318, 127 p.

Brown, A.V. and Jenner, G.A., 1989. Geological setting, petrology and chemistry of Cambrian boninite and low-Ti tholeiite lavas in western Tasmania. In: A.J. Crawford (Editor), Boninites. University of Tasmania, Geology Department, Hobart, Tasmania, 232-263.

Cameron, W.E., 1989. Contrasting boninite-tholeiite associations from New Caledonia. In: A.J. Crawford (Editor), Boninites. University of Tasmania, Geology Department, Hobart, Tasmania, 314-338.

Cameron, W.E., McCulloch, M.T. and Walker, D.A., 1983. Boninite petrogenesis: chemical and Nd-Sr isotopic constraints. Earth and Planetary Science Letters, 65, 75-89.

Campbell, F.H.A., 1971, Stratigraphy and sedimentation of part of the Rice Lake Group, Manitoba, In; W.D. McRitchie and W.Weber (eds), Geology and Geophysics of the Rice Lake region, southeastern Manitoba, Manitoba Department of Mines and Natural Resources, Mines Branch Publication 71-1, 135-188.

Campbell, I.H. and Griffiths, R.W., 1992. The changing nature of mantle hotspots through time: Implications for the chemical evolution of the mantle. Journal of Geology, 92, 497-523.

Campbell, I.H., Coad, P., Franklin, J.M., Gorton, M.P., Hart, T.R., Scott, S.D., Sowa, J., 1981. Rare earth elements in felsic volcanic rocks associated with Cu-Zn massive sulphide mineralization. Ontario Geological Survey, Miscellaneous Paper

98, 45-53.

Campbell, I.H., Griffiths, R.W. and Hill, R.I., 1989. Melting in an Archean mantle plume: heads it's basalts, tails it's komatiites. Nature, 369, 697-699.

Capdevila, R., Goodwin, A.M., Ujike, O. and Gorton, M.P., 1982. Trace-element geochemistry of Archean volcanic rocks and crustal growth in southwestern Abitibi Belt, Canada. Geology, 10, 418-422.

Card, K.D. and Ciesielski, A., 1986. DNAG#1, Subdivisions of the Superior Province of the Canadian Shield. Geoscience Canada 13, 5-13.

Cattell, A. and Arndt, N., 1987. Low- and high-alumina komatiites from a Late Archean sequence, Newton Township, Ontario. Contributions to Mineralogy and Petrology 97, 218-227.

Cawood, P.A., and Suhr, G., 1992. Generation and obduction of ophiolites: constraints from the Bay of Islands Complex, Western Newfoundland. Tectonics, 11, 884-897.

Class, C., Goldstein, S.L., and Galer, S.J.G., 1996. Temporal evolution of the Kerguelen plume: Geochemical evidence from approximate to 38 to 82 Ma lavas forming the Ninetyeast Ridge - Discussion. Contributions to Mineralogy and Petrology, 124, 98-103.

Clifford, P.M., 1969. Geology of the Western Lake St. Joseph area, Kenora and Thunder Bay Districts. Ontario Department of Mines, Geological Report 70, 57p.

Clifford, P.M. and McNutt, R.H., 1971. Evolution of Mt. St. Joseph - an Archaean volcano. Canadian Journal of Earth Sciences, 8, 150-161.

Condie, K.C., 1981. Archean greenstone belts. Elsevier, Amsterdam, 434pp.

Condie, K.C., 1997. Contrasting sources for upper an lower continental crust: The greenstone connection. The Journal of Geology, 105, 729-736.

Corfu, F. and Andrews, A.J., 1987. Geochronological constraints on the timing of magmatism, deformation and gold mineralization on the Red Lake greenstone belt, northwestern Ontario. Canadian Journal of Earth Sciences, 24, 1302-1320.

Corfu, F. and Davis, D.W., 1992. A U-Pb geochronological framework for the western Superior Province, Ontario. In: Geology of Ontario: Ontario Geological Survey, Special Volume 4, part 2, 1335-1348.

Corfu, F. and Stott, G.M., 1989. U-Pb geochronology of the central Uchi Subprovince, NW Ontario. *In*; Program with Abstracts, Geological Association of Canada-Mineralogical Association of Canada 14, A55.

Corfu, F. and Stott, G.M., 1993a. Age and petrogenesis of two late Archean magmatic suites, northwestern Superior Province, Canada; zircon U-Pb and Lu-Hf isotopic

relations. Journal of Petrology, 34, 817-838.

Corfu, F. and Stott, G.M., 1993b. U-Pb geochronology of the central Uchi Subprovince, Superior Province. Canadian Journal of Earth Sciences, 30, 1179-1196.

Corfu, F. and Wallace, H., 1986. U-Pb zircon ages for magmatism in the Red Lake greenstone belt, northwestern Ontario. Canadian Journal of Earth Sciences, 23, 27-42.

Davies, J.F., 1963. Geology and gold deposits of the Rice Lake - Wanipigow River area, Manitoba. Unpublished PhD thesis, University of Toronto, 142 pp.

Davies, H.L., Sun, S.-s., Frey, F.A., Gautier, I., McCulloch, M.T., Price, R.C., Bassias, Y., Klootwijk, C.T., and LeClaire, L., 1989. Basalt basement from the Kerguelen Plateau and the trail of a Dupal plume. Contributions to Mineralogy and Petrology, 103, 457-469.

Davis, D.W. and Jackson, M.C., 1988. Geochronology of the Lumby Lake greenstone belt: a 3 Ga complex within the Wabigoon Subprovince, northwest Ontario. Geological Society of America Bulletin, 100, 818-824.

Davis, D.W., Sutcliffe, R.H. and Trowell, N.F., 1988. Geochronological constraints on the tectonic evolution of alate Archaean greenstone belt, Wabigoon subprovince, Northwest Ontario, Canada. Precambrian Research, 39, 171-191.

Defant, M.J., Jackson, T.E., Drummond, M.S., De Boer, J.Z., Bellon, H., Feigenson, M.D., Maury, R.C. and Stewart, R.H., 1992. The geochemistry of young volcanism throughout western Panama and southeastern Costa Rica: an overview. Journal of the Geological Society of London, 149, 569-579.

deKemp, E.A., 1987. Stratigraphy, provenance and geochronology of Archean supracrustal rocks of western Eyapamikama Lake area, northwestern Ontario. Unpublished MSc thesis, Carlton University, Ottawa, Ontario, 98p.

DePaolo, D. J., 1981. Trace element and isotopic effects of combined wallrock assimilation and fractional crystallization. Earth and Planetary Science Letters, 53, 189-202.

Desrochers, J.-P., Hubert, C., Ludden, J.N. and Pilote, P., 1993. Accretion of Archean oceanic plateau fragments in the Abitibi greenstone belt, Canada. Geology, 21, 452-454.

Dostal, J. and Mueller, W.U., 1997. Komatiite flooding of a rifted rhyolitic arc complex: geochemical signature and tectonic significance of the Stoughton-Roquemaure Group Abitibi Greenstone Belt, Canada. Journal of Geology, 105, 545-563.

Drummond, M.S. and Defant, M.J., 1990. A model for trondhjehmite-tonalite-dacite genesis and crustal growth via slab melting: Archean to modern comparisons.

Journal of Geophysical Research, B95, 21503-21521.

Eggins, S.M., 1992. Petrogenesis of Hawaiian tholeiites. Contributions to Mineralogy and Petrology, 110: 387-397.

Elliot, T.R., Hawkesworth, C.J. and Gronvold, K., 1991. Dynamic melting of the Iceland plume. Nature, 351, 201-206.

Ewart, A., Hergt, J.M. and Hawkins, J.W., 1994. Major element, trace element, and isotope (Pb, Sr, and Nd) geochemistry of site 839 basalts and basaltic andesites: Implications for arc volcanism. Proceedings of the Ocean Drilling Program, Scientific Results, 135, 519-531.

Fan, J. and Kerrich, R., 1997. Geochemical characteristics of Al-depleted and undepleted komatiites and HREE-enriched low-Ti tholeiites, western Abitibi greenstone belt: A heterogeneous mantle-plume-convergent margin environment. Geochimica Cosmochimica Acta, 61, 4723-4744.

Farley, K.A., 1995. Rapid recycling of subducted sediments into the Samoan mantle plume. Geology, 23, 531-534.

Feng, R. and Kerrich, R., 1992. Geodynamic evolution of the southern Abitibi and Pontiac terranes; evidence from geochemistry of granitoid magma series (2700-2630 Ma). Canadian Journal of Earth Sciences, 29, 2266-2286.

Ferguson, S.A., Groen, H.A., and Haynes, R., 1971. Gold deposits of Ontario, Ontario Department of Mines and Northern Affairs, Mineral Resources Circular 13, 315p.

Floyd, P.A., 1989. Geochemical features of intraplate oceanic basalts. In: A.D. Saunders and M.J. Norry (Eds), Magmatism in the ocean basins. Geological Society Special Publication 42, London, 215-230.

Fralick, P. and King, D., 1996. MesoArchean evolution of Western Superior Province: Evidence from metasedimentary sequences near Atikokan. in Harrap, R.M. and Helmstaedt, H. (Eds.), 1996 Western Superior Transect Second Annual Workshop, Lithoprobe Report #53, 29-35.

Garland, F., Hawkesworth, C.J. and Mantovani, M.S.M., 1995. Description and petrogenesis of the Parana rhyolites, Southern Brazil. Journal of Petrology, 36, 1193-1227.

Gill, J.B., 1987. Early geochemical evolution of an oceanic island arc: Fiji and South Fiji Basin. Journal of the Geological Society of London, 95, 589-615.

Gill, J. and Whelan, P., 1989. Postsubduction ocean island alkali basalts in Fiji. Journal of Geophysical Research, 94, 4579-4588.

Gill, R.C.O., Holm, P.M., Nielsen, T.F.D., 1995. Was a short-lived Baffin Bay plume active prior to initiation of the present Icelandic plume? Clues from the high-Mg

picrites of West Greenland. Lithos, 34, 27-39.

Good, D.J.,1988. Geology of the east half of the Birch Lake area, District of Kenora, Patricia Portion. Ontario Geological Survey, Open File Report 5685, 1331p.

Goodwin, A.M., 1965. Geology of Pashkakogan Lake-Eastern Lake St. Joseph area. Ontario Department of Mines, Geological Report 42, 58p.

Goodwin, A.M., 1967. Volcanic studies in the Birch-Uchi lakes area of Ontario. Ontario Department of Mines, Miscellaneous Paper 6, 96p.

Goodwin, A.M., 1991. Precambrian geology, the dynamic evolution of the continental crust. Academic Press, London.

Grand, S.P., 1987. Tomographic inversion for shear velocity beneath the North American plate. Journal of Geophysical Research, 92, 14065-14090.

Gruau, G., Chauvel, C., Arndt, N., Cornichet, J., 1990. Aluminum depletion in komatiites and garnet fractionation in the early Archean mantle: Hafnium isotope constraints. Geochimica et Cosmochimica Acta, 54, 3095-3101.

Gribble, R.F., Stern, R.J., Bloomer, S.H., Stuben, D., O'Hearn, T., and Newman, S., 1996. MORB mantle and subduction components interact to generate basalts in the southern Mariana Trough back-arc basin. Geochimica et Cosmochimica Acta, 60, 2153-2166.

Gromet, L.P. and Silver, L.T., 1987. REE variations across the Peninsular Ranges Batholith: Implications for batholithic petrogenesis and crustal growth. Journal of Petrology, 28, 75-125.

Grove, T.L., de Wit, M.J., and Dann, J.C., 1997. Komatiites from the Komati type section, Barberton South Africa, *in* De Wit, M.J., and Ashwal, L.D. (eds.), Greenstone Belts, Oxford University Press, Oxford, 435-450.

Hall, D.H. and Hajnal, Z., 1969. Crustal structure of northwestern Ontaio: refraction seismology. Canadian Journal of Earth Sciences, 6, 81-99.

Hamilton, W.B., 1998. Archean Tectonics and Magmatism. International Geology Review, 40, 1-39.

Hanski, E.J., 1992. Petrology of Pechenga ferropicrites and cogenetic, Ni-bearing gabbro-wehrlite intrusions, Kola Peninsular, Russia, 367. Geological Survey of Finland Bulletin, 192 pp.

Hanski, E.J. and Smolkin, V.F., 1989. Pechenga ferropicrites and other Early Proterozoic picrites in the eastern part of the Baltic Shield. Precambrian Research, 45, 63-82.

Harris, R.A., 1992. Peri-collisional extensionand the formation of Oman-type ophiolites in the Banda arc and Brooks Range. In; Parson, L.M., Murton, B.J. And

Browning, P. (Eds), Ophiolites and their oceanic analogues, Geological Society Special Publication 60, 301-325.

Hawkesworth, C. J., Gallagher, K., Hergt, J. M. and McDermott, F., 1993. Mantle and slab contributions in arc magmas. Annual Review Earth Planetary Sciences, 21, 175-204.

Hawkesworth, C.J., Turner, S.P., McDermott, F., Peate, D.W. and van Calsteren, P., 1997. U-Th isotopes in Arc magmas: implications for element transfer from the subducted crust. Science, 276, 551-555.

Hawkins, J.W., 1994. Petrological synthesis: Lau basin transect (Leg 135). In: J. Hawkins, Parson, L., Allan, J. et al. (Ed.), Proceedings of the Ocean Drilling Program, Scientific Results, 135, 879-905.

Hawkins, J.W. and Allan, J.F., 1994, Petrologic evolution of Lau Basin Sites 834 through 839, *in*, Hawkins, J., Parson, L., Allan, J. et al., Proceedings of the Ocean Drilling Program, Scientific Results, 135, 427-470.

Henry, P., Stevenson, R.K., Larbi, Y., Gariepy, C., 1997a. Use of Nd isotopes to quantify 700 Ma of crustal growth from 3.4-2.7 Ga. In: Harrap, R.M. And Helmsteadt, H. (Eds), 1997 Western Superior Transect Third Annual Workshop, Lithoprobe report 54. Lithoprobe Secretatiat, University of British Columbia, Canada.

Henry, P., Stevenson, R.K., Larbi, Y., Gariepy, C., 1997b. Nd and Pb isotopic constraints for the crustal growth during the Archean in the western Superior Province (Ontario, Canada). EUG '97, Strasbourg, France, 23-27 March, 1997, Abstract supplement 1, Terra Nova 9, 256.

Herzberg, C, 1992. Depth and degree of melting of komatiites. Journal of Geophysical Research, 97, 4521-4540.

Herzberg, C., Gasparik, T., and Sawamoto, H, 1990. Origin of mantle peridotite: constraints from melting experiments to 16 Gpa. Journal of Geophysical Research 95, 15,779-15,803.

Hofmann, H.J. and Masson, M., 1994. Archean stromatolites from Abitibi greenstone belt, Quebec, Canada. Geological Society of America Bulletin, 106, 424-429.

Hoffman, H.J., Thurston, P.C. and Wallace, H., 1985. Archean stromatolites from the Uchi greenstone belt, northwestern Ontario,*In* Evolution of Archean supracrustal sequences. Geological Association of Canada, Special Paper 28, 125-132.

Hoffman, P.F., 1989. Precambrian geology and tectonic history of North America. In: A.W. Bally and A.R. Palmers (Eds.), The geology of North America - An overview. The Geological Society of America, Boulder, Colorado, pp. 447-512.

Hole, M.J., Saunders, A.D., Rogers, G. and Sykes, M.A., 1995. The relationship between alkaline magmatism, lithospheric extension and slab window formation along continental destructive plate margins. In: J.L. Smellie (Ed.), Volcanism associated with extension at consuming plate margins, Geological Society of London Special Publication 81, 265-285.

Hollings, P. and Kerrich, R., 1998. Trace Element Systematics of Ultramafic and Mafic Volcanic Rocks from the 3 Ga North Caribou Greenstone Belt, Northwestern Superior Province. Precambrian Research: In Press.

Hollings, P. and Wyman, D., 1997. Geochemistry of 3 Ga Terranes of the Superior Province, Canada: Generation of Felsic Melts in Archean Oceanic Plateaux ? Goldschmidt International Conference Abstracts, p. 95.

Hollings, P. and Wyman, D., 1998. Trace element systematics of volcanic and intrusive rocks from the 3 Ga Lumby Lake greenstone belt, Superior Province: Evidence for Archean plume-arc interaction. Lithos, in review.

Hollings, P., Polat, A. and Kerrich, R., 1997. Archean komatiites and alkaline basalts with majorite garnet and HIMU-like signatures in Superior Province ocean plateau volcanic belts. GSA Abstracts with Programs, v. 29, No. 6.

Hollings, P., Wyman, D., Kerrich, R., and Polat, A., 1997. Subduction at the Margins of an Active Oceanic Plateau: Geochemical Evidence From the 2.7 Ga Confederation Assemblage, Uchi Subprovince, Northern Superior Province, Canada. Goldschmidt International Conference Abstracts, p. 96.

Hollings, P., Wyman, D., Kerrich, R., and Polat, A., 1996. Trace element and Sm-Nd systematics of the 3 Ga Lumby Lake greenstone belt, Superior Province, Canada: Conjunction of an Archean Plateau and oceanic volcanic arc. EOS, Transactions, 77, p. 849.

Hughes, D.J., Tomlinson, K.Y., Thurston, P.C., and Davis, D.W., 1997. The Lumby Lake greenstone belt: geochemistry and crustal evolution. Western Superior Lithoprobe Transect, Third Workshop: Toronto, p. 14-15.

Humphris, S.E., 1984. The mobility of the rare earth elements in the crust. In: P. Henderson (Ed.), Rare earth element geochemistry. Elesevier, pp. 317-342.

Huppert, H. E., and Sparks, R. S. J., 1985a. Komatiites I: Eruption and flow. Journal of Petrology, 26, 694-725.

Huppert, H. E., and Sparks, R. S. J., 1985b. Cooling and contamination of mafic and ultramafic magmas during ascent through continental crust. Earth and Planetary Science Letters, 74, 371-386.

Jackson, M.C., 1985a. Precambrian geology of the Lumby Lake area, western part,

Kenora and Rainy River Districts. Ontario Geological Survey, Map P.2828, scale 1:15840.

Jackson, M.C., 1985b. Precambrian geology of the Lumby Lake area, eastern part, Kenora and Rainy River Districts. Ontario Geological Survey, Map P.2829, scale 1:15840.

Jackson, M.C., 1985c. Geology of the Lumby Lake area, Eastern part. Districts of Kenora and Rainy River. Ontario Geological Survey, Open File Report 5535, 122 p.

Jackson, M.C., 1985d. Geology of the Lumby Lake area, Western Part, districts of Kenora and Rainy River. Ontario Geological Survey, Open File Report 5534, 151 p.

Jackson, S.L. and Fyon, J.A., 1991. The western Abitibi Subprovince in Ontario. In, Geology of Ontario, Ontario Geological Survey, Special Volume 4, 405-484.

Jackson, S.L., Fyon, J.A. and Corfu, F., 1994. Review of Archean supracrustal assemblages of the southern Abitibi greenstone belt in Ontario, Canada: Products of microplate interaction within a large-scale plate-tectonic setting. Precambrian Research, 65, 183-205.

Jahn, B.-M., Auvray, B., Blais, S., Capdevila, R., Cornichet, J., Vidal, F., and Hameurt, J., 1980. Trace element geochemistry and petrogenesis of Finnish greenstone belts. Journal of Petrology, 21, 201-244.

Jahn, B., Gruau, G. and Glikson, A.Y., 1982. Komatiites of the Onverwacht Group, S. Africa; REE geochemistry, Sm/ Nd age and mantle evolution. Contributions to Mineralogy and Petrology, 80, 25-40.

Jenner, G.A. 1996. Trace element geochemistry of igneous rocks: geochemical nomenclature and analytical geochemistry. In Wyman, D.A. (Ed.) Trace element geochemistry of volcanic rocks: Applications for massive sulphide exploration. Geological Association of Canada, Short Course Notes, 12, 51-77.

Jenner, G.A., Longerich, H.P., Jackson, S.E. and Fryer, B.J., 1990. ICP-MS - A powerful tool for high precision trace-element analysis in earth sciences: Evidence from analysis of selected USGS reference samples. Chemical Geology, 83, 133-148.

Jochum, K.P., Arndt, N.T. and Hofman, A.W., 1991. Nb-Th-La in komatiites and basalts: constraints on komatiites petrogenesis and mantle evolution. Earth and Planetary Science Letters, 107, 272-289.

Kent, R.W., Hardarson, B.S., Saunders, A.D. and Storey, M., 1996. Plateaux ancient and modern: geochemical and sedimentological perspectives on Archaean oceanic

magmatism. Lithos, 37, 120-142.

Kepezhinkas, P. 1995. Diverse shoshonitic magma series in the Kamchatka arc: relationships between intra-arc extension and the composition of alkaline magmas. In: Smellie, J.L (Ed.), Volcanism associated with extension at consuming plate margins, Geological Society of London Special Publication 81, 249-264.

Kerr, A.C., Marriner, G.F., Arndt, N.T., Tarney, J., Nivia, A., Saunders, A.D., Duncan, R.A., 1996. The petrogenesis of Gorgona komatiites, picrites and basalts: new field, petrographic and geochemical constraints. Lithos, 37, 245-260.

Kerrich, R., Polat, A., Wyman, D., and Hollings, P. 1998. Trace element systematics of Mg-, to Fe-tholeiite suites of the 2.9-2.7 Ga Superior Province greenstone belts: implications for multi-component mantle plumes. Lithos, in press.

Kimura, G., Ludden, J., Desrochers, J.P. and Hori, R., 1993. A model of ocean crust accretion for the Superior Province. Lithos, 30: 337-355.

Kröner A., 1985. Evolution of the Archean continental crust. Annual Review of Earth and Planetary Sciences, 13, 49-74.

Kröner A. and Layer P. W., 1992. Crust formation and plate motion in the Early Archean. Science, 256, 1405-1411.

Lafleche, M.R., Dupuy, C. and Dostal, J., 1992. Tholeiitic volcanic rocks of the Late Archean Blake River Group, southern Abitibi greenstone belt: Origin and geodynamic implications. Canadian Journal of Earth Sciences, 29, 1448-1458.

Lafleche, C., Dupuy, C. and Bougault, H., 1991. Geochemistry and petrogenesis of Archean mafic volcanic rocks of the southern Abitibi Belt, Québec. Precambrian Research, 57, 207-241.

Lahaye, Y., Arndt, N., Byerly, G., Chauvel, C., Fourcade, S. and Gruau, G., 1995. The influence of alteration on the trace-element and nd isotopic compositions of komatiites. Chemical Geology, 126, 43-64.

Leeman, W.P., Smith, D.R., Hildreth, W., Palacz, Z. and Rogers, N., 1990. Compositional diversity of Late Cenozoic basalts in a transect across the Southern Washington Cascades: implications for subduction zone magmatism. Journal of Geophysical Research, 95, 19561-19582.

Lesher, C.M. and Arndt, N.T., 1995. Trace element and Nd isotope geochemistry, petrogenesis, and volcanic evolution of contaminated komatiites at Kambalda, Western Australia. Lithos, 34, 127-157.

Lesher, C.M., Goodwin, A.M., Campbell, I.H. and Gorton, M.P., 1986. Trace-element geochemistry of ore-associated and barren, felsic metavolcanic rocks in the Superior Province, Canada. Canadian Journal of Earth Sciences, 23, 222-237.

Longerich, H.P., Jenner, G.A., Fryer, B.J. and Jackson, S.E., 1990. Inductively coupled plasma-mass spectrometric analysis of geological samples: a critical evaluation based on case studies. Chemical Geology, 83, 105-118.

Ludden, J., Gelinas, L. and Trudel, P., 1982. Archean metavolcanics from the Rouyn-Noranda District, Abitibi greenstone belt, Quebec; 2, Mobility of trace elements and petrogenetic constraints. Canadian Journal of Earth Sciences, 19, 2276-2287.

MacDonald, W., Estrada, J., Gonzalez, H. and Ingeominas, A., 1997. Paleoplate affiliations of volcanic accretionary terranes of the Northern Andes. GSA Abstracts with program, 29, A245.

Mahoney, J.J., Jones, W.B., Frey, F.A., Salters, V.J.M., Pyle, D.G. and Davies, H.L., 1995. Geochemical characteristics of lavas from Broken Ridge, the Naturaliste Plateau and southernmost Kerguelen Plateau: Cretaceous plateau volcanism in the southeast Indian Ocean. Chemical Geology, 120, 315-345.

Mahoney, J.J., Storey, M., Duncan, R.A., Spencer, K.J. and Pringle, M., 1993. Geochemistry and geochronolgy of Leg 130 basement lavas: nature and origin of the Ontong Java plateau. In; Berger, W.H., Kroenke, L.W. and Mayer, L.A. (eds.), Proceedings of the Ocean Drilling Program, Scientific Results, 130, 3-22.

Martin, H., 1986. effect of steeper Archean geothermal gradient on geochemistry of subduction-zone magmas. Geology, 14, 753-756.

Martin, H., 1993. The mechanisms of petrogenesis of the Archaean continental crust - Comparison with modern processes. Lithos, 30, 373-388.

Martin, H., 1994. The Archean grey gneisses and the genesis of continental crust. In: K.C. Condie (Editor), Archean crustal evolution. Elsevier, 205-259.

Martin, H., Peucat, J.J., Sabate, P. and Cunha, J.C., 1997. Crustal evolution in the early Archean of South America: example of the Sete Voltas Massif, Bahia State, Brazil. Precambrian Research, 82, 35-62.

McCuaig, T.C., Kerrich, R., and Xie, Q., 1994. Phosphorous and high field strength anomalies in Archean high-magnesian magmas as possible indicators of source mineralogy and depth. Earth and Planetary Science Letters, 124, 221-239.

McCulloch, M.T., 1993. The role of subducted slabs in an evolving earth. Earth and Planetary Science Letters, 115, 89-100.

McCulloch, M.T. and Bennett, V.C., 1994. Progressive growth of the Earth's continental crust and depleted mantle. Geochimica et Cosmochimica Acta, 58, 4717-4738.

McCulloch, M.T., Gregory, R.T., Wasserburg, G.J., and Taylor, H.P., 1981. Sm-Nd, Rb-Sr, and $^{18}O/^{16}O$ isotopic systematics in an oceanic crustal section: Evidence

from the Samail ophiolite. Journal of Geophysical Research. 86, 2721-2735.

McRitchie, W.D., 1971. Geology of the Wallace Lake-Siderock Lake area; In W.D. McRitchie and W.Weber (eds), Geology and Geophysics of the Rice Lake region, southeastern Manitoba, Manitoba Department of Mines and Natural Resources, Mines Branch Publication 71-1, Map 71-1/6, scale one inch to one mile.

McRitchie, W.D. and Weber, W. Eds., 1971. Geology and geophysics of the Rice Lake region, southeastern Manitoba (Project Pioneer), Manitoba Department of Mines and Natural Resources, Mines Branch Publication 71-1, 430 p.

Meyn, H.D. and Palonen, P.A., 1980. Stratigraphy of an Archean submarine fan. Precambrian Research, 12, 257-285.

Nelson, E.P. and Forsythe, R.D., 1989. Ridge collision at convergent margins: implications for Archean and post-Archean crustal growth. Tectonophysics, 161, 307-315.

Nelson, D.R., Trendall, A.F., deLaeter, J.R., Grobler, N.J., Fletcher, I.R., 1992. A comparitive study of the geochemical and isotopic systematics of Late Archean flood basalts from the Pilbara and Kaapvaal cratons. Precambrian Research, 54, 231-256.

Nesbitt, R.W., Sun, S.S. and Purvis, A.C., 1979. Komatiites: geochemistry and genesis. Canadian Mineralogist, 17, 165-186.

Nesbitt, R.W. and Sun, S.S., 1976. Geochemistry of Archean spinifex textured peridotites and magnesian and low magnesian tholeiites. Earth and Planetary Science Letters, 31, 433-453.

Noble, S.R., 1989. Geology, geochemistry and isotope geology of the Trout Lake batholith and the Uchi-Confederation lakes greenstone belt, northwestern Ontario, Canada. Unpublished PhD thesis, University of Toronto, Ontario, 288p.

Noble, S.R., Krogh, T.E. and Evensen, N.M., 1989. U-Pb age constraints on the evolution of the Trout Lake-Uchi-Confederation lakes granite-greenstone terrane, Superior Province, Canada. Geological Association of Canada-Mineralogical Association of Canada, Joint Annual Meeting, Program with Abstracts, 14, p.A56.

Nunes, P.D. and Thurston, P.C., 1980. Two hundred and twenty million years of Archean evolution: a zircon U-Pb age stratigraphic study of the Uchi-Confederation lakes greenstone belt, Northwestern Ontario. Canadian Journal of Earth Sciences, 17, 710-721.

OGS, 1992. Tectonic assemblages of Ontario, west-central sheet. Ontario Geological Survey, Map 2576, 1:1,000,000.

Operto, S. and Charvis, P., 1995. Kerguelen plateau: A volcanic passive margin

fragment?. Geology, 23, 137-140

Parman, S.W., Dann, J.C., Grove, T.L., and deWit, M.J., 1997. Emplacement conditions of komatiite magmas from the 3.49 Ga Komati Formation, Barberton Greenstone Belt, South Africa. Earth and Planetary Science Letters, 150, 303-323.

Parsons, T., Thompson, G.A. and Sleep, N.H., 1994. Mantle plume influence on the Neogene uplift and extension of the U.S. western Cordillera. Geology, 22: 83-86.

Patterson, G.C., and Watkinson, G.H., 1984a. The geology of the Thierry Cu-Ni mine, northwestern Ontario. Canadian Mineralogist, 22, 3-11.

Patterson, G.C., and Watkinson, G.H., 1984b. Metamorphism and supergene alteration of Cu-Ni sulfides, Thierry mine, northwestern Ontario. Canadian Mineralogist, 22, 13-21.

Pearce, J.A., Ernewein, M., Bloomer, S.H., Parson, L.M., Murton, B.J., Johnson, L.E., 1995. Geochemistry of Lau Basin volcanic rocks. In: J. Smellie (Editor), Volcanism associated with extension at consuming plate margins. Geological Society of London Special Publication, 81, 53-75.

Pearce, J.A. and Parkinson, I.J., 1993. Trace element models for mantle melting: application to volcanic arc petrogenesis. In: H.M. Prichard, T. Alabaster, N.B.W. Harris and C.R. Neary (Editors), Magmatic processes and plate tectonics, 373-403.

Pearce, J. A. and Peate, D. W., 1995. Tectonic implications of the composition of volcanic arc magmas. Annual Review Earth Planetary Sciences, 23, 251-285.

Perring, C.S., Barnes, S.J. and Hill, R.E.T., 1996. Geochemistry of komatiites from Forrestania, Southern Cross Province, Western Australia: Evidence for crustal contamination. Lithos, 37, 181-197.

Pirie, J., 1981. Regional setting of gold deposits in the Red Lake area, northwestern Ontario. In; Genesis of Archean volcanic-hosted gold deposits, Symposium held at University of Waterloo, March 7, 1980, Ontario Geological Survey, Miscellaneous Paper 97, 71-93.

Polat, A., 1998. Geodynamics of the late Archean Schreiber-Hemlo and White River-Dayohessarah greenstone belts, Superior Province, Canada. Unpublished PhD. Thesis, University of Saskatchewan, Canada.

Polat, A., Kerrich, R. and Wyman, D., 1997. Geochemical diversity in oceanic komatiites and basalts from the Late Archean Wawa greenstone belt, Superior Province, Canada: Evidence for multiple mantle components in a heterogeneous plume. Precambrian Research: In Press.

Pouclet, A., Lee, J., Vidal, P., Cousens, B. and Bellon, H., 1995. Cretaceous to Cenozoic volcanism in South Korea and in the Sea of Japan: magmatic constraints

on the opening of the back-arc basin. In: J.L. Smellie (Editor), Volcanism associated with extension at consuming plate margins, Geological Society of London Special Publication 81, 169-191.

Poulsen, K.H., Davis, D.W., Weber, W., and Scoates, R.F.J., 1993. Geological and geochronological studies in the Rice Lake belt. Manitoba Energy and Mines, Minerals Division, Report of Activities, 1993, p. 152.

Poulsen, K.H., Weber, W., Garson, D.F. and Scoates, R.F.J., 1994. Digital database for Rice lake belt geology and mineral deposits: a progress report. In; Manitoba Energy and Mines, Minerals Division, Report of Activities, 1994, 163-166.

Poulsen, K.H., Weber, W., Brommecker, R., and Seneshen, D.N., 1996. Lithostratigraphic assembly and structural setting of gold mineralisation in the eastern Rice Lake greenstone belt, Manitoba, Field Trip Guidebook A4, Geological Association of Canada/Mineralogical Association of Canada Annual Meeting, Winnipeg, Manitoba.

Prest, V.K., 1939. Geology of the Keezik-Miminiska Lakes Area, Ontario Department of Mines, Annual Report 48, part 6, 21p.

Pryslak, A.P., 1971a, Corless Township, District of Kenora (Patricia Portion), Ontario Department of Mines and Northern Affairs, Preliminary Map, P.634, 1:50,000.

Pryslak, A.P., 1971b, Knott Township, District of Kenora (Patricia Portion), Ontario Department of Mines and Northern Affairs, Preliminary Map, P.635, 1:50,000.

Puchtel, I.S., Arndt, N.T., Hofmann, A.W., Haase, K.M., Kroner, A., Kulikov, V.S., Kulikova, V.V., Garbe-Schonberg, C.-D., and Nemchin, A.A., 1998. Petrology of mafic lavas within the Onega plateau, central Karelia: evidence for 2.0 Ga plume-related continental growth in the Baltic Shield. Contributions to Mineralogy and Petrology, 130, 134-153.

Puchtel, I.S., Haase, K.M., Hofmann, A.W., Chauvel, C., Kulikov, V.S., Garbe-Schonberg, C.-D., and Nemchin, A.A., 1997. Petrology and geochemistry of crustally contaminated komatiitic basalts from the Vetreny belt, southeastern Baltic shield: evidence for an early Proterozoic mantle plume beneath rifted Archean continental lithosphere. Geochimica et Cosmochimica Acta, 61, 1205-1222.

Pye, E.G., 1956. Geology and Mineral deposits of the Crow River area, Unpublished report prepared for Ontario Department of Mines, 239p., Accompanied by Map 47b, revised 1956, Published by the Ontario Department of Mines in 1976 as Open File Report 5152.

Rajamani, V., Shivkumar, K., Hanson, G.N., and Shirey, S.B., 1985. Geochemistry and petrogenesis of amphibolites, Kolar Schist Belt, South India: Evidence for

komatiitic magma derived by low percentages of melting of the mantle. Journal of Petrology, 26, 92-123.

Rapp R. P., Watson E. B., and Miller C. F., 1991. Partial melting of amphibolite/eclogite and the origin of Archean trondhjemites and tonalites. Precambrian Research, 51, 1-25.

Reagan, M.K. and Gill, J.B., 1989. Coexisting calc alkaline and high-niobium basalts from Turrialba volcano, Costa Rica: Implications for residual titanites in arc magma sources. Journal of Geophysical Research, 94, 4619-4633.

Richardson, D.J. and Ostry, G., 1996. Gold Deposits of Manitoba. Economic Geology Report ER86-1 (2nd edition), Manitoba Energy and Mines, 114p.

Rogers, N.W., MacLeod, C.J. and Murton, B.J., 1989. Petrogenesis of boninitic lavas from Limassol Forest Complex, Cyprus. In: A.J. Crawford (Editor), Boninites. University of Tasmania, Geology Department, Hobart, Tasmania, 288-311.

Rollinson, H., 1993. Using geochemical data: Evaluation, presentation, interpretation. Longman, Harlow, England, 352 pp.

Sage, R.P. and Breaks, F.W., 1982. Geology of the Cat Lake-Pickle Lake area, districts of Kenora and Thunder Bay. Ontario Geological Survey, Report 207, 238p.

Sage, R.P., Lightfoot, P.C., and Doherty, W., 1996. Bimodal cyclical Archean basalts and rhyolites from the Micipicoten (Wawa) greenstone belt, Ontario: evidence for magma contributions from the asthenospheric mantle and ancient continental lithosphere near the southern margin of the Superior Province. Precambrian Research, 76, 119-153.

Sajona, F.G., Maury, R.C., Bellon, H., Cotten, J., Defant, M.J., Pubellier, M., 1993. Initiation of subduction and the generation of slab melts in western and eastern Mindanao, Philippines. Geology, 21, 1007-1010.

Sajona, F.G., Maury, R.C., Bellon, H., Cotten, J., and Defant, M., 1996. High field strength element enrichment of Pliocene-Pleistocene island arc basalts, Zamboanga Peninsula, Western Mindanao (Philippines). Journal of Petrology, 37, 693-726.

Saunders, A.D. and Tarney, J., 1991. Back-arc basins. In: P.A. Floyd (Editor), Oceanic basalts. Blackie, 219-263.

Saunders, A.D., Norry, M.J., and Tarney, J., 1988. Origin of MORB and chemically-depleted mantle reservoirs: trace element constraints. Journal of Petrology, 29, 415-445.

Saunders, A.D., Tarney, J., Kerr, A.C. and Kent, R.W., 1996. The formation and fate of large oceanic igneous provinces. Lithos, 37, 81-95.

Schaefer, S.J., and Morton, P., 1991. Two komatiitic pyroclastic units, Superior

province, northwestern Ontario: their geology, petrography, and correlation. Canadian Journal of Earth Sciences, 28, 1455-1470.

Scharer, U., 1989. Age, origin and metamorphic overprint of volcanic and plutonic rocks in the Central uchi Subprovince, Superior province, Canada. Geological Association of Canada-Mineralogical Association of Canada, Joint Annual Meeting, Program with Abstracts, 14, p. A55.

Seneshen, D.M., 1990. The genesis of Archean rocks of the Manigotgan River Formation, southeastern Manitoba, unpublished Msc thesis, University of Manitoba, 173p.

Seneshen, D.M., and Owens, O.J., 1985. Geological investigations in the Stormy Lake area. In Manitoba Energy and Mines, Geological Services Branch, Report of Field Activities, 1985, 112-120.

Sharkov, E.V. and Smolkin, V.F., 1997. The early proterozoic Pechenga-Varzuga Belt: a case of Precambrian back-arc spreading. Precambrian Research, 82, 133-151.

Sigmarsson, O., Hémond, C., Condomines, M., Fourcade, S., and Oskarsson, N., 1991. Origin of silicic magma in Iceland revealed by Th isotopes. Geology, 19, 621-624.

Silver, P.G., and Chan, W.W, 1988. Implications for continental structure and evolution from seismic anisotropy. Nature, 335, 34-39.

Skufin, P.K., 1980. Characteristics of the volcanism in the Proterozoic Pechenga Structure. Byull. Mosk. Ova Ispyt. Ptir. Otd. Geol, 55: 120-131 (in Russian).

Sparks, R.J.S. 1986. The role of crustal contamination in magma evolution through geological time. Earth and Planetary Science Letters, 78, 211-223.

Stein, M. and Goldstein, S.L., 1996. From plume head to continental lithosphere in the Arabian Nubian shield. Nature, 382, 773-778.

Stein, M. and Hofmann, A.W., 1994. Mantle plumes and episodic crustal growth. Nature, 372, 63-68.

Stern, R.J. Lin, P., Morris, J.D., Jackson, M.C., Fryer, P., Bloomer, S.H., Ito, E., 1990. Enriched back-arc basin basalts from the northern Mariana Trough: implications for the magmatic evolution of back-arc basins. Earth and Planetary Science Letters, 100, 210-225.

Stern, R.A., Syme, E.C. and Lucas, S.B., 1995. Geochemistry of 1.9 Ga MORB- and OIB-like basalts from the Amisk collage, Flin Flon belt, Canada: Evidence for an intra-oceanic origin. Geochimica et Cosmochimica Acta, 59, 3131-3154.

Stevenson, R., 1995. Crust and mantle evolution in the Late Archean: Evidence from a Sm-Nd isotopic study of the North Spirit Lake greenstone belt, northwestern

Ontario, Canda. GSA Bulletin, 107, 1458-1467.

Stix, J. and Gorton. A.P., 1989. Physical and chemical processes of Archean subaqueous pyroclastic rocks. *in* Geoscience Research Grant Program, Summary of Research 1988-1989, Ontario Geological Survey, Miscellaneous Paper 143, 231-238.

Stone, D., Kamineni, D.C. and Jackson, M.C., 1992. Precambrian geology of the Atikokan area, northwestern Ontario. Geological Society of Canada Bulletin 405, 106p.

Stone, W.E., Crocket, J.H., Dickin, A.P., and Fleet, M.E., 1995. Origin of Archean ferropicrites: geochemical constraints from the Boston Creek flow, Abitibi greenstone belt, Ontario, Canada. Chemical Geology, 121, 51-71.

Storey, B.C., 1995. The role of mantle plumes in continental breakup: Case histories from Gondwanaland. Nature, 377, 301-308.

Storey, M., Mahoney, J.J., Kroenke, L.W., and Saunders, A.D., 1991. Are oceanic plateaus sites of komatiite formation. Geology, 19, 376-379.

Storey, M., Kent, R.W., Saunders, A.D., Salters, V.J., Hergt, J., Whitechurch, H., Sevigny, J.H., Thirlwall, M.F., Leat, P., Ghose, N.C. and Gifford, M., 1992. Lower Cretaceous volcanic rocks on continental margins and their relationship to the Kerguelen Plateau. In; Wise, S.W., Schlich, R., et al., Proceedings of the Ocean Drilling Program, Scientific Results 120, 33-53.

Stott, G., 1996. The geology and tectonic history of the Central Uchi subprovince, Ontario Geological Survey, open File Report 5952, 178p.

Stott, G., 1997. The Superior Province, Canada. in deWit, M.J., and Ashwal, L.D., eds., The tectonic evolution of greenstone belts, Oxford University Press, 480-507.

Stott, G.M. and Corfu, F., 1991. Uchi Subprovince. In ; Geology of Ontario, Ontario Geological Survey, Special Volume 4, Part 1, 145-238.

Stott, G.M. and LaRocque, C., 1983a. Precambrian geology of the Meen Lake area, Eastern part. Ontario Geological Survey, Preliminary Map P. 2620, scale 1:15 840.

Stott, G.M. and LaRocque, C., 1983b. Precambrian geology of the Meen Lake area, western part. Ontario Geological Survey, Preliminary Map P. 2619, scale 1:15 840.

Stott, G.M., and Wallace, H., 1984. Regional stratigraphy and structure of the central Uchi Subprovince: Meen Lake-Kasagiminnis Lake and Pashkokogan Lake section. in Summary of Field Work 1984, Ontario Geological Survey, Miscellaneous Paper 119, 7-13.

Stott, G.M., Kay, S.V., and Sanborn, M.M., 1987a. Precambrian geology of the Lake St. Joseph area, west half. Ontario Geological Survey, Map P3050, scale 1:50,000.

Stott, G.M., Kay, S.V., and Sanborn, M.M., 1987b. Precambrian geology of the Lake

St. Joseph area, east half. Ontario Geological Survey, Map P3051, scale 1:50,000.

Stott, G.M., Brown, G.H., Coleman, V.J., Green, G.M. and Reilly, B.A., 1989a. Precambrian geology of the Pickle Lake area, western part. Ontario Geological Survey, Preliminary Map P.5056, scale 1:50 000.

Stott, G.M., Brown, G.H., Coleman, V.J., Green, G.M. and Reilly, B.A., 1989b. Precambrian geology of the Pickle Lake area, eastern part. Ontario Geological Survey, Preliminary Map P.5057, scale 1:50 000.

Sun, S.S. and Nesbitt, R.W., 1976. Geochemical regularities and genetic significance of ophiolitic basalts. Geology, 6, 689-693.

Sun, S.-s. and McDonough, W.F., 1989. Chemical and isotopic systematics of oceanic basalts: implications for mantle composition and processes. In: A.D. Saunders and M.J. Norry (Editors), Magmatism in the ocean basins. Geological Society Special Publication, 313-345.

Sun, S.S., Nesbitt, R.W. and McCulloch, M.T., 1989. Geochemistry and petrogenesis of Archaean and early Proterozoic siliceous high-magnesian basalts, in Crawford, A.J., ed, Boninites: University of Tasmania, Geol. Dep., Hobart, Tasmania, Australia, 148-173.

Sutcliffe, R.H., Barrie, C.T., Burrows, D.R., and Beakhouse, G.P., 1993. Plutonism in the Southern Abitibi subprovince: A tectonic and petrogenetic framework. Economic Geology, 88, 1359-1375.

Tarney, J. and Jones, C.E., 1994. Trace element geochemistry of orogenic igneous rocks and crustal growth models. Journal of the Geological Society of London, 151, 855-868.

Taylor, S.R. and McLennan, S.M., 1985. The continental crust: its composition and evolution. Blackwell.

Taylor, S. R. and McLennan, S. M., 1995. The geochemical evolution of the continental crust. Reviews in Geophysics, 33, 241-265.

Taylor, R.N., Thirlwall, M.F., Murton, B.J., Hilton, D.R., and Gee, M.A.M., 1997. Isotopic constraints on the influence of the Icelandic plume. Earth and Planetary Science Letters, 148, E1-E8

Tejada, M.L.G., Mahoney, J.J., Duncan, R.A. and Hawkins, M.P., 1996. Age and geochemistry of basement and alkalic rocks of Malaita and Santa Isabel, Solomon Islands, southern margin of Ontong Java plateau. Journal of Petrology, 37, 361-394.

Theyer, P., 1983. Geology and gold environments in the Bissett-Wallace Lake portion of the Rice Lake greenstone belt. in Manitoba Energy and Mines, Mineral resources

Division, Report of Field Activities 1983, 101-106.

Thurston, P.C., 1985b. Geology of the Earngey-Costello area, District of Kenora, Patricia Portion; Ontario Geological Survey, Report 234, 125p.

Thurston, P.C., 1986. Volcanic cyclicity in mineral exploration; the caldera cycle and zoned magma chambers; *in* Volcanology and Mineral deposits, Ontario Geological Survey, Miscellaneous Paper 129, 104-123.

Thurston, P.C. and Chivers, K.M., 1990. Secular variation in greenstone development: Precambrian Research, 46, 21-58.

Thurston, P.C. and Fryer, B.J., 1983. The geochemistry of repetitive cyclical volcanism from basalt through rhyolite in the Uchi-Confederation greenstone belt, Canada. Contributions to Mineralogy and Petrology, 83, 204-226.

Thurston, P.C., Wan, J., Squair, H.S., Warburton, A.F. and Wierzbicki, V.W., 1978. Volcanology and mineral deposits of the Uchi-Confederation Lakes area, northwestern Ontario, Geological Society of America-Geological Association of Canada-Mineralogical Association of Canada, Joint Annual Meeting, Field Trips Guidebook, 302-324.

Thurston, P.C., Cortis, A.L. and Chivers, K.M., 1987. Reconnaissance re-evaluation of a number of northwestern greenstone belts, evidence for an early Archean sialic crust, Summary of fieldwork and other activities 1987. Ontario Geological Survey, pp. 4-24.

Thurston, P.C., Osmani, I.A and Stone, D., 1991. Northwestern Superior Province: Review and terrane analysis. In; Geology of Ontario, Ontario Geological Survey, Special Volume 4, Part 2, 81-144.

Thurston, P.C., 1985a. Physical volcanology and stratigraphy of the Confederation Lake area, District of Kenora (Patricia Portion); Ontario Geological Survey, Report 236, 117p.

Tomlinson, K.Y., 1996. The geochemistry and tectonic setting of early Precambrian greenstone belts, Northern Ontario, Canada. Unpublished Phd thesis, University of Portsmouth, UK, 287p.

Tomlinson, K.Y., Stevenson, R.K., Hughes, D.J., Hall, R.P., Thuston, P.C., and Henry, P., 1998. The Red Lake greenstone belt, Superior Province: evidence of plume-related magmatism at 3 Ga and evidence of an older enriched source. Precambrian Research, 89, 59-76.

Tomlinson, K.Y., Thurston, P.C., Hughes, D.J. and Keays, R.R., 1996, The central Wabigoon region: Petrogenesis of mafic-ultramafic rocks in the Steep Rock, Lumby Lake and Obonga greenstone belts (Continental rifting and rifting in the Archean),

in Harrap, R.M. and Helmstaedt, H. (Eds.), 1996 Western Superior Transect Second Annual Workshop, Lithoprobe Report #53, 65-73.

Turek, A., Keller, R. Van Schmus, W.R., and Weber, W., 1989. U-Pb zircon ages for the Rice Lake area, Southeastern Manitoba. Canadian Journal of Earth Sciences, 26, 23-30.

Wallace, H., Thurston, P.C. and Corfu, F., 1986. Developments in stratigraphic correlation: Western Uchi Subprovince, *In*; Volcanology and mineral deposits, Ontario Geological Survey, Miscellaneous Paper 129, 88-102.

Weaver, S.D., Storey, B.C., Pankhurst, R.J., Mukasa, S.B., DiVenere, V.J., Bradshaw, J.D., 1994. Antarctica-New Zealand rifting and marie Byrd Land lithospheric magmatism linked to ridge subduction and mantle plume activity. Geology, 22, 811-814.

Weber, W., 1971a. Geology of the Wanipigow River-Manigotagan River region, Winnipeg Mining District. In W.D. McRitchie and W.Weber (eds), Geology and Geophysics of the Rice Lake region, southeastern Manitoba, Manitoba Department of Mines and Natural Resources, Mines Branch Publication 71-1, Map 71-1/4, scale one inch to one mile.

Weber, W., 1971b. Geology of the Long Lake-Gem Lake area. In W.D. McRitchie and W.Weber (eds), Geology and Geophysics of the Rice Lake region, southeastern Manitoba, Manitoba Department of Mines and Natural Resources, Mines Branch Publication 71-1, 63-106.

Wharton, M.R., Hathway, B., and Colley, H., 1995. Volcanism associated with extension in an Oligocene-Miocene arc, southwestern Viti Levu, Fiji. In, Smellie, J.L. (Ed) Volcanism associated with extension at consuming plate margins, Geological Society Special Publication 81, 95-114.

Williams, S.R., Stott, G.M., Heather, K.B., Muir, T.L. and Sage, R.P., 1991. Wawa Subprovince, Geology of Ontario. Ontario Geological Survey, 485-542.

Wilson, M., 1989. Igneous Petrogenesis.Unwin Hyman, 466 p.

Wyman, D. and Hollings, P., 1998. Long-lived mantle plume influence on an Archean proto-continent: Geochemical evidence from the 3 Ga Lumby Lake greenstone belt. Geology. In Review.

Wyman, D.A., Bleeker, W., and Kerrich, R., 1997. A 2.7 Ga plume, proto-arc, to arc transition and the geodynamic setting of the Kidd Creek deposit: evidence from precise ICP MS trace element data. Economic Geology, in press.

Wyman, D.A., Ayer, J., and Devaney, J., 1998. Volcanic Geochemistry of the Sturgeon Lake and Sioux Lookout areas. In Prep.

Xie, Q. and Kerrich, R., 1994. Silicate-perovskite and majorite signature komatiites from the Archean Abitibi Greenstone Belt: Implications for early mantle differentiation and stratification: Journal of Geophysical Research, 99, 15,799-15,812.

Xie, Q., McCuaig, T.C., and Kerrich, R., 1995. Secular trends in the melting depths of mantle plumes: evidence from HFSE/REE systematics of Archean high-Mg lavas and modern oceanic basalts. Chemical Geology, 126, 29-42.

Xie, Q., Kerrich, R. and Fan, J., 1993. HFSE/REE fractionations in three komatiite-basalt sequences, Archean Abitibi greenstone belt: implications for multiple sources and depths. Geochimica et Cosmochimica Acta, 57, 4111-4118.

Yogodzinski, G.M., Jay, R.W., Volynets, O.N., Koloskov, A.V., Kay, S.M., 1995. Magnesian andesite in the western Aleutian Komandorsky region:Implications for slab melting and processes in the mantle wedge. GSA Bulletin, 197, 505-519.

Appendix A

Results for the analyses of selected elements in international reference material BIR-1

Results for the analyses of selected trace elements in BIR-1 during the period of data acquisition for this study.

	Govindaraju 1994	Univ. Saskatchewan (n=90) Na_2O_2 sinter			Xie et al., 1993	
		$\bar{x}$	σ	RSD(%)	$HF-HNO_3$	Na_2O_2 sinter
Y	16	15.09	0.75	5	14.6	14.7
Zr	15.5	14.99	0.56	4	15.7	15.1
Nb	0.6	0.61	0.05	8	0.738	0.648
La	0.62	0.63	0.04	6	0.614	0.628
Ce	1.95	1.91	0.10	5	1.93	1.92
Pr	0.38	0.36	0.02	4	0.382	0.357
Nd	2.5	2.33	0.11	5	2.47	2.29
Sm	1.1	1.10	0.05	5	1.14	1.08
Eu	0.54	0.52	0.03	6	0.524	0.516
Gd	1.85	1.82	0.09	5	1.91	1.81
Tb	0.36	0.35	0.02	5	0.351	0.353
Dy	2.5	2.56	0.11	4	2.63	2.53
Ho	0.57	0.58	0.02	4	0.567	0.57
Er	1.7	1.68	0.07	4	1.72	1.68
Tm	0.26	0.25	0.01	5	0.26	0.252
Yb	1.65	1.63	0.07	4	1.71	1.59
Lu	0.26	0.25	0.02	8	0.259	0.248
Hf	0.6	0.61	0.05	8	0.639	0.62
Ta	0.04	0.03	0.01	30		
Th	0.03	0.04	0.01	32	0.06	0.04

Appendix B

Data for 2.9-3.0 Ga Ball, Balmer, Garner Lake and Northern Pickle assemblages

Red Lake belt - Ball assemblage

	Komatiites						Komatiitic basalts		
	NDC87-01B	NDC87-09A	NDC87-01C	NDC87-02A	NDC87-09E	NDC87-09D	NDC87-02C	NDC87-09C	NDC87-12B
SiO_2	46.33	60.65	51.85	51.34	52.79	50.16	50.38	52.98	52.08
TiO_2	0.14	0.08	0.21	0.15	0.17	0.28	0.39	0.22	0.32
Al_2O_3	2.91	2.13	5.55	5.89	5.05	7.78	13.18	6.91	8.76
Fe_2O_3	12.66	7.60	11.37	9.47	10.47	13.01	14.88	10.70	11.80
MnO	0.25	0.05	0.13	0.14	0.16	0.21	0.07	0.21	0.22
MgO	32.81	29.42	25.33	24.46	23.38	21.09	14.99	16.31	14.81
CaO	4.87	0.04	5.47	8.42	7.87	7.20	2.15	12.05	10.35
K_2O	0.00	0.00	0.00	0.03	0.00	0.02	3.18	0.25	0.94
Na_2O	0.06	0.04	0.12	0.11	0.11	0.23	0.73	0.35	0.67
P_2O_5	0.00	0.00	0.00	0.00	0.02	0.02	0.04	0.02	0.03
LOI	20.23	5.04	5.94	3.84	3.41	3.47	4.33	2.20	1.78
Mg#	85	89	83	85	83	78	69	77	73
Ti	780	545	1309	982	1184	1783	2555	1524	2006
P	29	0	82	180	53	191	252	66	154
Cr	4955	4538	2525	5055	2553	3222	2016	1996	1305
Co	148	113	94	104	99	93	79	73	55
Ni	2036	1619	1079	1801	1069	652	475	211	253
Rb	1	1	1	1	1	1	210	8	37
Sr	57	2	35	9	11	38	124	127	93
Cs	0	0	0	0	1	0	30	1	2
Ba	5	2	2	2	2	4	99	18	96
Sc	19	14	28	28	23	43	36	55	40
V	85	62	132	123	123	196	185	193	201
Ta	0.02	0.02	0.04	0.08	0.06	0.08	0.20	0.06	0.10
Nb	0.41	0.13	0.51	0.97	0.72	1.06	2.61	0.67	1.28
Zr	9	4	12	13	15	24	60	20	32
Hf	0.24	0.14	0.39	0.39	0.35	0.70	1.53	0.58	0.91
Th	0.14	0.06	0.21	0.14	0.17	0.29	1.45	0.43	0.41
U	0.10	0.01	0.07	0.14	0.04	0.08	0.51	0.11	0.13
Y	1.57	0.27	5.32	4.79	4.16	6.80	3.80	5.50	7.03
La	0.84	0.11	1.58	0.54	0.95	1.37	6.96	2.46	2.21
Ce	1.77	0.23	3.56	1.59	2.47	3.47	13.91	4.84	5.57
Pr	0.23	0.03	0.43	0.27	0.34	0.50	1.53	0.55	0.68
Nd	1.04	0.14	2.05	1.35	1.59	2.20	5.36	2.44	2.92
Sm	0.25	0.02	0.66	0.53	0.52	0.61	0.89	0.60	0.84
Eu	0.11	0.01	0.23	0.14	0.14	0.28	0.24	0.20	0.32
Gd	0.28	0.05	0.82	0.71	0.61	0.97	0.76	0.81	1.09
Tb	0.05	0.01	0.14	0.12	0.12	0.17	0.10	0.13	0.17
Dy	0.31	0.05	1.01	0.86	0.81	1.18	0.73	0.97	1.24
Ho	0.06	0.01	0.20	0.19	0.18	0.27	0.15	0.20	0.26
Er	0.18	0.04	0.58	0.56	0.50	0.78	0.44	0.56	0.80
Tm	0.02	0.01	0.08	0.08	0.07	0.11	0.07	0.09	0.12
Yb	0.22	0.04	0.65	0.58	0.49	0.77	0.49	0.61	0.73
Lu	0.04	0.01	0.10	0.08	0.07	0.13	0.07	0.09	0.12
Cu	35	3	81	115	20	10	309	3	12
Zn	79	38	52	84	54	107	93	65	72
Mo	7.02	0.06	1.52	0.50	0.37	0.05	1.34	0.24	4.30
Ag	0.06	0.01	0.02	0.45	0.02	0.41	0.11	0.02	0.29
Tl	0.01	0.03	0.03	0.05	0.03	0.04	1.14	0.06	0.27
Pb	1.11	0.13	0.67	1.80	0.67	0.51	1.34	0.74	0.70
Sn	0.40	0.38	0.44	-	0.30	0.00	1.01	0.41	-
Sb	0.53	0.32	0.33	-	1.03	0.00	0.18	0.24	-
	NDC87-01B	NDC87-09A	NDC87-01C	NDC87-02A	NDC87-09E	NDC87-09D	NDC87-02C	NDC87-09C	NDC87-12B
(La/Yb)n	2.79	1.79	1.75	0.67	1.40	1.28	10.18	2.88	2.15
(La/Sm)n	2.15	3.23	1.55	0.66	1.19	1.46	5.07	2.64	1.70
(Gd/Yb)n	1.06	1.03	1.04	1.00	1.04	1.05	1.28	1.09	1.23
(La/Y)n	3.57	2.55	1.97	0.75	1.52	1.34	12.14	2.97	2.08
(Tb/Yb)n	1.01	1.14	0.97	0.97	1.16	0.99	0.97	0.98	1.06
(Tb/Y)n	1.29	1.61	1.09	1.09	1.25	1.03	1.15	1.01	1.02
(Eu/Eu*)n	1.25	0.92	0.97	0.67	0.79	1.12	0.87	0.90	1.04
AL_2O_3/TiO_2	22	23	25	35	25	26	30	27	26
Zr/Hf	37	30	31	33	42	34	39	34	35
La/Nb	2.06	0.83	3.10	0.56	1.31	1.30	2.67	3.65	1.72
Th/Nb	0.35	0.50	0.42	0.14	0.23	0.28	0.56	0.64	0.32
Th/La	0.17	0.60	0.13	0.25	0.17	0.21	0.21	0.17	0.19
Zr/Y	6	15	2	3	4	3	16	4	5
Ti/Zr	87	134	109	76	80	75	43	77	63
Ti/Sm	3085	25939	1991	1854	2288	2946	2880	2527	2389
P/Nd	28	0	40	133	33	87	47	27	53
Ti/V	9	9	10	8	10	9	14	8	10
Sc/Lu	516	1364	296	339	320	337	498	601	341
Nb/Nb*	0.38	0.98	0.27	1.97	0.74	0.73	0.28	0.20	0.55
Zr/Zr*	1.21	5.27	0.72	1.05	1.13	1.42	1.89	1.12	1.40
Hf/Hf*	1.18	6.40	0.85	1.17	0.97	1.51	1.77	1.20	1.46
Ti/Ti*	1.17	6.49	0.71	0.64	0.83	0.92	1.23	0.86	0.83
UTM Zone	15	15	15	15	15	15	15	15	15
Easting	341140	341135	341140	341150	34135	341135	341150	341135	341100
Northing	5656450	5656100	5656450	3656900	5656100	5656100	3656900	5656100	5655550

Red Lake belt - Balmer assemblage

	Komatiites				Komatiitic basalts			
	RL95-51	AB94-155B	AB94-168B	GC94-42	AB94-147B	RL95-40	RL95-50	RL95-39
SiO_2	46.06	45.71	50.82	43.95	46.86	49.84	51.32	53.59
TiO_2	0.28	0.32	0.25	0.19	0.31	0.32	0.68	0.32
Al_2O_3	9.55	7.91	4.64	3.34	9.22	9.29	9.21	9.38
Fe_2O_3	14.92	14.52	13.47	13.50	13.93	12.97	13.92	13.16
MnO	0.23	0.15	0.23	0.14	0.23	0.21	0.22	0.17
MgO	21.69	28.13	26.82	37.55	15.87	16.61	16.04	12.62
CaO	7.14	3.16	2.91	1.27	10.12	9.87	7.92	8.99
K_2O	0.02	0.00	0.76	0.00	1.91	0.09	0.33	0.05
Na_2O	0.13	0.12	0.09	0.08	1.52	0.78	0.29	1.69
P_2O_5	0.00	0.00	0.02	0.00	0.02	0.02	0.06	0.02
LOI	5.16	13.24	13.12	18.33	6.50	5.94	4.99	6.28
Mg#	76	81	81	86	71	74	72	68
Ti	1480	1658	1406	1024	1885	1954	4311	2367
P	140	49	158	113	187	0	425	194
Cr	2064	3898	2657	3220	1480	2193	1821	1103
Co	75	92	112	110	74	90	76	84
Ni	454	954	1392	1860	326	524	551	216
Rb	2	0	20	0	55	1	9	4
Sr	5	40	30	7	36	15	30	38
Cs	1	0	3	1	14	0	2	1
Ba	7	2	46	2	125	8	25	18
Sc	45	41	26	19	56	46	48	56
V	190	191	135	104	237	219	268	273
Ta	0.03	0.04	0.07	0.04	0.04	0.04	0.16	0.05
Nb	0.38	0.49	0.85	0.33	0.53	0.43	2.70	0.56
Zr	9	14	15	7	15	13	45	15
Hf	0.42	0.38	0.36	0.27	0.43	0.42	1.03	0.46
Th	0.35	0.14	0.14	0.04	0.11	0.10	0.54	0.17
U	0.03	0.03	0.03	0.01	0.03	0.02	0.07	0.04
Y	6.25	8.18	6.47	3.60	8.20	8.04	14.01	7.88
La	0.29	0.81	1.07	0.37	0.83	0.63	2.83	0.95
Ce	0.83	2.06	2.56	1.04	1.91	1.71	7.65	2.35
Pr	0.15	0.32	0.36	0.18	0.30	0.28	1.10	0.35
Nd	0.91	1.58	1.85	0.98	1.60	1.37	5.48	1.77
Sm	0.46	0.66	0.63	0.44	0.62	0.64	1.81	0.65
Eu	0.20	0.14	0.18	0.12	0.27	0.26	0.66	0.29
Gd	0.86	0.88	0.83	0.60	0.91	0.94	2.28	0.93
Tb	0.16	0.17	0.15	0.11	0.17	0.18	0.38	0.18
Dy	1.13	1.18	0.95	0.67	1.26	1.23	2.62	1.29
Ho	0.25	0.28	0.20	0.15	0.29	0.30	0.56	0.29
Er	0.77	0.85	0.63	0.40	0.86	0.83	1.60	0.85
Tm	0.12	0.12	0.10	0.06	0.13	0.13	0.25	0.13
Yb	0.75	0.86	0.62	0.43	0.90	0.81	1.59	0.87
Lu	0.14	0.14	0.09	0.06	0.14	0.13	0.24	0.13
Cu	3	57	97	8	68	114	20	85
Zn	120	69	63	63	75	80	95	80
Mo	0.16	0.08	0.14	0.19	0.30	0.24	0.83	0.09
Ag	0.11	0.95	0.69	-	0.25	0.07	0.46	0.18
Tl	-	-	0.13	0.01	0.40	-	0.10	0.05
Pb	0.38	0.40	1.04	0.15	1.02	0.37	0.79	1.10
Sn	0.32	0.17	1.98	1.88	1.48	0.14	0.41	0.27
Sb	0.46	0.97	2.73	7.15	2.61	0.21	2.09	0.12
	RL95-51	AB94-155B	AB94-168B	GC94-42	AB94-147B	RL95-40	RL95-50	RL95-39
(La/Yb)n	0.26	0.68	1.24	0.62	0.67	0.56	1.28	0.78
(La/Sm)n	0.36	0.80	1.10	0.54	0.87	0.64	1.01	0.94
(Gd/Yb)n	0.79	0.85	1.10	1.17	0.84	0.97	1.19	0.88
(La/Y)n	0.26	0.66	1.10	0.68	0.67	0.51	1.34	0.80
(Tb/Yb)n	0.95	0.90	1.07	1.14	0.87	1.02	1.08	0.94
(Tb/Y)n	0.95	0.87	0.95	1.24	0.87	0.94	1.13	0.96
(Eu/Eu*)n	0.86	0.55	0.76	0.70	1.09	1.04	1.00	1.13
AL_2O_3/TiO_2	38	29	20	20	29	28	13	23
Zr/Hf	38	37	41	27	34	31	44	34
La/Nb	0.72	1.67	1.27	1.11	1.56	1.44	1.05	1.68
Th/Nb	0.17	0.29	0.16	0.11	0.20	0.22	0.20	0.30
Th/La	0.23	0.17	0.13	0.10	0.13	0.15	0.19	0.18
Zr/Y	1.49	1.74	2.27	2.04	1.78	1.63	3.20	1.95
Ti/Zr	142	117	96	140	129	149	96	154
Ti/Sm	2992	2525	2220	2340	3050	3072	2386	3648
P/Nd	167	31	85	115	117	0	78	110
Ti/V	8	9	10	10	8	9	16	9
Sc/Lu	391	303	292	322	401	362	198	440
Nb/Nb*	1.37	0.56	0.70	0.96	0.55	0.71	0.96	0.55
Zr/Zr*	1.11	0.96	0.94	0.77	1.01	0.98	0.99	0.99
Hf/Hf*	1.06	0.95	0.84	1.04	1.08	1.14	0.82	1.07
Ti/Ti*	0.98	0.86	0.77	0.79	1.00	1.00	0.84	1.21
UTM Zone	15	15	15	15	15	15	15	15
Easting	442739	445750	445950	449650	447000	445511	444872	445503
Northing	5664809	565750	565950	5656750	5661550	5664750	5664001	5664798

	Rice Lake belt - Garner Lake assemblage Komatiitic basalts				Red Lake belt - Balmer assemblage Serpentinites			
	RC96-5	RC96-3	RC96-4	RC96-2	RL95-10A	RL95-10B	RL95-13	AB94-147A
SiO_2	52.76	52.39	52.86	53.44	45.41	45.51	49.58	50.97
TiO_2	0.28	0.31	0.31	0.28	0.22	0.17	1.30	1.16
Al_2O_3	9.12	9.89	9.60	9.14	4.14	2.33	14.49	13.92
Fe_2O_3	13.68	11.11	13.24	12.10	14.13	14.33	16.56	15.49
MnO	0.19	0.20	0.17	0.24	0.22	0.22	0.22	0.22
MgO	13.58	13.34	12.72	12.41	29.66	34.02	8.18	6.83
CaO	7.98	10.55	8.42	10.57	5.93	3.35	5.19	6.09
K_2O	0.05	0.05	0.13	0.17	0.02	0.00	0.28	0.19
Na_2O	2.36	2.17	2.56	1.62	0.27	0.10	4.07	5.02
P_2O_5	0.00	0.00	0.00	0.02	0.00	0.00	0.13	0.09
LOI	2.72	3.84	3.95	1.63	8.10	9.23	2.56	3.84
Mg#	69	73	68	69	82	84	52	49
Ti	1682	2055	1957	1838	1287	964	7872	7534
P	158	15	2	12	464	470	441	602
Cr	1303	1673	648	1499	2900	3613	209	191
Co	78	63	45	59	128	132	50	55
Ni	216	402	113	347	1529	1659	71	81
Rb	0	1	1	2	1	0	6	7
Sr	20	132	39	101	5	17	84	138
Cs	0	0	0	0	0	0	2	2
Ba	8	30	15	31	6	3	52	56
Sc	54	56	58	48	31	29	46	56
V	243	267	273	229	139	119	391	372
Ta	0.03	0.04	0.04	0.04	0.04	0.03	0.34	0.24
Nb	0.35	0.55	0.32	0.43	0.37	0.23	5.92	4.39
Zr	11	13	11	13	10	7	99	73
Hf	0.37	0.39	0.37	0.37	0.27	0.16	2.70	1.95
Th	0.10	0.07	0.06	0.06	0.05	0.04	1.06	0.52
U	0.02	0.01	0.01	0.01	0.00	0.69	0.31	0.12
Y	5.99	8.41	6.06	7.47	5.41	4.03	29.08	26.02
La	0.42	0.84	0.31	0.62	1.15	0.47	6.74	4.48
Ce	1.23	2.25	0.89	1.71	2.66	1.16	16.68	11.64
Pr	0.22	0.35	0.16	0.28	0.33	0.17	2.09	1.71
Nd	1.16	1.82	0.97	1.61	1.43	0.87	10.56	8.66
Sm	0.48	0.68	0.56	0.61	0.49	0.34	3.38	2.69
Eu	0.17	0.44	0.23	0.22	0.26	0.15	1.08	1.03
Gd	0.86	1.00	0.81	1.03	0.68	0.48	4.19	3.60
Tb	0.16	0.20	0.17	0.19	0.14	0.10	0.75	0.65
Dy	1.21	1.31	1.16	1.28	0.92	0.60	4.89	4.34
Ho	0.29	0.30	0.26	0.29	0.21	0.13	1.10	0.97
Er	0.80	0.88	0.77	0.85	0.56	0.35	3.32	2.74
Tm	0.12	0.14	0.11	0.12	0.08	0.04	0.49	0.43
Yb	0.83	0.90	0.76	0.83	0.52	0.32	3.24	2.73
Lu	0.13	0.14	0.11	0.12	0.08	0.04	0.50	0.43
Cu	95	189	103	67	71	87	346	126
Zn	57	51	44	50	103	108	87	133
Mo	0.10	0.17	0.09	0.22	1.29	2.71	1.01	0.63
Ag	0.26	0.27	0.20	0.23	1.30	1.13	1.09	1.76
Tl	0.02	0.04	0.03	0.06	-	-	0.10	0.07
Pb	0.56	0.36	0.68	0.53	0.98	0.80	2.40	3.47
Se	-	-	-	-	-	-	-	2.11
Sb	-	-	-	-	-	-	-	1.06
	RC96-5	RC96-3	RC96-4	RC96-2	RL95-10A	RL95-10B	RL95-13	AB94-147A
(La/Yb)n	0.36	0.67	0.29	0.54	1.58	1.06	1.49	1.18
(La/Sm)n	0.56	0.81	0.36	0.66	1.52	0.90	1.29	1.08
(Gd/Yb)n	0.86	0.91	0.88	1.03	1.09	1.25	1.07	1.09
(La/Y)n	0.47	0.66	0.34	0.55	1.40	0.77	1.53	1.14
(Tb/Yb)n	0.90	0.99	1.00	1.02	1.23	1.41	1.05	1.09
(Tb/Y)n	1.15	0.99	1.15	1.05	1.09	1.02	1.08	1.06
(Eu/Eu*)n	0.82	1.62	1.04	0.84	1.38	1.16	0.88	1.01
AL_2O_3/TiO_2	32	28	29	30	19	14	11	11
Zr/Hf	29	33	29	35	38	43	37	38
La/Nb	1.21	1.53	0.96	1.43	3.15	2.04	1.14	1.02
Th/Nb	0.29	0.14	0.19	0.15	0	0.19	0.18	0.12
Th/La	0.24	0.09	0.20	0.10	0.0	0.09	0.16	0.12
Zr/Y	1.79	1.54	1.78	1.72	1.88	1.77	3.41	2.82
Ti/Zr	157	159	182	143	127	135	79	103
Ti/Sm	3484	3043	3487	3026	2646	2848	2332	2801
P/Nd	136	8	2	8	326	538	42	69
Ti/V	7	8	7	8	9	8	20	20
Sc/La	405	418	509	404	415	653	93	132
Nb/Nb*	0.90	0.65	1.11	0.72	0.28	0.45	0.81	0.95
Zr/Zr*	0.99	0.81	1.01	0.90	0.85	0.91	1.15	1.05
Hf/Hf*	1.24	0.89	1.27	0.93	0.81	0.76	1.13	1.02
Ti/Ti*	1.03	0.99	1.15	0.92	0.88	0.95	0.83	0.96
UTM Zone	15	15	15	15	15	15	15	15
Easting	342823	342752	342752	342696	444715	444715	444571	447000
Northing	5633515	5634075	5634075	5634227	5661165	5661165	5661118	5661550

Red Lake belt - Balmer assemblage
Serpentinites

	AB94-152A	AB94-152B	AB94-152C	AB94-155A	AB94-168A	GC94-45	GC95-22A
SiO_2	48.84	47.98	46.86	65.08	51.76	41.64	43.54
TiO_2	1.91	0.26	0.38	0.26	0.34	0.26	0.26
Al_2O_3	13.96	6.83	8.50	7.47	8.66	2.71	3.86
Fe_2O_3	18.21	14.23	13.09	13.24	12.29	11.51	15.93
MnO	0.23	0.09	0.05	0.26	0.15	0.27	0.24
MgO	5.32	29.01	30.58	8.64	16.92	30.42	33.69
CaO	5.57	1.54	0.41	4.75	4.42	13.09	2.42
K_2O	0.23	0.00	0.00	0.28	4.89	0.00	0.00
Na_2O	4.49	0.09	0.12	0.03	0.64	0.06	0.09
P_2O_5	0.23	0.00	0.02	0.00	0.02	0.04	0.00
LOI	7.13	9.89	9.00	10.49	8.88	25.12	21.77
Mg#	39	82	84	59	75	85	82
Ti	11419	1546	2240	1281	1928	1495	1392
P	992	45	246	9	209	418	127
Cr	37	2805	1899	3732	1687	2383	3756
Co	48	90	103	58	66	88	120
Ni	34	1047	1129	694	295	1198	1851
Rb	8	0	1	8	168	0	0
Sr	101	22	11	38	147	139	38
Cs	0	0	1	0	37	0	0
Ba	34	1	4	47	213	2	3
Sc	44	17	44	29	48	24	22
V	324	159	170	232	215	109	127
Ta	0.57	0.04	0.07	0.02	0.05	0.04	0.03
Nb	8.89	0.36	1.16	0.34	0.58	0.57	0.41
Zr	163	9	13	11	16	15	7
Hf	4.34	0.32	0.37	0.34	0.45	0.44	0.26
Th	1.20	0.05	0.25	0.17	0.13	0.16	0.05
U	0.25	0.01	0.05	0.07	0.04	0.02	0.01
Y	47.55	4.64	4.62	4.03	10.74	5.01	4.27
La	10.61	0.36	0.46	0.96	1.20	0.77	0.56
Ce	26.50	0.99	1.08	2.04	2.78	1.91	1.28
Pr	3.90	0.15	0.16	0.28	0.44	0.29	0.19
Nd	18.48	0.75	0.86	1.34	2.11	1.41	1.01
Sm	5.56	0.34	0.34	0.39	0.78	0.60	0.41
Eu	1.84	0.07	0.05	0.19	0.21	0.26	0.18
Gd	7.24	0.53	0.51	0.42	1.19	0.72	0.58
Tb	1.24	0.11	0.10	0.08	0.23	0.14	0.11
Dy	8.17	0.77	0.81	0.63	1.61	0.94	0.74
Ho	1.81	0.18	0.19	0.15	0.38	0.19	0.16
Er	5.11	0.57	0.56	0.49	1.17	0.60	0.55
Tm	0.79	0.09	0.10	0.07	0.17	0.09	0.07
Yb	4.99	0.57	0.64	0.49	1.18	0.52	0.47
Lu	0.79	0.09	0.11	0.07	0.17	0.07	0.07
Cu	67	29	4	58	116	5	69
Zn	109	45	37	37	66	54	104
Mo	0.85	0.19	0.13	0.18	0.08	0.10	0.15
Ag	1.76	0.05	0.20	0.20	1.25	0.20	0.13
Tl	0.09	0.01	0.02	0.06	1.38	-	0.01
Pb	5.65	0.25	0.27	0.64	2.53	1.35	0.47
Sn	3.17	2.48	1.92	1.41	0.29	1.04	1.89
Sb	6.45	2.07	0.85	9.68	3.86	3.24	14.42

	AB94-152A	AB94-152B	AB94-152C	AB94-155A	AB94-168A	GC94-45	GC95-22A
(La/Yb)n	1.52	0.46	0.51	1.42	0.73	1.06	0.85
(La/Sm)n	1.23	0.69	0.88	1.61	0.99	0.83	0.87
(Gd/Yb)n	1.20	0.76	0.66	0.71	0.83	1.14	1.02
(La/Y)n	1.48	0.52	0.66	1.58	0.74	1.02	0.87
(Tb/Yb)n	1.13	0.87	0.69	0.72	0.88	1.19	1.05
(Tb/Y)n	1.10	0.99	0.89	0.81	0.89	1.15	1.08
(Eu/Eu*)n	0.89	0.47	0.40	1.42	0.65	1.22	1.13
AL_2O_3/TiO_2	7	30	23	35	27	11	17
Zr/Hf	37	27	34	34	35	34	27
La/Nb	1.19	1.00	0.40	2.81	2.08	1.35	1.35
Th/Nb	0.14	0.15	0.21	0.51	0.23	0.28	0.12
Th/La	0.11	0.15	0.54	0.18	0.11	0.21	0.09
Zr/Y	3.42	1.86	2.74	2.81	1.46	3.01	1.62
Ti/Zr	70	156	177	113	123	99	202
Ti/Sm	2055	3951	6626	3314	2459	2493	3367
P/Nd	54	60	286	7	99	296	126
Ti/V	35	8	13	6	9	14	11
Sc/La	56	420	408	430	273	326	308
Nb/Nb*	0.78	1.02	2.22	0.28	0.42	0.68	0.63
Zr/Zr*	1.11	1.18	1.62	1.09	0.84	1.13	0.74
Hf/Hf*	1.08	1.58	1.72	1.18	0.87	1.19	0.99
Ti/Ti*	0.71	1.26	2.13	1.26	0.79	0.90	1.12
UTM Zone	15	15	15	15	15	15	15
Easting	446050	446050	446050	445750	445950	449450	449300
Northing	5660600	5660600	5660600	565750	565950	5656800	5656800

Red Lake - Balmer assemblage

Tholeiites

	RL95-42	RL95-17	RL95-47	RL95-38	RL95-12A	RL95-8	RL95-9	RL95-23	RL95-20
SiO_2	53.88	52.25	50.30	51.79	50.12	49.79	50.23	48.94	47.34
TiO_2	0.41	0.96	0.36	0.64	0.96	0.88	1.13	1.03	0.61
Al_2O_3	5.78	10.43	15.11	11.43	15.37	13.90	14.37	15.01	11.41
Fe_2O_3	10.67	14.40	11.90	12.71	12.89	14.13	13.75	14.19	12.26
MnO	0.25	0.23	0.17	0.20	0.19	0.28	0.20	0.22	0.33
MgO	12.91	13.12	10.45	7.88	7.76	8.21	7.73	7.38	6.33
CaO	14.94	7.56	7.38	13.99	10.73	9.63	8.82	10.28	21.13
K_2O	0.09	0.54	1.55	0.11	0.09	0.06	0.11	0.14	0.12
Na_2O	1.06	0.42	2.74	1.21	1.83	3.05	3.56	2.72	0.44
P_2O_5	0.02	0.09	0.03	0.05	0.08	0.07	0.12	0.09	0.04
LOI	5.32	5.49	1.52	5.32	1.73	14.28	1.99	0.35	1.99
Mg#	73	67	66	58	57	56	55	53	53
Ti	2794	4857	2107	4328	5326	5499	6528	6103	3624
P	178	379	236	383	689	78	512	389	315
Cr	1884	1167	533	525	439	293	210	219	2622
Co	69	57	52	60	53	48	42	50	84
Ni	308	338	143	128	132	88	87	127	572
Rb	1	16	52	1	0	2	1	1	3
Sr	50	41	97	81	137	99	190	131	790
Cs	0	3	12	0	0	0	0	0	0
Ba	9	35	329	18	20	23	31	39	216
Sc	70	48	63	50	40	54	39	42	42
V	278	320	256	363	336	349	319	296	347
Ta	0.04	0.22	0.16	0.08	0.19	0.17	0.31	0.20	0.10
Nb	0.65	3.46	0.86	1.16	3.33	2.76	5.17	3.48	1.69
Zr	17	62	21	35	99	55	72	63	33
Hf	0.50	1.45	0.62	1.01	1.85	1.57	1.56	1.78	0.96
Th	0.28	0.51	0.26	0.23	0.40	0.47	0.95	0.45	0.26
U	0.04	0.11	0.08	0.07	0.00	0.06	0.23	0.09	0.09
Y	11.25	17.84	10.12	13.66	20.72	9.52	24.59	22.13	16.59
La	0.75	4.16	1.08	1.62	3.75	3.04	6.23	3.71	2.23
Ce	2.34	11.17	2.31	4.03	10.06	7.94	15.94	9.91	5.36
Pr	0.40	1.60	0.32	0.60	1.33	1.09	2.26	1.54	0.86
Nd	2.04	7.48	1.70	3.20	7.43	5.75	10.87	7.66	4.52
Sm	0.89	2.29	0.68	1.26	2.45	1.79	3.30	2.67	1.53
Eu	0.38	0.84	0.19	0.58	0.89	0.65	1.19	0.88	0.66
Gd	1.33	2.97	1.02	1.88	3.29	1.94	4.14	3.30	2.08
Tb	0.24	0.51	0.20	0.35	0.55	0.30	0.68	0.56	0.37
Dy	1.78	3.13	1.45	2.41	3.58	1.83	4.30	3.90	2.48
Ho	0.39	0.69	0.37	0.52	0.83	0.41	0.94	0.85	0.54
Er	1.04	1.91	1.11	1.52	2.36	1.17	2.74	2.40	1.54
Tm	0.16	0.31	0.18	0.22	0.34	0.20	0.42	0.37	0.26
Yb	0.92	1.96	1.13	1.39	2.22	1.16	2.66	2.37	1.55
Lu	0.13	0.28	0.19	0.21	0.30	0.20	0.40	0.38	0.24
Cu	29	28	10	116	122	92	34	161	10
Zn	68	83	90	88	89	106	77	96	98
Mo	0.15	0.40	0.10	4.47	1.67	1.18	0.90	0.58	2.57
Ag	0.14	0.20	0.20	0.14	0.91	1.37	0.24	0.24	0.10
Tl	-	0.13	0.38	0.00	-	0.17	0.01	0.01	-
Pb	4.30	0.97	2.43	0.85	0.78	0.81	0.81	1.39	10.08
Se	0.24	0.54	0.32	0.49	-	-	0.94	0.66	0.40
Sb	0.40	2.78	0.18	0.29	-	-	7.38	0.37	2.09
	RL95-42	RL95-17	RL95-47	RL95-38	RL95-12A	RL95-8	RL95-9	RL95-23	RL95-20
(La/Yb)n	0.59	1.52	0.68	0.84	1.21	1.02	1.68	1.12	1.03
(La/Sm)n	0.55	1.17	1.02	0.83	0.99	0.92	1.22	0.90	0.94
(Gd/Yb)n	1.20	1.25	0.75	1.12	1.22	1.06	1.29	1.15	1.11
(La/Y)n	0.44	1.54	0.70	0.79	1.20	2.04	1.68	1.11	0.89
(Tb/Yb)n	1.20	1.17	0.82	1.14	1.12	1.10	1.17	1.08	1.08
(Tb/Y)n	0.90	1.19	0.84	1.07	1.11	2.22	1.17	1.07	0.93
(Eu/Eu*)n	1.07	0.99	0.71	1.15	0.96	0.98	0.99	0.91	1.14
AL_2O_3/TiO_2	12	13	42	16	17	16	13	14	18
Zr/Hf	35	43	35	34	32	35	39	35	34
La/Nb	1.15	1.20	1.25	1.40	1.13	1.07	1.21	1.07	1.32
Th/Nb	0.43	0.15	0.31	0.20	0.12	0.17	0.18	0.13	0.16
Th/La	0.38	0.12	0.25	0.14	0.11	0.16	0.15	0.12	0.12
Zr/Y	1.54	3.46	2.11	2.54	2.87	5.79	3.04	2.84	1.97
Ti/Zr	161	79	99	125	90	93	87	97	111
Ti/Sm	3156	2121	3097	3422	2175	2466	1981	2285	2367
P/Nd	87	51	139	119	93	13	47	51	70
Ti/V	10	15	8	12	16	15	20	21	10
Sc/La	556	170	325	239	132	188	97	111	170
Nb/Nb*	1.02	0.83	0.64	0.66	0.89	0.92	0.79	0.93	0.68
Zr/Zr*	0.89	1.03	1.38	1.19	0.96	1.09	0.86	0.96	0.86
Hf/Hf*	0.92	0.88	1.45	1.26	1.09	1.13	0.81	0.99	0.92
Ti/Ti*	1.02	0.74	1.00	1.11	0.74	0.86	0.70	0.81	0.80
UTM Zone	15	15	15	15	15	15	15	15	15
Easting	448118	447042	446629	444885	446532	444606	444768	455277	451281
Northing	5666537	5659424	5667673	5663822	566739	5660405	5661101	5670357	5665637

Red Lake - Balmer assemblage

Tholeiites

	RL95-19	RL95-43	RL95-7B	RL95-12B	RL95-22	RL95-25	RL95-18A	RL95-18B	RL95-24	RL95-11
SiO_2	48.34	49.90	47.16	48.95	50.46	51.33	50.11	52.64	53.28	48.92
TiO_2	1.97	1.17	1.14	1.01	1.12	1.66	1.70	1.69	1.56	1.08
Al_2O_3	14.07	15.37	15.64	15.94	16.27	13.61	14.65	14.33	12.71	14.73
Fe_2O_3	13.15	13.53	13.69	13.30	11.46	16.08	15.78	16.57	15.17	14.42
MnO	0.22	0.22	0.30	0.21	0.24	0.29	0.25	0.26	0.23	0.16
MgO	6.60	6.66	6.67	6.32	5.21	7.25	6.12	5.58	4.73	4.41
CaO	6.15	10.45	9.79	11.17	11.98	6.94	9.05	4.65	10.18	13.08
K_2O	0.09	0.19	1.88	0.14	0.26	1.23	0.98	3.38	0.10	0.25
Na_2O	3.21	2.41	3.62	2.88	2.91	1.45	1.20	0.74	1.91	2.83
P_2O_5	0.20	0.10	0.10	0.08	0.10	0.18	0.16	0.15	0.14	0.11
LOI	0.50	0.65	15.33	1.32	1.11	1.63	0.96	0.55	0.65	1.63
Mg#	52	52	52	51	90	90	46	43	41	40
Ti	13820	5591	6093	5437	6596	10737	9542	10733	8913	6016
P	1061	457	426	670	427	1182	545	808	786	566
Cr	54	206	381	446	283	216	124	67	20	196
Co	51	46	34	54	51	61	52	52	62	44
Ni	54	112	94	132	143	35	52	56	47	70
Rb	2	4	65	0	3	51	33	91	1	2
Sr	82	131	75	204	139	77	102	46	116	170
Cs	0	1	2	0	0	3	4	3	0	0
Ba	42	32	97	38	75	168	361	283	19	24
Sc	47	35	42	52	45	58	48	44	46	38
V	467	272	293	344	355	481	440	407	470	319
Ta	0.54	0.27	0.24	0.21	0.28	0.41	0.37	0.39	0.33	0.32
Nb	8.34	3.95	3.35	3.44	3.99	7.00	6.56	5.52	4.89	4.98
Zr	143	73	62	63	65	124	112	102	107	64
Hf	3.35	2.11	1.71	1.87	1.88	3.45	2.65	2.88	2.81	1.79
Th	1.23	0.46	0.65	0.64	0.49	1.23	0.82	1.00	0.95	1.02
U	0.31	0.11	0.22	-0.09	0.10	1.01	0.20	0.19	0.17	0.29
Y	39.54	27.30	14.87	21.53	24.01	34.92	35.67	31.53	33.57	19.18
La	10.29	3.95	4.01	4.06	3.76	8.59	6.96	8.07	6.32	5.89
Ce	26.85	10.63	10.71	10.32	10.01	22.15	19.17	21.01	16.97	16.30
Pr	3.78	1.62	1.56	1.37	1.55	2.92	2.79	3.00	2.46	2.30
Nd	17.59	8.21	7.89	7.81	7.75	15.50	13.49	14.38	11.84	10.58
Sm	4.76	2.76	2.44	2.62	2.55	4.34	4.20	4.42	3.92	2.68
Eu	1.44	1.00	0.89	1.01	1.07	1.38	1.41	1.26	1.40	1.67
Gd	5.91	3.66	3.09	3.57	3.30	5.66	5.46	5.36	5.01	3.36
Tb	1.06	0.64	0.51	0.57	0.56	0.96	0.96	0.93	0.87	0.53
Dy	6.99	4.34	2.94	3.78	3.78	6.16	6.16	5.96	5.87	3.33
Ho	1.57	0.96	0.63	0.87	0.83	1.36	1.43	1.35	1.28	0.72
Er	4.80	2.73	1.87	2.45	2.34	4.11	4.01	3.91	3.58	2.07
Tm	0.71	0.43	0.29	0.34	0.34	0.62	0.64	0.61	0.53	0.32
Yb	4.91	2.68	1.97	2.28	2.29	3.94	3.93	3.89	3.57	2.11
Lu	0.75	0.39	0.30	0.31	0.35	0.64	0.62	0.58	0.52	0.35
Cu	124	128	180	129	142	170	87	125	148	56
Zn	118	81	83	88	95	187	162	103	152	38
Mo	1.57	0.35	0.53	0.87	0.59	1.41	1.03	1.23	0.42	0.69
Ag	0.70	0.75	0.46	0.96	0.15	1.29	0.42	0.46	0.85	0.25
Tl	0.01	0.05	0.46	-	0.02	0.50	0.21	0.53	0.04	-
Pb	2.87	1.48	3.27	0.90	0.64	6.52	2.43	2.28	2.18	10.84
Sn	1.66	0.67	0.55	-	0.80	-	1.06	1.06	0.99	0.98
Sb	0.65	0.88	3.87	-	0.16	-	4.96	3.56	0.49	12.12

	RL95-19	RL95-43	RL95-7B	RL95-12B	RL95-22	RL95-25	RL95-18A	RL95-18B	RL95-24	RL95-11
(La/Yb)n	1.50	1.06	1.46	1.27	1.18	1.56	1.27	1.49	1.27	2.00
(La/Sm)n	1.40	0.92	1.06	1.00	0.95	1.28	1.07	1.18	1.04	1.42
(Gd/Yb)n	0.99	1.13	1.30	1.29	1.19	1.19	1.15	1.14	1.16	1.32
(La/Y)n	1.72	0.96	1.79	1.25	1.04	1.63	1.29	1.70	1.25	2.03
(Tb/Yb)n	0.98	1.09	1.17	1.14	1.11	1.11	1.11	1.08	1.10	1.14
(Tb/Y)n	1.12	0.99	1.43	1.12	0.97	1.16	1.13	1.23	1.08	1.16
(Eu/Eu*)n	0.83	0.96	0.99	1.01	1.13	0.85	0.90	0.79	0.97	1.70
Al_2O_3/TiO_2	6	16	15	18	15	7	9	8	8	14
Zr/Hf	43	35	36	33	34	36	42	35	38	36
La/Nb	1.23	1.00	1.20	1.18	0.94	1.23	1.06	1.46	1.29	1.18
Th/Nb	0.15	0.12	0.19	0.19	0.12	0.18	0.12	0.18	0.19	0.20
Th/La	0.12	0.12	0.16	0.16	0.13	0.14	0.12	0.12	0.15	0.17
Zr/Y	3.62	2.68	4.17	2.91	2.70	3.54	3.13	3.23	3.18	3.33
Ti/Zr	97	76	98	87	102	87	85	106	84	94
Ti/Sm	2901	2027	2493	2075	2588	2473	2272	2426	2276	2242
P/Nd	60	56	54	86	55	76	40	56	66	53
Ti/V	30	21	21	16	19	22	22	26	19	19
Sc/La	62	89	141	165	128	90	77	75	88	109
Nb/Nb*	0.79	1.00	0.83	0.81	1.05	0.78	0.97	0.66	0.77	0.87
Zr/Zr*	1.08	1.07	0.98	0.96	1.01	1.04	1.03	0.88	1.08	0.83
Hf/Hf*	0.92	1.11	0.98	1.04	1.06	1.06	0.88	0.91	1.03	0.84
Ti/Ti*	1.03	0.70	0.88	0.70	0.90	0.86	0.79	0.87	0.80	0.79
UTM Zone	15	15	15	15	15	15	15	15	15	15
Easting	450043	450540	445012	446532	454053	454187	448977	448977	455982	445060
Northing	5662909	5668364	5660193	566739	5669480	5670969	5661098	5661098	5671004	5661466

	Red Lake - Balmer assemblage LREE enriched tholeiites					Birch-Uchi belt Balmer assemblage	Rice Lake belt Balmer assemblage	
	RL95-44	RL95-26	RL95-45	RL95-21	RL95-41	SB95-1	RC96-6	RC96-7
SiO_2	50.45	50.23	51.02	51.41	58.56	50.18	52.50	49.65
TiO_2	0.60	0.93	0.62	0.71	1.03	1.24	0.75	0.66
Al_2O_3	13.08	14.50	13.62	14.75	17.73	14.25	16.53	14.88
Fe_2O_3	11.84	13.27	11.78	11.98	6.43	14.35	11.27	13.89
MnO	0.21	0.20	0.17	0.18	0.23	0.22	0.25	0.23
MgO	11.02	7.37	10.65	6.57	2.85	6.52	3.83	7.91
CaO	11.12	10.82	8.82	10.85	9.84	10.59	11.81	10.16
K_2O	0.09	0.19	0.22	0.18	1.66	0.35	0.16	0.14
Na_2O	1.54	2.42	3.04	3.29	1.54	2.18	2.86	2.42
P_2O_5	0.05	0.06	0.05	0.07	0.12	0.11	0.04	0.04
LOI	0.96	0.20	0.65	0.76	3.52	0.55	6.56	11.60
Mg#	67	55	67	55	49	50	43	56
Ti	3980	4110	3809	4025	5379	7245	5152	4331
P	224	320	324	391	481	542	88	100
Cr	878	201	821	283	271	215	333	305
Co	67	44	55	48	21	64	45	50
Ni	247	90	243	100	139	88	155	131
Rb	2	8	4	1	40	4	5	2
Sr	236	142	179	215	98	126	112	56
Cs	0	0	0	0	6	0	0	0
Ba	23	46	87	37	102	66	46	16
Sc	47	40	49	38	37	53	54	50
V	279	266	256	235	273	398	367	330
Ta	0.15	0.23	0.14	0.19	0.13	0.29	0.13	0.12
Nb	2.16	3.09	2.47	3.17	2.07	3.86	1.87	1.72
Zr	47	52	44	47	78	82	41	36
Hf	1.46	1.45	1.04	1.32	2.11	2.30	1.20	0.99
Th	1.29	0.94	1.26	0.76	0.73	1.57	0.24	0.20
U	0.22	0.16	0.24	0.15	0.27	0.10	0.06	0.06
Y	17.09	17.08	16.30	15.14	25.22	27.69	17.46	16.17
La	3.81	4.77	4.24	4.41	4.13	4.65	2.17	1.64
Ce	9.09	11.40	10.12	10.69	10.65	12.75	6.02	4.89
Pr	1.15	1.57	1.35	1.52	1.63	1.83	0.95	0.78
Nd	5.12	7.63	6.44	6.81	7.91	8.56	5.00	3.82
Sm	1.67	2.14	2.01	1.92	2.96	2.80	1.65	1.36
Eu	0.56	0.76	0.82	0.75	0.98	0.99	0.67	0.47
Gd	2.38	2.56	2.71	2.31	3.80	3.94	2.50	2.09
Tb	0.39	0.43	0.46	0.40	0.66	0.66	0.44	0.39
Dy	2.81	2.91	3.15	2.54	4.42	4.57	3.12	2.59
Ho	0.62	0.63	0.69	0.57	0.98	1.07	0.68	0.61
Er	1.79	1.85	2.05	1.63	2.79	3.10	2.04	1.74
Tm	0.26	0.27	0.32	0.24	0.42	0.45	0.30	0.26
Yb	1.65	1.77	2.06	1.59	2.67	3.00	1.94	1.72
Lu	0.27	0.27	0.29	0.24	0.43	0.45	0.31	0.26
Cu	109	48	99	114	78	159	66.27	154.50
Zn	84	66	72	77	96	136	87.37	124.67
Mo	0.25	0.49	0.30	0.83	0.68	0.71	0.24	0.24
Ag	0.41	0.26	0.50	0.12	0.74	0.62	0.28	0.37
Tl	0.00	0.07	0.03	0.00	0.25	1.26	0.05	0.04
Pb	11.60	1.52	3.58	1.25	4.35	0.32	1.67	2.98
Se	0.50	0.63	0.57	0.55	0.62	0.00	-	-
Sb	0.34	4.06	0.63	0.57	0.56	0.00	-	-
	RL95-44	RL95-26	RL95-45	RL95-21	RL95-41	SB95-1	RC96-6	RC96-7
(La/Yb)n	1.66	1.93	1.47	1.99	1.11	1.11	0.80	0.69
(La/Sm)n	1.48	1.44	1.36	1.48	0.90	1.07	0.85	0.78
(Gd/Yb)n	1.20	1.19	1.09	1.20	1.18	1.09	1.07	1.00
(La/Y)n	1.48	1.85	1.72	1.93	1.09	1.11	0.82	0.67
(Tb/Yb)n	1.09	1.10	1.02	1.15	1.13	1.01	1.02	1.03
(Tb/Y)n	0.97	1.06	1.19	1.12	1.10	1.01	1.05	1.01
(Eu/Eu*)n	0.85	0.99	1.07	1.08	0.90	0.91	1.01	0.85
AL_2O_3/TiO_2	19	21	21	22	20	12	19	21
Zr/Hf	32	36	42	35	37	36	34	36
La/Nb	1.76	1.55	1.72	1.39	2.00	1.20	1.16	0.96
Th/Nb	0.60	0.30	0.51	0.24	0.35	0.41	0.13	0.12
Th/La	0.34	0.20	0.30	0.17	0.18	0.34	0.11	0.12
Zr/Y	2.76	3.04	2.68	3.09	3.08	2.96	2.32	2.22
Ti/Zr	84	79	87	86	69	88	127	121
Ti/Sm	2389	1917	1892	2091	1816	2592	3131	3186
P/Nd	44	42	50	57	61	63	18	26
Ti/V	14	15	15	17	20	18	14	13
Sc/Lu	174	148	169	156	85	117	176	193
Nb/Nb*	0.51	0.58	0.52	0.65	0.48	0.85	0.89	1.16
Zr/Zr*	1.12	0.89	0.84	0.89	1.11	1.16	0.98	1.09
Hf/Hf*	1.25	0.90	0.72	0.91	1.09	1.18	1.05	1.09
Ti/Ti*	0.79	0.69	0.65	0.76	0.63	0.86	1.00	1.02
UTM Zone	15	15	15	15	15	15	15	15
Easting	452597	453200	451967	453492	447756	500619	342749	342524
Northing	5668911	5670591	5668570	5668718	5665723	5647239	5634394	5634224

Red Lake belt
Ball assemblage

	NDC87-06A	NDC87-01E	NDC87-15C
SiO_2	90.82	62.87	56.27
TiO_2	0.35	0.48	0.40
Al_2O_3	10.49	13.65	12.71
Fe_2O_3	12.65	6.69	11.07
MnO	0.25	0.08	0.18
MgO	13.06	6.69	8.08
CaO	11.21	4.18	9.11
K_2O	0.31	1.95	0.29
Na_2O	0.81	3.23	1.81
P_2O_5	0.04	0.17	0.07
LOI	0.91	0.81	1.57
Mg#	69	69	62
Ti	2253	3262	2549
P	132	745	210
Cr	1304	556	302
Co	80	32	37
Ni	395	151	93
Rb	6	150	7
Sr	87	251	538
Cs	1	10	2
Ba	17	56	41
Sc	30	17	44
V	190	104	241
Ta	0.10	0.43	0.18
Nb	1.68	6.87	2.86
Zr	29	128	62
Hf	0.83	3.25	1.62
Th	0.54	3.20	0.89
U	0.14	0.81	0.24
Y	8.86	12.98	12.56
La	2.45	16.59	4.14
Ce	5.58	38.37	9.47
Pr	0.69	4.58	1.13
Nd	3.07	17.46	4.53
Sm	0.89	3.14	1.19
Eu	0.29	1.03	0.54
Gd	1.32	2.68	1.82
Tb	0.23	0.41	0.29
Dy	1.59	2.44	2.00
Ho	0.36	0.49	0.44
Er	1.04	1.46	1.22
Tm	0.16	0.20	0.18
Yb	1.06	1.40	1.26
Lu	0.17	0.22	0.18
Cu	74	6	10
Zn	81	43	62
Mo	0.13	0.70	0.21
Ag	0.05	0.11	0.35
Tl	0.08	0.89	0.07
Pb	1.30	3.19	3.13
Sn	0.51	0.60	-
Sb	0.12	0.96	-
	NDC87-06A	NDC87-01E	NDC87-15C
$(La/Yb)_N$	1.66	8.49	2.36
$(La/Sm)_N$	1.78	3.42	2.24
$(Gd/Yb)_N$	1.03	1.58	1.20
(La/Y)$_N$	1.83	8.47	2.18
(Tb/Yb)$_N$	1.00	1.34	1.05
(Tb/Y)$_N$	1.10	1.34	0.97
$(Eu/Eu^*)_N$	0.82	1.06	1.11
Al_2O_3/TiO_2	27	25	30
Zr/Hf	35	39	38
La/Nb	1.46	2.42	1.45
Th/Nb	0.33	0.47	0.31
Th/La	0.22	0.19	0.21
Zr/Y	3	10	5
Ti/Zr	77	26	41
Ti/Sm	2537	1041	2134
P/Nd	43	43	46
Ti/V	12	31	11
Sc/La	174	77	249
Nb/Nb^*	0.58	0.36	0.59
Zr/Zr^*	1.22	1.19	1.84
Hf/Hf^*	1.26	1.10	1.75
Ti/Ti^*	0.82	0.45	0.68
UTM Zone	15	15	15
Easting	341150	341140	341080
Northing	5655050	5656450	5656300

Red Lake belt - Ball assemblage

FI

	NDC87-01A	NDC87-01D	NDC87-02B	NDC87-02D	NDC87-06B	NDC87-06C	NDC87-09B	NDC87-12A	NDC87-15A	NDC87-15B
SiO_2	72.61	76.62	73.45	73.25	73.82	73.78	72.47	72.04	73.09	72.95
TiO_2	0.30	0.20	0.20	0.29	0.21	0.19	0.26	0.27	0.31	0.29
Al_2O_3	15.31	14.99	14.87	15.00	13.75	15.02	15.68	14.53	14.87	15.04
Fe_2O_3	2.47	1.54	1.98	1.86	2.28	1.43	2.01	2.77	2.17	2.62
MnO	0.03	0.00	0.03	0.00	0.04	0.03	0.02	0.05	0.04	0.04
MgO	1.26	1.25	0.89	0.81	2.49	0.56	1.68	1.57	1.65	1.55
CaO	1.80	0.34	1.99	1.24	3.11	1.98	1.21	2.18	1.67	1.68
K_2O	2.45	4.80	2.47	1.59	2.57	2.40	2.77	3.71	3.51	3.08
Na_2O	3.72	0.20	4.11	5.88	1.67	4.58	3.81	2.80	2.60	2.67
P_2O_5	0.08	0.06	0.06	0.09	0.06	0.06	0.08	0.07	0.08	0.08
LOI	1.27	2.25	1.27	0.91	1.31	1.37	1.16	2.04	1.89	1.73
Mg#	53	64	50	49	71	46	65	56	63	56
Ti	1917	1057	1326	1793	1359	1088	1784	1640	1788	1819
P	627	221	459	369	237	440	312	311	327	357
Cr	10	28	48	14	74	10	9	13	21	13
Co	12	5	14	10	12	4	6	8	7	11
Ni	4	16	18	5	45	9	7	6	11	6
Rb	72	119	83	65	65	60	67	90	66	99
Sr	130	66	262	204	97	139	94	111	83	103
Cs	2	3	2	1	3	3	6	4	4	3
Ba	324	685	458	119	229	524	489	544	345	312
Sc	3	3	3	2	4	3	4	4	3	3
V	25	14	21	23	22	16	30	28	24	24
Ta	0.33	0.57	0.26	0.33	0.35	0.59	0.33	0.38	0.34	0.35
Nb	4.24	5.15	3.37	4.23	3.81	4.93	3.85	4.37	4.05	4.05
Zr	142	110	108	130	121	115	123	114	129	124
Hf	3.54	3.34	2.89	3.22	3.33	3.51	3.21	3.18	3.38	3.19
Th	4.64	7.85	4.14	4.74	5.14	7.66	3.55	4.90	4.57	5.00
U	1.09	2.45	1.26	0.96	1.13	2.30	0.97	1.23	0.97	1.03
Y	3.31	3.13	3.34	3.33	3.47	3.55	3.99	4.00	3.01	3.37
La	25.20	16.17	17.87	22.67	17.01	16.39	16.46	18.39	18.13	21.23
Ce	45.12	28.02	33.34	41.26	29.24	28.28	31.27	32.51	33.95	38.90
Pr	4.47	2.75	3.33	4.21	2.88	2.65	3.25	3.31	3.39	3.95
Nd	14.90	9.20	10.55	13.82	9.72	8.80	11.31	11.53	11.40	12.97
Sm	2.19	1.52	1.57	2.10	1.53	1.49	1.76	1.79	1.77	2.01
Eu	0.60	0.40	0.47	0.57	0.46	0.44	0.42	0.62	0.55	0.62
Gd	1.47	1.19	1.09	1.38	1.18	1.14	1.35	1.48	1.31	1.33
Tb	0.15	0.13	0.11	0.14	0.13	0.12	0.16	0.14	0.13	0.14
Dy	0.71	0.64	0.56	0.69	0.64	0.68	0.85	0.78	0.69	0.64
Ho	0.11	0.11	0.10	0.10	0.12	0.12	0.15	0.14	0.11	0.10
Er	0.28	0.28	0.24	0.25	0.27	0.24	0.36	0.37	0.25	0.28
Tm	0.04	0.04	0.04	0.04	0.04	0.03	0.06	0.05	0.03	0.04
Yb	0.27	0.25	0.27	0.17	0.22	0.26	0.30	0.30	0.21	0.24
Lu	0.04	0.03	0.04	0.03	0.03	0.04	0.05	0.04	0.03	0.03
Cu	466	22	399	111	4	10	17	11	57	48
Zn	21	25	22	14	28	28	16	25	56	28
Mo	0.39	0.24	0.80	0.37	0.35	0.22	0.15	0.35	0.17	0.16
Ag	0.28	0.10	0.95	0.12	0.09	0.64	0.10	0.09	0.13	0.12
Tl	0.28	0.43	0.28	0.23	0.36	0.34	0.29	0.55	0.33	0.26
Pb	2.67	4.08	3.85	2.11	5.80	13.03	1.66	2.20	15.60	6.16
Sn	0.75	0.78	-	0.48	0.70	-	0.87	0.71	0.65	0.80
Sb	0.11	0.07	-	0.57	0.11	-	0.15	0.15	0.08	0.05

	NDC87-01A	NDC87-01D	NDC87-02B	NDC87-02D	NDC87-06B	NDC87-06C	NDC87-09B	NDC87-12A	NDC87-15A	NDC87-15B
(La/Yb)n	66.07	47.23	46.98	94.73	54.82	45.12	38.89	44.55	60.74	62.35
(La/Sm)n	7.44	6.85	7.35	6.98	7.20	7.10	6.04	6.65	6.60	6.81
(Gd/Yb)n	4.44	4.00	3.30	6.66	4.40	3.63	3.67	4.14	5.08	4.51
(La/Y)n	50.40	34.22	35.46	45.08	32.48	30.56	27.35	30.45	39.95	41.77
(Tb/Yb)n	2.53	2.46	1.78	3.74	2.69	2.18	2.42	2.19	2.81	2.65
(Th/Y)n	1.93	1.78	1.34	1.78	1.59	1.47	1.70	1.50	1.85	1.78
(Eu/Eu*)n	0.96	0.87	1.04	0.95	1.00	1.00	0.81	1.14	1.06	1.09
Al_2O_3/TiO_2	48	84	67	50	61	82	53	53	49	49
Zr/Hf	40	33	38	40	36	33	38	36	38	39
La/Nb	5.94	3.14	5.30	5.36	4.46	3.33	4.27	4.21	4.48	5.24
Th/Nb	1.09	1.52	1.23	1.12	1.35	1.56	0.92	1.12	1.13	1.23
Th/La	0.18	0.49	0.23	0.21	0.30	0.47	0.22	0.27	0.25	0.24
Zr/Y	43	35	32	39	35	32	31	29	43	37
Ti/Zr	13	10	12	14	11	9	15	14	14	15
Ti/Sm	877	693	845	854	890	730	1014	918	1008	903
P/Nd	42	24	43	27	24	50	28	27	29	27
Ti/V	76	73	63	79	61	70	59	58	75	75
Sc/La	72	85	70	82	121	75	75	108	100	99
Nb/Nb*	0.11	0.21	0.13	0.13	0.14	0.19	0.17	0.16	0.16	0.13
Zr/Zr*	1.72	2.04	1.84	1.67	2.18	2.19	1.90	1.74	1.99	1.68
Hf/Hf*	1.56	2.24	1.78	1.50	2.17	2.44	1.80	1.76	1.89	1.57
Ti/Ti*	0.42	0.31	0.40	0.42	0.40	0.33	0.46	0.40	0.46	0.44
UTM Zone	15	15	15	15	15	15	15	15	15	15
Easting	341140	341140	341150	341150	341050	341050	341350	341100	341080	341080
Northing	5656450	5656450	5656900	5656900	5655050	5655050	5656100	5655550	5656300	5656300

Red Lake belt - Balmer assemblage

		FII		FIII	
	RL95-48	RL95-49	RL95-7A	RL95-16	RL95-6
SiO_2	74.03	74.19	76.37	[illegible]	[illegible]
TiO_2	0.39	0.52	0.20	0.84	1.52
Al_2O_3	10.75	10.08	14.33	11.66	12.52
Fe_2O_3	4.52	7.06	2.74	8.25	17.31
MnO	0.17	0.11	0.03	0.16	0.24
MgO	2.39	2.60	1.10	0.95	1.84
CaO	4.66	2.63	0.95	3.75	6.29
K_2O	0.80	0.95	4.08	0.44	0.89
Na_2O	2.23	1.83	0.15	4.38	2.88
P_2O_5	0.06	0.06	0.05	0.24	0.51
LOI	1.20	1.42	2.72	0.96	0.15
Mg#	54	45	47	20	19
Ti	2478	3034	934	4893	8862
P	379	360	382	1256	1788
Cr	201	345	30	92	10
Co	20	33	3	9	23
Ni	63	82	12	6	1
Rb	35	37	133	8	25
Sr	121	90	14	68	191
Cs	3	2	4	1	3
Ba	282	167	193	115	228
Sc	13	12	1	21	30
V	82	83	2	19	17
Ta	0.48	0.62	0.77	1.27	1.19
Nb	4.75	6.62	10.97	23.17	17.87
Zr	98	179	165	480	286
Hf	2.54	4.84	4.96	11.90	6.81
Th	6.87	9.24	6.12	4.04	3.22
U	2.50	2.24	1.51	0.82	0.82
Y	19.20	12.73	19.50	106.89	84.86
La	18.70	16.56	27.25	30.24	25.76
Ce	34.35	31.00	54.58	73.26	63.47
Pr	3.64	3.12	5.64	9.07	8.91
Nd	13.39	10.87	24.12	46.20	40.98
Sm	2.59	2.25	4.80	13.52	11.88
Eu	0.73	0.70	1.11	3.23	3.49
Gd	2.95	2.39	4.17	16.06	15.08
Tb	0.44	0.36	0.64	2.82	2.50
Dy	2.94	2.04	3.63	17.94	16.19
Ho	0.64	0.43	0.75	4.06	3.57
Er	1.81	1.25	2.18	12.10	10.07
Tm	0.32	0.19	0.33	1.82	1.49
Yb	1.89	1.23	2.06	12.02	9.55
Lu	0.31	0.19	0.31	1.81	1.50
Cu	52	117	3	14	29
Zn	67	67	37	127	158
Mo	1.48	1.97	0.74	1.92	3.99
Ag	1.16	1.41	1.14	2.20	0.99
Tl	0.28	0.26	0.82	0.30	0.19
Pb	9.64	9.58	3.71	2.61	4.27
Sn	0.91	-	-	-	2.38
Sb	0.08	-	-	-	0.38
	RL95-48	RL95-49	RL95-7A	RL95-16	RL95-6
$(La/Yb)_N$	7.10	9.69	9.46	1.80	1.93
$(La/Sm)_N$	4.66	4.75	3.67	1.44	1.40
$(Gd/Yb)_N$	1.29	1.61	1.67	1.11	1.31
(La/Y)N	6.45	8.62	9.26	1.87	2.01
(Tb/Yb)N	1.07	1.34	1.40	1.07	1.19
(Tb/Y)N	0.97	1.19	1.37	1.11	1.24
$(Eu/Eu^*)_N$	0.81	0.92	0.74	0.67	0.80
AL_2O_3/TiO_2	26	20	92	14	8
Zr/Hf	39	37	33	40	42
La/Nb	3.94	2.50	2.48	1.31	1.44
Th/Nb	1.45	1.40	0.56	0.17	0.18
Th/La	0.37	0.56	0.22	0.13	0.13
Zr/Y	5.10	14.09	8.48	4.49	3.37
Ti/Zr	25	17	6	10	31
Ti/Sm	957	1348	195	362	746
Pr/Nd	28	33	16	27	44
Ti/V	30	37	552	263	520
Sc/Lu	42	62	2	12	20
Nb/Nb^*	0.17	0.28	0.30	0.69	0.64
Zr/Zr^*	1.15	2.51	1.06	1.33	0.90
Hf/Hf^*	1.08	2.45	1.16	1.19	0.77
Ti/Ti^*	0.35	0.52	0.08	0.13	0.26
UTM Zone	15	15	15	15	15
Easting	444971	444992	445012	435489	439275
Northing	5665249	5665012	5660193	5645824	5648148

Northern Pickle assemblage

Tholeiites

	PL95-32	PL4	PL5	PL95-31	PL95-29	PL2
SiO_2	49.26	49.47	49.61	48.80	48.48	48.57
TiO_2	0.99	1.04	0.99	1.09	2.02	2.03
Al_2O_3	15.31	14.88	14.95	15.58	12.71	12.67
Fe_2O_3	13.38	13.98	13.94	13.43	19.58	19.41
MnO	0.22	0.27	0.21	0.26	0.26	0.26
MgO	5.90	5.80	5.40	4.58	4.62	4.33
CaO	12.26	11.56	12.12	13.43	9.02	9.36
K_2O	0.17	0.24	0.17	0.16	0.45	0.48
Na_2O	2.42	2.66	2.52	2.57	2.71	2.67
P_2O_5	0.08	0.09	0.08	0.09	0.16	0.20
LOI	0.45	0.70	0.50	0.96	0.91	0.70
Mg#	49	48	46	43	34	33
Ti	6620	6969	5397	7652	14301	12589
P	438	396	351	549	947	879
Cr	379	385	360	421	198	51
Co	52	54	48	63	58	64
Ni	114	106	95	124	49	52
Rb	3	4	5	1	7	7
Sr	137	140	164	168	285	257
Cs	0	0	0	0	0	0
Ba	37	60	35	41	99	107
Sc	53	39	39	60	53	25
V	389	334	283	364	450	389
Ta	0.18	0.23	0.18	0.24	0.59	0.73
Nb	3.21	4.18	3.61	3.97	11.02	11.71
Zr	62	69	61	69	140	148
Hf	1.92	1.89	1.70	2.09	3.61	4.11
Th	0.37	0.44	0.37	0.49	1.34	1.43
U	0.16	0.09	0.08	0.25	0.36	0.41
Y	23.44	24.44	23.58	25.54	29.73	29.25
La	3.94	4.05	3.39	4.35	11.45	13.71
Ce	17	10.94	9.23	11.19	29.21	34.29
Pr	1.5	1.59	1.30	1.60	3.71	4.83
Nd	7.47	8.06	6.80	8.70	18.47	22.25
Sm	2.47	2.54	2.31	2.88	5.31	5.78
Eu	1.01	0.82	0.80	1.03	1.70	1.73
Gd	3.31	3.12	2.68	4.02	6.16	6.27
Tb	0.59	0.58	0.46	0.61	0.86	0.98
Dy	3.82	3.97	3.44	4.16	5.55	6.22
Ho	0.83	0.85	0.76	0.95	1.13	1.20
Er	2.53	2.45	2.20	2.61	3.04	3.57
Tm	0.41	0.39	0.33	0.46	0.46	0.48
Yb	2.23	2.57	2.32	2.70	2.72	3.18
Lu	0.34	0.41	0.35	0.42	0.39	0.45
Cu	17	-	-	59	188	-
Zn	120	-	-	113	132	-
Mo	1.08	-	-	1.97	1.26	-
Ag	-	-	-	-	0.92	-
Tl	0.02	-	-	-	0.71	-
Pb	0.57	-	-	0.78	2.12	-
Se	0.82	-	-	0.87	-	-
Sb	-	-	-	-	-	-
	PL95-32	PL4	PL5	PL95-31	PL95-29	PL2
(La/Yb)n	1.27	1.13	1.05	1.16	3.02	3.09
(La/Sm)n	1.03	1.03	0.95	0.97	1.39	1.53
(Gd/Yb)n	1.23	1.01	0.96	1.23	1.87	1.63
(La/Y)n	1.11	1.10	0.95	1.13	2.55	3.10
(Tb/Yb)n	1.21	1.03	0.91	1.03	1.43	1.40
(Tb/Y)n	1.06	1.00	0.82	1.01	1.21	1.40
(Eu/Eu*)n	1.08	0.89	0.98	0.92	0.90	0.87
AL_2O_3/TiO_2	14	15	17	12	5	6
Zr/Hf	32	37	36	33	39	36
La/Nb	1.23	0.97	0.94	1.10	1.04	1.17
Th/Nb	0.11	0.11	0.10	0.12	0.12	0.12
Th/La	0.09	0.11	0.11	0.11	0.12	0.10
Zr/Y	2.63	2.83	2.59	2.71	4.69	5.08
Ti/Zr	107	88	88	111	103	85
Ti/Sm	2677	2392	2335	2653	2692	2178
P/Nd	59	49	52	63	51	40
Ti/V	17	18	19	21	32	32
Sc/La	155	95	111	143	134	54
Nb/Nb*	0.80	1.04	1.08	0.87	0.91	0.80
Zr/Zr*	0.99	1.06	1.07	0.96	0.98	0.91
Hf/Hf*	1.12	1.05	1.07	1.05	0.91	0.91
Ti/Ti*	0.92	0.85	0.86	0.89	0.99	0.83
UTM Zone	15	16	16	16	15	16
Easting	297430	297200	297500	297023	703943	287600
Northing	5725396	5725650	5725600	5725499	5717867	5718150

Northern Pickle assemblage

OIB-like

	GPT88-8B	GPT88-8A	PL-3	PL95-30	CB90-12A	CB90-6A	CGR91-18A	CGR91-18C	CB90-6B
SiO_2	48.78	49.70	50.64	50.28	51.72	50.12	49.02	49.01	48.98
TiO_2	1.01	1.06	1.08	1.16	0.94	1.13	1.39	1.39	1.54
Al_2O_3	11.30	15.16	15.43	16.22	16.32	15.60	14.24	14.42	13.87
Fe_2O_3	14.34	13.51	12.84	15.20	13.67	13.94	16.63	18.65	17.71
MnO	0.22	0.16	0.16	0.16	0.18	0.19	0.22	0.25	0.21
MgO	8.70	6.28	4.90	5.43	4.82	4.33	4.78	5.03	4.75
CaO	13.19	10.62	10.17	6.85	9.86	10.01	9.03	7.20	6.74
K_2O	0.42	0.33	0.45	0.23	0.32	0.69	0.12	0.36	1.76
Na_2O	1.98	3.11	4.21	4.32	2.11	3.88	4.42	3.59	4.28
P_2O_5	0.06	0.07	0.12	0.14	0.06	0.12	0.14	0.11	0.16
LOI	3.41	1.83	3.09	2.20	6.44	10.74	8.93	8.69	6.89
Mg#	57	51	46	44	44	41	39	37	37
Ti	6526	6283	7134	6577	5298	6681	7372	8587	9499
P	340	497	540	462	501	605	592	676	868
Cr	287	65	206	174	7	29	52	19	10
Co	84	63	53	51	48	66	51	83	65
Ni	196	117	118	99	53	107	53	77	35
Rb	11	8	13	6	78	14	2	12	40
Sr	384	513	476	433	313	542	328	451	456
Cs	0	0	0	0	32	1	0	1	14
Ba	70	73	141	64	627	438	34	103	259
Sc	46	27	20	36	20	28	19	25	23
V	307	260	190	200	161	225	237	280	269
Ta	0.27	0.40	0.57	0.63	0.54	0.55	0.76	0.68	0.66
Nb	4.87	6.26	11.02	11.19	9.40	9.94	11.96	11.58	11.73
Zr	54	65	94	94	89	86	111	100	104
Hf	1.58	1.89	2.30	2.24	2.17	2.31	2.96	2.62	2.68
Th	0.57	0.81	1.11	1.34	1.12	1.17	1.67	1.51	1.36
U	0.13	0.19	0.22	0.35	0.26	0.24	0.35	0.30	0.29
Y	14.53	14.44	17.77	15.67	7.68	13.37	17.84	12.83	15.03
La	5.93	7.93	14.57	13.67	14.10	14.05	16.56	14.55	17.54
Ce	15.46	18.14	34.88	31.89	34.04	32.75	35.21	34.50	40.50
Pr	2.20	2.70	4.52	3.91	4.21	4.07	4.85	4.30	4.94
Nd	10.38	12.28	19.65	19.01	18.26	17.44	20.91	18.64	20.73
Sm	2.93	3.16	3.98	3.88	3.85	3.73	4.49	4.05	4.56
Eu	0.85	1.17	1.33	1.09	1.16	1.21	1.56	1.35	1.23
Gd	2.76	3.54	3.65	3.48	2.69	3.43	4.78	3.58	3.91
Tb	0.42	0.61	0.51	0.55	0.32	0.47	0.76	0.50	0.51
Dy	2.57	2.86	2.83	2.85	1.54	2.62	3.73	2.77	2.92
Ho	0.49	0.66	0.55	0.53	0.30	0.48	0.89	0.52	0.56
Er	1.32	1.51	1.51	1.51	0.85	1.33	2.06	1.37	1.62
Tm	0.20	0.22	0.25	0.24	0.15	0.21	0.29	0.22	0.25
Yb	1.23	1.58	1.35	1.41	1.00	1.32	2.28	1.39	1.70
Lu	0.16	0.20	0.21	0.19	0.18	0.20	0.29	0.24	0.24
Cu	208	191	-	141	150	228	195	247	275
Zn	119	73	-	93	90	113	125	168	149
Mo	0.63	0.13	-	1.20	0.85	0.45	12.24	0.73	0.47
Ag	0.21	0.29	-	-	0.24	0.34	0.33	0.44	0.42
Tl	0.04	0.06	-	0.03	0.70	0.07	0.03	0.13	0.26
Pb	4.23	3.00	-	2.33	2.84	2.72	2.26	3.29	2.29
Se	0.98	0.61	-	0.96	0.83	0.69	0.96	1.48	1.57
Sb	0.21	0.30	-	-	0.69	0.75	0.44	0.77	0.54
	GPT88-8B	GPT88-8A	PL-3	PL95-30	CB90-12A	CB90-6A	CGR91-18A	CGR91-18C	CB90-6B
(La/Yb)n	3.45	3.60	7.73	6.93	10.11	7.65	5.22	7.55	7.40
(La/Sm)n	1.31	1.62	2.36	2.27	2.36	2.43	2.38	2.33	2.48
(Gd/Yb)n	1.86	1.86	2.23	2.04	2.23	2.15	1.74	2.13	1.90
(La/Y)n	2.70	3.64	5.43	5.78	12.16	6.96	6.15	7.56	7.73
(Tb/Yb)n	1.57	1.76	1.70	1.78	1.45	1.60	1.52	1.63	1.37
(Th/Y)n	1.23	1.78	1.19	1.48	1.74	1.46	1.79	1.64	1.43
(Eu/Eu*)n	0.90	1.07	1.05	0.89	1.04	1.01	1.02	1.06	0.87
AL_2O_3/TiO_2	10	14	13	15	19	14	12	10	9
Zr/Hf	34	34	41	42	41	37	37	38	39
La/Nb	1.22	1.27	1.32	1.22	1.50	1.41	1.39	1.26	1.49
Th/Nb	0.12	0.13	0.10	0.12	0.12	0.12	0.14	0.13	0.12
Th/La	0.10	0.10	0.08	0.10	0.08	0.08	0.10	0.10	0.08
Zr/Y	3.73	4.50	5.31	6.03	11.55	6.46	6.20	7.80	6.95
Ti/Zr	121	97	76	70	60	77	67	86	91
Ti/Sm	2229	1990	1793	1694	1375	1790	1643	2119	2081
P/Nd	33	40	27	24	27	35	28	36	42
Ti/V	21	24	37	33	33	30	31	31	35
Sc/La	297	133	99	192	112	139	65	105	99
Nb/Nb*	0.80	0.67	0.68	0.71	0.60	0.62	0.57	0.69	0.58
Zr/Zr*	0.68	0.72	0.74	0.76	0.73	0.74	0.79	0.80	0.74
Hf/Hf*	0.72	0.76	0.65	0.66	0.65	0.72	0.77	0.76	0.69
Ti/Ti*	0.91	0.74	0.74	0.71	0.65	0.74	0.63	0.89	0.89
UTM Zone	15	15	16	16	15	15	15	15	15
Easting	706450	706450	293150	293163	702150	701450	706900	706900	701450
Northing	5720600	5720600	5724050	5723760	5712400	5711400	5712350	5712350	5711400

Northern Pickle assemblage

OIB-like

	CB90-6C	CB90-12B	CGR91-18B	GPT88-7A	GPT88-7B	CB90-12C	PL95-28	PL95-27
SiO_2	52.02	51.76	47.40	51.94	50.61	50.81	50.93	53.54
TiO_2	1.56	1.55	1.90	1.36	1.50	1.35	1.58	1.29
Al_2O_3	14.28	14.38	14.03	14.46	13.90	16.03	14.66	11.98
Fe_2O_3	16.58	18.57	18.01	14.57	16.25	15.93	15.56	13.66
MnO	0.20	0.25	0.29	0.22	0.18	0.17	0.22	0.17
MgO	4.32	4.80	4.59	3.53	3.69	3.58	3.09	2.52
CaO	5.69	5.97	10.38	7.91	10.34	7.45	8.51	11.12
K_2O	0.54	1.28	0.24	1.65	0.03	1.48	0.55	0.59
Na_2O	4.64	1.28	3.43	4.19	3.71	3.03	4.75	4.77
P_2O_5	0.17	0.16	0.13	0.18	0.16	0.15	0.15	0.15
LOI	2.88	8.99	10.68	11.48	10.49	8.58	12.35	12.23
Mg#	36	36	36	35	33	33	30	29
Ti	9476	9469	8898	7520	8447	7428	10084	7806
P	845	877	906	869	773	680	837	785
Cr	9	21	69	26	42	8	134	116
Co	56	73	59	45	59	59	54	41
Ni	32	57	62	54	68	77	44	47
Rb	13	38	6	42	1	26	13	16
Sr	354	374	474	361	512	206	555	471
Cs	9	19	0	1	0	1	1	0
Ba	236	587	61	352	18	235	160	190
Sc	26	20	22	30	22	25	40	34
V	265	233	313	195	185	222	280	206
Ta	0.68	0.77	0.68	0.84	0.84	0.65	0.77	0.78
Nb	12.97	13.09	11.39	12.35	15.64	11.23	15.17	14.28
Zr	107	117	105	136	150	106	134	120
Hf	2.40	3.08	2.76	3.80	3.25	2.47	3.07	2.81
Th	1.44	1.80	1.57	2.88	2.78	1.32	1.85	1.77
U	0.31	0.38	0.33	0.51	0.49	0.29	0.36	0.28
Y	21.23	13.22	20.49	13.29	20.48	11.33	15.79	14.94
La	17.39	19.36	16.95	21.80	22.27	15.05	17.70	14.97
Ce	40.65	44.20	36.38	43.74	50.29	36.89	40.14	33.76
Pr	5.16	5.48	5.02	5.68	5.90	4.44	4.63	3.99
Nd	21.15	24.08	21.81	23.30	24.87	19.07	22.27	17.90
Sm	4.63	4.82	4.56	4.69	5.47	4.32	4.82	4.05
Eu	1.37	1.49	1.44	1.39	1.49	1.12	1.35	1.26
Gd	4.29	4.15	5.06	4.30	4.67	3.20	3.85	4.19
Tb	0.64	0.50	0.87	0.61	0.62	0.41	0.53	0.49
Dy	3.77	2.72	4.13	2.81	3.91	2.24	2.86	2.49
Ho	0.78	0.46	0.96	0.64	0.73	0.42	0.53	0.53
Er	2.18	1.44	2.26	1.60	2.09	1.29	1.52	1.58
Tm	0.32	0.21	0.32	0.27	0.30	0.18	0.25	0.26
Yb	1.77	1.35	2.25	2.06	2.04	1.43	1.50	1.53
Lu	0.25	0.23	0.30	0.29	0.30	0.22	0.27	0.25
Cu	285	309	327	192	326	235	277	192
Zn	129	158	152	93	165	128	105	60
Mo	0.87	0.74	20.07	0.20	6.34	1.49	1.30	1.39
Ag	0.26	0.44	0.44	0.42	0.39	0.29	1.13	1.24
Tl	0.06	0.40	0.04	0.25	0.00	0.15	0.77	1.13
Pb	2.32	2.17	5.97	3.25	3.79	2.46	2.67	2.82
Sn	1.10	1.34	0.48	1.20	0.54	1.04	-	-
Sb	0.57	0.75	0.66	0.40	0.55	0.84	-	-
	CB90-6C	CB90-12B	CGR91-18B	GPT88-7A	GPT88-7B	CB90-12C	PL95-28	PL95-27
(La/Yb)n	7.04	10.27	5.41	7.58	7.82	7.53	8.45	7.01
(La/Sm)n	2.43	2.60	2.40	3.00	2.63	2.25	2.37	2.39
(Gd/Yb)n	2.00	2.54	1.86	1.73	1.89	1.85	2.12	2.27
(La/Y)n	5.43	9.70	5.48	10.87	7.20	8.79	7.43	6.64
(Tb/Yb)n	1.64	1.69	1.77	1.35	1.38	1.31	1.59	1.46
(Tb/Y)n	1.26	1.59	1.79	1.94	1.27	1.53	1.40	1.38
(Eu/Eu*)n	0.92	1.00	0.91	0.93	0.88	0.88	0.92	0.92
AL_2O_3/TiO_2	9	9	9	12	10	13	9	9
Zr/Hf	45	38	38	36	46	43	44	43
La/Nb	1.34	1.48	1.49	1.77	1.42	1.34	1.17	1.05
Th/Nb	0.11	0.14	0.14	0.23	0.18	0.12	0.12	0.12
Th/La	0.08	0.09	0.09	0.13	0.12	0.09	0.10	0.12
Zr/Y	5.03	8.88	5.14	10.21	7.35	9.36	8.49	8.00
Ti/Zr	89	81	85	55	56	70	75	65
Ti/Sm	2046	1966	1952	1603	1545	1719	2094	1927
P/Nd	40	36	42	37	31	36	38	44
Ti/V	36	41	28	39	46	33	36	38
Sc/La	104	89	73	69	74	115	152	137
Nb/Nb*	0.65	0.58	0.54	0.42	0.59	0.68	0.72	0.80
Zr/Zr*	0.75	0.75	0.73	0.90	0.89	0.81	0.90	0.97
Hf/Hf*	0.61	0.72	0.69	0.91	0.70	0.68	0.74	0.83
Ti/Ti*	0.84	0.84	0.73	0.66	0.66	0.79	0.93	0.75
UTM Zone	15	15	15	15	15	15	15	15
Easting	701450	702150	706900	706750	706750	702150	699125	699756
Northing	5711400	5712400	5712350	5720650	5720650	5712400	5711172	5711672

Appendix C

Data for 2.8-2.9 Ga Pickle Crow, Woman and Meen assemblages

Pickle Crow assemblage

	Komatiite				Tholeiites				
	KAF89-34B	KAF89-34A	PL95-23	KAF87-18A	PL95-37	PL-9	KAF89-34C	PL95-12B	KAF89-35B
SiO_2	45.85	50.31	49.29	49.27	49.58	50.32	47.96	49.66	51.01
TiO_2	0.66	0.46	0.61	0.62	0.57	0.71	0.65	0.64	1.09
Al_2O_3	4.77	11.93	14.92	14.84	17.11	15.55	15.85	15.18	14.16
Fe_2O_3	18.74	11.01	12.19	11.96	10.18	12.01	13.09	12.31	12.62
MnO	0.23	0.19	0.19	0.20	0.13	0.17	0.18	0.19	0.23
MgO	23.41	12.45	10.51	10.31	8.38	9.61	10.09	8.65	8.58
CaO	6.19	12.55	10.61	10.51	11.27	9.38	9.77	11.49	9.83
K_2O	0.00	0.11	0.05	0.29	0.20	1.01	0.11	0.11	0.91
Na_2O	0.09	0.97	1.58	1.97	2.54	1.20	2.24	1.71	2.50
P_2O_5	0.04	0.03	0.04	0.04	0.04	0.05	0.05	0.05	0.07
LOI	10.08	0.86	1.09	1.06	0.60	14.67	1.21	0.81	0.60
Mg#	73	71	65	65	64	64	63	61	60
Ti	3774	2641	3845	7643	3886	4946	3977	3518	6380
P	206	97	471	600	356	200	221	326	294
Cr	2658	385	565	316	431	551	375	452	419
Co	150	60	54	69	50	56	73	45	55
Ni	1406	89	209	116	134	159	252	134	97
Rb	0	2	2	10	5	33	1	1	23
Sr	35	66	74	90	191	72	168	117	109
Cs	0	0	1	2	3	2	0	0	5
Ba	2	15	27	43	33	202	52	20	242
Sc	27	72	67	46	56	43	37	74	58
V	197	280	318	252	215	275	243	298	367
Ta	0.21	0.12	0.09	0.13	0.16	0.08	0.12	0.09	0.21
Nb	3.10	1.03	1.48	1.61	1.90	1.57	1.80	1.59	2.90
Zr	99	23	32	54	33	35	37	34	58
Hf	1.11	0.70	1.01	1.08	1.02	1.17	1.06	1.13	1.64
Th	0.28	0.13	0.18	0.21	0.22	0.23	0.26	0.28	0.33
U	0.08	0.03	0.09	0.04	0.06	0.01	0.05	0.04	0.06
Y	9.10	11.58	16.26	14.46	11.58	10.98	14.78	17.23	21.70
La	2.63	1.38	1.50	1.46	2.24	1.70	2.61	1.81	2.94
Ce	7.27	3.72	4.24	4.30	5.50	4.61	6.72	4.66	8.49
Pr	1.05	0.55	0.61	0.68	0.72	0.70	0.99	0.64	1.33
Nd	5.33	3.00	3.59	3.76	4.38	3.73	4.95	3.97	7.20
Sm	1.73	1.11	1.33	1.38	1.42	1.22	1.65	1.46	2.63
Eu	0.50	0.39	0.50	0.58	0.63	0.41	0.68	0.60	0.96
Gd	1.87	1.49	1.95	2.10	1.96	1.80	2.21	1.95	3.45
Tb	0.29	0.29	0.37	0.36	0.33	0.30	0.39	0.40	0.61
Dy	1.77	2.09	2.59	2.45	1.89	2.03	2.72	2.52	4.17
Ho	0.37	0.44	0.58	0.56	0.44	0.44	0.62	0.59	0.89
Er	0.99	1.30	1.69	1.61	1.44	1.35	1.84	1.81	2.56
Tm	0.13	0.19	0.27	0.24	0.22	0.22	0.27	0.27	0.38
Yb	0.93	1.30	1.80	1.60	1.22	1.49	1.75	1.71	2.56
Lu	0.13	0.19	0.26	0.24	0.19	0.22	0.25	0.26	0.35
Cu	123	85	97	131	66	-	189	93	124
Zn	107	51	75	107	62	-	103	70	74
Mo	0.18	0.28	0.39	0.19	1.64	-	0.17	0.86	0.31
Ag	0.12	0.05	0.92	0.30	-	-	0.14	-	0.16
Tl	0.03	0.01	0.13	0.05	0.22	-	0.01	-	0.04
Pb	0.57	0.50	0.40	1.39	2.16	-	1.23	0.72	0.68
Se	0.40	0.44	-	0.57	0.71	-	0.54	0.55	0.53
Sb	0.10	0.10	-	0.15	-	-	0.12	-	0.30
	KAF89-34B	KAF89-34A	PL95-23	KAF87-18A	PL95-37	PL-9	KAF89-34C	PL95-12B	KAF89-35B
(La/Yb)n	2.04	0.76	0.59	0.65	1.32	0.82	1.07	0.76	0.82
(La/Sm)n	0.98	0.80	0.73	0.68	1.02	0.90	1.02	0.80	0.72
(Gd/Yb)n	1.67	0.95	0.89	1.09	1.33	1.00	1.04	0.94	1.12
(La/Y)n	1.92	0.79	0.61	0.67	1.28	1.02	1.17	0.69	0.90
(Tb/Yb)n	1.41	1.02	0.92	1.04	1.23	0.91	1.02	1.06	1.09
(Tb/Y)n	1.32	1.06	0.94	1.06	1.20	1.14	1.12	0.98	1.19
(Eu/Eu*)n	0.84	0.93	0.95	1.03	1.16	0.85	1.09	1.08	0.97
Al_2O_3/TiO_2	7	27	23	11	26	21	24	25	13
Zr/Hf	35	32	32	31	32	30	35	30	35
La/Nb	0.85	1.34	1.01	0.91	1.18	1.08	1.45	1.13	1.01
Th/Nb	0.09	0.13	0.12	0.13	0.12	0.15	0.15	0.17	0.11
Th/La	0.10	0.09	0.12	0.15	0.10	0.14	0.10	0.15	0.11
Zr/Y	4.33	1.95	1.97	2.34	2.81	3.22	2.53	1.97	2.67
Ti/Zr	96	117	120	225	119	129	106	104	110
Ti/Sm	2182	2380	2889	5519	2738	3741	2410	2402	2429
Pr/Nd	39	32	131	159	81	54	45	82	41
Ti/V	19	9	12	30	18	17	16	12	17
Sc/La	207	375	263	190	303	198	148	283	165
Nb/Nb*	1.21	0.75	1.04	1.22	0.77	0.94	0.66	0.85	1.06
Zr/Zr*	0.90	0.86	1.02	1.03	0.90	1.15	0.91	0.97	0.92
Hf/Hf*	0.92	0.96	1.16	1.19	1.02	1.38	0.93	1.17	0.95
Ti/Ti*	0.83	0.81	0.94	1.77	0.92	1.22	0.82	0.82	0.84
UTM Zone	16	16	15	16	15	15	16	15	16
Easting	297850	297850	704501	295700	701900	703100	297850	696881	293800
Northing	5712900	5712900	5709801	5712200	5699300	5708516	5712900	5703397	5710800

Pickle Crow assemblage

Tholeiites

	PL95-22	PL95-36	PL95-15	PL95-24	PL95-39	PL95-7	PL95-8	PL95-12C	PL-8A	PL95-14
SiO_2	52.21	49.35	48.94	48.89	49.03	48.15	48.09	49.65	49.94	47.72
TiO_2	1.02	0.83	0.69	0.67	1.22	0.89	0.90	0.80	0.82	0.99
Al_2O_3	15.55	15.98	15.46	15.17	14.25	15.33	15.00	15.00	14.84	15.64
Fe_2O_3	11.97	12.92	12.80	12.51	13.65	14.72	14.70	13.48	13.92	14.20
MnO	0.14	0.18	0.19	0.19	0.16	0.16	0.17	0.20	0.19	0.19
MgO	7.95	8.58	8.36	8.12	8.75	9.22	9.19	8.00	8.04	8.18
CaO	8.83	9.61	11.16	12.61	8.00	8.32	9.58	11.15	9.71	10.63
K_2O	0.00	0.48	0.18	0.15	1.22	0.18	0.17	0.09	0.10	0.14
Na_2O	2.23	2.00	2.16	1.64	3.62	2.95	2.12	1.57	2.34	2.15
P_2O_5	0.12	0.07	0.05	0.04	0.09	0.07	0.07	0.06	0.08	0.08
LOI	4.60	0.91	0.45	0.86	0.40	1.42	1.27	0.91	2.35	1.11
Mg#	59	59	59	59	59	58	58	57	56	56
Ti	6187	5364	4180	4115	7359	6489	5228	4528	4840	5263
P	708	367	309	468	492	0	110	182	357	346
Cr	397	270	250	486	304	253	299	343	277	343
Co	48	52	56	52	45	45	54	50	54	55
Ni	143	157	170	112	107	102	120	134	150	167
Rb	0	23	2	1	34	6	5	3	2	2
Sr	165	202	107	108	144	155	104	166	128	116
Cs	1	4	0	0	13	0	0	0	0	0
Ba	12	151	18	18	404	71	44	15	35	31
Sc	43	71	52	76	65	57	66	99	42	58
V	260	314	286	306	347	324	343	325	286	348
Ta	0.42	0.14	0.10	0.13	0.27	0.15	0.16	0.12	0.18	0.14
Nb	7.29	2.75	2.00	2.05	4.64	2.66	2.71	2.41	2.12	2.44
Zr	129	51	37	39	79	50	51	48	42	48
Hf	3.61	1.32	1.24	1.13	2.17	1.67	1.64	1.46	1.66	1.61
Th	0.98	0.29	0.21	0.29	0.55	0.25	0.39	0.42	0.26	0.26
U	0.26	0.10	0.02	0.11	0.15	0.13	0.13	0.06	0.08	0.05
Y	36.33	19.57	14.57	16.99	35.28	20.25	19.74	20.44	16.53	18.77
La	7.54	2.43	1.72	2.08	5.10	2.29	2.96	2.84	2.46	2.60
Ce	19.90	6.43	5.00	5.60	13.17	5.83	7.32	7.49	6.95	7.39
Pr	2.70	0.92	0.71	0.81	1.83	0.82	1.04	1.01	1.12	1.06
Nd	14.37	5.19	4.22	4.79	9.83	4.17	5.33	5.67	5.72	5.82
Sm	4.31	2.03	1.44	1.72	3.18	2.13	1.99	1.93	1.89	1.97
Eu	1.22	0.74	0.57	0.61	1.11	0.62	0.73	0.76	0.73	0.78
Gd	5.47	2.74	2.03	2.37	4.09	2.31	3.05	2.45	2.59	2.83
Tb	0.94	0.48	0.37	0.45	0.70	0.42	0.46	0.47	0.48	0.53
Dy	6.26	3.18	2.54	2.82	4.42	2.89	2.90	3.18	3.38	3.46
Ho	1.43	0.73	0.60	0.62	0.97	0.65	0.66	0.69	0.71	0.79
Er	4.14	1.99	1.67	1.91	2.76	2.00	2.07	2.07	2.15	2.30
Tm	0.61	0.29	0.24	0.27	0.43	0.30	0.31	0.32	0.31	0.34
Yb	4.14	2.02	1.52	1.84	2.44	1.73	1.85	1.97	2.10	2.05
Lu	0.63	0.30	0.24	0.28	0.40	0.27	0.25	0.31	0.27	0.31
Cu	80	118	135	83	74	26	86	145	-	155
Zn	90	77	83	79	64	75	89	86	-	92
Mo	0.84	1.09	0.48	0.26	1.06	0.83	1.37	0.89	-	0.98
Ag	1.16	-	0.66	1.01	-	-	-	-	-	0.55
Tl	0.08	0.30	-	0.10	0.11	0.05	-	0.01	-	0.00
Pb	1.68	1.75	1.51	0.82	0.52	0.43	0.41	0.97	-	0.94
Sn	-	0.60	-	-	0.78	0.56	0.63	0.63	-	-
Sb	-	-	-	-	-	-	-	-	-	-
	PL95-22	PL95-36	PL95-15	PL95-24	PL95-39	PL95-7	PL95-8	PL95-12C	PL-8A	PL95-14
(La/Yb)n	1.30	0.86	0.81	0.81	1.50	0.95	1.15	1.03	0.84	0.91
(La/Sm)n	1.13	0.77	0.77	0.78	1.04	0.69	0.96	0.95	0.84	0.85
(Gd/Yb)n	1.09	1.12	1.10	1.07	1.38	1.11	1.37	1.03	1.02	1.14
(La/Y)n	1.38	0.82	0.78	0.81	1.34	0.75	0.99	0.92	0.98	0.92
(Tb/Yb)n	1.03	1.08	1.10	1.12	1.29	1.11	1.12	1.08	1.04	1.17
(Tb/Y)n	1.09	1.02	1.07	1.11	1.15	0.87	0.97	0.97	1.22	1.18
(Eu/Eu*)n	0.77	0.96	1.02	0.93	0.94	0.85	0.91	1.07	1.00	1.02
Al_2O_3/TiO_2	15	18	22	22	12	20	17	20	18	18
Zr/Hf	36	38	30	35	37	30	31	33	26	30
La/Nb	1.03	0.88	0.86	1.01	1.10	0.86	1.09	1.18	1.16	1.06
Th/Nb	0.13	0.11	0.11	0.14	0.12	0.10	0.14	0.17	0.12	0.11
Th/La	0.13	0.12	0.12	0.14	0.11	0.11	0.13	0.15	0.10	0.10
Zr/Y	3.56	2.59	2.57	2.30	3.14	2.47	2.60	2.34	2.56	2.57
Ti/Zr	48	106	112	105	93	90	102	95	114	109
Ti/Sm	1434	2647	2903	2388	2314	2108	2629	2351	2556	2668
Pr/Nd	49	71	73	98	50	-4	21	67	62	59
Ti/V	24	17	15	13	21	14	15	14	17	15
Sc/La	69	237	219	270	164	207	264	187	159	185
Nb/Nb*	0.95	1.12	1.26	0.99	0.88	1.10	0.84	0.84	0.91	1.00
Zr/Zr*	1.14	1.08	1.05	0.94	0.98	1.16	1.09	1.00	0.89	0.98
Hf/Hf*	1.15	1.02	1.26	0.99	0.97	1.41	1.26	1.11	1.26	1.19
Ti/Ti*	0.50	0.90	0.97	0.81	0.81	0.80	0.84	0.83	0.86	0.88
UTM Zone	15	15	15	15	15	15	15	15	16	15
Easting	698146	702175	697156	694630	706877	692257	692287	696800	280950	696665
Northing	5708776	5699731	5696379	5672135	5711990	5702943	5702982	5703347	5707850	5703506

Pickle Crow assemblage

Tholeiites

	PL-8B	PL-14	KAF89-33A	KAF89-33C	PL95-12A	KAF89-33B	KAF87-15B	PL-10	PL95-16	PL95-6
SiO_2	46.26	52.11	47.17	50.88	47.35	50.93	53.16	49.30	48.45	48.83
TiO_2	1.08	0.85	1.08	1.11	0.62	0.83	0.80	0.85	0.92	0.83
Al_2O_3	18.65	14.71	16.24	16.79	15.90	14.01	16.09	15.36	16.25	14.62
Fe_2O_3	17.38	11.34	13.65	11.36	11.84	13.81	10.49	13.70	13.49	13.91
MnO	0.19	0.21	0.21	0.19	0.23	0.20	0.22	0.22	0.28	0.22
MgO	9.71	6.25	7.48	6.20	6.33	7.36	5.47	7.28	7.12	7.18
CaO	4.52	12.26	11.79	10.24	17.28	10.53	11.00	10.90	10.83	11.57
K_2O	0.44	0.12	0.33	0.31	0.09	0.16	0.24	0.05	0.28	0.36
Na_2O	1.67	2.07	1.99	2.84	0.71	2.11	2.36	2.28	2.30	2.42
P_2O_5	0.10	0.07	0.07	0.09	0.04	0.06	0.06	0.07	0.07	0.06
LOI	5.82	1.73	0.71	0.40	3.25	0.45	0.50	1.90	0.65	0.86
Mg#	55	55	55	55	54	54	54	54	54	53
Ti	6314	4862	6374	7992	3729	4150	5220	5086	5620	6146
P	416	311	160	995	456	237	335	317	410	341
Cr	358	448	250	314	481	37	128	306	434	288
Co	76	48	60	48	50	53	78	45	51	54
Ni	193	100	142	115	147	69	103	115	131	132
Rb	10	1	12	7	1	1	6	0	5	13
Sr	80	158	128	178	262	122	132	157	156	195
Cs	2	1	2	2	0	0	0	0	10	0
Ba	274	34	32	50	12	54	94	25	43	94
Sc	53	48	50	49	81	54	59	42	68	69
V	369	319	314	404	548	244	373	298	383	344
Ta	0.21	0.10	0.19	0.23	0.07	0.14	0.11	0.16	0.12	0.23
Nb	2.78	2.04	3.28	1.84	1.51	2.44	1.64	2.81	1.93	2.37
Zr	96	48	61	65	34	47	46	49	53	49
Hf	1.48	1.36	1.85	1.84	1.18	1.38	1.45	1.31	1.81	1.56
Th	0.33	0.35	0.29	0.55	0.32	0.29	0.23	0.32	0.36	0.33
U	0.23	0.07	0.07	0.14	0.05	0.06	0.08	0.06	0.06	0.16
Y	21.09	22.19	23.20	19.07	16.67	18.07	21.81	20.81	19.84	20.27
La	3.00	2.68	3.93	4.04	1.41	3.51	2.26	2.93	3.11	3.09
Ce	8.09	6.95	9.29	10.80	3.89	9.84	6.17	7.95	8.16	7.62
Pr	1.23	0.97	1.33	1.53	0.60	1.23	0.91	1.19	1.08	1.10
Nd	6.39	5.13	7.48	7.70	3.30	6.03	4.91	6.21	6.00	6.63
Sm	2.22	1.82	2.52	2.38	1.49	1.96	1.76	1.98	2.11	2.11
Eu	0.84	0.68	0.92	0.90	0.53	0.74	0.70	0.75	0.81	0.78
Gd	3.17	2.62	3.41	3.03	1.97	2.56	2.63	2.85	2.92	3.04
Tb	0.56	0.47	0.60	0.50	0.37	0.44	0.46	0.49	0.54	0.52
Dy	3.98	3.35	4.05	3.59	2.42	2.93	3.60	3.44	3.67	3.63
Ho	0.88	0.76	0.88	0.76	0.56	0.70	0.79	0.68	0.82	0.81
Er	2.71	2.18	2.63	2.16	1.74	2.06	2.32	1.97	2.29	2.39
Tm	0.39	0.34	0.37	0.32	0.27	0.28	0.36	0.31	0.35	0.36
Yb	2.64	2.13	2.47	2.18	1.63	2.02	2.20	2.05	2.30	2.34
Lu	0.37	0.32	0.35	0.31	0.26	0.27	0.33	0.30	0.34	0.33
Cu	-	-	113	130	87	169	154	-	50	54
Zn	-	-	91	106	73	68	128	-	110	93
Mo	-	-	1.24	1.40	1.11	1.36	0.55	-	0.57	1.39
Ag	-	-	0.12	0.30	-	0.09	0.11	-	0.45	-
Tl	-	-	0.03	0.07	0.04	-	0.03	-	0.02	0.04
Pb	-	-	1.31	2.33	1.10	0.92	0.75	-	1.48	1.05
Sn	-	-	0.68	0.57	0.59	0.55	0.63	-	-	1.18
Sb	-	-	0.14	0.15	-	0.15	0.04	-	-	-

	PL-8B	PL-14	KAF89-33A	KAF89-33C	PL95-12A	KAF89-33B	KAF87-15B	PL-10	PL95-16	PL95-6
(La/Yb)n	0.81	0.90	0.97	1.33	0.62	1.24	0.74	1.03	0.97	0.95
(La/Sm)n	0.87	0.95	0.86	1.10	0.61	1.16	0.83	0.95	0.95	0.95
(Gd/Yb)n	0.99	1.02	1.14	1.15	1.00	1.05	0.99	1.15	1.05	1.07
(La/Y)n	0.94	0.80	0.95	1.40	0.56	1.29	0.69	0.93	1.04	1.01
(Tb/Yb)n	0.97	1.00	1.11	1.05	1.04	0.99	0.95	1.08	1.08	1.01
(Tb/Y)n	1.12	0.89	1.09	1.11	0.94	1.03	0.89	0.99	1.15	1.08
(Eu/Eu*)n	0.96	0.95	0.96	1.03	0.94	1.01	1.00	0.96	1.00	0.94
AL_2O_3/TiO_2	18	18	15	13	25	20	18	24	17	14
Zr/Hf	37	36	33	35	29	34	32	37	29	31
La/Nb	1.08	1.31	1.02	1.05	0.93	1.44	1.38	1.04	1.61	1.31
Th/Nb	0.12	0.17	0.09	0.14	0.21	0.12	0.14	0.11	0.19	0.14
Th/La	0.11	0.13	0.09	0.14	0.23	0.08	0.10	0.11	0.12	0.11
Zr/Y	2.63	2.19	2.61	3.40	2.02	2.62	2.13	2.34	2.65	2.40
Ti/Zr	114	100	105	117	111	88	112	80	107	126
Ti/Sm	2840	2670	2531	3190	2501	2118	2968	1958	2662	2915
P/Nd	65	61	48	77	138	39	68	51	68	51
Ti/V	17	15	20	19	11	17	14	13	15	18
Sc/La	144	152	143	190	311	198	178	139	199	209
Nb/Nb*	0.94	0.74	1.02	0.95	1.10	0.65	0.74	0.97	0.61	0.70
Zr/Zr*	1.02	1.10	0.97	1.05	1.05	0.95	1.09	0.96	1.02	0.90
Hf/Hf*	0.99	1.12	1.07	1.08	1.33	1.01	1.24	0.94	1.28	1.05
Ti/Ti*	0.94	0.88	0.86	1.12	0.86	0.73	0.96	0.65	0.89	0.96
UTM Zone	16	15	16	16	15	16	16	Grab sample	15	15
Easting	280950	652950	294400	294400	696831	294400	292750		692964	692758
Northing	5707850	5689250	5711200	5711200	5703357	5711200	5708500		5688906	5703269

Pickle Crow assemblage

Tholeiites

	PL95-13	PL95-6	KAF87-15C	PL95-3	PL-6	KAF89-34D	PL-13B	KAF87-15A	PL-13A	PL95-4
SiO_2	47.36	47.08	49.18	61.06	49.78	49.76	46.02	51.11	50.40	61.20
TiO_2	0.87	0.89	1.19	1.10	0.87	1.16	0.87	1.01	0.89	1.01
Al_2O_3	15.48	15.69	14.49	17.99	18.21	14.38	13.73	13.29	14.50	19.32
Fe_2O_3	14.15	14.98	14.39	7.18	8.35	14.38	13.41	14.92	13.37	5.82
MnO	0.26	0.23	0.19	0.18	0.26	0.21	0.29	0.22	0.21	0.14
MgO	7.00	7.38	7.07	3.49	4.05	6.86	6.25	6.82	5.97	2.34
CaO	13.12	10.39	10.92	5.42	15.12	10.71	16.31	10.73	11.01	5.89
K_2O	0.19	0.40	0.15	0.22	0.52	0.05	0.36	0.10	0.20	0.71
Na_2O	1.51	2.89	2.32	3.89	2.74	2.41	2.69	1.73	3.38	3.51
P_2O_5	0.07	0.07	0.09	0.08	0.09	0.09	0.06	0.06	0.07	0.07
LOI	1.21	0.55	0.40	3.84	10.86	0.35	7.64	0.40	1.73	2.88
Mg#	52	52	52	52	52	51	51	50	50	47
Ti	5295	5050	7549	6364	5391	6789	4382	5804	4497	6251
P	358	313	493	320	387	365	282	232	311	319
Cr	351	326	167	221	310	157	267	476	279	277
Co	60	54	60	48	45	51	49	67	50	64
Ni	179	134	108	123	140	88	105	200	106	168
Rb	5	15	1	8	14	1	23	1	3	14
Sr	140	153	138	104	117	198	128	96	216	169
Cs	0	2	0	1	1	0	2	0	0	1
Ba	38	92	19	101	170	26	124	15	77	136
Sc	62	77	55	51	46	46	45	64	41	17
V	359	324	372	324	320	390	336	441	313	232
Ta	0.13	0.12	0.22	0.20	0.23	0.23	0.13	0.18	0.15	0.21
Nb	2.49	2.64	3.95	3.32	2.57	3.73	3.16	2.55	3.24	2.95
Zr	49	51	70	64	39	67	47	51	53	52
Hf	1.53	1.62	2.05	2.03	1.25	2.11	1.37	1.54	1.37	1.75
Th	0.25	0.26	0.43	0.41	0.33	0.43	0.32	0.37	0.33	0.70
U	0.05	0.05	0.10	0.14	0.10	0.09	0.09	0.08	0.07	0.22
Y	19.18	21.57	26.38	18.19	20.09	22.59	21.38	20.77	22.39	6.82
La	2.72	2.17	4.01	3.46	3.25	4.12	3.91	2.55	1.42	3.73
Ce	7.37	6.12	10.87	9.45	8.57	10.00	9.84	7.58	9.12	9.80
Pr	1.07	0.90	1.65	1.31	1.35	1.62	1.33	1.16	1.26	1.26
Nd	6.08	5.51	8.51	7.38	6.86	8.74	7.03	6.59	6.83	6.55
Sm	2.02	2.02	2.91	2.33	2.21	2.88	2.18	2.36	2.12	1.95
Eu	0.76	0.68	0.95	0.80	0.94	1.02	0.70	0.81	0.83	0.79
Gd	2.77	2.49	3.64	2.96	3.22	4.03	2.80	3.31	2.63	1.97
Tb	0.49	0.48	0.64	0.52	0.55	0.78	0.46	0.57	0.44	0.32
Dy	3.29	3.26	4.44	3.25	3.95	4.28	3.49	4.14	3.30	1.64
Ho	0.72	0.72	0.94	0.68	0.82	1.10	0.73	0.91	0.72	0.42
Er	2.04	2.07	2.87	2.01	2.46	2.82	2.22	2.69	2.19	0.91
Tm	0.35	0.33	0.43	0.28	0.38	0.42	0.31	0.39	0.32	0.16
Yb	2.00	1.98	2.75	1.63	2.49	3.23	2.10	2.55	2.16	0.93
Lu	0.31	0.31	0.40	0.20	0.34	0.44	0.30	0.37	0.33	0.13
Cu	155	43	123	139	-	116	-	83	-	171
Zn	101	87	100	67	-	91	-	83	-	72
Mo	0.66	0.89	0.64	0.76	-	0.36	-	0.27	-	1.04
Ag	0.69	-	0.10	-	-	0.08	-	0.12	-	-
Tl	0.06	0.23	0.02	0.23	-	0.02	-	-	-	0.51
Pb	0.68	0.70	0.63	1.23	-	0.62	-	0.70	-	2.72
Sn	-	0.66	0.67	0.65	-	0.58	-	0.44	-	0.92
Sb	-	-	0.02	-	-	0.06	-	0.09	-	-

	PL95-13	PL95-6	KAF87-15C	PL95-3	PL-6	KAF89-34D	PL-13B	KAF87-15A	PL-13A	PL95-4
(La/Yb)n	0.98	0.79	1.04	1.52	0.93	0.92	1.33	0.72	1.14	2.88
(La/Sm)n	0.87	0.69	0.89	0.96	0.95	0.93	1.16	0.70	1.04	1.24
(Gd/Yb)n	1.14	1.04	1.10	1.50	1.07	1.03	1.10	1.07	1.01	1.75
(La/Y)n	0.94	0.67	1.01	1.26	1.07	1.21	1.21	0.81	1.01	3.63
(Tb/Yb)n	1.11	1.11	1.06	1.46	1.01	1.10	1.00	1.02	0.92	1.58
(Tb/Y)n	1.07	0.94	1.02	1.21	1.16	1.45	0.91	1.16	0.82	1.99
(Eu/Eu*)n	0.99	0.92	0.89	0.93	1.08	0.92	0.86	0.89	1.08	1.23
Al_2O_3/TiO_2	17	18	11	16	20	15	19	20	19	18
Zr/Hf	32	32	34	31	31	32	34	33	38	30
La/Nb	1.09	0.82	1.02	1.04	1.26	1.10	1.23	1.00	1.06	1.26
Th/Nb	0.10	0.10	0.11	0.12	0.13	0.12	0.10	0.15	0.10	0.24
Th/La	0.09	0.12	0.11	0.12	0.10	0.10	0.08	0.15	0.10	0.19
Zr/Y	2.55	2.37	2.66	3.50	1.93	2.97	2.20	2.45	2.35	7.65
Ti/Zr	108	99	108	100	139	86	93	76	87	120
Ti/Sm	2617	2496	2593	2726	2445	2010	2006	1650	2172	3206
Pr/Nd	59	57	58	43	56	42	40	35	46	49
Ti/V	15	16	20	20	17	15	13	9	15	27
Sc/La	202	248	138	251	135	103	148	172	125	283
Nb/Nb*	0.92	1.32	1.00	0.98	0.78	0.82	0.76	1.11	0.94	0.77
Zr/Zr*	0.97	1.06	0.97	1.06	0.69	0.93	0.83	0.89	0.96	1.01
Hf/Hf*	1.09	1.22	1.03	1.23	0.81	9.05	0.88	0.98	0.91	1.23
Ti/Ti*	0.89	0.89	0.92	0.96	0.80	0.67	0.70	0.55	0.77	1.26
UTM Zone	15	15	16	15	16	16	15	16	15	15
Easting	696560	692614	292750	703559	281700	297850	696250	292750	696250	703866
Northing	5703755	5703212	5708500	5707967	5707550	5712900	5703750	5708500	5703730	5707269

Pickle Crow assemblage

Tholeiites

	PL95-11	PL95-1	KAF87-23B	PL95-35	PL-7	PL95-2	PL95-33
SiO_2	47.14	52.73	49.84	50.73	52.21	54.48	49.15
TiO_2	1.72	0.90	1.22	1.42	0.90	1.08	1.71
Al_2O_3	15.13	17.50	13.71	13.56	16.68	16.88	19.45
Fe_2O_3	16.26	9.48	16.78	16.17	11.37	10.51	7.17
MnO	0.26	0.26	0.24	0.22	0.27	0.29	0.19
MgO	6.31	3.64	6.20	5.78	3.66	3.15	1.39
CaO	10.43	12.10	9.35	10.05	12.35	10.12	6.18
K_2O	0.26	0.06	0.10	0.05	0.36	0.48	1.60
Na_2O	2.36	1.25	2.48	1.72	2.11	2.94	2.99
P_2O_5	0.13	0.06	0.08	0.11	0.09	0.09	0.16
LOI	1.06	0.28	0.35	0.91	0.34	0.05	1.63
Mg#	46	46	45	44	41	40	30
Ti	10928	9925	8121	8770	9205	9988	10162
P	422	359	998	981	378	353	466
Cr	221	376	15	164	218	248	243
Co	48	57	73	51	56	52	53
Ni	47	158	42	35	125	113	118
Rb	7	2	1	1	11	16	58
Sr	178	175	62	94	126	136	128
Cs	0	0	0	0	1	2	5
Ba	54	35	16	13	356	139	171
Sc	80	72	64	80	43	76	48
V	425	359	457	428	302	364	302
Ta	0.47	0.16	0.24	0.27	0.21	0.20	0.33
Nb	7.81	2.70	3.46	4.58	2.54	3.44	5.75
Zr	115	51	71	79	45	65	107
Hf	3.29	1.58	2.09	2.44	1.44	2.07	2.64
Th	1.10	0.37	0.46	0.70	0.35	0.44	0.70
U	0.35	0.16	0.13	0.18	0.07	0.12	0.21
Y	34.18	21.34	26.93	25.68	17.88	22.52	24.88
La	8.51	3.32	2.92	4.93	2.94	4.02	7.06
Ce	21.49	8.70	8.94	12.81	7.82	10.30	19.08
Pr	2.72	1.23	1.43	1.75	1.24	1.39	2.70
Nd	16.24	6.99	7.96	9.66	6.38	8.37	14.37
Sm	4.84	2.41	2.84	3.27	2.05	2.83	4.15
Eu	1.63	0.86	1.10	1.03	0.76	1.02	1.39
Gd	5.80	3.16	4.19	4.20	2.75	3.38	5.38
Tb	0.94	0.55	0.75	0.74	0.49	0.62	0.84
Dy	5.84	3.56	5.14	4.46	3.52	3.80	5.25
Ho	1.28	0.81	1.15	1.00	0.73	0.84	1.04
Er	3.77	2.40	3.30	2.91	2.16	2.47	3.06
Tm	0.54	0.37	0.49	0.46	0.34	0.35	0.43
Yb	3.19	2.10	3.21	2.72	2.21	1.96	3.03
Lu	0.46	0.28	0.47	0.41	0.31	0.31	0.33
Cu	97	159	93	71	-	140	13
Zn	117	70	78	75	-	79	51
Mo	1.18	0.87	0.21	1.02	-	1.00	35.34
Ag	-	-	0.15	-	-	-	0.00
Tl	0.10	0.17	0.01	0.11	-	0.06	1.24
Pb	1.36	4.05	0.49	0.42	-	0.79	2.78
Sn	0.72	0.67	0.40	0.66	-	0.51	0.89
Sb	-	-	0.21	-	-	-	0.00
	PL95-11	PL95-1	KAF87-23B	PL95-35	PL-7	PL95-2	PL95-33
$(La/Yb)_N$	1.91	1.13	0.65	1.30	0.95	1.47	1.67
$(La/Sm)_N$	1.14	0.89	0.66	0.97	0.93	0.92	1.10
$(Gd/Yb)_N$	1.50	1.24	1.08	1.28	1.03	1.43	1.47
(La/Yb	1.65	1.03	0.72	1.27	1.09	1.18	1.88
$(Tb/Yb)_N$	1.33	1.20	1.07	1.34	1.00	1.45	1.26
(Tb/Y	1.15	1.09	1.17	1.22	1.14	1.16	1.41
$(Eu/Eu^*)_N$	0.94	0.95	0.98	0.85	0.98	1.00	0.90
AL_2O_3/TiO_2	8	18	10	9	19	17	11
Zr/Hf	35	32	34	32	31	31	40
La/Nb	1.09	1.23	0.84	1.08	1.16	1.17	1.23
Th/Nb	0.14	0.14	0.13	0.15	0.14	0.13	0.12
Th/La	0.13	0.11	0.16	0.14	0.12	0.11	0.10
Zr/Y	3.36	2.38	2.63	3.08	2.52	2.87	4.30
Ti/Zr	95	117	115	111	115	93	95
Ti/Sm	2258	2463	2859	2678	2542	2116	2448
P/Nd	26	51	75	60	59	42	32
Ti/V	26	17	18	20	17	16	34
Sc/La	172	253	136	195	136	245	145
Nb/Nb^*	0.87	0.79	1.35	0.90	0.86	0.82	0.82
Zr/Zr^*	0.90	0.86	1.03	0.97	0.86	0.92	0.96
Hf/Hf^*	0.93	0.97	1.10	1.09	1.00	1.07	0.86
Ti/Ti^*	0.82	0.85	0.93	0.94	0.87	0.77	0.85
UTM Zone	15	15	16	15	16	15	15
Easting	697352	703750	299450	702800	281720	703520	705842
Northing	5704337	5709060	5713950	5700600	5707500	5707965	5710842

Pickle Crow assemblage

Calc alkaline

	PL95-9	KAF87-18B	KAF89-35C	PL-12	KAF87-21C	PL95-10	PL-11	KAF87-21B	KAF87-23A	KAF89-35A	KAF87-21A
SiO_2	50.83	53.10	53.44	52.45	52.69	53.19	53.21	54.89	55.81	56.06	55.85
TiO_2	0.85	0.56	0.52	0.85	0.58	0.72	0.73	0.65	0.64	0.90	1.16
Al_2O_3	13.10	15.29	15.33	13.95	16.23	12.21	11.80	15.13	14.98	14.63	13.40
Fe_2O_3	10.71	10.03	8.90	9.96	9.59	12.01	13.02	10.84	10.77	11.95	15.55
MnO	0.19	0.14	0.18	0.18	0.15	0.21	0.26	0.16	0.17	0.18	0.20
MgO	10.38	9.19	8.07	8.45	7.84	8.62	8.64	6.13	5.36	4.79	3.22
CaO	10.27	9.05	7.99	10.06	8.96	11.10	9.55	6.84	6.87	7.78	6.41
K_2O	0.58	0.54	2.54	0.39	0.84	0.20	1.05	0.61	0.71	0.65	1.27
Na_2O	2.66	2.04	2.98	3.24	3.05	1.66	1.67	2.65	2.70	2.96	2.80
P_2O_5	0.44	0.06	0.05	0.46	0.06	0.07	0.07	0.09	0.09	0.10	0.14
LOI	1.83	1.47	1.99	1.06	0.65	0.60	1.21	0.30	0.45	1.01	0.90
Mg#	68	67	67	65	64	61	59	55	52	47	31
Ti	5184	6661	9037	4981	3349	4690	4079	4009	3917	6126	6640
P	1981	501	247	2029	186	259	109	401	435	648	790
Cr	711	24	544	554	583	716	733	47	38	13	5
Co	49	68	48	41	46	56	50	55	44	54	60
Ni	176	56	109	116	121	147	135	74	59	39	8
Rb	24	23	113	13	26	4	34	14	21	18	45
Sr	619	191	122	640	203	219	203	190	236	236	224
Cs	2	2	2	1	2	0	0	2	1	1	1
Ba	353	107	621	241	167	98	331	157	219	141	328
Sc	44	39	34	27	32	41	35	39	40	39	37
V	253	212	176	199	212	288	218	232	190	266	424
Ta	0.37	0.22	0.20	0.47	0.19	0.26	0.27	0.25	0.25	0.30	0.39
Nb	7.52	3.38	2.66	7.86	2.58	4.55	4.08	3.84	4.08	4.42	5.99
Zr	114	58	54	111	58	61	70	77	89	98	129
Hf	3.23	1.50	1.32	2.89	1.75	1.68	1.77	1.93	2.25	2.84	3.63
Th	8.90	1.89	1.77	9.69	1.90	2.67	2.60	2.96	3.03	2.93	4.01
U	1.80	0.44	0.40	2.89	0.44	0.61	0.50	0.66	0.73	0.75	0.96
Y	17.45	13.29	11.15	16.99	11.73	18.37	16.43	17.03	17.64	20.25	23.15
La	41.20	6.64	7.55	43.46	6.66	10.05	9.90	10.96	11.64	11.24	17.52
Ce	82.04	14.93	15.49	87.43	13.15	20.51	20.09	22.80	24.05	23.56	32.41
Pr	8.58	1.79	1.77	10.09	1.68	2.28	2.38	2.52	2.60	2.70	3.98
Nd	35.46	7.59	7.18	37.43	7.03	10.05	9.86	9.92	10.44	11.53	16.30
Sm	6.18	1.92	1.69	6.48	1.82	2.50	2.66	2.30	2.29	2.79	3.53
Eu	1.72	0.63	0.64	1.72	0.68	0.76	0.88	0.71	0.69	0.91	1.13
Gd	5.34	2.14	1.90	5.13	2.31	3.17	3.10	2.59	2.83	3.45	4.26
Tb	0.61	0.35	0.33	0.62	0.46	0.47	0.48	0.43	0.42	0.55	0.80
Dy	3.41	2.28	2.15	3.63	2.40	2.94	3.12	2.97	2.78	3.74	4.30
Ho	0.66	0.50	0.44	0.68	0.56	0.72	0.61	0.64	0.61	0.78	1.09
Er	1.76	1.37	1.28	1.90	1.43	1.80	1.86	1.84	1.77	2.18	2.89
Tm	0.25	0.21	0.19	0.27	0.22	0.30	0.25	0.27	0.26	0.32	0.42
Yb	1.55	1.44	1.31	1.76	1.73	1.60	1.72	1.75	1.67	2.10	3.35
Lu	0.22	0.21	0.18	0.25	0.23	0.25	0.25	0.25	0.22	0.31	0.45
Cu	61	180	78	-	88	112	-	71	70	52	55
Zn	85	87	130	-	75	88	-	85	73	90	121
Mo	0.49	0.53	2.79	-	0.13	0.98	-	0.55	0.78	1.10	0.37
Ag	0.62	0.15	0.30	-	0.21	-	-	0.24	0.11	0.31	0.37
Tl	0.18	0.18	0.62	-	0.19	0.07	-	0.06	0.09	0.14	0.30
Pb	6.91	4.21	2.69	-	3.41	4.43	-	4.25	4.96	2.15	7.67
Sn	-	0.47	0.37	-	0.54	0.65	-	0.67	0.65	0.54	2.98
Sb	-	0.23	0.06	-	0.30	-	-	0.22	0.11	0.30	0.93
	PL95-9	KAF87-18B	KAF89-35C	PL-12	KAF87-21C	PL95-10	PL-11	KAF87-21B	KAF87-23A	KAF89-35A	KAF87-21A
(La/Yb)n	19.01	3.30	4.15	17.72	2.76	4.52	4.12	4.50	5.01	3.84	3.75
(La/Sm)n	4.31	2.24	2.88	4.33	2.36	2.59	2.40	3.08	3.28	2.61	3.21
(Gd/Yb)n	2.84	1.23	1.20	2.41	1.10	1.64	1.49	1.23	1.40	1.36	1.05
(La/Y)n	15.64	3.31	4.48	16.94	3.76	3.62	3.99	4.26	4.37	3.68	5.01
(Tb/Yb)n	1.80	1.09	1.14	1.59	1.22	1.34	1.26	1.12	1.15	1.18	1.09
(Tb/Y)n	1.48	1.09	1.23	1.52	1.66	1.07	1.22	1.06	1.00	1.13	1.46
(Eu/Eu*)n	0.90	0.95	1.09	0.88	1.02	0.82	0.94	0.89	0.83	0.90	0.89
Al_2O_3/TiO_2	15	14	29	17	28	16	17	22	26	14	12
Zr/Hf	35	39	41	38	33	37	39	40	40	35	35
La/Nb	5.48	1.96	2.84	5.53	2.59	2.21	2.43	2.85	2.85	2.55	2.92
Th/Nb	1.18	0.56	0.66	1.23	0.74	0.59	0.64	0.77	0.74	0.66	0.67
Th/La	0.22	0.28	0.23	0.22	0.29	0.27	0.26	0.27	0.26	0.26	0.23
Zr/Y	6.51	4.38	4.86	6.54	4.92	3.34	4.25	4.54	5.06	4.85	5.56
Ti/Zr	46	115	56	45	58	76	58	52	37	62	52
Ti/Sm	839	3472	1793	769	1838	1873	1532	1745	1448	2197	1882
Pr/Nd	56	66	34	54	55	26	31	40	42	56	48
Ti/V	20	31	17	25	16	16	19	17	17	23	16
Sc/La	195	183	187	108	137	326	138	156	180	126	83
Nb/Nb*	0.14	0.43	0.27	0.14	0.28	0.34	0.31	0.27	0.27	0.31	0.34
Zr/Zr*	0.53	1.05	1.08	0.49	1.12	0.85	0.94	1.12	1.26	1.20	1.18
Hf/Hf*	0.55	0.99	0.95	0.47	1.23	0.84	0.87	1.01	1.15	1.26	1.20
Ti/Ti*	0.36	1.30	0.67	0.34	0.65	0.66	0.56	0.65	0.52	0.78	0.68
UTM Zone	15	16	16	16	16	15	16	16	16	16	16
Easting	698955	295700	293800	279500	296500	697072	279800	296500	299450	293800	296500
Northing	5704224	571200	5710800	5703450	5712950	5704606	5703800	5712950	5713950	5710800	5712950

	Pickle Crow assemblage		Woman assemblage			
	Felsic		Red Lake belt			
	KAF89-35D	PL95-34	RL95-34	RL95-36	RL95-35	RL95-37
SiO_2	78.34	64.20	61.75	68.40	70.71	70.84
TiO_2	0.04	0.03	0.71	0.37	0.44	0.41
Al_2O_3	13.89	0.35	17.38	14.99	14.89	15.30
Fe_2O_3	0.75	31.11	6.25	3.70	3.78	3.40
MnO	0.03	0.27	0.09	0.09	0.07	0.05
MgO	0.20	2.53	2.62	1.46	1.00	0.80
CaO	1.10	1.41	4.17	5.90	4.00	3.32
K_2O	2.29	0.00	1.93	1.73	2.08	2.59
Na_2O	3.34	0.05	4.95	3.28	2.92	3.21
P_2O_5	0.02	0.06	0.14	0.08	0.10	0.09
LOI	1.11	0.00	0.91	2.30	0.96	0.86
Mg#	38	15	48	46	37	34
Ti	174	136	4425	2368	2905	2125
P	0	196	665	445	533	361
Cr	4	312	22	110	56	41
Co	1	10	23	12	14	6
Ni	2	8	20	41	27	19
Rb	71	0	110	61	80	84
Sr	61	5	576	417	352	293
Cs	1	0	11	6	5	6
Ba	568	2	371	550	448	503
Sc	2	15	13	10	8	6
V	6	7	109	62	58	38
Ta	0.53	0.02	0.32	0.53	0.66	0.64
Nb	5.71	0.25	4.30	5.43	7.06	6.21
Zr	37	6	118	138	137	120
Hf	2.19	0.10	3.06	3.46	3.68	2.93
Th	4.10	0.23	1.53	8.90	10.79	10.57
U	2.84	0.18	0.93	2.62	3.17	2.63
Y	5.50	5.49	13.10	14.94	11.87	9.53
La	4.26	1.37	22.62	23.77	26.02	25.99
Ce	8.50	2.07	49.20	46.04	50.63	50.64
Pr	1.01	0.24	5.72	4.75	5.09	5.06
Nd	4.10	1.18	22.39	16.46	17.88	17.40
Sm	1.37	0.29	3.96	3.03	3.09	2.99
Eu	0.23	0.22	1.19	0.84	0.83	0.80
Gd	1.34	0.48	3.26	2.67	2.58	2.30
Tb	0.19	0.07	0.41	0.38	0.34	0.28
Dy	1.08	0.66	2.34	2.29	2.06	1.76
Ho	0.21	0.13	0.45	0.48	0.40	0.33
Er	0.56	0.46	1.27	1.47	1.09	0.95
Tm	0.08	0.08	0.18	0.24	0.18	0.14
Yb	0.50	0.46	1.08	1.56	1.11	0.97
Lu	0.07	0.06	0.18	0.25	0.15	0.14
Cu	2	295	8	31	11	19
Zn	37	259	89	68	67	50
Mo	12.10	1.18	0.16	1.60	1.28	0.84
Ag	0.10	-	0.73	1.11	0.96	0.95
Tl	0.39	0.05	0.75	0.41	0.51	0.59
Pb	6.37	0.29	5.62	18.23	10.76	13.47
Sn	0.88	0.72	0.59	0.88	0.65	0.92
Sb	0.11	-	0.41	0.49	0.49	0.48
	KAF89-35D	PL95-34	RL95-34	RL95-36	RL95-35	RL95-37
(La/Yb)n	6.16	2.12	15.02	10.96	16.80	19.25
(La/Sm)n	2.01	3.04	3.69	5.07	5.44	5.62
(Gd/Yb)n	2.24	0.87	2.50	1.42	1.92	1.96
(La/Y)n	5.13	1.65	11.44	10.54	14.52	18.06
(Tb/Yb)n	1.76	0.68	1.74	1.11	1.40	1.33
(Tb/Y)n	1.47	0.53	1.33	1.06	1.21	1.24
(Eu/Eu*)n	0.52	1.82	0.98	0.88	0.87	0.89
AL_2O_3/TiO_2	474	15	23	37	31	42
Zr/Hf	17	65	39	40	37	41
La/Nb	0.75	5.50	5.26	4.37	3.69	4.18
Th/Nb	0.72	0.91	0.82	1.64	1.53	1.70
Th/La	0.96	0.17	0.16	0.37	0.41	0.41
Zr/Y	6.81	1.18	9.01	9.22	11.55	12.63
Ti/Zr	5	21	38	17	21	18
Ti/Sm	128	466	1119	782	940	712
P/Nd	0	165	30	27	30	21
Ti/V	31	20	41	38	50	56
Sc/La	34	343	70	41	51	39
Nb/Nb*	1.00	0.10	0.15	0.17	0.20	0.17
Zr/Zr*	1.10	0.76	0.87	1.35	1.28	1.16
Hf/Hf*	2.33	0.43	0.82	1.23	1.24	1.02
Ti/Ti*	0.05	0.14	0.49	0.33	0.41	0.32
UTM Zone	16	15	15	15	15	15
Easting	293800	706233	437584	438243	437896	438719
Northing	5710800	5711502	5657296	5657715	5657624	5658016

	Mafic							Intermediate		
	MLBB-11	MLBB-10	MLBB-05	SB95-38	SB95-42	SB95-32	MLBB-07	SB95-39	SB95-41	MLBB-08
SiO_2	50.56	48.00	49.47	49.21	51.99	47.53	49.29	57.10	57.62	60.67
TiO_2	0.69	1.11	0.92	1.03	0.71	1.33	1.02	0.96	0.62	0.60
Al_2O_3	11.99	17.19	15.61	15.18	15.70	15.74	14.18	17.00	17.45	15.22
Fe_2O_3	12.45	14.38	14.03	14.84	12.31	15.23	15.40	10.66	9.76	6.62
MnO	0.21	0.19	0.23	0.17	0.24	0.28	0.24	0.12	0.13	0.18
MgO	13.43	8.05	7.67	8.09	6.67	7.21	7.01	2.78	6.25	4.20
CaO	8.38	10.76	8.58	9.17	10.61	10.32	10.10	2.13	2.60	4.54
K_2O	0.40	0.00	0.05	0.08	0.00	0.26	0.35	0.83	0.34	2.10
Na_2O	2.24	0.22	3.27	2.15	1.72	1.98	2.34	3.22	3.11	3.75
P_2O_5	0.25	0.11	0.07	0.08	0.05	0.13	0.07	0.19	0.15	0.12
LOI	0.16	0.73	3.47	11.85	5.04	0.40	11.11	5.77	4.77	10.86
Mg#	70	55	55	55	54	51	50	62	58	58
Tl	9979	6316	4872	6205	4824	8114	5828	4567	9649	3387
P	1393	683	570	422	310	760	483	822	726	546
Cr	1183	204	244	258	452	176	275	272	122	26
Co	65	76	56	64	70	74	61	42	40	23
Ni	172	193	131	134	159	207	74	85	96	30
Rb	9	1	1	2	0	3	8	24	11	71
Sr	101	176	291	200	283	108	222	83	136	117
Cs	1	0	0	0	0	0	1	2	0	2
Ba	176	5	32	21	22	51	79	166	114	236
Sc	32	41	36	40	48	39	46	26	16	12
V	241	289	278	322	337	225	373	179	151	85
Ta	0.32	0.27	0.22	0.19	0.09	0.41	0.21	0.38	0.58	0.74
Nb	5.89	3.92	3.49	3.34	1.37	5.89	3.31	8.08	8.42	9.22
Zr	77	74	58	64	44	112	52	161	164	190
Hf	2.24	2.07	1.71	1.72	1.26	2.59	1.57	3.21	3.75	5.19
Th	2.98	1.21	0.85	0.40	0.33	1.85	0.49	3.66	7.15	10.38
U	0.95	0.28	0.20	0.10	0.07	0.40	0.11	0.73	1.69	2.58
Y	16.93	20.12	18.66	22.24	18.14	28.68	21.32	16.57	18.18	24.57
La	7.93	6.18	5.04	4.01	2.00	4.97	4.10	17.96	15.57	31.60
Ce	17.39	13.70	12.32	10.81	5.38	14.21	9.85	43.07	36.35	58.12
Pr	2.45	2.02	1.74	1.52	0.78	2.17	1.57	5.10	4.12	6.79
Nd	11.29	9.61	8.10	7.74	4.18	10.00	7.65	20.16	15.52	25.10
Sm	2.95	2.54	2.44	2.35	1.50	3.26	2.51	3.80	3.11	4.69
Eu	0.84	0.97	0.85	0.76	0.66	0.97	0.92	1.07	0.87	1.19
Gd	3.01	3.32	3.23	3.13	2.41	4.34	3.11	3.14	3.19	4.39
Tb	0.48	0.51	0.55	0.50	0.42	0.70	0.52	0.51	0.49	0.64
Dy	2.88	3.55	3.75	3.70	3.10	4.93	3.94	3.05	2.97	4.37
Ho	0.65	0.80	0.86	0.83	0.68	1.08	0.82	0.66	0.64	0.90
Er	1.79	2.28	2.43	2.44	1.94	3.12	2.49	1.80	1.81	2.55
Tm	0.27	0.37	0.37	0.39	0.28	0.49	0.38	0.31	0.27	0.38
Yb	1.76	2.34	2.42	2.47	1.89	3.02	2.42	1.79	1.84	2.33
Lu	0.24	0.35	0.36	0.36	0.27	0.43	0.38	0.28	0.26	0.37
Cu	38	185	100	177	130	264	157	53	68	8
Zn	75	92	113	104	108	130	101	88	79	74
Mo	0.13	0.20	0.51	0.46	17.93	6.33	0.10	0.56	0.43	0.09
Ag	0.23	0.20	0.19	0.58	0.28	0.69	0.20	0.68	0.96	0.51
Tl	0.06	0.00	0.01	-	-	-	0.04	0.05	0.03	0.29
Pb	1.26	2.51	4.97	3.50	1.15	3.70	2.78	2.01	4.45	8.84
Sn	0.39	0.60	0.51	0.44	0.57	0.97	0.59	0.80	1.14	1.42
Sb	2.38	7.98	1.07	2.35	2.75	0.16	1.95	2.83	1.55	0.36
	MLBB-11	MLBB-10	MLBB-05	SB95-38	SB95-42	SB95-32	MLBB-07	SB95-39	SB95-41	MLBB-08
(La/Yb)n	3.22	1.90	1.49	1.16	0.76	1.18	1.21	7.20	6.05	9.74
(La/Sm)n	1.73	1.57	1.33	1.10	0.86	0.98	1.05	3.05	3.23	4.36
(Gd/Yb)n	1.41	1.17	1.10	1.05	1.05	1.19	1.06	1.45	1.43	1.56
(La/Y)n	3.10	2.04	1.79	1.20	0.73	1.15	1.27	7.18	5.67	8.52
(Tb/Yb)n	1.23	1.00	1.03	0.93	1.01	1.06	0.98	1.29	1.21	1.26
(Tb/Y)n	1.19	1.07	1.23	0.95	0.97	1.03	1.03	1.29	1.14	1.10
(Eu/Eu*)n	0.85	1.02	0.92	0.86	1.06	0.79	1.01	0.92	0.84	0.79
AL_2O/TiO_2	17	16	19	15	19	11	15	22	26	27
Zr/Hf	34	36	34	37	35	43	33	50	44	37
La/Nb	2.04	1.58	1.45	1.20	1.46	0.84	1.24	2.22	1.85	3.43
Th/Nb	0.77	0.31	0.24	0.12	0.24	0.31	0.15	0.45	0.85	1.13
Th/La	0.38	0.20	0.17	0.10	0.16	0.37	0.12	0.20	0.46	0.33
Zr/Y	4.53	3.70	3.09	2.86	2.45	3.89	2.44	9.70	9.01	7.74
Ti/Zr	52	85	85	98	109	73	112	28	24	18
Ti/Sm	1347	2485	1904	2643	3210	3486	2322	1202	1269	723
Pr/Nd	123	71	70	55	74	76	63	41	47	22
Ti/V	16	22	18	19	14	36	16	26	26	40
Sc/La	131	117	100	111	175	89	123	94	61	34
Nb/Nb*	0.40	0.52	0.63	0.84	0.69	1.26	0.72	0.40	0.47	0.20
Zr/Zr*	0.92	1.04	0.90	1.03	1.23	1.35	0.82	1.27	1.63	1.21
Hf/Hf*	0.97	1.05	0.96	1.01	1.26	1.14	0.90	0.92	1.35	1.20
Ti/Ti*	0.53	0.86	0.69	0.91	1.00	0.85	0.83	0.52	0.50	0.30
UTM Zone	15	15	15	15	15	15	15	15	15	15
Easting	512450	513450	512300	517377	516552	514110	514150	516927	516088	515300
Northing	5678850	5678900	5676750	5669218	5675993	5661561	5677900	5673644	5676701	5677050

Birch-Uchi belt - Woman assemblage

	Intermediate						Felsic
	SB95-36	SB95-33	MLB8-15	SB95-37	SB95-40	MLB8-16	MLB7-02
SiO_2	[illegible]	59.15	58.10	61.99	54.19	53.62	74.82
TiO_2	[illegible]	0.84	0.65	0.89	0.87	2.11	0.31
Al_2O_3	16.78	17.81	15.64	17.11	18.31	12.13	13.72
Fe_2O_3	10.87	5.77	8.18	6.38	11.05	18.73	2.71
MnO	0.14	0.08	0.15	0.09	0.21	0.24	0.05
MgO	5.70	2.79	3.71	3.18	4.01	3.21	1.42
CaO	5.62	5.65	7.07	3.07	6.22	6.05	1.43
K_2O	3.23	5.18	1.85	2.46	3.33	0.24	4.96
Na_2O	1.00	2.51	4.41	2.57	1.61	3.03	0.14
P_2O_5	0.26	0.21	0.23	0.26	0.21	0.63	0.04
LOI	2.72	5.49	5.49	4.77	3.58	6.10	4.77
Mg#	54	52	50	46	44	27	54
Ti	3811	4488	3838	4403	4950	12815	1622
P	843	791	1309	992	911	2754	106
Cr	244	29	40	128	143	6	3
Co	42	21	32	29	38	39	5
Ni	235	52	23	93	117	8	5
Rb	121	110	37	73	50	6	105
Sr	97	163	847	57	180	158	39
Cs	9	3	2	2	2	0	4
Ba	575	992	555	371	250	92	682
Sc	19	14	19	16	20	36	6
V	161	131	169	135	161	100	3
Ta	0.67	0.62	0.36	0.74	0.49	0.62	1.24
Nb	9.30	8.10	6.04	9.60	7.71	10.24	15.73
Zr	177	171	131	201	131	293	515
Hf	4.23	4.27	3.28	5.06	3.35	5.75	8.47
Th	6.64	7.56	7.44	10.17	3.82	1.77	16.20
U	1.50	1.87	1.45	2.06	0.79	0.45	3.70
Y	17.78	19.16	14.46	20.18	12.06	53.59	34.51
La	30.90	31.50	27.42	25.81	17.96	15.24	50.99
Ce	64.33	64.20	54.17	57.37	40.83	35.36	98.56
Pr	7.34	7.21	5.94	6.63	4.67	5.42	11.98
Nd	27.74	27.92	21.81	25.10	18.04	26.23	42.56
Sm	5.05	5.38	4.25	4.82	3.48	7.62	7.61
Eu	1.43	1.42	1.32	1.08	1.14	2.80	1.48
Gd	4.16	4.48	3.64	3.82	3.21	9.58	6.15
Tb	0.54	0.65	0.42	0.53	0.42	1.44	0.86
Dy	3.39	3.96	2.60	3.51	2.46	10.46	5.89
Ho	0.66	0.76	0.52	0.73	0.48	2.05	1.18
Er	1.75	2.19	1.44	1.99	1.31	6.17	3.43
Tm	0.27	0.31	0.22	0.32	0.21	0.94	0.53
Yb	1.62	2.07	1.27	2.07	1.28	6.36	3.40
Lu	0.26	0.32	0.20	0.32	0.19	0.94	0.56
Cu	81	29	47	77	41	38	5
Zn	88	90	82	101	87	178	57
Mo	9.46	0.71	1.64	0.50	0.57	7.99	0.31
Ag	0.44	0.69	0.43	0.77	0.77	0.54	0.89
Tl	0.83	0.47	0.27	0.30	0.17	0.04	0.28
Pb	6.19	10.47	23.86	5.95	4.27	2.12	10.07
Se	1.02	1.46	1.13	1.21	1.02	1.36	2.03
Sb	0.17	0.12	1.79	0.31	3.22	1.20	2.25
	SB95-36	SB95-33	MLB8-15	SB95-37	SB95-40	MLB8-16	MLB7-02
(La/Yb)n	13.65	10.92	15.52	8.92	10.02	1.72	10.77
(La/Sm)n	3.95	3.78	4.16	3.46	3.33	1.29	4.33
(Gd/Yb)n	2.12	1.79	2.38	1.52	2.07	1.25	1.50
(La/Y)n	11.51	10.89	12.56	8.47	9.86	1.88	9.79
(Tb/Yb)n	1.52	1.44	1.52	1.17	1.50	1.03	1.15
(Tb/Y)n	1.29	1.43	1.23	1.11	1.48	1.13	1.05
(Eu/Eu*)n	0.92	0.86	1.00	0.74	1.02	1.00	0.64
Al_2O_3/TiO_2	26	24	24	23	22	6	50
Zr/Hf	42	40	40	40	39	35	37
La/Nb	3.32	3.89	4.54	2.69	2.33	1.49	3.24
Th/Nb	0.71	0.93	1.23	1.06	0.50	0.17	1.03
Th/La	0.21	0.24	0.27	0.39	0.21	0.12	0.32
Zr/Y	9.95	8.92	9.06	9.98	10.89	3.79	9.11
Ti/Zr	22	26	29	22	38	63	5
Ti/Sm	754	834	902	914	1422	1682	213
P/Nd	30	28	60	40	51	105	2
Ti/V	24	34	23	33	31	128	496
Sc/La	75	44	97	50	105	38	11
Nb/Nb*	0.23	0.20	0.16	0.31	0.36	0.58	0.22
Zr/Zr*	1.03	0.97	0.94	1.27	1.15	0.99	1.21
Hf/Hf*	0.90	0.87	0.86	1.15	1.06	1.02	1.18
Ti/Ti*	0.33	0.36	0.39	0.41	0.59	0.59	0.09
UTM Zone	15	15	15	15	15	[illegible]	15
Easting	516993	515791	514000	516149	516173	[illegible]	515900
Northing	5666341	5662422	5679400	5667818	5675198	5678750	5675350

Meen-Dempster belt - Woman assemblage

	84GRS-1166	84GRS-0047	84GRS-0075	84GRS-1283	84GRS-1056	84GRS-1225	82GRS-0835	82GRS-1582	82GRS-0139
SiO_2	53.68	55.12	55.59	55.06	56.00	55.31	47.51	49.94	52.84
TiO_2	0.68	0.88	1.26	1.19	1.93	0.92	0.74	0.64	1.08
Al_2O_3	17.21	16.63	18.18	16.52	16.49	17.18	16.01	15.06	15.38
Fe_2O_3	2.47	2.39	2.43	3.33	4.15	3.51	11.62	11.93	12.97
MnO	0.18	0.19	0.21	0.22	0.24	0.25	0.18	0.21	0.17
MgO	10.31	9.44	8.45	8.73	7.55	6.36	8.48	6.80	5.02
CaO	13.63	13.55	10.64	11.30	10.42	14.34	13.66	13.55	10.35
K_2O	0.12	0.07	0.13	0.29	0.21	0.18	0.19	0.27	0.21
Na_2O	1.73	1.70	3.01	3.26	2.86	1.91	1.55	1.57	1.87
P_2O_5	0.02	0.03	0.08	0.10	0.15	0.03	0.04	0.02	0.12
LOI	1.21	1.01	1.42	1.01	2.04	2.78	0.40	0.50	0.81
Mg#	90	90	88	85	80	80	62	56	46
Ti	4149	4087	7079	5530	11435	5230	4234	4007	6433
P	221	222	408	333	765	274	283	195	527
Cr	410	289	197	196	227	268	358	194	240
Co	61	57	64	55	66	63	50	61	53
Ni	189	162	112	109	87	157	133	135	106
Rb	2	1	2	7	5	1	3	5	2
Sr	105	81	243	248	149	150	135	130	123
Cs	0	0	0	0	1	0	0	0	0
Ba	45	23	116	48	47	42	39	47	53
Sc	39	40	49	38	53	43	34	42	34
V	233	256	355	284	441	283	211	243	250
Ta	0.14	0.13	0.21	0.13	0.32	0.13	0.18	0.11	0.37
Nb	2.16	1.76	3.05	3.07	5.44	2.43	2.57	1.65	6.45
Zr	84	82	98	97	93	48	56	51	119
Hf	0.94	0.87	1.56	1.53	2.51	1.40	1.00	0.85	3.06
Th	0.25	0.26	0.42	0.32	0.75	0.28	0.46	0.23	0.88
U	0.17	0.04	0.09	0.08	0.16	0.06	0.07	0.05	0.22
Y	14.84	15.01	21.67	23.03	33.29	20.01	17.07	14.23	34.66
La	2.00	1.83	3.46	2.32	6.68	2.69	1.75	1.91	7.62
Ce	5.19	4.98	9.22	7.28	17.23	6.89	8.87	4.89	18.99
Pr	0.77	0.77	1.41	1.21	2.63	1.10	1.29	0.78	2.85
Nd	4.01	3.95	6.70	6.59	12.95	5.55	6.20	4.01	13.22
Sm	1.39	1.47	2.16	2.34	4.12	1.88	1.81	1.43	3.94
Eu	0.56	0.59	0.79	0.84	1.23	0.70	0.64	0.51	1.17
Gd	1.81	1.97	2.84	3.09	4.95	2.60	2.28	1.87	5.06
Tb	0.34	0.37	0.53	0.57	0.89	0.47	0.42	0.35	0.88
Dy	2.44	2.58	3.63	3.90	5.91	3.16	2.88	2.30	6.23
Ho	0.53	0.58	0.80	0.86	1.29	0.73	0.61	0.52	1.35
Er	1.46	1.66	2.31	2.49	3.76	2.12	1.81	1.43	3.85
Tm	0.23	0.25	0.36	0.38	0.54	0.32	0.27	0.23	0.59
Yb	1.53	1.65	2.25	2.51	3.37	2.06	1.71	1.46	3.83
Lu	0.20	0.23	0.33	0.36	0.50	0.32	0.26	0.21	0.55
Cu	101	124	182	143	128	149	58	88	73
Zn	83	78	101	79	140	92	62	78	88
Mo	4.67	0.10	0.24	0.18	0.49	0.17	1.11	2.18	0.20
Ag	0.06	1.56	0.07	0.09	0.11	0.05	0.04	0.08	0.24
Tl	-	-	-	-	-	-	-	0.09	-
Pb	12.68	23.01	5.58	3.13	9.54	11.53	200.46	218.77	69.98
Se	2.83	3.27	4.64	1.49	1.97	2.65	3.92	6.62	7.04
Sb	0.17	0.36	0.76	0.09	0.18	0.14	28.26	37.10	10.96

	84GRS-1166	84GRS-0047	84GRS-0075	84GRS-1283	84GRS-1056	84GRS-1225	82GRS-0835	82GRS-1582	82GRS-0139
(La/Yb)n	0.94	0.80	1.10	0.66	1.42	0.94	1.57	0.94	1.43
(La/Sm)n	0.93	0.80	1.03	0.64	1.05	0.92	1.34	0.86	1.25
(Gd/Yb)n	0.98	0.99	1.04	1.02	1.22	1.05	1.10	1.06	1.09
(La/Y)n	0.89	0.81	1.06	0.67	1.33	0.89	1.45	0.89	1.46
(Tb/Yb)n	1.02	1.03	1.06	1.03	1.20	1.05	1.12	1.10	1.04
(Tb/Y)n	0.97	1.05	1.02	1.03	1.12	0.99	1.04	1.04	1.06
(Eu/Eu*)n	1.07	1.05	0.98	0.95	0.83	0.97	0.97	0.96	0.80
Al_2O_3/TiO_2	23	22	13	16	7	18	22	22	14
Zr/Hf	36	37	37	37	37	34	36	36	39
La/Nb	0.93	1.04	1.13	0.76	1.23	1.11	1.46	1.16	1.18
Th/Nb	0.12	0.15	0.14	0.11	0.14	0.11	0.18	0.14	0.14
Th/La	0.13	0.14	0.12	0.14	0.11	0.10	0.12	0.12	0.12
Zr/Y	2.28	2.13	2.66	2.46	2.78	2.39	2.11	2.17	3.43
Ti/Zr	123	128	123	98	124	109	118	130	54
Ti/Sm	2992	2771	3277	2360	2773	2780	2343	2807	1632
P/Nd	55	56	61	51	59	49	46	49	40
Ti/V	18	16	20	19	26	18	20	16	26
Sc/La	194	173	146	105	105	136	131	198	62
Nb/Nb*	1.04	0.98	0.88	1.55	0.78	0.86	0.61	0.83	0.79
Zr/Zr*	0.99	0.92	1.05	1.00	0.88	1.02	0.75	0.89	1.14
Hf/Hf*	1.00	0.90	1.03	0.97	0.86	1.09	0.75	0.90	1.06
Ti/Ti*	1.04	0.95	1.13	0.81	1.00	0.94	0.83	0.97	0.57
UTM Zone	15	15	15	15	15	15	15	15	15
Easting	646275	636275	637415	653175	636345	645770	606893	610703	615902
Northing	5685270	5686730	5683600	5685465	5685880	5684355	5704634	5703388	5700536

	Lake St. Joseph belt - Woman assemblage				Meen-Dempster belt - Meen assemblage				
	PL95-24	PL95-25	PL95-41	PL95-26	84GRS-1206	82GRS-0120	84GRS-0022	82GRS-0224	82GRS-1022
SiO_2	48.89	49.29	51.40	53.68	57.60	72.54	73.06	74.79	75.77
TiO_2	0.67	0.79	1.09	1.44	0.77	0.48	0.43	0.46	0.12
Al_2O_3	15.17	15.16	15.90	12.04	15.91	16.40	16.24	16.75	14.35
Fe_2O_3	12.51	12.60	11.46	14.49	2.12	2.35	0.37	0.19	0.97
MnO	0.19	0.19	0.23	0.31	0.18	0.11	0.01	0.02	0.02
MgO	6.12	7.70	4.68	3.14	8.08	0.69	0.99	0.54	0.50
CaO	12.61	12.40	13.11	11.94	12.73	1.88	2.42	2.10	0.83
K_2O	0.15	0.13	0.12	0.27	0.23	2.58	1.46	2.46	2.50
Na_2O	1.64	1.67	1.94	2.55	2.32	2.82	3.97	2.84	5.11
P_2O_5	0.04	0.06	0.07	0.14	0.08	0.13	0.14	0.04	0.03
LOI	0.86	0.45	2.09	1.73	1.21	1.32	1.32	1.21	0.70
Mg#	49	57	47	32	89	39	85	80	53
Ti	4115	4681	7888	8576	4360	2688	1877	1181	517
P	468	492	420	735	311	546	626	552	422
Cr	486	428	344	105	372	12	11	17	3
Co	52	55	69	41	55	10	8	5	2
Ni	112	139	192	16	105	13	11	11	2
Rb	1	2	1	3	7	53	24	50	31
Sr	108	129	128	230	155	252	233	233	170
Cs	0	0	0	0	1	1	0	1	0
Ba	18	29	24	47	91	583	285	538	776
Sc	76	65	51	55	42	7	4	7	1
V	306	290	366	398	237	50	30	50	3
Ta	0.13	0.16	0.20	0.33	0.19	0.36	0.47	0.37	0.54
Nb	2.05	2.47	3.36	5.54	3.06	5.71	5.22	5.83	5.17
Zr	89	95	64	103	97	97	111	100	89
Hf	1.13	1.30	1.91	3.02	1.44	2.49	2.93	2.40	2.70
Th	0.29	0.41	0.28	2.43	1.54	5.11	5.82	4.84	6.57
U	0.11	0.12	0.07	0.54	0.35	1.06	1.32	1.14	1.82
Y	16.99	16.90	24.00	25.55	16.95	5.40	5.43	4.35	5.04
La	2.08	2.67	3.15	12.45	6.47	18.13	8.65	13.68	16.85
Ce	5.60	7.37	9.15	27.67	13.39	36.44	19.26	29.79	30.42
Pr	0.81	1.08	1.37	3.11	1.68	3.94	2.01	3.33	3.06
Nd	4.79	5.93	7.63	14.98	7.13	13.60	7.18	12.30	9.76
Sm	1.72	1.98	2.54	3.77	1.87	2.22	1.50	2.41	1.51
Eu	0.61	0.73	0.90	1.30	0.60	0.66	0.35	0.71	0.30
Gd	2.37	2.63	3.30	4.44	2.30	1.69	1.24	1.57	1.14
Tb	0.45	0.45	0.59	0.67	0.41	0.21	0.20	0.19	0.15
Dy	2.82	2.92	4.01	4.27	2.74	1.09	1.23	0.95	0.87
Ho	0.62	0.64	0.91	0.98	0.59	0.20	0.25	0.15	0.16
Er	1.91	1.89	2.54	2.93	1.73	0.57	0.65	0.39	0.48
Tm	0.27	0.31	0.38	0.42	0.25	0.09	0.10	0.06	0.08
Yb	1.84	1.78	2.58	2.85	1.66	0.55	0.61	0.32	0.47
Lu	0.28	0.30	0.33	0.41	0.24	0.09	0.08	0.05	0.07
Cu	83	122	108	31	88	17	19	8	51
Zn	79	83	101	105	82	27	37	44	11
Mo	0.26	0.41	0.30	1.97	0.30	0.34	0.48	0.47	1.73
Ag	1.01	0.67	0.09	0.87	0.05	0.11	0.21	0.19	0.26
Tl	0.10	0.08	0.02	1.10	0.07	0.21	0.05	0.27	0.09
Pb	0.82	0.64	0.93	5.00	4.66	61.09	29.86	29.02	7.90
Sn	-	-	0.66	-	2.04	4.12	1.14	2.81	2.62
Sb	-	-	0.09	-	0.09	8.80	0.19	3.74	0.24
	PL95-24	PL95-25	PL95-41	PL95-26	84GRS-1206	82GRS-0120	84GRS-0022	82GRS-0224	82GRS-1022
(La/Yb)n	0.81	1.08	0.87	3.13	2.79	23.75	10.21	30.27	25.52
(La/Sm)n	0.78	0.87	0.80	2.13	2.23	5.28	3.73	3.67	7.21
(Gd/Yb)n	1.07	1.22	1.06	1.29	1.14	2.56	1.68	4.01	1.99
(La/Y)n	0.81	1.05	0.87	3.23	2.53	22.23	10.55	20.81	22.16
(Tb/Yb)n	1.12	1.15	1.04	1.07	1.14	1.77	1.52	2.70	1.45
(Tb/Y)n	1.11	1.11	1.04	1.11	1.03	1.65	1.57	1.85	1.26
(Eu/Eu*)n	0.93	0.97	0.95	0.97	0.88	1.00	0.77	1.05	0.68
Al_2O_3/TiO_2	22	19	12	8	20	36	51	32	166
Zr/Hf	35	34	33	34	40	39	38	42	33
La/Nb	1.01	1.08	0.94	2.25	2.12	3.18	1.66	2.35	3.26
Th/Nb	0.14	0.16	0.08	0.44	0.50	0.90	1.11	0.83	1.27
Th/La	0.14	0.15	0.09	0.20	0.24	0.28	0.67	0.35	0.39
Zr/Y	2.30	2.66	2.66	4.03	3.36	17.91	20.44	22.90	17.74
Ti/Zr	105	105	123	83	77	28	17	32	6
Ti/Sm	2388	2368	3102	2276	2329	1211	1252	1320	342
P/Nd	98	83	55	49	44	40	87	45	43
Ti/V	13	16	22	22	18	54	62	54	155
Sc/La	270	220	156	136	175	80	51	145	18
Nb/Nb*	0.99	0.95	1.16	0.37	0.36	0.24	0.50	0.35	0.21
Zr/Zr*	0.94	0.90	1.00	0.95	1.08	1.22	2.34	1.27	1.61
Hf/Hf*	0.99	0.95	1.09	1.01	0.99	1.14	2.24	1.11	1.76
Ti/Ti*	0.81	0.81	1.08	0.83	0.83	0.55	0.55	0.65	0.16
UTM Zone	15	15	15	15	15	15	15	15	15
Easting	694630	694850	696509	694650	653890	613611	635525	614771	607213
Northing	5672135	5672900	5668207	5675000	5685050	5700236	5689930	5699305	5702280

Appendix D

Data for the ~2.7 Ga Confederation assemblage

	Rice Lake - Tinney Formation				Rice Lake - Stormy Lake Formation						
	RC95-11	RC95-9	RC95-12	RC95-10	RC95-8	RC96-1	RC95-6	RC95-5	RC95-7	RC96-16	RC96-14
SiO_2	51.52	49.22	61.11	49.85	50.63	49.92	51.15	49.83	49.08	50.82	51.04
TiO_2	0.67	0.67	0.86	1.01	0.81	0.92	0.95	1.14	1.22	0.99	1.02
Al_2O_3	15.20	15.46	15.38	14.03	13.96	14.72	14.18	14.36	15.83	14.43	13.89
Fe_2O_3	10.53	12.41	7.90	14.56	13.54	13.69	13.34	15.61	14.34	14.43	14.61
MnO	0.18	0.19	0.11	0.27	0.20	0.23	0.20	0.23	0.20	0.21	0.25
MgO	9.16	8.36	5.03	5.65	8.32	7.20	6.77	7.69	6.82	6.41	6.08
CaO	9.52	12.31	4.60	12.57	10.19	11.01	11.45	9.02	10.25	10.51	9.98
K_2O	0.08	0.03	0.50	0.18	0.11	0.20	0.04	0.09	0.07	0.06	0.30
Na_2O	2.80	1.31	4.25	1.81	2.17	2.15	1.84	1.94	2.08	2.04	2.75
P_2O_5	0.04	0.04	0.26	0.07	0.06	0.06	0.07	0.09	0.10	0.08	0.07
LOI	2.15	3.63	2.09	3.09	2.46	1.73	3.15	3.04	4.82	2.09	2.04
Mg#	65	60	58	46	57	54	53	52	51	49	48
Ti	3812	3558	5416	5238	4960	5288	5107	7118	6971	7100	6647
P	126	127	1231	287	362	362	479	607	549	769	473
Cr	361	337	109	244	97	336	119	72	234	300	218
Co	47	51	25	47	53	61	46	55	48	91	58
Ni	145	141	74	73	73	110	58	59	92	155	110
Rb	1	0	18	3	2	5	0	1	1	1	8
Sr	121	144	254	123	136	137	127	154	144	142	134
Cs	0	0	0	0	0	0	0	0	0	0	0
Ba	72	6	224	58	18	54	12	12	14	19	60
Sc	40	37	16	43	47	55	42	51	37	49	52
V	285	308	138	365	332	329	361	401	356	352	400
Ta	0.09	0.10	0.54	0.20	0.15	0.16	0.23	0.26	0.27	0.21	0.21
Nb	1.81	1.84	9.08	3.15	2.50	2.50	3.07	3.83	4.33	3.11	3.03
Zr	57	57	358	55	48	49	62	77	78	61	53
Hf	1.11	1.14	3.83	1.57	1.44	1.40	1.72	2.18	2.17	1.75	1.56
Th	0.29	0.56	3.36	0.50	0.46	0.36	0.83	0.86	0.62	0.34	0.34
U	0.05	0.05	0.55	0.08	0.08	0.08	0.09	0.15	0.10	0.07	0.07
Y	14.65	16.65	16.19	21.12	17.49	19.20	19.64	24.24	26.29	23.25	23.38
La	1.55	1.92	24.06	3.58	2.73	3.14	4.45	5.27	4.74	3.58	3.65
Ce	4.21	5.36	55.81	9.63	7.27	8.31	11.10	13.54	12.68	9.69	9.84
Pr	0.65	0.83	6.85	1.44	1.11	1.29	1.61	1.86	1.84	1.43	1.43
Nd	3.77	4.28	27.19	7.29	5.57	6.43	7.24	9.18	8.95	7.01	6.95
Sm	1.29	1.47	5.02	2.37	1.94	2.10	2.35	2.84	2.97	2.19	2.42
Eu	0.41	0.58	1.40	0.90	0.74	0.77	0.65	1.04	1.04	0.94	0.93
Gd	1.75	2.18	4.08	3.16	2.52	2.70	3.14	3.90	3.92	3.32	3.21
Tb	0.32	0.39	0.49	0.55	0.44	0.48	0.53	0.63	0.65	0.56	0.59
Dy	2.18	2.69	2.91	3.83	3.06	3.21	3.67	4.49	4.32	3.90	4.09
Ho	0.48	0.62	0.54	0.81	0.67	0.72	0.78	0.95	0.96	0.88	0.92
Er	1.34	1.76	1.44	2.40	1.96	2.13	2.32	2.77	2.76	2.57	2.64
Tm	0.20	0.28	0.21	0.34	0.32	0.33	0.36	0.43	0.40	0.39	0.41
Yb	1.41	1.70	1.40	2.31	2.01	2.12	2.35	2.80	2.62	2.50	2.67
Lu	0.20	0.26	0.21	0.34	0.28	0.31	0.36	0.43	0.39	0.39	0.41
Cu	88	115	46	137	128	158	98	120	74	212	14
Zn	72	65	116	79	86	91	71	104	104	123	112
Mo	0.04	0.35	0.63	0.11	0.28	1.65	0.44	0.23	0.34	0.34	2.65
Ag	0.14	0.13	0.72	0.25	0.15	0.42	0.19	0.17	0.13	0.48	0.34
Tl	-	-	0.06	-	0.01	0.08	-	-	-	0.02	0.07
Pb	0.38	0.69	3.01	0.74	0.55	1.60	0.79	0.92	0.95	0.68	5.83
Sn	0.29	0.43	0.86	0.51	0.48	-	0.42	0.56	0.75	-	-
Sb	0.01	0.19	0.11	0.06	0.10	-	0.11	0.13	0.17	-	-
	RC95-11	RC95-9	RC95-12	RC95-10	RC95-8	RC96-1	RC95-6	RC95-5	RC95-7	RC96-16	RC96-14
(La/Yb)n	0.79	0.81	12.33	1.11	0.97	1.06	1.36	1.35	1.30	1.03	0.98
(La/Sm)n	0.78	0.84	3.09	0.97	0.91	0.97	1.22	1.20	1.03	1.06	0.98
(Gd/Yb)n	1.02	1.06	2.41	1.13	1.04	1.05	1.10	1.15	1.24	1.10	0.99
(La/Y)n	0.70	0.76	9.84	1.12	1.03	1.08	1.50	1.44	1.19	1.02	1.04
(Tb/Yb)n	1.02	1.05	1.59	1.08	1.00	1.03	1.02	1.02	1.13	1.03	1.01
(Tb/Y)n	0.91	0.99	1.27	1.09	1.06	1.05	1.12	1.09	1.04	1.02	1.06
(Eu/Eu*)n	0.83	0.99	0.92	1.00	1.02	0.98	0.73	0.96	0.93	1.07	1.02
Al_2O_3/TiO_2	23	26	17	16	17	16	16	12	13	12	12
Zr/Hf	34	32	41	35	33	35	36	35	36	35	34
La/Nb	0.86	1.05	2.65	1.14	1.09	1.26	1.45	1.37	1.09	1.15	1.21
Th/Nb	0.16	0.31	0.37	0.16	0.18	0.14	0.27	0.22	0.14	0.11	0.11
Th/La	0.18	0.29	0.14	0.14	0.17	0.11	0.19	0.16	0.13	0.09	0.09
Zr/Y	2.55	2.23	9.74	2.62	2.75	2.54	3.16	3.16	2.98	2.62	2.27
Ti/Zr	102	96	34	95	103	108	82	93	89	117	125
Ti/Sm	2961	2417	1078	2208	2560	2522	2170	2502	2349	3247	2751
P/Nd	34	30	45	39	65	56	66	66	61	110	68
Ti/V	13	12	39	14	15	16	14	18	20	20	17
Sc/La	198	144	76	125	171	181	117	118	96	127	128
Nb/Nb*	1.18	1.00	0.33	0.88	0.91	0.79	0.64	0.70	0.91	0.88	0.83
Zr/Zr*	1.17	1.02	0.93	0.92	1.02	0.92	1.04	1.04	1.05	1.08	0.90
Hf/Hf*	1.26	1.14	0.82	0.94	1.10	0.96	1.04	1.07	1.08	1.12	0.96
Ti/Ti*	1.01	0.79	0.47	0.76	0.89	0.88	0.74	0.85	0.81	1.04	0.94
UTM Zone	15	15	15	15	15	15	15	15	15	15	15
Easting	336024	337530	335902	336742	336936	341049	335939	335174	336496	336180	341078
Northing	5642207	5644487	5641076	5643222	5646097	5636451	5647345	5647795	5646576	5638865	5636300

	Rice Lake - Gunnar Fm		Rice Lake - Narrows Formation								
	RC96-15	RC96-17	RC95-14	RC96-9	RC95-1	RC95-3	RC95-4A	RC96-13	RC96-12	RC95-13	RC95-16
SiO_2	65.92	68.13	61.09	64.99	64.26	65.51	65.28	60.82	62.99	50.08	62.18
TiO_2	0.45	0.46	0.67	0.50	0.55	0.67	0.53	0.52	0.53	1.39	0.54
Al_2O_3	16.95	16.03	17.17	17.10	16.54	15.30	16.14	19.44	17.17	17.16	16.68
Fe_2O_3	5.08	4.86	7.72	5.42	5.42	5.65	5.09	5.72	5.08	13.19	5.49
MnO	0.05	0.06	0.11	0.05	0.08	0.07	0.07	0.04	0.05	0.19	0.11
MgO	2.68	1.18	4.15	2.75	2.72	2.62	2.33	2.53	2.09	5.19	2.12
CaO	2.29	4.10	3.03	2.93	4.86	5.11	5.27	4.26	5.93	9.50	6.91
K_2O	0.61	0.47	0.56	1.89	1.18	0.79	0.80	0.65	1.43	0.62	1.95
Na_2O	5.85	4.56	5.36	4.26	4.27	4.08	4.39	5.87	4.58	2.51	3.92
P_2O_5	0.11	0.13	0.14	0.10	0.12	0.21	0.11	0.13	0.15	0.17	0.12
LOI	3.25	2.88	3.90	3.09	2.72	1.68	1.78	2.78	5.48	6.44	7.13
Mg#	54	35	54	53	52	51	50	49	47	46	46
Ti	3110	3023	4474	2911	3390	3974	3166	3155	2930	8948	2657
P	254	615	578	487	465	905	466	475	489	1073	776
Cr	19	7	59	31	38	30	31	42	31	76	33
Co	13	15	26	17	19	16	17	23	17	44	12
Ni	24	5	60	36	38	24	35	38	30	93	23
Rb	13	9	18	46	38	19	21	14	26	17	46
Sr	272	492	186	289	352	449	357	421	202	344	219
Cs	0	0	0	1	0	0	0	0	1	2	1
Ba	119	108	167	397	340	221	403	125	159	154	258
Sc	14	9	17	14	13	11	12	10	9	34	10
V	98	50	156	103	101	102	105	78	67	286	84
Ta	0.47	0.32	0.53	0.34	0.38	0.52	0.42	0.28	0.32	0.35	0.24
Nb	7.00	5.16	7.44	4.31	4.71	8.31	5.67	4.26	4.61	5.61	3.68
Zr	151	98	144	90	111	157	125	71	80	114	105
Hf	3.49	2.53	3.19	2.71	3.30	3.49	3.13	1.89	2.07	2.96	2.90
Th	2.33	2.45	3.01	2.77	3.64	3.74	4.42	1.61	1.89	1.77	2.00
U	0.54	0.57	0.65	0.67	0.73	0.66	0.88	0.38	0.40	0.36	0.44
Y	10.76	15.63	13.51	9.29	9.82	13.13	11.39	6.43	6.75	19.45	8.41
La	14.33	19.30	15.62	13.37	15.17	23.73	17.78	11.91	12.28	11.34	11.69
Ce	30.15	42.56	31.78	27.76	32.32	55.96	37.18	24.76	26.73	25.60	25.05
Pr	3.48	4.96	3.56	3.15	3.66	6.63	4.08	2.78	3.17	3.26	2.90
Nd	13.19	18.31	14.13	11.89	13.75	24.62	15.51	10.57	12.30	13.51	11.98
Sm	2.39	3.27	2.82	2.30	2.59	4.22	2.91	2.05	2.25	3.22	2.36
Eu	0.82	0.93	0.90	0.68	0.77	1.12	0.78	0.86	0.86	1.17	0.62
Gd	2.18	2.98	2.80	1.85	2.46	3.34	2.85	1.62	1.76	3.59	2.12
Tb	0.31	0.39	0.40	0.25	0.33	0.42	0.34	0.20	0.22	0.52	0.26
Dy	1.78	2.54	2.29	1.56	1.83	2.21	1.96	1.20	1.31	3.39	1.68
Ho	0.34	0.53	0.46	0.33	0.38	0.43	0.39	0.23	0.27	0.70	0.33
Er	0.94	1.49	1.32	0.92	0.99	1.15	1.07	0.61	0.73	2.00	0.89
Tm	0.13	0.25	0.19	0.14	0.15	0.17	0.14	0.09	0.11	0.29	0.15
Yb	0.94	1.49	1.17	0.80	0.98	1.02	0.96	0.51	0.66	1.92	0.94
Lu	0.14	0.23	0.20	0.14	0.15	0.16	0.14	0.08	0.09	0.27	0.16
Cu	11	9	68	45	42	30	38	12	12	80	38
Zn	58	46	86	82	70	62	54	30	64	112	59
Mo	0.83	0.33	0.86	0.16	0.37	0.59	0.86	0.43	0.49	0.25	0.75
Ag	0.40	0.08	0.70	0.54	0.58	0.49	0.50	0.06	0.07	0.39	0.33
Tl	0.07	0.07	0.07	0.18	0.13	0.03	0.10	0.08	0.14	0.10	0.19
Pb	1.62	2.66	3.39	4.12	4.32	3.34	4.49	2.02	2.13	3.30	2.00
Sn	-	0.62	0.80	-	0.61	0.77	0.71	0.59	1.20	0.64	0.61
Sb	-	0.35	0.65	-	0.13	0.16	0.13	0.39	0.19	0.99	0.29
	RC96-15	RC96-17	RC95-14	RC96-9	RC95-1	RC95-3	RC95-4A	RC96-13	RC96-12R	RC95-13	RC95-16
(La/Yb)n	10.93	9.28	9.54	11.96	11.14	16.73	13.32	16.62	13.25	4.24	8.89
(La/Sm)n	3.88	3.81	3.58	3.75	3.78	3.63	3.94	3.76	3.53	2.28	3.20
(Gd/Yb)n	1.92	1.65	1.97	1.91	2.08	2.71	2.46	2.61	2.19	1.55	1.86
(La/Y)n	8.82	8.18	7.66	9.54	10.23	11.97	10.34	12.26	12.05	3.86	9.20
(Tb/Yb)n	1.50	1.19	1.53	1.41	1.53	1.86	1.60	1.73	1.52	1.24	1.24
(Tb/Y)n	1.21	1.05	1.23	1.12	1.41	1.33	1.24	1.27	1.38	1.13	1.28
(Eu/Eu*)n	1.07	0.89	0.97	0.97	0.92	0.88	0.82	1.40	1.28	1.05	0.83
AL_2O_3/TiO_2	33	32	23	35	29	23	30	37	35	11	37
Zr/Hf	43	39	45	33	34	45	40	37	39	38	36
La/Nb	2.05	3.74	2.10	3.11	3.22	2.86	3.13	2.80	2.66	2.02	3.18
Th/Nb	0.33	0.47	0.41	0.64	0.77	0.45	0.78	0.38	0.41	0.31	0.54
Th/La	0.16	0.13	0.19	0.21	0.24	0.16	0.25	0.14	0.15	0.16	0.17
Zr/Y	14.02	6.26	10.62	9.65	11.29	11.97	11.00	11.02	11.92	5.85	12.47
Ti/Zr	21	31	31	32	31	25	25	45	36	79	25
Ti/Sm	1304	924	1588	1264	1309	942	1087	1543	1304	2782	1127
P/Nd	19	34	41	41	34	37	30	45	40	79	31
Ti/V	32	60	29	28	34	39	30	41	43	31	32
Sc/La	96	40	88	99	86	69	85	119	99	128	62
Nb/Nb*	0.38	0.22	0.36	0.25	0.25	0.31	0.25	0.28	0.30	0.42	0.25
Zr/Zr*	1.86	0.88	1.58	1.19	1.29	1.07	1.29	1.06	1.06	1.19	1.37
Hf/Hf*	1.56	0.82	1.27	1.30	1.39	0.86	1.17	1.02	0.99	1.13	1.37
Ti/Ti*	0.54	0.38	0.63	0.56	0.53	0.42	0.43	0.69	0.58	1.04	0.47
UTM Zone	15	15	15	15	15	15	15	15	15	15	15
Easting	339131	334062	297434	341200	313478	328687	333625	339848	339848	299457	312065
Northing	5636817	5637551	5661202	5634596	5655900	5633510	5650401	5635982	5635982	5660550	5655100

	Rice Lake - Narrows Formation				Red Lake belt			
	RC96-11	RC96-8	RC96-10	PRC95-15	RL95-27	RL95-30	RL95-14	RL95-28
SiO_2	67.92	72.22	67.90	57.79	51.49	51.77	47.77	52.12
TiO_2	0.44	0.35	0.41	1.30	0.80	0.58	0.59	1.17
Al_2O_3	15.57	12.64	14.59	13.76	21.30	17.78	17.59	15.89
Fe_2O_3	4.66	5.82	4.24	14.50	9.76	7.76	12.70	12.45
MnO	0.08	0.09	0.12	0.20	0.16	0.20	0.15	0.17
MgO	1.76	1.59	1.01	2.58	4.05	2.84	4.25	3.71
CaO	4.14	1.57	5.78	5.62	8.47	14.78	14.55	11.34
K_2O	0.49	2.94	0.45	0.15	0.10	0.36	0.30	0.60
Na_2O	4.91	2.74	5.38	3.89	4.21	4.27	2.03	2.46
P_2O_5	0.12	0.04	0.13	0.20	0.08	0.07	0.07	0.10
LOI	1.78	0.96	4.33	4.93	5.88	11.35	8.69	11.23
Mg#	45	38	34	28	49	46	42	40
Ti	2670	2005	2487	8134	4971	3421	3319	6935
P	341	240	888	764	311	386	61	556
Cr	14	21	40	3	98	116	176	185
Co	9	3	76	27	89	48	99	45
Ni	14	2	88	7	221	162	222	110
Rb	21	92	10	4	2	8	9	15
Sr	541	125	632	304	359	373	304	291
Cs	1	6	0	0	1	1	2	2
Ba	205	558	117	126	97	68	60	196
Sc	12	9	13	33	40	32	47	26
V	82	6	90	147	238	162	184	168
Ta	0.40	1.35	0.37	0.22	0.19	0.19	0.19	0.26
Nb	5.41	26.84	4.98	3.77	3.12	3.05	3.18	4.33
Zr	122	508	108	115	55	55	55	84
Hf	3.04	8.11	2.84	3.31	1.51	1.44	1.54	1.98
Th	3.33	6.86	3.10	4.49	1.33	1.45	1.46	1.64
U	0.71	1.52	0.65	0.69	0.28	0.28	1.15	0.34
Y	13.21	52.86	13.46	41.43	14.91	15.81	13.75	16.43
La	20.64	45.94	19.82	22.91	7.05	7.20	5.92	9.03
Ce	42.12	101.93	41.02	51.78	16.84	15.87	13.26	19.93
Pr	4.57	11.98	4.51	6.51	2.12	1.95	1.50	2.50
Nd	16.76	47.67	15.82	28.72	8.97	7.81	7.10	11.12
Sm	2.88	9.53	2.80	6.17	2.26	1.99	1.85	2.98
Eu	0.87	1.85	0.79	1.87	0.87	0.76	0.67	1.11
Gd	2.55	9.01	2.50	6.84	2.49	2.32	2.12	3.27
Tb	0.34	1.39	0.33	1.04	0.39	0.36	0.35	0.49
Dy	1.97	9.43	2.04	7.06	2.63	2.47	2.38	2.98
Ho	0.41	1.96	0.41	1.56	0.53	0.55	0.50	0.56
Er	1.10	5.26	1.14	4.56	1.49	1.38	1.42	1.61
Tm	0.16	0.84	0.17	0.69	0.22	0.23	0.22	0.23
Yb	1.14	5.47	1.13	4.55	1.37	1.44	1.37	1.52
Lu	0.17	0.88	0.18	0.68	0.20	0.21	0.19	0.23
Cu	25	12	288	206	141	130	112	89
Zn	50	95	89	124	105	66	75	100
Mo	1.44	2.13	0.66	0.82	0.42	0.21	0.91	0.46
Ag	0.56	0.90	1.27	0.41	0.44	0.48	0.85	0.64
Tl	0.05	0.38	0.04	0.01	0.04	0.06	0.10	0.12
Pb	4.92	8.70	7.49	2.85	2.67	15.56	2.13	3.03
Sn	-	-	0.00	0.96	0.39	0.36	-	0.78
Sb	-	-	0.00	0.42	4.94	1.07	-	0.95
	RC96-11	RC96-8	RC96-10	PRC95-15	RL95-27	RL95-30	RL95-14	RL95-28
(La/Yb)n	12.95	6.02	12.60	3.61	3.70	3.60	3.10	4.25
(La/Sm)n	4.63	3.11	4.57	2.40	2.02	2.33	2.07	2.03
(Gd/Yb)n	1.84	1.36	1.83	1.24	1.51	1.33	1.28	1.77
(La/Y)n	10.34	5.76	9.75	3.66	3.13	3.02	2.85	3.64
(Tb/Yb)n	1.36	1.15	1.35	1.04	1.30	1.13	1.17	1.46
(Tb/Y)n	1.09	1.10	1.04	1.05	1.10	0.95	1.08	1.25
(Eu/Eu*)n	0.96	0.60	0.90	0.87	1.12	1.07	1.03	1.10
Al_2O_3/TiO_2	35	38	35	10	26	31	32	14
Zr/Hf	40	38	38	35	36	38	35	42
La/Nb	3.81	1.71	3.98	6.08	2.26	2.36	1.86	2.09
Th/Nb	0.61	0.26	0.62	1.19	0.42	0.48	0.46	0.38
Th/La	0.16	0.15	0.16	0.20	0.19	0.20	0.25	0.18
Zr/Y	9.20	5.82	8.04	2.78	3.68	3.49	3.97	5.11
Ti/Zr	22	7	23	71	91	62	61	83
Ti/Sm	927	210	887	1318	2204	1717	1792	2408
P/Nd	20	5	56	27	35	49	9	50
Ti/V	33	317	28	55	21	21	18	41
Sc/La	70	10	71	49	200	153	248	111
Nb/Nb*	0.20	0.48	0.19	0.14	0.39	0.35	0.45	0.39
Zr/Zr*	1.21	1.00	1.12	0.60	0.84	0.97	1.04	1.03
Hf/Hf*	1.10	0.95	1.07	0.62	0.84	0.91	1.07	0.88
Ti/Ti*	0.39	0.09	0.37	0.50	0.83	0.63	0.66	0.89
UTM Zone	15	15	15	15	15	15	15	15
Easting	338366	341268	340017	296334	445175	443550	445822	446600
Northing	5634238	5635011	5634760	5661330	5654341	5654476	5654403	5654100

Red Lake belt

	RL95-5	RL95-29	RL95-15	RL95-3	RL95-2	RL95-1	RL95-4
SiO_2	53.25	49.73	58.14	59.20	60.98	64.95	72.74
TiO_2	1.69	0.65	1.59	0.87	1.13	0.18	0.17
Al_2O_3	13.92	16.88	13.04	14.60	14.58	12.76	13.87
Fe_2O_3	15.20	10.44	14.82	9.67	10.40	9.40	2.86
MnO	0.31	0.25	0.34	0.18	0.16	0.38	0.06
MgO	3.87	2.43	2.23	3.44	1.78	0.38	0.77
CaO	7.95	14.85	5.11	7.11	5.04	7.16	2.43
K_2O	0.35	1.60	0.67	0.68	1.13	3.57	1.57
Na_2O	3.31	3.08	3.66	4.07	4.36	1.22	5.24
P_2O_5	0.16	0.09	0.41	0.19	0.42	0.00	0.08
LOI	5.77	12.74	4.88	0.45	0.30	5.93	2.04
Mg#	36	34	25	44	27	8	37
Ti	10398	3377	9503	4683	6963	1037	2148
P	971	399	1913	621	1683	126	379
Cr	31	103	144	52	4	3	8
Co	56	49	24	27	22	3	5
Ni	50	151	7	45	5	2	5
Rb	6	38	16	16	26	125	43
Sr	144	204	229	263	349	130	470
Cs	0	2	1	1	1	2	1
Ba	83	210	260	137	385	323	605
Sc	52	25	46	25	17	2	7
V	411	158	73	159	38	1	17
Ta	0.44	0.29	0.61	0.59	0.93	2.77	0.72
Nb	7.36	4.26	9.83	9.47	16.00	40.19	11.14
Zr	121	76	120	164	239	372	223
Hf	2.83	1.99	3.19	3.82	5.24	10.39	5.42
Th	1.70	2.92	3.54	4.03	6.74	14.43	11.98
U	0.41	0.66	0.76	0.92	1.63	3.48	2.06
Y	17.18	15.70	28.75	32.96	40.49	102.91	27.70
La	10.93	12.39	17.08	21.92	52.70	89.15	54.28
Ce	26.42	27.97	36.88	49.73	113.56	185.58	120.58
Pr	3.49	3.26	4.19	6.09	13.68	21.56	13.88
Nd	16.64	12.77	19.56	23.90	54.69	78.70	52.09
Sm	4.56	2.75	4.51	5.16	10.58	16.95	8.60
Eu	1.50	0.90	1.79	1.47	2.79	2.12	1.58
Gd	6.02	3.01	5.44	5.71	9.88	17.81	7.07
Tb	1.00	0.46	0.84	0.86	1.29	2.69	0.90
Dy	6.60	2.96	5.21	5.59	7.46	17.46	5.19
Ho	1.46	0.63	1.08	1.27	1.53	3.72	1.03
Er	3.95	1.67	2.90	3.60	4.11	10.95	2.85
Tm	0.65	0.26	0.44	0.55	0.60	1.74	0.44
Yb	4.02	1.78	2.70	3.82	3.94	11.53	2.82
Lu	0.65	0.25	0.40	0.58	0.59	1.75	0.47
Cu	95	76	21	40	93	7	27
Zn	458	58	330	88	120	129	34
Mo	1.48	0.17	1.47	3.94	2.57	2.69	2.16
Ag	0.47	0.64	1.15	0.58	0.84	1.34	0.79
Tl	0.06	0.23	0.46	0.02	0.11	0.11	0.17
Pb	5.81	3.74	6.26	4.24	8.32	8.43	8.62
Sn	1.11	0.77	-	1.29	1.99	5.91	1.50
Sb	0.82	1.82	-	0.35	0.37	0.16	0.67
	RL95-5	RL95-29	RL95-15	RL95-3	RL95-2	RL95-1	RL95-4
$(La/Yb)_N$	1.95	4.99	4.54	4.12	9.59	5.54	13.82
$(La/Sm)_N$	1.55	2.91	2.44	2.74	3.22	3.40	4.08
$(Gd/Yb)_N$	1.24	1.40	1.67	1.24	2.07	1.28	2.08
$(La/Y)_N$	1.95	5.23	3.94	4.41	8.62	5.74	12.98
$(Tb/Yb)_N$	1.14	1.18	1.41	1.03	1.49	1.06	1.45
$(Tb/Y)_N$	1.13	1.24	1.22	1.10	1.34	1.10	1.36
$(Eu/Eu^*)_N$	0.88	0.95	1.10	0.82	0.82	0.37	0.60
AL_2O_3/TiO_2	8	30	8	19	12	74	38
Zr/Hf	43	38	38	43	46	36	41
La/Nb	1.48	2.91	1.74	2.31	3.29	2.22	4.87
Th/Nb	0.23	0.69	0.36	0.42	0.42	0.36	1.07
Th/La	0.16	0.24	0.21	0.18	0.13	0.16	0.22
Zr/Y	3.26	4.86	4.17	4.97	5.91	3.61	8.04
Ti/Zr	86	44	79	29	29	3	10
Ti/Sm	2281	1228	2105	907	658	61	250
P/Nd	58	31	98	26	31	2	7
Ti/V	25	21	131	29	181	1067	124
Sc/La	80	99	115	43	29	1	14
Nb/Nb^*	0.61	0.29	0.46	0.37	0.24	0.35	0.17
Zr/Zr^*	0.96	0.89	0.88	1.02	0.69	0.70	0.73
Hf/Hf^*	0.81	0.84	0.85	0.86	0.55	0.71	0.64
Ti/Ti^*	0.79	0.46	0.76	0.34	0.27	0.02	0.11
UTM Zone	15	15	15	15	15	15	15
Easting	440099	443869	444008	446243	444581	444041	440676
Northing	5650556	5654598	5650490	5643940	5648993	5650116	5651022

Birch-Uchi belt - Tholeiites

	SL87-03	SL88-15	SL88-06	SH87-05	SB95-22	SL87-04
SiO_2	45.02	49.65	50.38	48.04	51.65	50.73
TiO_2	0.74	0.94	1.31	0.93	2.07	2.26
Al_2O_3	15.73	14.71	16.97	15.03	12.02	12.74
Fe_2O_3	14.59	10.93	16.54	13.76	18.71	19.63
MnO	0.23	0.19	0.20	0.24	0.24	0.28
MgO	9.71	5.35	7.51	5.75	3.87	3.10
CaO	11.51	14.06	3.68	13.54	8.37	7.29
K_2O	1.39	0.03	1.13	0.29	0.45	0.46
Na_2O	1.03	4.06	2.18	2.38	2.34	3.16
P_2O_5	0.05	0.06	0.09	0.05	0.27	0.35
LOI	14.54	6.00	6.39	4.50	4.33	6.49
Mg#	59	52	50	48	31	26
Ti	4404	5209	8809	4610	9254	13990
P	324	311	419	807	1077	1674
Cr	179	112	247	395	24	3
Co	79	62	80	81	45	46
Ni	228	116	214	191	30	2
Rb	2	1	33	5	13	15
Sr	116	121	33	453	94	103
Cs	0	0	1	0	1	12
Ba	88	30	185	85	93	134
Sc	45	34	37	47	33	33
V	236	230	287	309	281	112
Ta	0.07	0.27	0.20	0.18	0.65	0.69
Nb	1.72	4.36	3.54	3.03	9.61	11.47
Zr	35	99	63	94	168	197
Hf	1.05	1.64	1.89	1.67	4.46	5.85
Th	0.21	0.38	0.57	0.47	1.68	1.76
U	0.05	0.11	0.13	0.10	0.41	0.43
Y	11.79	16.47	21.14	24.14	46.13	59.98
La	2.01	5.11	4.64	4.24	12.66	14.72
Ce	5.93	12.92	11.21	11.19	32.71	34.27
Pr	0.90	1.81	1.78	1.64	4.54	5.31
Nd	4.88	9.10	9.13	8.02	21.60	25.38
Sm	1.68	2.47	2.79	2.58	6.44	7.52
Eu	0.92	0.84	1.11	0.96	2.11	2.32
Gd	2.32	3.19	3.40	3.31	8.05	9.70
Tb	0.38	0.46	0.52	0.59	1.35	1.51
Dy	2.34	2.84	3.58	3.88	8.65	9.84
Ho	0.47	0.64	0.78	0.86	1.92	2.24
Er	1.28	1.67	2.13	2.46	5.61	6.86
Tm	0.17	0.23	0.32	0.37	0.83	0.94
Yb	1.06	1.47	1.89	2.30	5.22	5.63
Lu	0.16	0.23	0.32	0.33	0.79	0.92
Cu	134	164	126	146	126	51
Zn	112	68	140	100	174	193
Mo	1.13	1.07	0.29	2.36	0.94	0.69
Ag	0.11	0.24	0.21	0.25	0.62	0.60
Tl	0.16	0.00	0.18	0.04	0.08	0.02
Pb	1.37	0.55	0.57	2.95	3.08	1.63
Sn	0.57	0.69	0.93	0.69	2.14	1.71
Sb	0.72	0.51	1.39	2.14	0.29	0.89
	SL87-03	**SL88-15**	**SL88-06**	**SH87-05**	**SB95-22**	**SL87-04**
$(La/Yb)_N$	1.36	2.49	1.76	1.32	1.74	1.87
$(La/Sm)_N$	0.77	1.34	1.08	1.06	1.27	1.27
$(Gd/Yb)_N$	1.81	1.79	1.48	1.19	1.28	1.42
$(La/Y)_N$	1.13	2.06	1.45	1.16	1.82	1.63
$(Tb/Yb)_N$	1.61	1.41	1.25	1.16	1.17	1.22
$(Tb/Y)_N$	1.34	1.16	1.04	1.02	1.22	1.06
$(Eu/Eu^*)_N$	1.42	0.91	1.10	1.00	0.89	0.83
Al_2O_3/TiO_2	22	17	11	13	8	6
Zr/Hf	34	36	33	32	38	34
La/Nb	1.17	1.17	1.31	1.40	1.32	1.28
Th/Nb	0.12	0.09	0.16	0.16	0.17	0.15
Th/La	0.10	0.07	0.12	0.11	0.13	0.12
Zr/Y	3.00	3.61	2.97	2.25	3.64	3.29
Ti/Zr	124	88	140	122	55	68
Ti/Sm	2617	2107	3159	2560	1438	1781
P/Nd	66	34	46	101	50	66
Ti/V	19	23	31	21	33	120
Sc/La	278	144	115	140	42	36
Nb/Nb^*	0.94	0.80	0.69	0.70	0.73	0.68
Zr/Zr^*	0.86	0.87	0.86	0.82	0.99	0.99
Hf/Hf^*	0.92	0.87	0.94	0.92	0.95	1.06
Ti/Ti^*	0.88	0.73	1.13	0.89	0.51	0.62
UTM Zone	15	15	15	15	15	15
Easting	519950	524000	519750	522100	519339	519500
Northing	5673750	5678800	5675250	5681500	5665794	5673550

Birch-Uchi belt - Calc alkaline

	SB95-1	SB95-4	SB95-5	SB95-6	SB95-18	SB95-20	SB95-21	SB95-23	SB95-26	SB95-27	SB95-35
SiO_2	50.18	48.66	49.83	52.34	47.03	46.58	47.99	47.67	48.35	47.52	51.33
TiO_2	1.23	0.59	0.94	0.80	0.69	1.43	0.82	0.92	0.89	0.61	0.73
Al_2O_3	14.25	16.29	14.64	16.69	17.14	17.76	15.48	15.44	16.43	16.02	15.64
Fe_2O_3	14.35	11.53	14.02	11.13	12.02	14.21	13.50	15.23	12.48	11.48	11.97
MnO	0.22	0.15	0.21	0.22	0.18	0.17	0.20	0.25	0.19	0.18	0.18
MgO	6.52	9.60	7.55	5.15	8.35	6.97	8.26	8.95	7.67	10.28	6.18
CaO	10.59	11.85	10.49	9.12	12.96	9.70	11.43	8.22	10.61	10.85	10.89
K_2O	0.35	0.12	0.46	0.53	0.10	0.21	0.30	0.63	1.11	1.76	1.57
Na_2O	2.18	1.17	1.78	4.00	1.48	2.84	1.97	2.64	2.20	1.26	1.26
P_2O_5	0.11	0.04	0.09	0.04	0.05	0.14	0.06	0.06	0.07	0.03	0.05
LOI	0.55	3.95	2.72	1.42	2.41	3.09	2.46	2.88	2.30	3.79	6.78
Mg#	50	65	54	50	60	52	57	56	58	66	53
Ti	7245	3506	5803	4704	4047	8040	4133	4996	4948	2848	3906
P	542	169	408	226	328	777	361	393	454	183	264
Cr	215	398	190	348	205	337	282	268	242	389	348
Co	64	67	72	54	73	60	65	74	61	61	59
Ni	88	171	93	176	204	235	177	211	191	248	131
Rb	4	1	13	12	2	4	5	5	20	27	74
Sr	126	125	202	148	234	417	114	86	143	144	46
Cs	0	0	1	0	0	0	0	0	0	0	5
Ba	66	16	131	134	28	74	56	83	134	252	48
Sc	53	44	35	40	26	39	33	35	35	29	52
V	398	204	263	259	191	267	224	241	243	188	318
Ta	0.29	0.21	0.31	0.14	0.25	0.38	0.15	0.26	0.30	0.10	0.09
Nb	3.86	2.16	3.54	1.44	2.73	7.67	2.25	3.93	4.85	1.56	1.28
Zr	82	43	61	39	44	85	51	55	71	30	47
Hf	2.30	1.14	1.61	1.11	1.28	2.32	1.50	1.60	2.14	0.82	1.32
Th	1.57	1.44	1.15	1.15	2.51	2.21	1.08	0.64	1.30	0.67	0.53
U	0.10	0.08	0.16	0.09	0.12	0.31	0.11	0.10	0.30	0.05	0.06
Y	27.69	13.72	17.10	18.08	11.44	22.45	16.40	14.42	19.69	10.11	17.77
La	4.65	3.46	5.84	2.59	4.49	11.50	2.81	4.33	6.12	1.91	2.20
Ce	12.75	8.43	13.69	6.84	11.16	27.44	7.46	11.29	15.11	5.05	5.59
Pr	1.83	1.11	1.83	0.95	1.56	3.43	1.10	1.60	2.08	0.72	0.81
Nd	8.56	5.15	7.97	5.31	7.20	13.93	6.08	7.95	9.24	3.54	4.17
Sm	2.80	1.55	2.14	1.82	1.86	3.34	2.10	2.42	2.53	1.17	1.63
Eu	0.99	0.61	0.86	0.81	0.88	1.22	0.70	0.82	0.86	0.51	0.57
Gd	3.94	2.19	3.27	3.01	2.32	3.63	2.88	2.83	3.30	1.63	2.35
Tb	0.66	0.36	0.49	0.46	0.34	0.61	0.44	0.45	0.55	0.25	0.45
Dy	4.57	2.29	3.14	3.23	2.11	3.92	2.90	2.76	3.61	1.64	3.11
Ho	1.07	0.50	0.66	0.71	0.42	0.85	0.61	0.54	0.80	0.35	0.66
Er	3.10	1.28	1.79	2.08	1.19	2.31	1.66	1.49	2.05	0.99	1.96
Tm	0.45	0.19	0.26	0.32	0.17	0.34	0.26	0.24	0.32	0.15	0.31
Yb	3.00	1.18	1.56	2.02	1.12	2.06	1.62	1.36	1.85	0.83	2.05
Lu	0.45	0.16	0.27	0.34	0.16	0.30	0.26	0.21	0.30	0.11	0.31
Cu	159	154	217	77	136	62	115	46	86	101	45
Zn	136	76	96	171	66	117	81	139	111	68	83
Mo	0.71	0.55	0.25	0.81	0.35	0.46	0.57	0.45	4.59	1.98	0.92
Ag	0.62	0.99	0.29	0.23	0.19	0.25	0.06	0.19	0.43	0.19	0.16
Tl	1.26	0.52	0.54	1.17	0.74	0.06	-	0.02	0.10	0.04	0.57
Pb	0.32	1.94	1.32	1.21	0.48	2.99	0.99	1.47	2.92	3.12	1.42
Sn	-	-	-	-	-	0.84	0.61	0.63	1.19	0.32	0.32
Sb	-	-	-	-	-	0.27	1.61	0.30	1.12	1.03	0.06
	SB95-1	SB95-4	SB95-5	SB95-6	SB95-18	SB95-20	SB95-21	SB95-23	SB95-26	SB95-27	SB95-35
(La/Yb)n	1.11	2.11	2.68	0.92	2.88	4.00	1.24	2.29	2.37	1.65	0.77
(La/Sm)n	1.07	1.44	1.76	0.92	1.55	2.22	0.86	1.16	1.56	1.05	0.87
(Gd/Yb)n	1.09	1.54	1.73	1.23	1.71	1.46	1.47	1.72	1.47	1.62	0.95
(La/Y)n	1.11	1.67	2.26	0.95	2.60	3.39	1.13	1.99	2.06	1.25	0.82
(Tb/Yb)n	1.01	1.41	1.44	1.03	1.38	1.34	1.24	1.52	1.36	1.36	0.99
(Tb/Y)n	1.01	1.11	1.21	1.06	1.24	1.14	1.13	1.32	1.18	1.03	1.06
(Eu/Eu*)n	0.91	1.02	1.00	1.05	1.30	1.06	0.87	0.96	0.91	1.12	0.88
Al_2O_3/TiO_2	12	27	15	21	25	13	22	18	20	33	24
Zr/Hf	36	38	38	36	35	37	34	35	33	37	36
La/Nb	1.20	1.60	1.65	1.79	1.64	1.50	1.25	1.10	1.26	1.23	1.72
Th/Nb	0.41	0.66	0.32	0.79	0.92	0.29	0.48	0.16	0.27	0.43	0.41
Th/La	0.34	0.41	0.20	0.44	0.56	0.19	0.38	0.15	0.21	0.35	0.24
Zr/Y	2.96	3.16	3.56	2.17	3.86	3.78	3.13	3.83	3.59	2.97	2.65
Ti/Zr	88	81	95	120	92	95	80	90	70	95	83
Ti/Sm	2592	2262	2715	2591	2170	2406	1967	2066	1958	2427	2389
P/Nd	63	33	51	43	46	56	59	49	49	52	63
Ti/V	18	17	22	18	21	30	18	21	20	15	12
Sc/La	117	279	132	116	160	131	130	171	117	253	168
Nb/Nb*	0.85	0.57	0.53	0.55	0.56	0.59	0.80	0.88	0.73	0.80	0.55
Zr/Zr*	1.16	1.06	1.02	0.88	0.84	0.86	0.99	0.87	1.01	1.02	1.25
Hf/Hf*	1.18	1.02	0.98	0.89	0.88	0.85	1.05	0.91	1.11	1.01	1.27
Ti/Ti*	0.86	0.75	0.87	0.80	0.77	0.91	0.66	0.76	0.68	0.81	0.79
UTM Zone	15	15	15	15	15	15	15	15	15	15	15
Easting	500619	515001	518972	516843	517249	520991	519065	521992	523217	521948	517445
Northing	5647239	5655576	5656148	5655261	5658094	5663938	5664014	5667642	5667035	5665952	5663524

Birch-Uchi belt - Calc alkaline

	SB95-43	SL87-05	SL88-09	SB95-34	SB95-3	SB95-17	SH87-12
SiO_2	51.98	49.95	49.82	52.84	55.06	55.61	61.78
TiO_2	0.45	0.57	0.60	0.79	0.64	0.69	0.60
Al_2O_3	17.75	18.02	16.61	17.25	19.38	17.50	16.42
Fe_2O_3	9.82	10.54	13.22	10.73	7.90	9.28	6.60
MnO	0.29	0.27	0.28	0.18	0.11	0.15	0.11
MgO	4.41	8.57	7.71	6.18	4.18	4.53	2.23
CaO	10.02	8.09	10.33	9.07	8.51	8.37	4.96
K_2O	0.05	0.05	0.00	0.06	0.28	0.53	1.62
Na_2O	5.20	3.90	1.38	2.83	3.81	3.23	5.49
P_2O_5	0.03	0.04	0.05	0.05	0.13	0.11	0.21
LOI	5.54	3.74	8.11	7.41	4.33	7.12	7.18
Mg#	50	64	56	56	54	52	43
Tl	2325	1744	1674	5069	1885	4097	3495
P	103	238	313	301	604	533	1155
Cr	171	496	392	459	57	147	15
Co	43	78	70	70	41	47	20
Ni	91	273	221	163	78	110	7
Rb	1	1	0	2	5	12	36
Sr	210	184	303	101	612	262	202
Cs	0	0	0	0	0	0	1
Ba	45	59	12	24	81	138	226
Sc	32	42	30	71	20	21	14
V	146	262	187	393	124	167	119
Ta	0.18	0.22	0.19	0.09	0.29	0.48	0.54
Nb	2.45	2.98	3.30	1.56	4.81	4.95	6.89
Zr	34	47	43	48	77	89	137
Hf	0.86	1.22	1.09	1.41	1.98	1.79	3.71
Th	1.02	1.19	0.97	0.65	2.05	4.87	9.37
U	0.36	0.36	0.26	0.08	0.25	0.88	2.61
Y	9.00	10.59	12.73	22.53	12.53	13.74	14.75
La	3.34	4.66	5.33	2.14	9.26	13.97	28.00
Ce	7.98	9.82	12.02	5.67	21.95	28.36	56.29
Pr	0.99	1.40	1.48	0.82	2.69	3.13	6.07
Nd	4.38	6.17	6.21	4.93	11.61	11.48	23.28
Sm	1.26	1.65	1.70	1.60	2.37	2.47	4.57
Eu	0.40	0.74	0.64	0.66	0.87	0.77	1.16
Gd	1.45	1.79	2.01	2.70	2.51	2.24	3.25
Tb	0.24	0.28	0.32	0.49	0.33	0.35	0.42
Dy	1.49	1.86	2.02	3.57	2.13	2.23	2.56
Ho	0.33	0.37	0.43	0.83	0.45	0.48	0.51
Er	0.86	0.95	1.17	2.34	1.22	1.36	1.44
Tm	0.13	0.16	0.17	0.38	0.18	0.20	0.20
Yb	0.76	0.90	1.10	2.13	1.18	1.26	1.34
Lu	0.12	0.13	0.16	0.33	0.20	0.18	0.19
Cu	95	129	131	154	55	45	20
Zn	57	88	79	101	62	76	79
Mo	7.64	12.87	0.61	0.20	0.40	0.45	0.94
Ag	0.17	0.11	0.18	0.13	0.32	0.40	0.50
Tl	0.01	-	-	0.00	0.64	0.58	0.47
Pb	1.40	1.07	1.84	1.05	1.98	0.24	11.42
Sn	0.40	0.67	0.65	0.55	-	-	1.38
Sb	0.65	0.44	1.55	0.42	-	-	1.10
	SB95-43	**SL87-05**	**SL88-09**	**SB95-34**	**SB95-3**	**SB95-17**	**SH87-12**
(La/Yb)n	3.15	3.70	3.47	0.72	5.63	7.92	14.98
(La/Sm)n	1.72	1.82	2.03	0.86	2.52	3.65	3.96
(Gd/Yb)n	1.57	1.63	1.51	1.05	1.76	1.46	2.00
(La/Y)n	2.46	2.91	2.77	0.63	4.90	6.73	12.57
(Tb/Yb)n	1.45	1.41	1.34	1.06	1.29	1.27	1.42
(Tb/Y)n	1.13	1.11	1.07	0.92	1.12	1.08	1.19
(Eu/Eu*)n	0.91	1.30	1.05	0.96	1.08	0.98	0.87
AL_2O_3/TiO_2	45	28	27	20	29	26	28
Zr/Hf	39	38	39	34	39	49	37
La/Nb	1.36	1.56	1.62	1.37	1.92	2.82	4.06
Th/Nb	0.42	0.40	0.30	0.42	0.43	0.98	1.36
Th/La	0.31	0.26	0.18	0.30	0.22	0.35	0.33
Zr/Y	3.74	4.44	3.37	2.14	6.17	6.45	9.29
Ti/Zr	69	80	86	105	50	46	26
Ti/Sm	1851	2269	2163	3167	1640	1655	765
Pr/Nd	23	39	50	61	52	46	50
Ti/V	16	14	20	13	31	24	29
Sc/La	279	311	184	212	102	116	74
Nb/Nb*	0.66	0.50	0.52	0.72	0.46	0.27	0.18
Zr/Zr*	0.99	1.02	0.91	1.19	1.02	1.15	0.92
Hf/Hf*	0.91	0.96	0.84	1.26	0.95	0.84	0.90
Ti/Ti*	0.68	0.86	0.79	0.97	0.63	0.69	0.36
UTM Zone	15	15	15	15	15	15	15
Easting	518674	519250	519250	516632	514558	515260	522650
Northing	5672504	5673400	5677800	5662222	5655205	5656332	5682400

Birch-Uchi belt - Felsic

	SB95-10	SB95-19	SB95-9	SL87-02	SH87-02	SH87-04	SH87-09	SH88-13	SH87-07	SB95-25	SB95-29
SiO_2	63.65	63.89	64.42	66.01	68.18	69.39	69.75	69.76	69.89	70.14	70.21
TiO_2	0.64	0.70	0.68	0.76	0.78	0.47	0.69	0.68	0.42	0.42	0.40
Al_2O_3	15.52	14.86	16.05	11.70	11.47	10.36	10.67	10.72	14.06	12.35	12.33
Fe_2O_3	5.83	8.01	4.88	9.01	9.93	10.46	9.67	10.23	3.52	8.05	7.93
MnO	0.15	0.12	0.07	0.16	0.16	0.39	0.14	0.17	0.05	0.15	0.17
MgO	2.35	3.82	2.72	2.84	1.16	0.75	1.34	1.32	1.73	0.82	0.78
CaO	4.99	3.95	5.24	5.46	3.40	5.15	3.47	3.43	3.94	2.82	3.48
K_2O	3.36	1.62	1.33	0.11	1.98	2.82	0.49	1.00	1.53	0.50	0.44
Na_2O	3.34	2.93	4.45	3.85	2.77	0.13	3.62	2.52	4.74	4.70	4.71
P_2O_5	0.15	0.08	0.15	0.11	0.18	0.10	0.17	0.17	0.11	0.06	0.06
LOI	2.67	1.63	0.50	5.65	5.49	6.32	3.84	4.22	4.28	2.83	0.60
Mg#	47	51	55	41	20	14	23	22	52	18	7
Ti	3952	4294	4034	4629	4599	2577	4624	4424	2263	1912	2236
P	663	431	667	553	977	382	1090	1042	597	232	225
Cr	40	105	48	72	2	1	2	1	77	4	14
Co	25	40	23	24	15	5	15	14	14	8	9
Ni	42	56	42	27	1	1	1	2	47	1	2
Rb	74	64	30	1	35	60	11	24	44	9	9
Sr	270	106	268	44	87	182	100	112	225	88	292
Cs	2	1	1	0	1	1	0	1	3	0	1
Ba	740	335	718	26	395	648	169	138	412	116	212
Sc	13	19	13	16	18	10	19	19	8	8	9
V	90	132	94	83	4	2	3	3	67	1	1
Ta	0.94	0.93	0.91	1.29	1.75	2.06	1.66	1.69	0.20	1.35	1.39
Nb	10.38	8.46	10.78	19.49	31.62	34.14	29.31	30.03	2.97	22.11	22.83
Zr	159	151	178	387	507	545	468	481	103	515	439
Hf	4.15	2.70	4.46	11.48	13.95	14.64	13.40	12.80	2.71	10.94	10.13
Th	6.13	6.64	5.99	3.67	5.72	6.93	5.55	5.41	2.70	4.02	4.34
U	1.41	2.05	1.44	0.87	1.46	1.61	1.36	1.33	0.73	0.93	1.05
Y	22.41	22.97	25.10	78.25	129.07	138.55	120.33	127.01	5.89	116.78	101.39
La	23.33	21.49	25.91	22.57	41.29	43.05	18.99	41.21	13.49	29.99	12.94
Ce	49.89	43.27	56.87	53.07	101.94	107.28	97.28	103.30	27.14	74.86	76.18
Pr	5.45	4.67	6.21	8.07	13.40	14.18	13.04	13.67	3.06	10.06	9.82
Nd	21.20	17.45	23.74	36.93	60.03	61.79	59.81	61.43	11.59	43.99	43.62
Sm	4.34	3.80	5.16	10.48	16.47	16.74	17.24	16.44	2.04	12.02	13.01
Eu	1.04	0.84	1.37	2.41	3.91	3.06	4.08	3.73	0.67	3.70	3.78
Gd	4.27	3.88	4.99	12.29	19.50	19.94	18.95	18.34	1.59	15.50	16.04
Tb	0.63	0.61	0.71	2.10	3.28	3.37	3.05	3.17	0.22	2.61	2.67
Dy	4.06	3.71	4.37	14.35	22.77	22.76	20.50	20.24	1.09	18.26	18.31
Ho	0.82	0.80	0.91	3.10	5.00	5.03	4.26	4.51	0.21	4.07	3.84
Er	2.45	2.24	2.45	9.11	14.93	15.13	12.44	13.01	0.56	11.86	11.50
Tm	0.37	0.32	0.38	1.40	2.33	2.34	2.00	2.03	0.07	1.71	1.79
Yb	2.40	2.10	2.37	9.23	14.95	14.91	13.02	13.80	0.51	11.01	11.29
Lu	0.36	0.32	0.35	1.43	2.29	2.30	1.97	2.05	0.06	1.68	1.74
Cu	35	69	31	132	13	6	23	8	18	2	10
Zn	82	88	74	227	173	129	113	127	36	92	427
Mo	4.92	2.60	0.78	1.13	2.05	1.96	11.76	4.26	1.69	0.70	3.22
Ag	1.18	0.80	0.64	1.25	1.49	2.57	1.45	1.42	0.31	1.04	1.37
Tl	1.64	1.54	1.69	-	0.17	0.24	0.05	0.13	0.29	0.02	0.06
Pb	0.40	0.19	0.54	11.65	3.21	4.25	3.38	3.53	6.75	3.12	4.54
Sn	-	-	-	2.02	4.22	4.54	3.22	3.67	0.50	1.20	2.93
Sb	-	-	-	0.57	1.11	0.73	0.82	0.72	2.29	0.07	0.24
	SB95-10	SB95-19	SB95-9	SL87-02	SH87-02	SH87-04	SH87-09	SH88-13	SH87-07	SB95-25	SB95-29
(La/Yb)n	6.96	7.32	7.83	1.75	1.98	2.07	2.15	2.14	18.92	1.95	2.09
(La/Sm)n	3.47	3.65	3.25	1.39	1.62	1.66	1.46	1.62	4.26	1.61	1.64
(Gd/Yb)n	1.47	1.53	1.74	1.10	1.08	1.11	1.20	1.10	2.57	1.16	1.17
(La/Y)n	6.90	6.20	6.84	1.91	2.12	2.06	2.15	2.15	15.16	1.70	2.15
(Tb/Yb)n	1.18	1.32	1.37	1.03	1.00	1.03	1.07	1.04	1.95	1.08	1.07
(Tb/Y)n	1.17	1.11	1.19	1.13	1.07	1.02	1.07	1.05	1.56	0.94	1.10
(Eu/Eu*)n	0.73	0.67	0.81	0.65	0.67	0.51	0.69	0.65	1.09	0.83	0.80
Al_2O_3/TiO_2	23	20	24	15	15	24	14	15	37	38	33
Zr/Hf	38	56	40	34	36	37	35	38	38	47	43
La/Nb	2.25	2.54	2.40	1.16	1.31	1.26	1.33	1.37	4.54	1.36	1.44
Th/Nb	0.59	0.78	0.56	0.19	0.18	0.20	0.19	0.18	0.91	0.18	0.19
Th/La	0.26	0.31	0.23	0.16	0.14	0.16	0.14	0.13	0.20	0.13	0.13
Zr/Y	7.07	6.59	7.09	4.95	3.93	3.93	3.89	3.79	17.43	4.41	4.33
Ti/Zr	25	28	23	12	9	5	10	9	22	4	5
Ti/Sm	910	1129	782	442	279	154	268	269	1107	161	172
P/Nd	31	25	28	15	16	6	18	17	51	5	5
Ti/V	44	33	43	56	1193	1506	1445	1685	34	1739	2039
Sc/La	35	61	38	11	8	4	9	9	135	5	5
Nb/Nb*	0.35	0.30	0.34	0.76	0.71	0.74	0.70	0.68	0.17	0.69	0.60
Zr/Zr*	1.14	1.29	1.11	1.36	1.12	1.17	1.01	1.05	1.46	1.55	1.27
Hf/Hf*	1.08	0.83	1.01	1.46	1.11	1.14	1.05	1.01	1.40	1.19	1.07
Ti/Ti*	0.36	0.44	0.31	0.16	0.10	0.06	0.10	0.10	0.50	0.06	0.06
UTM Zone	15	15	15	15	15	15	15	15	15	15	15
Easting	524500	518600	524500	519550	522550	522350	522250	522450	527100	522955	521947
Northing	5654450	5659430	5654450	5673750	5681600	5681550	5680750	5680700	5682750	5669240	5662139

Birch-Uchi belt - Felsic

	SH88-14	SB95-28	SL88-08	SH88-16	SL88-16	SB95-24	SB95-49	SL88-11	SL88-07	SB95-16	SB95-44
SiO_2	70.41	71.72	72.66	72.67	72.76	73.19	73.28	74.01	74.17	74.81	75.05
TiO_2	0.73	0.56	0.58	0.73	0.58	0.53	0.40	0.48	0.43	0.22	0.67
Al_2O_3	10.78	11.25	11.11	11.16	11.36	11.09	10.95	10.80	11.06	11.95	10.57
Fe_2O_3	9.31	7.57	6.99	7.44	6.64	6.78	7.16	6.02	6.47	1.75	5.00
MnO	0.13	0.13	0.08	0.06	0.09	0.14	0.13	0.08	0.08	0.03	0.13
MgO	1.33	0.98	1.39	0.98	1.52	0.52	0.59	0.53	0.56	0.46	0.53
CaO	2.52	2.92	1.88	1.69	1.68	2.34	2.89	1.20	1.79	1.93	2.94
K_2O	0.82	0.64	0.47	0.52	0.22	0.63	0.92	0.37	0.90	2.56	1.12
Na_2O	3.83	4.12	4.72	4.58	5.02	4.67	3.65	4.39	4.49	4.23	3.87
P_2O_5	0.16	0.10	0.13	0.17	0.13	0.11	0.04	0.12	0.04	0.06	0.12
LOI	2.72	2.30	4.33	2.72	2.30	1.06	3.57	4.49	3.20	1.94	1.57
Mg#	24	22	30	22	34	15	15	16	16	17	19
Ti	3749	3399	3404	4410	3394	2472	2286	2622	2685	1180	3377
P	737	438	596	992	558	306	149	489	237	264	163
Cr	2	10	8	5	6	6	3	4	10	7	11
Co	11	11	10	9	9	9	4	8	8	6	7
Ni	2	4	2	1	2	2	0	2	5	3	1
Rb	15	8	6	9	5	15	20	8	18	86	19
Sr	99	104	54	99	95	101	77	131	80	196	92
Cs	1	0	0	1	0	1	0	0	1	2	0
Ba	237	229	168	151	93	58	183	124	121	610	177
Sc	15	12	10	17	11	14	6	9	7	3	10
V	2	3	8	3	7	4	0	4	4	15	3
Ta	1.65	1.70	1.97	1.76	2.05	1.58	1.82	1.93	2.39	0.60	1.99
Nb	27.18	26.95	31.10	31.95	32.13	22.23	30.15	37.33	39.24	5.28	29.93
Zr	433	521	555	511	537	423	599	616	702	103	523
Hf	12.53	12.13	16.57	13.88	16.68	11.69	15.30	15.53	20.40	2.87	16.00
Th	5.42	4.69	6.71	5.64	6.80	4.98	5.84	6.54	8.38	7.94	6.69
U	1.34	1.19	1.65	1.35	1.65	1.13	1.26	1.65	2.07	1.65	1.69
Y	117.26	110.39	152.53	97.07	137.88	94.02	65.91	131.47	162.85	5.58	142.82
La	37.17	31.40	44.94	39.58	46.82	29.85	36.45	43.85	55.98	17.72	51.36
Ce	95.15	77.51	109.77	99.93	104.22	74.36	90.00	107.57	137.49	32.29	126.60
Pr	12.79	10.03	14.50	13.48	14.91	10.29	11.62	14.08	17.93	3.06	16.35
Nd	57.56	44.88	66.02	60.81	67.98	46.41	53.59	64.08	78.21	10.68	72.01
Sm	16.40	13.12	18.04	16.27	18.26	13.24	14.75	17.18	21.15	1.73	18.52
Eu	3.95	3.36	3.82	3.89	3.85	2.81	2.99	3.54	3.72	0.40	3.49
Gd	18.95	16.78	21.39	17.85	21.11	16.17	13.08	19.60	24.57	1.36	21.20
Tb	3.29	2.85	3.78	2.92	3.60	2.86	1.92	3.22	4.25	0.17	3.89
Dy	22.17	19.55	25.58	18.22	25.10	18.48	12.67	21.57	28.58	0.97	24.52
Ho	4.86	4.26	5.78	4.09	5.25	4.09	2.64	4.61	6.34	0.19	5.51
Er	14.19	12.28	16.76	11.63	16.08	12.10	8.48	13.87	18.76	0.49	16.37
Tm	2.15	1.95	2.39	1.83	2.35	1.81	1.60	2.16	2.88	0.07	2.43
Yb	14.27	12.18	15.92	11.79	15.81	11.81	11.00	14.58	18.99	0.42	16.69
Lu	2.09	1.85	2.46	1.81	2.47	1.77	1.85	2.17	2.92	0.06	2.46
Cu	14	6	5	8	8	5	29	6	7	8	20
Zn	236	108	88	135	124	112	382	148	139	28	50
Mo	2.01	3.13	1.38	2.27	0.59	2.18	2.40	2.92	2.54	0.14	25.80
Ag	1.17	2.01	2.77	1.35	1.45	1.25	2.61	2.47	3.89	0.40	2.35
Tl	0.08	0.02	0.01	0.04	0.01	0.06	0.08	0.00	0.06	0.73	0.13
Pb	4.95	2.44	3.37	2.49	3.37	3.05	9.18	3.39	5.23	0.12	3.00
Sn	3.85	3.24	4.55	3.69	4.42	3.13	3.83	4.16	6.05	-	4.95
Sb	0.69	0.15	3.15	0.79	0.82	0.60	0.18	2.61	1.46	-	0.38
	SH88-14	SB95-28	SL88-08	SH88-16	SL88-16	SB95-24	SB95-49	SL88-11	SL88-07	SB95-16	SB95-44
(La/Yb)n	1.87	1.85	2.02	2.41	2.12	1.81	2.38	2.16	2.11	30.39	2.21
(La/Sm)n	1.46	1.55	1.61	1.57	1.66	1.46	1.60	1.65	1.71	6.60	1.79
(Gd/Yb)n	1.10	1.14	1.11	1.25	1.10	1.13	0.98	1.11	1.07	2.68	1.05
(La/Y)n	2.10	1.88	1.95	2.70	2.25	2.10	3.66	2.21	2.28	21.04	2.38
(Tb/Yb)n	1.05	1.07	1.08	1.13	1.04	1.10	0.79	1.00	1.02	1.88	1.06
(Tb/Y)n	1.18	1.09	1.04	1.26	1.10	1.28	1.22	1.03	1.10	1.30	1.14
(Eu/Eu*)n	0.68	0.69	0.59	0.70	0.60	0.59	0.64	0.59	0.50	0.76	0.54
AL_2O_3/TiO_2	17	20	19	15	20	26	29	25	24	70	19
Zr/Hf	35	43	33	37	32	36	39	40	34	36	33
La/Nb	1.37	1.17	1.36	1.24	1.46	1.34	1.21	1.17	1.43	3.36	1.72
Th/Nb	0.20	0.17	0.20	0.18	0.21	0.22	0.19	0.18	0.21	1.50	0.22
Th/La	0.15	0.15	0.15	0.14	0.15	0.17	0.16	0.15	0.15	0.45	0.13
Zr/Y	3.69	4.72	3.64	5.26	3.90	4.50	9.09	4.69	4.31	18.47	3.66
Ti/Zr	9	7	6	9	6	6	4	4	4	11	6
Ti/Sm	229	259	189	271	186	187	155	153	127	681	182
P/Nd	13	10	9	16	8	7	3	8	3	25	5
Ti/V	1716	1221	414	1623	453	574	8487	619	685	77	1081
Sc/La	7	7	4	9	4	8	3	4	2	52	4
Nb/Nb*	0.70	0.79	0.67	0.76	0.57	0.69	0.76	0.78	0.64	0.20	0.54
Zr/Zr*	0.98	1.49	1.11	1.12	1.06	1.18	1.47	1.29	1.19	1.66	0.99
Hf/Hf*	1.02	1.25	1.20	1.11	1.19	1.18	1.37	1.17	1.26	1.67	1.10
Ti/Ti*	0.08	0.09	0.07	0.10	0.07	0.07	0.07	0.06	0.05	0.30	0.07
UTM Zone	15	15	15	15	15	15	15	15	15	15	15
Easting	525500	521569	519450	522800	523650	521741	523596	522750	522350	514197	523084
Northing	5682700	5662301	5678900	56815500	5679250	5670215	5659637	5678800	5678500	5655891	5660913

Birch-Uchi belt - Felsic

	SB95-50	SB95-14	SB95-2	SB95-7	SB95-13	SB95-47	SB95-8	SB95-51	SB95-48	SB95-11	SB95-12	SB95-15
SiO_2	75.33	76.37	76.44	76.50	76.78	77.07	77.77	77.97	79.20	79.34	79.36	79.70
TiO_2	0.47	0.30	0.17	0.18	0.47	0.48	0.16	0.09	0.19	0.40	0.38	0.39
Al_2O_3	11.24	10.95	11.45	15.15	10.70	10.07	11.52	11.79	10.72	11.13	11.16	9.52
Fe_2O_3	4.69	5.47	2.91	1.36	4.99	4.96	3.21	2.62	2.89	2.58	1.52	1.66
MnO	0.15	0.12	0.08	0.03	0.11	0.05	0.11	0.03	0.06	0.02	0.03	0.11
MgO	0.45	0.65	0.53	1.07	0.76	4.03	1.11	0.37	0.34	0.20	0.26	0.23
CaO	1.35	1.20	1.39	0.16	1.57	0.03	1.75	0.32	1.17	0.80	0.98	1.31
K_2O	0.92	1.49	5.11	5.41	1.97	1.09	3.45	1.76	1.02	1.68	1.67	1.82
Na_2O	5.34	3.43	1.90	0.13	2.60	0.18	0.93	4.72	4.39	3.81	4.59	3.22
P_2O_5	0.07	0.02	0.02	0.00	0.04	0.04	0.00	0.03	0.02	0.04	0.03	0.04
LOI	2.09	2.20	1.21	2.25	3.04	2.93	1.47	0.96	1.37	0.60	1.32	2.62
Mg#	17	21	29	63	25	56	43	23	20	15	28	23
Ti	2903	1772	1140	1189	2617	2170	914	2332	1341	2285	2240	2444
P	282	97	94	48	213	131	51	0	67	139	107	184
Cr	14	4	12	5	13	4	6	2	6	6	10	9
Co	4	9	6	3	7	7	5	2	2	4	2	3
Ni	2	0	2	3	1	1	2	1	1	1	0	1
Rb	21	26	96	83	32	17	72	31	22	32	22	16
Sr	73	90	54	16	49	6	44	44	88	64	45	71
Cs	0	1	0	1	1	0	1	0	1	2	0	0
Ba	328	485	979	891	405	185	588	400	292	415	421	476
Sc	10	5	4	3	9	10	3	7	3	6	8	7
V	3	0	5	2	1	0	1	1	1	1	0	0
Ta	1.80	1.96	2.01	4.89	3.33	2.34	3.99	1.82	2.11	2.40	3.76	2.64
Nb	29.27	49.31	26.33	62.77	40.30	38.85	55.17	48.46	33.92	34.84	49.22	37.71
Zr	580	656	278	669	713	821	916	936	389	421	944	707
Hf	14.30	14.90	5.20	17.99	13.48	18.76	9.88	23.57	10.98	9.09	15.76	16.58
Th	5.28	10.43	12.46	12.68	7.55	7.37	11.70	8.96	10.65	5.75	9.03	7.71
U	1.24	2.35	3.75	3.71	1.74	1.82	2.79	0.67	1.79	1.53	2.30	1.71
Y	115.41	183.44	38.61	146.06	153.86	220.90	223.52	238.67	211.40	114.13	156.77	142.61
La	35.66	71.63	53.98	117.95	53.99	75.05	91.06	71.08	81.09	47.15	66.41	45.29
Ce	90.32	176.66	117.13	276.18	133.74	195.12	212.27	171.49	199.16	116.91	169.42	109.50
Pr	11.93	24.55	13.02	31.76	17.77	25.74	25.87	21.61	25.57	14.76	23.45	14.06
Nd	54.03	105.68	49.55	133.32	74.25	112.98	111.63	96.64	115.22	61.85	103.45	61.94
Sm	15.27	27.76	9.32	30.78	18.64	28.39	28.62	24.80	28.74	16.35	27.99	16.60
Eu	3.22	4.33	1.55	3.74	3.86	6.10	3.36	4.72	3.52	3.67	4.51	3.87
Gd	17.92	28.95	8.30	31.13	23.55	32.34	35.88	32.63	32.53	20.60	31.33	19.41
Tb	3.05	4.54	1.06	4.60	3.70	5.40	5.81	5.59	5.17	3.34	4.62	3.42
Dy	20.42	32.56	6.56	30.06	27.25	34.45	40.14	39.67	34.30	21.54	33.17	23.28
Ho	4.52	6.76	1.35	6.21	5.87	7.24	9.14	8.66	7.68	4.57	6.90	4.98
Er	13.16	19.54	3.88	18.03	16.68	21.39	27.42	25.24	21.36	12.26	19.13	14.69
Tm	2.13	3.35	0.63	2.90	2.74	3.08	4.17	3.74	3.11	1.81	3.03	2.25
Yb	13.90	20.09	4.02	19.77	16.09	20.46	27.47	23.26	19.36	10.85	18.46	14.60
Lu	2.14	3.23	0.64	3.18	2.60	3.14	4.19	3.71	2.82	1.70	3.10	2.17
Cu	16	3	11	5	3	3	13	7	2	6	16	9
Zn	284	125	53	66	31	129	59	99	79	64	73	147
Mo	2.34	3.08	3.00	1.91	2.81	4.23	1.67	2.93	0.66	1.57	3.49	3.25
Ag	2.80	2.93	1.38	2.69	2.86	2.55	2.58	3.97	1.67	1.97	3.92	2.89
Tl	0.15	4.45	2.89	14.06	5.66	0.07	9.47	0.05	0.08	5.01	6.25	4.87
Pb	85.19	0.22	2.89	0.40	0.26	3.05	0.31	3.50	3.41	0.33	0.39	0.37
Sn	4.26	-	-	-	-	7.21	-	7.82	4.53	-	-	-
Sb	0.29	-	-	-	-	0.14	-	0.18	0.09	-	-	-
	SB95-50	SB95-14	SB95-2	SB95-7	SB95-13	SB95-47	SB95-8	SB95-51	SB95-48	SB95-11	SB95-12	SB95-15
(La/Yb)n	1.84	2.56	9.63	4.28	2.41	2.63	2.38	2.19	3.00	3.11	2.58	2.22
(La/Sm)n	1.51	1.67	3.74	2.48	1.87	1.71	2.06	1.85	1.82	1.86	1.53	1.76
(Gd/Yb)n	1.07	1.19	1.71	1.30	1.21	1.31	1.08	1.16	1.39	1.57	1.40	1.10
(La/Y)n	2.05	2.59	9.26	5.35	2.32	2.25	2.70	1.97	2.54	2.74	2.81	2.10
(Tb/Yb)n	1.00	1.03	1.20	1.06	1.05	1.20	0.96	1.09	1.21	1.40	1.14	1.06
(Tb/Y)n	1.11	1.04	1.16	1.32	1.01	1.03	1.09	0.98	1.03	1.23	1.24	1.01
(Eu/Eu*)n	0.59	0.46	0.53	0.37	0.56	0.61	0.32	0.51	0.35	0.61	0.46	0.60
AL_2O_3/TiO_2	23	37	60	76	24	28	75	30	48	29	30	23
Zr/Hf	41	44	53	37	53	44	52	40	35	46	60	43
La/Nb	1.22	1.45	2.05	1.88	1.34	1.93	1.65	1.47	2.39	1.35	1.35	1.20
Th/Nb	0.18	0.21	0.47	0.20	0.19	0.19	0.21	0.18	0.31	0.17	0.18	0.20
Th/La	0.15	0.15	0.23	0.11	0.14	0.10	0.13	0.13	0.13	0.12	0.14	0.17
Zr/Y	5.03	3.58	7.19	4.58	4.63	3.72	2.31	3.92	1.84	3.69	6.02	4.96
Ti/Zr	5	3	4	2	4	3	2	2	3	5	2	3
Ti/Sm	190	64	122	39	140	76	32	94	47	140	80	147
P/Nd	5	1	2	0	3	1	0	0	1	2	1	3
Ti/V	970	10541	231	566	2738	8431	824	4529	965	3837	5988	7161
Sc/La	5	1	5	1	3	3	1	2	1	3	2	3
Nb/Nb*	0.78	0.63	0.39	0.46	0.69	0.50	0.53	0.61	0.38	0.68	0.71	0.75
Zr/Zr*	1.40	0.84	0.89	0.72	1.33	1.00	0.63	1.32	0.47	0.92	1.21	1.53
Hf/Hf*	1.25	0.69	0.61	0.70	0.91	0.83	0.44	1.21	0.48	0.72	0.73	1.30
Ti/Ti*	0.07	0.02	0.05	0.02	0.05	0.03	0.01	0.03	0.02	0.05	0.03	0.05
UTM Zone	15	15	15	15	15	15	15	15	15	15	15	15
Easting	523632	522735	513153	524500	522763	523420	524500	523431	523707	522614	522972	523258
Northing	5659611	5660505	5655053.00	5654450	5660997	5658242	5654450	5659482	5659877	5662025	5661346	5659341

Birch-Uchi - Altered felsics

	SB95-30	SB95-45	SB95-46
SiO_2	74.58	73.71	79.62
TiO_2	0.15	0.18	0.14
Al_2O_3	10.18	13.37	10.01
Fe_2O_3	8.94	5.26	6.02
MnO	0.05	0.05	0.06
MgO	4.45	1.08	2.14
CaO	0.45	0.11	0.03
K_2O	1.09	1.76	1.72
Na_2O	0.12	2.45	0.27
P_2O_5	0.00	0.02	0.00
LOI	3.52	2.88	2.62
Mg#	52	56	44
Ti	861	832	512
P	116	35	76
Cr	7	2	1
Co	14	5	5
Ni	6	0	0
Rb	21	29	22
Sr	10	99	9
Cs	0	1	0
Ba	398	291	369
Sc	3	2	2
V	5	3	0
Ta	3.30	4.00	2.83
Nb	47.84	61.02	47.12
Zr	417	515	417
Hf	15.25	17.83	12.70
Th	9.82	12.73	8.74
U	2.45	2.40	2.32
Y	124.56	171.59	89.12
La	17.09	3.83	0.82
Ce	43.87	11.15	2.50
Pr	6.00	1.83	0.40
Nd	29.49	11.02	2.35
Sm	10.24	6.66	1.81
Eu	1.05	0.75	0.21
Gd	13.58	17.60	5.87
Tb	2.90	4.37	1.53
Dy	21.17	31.46	13.47
Ho	5.02	7.61	3.31
Er	14.66	22.16	11.84
Tm	2.34	3.88	2.04
Yb	15.09	25.76	14.22
Lu	2.27	3.87	2.31
Cu	5	6	22
Zn	327	63	3005
Mo	35.18	3.13	1.91
Ag	1.88	2.41	1.34
Tl	0.09	0.12	0.05
Pb	91.24	14.81	2.54
Se	5.70	9.15	23.23
Sb	0.46	0.21	0.19
	SB95-30	**SB95-45**	**SB95-46**
(La/Yb)n	0.81	0.11	0.04
(La/Sm)n	1.08	0.37	0.29
(Gd/Yb)n	0.74	0.56	0.34
(La/Y)n	0.91	0.15	0.06
(Tb/Yb)n	0.87	0.77	0.49
(Tb/Y)n	0.98	1.07	0.72
(Eu/Eu*)n	0.27	0.20	0.18
AL_2O_3/TiO_2	71	96	116
Zr/Hf	27	29	33
La/Nb	0.36	0.06	0.02
Th/Nb	0.21	0.21	0.19
Th/La	0.57	3.33	10.64
Zr/Y	3.35	3.00	4.67
Ti/Zr	2	2	1
Ti/Sm	84	125	283
P/Nd	4	3	32
Ti/V	184	256	1994
Sc/La	1	1	1
Nb/Nb*	2.68	17.32	65.26
Zr/Zr*	1.66	4.16	13.99
Hf/Hf*	2.20	5.22	15.46
Ti/Ti*	0.03	0.03	0.06
UTM Zone	15	15	15
Easting	522548	522986	523106
Northing	5660691	5658207	5657713

South Bay mine site DDH FIII

	SB95-4A	SB95-4B	SB95-4C	SB95-4D	SB95-4E	SB95-4F	SB95-4G	SB95-4H	SB95-4I
SiO_2	72.01	72.71	69.03	72.93	72.34	73.01	70.93	71.91	72.39
TiO_2	0.43	0.42	0.44	0.42	0.42	0.44	0.44	0.41	0.43
Al_2O_3	10.98	11.01	11.01	11.13	10.93	11.64	11.14	10.76	11.10
Fe_2O_3	7.88	7.79	6.68	6.64	7.26	6.11	7.47	7.11	7.51
MnO	0.11	0.12	0.14	0.11	0.12	0.09	0.12	0.14	0.15
MgO	1.13	0.91	0.45	0.49	0.92	0.62	0.50	0.59	0.58
CaO	3.09	2.09	6.94	2.97	2.71	2.33	4.14	4.34	2.67
K_2O	0.88	1.28	1.12	0.74	1.49	1.04	1.36	1.71	1.17
Na_2O	3.39	3.57	4.08	4.47	3.71	4.62	3.79	2.93	3.90
P_2O_5	0.10	0.10	0.10	0.09	0.10	0.10	0.10	0.09	0.10
LOI	1.32	0.55	4.55	2.51	1.21	1.11	1.83	2.09	1.42
Mg#	24	20	13	14	22	18	13	16	14
Ti	2352	2534	2540	2471	2325	2547	2313	2152	2311
P	318	373	364	346	322	367	280	266	312
Cr	4	13	8	6	4	8	8	5	3
Co	9	10	9	9	10	9	8	10	9
Ni	3	5	2	2	2	2	2	2	2
Rb	16	22	15	12	20	15	17	21	14
Sr	149	133	155	112	98	101	119	124	124
Cs	1	1	1	0	1	1	1	1	0
Ba	172	298	265	135	321	263	385	465	352
Sc	8	9	9	9	8	9	8	7	8
V	4	6	5	5	4	5	4	4	4
Ta	1.65	1.59	1.59	1.66	1.63	1.75	1.68	1.60	1.66
Nb	29.75	29.81	30.99	31.41	31.85	30.33	29.48	32.11	31.56
Zr	628	631	669	707	675	633	600	677	676
Hf	15.46	15.31	15.78	16.08	15.49	16.04	15.68	15.21	15.89
Th	4.97	4.99	4.84	5.04	4.92	5.28	5.36	4.93	5.03
U	1.25	1.28	1.22	1.28	1.27	1.31	1.38	1.28	1.31
Y	130.39	129.74	153.37	135.77	132.74	122.57	134.49	146.25	134.78
La	36.22	35.47	38.24	36.57	37.12	34.94	37.27	35.67	37.00
Ce	89.57	88.48	90.83	90.27	91.41	86.91	91.40	87.40	90.99
Pr	12.26	12.03	12.36	12.42	12.62	11.94	12.51	12.05	12.36
Nd	55.61	54.68	55.29	56.34	57.07	54.68	57.74	54.80	56.74
Sm	15.70	15.52	16.14	16.25	15.83	15.19	16.38	15.66	16.07
Eu	3.71	3.69	3.69	3.75	3.63	3.75	3.97	3.77	3.77
Gd	19.13	18.94	19.84	19.21	18.86	18.28	20.12	19.64	19.37
Tb	3.27	3.28	3.46	3.34	3.34	3.26	3.53	3.39	3.37
Dy	22.55	22.28	23.99	22.30	21.92	21.52	23.54	22.81	22.70
Ho	5.02	4.98	5.41	4.91	4.80	4.75	5.17	4.98	5.01
Er	14.72	14.27	16.32	14.54	14.16	14.02	15.16	14.78	14.49
Tm	2.29	2.20	2.59	2.23	2.22	2.14	2.36	2.26	2.25
Yb	14.25	14.39	16.64	14.81	14.43	14.04	14.86	14.21	14.53
Lu	2.18	2.10	2.53	2.21	2.13	2.04	2.29	2.14	2.18
Cu	22	24	26	14	17	20	28	69	10
Zn	165	109	109	154	161	173	272	71	127
Mo	1.62	1.52	2.01	2.93	1.59	1.46	1.53	1.81	1.52
Ag	1.32	1.26	1.35	1.40	1.21	1.38	1.32	1.33	1.21
Tl	0.12	0.13	0.05	0.08	0.13	0.11	0.11	0.14	0.12
Pb	5.37	4.60	5.14	4.20	4.37	4.52	7.49	12.40	4.50
Sn	4.15	3.79	3.51	3.79	4.58	3.36	6.29	2.87	15.69
Sb	0.29	0.32	0.31	0.18	0.27	0.28	0.31	0.54	0.22

	SB95-4A	SB95-4B	SB95-4C	SB95-4D	SB95-4E	SB95-4F	SB95-4G	SB95-4H	SB95-4I
(La/Yb)n	1.82	1.77	1.65	1.77	1.84	1.78	1.80	1.80	1.83
(La/Sm)n	1.49	1.48	1.53	1.45	1.52	1.49	1.47	1.47	1.49
(Gd/Yb)n	1.11	1.09	0.99	1.07	1.08	1.08	1.12	1.14	1.10
(La/Y)n	1.84	1.81	1.65	1.78	1.85	1.89	1.84	1.62	1.82
(Tb/Yb)n	1.04	1.04	0.95	1.03	1.05	1.05	1.08	1.08	1.05
(Tb/Y)n	1.05	1.06	0.95	1.03	1.06	1.12	1.10	0.97	1.05
(Eu/Eu*)n	0.65	0.66	0.63	0.65	0.64	0.69	0.67	0.66	0.65
Al_2O_3/TiO_2	28	26	26	27	28	27	29	30	28
Zr/Hf	41	41	42	44	44	39	38	45	43
La/Nb	1.22	1.19	1.23	1.16	1.17	1.15	1.26	1.11	1.17
Th/Nb	0.17	0.17	0.16	0.16	0.15	0.17	0.18	0.15	0.16
Th/La	0.14	0.14	0.13	0.14	0.13	0.15	0.14	0.14	0.14
Zr/Y	4.81	4.86	4.36	5.21	5.08	5.16	4.46	4.63	5.01
Ti/Zr	4	4	4	3	3	4	4	3	3
Ti/Sm	150	163	157	152	147	168	141	137	144
P/Nd	6	7	7	6	6	7	5	5	6
Ti/V	533	452	525	490	553	560	577	558	563
Sc/Lu	4	4	3	4	4	4	3	3	4
Nb/Nb*	0.76	0.78	0.72	0.79	0.79	0.81	0.72	0.82	0.78
Zr/Zr*	1.47	1.50	1.55	1.62	1.55	1.52	1.35	1.60	1.55
Hf/Hf*	1.31	1.32	1.33	1.33	1.29	1.40	1.28	1.30	1.32
Ti/Ti*	0.05	0.06	0.06	0.06	0.05	0.06	0.05	0.05	0.05
UTM Zone	•	•	•	•	•	•	•	•	•
Easting									
Northing									

* Samples from Noranda Exploration core library

	South Bay mine site DDH Tholeiites						Horseshoe Lake DDH FIIIa				
	SB95-4K	SB95-4L	SB95-4M	SB95-4N	SB95-4O	SB95-4P	HL96-1A	HL96-1B	HL96-1C	HL96-1D	HL96-1E
SiO_2	72.87	72.81	52.32	49.68	49.45	55.50	74.29	81.61	77.55	74.66	77.27
TiO_2	0.43	0.42	1.76	1.48	1.40	1.48	0.34	0.23	0.29	0.34	0.30
Al_2O_3	11.72	11.21	13.57	12.19	12.26	12.69	10.71	8.95	10.65	11.64	10.91
Fe_2O_3	6.80	6.61	17.47	19.62	13.09	16.61	7.62	2.84	3.90	5.77	3.31
MnO	0.11	0.11	0.22	0.26	0.28	0.22	0.15	0.05	0.07	0.09	0.06
MgO	1.02	0.80	4.08	5.31	2.24	3.45	0.50	0.19	0.28	0.40	0.33
CaO	2.81	2.57	7.61	8.01	6.10	6.57	0.90	1.22	1.10	1.25	1.42
K_2O	1.00	1.11	0.56	0.37	0.53	0.55	2.57	1.29	2.26	2.81	1.02
Na_2O	3.54	4.24	2.21	2.52	4.24	2.67	2.88	3.61	3.88	3.01	5.34
P_2O_5	0.10	0.10	0.22	0.15	0.39	0.27	0.03	0.02	0.02	0.03	0.03
LOI	0.76	0.96	2.56	2.51	2.51	2.15	1.16	1.06	1.21	1.47	1.32
Mg#	25	21	34	37	27	31	13	13	14	13	18
Ti	2514	2396	9008	9818	7626	7581	1708	1445	1710	1899	1781
P	385	322	740	542	1520	967	70	32	31	76	55
Cr	8	6	12	42	5	3	5	4	6	5	3
Co	10	9	49	63	25	48	8	3	5	7	4
Ni	2	2	27	71	5	9	1	1	1	2	1
Rb	15	13	11	6	9	10	45	18	28	46	14
Sr	125	92	235	148	120	147	64	52	49	77	30
Cs	0	0	1	0	1	1	1	0	1	1	0
Ba	263	332	80	42	63	100	555	277	396	600	163
Sc	9	8	30	33	26	29	5	3	4	5	5
V	5	4	269	461	53	157	1	0	0	0	1
Ta	1.64	1.65	0.54	0.45	0.76	0.58	2.40	1.88	2.29	2.42	2.35
Nb	30.56	29.81	9.01	7.13	13.23	9.66	42.42	31.81	41.68	40.54	42.05
Zr	646	631	156	129	257	178	756	535	712	724	744
Hf	15.79	16.14	4.61	3.91	6.56	4.97	19.38	15.22	18.49	20.18	19.40
Th	5.04	4.95	1.65	1.36	2.28	2.18	8.23	6.34	7.80	8.43	7.39
U	1.27	1.28	0.42	0.34	0.56	0.57	2.10	1.60	1.97	2.17	2.22
Y	128.97	126.75	43.46	37.90	73.75	57.37	172.81	80.24	106.93	170.55	123.07
La	36.75	36.42	12.62	11.02	18.68	19.20	58.53	40.73	55.28	60.27	53.34
Ce	89.97	89.39	31.58	26.89	46.44	45.13	139.15	96.55	133.58	143.25	127.10
Pr	12.21	12.36	4.41	3.67	6.49	6.04	18.50	12.96	17.90	18.95	16.81
Nd	55.89	56.72	20.32	17.62	31.02	27.34	82.13	59.82	79.99	84.60	74.37
Sm	16.20	16.25	5.89	5.01	8.97	7.66	22.12	15.62	20.42	22.69	19.91
Eu	3.75	3.80	1.90	1.56	3.10	2.21	4.00	2.67	3.46	4.25	3.62
Gd	19.17	19.15	7.21	6.20	11.50	9.44	25.20	15.88	20.27	26.67	20.84
Tb	3.36	3.38	1.22	1.04	1.96	1.62	4.32	2.46	3.06	4.50	3.31
Dy	22.51	22.38	8.31	7.04	12.92	10.80	29.07	16.03	20.08	30.36	21.58
Ho	4.99	5.01	1.79	1.51	2.79	2.30	6.29	3.32	4.26	6.72	4.73
Er	14.60	14.61	5.20	4.53	7.96	6.59	18.44	9.78	13.25	19.79	13.70
Tm	2.21	2.19	0.77	0.69	1.25	1.00	2.95	1.62	2.05	3.04	2.12
Yb	14.40	14.58	4.94	4.27	7.68	6.30	19.35	10.45	13.79	19.84	13.86
Lu	2.15	2.17	0.72	0.62	1.14	0.90	2.82	1.59	2.10	2.84	2.12
Cu	28	9	12	129	20	48	7	15	8	57	7
Zn	136	150	117	140	138	121	223	73	171	169	113
Mo	1.39	1.41	0.56	0.38	1.10	0.91	3.12	1.12	1.59	3.45	1.06
Ag	1.33	1.30	0.25	0.37	0.58	0.39	1.49	1.23	1.47	1.79	1.48
Tl	0.13	0.22	0.27	0.19	0.13	0.21	0.24	0.10	0.16	0.23	0.07
Pb	5.50	5.33	4.78	2.69	2.61	2.66	5.88	3.28	6.04	12.67	4.95
Se	3.54	4.63	1.60	1.35	1.97	1.59	7.84	44.59	6.23	6.72	6.54
Sb	0.41	0.38	1.33	0.44	0.35	0.43	0.22	0.32	0.23	0.35	0.25
	SB95-4K	SB95-4L	SB95-4M	SB95-4N	SB95-4O	SB95-4P	HL96-1A	HL96-1B	HL96-1C	HL96-1D	HL96-1E
(La/Yb)n	1.83	1.79	1.83	1.85	1.74	2.18	2.17	2.80	2.87	2.18	2.76
(La/Sm)n	1.47	1.45	1.38	1.42	1.35	1.62	1.71	1.68	1.75	1.72	1.73
(Gd/Yb)n	1.10	1.09	1.21	1.20	1.24	1.24	1.08	1.26	1.22	1.11	1.24
(La/Y)n	1.89	1.90	1.92	1.93	1.68	2.22	2.24	3.36	3.42	2.34	2.87
(Tb/Yb)n	1.06	1.05	1.12	1.10	1.16	1.17	1.01	1.07	1.01	1.03	1.09
(Tb/Y)n	1.09	1.12	1.18	1.15	1.11	1.19	1.05	1.28	1.20	1.11	1.13
(Eu/Eu*)n	0.65	0.66	0.89	0.85	0.93	0.79	0.52	0.51	0.51	0.53	0.54
Al_2O_3/TiO_2	27	28	9	7	10	10	37	37	37	37	37
Zr/Hf	41	39	34	33	39	36	39	35	39	36	38
La/Nb	1.20	1.22	1.40	1.55	1.41	1.99	1.38	1.28	1.33	1.49	1.27
Th/Nb	0.16	0.17	0.18	0.19	0.17	0.23	0.19	0.20	0.19	0.21	0.18
Th/La	0.14	0.14	0.13	0.12	0.12	0.11	0.14	0.16	0.14	0.14	0.14
Zr/Y	5.01	4.98	3.58	3.40	3.48	3.10	4.37	6.67	6.66	4.25	6.05
Ti/Zr	4	4	58	76	30	43	2	3	2	3	2
Ti/Sm	155	147	1530	1958	850	989	77	92	84	84	89
P/Nd	7	6	36	31	49	35	1	1	0	1	1
Ti/V	525	548	33	21	144	48	2342	3759	3462	3853	2772
Sc/La	4	4	42	53	23	32	2	2	2	2	2
Nb/Nb*	0.76	0.75	0.67	0.59	0.66	0.44	0.64	0.69	0.68	0.60	0.70
Zr/Zr*	1.49	1.44	0.99	0.95	1.06	0.85	1.23	1.21	1.22	1.14	1.34
Hf/Hf*	1.32	1.33	1.06	1.04	0.99	0.86	1.14	1.25	1.15	1.16	1.27
Ti/Ti*	0.06	0.05	0.55	0.70	0.30	0.35	0.03	0.04	0.03	0.03	0.03
UTM Zone	•	•	•	•	•	•	•	•	•	•	•
Easting											
Northing											

* Samples from Noranda Exploration core library

Horseshoe Lake DDH

FIIIa

	HL96-1F	HL96-1G	HL96-1H	HL96-1I	HL96-1J	HL96-1K	HL96-1L	HL96-1M	HL96-1N	HL96-1O	HL96-1P
SiO_2	76.90	76.72	74.04	83.75	80.21	76.58	77.90	78.89	71.24	67.41	82.63
TiO_2	0.33	0.32	0.32	0.30	0.27	0.32	0.32	0.30	0.35	0.40	0.22
Al_2O_3	10.94	11.36	11.20	8.91	9.67	11.36	11.10	10.94	12.18	13.67	9.28
Fe_2O_3	4.23	4.24	5.77	1.57	2.71	4.46	2.67	3.10	6.90	8.65	3.60
MnO	0.08	0.04	0.12	0.03	0.07	0.07	0.05	0.04	0.10	0.09	0.01
MgO	0.42	0.41	0.15	0.13	0.22	0.39	0.39	0.24	2.17	1.43	1.57
CaO	0.74	0.33	2.17	0.71	1.41	0.63	1.29	0.26	1.94	1.98	0.35
K_2O	1.57	1.30	1.40	1.04	1.09	1.46	1.04	1.04	1.40	2.97	0.10
Na_2O	4.95	5.25	4.80	3.54	4.31	4.70	5.21	5.14	1.69	2.96	1.24
P_2O_5	0.04	0.03	0.03	0.02	0.03	0.03	0.03	0.03	0.03	0.03	0.02
LOI	0.70	0.30	1.83	0.81	1.12	0.96	1.11	0.35	1.06	0.86	1.01
Mg#	18	17	6	15	15	16	24	15	41	32	39
Ti	1731	1927	1782	1424	1574	1854	1734	1803	1969	2339	1304
P	36	55	60	0	0	37	32	32	51	86	17
Cr	4	3	5	4	7	3	5	3	3	4	4
Co	5	5	6	2	3	6	5	4	8	10	4
Ni	1	1	1	1	1	1	1	1	1	1	1
Rb	24	21	30	12	16	26	13	13	75	69	3
Sr	36	29	104	63	43	42	46	27	124	151	17
Cs	1	1	1	0	0	1	0	1	4	4	0
Ba	227	258	331	252	164	288	275	315	641	685	12
Sc	5	5	5	4	4	5	4	5	5	6	3
V	1	0	0	0	0	1	0	1	1	1	0
Ta	2.32	2.37	2.29	1.85	2.04	2.26	2.39	2.33	2.66	3.02	1.71
Nb	43.44	44.61	45.27	34.67	40.15	44.28	41.79	43.21	53.13	52.99	32.47
Zr	767	788	796	609	724	834	738	537	944	961	560
Hf	19.47	20.08	18.97	15.49	17.13	20.19	19.85	14.00	22.10	24.56	14.11
Th	7.51	7.79	7.82	6.16	6.82	7.75	7.77	7.49	9.30	9.96	5.55
U	1.92	2.00	2.02	1.54	1.70	1.92	2.02	2.03	2.33	2.55	1.48
Y	114.38	132.91	152.46	107.30	133.94	153.21	130.79	126.76	201.93	164.84	88.76
La	56.24	58.98	55.20	39.92	52.57	59.19	59.61	54.78	63.50	63.21	47.27
Ce	136.18	139.53	131.88	94.84	122.18	139.35	140.50	130.02	152.18	152.49	110.80
Pr	18.22	18.86	17.55	12.73	16.48	18.51	19.05	16.94	20.28	20.48	14.80
Nd	80.30	85.06	77.56	56.31	74.71	84.52	84.70	72.64	89.90	89.54	65.36
Sm	20.57	22.21	20.34	14.76	20.50	22.03	22.97	18.14	24.68	24.36	16.58
Eu	3.92	4.08	3.75	2.86	3.76	4.15	4.40	3.49	4.63	4.54	2.98
Gd	20.56	23.15	22.37	16.63	22.48	25.28	25.13	20.19	28.46	28.19	16.43
Tb	3.27	3.71	3.79	2.79	3.63	4.18	3.92	3.56	4.90	4.70	2.56
Dy	21.40	23.90	25.27	18.77	23.18	26.88	25.34	24.13	32.38	31.42	16.21
Ho	4.51	5.29	5.36	4.11	4.88	5.74	5.33	5.12	6.92	6.54	3.35
Er	13.01	15.46	16.06	12.49	13.99	16.21	14.90	14.95	19.77	18.48	10.11
Tm	2.10	2.47	2.55	1.93	2.17	2.48	2.35	2.24	3.08	2.85	1.66
Yb	13.92	16.61	16.62	12.70	14.31	16.43	15.76	14.37	19.73	18.58	11.70
Lu	2.18	2.52	2.51	1.88	2.13	2.46	2.32	2.12	2.89	2.77	1.74
Cu	2	2	8	6	2	3	3	4	15	16	5
Zn	106	142	154	61	73	151	244	263	269	231	143
Mo	0.83	0.70	1.76	0.70	0.68	0.79	0.70	1.77	2.88	3.05	1.76
Ag	1.28	1.42	1.34	1.13	1.23	1.42	1.36	1.35	1.59	1.79	1.00
Tl	0.11	0.14	0.12	0.08	0.13	0.17	0.10	0.14	0.90	0.95	0.18
Pb	2.61	3.21	6.51	5.83	3.94	4.02	4.26	4.37	10.74	10.81	4.65
Sn	5.34	6.23	5.74	4.79	5.45	5.38	5.88	6.30	7.04	8.60	3.75
Sb	0.27	0.27	0.34	0.27	0.26	0.35	0.25	0.19	0.43	0.27	0.65
	HL96-1F	HL96-1G	HL96-1H	HL96-1I	HL96-1J	HL96-1K	HL96-1L	HL96-1M	HL96-1N	HL96-1O	HL96-1P
(La/Yb)n	2.90	2.55	2.38	2.25	2.63	2.58	2.71	2.73	2.31	2.44	2.90
(La/Sm)n	1.77	1.72	1.75	1.75	1.66	1.74	1.68	1.95	1.66	1.68	1.84
(Gd/Yb)n	1.22	1.15	1.11	1.08	1.30	1.27	1.32	1.16	1.19	1.25	1.16
(La/Y)n	3.26	2.94	2.40	2.46	2.60	2.56	3.02	2.86	2.08	2.54	3.53
(Tb/Yb)n	1.07	1.02	1.04	1.00	1.15	1.16	1.13	1.13	1.13	1.15	0.99
(Tb/Y)n	1.20	1.17	1.04	1.09	1.14	1.15	1.26	1.18	1.02	1.20	1.21
(Eu/Eu*)n	0.58	0.55	0.53	0.56	0.53	0.54	0.56	0.56	0.53	0.53	0.55
Al_2O_3/TiO_2	38	36	38	38	37	37	38	36	37	34	38
Zr/Hf	39	39	42	39	42	41	37	38	43	39	40
La/Nb	1.29	1.32	1.22	1.15	1.31	1.34	1.43	1.27	1.20	1.19	1.46
Th/Nb	0.17	0.17	0.17	0.18	0.17	0.18	0.19	0.17	0.17	0.19	0.17
Th/La	0.13	0.13	0.14	0.15	0.13	0.13	0.13	0.14	0.15	0.16	0.12
Zr/Y	6.70	5.93	5.22	5.67	5.41	5.44	5.64	4.23	4.67	5.83	6.31
Ti/Zr	2	2	2	2	2	2	2	3	2	2	2
Ti/Sm	84	87	88	96	77	84	75	99	80	96	79
P/Nd	0	1	1	0	0	0	0	0	1	1	0
Ti/V	3213	4267	4969	3597	4044	2676	4133	2763	3732	4257	2695
Sc/La	2	2	2	2	2	2	2	2	2	2	2
Nb/Nb*	0.70	0.67	0.73	0.77	0.66	0.66	0.62	0.70	0.75	0.75	0.60
Zr/Zr*	1.31	1.26	1.39	1.46	1.28	1.34	1.16	1.02	1.39	1.42	1.18
Hf/Hf*	1.20	1.16	1.20	1.35	1.10	1.17	1.13	0.97	1.18	1.32	1.08
Ti/Ti*	0.03	0.03	0.03	0.04	0.03	0.03	0.03	0.04	0.03	0.04	0.03
UTM Zone	*	*	*	*	*	*	*	*	*	*	*
Easting											
Northing											

* Samples from Noranda Exploration core library

	Horseshoe Lake DDH FIIIb							Dixie 19 DDH OIB-like basalts		
	HL96-1Q	HL96-1R	HL96-1S	HL96-1T	HL96-2A	HL96-2B	HL96-2C	SJV91-1A	SJV91-1D	SJV91-1M
SiO_2	80.26	79.06	78.10	81.94	74.26	70.87	77.16	48.02	51.06	51.99
TiO_2	0.12	0.13	0.13	0.10	0.31	0.32	0.29	2.97	2.02	0.64
Al_2O_3	11.71	12.23	11.94	10.28	11.24	12.03	10.60	13.40	14.00	15.84
Fe_2O_3	1.97	1.54	1.26	0.69	6.39	7.82	4.97	18.07	17.91	12.59
MnO	0.07	0.03	0.00	0.00	0.06	0.13	0.09	0.34	0.28	0.17
MgO	2.38	1.24	0.26	0.08	0.84	1.54	0.29	3.84	3.09	7.27
CaO	0.43	1.27	0.31	0.31	0.98	2.19	1.55	7.97	7.20	8.11
K_2O	1.60	3.82	5.39	2.62	1.88	1.97	2.50	0.39	0.31	0.51
Na_2O	1.47	0.68	2.63	4.00	4.01	1.10	2.53	3.34	3.27	2.80
P_2O_5	0.00	0.00	0.00	0.00	0.03	0.02	0.02	1.66	0.86	0.07
LOI	1.99	1.52	0.65	0.45	1.16	1.94	1.21	0.00	0.91	0.60
Mg#	73	64	31	20	22	30	11	32	28	56
Ti	716	777	723	560	1704	1761	1655	17101	11915	3952
P	0	0	0	0	26	14	50	7078	3725	292
Cr	3	4	5	14	3	3	3	4	18	46
Co	3	3	2	1	7	9	6	39	49	75
Ni	2	2	2	2	1	2	1	2	14	146
Rb	54	105	102	50	27	76	45	7	5	10
Sr	56	65	42	28	50	118	79	406	575	164
Cs	1	2	2	0	1	1	1	0	0	0
Ba	205	465	965	414	218	521	473	137	106	271
Sc	2	2	2	2	4	5	4	31	30	33
V	2	2	2	1	0	0	0	40	38	215
Ta	2.54	2.68	2.52	1.98	2.47	2.73	2.29	0.91	1.01	0.31
Nb	14.66	15.13	13.39	26.91	46.13	48.05	43.56	13.69	18.42	8.57
Zr	183	159	164	144	797	908	721	68	128	50
Hf	7.54	7.04	7.16	6.00	19.86	21.11	18.39	1.56	3.35	1.54
Th	15.61	16.50	15.47	12.46	7.95	9.46	7.76	0.55	0.99	0.75
U	3.58	3.90	3.28	2.78	2.05	2.42	1.91	0.14	0.35	0.23
V	93.69	103.72	98.00	83.56	152.61	195.94	164.51	56.83	48.69	21.14
La	62.08	69.78	62.71	55.52	65.73	65.38	55.71	27.05	23.42	8.07
Ce	130.85	145.80	131.77	117.55	158.83	154.96	131.58	69.81	58.60	18.47
Pr	14.85	16.55	15.10	13.47	20.93	20.59	17.68	10.03	8.09	2.62
Nd	54.74	60.75	55.59	49.28	92.17	90.67	78.11	48.23	37.85	11.91
Sm	11.95	12.98	12.23	10.71	24.85	24.83	21.38	12.56	9.24	3.17
Eu	0.76	0.76	0.65	0.55	4.10	4.38	3.74	4.50	3.72	1.49
Gd	11.35	13.08	12.67	10.70	26.55	29.54	24.42	14.03	10.41	3.62
Tb	2.14	2.38	2.17	1.91	4.29	4.97	4.25	1.95	1.51	0.58
Dy	14.81	16.71	14.97	13.20	27.79	34.31	27.95	11.39	9.14	3.60
Ho	3.45	3.75	3.40	2.93	5.73	7.39	6.02	2.24	1.86	0.77
Er	10.64	11.97	10.70	9.12	15.66	22.08	17.34	5.74	5.11	2.15
Tm	1.71	1.95	1.78	1.46	2.40	3.36	2.72	0.78	0.71	0.32
Yb	10.94	13.17	12.06	9.54	15.76	21.92	18.07	4.59	4.36	2.01
Lu	1.52	1.96	1.86	1.40	2.47	3.27	2.60	0.66	0.67	0.32
Cu	3	6	8	9	2	4	6	27	16	44
Zn	58	49	38	26	74	218	145	146	136	139
Mo	1.63	0.86	0.37	0.46	0.87	4.40	1.53	1.97	0.59	1.41
Ag	0.36	0.34	0.34	0.35	1.39	1.50	1.31	0.14	0.08	0.09
Tl	1.79	1.55	0.96	0.42	0.13	0.37	0.20	0.02	0.03	0.03
Pb	14.35	11.65	10.63	13.13	3.13	22.15	5.04	2.38	1.61	1.61
Sn	7.07	6.93	6.97	4.40	3.89	6.83	5.79	3.96	2.32	6.47
Sb	0.18	0.19	0.24	0.26	0.12	0.31	0.24	0.18	0.32	0.12
	HL96-1Q	HL96-1R	HL96-1S	HL96-1T	HL96-2A	HL96-2B	HL96-2C	SJV91-1A	SJV91-1D	SJV91-1M
(La/Yb)n	4.07	3.80	3.73	4.17	2.99	2.14	2.21	4.23	3.85	2.88
(La/Sm)n	3.36	3.47	3.31	3.35	1.71	1.70	1.68	1.39	1.64	1.64
(Gd/Yb)n	0.86	0.82	0.87	0.93	1.39	1.11	1.12	2.53	1.97	1.49
(La/Y)n	4.39	4.46	4.24	4.40	2.85	2.21	2.24	3.15	3.19	2.53
(Tb/Yb)n	0.89	0.82	0.87	0.91	1.24	1.03	1.07	1.93	1.58	1.32
(Tb/Y)n	0.96	0.96	0.93	0.96	1.18	1.07	1.08	1.44	1.31	1.16
(Eu/Eu*)n	0.20	0.18	0.16	0.16	0.48	0.49	0.50	1.03	1.16	1.34
Al_2O_3/TiO_2	98	100	98	111	39	41	38	5	7	24
Zr/Hf	24	23	23	24	40	38	39	44	38	33
La/Nb	1.79	1.99	1.88	2.06	1.42	1.36	1.28	1.98	1.27	0.94
Th/Nb	0.45	0.47	0.46	0.46	0.17	0.20	0.18	0.04	0.05	0.09
Th/La	0.25	0.24	0.25	0.22	0.12	0.14	0.14	0.02	0.04	0.09
Zr/Y	1.96	1.53	1.67	1.72	5.22	4.12	4.38	1.20	2.62	2.38
Ti/Zr	4	5	4	4	2	2	2	251	93	79
Ti/Sm	60	57	59	52	69	71	77	1361	1289	1247
P/Nd	0	0	0	0	0	0	1	147	98	25
Ti/V	402	375	397	444	3778	3840	3948	425	311	18
Sc/La	1	1	1	1	2	1	2	47	45	103
Nb/Nb*	0.44	0.39	0.42	0.38	0.63	0.65	0.69	0.49	0.73	0.91
Zr/Zr*	0.50	0.39	0.44	0.43	1.15	1.18	1.22	0.19	0.47	0.57
Hf/Hf*	0.74	0.63	0.69	0.66	1.04	1.12	1.13	0.16	0.45	0.63
Ti/Ti*	0.02	0.02	0.02	0.02	0.03	0.03	0.03	0.51	0.48	0.46
UTM Zone	•	•	•	•	•	•	•	•	•	•
Easting										
Northing										

* Samples from Noranda Exploration core library

Dixie 19 DDH

	FI felsics		FIII felsics							
	SJV91-1B	SJV91-1Q	SJV91-1C	SJV91-1H	SJV91-1I	SJV91-1J	SJV91-1L	SJV91-1N	SJV91-1O	SJV91-1P
SiO_2	77.21	58.54	74.13	74.66	72.09	76.00	99.19	78.04	58.66	77.65
TiO_2	0.18	0.72	0.62	0.27	0.79	0.15	0.93	0.22	1.40	0.17
Al_2O_3	12.90	14.28	10.91	10.40	10.74	12.33	15.92	12.11	12.50	11.42
Fe_2O_3	1.75	7.44	6.10	2.70	4.04	0.66	12.80	4.27	14.72	2.91
MnO	0.02	0.12	0.05	0.02	0.06	0.00	0.10	0.01	0.19	0.00
MgO	0.33	6.98	4.28	11.13	5.80	0.81	9.35	3.55	5.45	1.30
CaO	1.94	6.72	0.96	0.17	0.84	1.44	0.26	0.26	4.03	1.21
K_2O	0.76	1.76	0.89	0.24	0.78	0.63	0.87	0.89	0.18	1.08
Na_2O	4.89	1.39	2.38	0.41	0.72	1.74	0.47	0.61	2.63	2.01
P_2O_5	0.02	0.23	0.07	0.02	0.15	0.03	0.11	0.03	0.23	0.06
LOI	0.76	0.50	0.76	4.33	2.35	1.84	1.68	0.96	0.00	1.21
Mg#	29	67	61	90	61	96	62	65	45	71
Ti	1130	4056	3581	1559	4861	1804	5276	978	8206	2203
P	59	908	253	76	907	64	315	66	896	184
Cr	6	499	3	3	5	3	3	6	8	7
Co	6	46	17	12	25	2	42	12	60	10
Ni	1	146	0	0	1	0	1	1	4	2
Rb	19	69	9	7	21	17	21	23	5	26
Sr	174	578	102	19	38	123	31	54	124	91
Cs	1	2	2	2	3	6	3	1	1	4
Ba	402	389	93	35	163	41	143	191	54	177
Sc	3	20	12	13	17	3	18	3	30	7
V	7	135	6	0	20	1	13	4	141	7
Ta	0.73	0.53	1.72	1.19	1.61	2.83	2.56	1.46	1.08	1.46
Nb	11.70	9.73	33.52	19.89	29.36	48.66	54.14	21.87	17.51	28.20
Zr	168	132	456	300	468	429	675	245	219	541
Hf	4.41	4.22	13.52	9.24	14.18	13.03	16.98	8.29	6.22	13.36
Th	5.57	3.81	7.24	14.79	8.01	13.52	11.62	14.01	2.27	7.62
U	0.93	1.14	0.73	1.36	0.64	1.54	1.04	1.86	0.79	1.24
Y	17.85	19.96	134.45	124.27	140.90	176.92	59.62	68.23	76.10	100.23
La	25.17	26.59	47.22	47.31	53.65	56.05	83.18	69.84	22.84	67.72
Ce	47.74	58.36	120.38	111.13	128.14	134.03	200.65	144.04	53.71	147.61
Pr	5.15	7.13	16.15	14.25	16.94	16.80	26.13	15.97	7.13	18.19
Nd	18.85	28.78	71.17	60.82	77.98	67.45	115.12	59.84	32.39	76.97
Sm	3.66	5.86	16.31	14.86	18.66	15.27	26.38	11.33	8.62	15.87
Eu	1.00	1.55	3.32	2.25	2.80	2.16	3.70	1.02	3.18	3.41
Gd	3.32	5.15	22.51	17.74	24.04	18.94	32.41	11.15	10.74	16.07
Tb	0.46	0.67	3.90	3.21	3.75	3.59	5.40	1.76	1.77	2.71
Dy	2.80	3.86	26.07	22.53	24.66	25.04	36.33	11.43	12.48	17.50
Ho	0.60	0.73	5.81	5.08	5.47	5.64	8.00	2.52	2.75	3.93
Er	1.77	1.99	16.97	15.01	15.65	16.85	23.75	7.47	8.33	11.77
Tm	0.28	0.29	2.53	2.40	2.34	2.60	3.68	1.15	1.31	1.84
Yb	1.82	1.79	16.37	15.50	15.09	16.84	23.69	7.59	8.73	12.17
Lu	0.30	0.25	2.34	2.14	2.34	2.33	3.61	1.09	1.39	1.81
Cu	2	10	4	3	173	2	4	9	137	3
Zn	24	93	74	53	108	31	134	245	110	133
Mo	0.39	0.28	0.88	0.89	0.42	1.60	5.75	0.61	1.36	1.26
Ag	0.30	0.25	0.73	0.96	0.74	0.90	1.46	0.44	0.61	1.21
Tl	0.05	0.34	0.04	0.02	0.11	0.06	0.10	0.09	0.03	0.10
Pb	5.06	5.95	2.19	2.84	1.80	3.28	2.38	4.30	6.70	2.86
Sn	0.89	1.80	2.23	7.09	6.70	10.28	2.61	5.92	8.22	3.93
Sb	0.18	0.26	0.05	0.12	0.12	0.15	0.08	0.08	0.05	0.03
	SJV91-1B	SJV91-1Q	SJV91-1C	SJV91-1R	SJV91-1I	SJV91-1J	SJV91-1L	SJV91-1N	SJV91-1O	SJV91-1P
(La/Yb)n	9.90	10.66	2.07	2.19	2.55	2.39	2.52	6.60	1.88	3.99
(La/Sm)n	4.45	2.93	1.87	2.06	1.86	2.37	2.04	3.98	1.71	2.76
(Gd/Yb)n	1.50	2.38	1.14	0.95	1.32	0.93	1.13	1.21	1.02	1.09
(La/Y)n	9.34	8.83	2.33	2.52	2.52	2.10	9.24	6.78	1.99	4.48
(Tb/Yb)n	1.16	1.71	1.08	0.94	1.13	0.97	1.04	1.05	0.92	1.01
(Tb/Y)n	1.09	1.42	1.22	1.09	1.12	0.85	1.80	1.08	0.98	1.14
(Eu/Eu*)n	0.86	0.84	0.53	0.42	0.40	0.39	0.39	0.27	1.01	0.65
Al_2O_3/TiO_2	67	21	18	40	13	40	18	74	9	31
Zr/Hf	38	31	34	32	33	33	40	30	35	40
La/Nb	2.15	2.73	1.41	2.38	1.83	1.15	1.54	3.19	1.30	2.40
Th/Nb	0.48	0.39	0.22	0.74	0.27	0.28	0.21	0.64	0.13	0.27
Th/La	0.22	0.14	0.15	0.31	0.15	0.24	0.14	0.20	0.10	0.11
Zr/Y	9.40	6.59	3.39	2.42	3.32	2.42	11.33	3.60	2.88	5.40
Ti/Zr	7	31	8	5	10	4	8	4	37	4
Ti/Sm	309	692	220	105	261	118	200	86	952	139
P/Nd	3	32	4	1	8	1	3	1	28	2
Ti/V	159	30	630	5749	248	1412	417	223	58	306
Sc/La	9	79	5	6	7	2	5	3	22	4
Nb/Nb*	0.33	0.30	0.67	0.37	0.49	0.77	0.59	0.24	0.67	0.34
Zr/Zr*	1.40	0.70	0.93	0.69	0.85	0.92	0.85	0.65	0.91	1.07
Hf/Hf*	1.33	0.82	1.00	0.77	0.93	1.02	0.77	0.80	0.93	0.96
Ti/Ti*	0.13	0.29	0.07	0.04	0.09	0.04	0.07	0.03	0.34	0.05
UTM Zone	•	•	•	•	•	•	•	•	•	•
Easting										
Northing										

* Samples from Noranda Exploration core library

	Dixie 19 DDH Outliers				Dixie South DDH OIB-like basalts		Dixie South DDH FIIIb felsic			
	SJV91-1E	SJV91-1F	SJV91-1G	SJV91-1K	D94-1A	D94-1V	D94-1B	D94-1C	D94-1E	D94-1F
SiO_2	52.15	64.52	45.92	50.50	52.12	51.65	78.13	78.37	79.07	78.53
TiO_2	1.97	0.70	1.69	1.01	2.24	2.11	0.17	0.15	0.17	0.14
Al_2O_3	10.51	14.14	17.35	12.83	13.21	12.76	11.57	11.27	11.06	10.61
Fe_2O_3	19.80	8.30	16.33	17.11	16.73	17.72	2.22	2.13	1.82	2.73
MnO	0.29	0.10	0.16	0.25	0.25	0.23	0.01	0.03	0.03	0.05
MgO	9.61	4.02	5.66	5.50	4.56	4.04	1.18	0.94	1.00	1.02
CaO	3.77	3.95	8.96	7.82	6.09	8.14	2.02	1.71	1.99	2.59
K_2O	0.13	0.07	0.85	0.54	0.39	0.31	1.30	1.77	2.79	2.09
Na_2O	2.42	4.17	3.00	2.32	4.21	2.82	3.37	3.65	2.08	2.22
P_2O_5	0.34	0.02	0.07	0.11	0.20	0.22	0.02	0.00	0.00	0.02
LOI	0.20	0.00	1.01	0.15	0.25	0.15	1.06	1.06	0.70	1.21
Mg#	53	52	43	41	37	33	54	49	55	45
Ti	11299	4089	10168	17571	12534	12591	1017	891	950	869
P	1457	1	308	424	824	916	79	39	38	67
Cr	6	5	10	4	1	6	5	3	7	6
Co	71	24	124	78	67	75	7	6	6	8
Ni	10	2	54	5	1	20	1	1	1	2
Rb	4	1	25	11	8	2	26	44	68	58
Sr	261	288	457	295	361	155	169	54	51	80
Cs	0	0	2	1	1	0	1	1	1	1
Ba	28	92	296	169	163	90	439	210	409	377
Sc	29	14	25	32	26	43	3	4	3	4
V	102	23	504	237	233	366	7	3	3	4
Ta	1.50	0.94	0.19	0.90	0.72	0.72	2.46	2.56	2.36	2.59
Nb	10.66	15.01	3.08	12.94	13.80	12.77	35.11	35.53	34.40	38.10
Zr	213	184	37	47	177	122	233	222	217	224
Hf	5.86	10.34	1.04	1.51	4.34	3.56	8.71	8.84	8.34	9.11
Th	1.53	0.92	0.53	1.10	2.59	2.03	13.51	13.13	12.18	13.00
U	0.44	0.58	0.13	0.35	0.65	0.50	3.26	3.22	2.96	3.33
Y	48.76	23.36	11.12	16.92	37.79	47.00	103.10	108.31	114.49	126.17
La	15.98	24.48	5.71	9.95	20.10	16.84	60.36	59.95	61.06	66.25
Ce	38.37	43.80	12.88	25.40	46.73	40.69	132.93	130.57	132.76	145.19
Pr	4.97	4.73	1.65	3.58	6.06	5.45	15.70	15.62	15.73	16.99
Nd	22.26	18.02	7.24	16.65	26.70	24.58	60.91	59.94	61.05	67.42
Sm	9.45	3.35	1.82	4.83	6.29	6.42	13.78	13.98	14.05	15.45
Eu	2.47	4.50	0.79	1.58	2.09	1.80	0.95	0.93	1.00	1.15
Gd	7.02	3.31	1.98	5.74	6.75	7.67	14.08	14.05	14.47	17.20
Tb	1.18	0.59	0.31	0.98	1.06	1.27	2.68	2.65	2.63	3.02
Dy	8.42	4.57	1.92	6.46	6.63	8.20	18.13	18.16	18.12	20.79
Ho	1.93	1.24	0.40	1.38	1.41	1.80	4.06	4.15	4.11	4.51
Er	6.06	4.43	1.09	3.96	4.07	5.26	12.27	13.08	12.49	13.76
Tm	1.02	0.84	0.16	0.61	0.61	0.79	2.00	2.08	2.03	2.18
Yb	7.04	6.70	1.07	3.90	3.90	5.01	13.39	13.53	13.58	14.06
Lu	1.13	1.21	0.15	0.58	0.57	0.74	1.87	1.87	1.89	2.08
Cu	445	15	181	52	14	78	5	13	5	13
Zn	147	79	119	143	141	157	44	36	100	367
Mo	0.36	0.39	0.16	0.67	0.57	0.68	0.48	2.61	1.41	2.73
Ag	0.18	0.67	0.20	0.11	0.34	0.33	0.53	0.43	0.45	0.51
Tl	0.02	0.00	0.08	0.03	0.03	0.02	0.10	0.20	0.35	0.93
Pb	1.80	1.71	3.09	2.01	3.15	2.54	8.72	6.71	10.24	22.62
Sn	2.06	0.63	1.33	3.75	1.94	2.57	5.12	3.72	6.29	9.67
Sb	0.09	0.04	0.44	0.20	0.63	0.18	0.23	0.26	0.18	0.34
	SJV91-1E	SJV91-1F	SJV91-1G	SJV91-1K	D94-1A	D94-1V	D94-1B	D94-1C	D94-1E	D94-1F
(La/Yb)n	1.63	2.62	3.82	1.83	3.70	2.41	3.23	3.18	3.22	3.38
(La/Sm)n	1.89	4.72	2.03	1.33	2.07	1.69	2.83	2.77	2.81	2.77
(Gd/Yb)n	0.82	0.41	1.53	1.22	1.43	1.27	0.87	0.86	0.88	1.01
(La/Y)n	2.17	6.94	3.40	1.78	3.52	2.37	3.88	3.67	3.53	3.48
(Tb/Yb)n	0.76	0.40	1.33	1.15	1.24	1.15	0.91	0.89	0.88	0.98
(Tb/Y)n	1.02	1.06	1.18	1.12	1.18	1.14	1.09	1.03	0.96	1.00
(Eu/Eu*)n	1.22	4.08	1.26	0.92	0.97	0.78	0.21	0.20	0.21	0.22
Al_2O_3/TiO_2	6	20	10	4	6	6	68	76	77	73
Zr/Hf	36	37	36	31	41	34	27	25	26	25
La/Nb	0.52	1.63	1.85	0.77	1.46	1.32	1.72	1.69	1.77	1.74
Th/Nb	0.05	0.06	0.17	0.09	0.19	0.16	0.38	0.37	0.35	0.34
Th/La	0.10	0.04	0.09	0.11	0.13	0.12	0.22	0.22	0.20	0.20
Zr/Y	4.36	16.45	3.33	1.28	4.68	2.60	2.26	2.05	1.90	1.78
Ti/Zr	53	11	274	372	71	103	4	4	4	4
Ti/Sm	2073	1222	5592	3640	1994	1961	74	64	61	56
P/Nd	65	0	42	25	31	38	1	1	1	1
Ti/V	111	178	20	74	54	22	138	315	310	207
Sc/La	25	12	162	56	45	57	2	2	2	2
Nb/Nb*	1.72	0.41	0.45	1.24	0.60	0.68	0.48	0.48	0.46	0.47
Zr/Zr*	1.34	3.43	0.71	0.36	0.95	0.67	0.56	0.53	0.51	0.48
Hf/Hf*	1.34	3.34	0.72	0.42	0.84	0.71	0.75	0.77	0.71	0.71
Ti/Ti*	0.72	0.49	2.12	1.32	0.76	0.71	0.03	0.03	0.02	0.02
UTM Zone	•	•	•	•	•	•	•	•	•	•
Easting										
Northing										

* Samples from Noranda Exploration core library

Dixie South DDH
FIIIb felsic

	D94-1G	D94-1H	D94-1I	D94-1J	D94-1K	D94-1L	D94-1M	D94-1N	D94-1O	D94-1P	D94-1Q	D94-1R	D94-1S	D94-1T
SiO_2	78.45	78.38	79.57	76.62	77.63	74.46	78.17	75.92	78.15	76.95	77.90	77.35	77.97	78.40
TiO_2	0.17	0.17	0.17	0.18	0.17	0.20	0.15	0.15	0.16	0.17	0.13	0.14	0.13	0.13
Al_2O_3	9.70	11.36	11.20	11.31	11.98	12.33	10.71	10.89	11.31	11.60	11.89	11.99	12.09	11.95
Fe_2O_3	4.88	2.87	1.65	3.28	2.28	3.30	3.08	4.56	2.70	2.77	1.65	1.86	1.63	1.38
MnO	0.16	0.03	0.01	0.08	<0.01	0.07	0.10	0.14	0.13	0.32	<0.01	0.02	0.00	0.00
MgO	0.84	0.44	0.27	0.42	0.20	2.94	4.50	6.49	0.32	0.37	0.21	0.62	0.16	0.49
CaO	2.09	1.64	0.60	3.39	0.54	0.61	0.05	0.00	0.78	0.67	0.80	0.62	0.49	0.58
K_2O	2.23	2.64	1.24	3.45	1.75	5.33	3.03	1.81	1.97	3.46	3.73	4.57	3.72	3.51
Na_2O	1.46	2.49	5.28	1.27	5.47	0.78	0.22	0.06	4.49	3.70	3.72	2.83	3.63	3.57
P_2O_5	0.02	0.00	0.00	0.00	0.00	0.00	0.00	0.00	0.00	0.00	0.00	0.00	0.00	0.00
LOI	0.76	0.96	0.50	1.42	0.35	1.32	1.16	1.94	0.96	0.55	0.60	0.76	0.81	0.60
Mg#	27	25	26	22	16	66	76	76	21	23	22	42	33	44
Ti	969	904	990	1001	1050	1055	915	939	958	1014	781	768	778	789
P	55	16	24	18	0	0	4	0	3	54	49	23	18	22
Cr	9	4	4	3	11	3	2	3	8	4	6	17	6	7
Co	15	7	4	8	6	8	7	11	7	7	5	6	5	4
Ni	5	0	0	0	1	0	0	2	1	0	2	2	1	1
Rb	62	58	22	56	20	113	55	33	36	58	3	126	92	94
Sr	53	69	50	81	61	39	18	4	37	29	71	32	47	40
Cs	2	1	0	0	0	2	2	1	0	1	0	1	1	1
Ba	529	544	240	572	444	529	328	208	433	564	623	742	633	525
Sc	4	3	2	3	2	3	2	2	2	3	7	3	3	3
V	6	1	1	1	3	0	0	0	1	1	0	2	2	3
Ta	2.39	2.84	3.10	2.82	3.24	3.19	2.63	2.81	2.95	3.07	1.32	2.62	2.53	2.60
Nb	44.56	50.07	50.03	50.44	52.63	56.80	45.59	47.60	48.59	52.09	25.07	36.05	34.90	35.83
Zr	405	469	465	414	501	538	450	470	480	509	132	182	160	175
Hf	13.35	16.32	13.78	13.60	18.10	18.37	15.27	16.65	17.50	17.89	5.25	7.78	6.91	7.03
Th	8.11	9.99	9.82	10.12	13.45	11.54	9.25	9.54	9.99	10.17	14.59	15.78	14.93	15.84
U	2.15	2.42	2.44	2.52	2.61	2.76	2.15	2.44	2.14	2.63	1.36	3.69	3.54	3.71
Y	171.93	196.89	167.37	214.87	127.29	206.40	200.39	161.17	128.33	167.73	99.88	87.39	82.95	110.04
La	59.11	72.24	61.75	72.36	84.05	78.81	56.86	58.40	63.88	75.74	67.62	66.96	64.38	66.80
Ce	141.57	172.66	153.21	172.43	205.15	185.02	134.90	148.82	155.46	181.59	141.14	143.62	137.87	145.44
Pr	18.59	22.82	20.54	23.19	27.50	24.66	18.15	20.07	20.72	24.15	15.96	16.39	15.93	16.67
Nd	82.03	102.37	91.63	101.25	121.35	107.21	85.68	91.43	91.52	106.60	57.70	61.42	59.74	61.75
Sm	22.02	27.44	22.68	27.06	30.71	29.30	22.68	23.40	23.69	28.12	12.53	13.45	12.96	13.65
Eu	2.80	3.38	3.04	3.46	3.90	4.02	1.08	1.82	3.30	3.64	0.71	0.78	0.71	0.68
Gd	25.50	31.71	25.76	32.09	30.02	31.04	25.35	23.07	24.12	28.67	12.07	13.30	12.63	14.00
Tb	4.40	5.33	4.79	5.44	5.03	5.75	4.55	4.51	4.15	4.98	2.31	2.26	2.12	2.42
Dy	30.37	35.00	31.53	36.96	30.57	37.55	29.38	30.96	25.45	32.45	15.85	14.89	13.96	16.56
Ho	6.68	7.64	6.59	8.14	5.99	8.04	6.09	6.61	5.18	6.96	3.61	3.30	3.07	3.71
Er	19.24	22.05	18.83	24.05	16.39	23.33	17.20	18.18	14.31	19.83	11.13	9.99	9.21	11.34
Tm	3.02	3.40	2.93	3.73	2.52	3.45	2.51	2.76	2.20	3.03	1.84	1.65	1.51	1.82
Yb	19.14	21.59	19.27	23.98	17.22	23.13	16.65	17.37	14.67	20.38	12.17	10.85	10.12	12.19
Lu	2.89	3.26	2.69	3.44	2.45	3.03	2.28	2.22	2.02	2.87	1.67	1.66	1.53	1.84
Cu	55	44	5	35	23	6	3	1	5	15	6	12	3	1
Zn	637	164	79	195	1826	174	377	130	155	317	39	76	32	28
Mo	3.31	2.15	0.66	10.50	0.74	2.73	0.67	1.36	0.52	0.95	0.55	1.54	1.78	2.11
Ag	1.12	1.10	1.02	0.89	1.12	1.08	0.88	0.98	0.96	1.13	0.36	0.36	0.29	0.41
Tl	0.89	0.25	0.09	0.15	0.10	0.65	0.19	0.11	0.16	0.27	0.26	0.41	0.29	0.29
Pb	16.62	10.92	5.25	8.64	149.46	19.22	3.61	3.68	6.39	24.68	8.86	10.03	7.88	6.94
Sn	8.81	6.04	6.86	8.22	6.41	9.79	8.25	14.12	6.79	10.05	3.88	7.01	4.55	22.29
Sb	0.10	0.10	0.17	0.42	0.26	0.09	0.05	0.20	0.13	0.12	0.12	0.13	0.08	0.19
	D94-1G	D94-1H	D94-1I	D94-1J	D94-1K	D94-1L	D94-1M	D94-1N	D94-1O	D94-1P	D94-1Q	D94-1R	D94-1S	D94-1T
(La/Yb)n	2.21	2.40	2.30	2.16	3.50	2.44	2.45	2.41	3.12	2.66	3.98	4.42	4.56	3.93
(La/Sm)n	1.73	1.70	1.76	1.73	1.77	1.74	1.62	1.61	1.74	1.74	3.49	3.22	3.21	3.16
(Gd/Yb)n	1.10	1.21	1.11	1.11	1.44	1.11	1.26	1.10	1.36	1.16	0.82	1.01	1.03	0.95
(La/Y)n	2.28	2.43	2.44	2.23	4.37	2.53	1.88	2.40	3.30	2.99	4.48	5.08	5.14	4.02
(Tb/Yb)n	1.05	1.12	1.13	1.03	1.33	1.13	1.24	1.18	1.29	1.11	0.86	0.95	0.95	0.90
(Tb/Y)n	1.08	1.14	1.20	1.06	1.66	1.17	0.95	1.17	1.36	1.25	0.97	1.08	1.07	0.92
(Eu/Eu*)n	0.36	0.35	0.38	0.36	0.39	0.41	0.14	0.24	0.42	0.39	0.18	0.18	0.17	0.15
Al_2O_3/TiO_2	60	75	68	67	68	69	70	70	71	68	91	93	93	91
Zr/Hf	30	29	34	30	28	29	29	28	27	28	25	23	23	25
La/Nb	1.33	1.44	1.23	1.43	1.60	1.39	1.25	1.23	1.31	1.45	2.70	1.86	1.84	1.86
Th/Nb	0.18	0.20	0.20	0.20	0.22	0.20	0.20	0.20	0.21	0.20	0.58	0.44	0.43	0.44
Th/La	0.14	0.14	0.16	0.14	0.14	0.15	0.16	0.16	0.16	0.13	0.22	0.24	0.23	0.24
Zr/Y	2.36	2.38	2.78	1.93	3.93	2.61	2.25	2.92	3.74	3.03	1.32	2.08	1.93	1.59
Ti/Zr	2	2	2	2	2	2	2	2	2	2	6	4	5	4
Ti/Sm	44	33	44	37	34	36	40	40	40	36	62	57	60	58
P/Nd	1	0	0	0	0	0	0	0	0	1	1	0	0	0
Ti/V	161	914	1059	1371	305	3063	3231	2710	759	1709	3374	333	348	309
Sc/La	1	1	1	1	1	1	1	1	1	1	4	2	2	1
Nb/Nb*	0.67	0.62	0.75	0.62	0.57	0.63	0.71	0.77	0.69	0.61	0.29	0.43	0.43	0.44
Zr/Zr*	0.66	0.61	0.71	0.55	0.57	0.66	0.71	0.70	0.71	0.64	0.34	0.44	0.40	0.42
Hf/Hf*	0.79	0.77	0.76	0.65	0.74	0.82	0.87	0.90	0.94	0.82	0.49	0.68	0.62	0.61
Ti/Ti*	0.02	0.01	0.02	0.01	0.01	0.01	0.02	0.02	0.02	0.01	0.03	0.02	0.02	0.02
UTM Zone	•	•	•	•	•	•	•	•	•	•	•	•	•	•
Easting														
Northing														

• Samples from Noranda Exploration core library

	Dixie South DDH FIIIa felsic					Dixie 18 DDH Dacites		
	D94-1D	D94-1U	D94-1W	D94-1X	D94-1Y	SJV91-2A	SJV91-2B	SJV91-2C
SiO_2	75.73	74.31	72.72	69.61	72.95	65.48	65.53	70.28
TiO_2	0.57	0.60	0.62	0.65	0.70	0.94	0.91	0.72
Al_2O_3	11.32	10.79	11.27	11.57	11.37	11.59	11.33	10.77
Fe_2O_3	4.61	5.83	5.75	9.08	6.35	10.78	11.02	9.19
MnO	0.05	0.09	0.09	0.18	0.07	0.08	0.14	0.18
MgO	0.96	1.00	1.21	1.20	1.41	1.67	1.60	0.74
CaO	1.93	1.87	3.11	2.28	1.34	4.29	4.67	3.15
K_2O	1.72	1.66	1.34	0.96	1.33	1.45	0.76	0.60
Na_2O	3.03	3.73	3.74	4.31	4.34	3.45	3.78	3.97
P_2O_5	0.08	0.13	0.14	0.14	0.15	0.27	0.26	0.19
LOI	0.35	0.60	1.42	0.30	0.10	0.60	0.91	0.76
Mg#	31	27	32	22	33	25	24	15
Ti	3456	3745	3962	3958	4251	5676	5460	4369
P	418	566	622	613	606	1169	1122	851
Cr	4	4	8	7	5	7	8	7
Co	16	17	19	26	19	29	29	24
Ni	1	1	2	1	1	3	3	0
Rb	38	44	36	21	25	30	16	20
Sr	42	56	60	91	45	109	123	135
Cs	1	2	1	0	1	5	2	6
Ba	211	196	217	346	133	222	95	280
Sc	12	12	12	13	13	22	21	18
V	12	13	18	17	17	35	35	4
Ta	2.11	1.69	1.74	1.78	1.92	1.14	1.14	1.36
Nb	34.68	30.15	29.59	31.31	30.60	19.68	17.98	25.37
Zr	479	464	452	492	486	390	386	540
Hf	13.24	12.61	13.32	13.54	15.00	10.68	10.46	13.11
Th	9.93	5.86	5.99	6.10	6.53	3.49	3.47	4.10
U	2.42	1.46	1.44	1.53	1.60	0.93	0.87	1.02
Y	112.20	110.76	111.15	117.88	107.72	98.05	75.17	115.32
La	52.16	37.43	40.14	39.60	39.18	24.05	24.13	29.85
Ce	118.81	90.67	99.17	96.32	102.90	60.98	61.23	74.59
Pr	14.86	12.15	13.30	13.00	14.24	8.72	8.56	10.37
Nd	62.39	53.74	59.76	57.32	66.20	40.97	39.88	46.85
Sm	15.21	14.55	16.14	15.42	17.29	12.05	11.39	13.95
Eu	2.49	2.67	3.07	3.16	3.34	4.35	3.39	3.87
Gd	17.74	16.90	18.82	18.31	19.79	15.72	13.43	17.39
Tb	2.90	2.96	3.05	3.05	3.24	2.74	2.13	2.96
Dy	19.52	20.00	20.47	20.54	21.44	18.00	13.04	19.77
Ho	4.16	4.31	4.37	4.42	4.38	3.83	2.90	4.29
Er	12.26	12.11	12.46	13.16	12.86	11.03	8.57	12.59
Tm	1.85	1.86	1.94	2.02	2.02	1.66	1.33	1.93
Yb	12.26	11.87	13.11	13.83	13.09	10.80	8.77	12.44
Lu	1.81	1.82	1.87	2.02	1.88	1.66	1.44	1.96
Cu	17	32	10	20	4	4	11	10
Zn	80	147	140	204	117	34	56	131
Mo	2.17	1.18	1.29	1.16	0.58	1.59	1.25	1.35
Ag	1.13	1.04	1.15	1.43	1.16	0.78	0.67	1.07
Tl	0.19	0.25	0.45	0.82	0.79	0.12	0.11	0.16
Pb	5.57	6.15	8.27	32.09	9.26	2.76	2.63	2.90
Sn	4.05	10.03	5.78	6.06	3.79	15.10	2.35	4.14
Sb	0.24	0.09	0.10	0.16	0.09	0.61	1.42	1.40
	D94-1D	D94-1U	D94-1W	D94-1X	D94-1Y	SJV91-2A	SJV91-2B	SJV91-2C
(La/Yb)n	3.05	2.26	2.19	2.05	2.15	1.60	1.97	1.72
(La/Sm)n	2.21	1.66	1.61	1.66	1.46	1.29	1.37	1.38
(Gd/Yb)n	1.20	1.18	1.19	1.09	1.25	1.20	1.27	1.16
(La/Y)n	3.08	2.24	2.39	2.23	2.41	1.62	2.13	1.71
(Tb/Yb)n	1.07	1.13	1.08	1.00	1.13	1.15	1.10	1.08
(Tb/Y)n	1.09	1.12	1.15	1.09	1.26	1.17	1.19	1.08
(Eu/Eu*)n	0.46	0.52	0.54	0.57	0.55	0.97	0.84	0.76
AL_2O_3/TiO_2	20	17	17	17	16	12	12	15
Zr/Hf	36	37	34	36	32	36	37	41
La/Nb	1.50	1.24	1.36	1.26	1.28	1.22	1.34	1.18
Th/Nb	0.29	0.19	0.20	0.19	0.21	0.18	0.19	0.16
Th/La	0.19	0.16	0.15	0.15	0.17	0.15	0.14	0.14
Zr/Y	4.27	4.19	4.07	4.18	4.51	3.97	5.14	4.68
Ti/Zr	7	8	9	8	9	15	14	8
Ti/Sm	227	257	246	257	246	471	479	313
P/Nd	7	11	10	11	9	29	28	18
Ti/V	297	283	216	229	256	162	157	1011
Sc/La	7	6	7	6	7	13	16	9
Nb/Nb*	0.56	0.73	0.68	0.72	0.77	0.77	0.71	0.79
Zr/Zr*	1.08	1.15	1.01	1.15	0.99	1.21	1.25	1.46
Hf/Hf*	1.08	1.13	1.08	1.14	1.11	1.21	1.23	1.29
Ti/Ti*	0.08	0.09	0.09	0.09	0.09	0.16	0.17	0.11
UTM Zone	•	•	•	•	•	•	•	•
Easting								
Northing								

* Samples from Noranda Exploration core library

	Dixie 18 DDH Icelandites				Dixie 18 DDH Calc alkaline			
	SJV91-2D	SJV91-2G	SJV91-2I	SJV91-2J	SJV91-2E	SJV91-2F	SJV91-2H	SJV91-2K
SiO_2	54.27	52.58	50.48	50.98	56.81	71.53	50.20	50.72
TiO_2	1.92	2.11	1.57	1.33	0.78	0.24	0.61	0.77
Al_2O_3	12.48	13.43	12.27	10.61	16.92	15.65	18.98	17.84
Fe_2O_3	15.72	14.75	16.43	17.02	8.94	2.16	12.24	8.92
MnO	0.36	0.51	0.56	0.33	0.15	0.05	0.33	0.14
MgO	3.49	4.39	2.52	7.30	3.56	0.70	3.17	3.52
CaO	8.15	7.93	6.21	1.62	6.48	2.81	9.06	6.76
K_2O	0.60	0.55	0.28	0.76	1.50	1.90	2.24	1.05
Na_2O	2.60	3.53	3.43	0.81	4.58	4.87	3.08	0.98
P_2O_5	0.43	0.22	0.25	0.22	0.27	0.08	0.08	0.28
LOI	0.20	0.15	0.00	0.25	1.01	0.76	0.45	0.15
Mg#	33	40	25	49	47	42	36	46
Ti	11276	12734	9383	8011	4521	1283	3466	4667
P	1875	997	1101	948	1122	355	376	1162
Cr	20	6	5	1	26	11	217	16
Co	53	54	38	55	37	9	44	39
Ni	21	20	2	2	11	4	121	10
Rb	6	20	2	58	49	53	64	34
Sr	148	149	221	47	635	476	186	970
Cs	0	1	0	14	5	6	6	16
Ba	193	210	78	91	671	1068	323	485
Sc	40	48	41	34	19	4	24	18
V	187	404	67	65	156	21	176	152
Ta	0.54	0.57	0.62	1.75	0.59	0.95	0.26	0.64
Nb	9.53	10.09	10.48	11.04	10.24	12.52	3.89	10.58
Zr	183	169	202	176	174	151	70	184
Hf	4.58	4.59	5.75	4.91	4.72	4.47	1.82	4.84
Th	1.43	1.67	2.20	2.10	3.77	5.21	1.98	3.99
U	0.36	0.43	0.58	0.59	1.02	2.38	0.50	1.08
Y	52.12	46.75	60.22	51.37	30.90	20.17	13.51	28.39
La	12.84	12.59	11.61	12.70	28.97	26.85	10.31	28.46
Ce	31.81	30.71	30.13	31.03	61.80	54.57	20.70	62.00
Pr	4.46	4.31	4.24	4.28	7.59	6.34	2.43	7.60
Nd	21.28	20.17	20.77	20.28	30.94	24.35	9.84	30.74
Sm	6.46	5.47	6.21	5.48	6.39	4.46	2.16	6.27
Eu	2.31	1.67	1.86	1.36	1.62	1.14	0.69	1.87
Gd	8.12	7.06	8.45	7.43	6.13	3.88	2.30	6.08
Tb	1.32	1.19	1.51	1.29	0.88	0.52	0.39	0.79
Dy	8.90	7.97	10.38	8.73	5.45	3.29	2.40	4.81
Ho	1.93	1.73	2.33	1.98	1.10	0.69	0.50	1.01
Er	5.43	4.93	6.94	5.89	3.25	2.04	1.46	2.92
Tm	0.82	0.76	1.06	0.91	0.48	0.31	0.22	0.44
Yb	5.32	4.95	7.01	5.96	3.08	2.25	1.44	2.85
Lu	0.78	0.74	1.04	0.89	0.48	0.34	0.22	0.46
Cu	39	8	28	54	4	14	5	26
Zn	190	192	189	925	103	42	116	168
Mo	0.74	0.54	0.80	0.24	0.15	0.12	0.29	0.22
Ag	0.42	0.36	0.46	0.55	0.32	0.33	0.17	0.49
Tl	0.13	0.22	0.04	0.88	0.41	0.32	0.84	0.59
Pb	2.67	2.42	14.59	12.41	6.29	9.30	5.47	35.72
Sn	1.48	1.21	1.71	2.04	1.73	1.35	0.82	1.60
Sb	3.90	2.74	2.60	0.08	0.84	0.35	2.00	0.05
	SJV91-2D	SJV91-2G	SJV91-2I	SJV91-2J	SJV91-2E	SJV91-2F	SJV91-2H	SJV91-2K
(La/Yb)n	1.73	1.82	1.19	1.53	6.74	8.57	5.14	7.15
(La/Sm)n	1.28	1.49	1.21	1.50	2.93	3.89	3.08	2.93
(Gd/Yb)n	1.26	1.18	1.00	1.03	1.65	1.43	1.32	1.76
(La/Y)n	1.63	1.78	1.28	1.64	6.21	8.82	5.05	6.64
(Tb/Yb)n	1.13	1.09	0.98	0.99	1.30	1.06	1.24	1.26
(Tb/Y)n	1.07	1.07	1.05	1.06	1.19	1.09	1.22	1.17
(Eu/Eu*)n	0.98	0.82	0.78	0.65	0.78	0.82	0.94	0.92
AL_2O_3/TiO_2	7	6	8	8	22	72	32	23
Zr/Hf	40	37	35	36	37	34	39	38
La/Nb	1.35	1.25	1.11	1.15	2.83	2.14	2.65	2.69
Th/Nb	0.15	0.17	0.21	0.19	0.37	0.42	0.51	0.38
Th/La	0.11	0.13	0.19	0.16	0.13	0.19	0.19	0.14
Zr/Y	3.50	3.62	3.36	3.43	5.63	7.49	5.21	6.47
Ti/Zr	62	75	46	45	26	8	49	25
Ti/Sm	1745	2329	1511	1461	707	287	1605	744
P/Nd	88	49	53	47	36	15	38	38
Ti/V	60	32	140	123	29	62	26	31
Sc/La	51	65	39	38	40	11	109	39
Nb/Nb*	0.69	0.73	0.87	0.79	0.28	0.35	0.28	0.30
Zr/Zr*	1.08	1.12	1.23	1.16	0.86	1.00	1.06	0.92
Hf/Hf*	0.98	1.10	1.27	1.17	0.84	1.08	0.99	0.87
Ti/Ti*	0.62	0.81	0.51	0.50	0.29	0.12	0.62	0.30
UTM Zone	•	•	•	•	•	•	•	•
Easting								
Northing								

* Samples from Noranda Exploration core library

Dixie 3 DDH
FIII felsics

	SJV91-4A	SJV91-4B	SJV91-4C	SJV91-4D	SJV91-4E	SJV91-4F	SJV91-4G	SJV91-4H	SJV91-4I	SJV91-4J	SJV91-4K
SiO_2	74.71	75.84	69.76	68.21	76.96	70.34	79.08	72.90	79.32	76.88	76.64
TiO_2	0.48	0.18	0.26	0.49	0.26	0.24	0.21	0.20	0.17	0.18	0.16
Al_2O_3	10.41	11.47	15.12	15.43	11.84	12.19	10.65	13.09	11.77	12.21	12.17
Fe_2O_3	7.17	4.46	3.88	4.14	1.55	6.81	2.33	3.74	2.70	2.00	2.25
MnO	0.10	0.06	0.03	0.09	0.02	0.11	0.06	0.05	0.02	0.01	0.02
MgO	4.46	1.01	1.81	1.55	0.85	1.97	1.50	1.36	1.29	0.19	0.41
CaO	0.28	1.31	1.23	3.22	1.08	1.91	1.72	1.75	0.23	0.59	1.24
K_2O	2.19	2.84	4.74	2.18	4.46	5.76	3.39	6.04	3.93	3.92	3.60
Na_2O	0.13	2.81	3.13	4.50	0.95	0.61	1.03	0.85	0.59	1.98	3.48
P_2O_5	0.06	0.02	0.04	0.19	0.03	0.04	0.03	0.03	0.00	0.03	0.03
LOI	1.63	0.96	0.96	0.91	1.47	0.70	0.70	1.16	1.63	0.10	1.01
Mg#	58	33	51	45	55	39	59	44	51	17	29
Ti	2835	1116	1604	3039	1616	1438	1273	1061	908	1037	1008
P	224	77	153	845	126	144	93	95	19	117	99
Cr	3	8	9	15	4	5	4	8	3	10	10
Co	18	13	20	16	6	17	7	11	6	6	6
Ni	1	4	8	9	1	4	3	5	0	1	3
Rb	43	71	118	79	119	155	100	117	118	58	63
Sr	18	163	281	415	152	138	128	173	43	110	65
Cs	4	5	7	5	2	15	5	4	7	2	1
Ba	331	576	732	715	406	617	522	841	536	775	640
Sc	10	4	7	7	5	5	4	4	2	3	3
V	3	8	56	67	8	16	6	10	1	4	4
Ta	1.86	2.59	3.05	0.82	2.37	2.02	1.96	1.13	2.59	2.40	2.30
Nb	34.85	42.21	35.53	12.91	37.39	29.82	28.04	28.21	38.56	38.91	38.20
Zr	415	323	305	231	349	272	253	268	339	282	269
Hf	8.86	10.66	11.53	6.42	11.09	9.35	8.51	8.83	11.18	9.22	8.87
Th	5.91	13.35	16.93	9.68	14.83	12.79	10.85	5.87	13.66	13.47	12.52
U	1.40	3.08	3.61	3.53	3.59	3.11	2.72	0.57	2.78	2.87	2.79
Y	127.11	78.06	108.74	37.00	92.99	95.12	68.34	94.95	77.24	50.04	93.70
La	41.43	72.99	77.38	38.29	63.11	57.40	49.15	71.56	73.31	70.21	71.82
Ce	100.51	158.32	169.74	79.80	141.30	124.68	107.56	155.59	158.52	148.99	153.90
Pr	13.72	18.32	19.74	9.32	16.60	14.81	12.69	17.95	18.87	17.12	17.61
Nd	61.12	69.40	74.92	36.45	63.47	56.93	50.10	68.27	72.19	63.94	65.66
Sm	16.75	14.66	15.36	7.42	14.13	12.65	11.38	14.33	15.31	12.60	13.53
Eu	3.99	1.30	2.03	1.73	1.35	1.86	1.20	1.23	1.62	1.38	1.42
Gd	19.20	12.54	14.06	6.97	13.77	13.82	11.33	13.82	14.94	11.76	13.78
Tb	3.48	2.14	2.62	1.01	2.30	2.33	1.86	2.47	2.38	1.78	2.27
Dy	23.48	14.02	18.22	6.41	15.15	15.72	12.10	16.49	15.13	10.85	14.56
Ho	5.15	3.04	4.06	1.37	3.34	3.48	2.58	3.54	3.12	2.15	3.07
Er	15.06	9.01	12.10	4.03	10.20	10.25	7.71	10.38	8.97	5.99	8.87
Tm	2.39	1.40	1.96	0.60	1.62	1.67	1.26	1.63	1.37	0.91	1.36
Yb	15.34	9.04	12.83	3.91	10.72	10.69	8.18	10.53	8.86	5.71	8.77
Lu	2.11	1.23	1.79	0.59	1.62	1.71	1.23	1.42	1.31	0.85	1.28
Cu	32	19	38	9	7	25	2	25	2	9	2
Zn	361	108	311	77	33	87	36	57	113	47	38
Mo	2.30	0.32	1.64	0.51	2.23	2.54	1.52	4.68	0.29	0.58	0.21
Ag	1.67	1.39	1.12	0.70	0.77	0.78	0.50	0.77	0.72	0.57	0.54
Tl	0.24	0.64	0.84	0.62	0.98	0.69	0.33	1.06	0.47	0.24	0.18
Pb	29.73	33.21	21.56	20.94	16.48	9.33	6.07	27.63	4.94	8.83	4.13
Se	5.49	6.39	8.06	3.67	7.49	7.60	5.76	7.13	6.16	5.08	5.28
Sb	0.11	0.10	0.12	1.34	0.16	0.13	0.12	0.14	0.14	0.13	0.07
	SJV91-4A	SJV91-4B	SJV91-4C	SJV91-4D	SJV91-4E	SJV91-4F	SJV91-4G	SJV91-4H	SJV91-4I	SJV91-4J	SJV91-4K
(La/Yb)n	1.94	5.79	4.32	7.03	4.22	3.85	4.31	4.87	5.93	8.82	5.87
(La/Sm)n	1.60	3.22	3.26	3.33	2.88	2.93	2.79	3.22	3.09	3.60	3.43
(Gd/Yb)n	1.04	1.15	0.91	1.48	1.06	1.07	1.15	1.09	1.39	1.70	1.30
(La/Y)n	2.16	6.19	4.71	6.85	4.50	4.00	4.76	4.99	6.29	9.29	5.68
(Tb/Yb)n	1.03	1.08	0.93	1.17	0.98	0.99	1.04	1.07	1.22	1.42	1.18
(Tb/Y)n	1.15	1.15	1.01	1.14	1.04	1.03	1.14	1.09	1.29	1.49	1.14
(Eu/Eu*)n	0.68	0.29	0.41	0.72	0.29	0.43	0.32	0.26	0.32	0.34	0.32
Al_2O_3/TiO_2	22	61	57	30	52	51	50	74	78	71	73
Zr/Hf	49	30	26	36	31	29	30	30	30	31	30
La/Nb	1.19	1.73	2.18	2.97	1.69	1.93	1.75	2.54	1.90	1.80	1.88
Th/Nb	0.17	0.32	0.48	0.75	0.40	0.43	0.39	0.21	0.35	0.35	0.33
Th/La	0.14	0.18	0.22	0.25	0.24	0.22	0.22	0.08	0.19	0.19	0.17
Zr/Y	3.42	4.14	2.80	6.24	3.75	2.86	3.71	2.82	4.38	5.64	3.22
Ti/Zr	7	3	5	13	5	5	5	4	3	4	4
Ti/Sm	169	76	104	410	114	114	112	74	59	82	74
P/Nd	4	1	2	23	2	3	2	1	0	2	1
Ti/V	869	147	29	45	207	90	224	107	1224	261	270
Sc/La	5	3	4	12	3	3	3	2	2	3	2
Nb/Nb*	0.76	0.47	0.38	0.26	0.49	0.42	0.47	0.32	0.42	0.44	0.42
Zr/Zr*	0.94	0.70	0.62	0.97	0.81	0.70	0.73	0.59	0.71	0.69	0.63
Hf/Hf*	0.70	0.84	0.85	0.98	0.93	0.87	0.89	0.71	0.84	0.81	0.75
Th/Th*	0.06	0.03	0.04	0.17	0.05	0.04	0.04	0.03	0.02	0.03	0.03
UTM Zone	•	•	•	•	•	•	•	•	•	•	•
Easting											
Northing											

* Samples from Noranda Exploration core library

	Dixie 3 DDH FIII felsics					Dixie 3 DDH OIB-like basalts	
	SJV91-4L	SJV91-4M	SJV91-4N	SJV91-4O	SJV91-4P	SJV91-4Q	SJV91-4R
SiO_2	76.39	80.23	78.50	75.63	76.98	50.34	51.63
TiO_2	0.18	0.16	0.16	0.24	0.25	1.92	1.90
Al_2O_3	12.38	11.16	11.52	13.01	13.10	17.47	17.35
Fe_2O_3	2.20	1.37	1.92	2.92	1.86	14.00	14.09
MnO	0.02	0.03	0.01	0.03	0.01	0.03	0.28
MgO	0.30	0.18	0.21	0.79	1.96	15.62	10.99
CaO	0.66	1.42	0.72	1.03	1.14	0.30	1.41
K_2O	3.37	1.33	2.85	2.32	2.79	0.02	0.06
Na_2O	4.47	4.09	4.10	4.00	1.91	0.09	1.03
P_2O_5	0.02	0.03	0.02	0.03	0.03	0.21	0.24
LOI	0.45	0.81	0.76	1.37	1.11	7.82	6.28
Mg#	23	23	20	37	70	71	62
Ti	1035	935	984	1593	1519	4919	10815
P	98	117	101	100	78	870	944
Cr	6	7	8	5	3	36	50
Co	6	4	6	8	5	51	48
Ni	1	1	1	1	1	63	70
Rb	63	28	50	74	78	1	2
Sr	83	202	103	136	99	3	58
Cs	2	1	2	1	3	0	0
Ba	714	1111	1123	330	363	2	12
Sc	3	3	3	4	5	19	21
V	4	3	3	6	6	152	182
Ta	2.42	2.15	2.38	2.17	1.98	0.43	0.68
Nb	38.85	37.87	46.09	34.13	30.26	13.22	12.95
Zr	272	278	272	305	277	146	143
Hf	9.28	8.53	8.72	9.80	9.64	3.53	3.52
Th	13.28	12.33	12.61	13.78	13.59	1.90	2.10
U	3.07	2.76	2.52	3.21	2.67	0.19	0.39
Y	82.05	78.07	48.85	117.30	93.08	22.74	24.03
La	73.20	70.31	67.12	51.61	61.85	17.44	19.80
Ce	154.76	148.72	144.04	115.51	133.91	39.97	46.36
Pr	17.79	17.25	16.58	13.71	15.50	5.05	5.88
Nd	67.62	66.85	62.86	54.07	59.07	21.26	24.89
Sm	14.08	13.47	13.19	11.88	12.52	4.97	5.32
Eu	1.40	1.30	1.46	1.14	1.20	1.56	1.72
Gd	13.41	13.43	11.97	13.25	13.22	4.88	5.63
Tb	2.15	2.17	1.88	2.54	2.30	0.71	0.81
Dy	14.24	14.19	11.27	17.43	15.43	4.26	4.82
Ho	3.00	3.03	2.23	3.86	3.40	0.83	0.96
Er	8.73	8.84	6.36	11.41	10.22	2.24	2.58
Tm	1.36	1.40	0.97	1.78	1.62	0.32	0.36
Yb	8.61	8.90	6.29	11.45	10.69	2.02	2.34
Lu	1.29	1.28	0.87	1.63	1.49	0.29	0.35
Cu	4	9	4	2	4	5	7
Zn	61	47	57	37	45	471	584
Mo	0.80	0.38	0.48	0.40	1.14	0.90	1.73
Ag	0.54	0.51	0.59	0.66	0.49	0.50	0.31
Tl	0.21	0.09	0.19	0.36	0.28	0.01	0.02
Pb	10.23	8.23	6.82	9.92	9.86	2.21	47.97
Sn	5.32	4.94	4.59	5.98	6.22	3.89	1.77
Sb	0.08	0.15	0.13	0.08	0.02	0.16	0.03
	SJV91-4L	SJV91-4M	SJV91-4N	SJV91-4O	SJV91-4P	SJV91-4Q	SJV91-4R
(La/Yb)n	6.10	5.66	7.65	3.23	4.15	6.20	6.07
(La/Sm)n	3.36	3.37	3.29	2.81	3.19	2.27	2.41
(Gd/Yb)n	1.29	1.25	1.57	0.96	1.02	2.00	1.99
(La/Y)n	5.91	5.97	9.10	2.91	4.40	5.08	5.46
(Tb/Yb)n	1.13	1.11	1.36	1.01	0.98	1.60	1.57
(Tb/Y)n	1.10	1.17	1.62	0.91	1.04	1.31	1.41
(Eu/Eu*)n	0.31	0.29	0.35	0.28	0.28	0.96	0.96
Al_2O_3/TiO_2	72	72	70	49	51	21	9
Zr/Hf	29	33	31	31	29	41	40
La/Nb	1.88	1.86	1.46	1.51	2.04	1.32	1.53
Th/Nb	0.34	0.33	0.27	0.40	0.45	0.14	0.16
Th/La	0.18	0.18	0.19	0.27	0.22	0.11	0.11
Zr/Y	3.31	3.56	5.58	2.60	2.98	6.43	5.93
Ti/Zr	4	3	4	5	5	34	76
Ti/Sm	73	69	75	134	121	989	2034
P/Nd	1	2	2	2	1	41	38
Ti/V	282	279	282	277	234	32	59
Sc/La	2	2	3	3	3	64	60
Nb/Nb*	0.42	0.42	0.55	0.55	0.40	0.65	0.57
Zr/Zr*	0.61	0.64	0.65	0.83	0.71	0.99	0.86
Hf/Hf*	0.75	0.71	0.76	0.97	0.89	0.86	0.77
Ti/Ti*	0.03	0.03	0.03	0.05	0.05	0.40	0.78
UTM Zone	•	•	•	•	•	•	•
Easting							
Northing							

* Samples from Noranda Exploration core library

Meen-Dempster belt

	Tholeiites					OIB-like		
	82GRS-0292	82GRS-0254	82GRS-0405	84GRS-1277	84GRS-0239	82GRS-1187	82GRS-0106	84GRS-0032
SiO_2	48.27	46.56	48.41	54.77	57.65	47.68	48.57	56.33
TiO_2	0.95	1.14	0.69	0.94	1.18	2.22	1.90	2.01
Al_2O_3	15.07	16.43	14.06	16.82	17.33	13.14	12.52	16.67
Fe_2O_3	13.24	14.91	13.04	2.84	2.31	19.87	19.09	4.37
MnO	0.19	0.18	0.25	0.33	0.28	0.25	0.22	0.26
MgO	8.44	7.25	6.85	7.83	6.55	4.38	5.36	7.14
CaO	11.92	10.96	13.45	13.75	11.55	9.49	8.34	8.63
K_2O	0.24	0.25	0.69	0.19	0.25	0.36	0.42	0.14
Na_2O	1.62	2.26	2.50	2.48	2.82	2.48	3.46	4.31
P_2O_5	0.05	0.05	0.05	0.06	0.08	0.13	0.11	0.13
LOI	0.60	0.70	0.71	0.50	0.50	0.30	0.00	0.30
Mg#	58	52	54	86	86	33	38	78
Ti	5535	7093	5443	5007	6618	14937	11747	10856
P	340	405	367	287	307	1052	789	594
Cr	307	186	493	273	243	5	43	58
Co	59	63	67	62	67	67	70	56
Ni	136.9	104.8	165.1	157.4	104.7	23.1	64.6	46.2
Rb	4	4	16	4	2	4	6	2
Sr	123	279	151	165	128	265	311	247
Cs	1	1	2	0	0	0	1	0
Ba	101	58	120	52	122	96	50	86
Sc	39	36	51	42	50	26	22	45
V	266	289	323	268	340	337	308	404
Ta	0.18	0.27	0.16	0.15	0.19	0.85	0.63	0.35
Nb	2.52	4.13	3.86	2.32	3.08	14.23	11.51	6.03
Zr	46	61	40	37	55	172	127	103
Hf	1.26	1.62	1.09	1.06	1.56	4.05	3.35	2.66
Th	0.28	0.49	0.31	0.32	0.41	1.79	1.27	0.93
U	0.08	0.10	0.31	0.19	0.08	0.40	0.31	0.20
Y	21.89	21.48	16.83	16.52	23.09	38.29	27.09	27.58
La	2.71	3.43	2.90	2.66	2.76	17.55	6.61	5.74
Ce	7.26	9.38	7.25	6.99	7.45	41.20	20.36	15.15
Pr	1.21	1.41	1.11	1.05	1.13	5.74	2.90	2.35
Nd	6.21	7.07	5.50	5.22	5.55	26.00	15.36	11.95
Sm	2.31	2.49	1.75	1.74	1.98	7.02	4.80	3.95
Eu	0.87	0.88	0.63	0.65	0.71	2.08	1.69	1.28
Gd	2.97	3.08	2.40	2.28	2.85	7.10	5.01	4.36
Tb	0.53	0.54	0.44	0.41	0.54	1.13	0.84	0.79
Dy	3.63	3.72	2.86	2.92	3.84	7.16	5.14	5.14
Ho	0.76	0.82	0.61	0.64	0.87	1.46	1.01	1.07
Er	2.28	2.31	1.82	1.86	2.48	4.04	2.74	2.93
Tm	0.34	0.34	0.26	0.28	0.38	0.58	0.40	0.42
Yb	2.25	2.13	1.84	1.81	2.49	3.69	2.60	2.76
Lu	0.29	0.31	0.25	0.26	0.35	0.52	0.34	0.39
Cu	114	95	59	79	102	158	90	75
Zn	86	102	126	112	112	156	134	118
Mo	0.76	0.16	3.28	0.28	0.65	0.75	0.34	0.32
Ag	0.07	0.10	0.09	0.04	0.09	0.29	0.30	0.17
Tl	0.01	-	-	0.06	-	0.00	0.01	-
Pb	41.91	54.93	141.16	8.41	22.44	99.49	38.38	3.16
Sn	3.82	3.26	5.82	1.21	2.52	5.69	3.35	1.45
Sb	6.64	9.11	26.75	0.04	0.56	16.34	5.88	0.21
	82GRS-0292	82GRS-0254	82GRS-0405	84GRS-1277	84GRS-0239	82GRS-1187	82GRS-0106	84GRS-0032
$(La/Yb)_N$	0.86	1.16	1.13	1.06	0.80	3.41	1.82	1.49
$(La/Sm)_N$	0.76	0.89	1.07	0.99	0.90	1.62	0.89	0.94
$(Gd/Yb)_N$	1.09	1.20	1.08	1.04	0.95	1.59	1.59	1.31
$(La/Y)_N$	0.82	1.06	1.14	1.07	0.79	3.04	1.62	1.38
$(Tb/Yb)_N$	1.08	1.16	1.09	1.04	0.99	1.40	1.47	1.31
$(Tb/Y)_N$	1.02	1.06	1.11	1.05	0.99	1.24	1.30	1.21
$(Eu/Eu^*)_N$	1.01	0.97	0.95	1.00	0.92	0.89	1.05	0.94
Al_2O_3/TiO_2	16	14	15	18	14	5	6	8
Zr/Hf	36.59	37.47	36.39	35.21	35.59	42.34	37.90	38.69
La/Nb	1.08	0.83	0.75	1.15	0.90	1.23	0.57	0.95
Th/Nb	0.11	0.12	0.08	0.14	0.13	0.13	0.11	0.15
Th/La	0.10	0.14	0.11	0.12	0.15	0.10	0.19	0.16
Zr/Y	2.10	2.83	2.35	2.25	2.40	4.48	4.69	3.73
Ti/Zr	120	117	138	135	119	87	93	106
Ti/Sm	2392	2851	3106	2880	3342	2127	2447	2747
P/Nd	54.69	57.29	66.66	54.96	55.31	40.48	51.36	49.74
Ti/V	20.82	24.51	16.84	18.69	19.48	44.30	38.11	26.85
Sc/La	134	115	201	162	142	50	64	115
Nb/Nb^*	0.93	1.22	1.24	0.85	1.12	0.71	2.00	1.03
Zr/Zr^*	0.84	1.00	0.88	0.85	1.16	0.88	1.02	1.04
Hf/Hf^*	0.83	0.97	0.88	0.88	1.18	0.75	0.98	0.97
Ti/Ti^*	0.84	1.01	1.05	0.99	1.10	0.84	0.95	1.03
UTM Zone	15	15		15	15	15	15	15
Easting	610032	609988	604520	662625	653625	613222	604558	625625
Northing	5697778	5698953	5697137	5683985	5675450	5699425	5700939	5690325

Meen-Dempster belt

	Subduction influenced tholeiites				Intermediate			
	82GRS-1026	82GRS-0168	82GRS-0088	82GRS-0284	82GRS-0056	82GRS-0297	84GRS-0235	82GRS-0366
SiO_2	49.88	50.12	50.81	51.43	47.93	55.69	61.38	59.46
TiO_2	0.73	0.72	0.84	0.73	0.31	0.71	1.14	1.14
Al_2O_3	15.16	15.07	14.30	14.78	11.49	13.77	16.50	11.75
Fe_2O_3	12.29	12.40	12.78	12.52	10.96	9.38	2.26	17.67
MnO	0.18	0.19	0.19	0.18	0.26	0.18	0.43	0.19
MgO	8.04	7.28	6.98	7.54	12.32	4.48	5.13	1.63
CaO	12.60	12.61	12.17	11.29	15.56	12.14	9.97	3.88
K_2O	0.18	0.17	0.21	0.22	0.49	2.02	0.15	0.16
Na_2O	0.89	1.35	1.62	1.25	0.57	1.48	3.01	3.94
P_2O_5	0.05	0.09	0.10	0.05	0.09	0.14	0.03	0.15
LOI	0.50	2.15	0.40	1.11	3.41	1.52	0.40	0.81
Mg#	59	56	55	57	71	51	83	17
Ti	4769	5012	5997	4617	2038	5227	6282	6881
P	267	273	318	251	273	1383	250	1293
Cr	378	437	364	374	880	505	225	2
Co	56	62	60	58	77	43	65	34
Ni	134.5	146.2	116.7	126.7	565.6	87.8	112.3	1.5
Rb	2	1	2	3	9	40	2	4
Sr	156	80	132	97	144	508	204	191
Cs	0	0	0	1	0	2	0	1
Ba	45	27	72	43	120	500	136	144
Sc	68	55	55	49	22	34	49	28
V	309	334	357	307	98	244	321	98
Ta	0.23	0.13	0.14	0.12	0.18	0.26	0.17	0.63
Nb	1.45	1.32	1.91	1.36	2.28	3.65	3.01	10.25
Zr	41	40	44	38	57	88	54	253
Hf	1.24	1.09	1.29	1.09	1.41	2.19	1.38	6.62
Th	0.38	0.28	0.38	0.30	1.36	5.05	0.32	2.10
U	0.09	0.07	0.10	0.06	0.43	1.28	0.07	0.59
Y	18.82	17.71	20.08	18.96	9.19	15.26	21.11	55.99
La	2.30	1.87	2.83	1.95	6.71	17.92	1.82	6.23
Ce	5.78	4.85	7.02	4.96	13.37	36.12	4.58	18.26
Pr	0.84	0.73	1.07	0.75	1.59	4.51	0.72	2.78
Nd	4.44	3.83	5.28	4.15	5.79	18.35	3.75	13.64
Sm	1.58	1.50	1.83	1.61	1.46	3.69	1.73	4.81
Eu	0.63	0.58	0.71	0.60	0.44	1.12	0.70	1.46
Gd	2.31	2.11	2.80	2.38	1.39	3.39	2.64	6.52
Tb	0.43	0.42	0.48	0.46	0.24	0.47	0.52	1.29
Dy	3.01	3.05	3.52	3.18	1.69	2.77	3.60	9.13
Ho	0.68	0.66	0.73	0.72	0.33	0.55	0.80	2.08
Er	2.07	1.88	2.19	2.00	0.99	1.48	2.36	6.13
Tm	0.30	0.30	0.34	0.32	0.14	0.22	0.35	0.95
Yb	2.04	2.00	2.23	2.17	1.11	1.49	2.26	6.74
Lu	0.29	0.27	0.27	0.30	0.17	0.20	0.32	0.98
Cu	107	102	106	130	76	112	48	65
Zn	86	92	97	77	77	78	94	63
Mo	0.15	0.33	0.23	0.22	0.60	0.69	0.31	0.41
Ag	0.12	0.15	0.04	0.09	0.13	0.19	0.08	0.39
Tl	0.00	-	-	-	0.02	0.22	-	0.06
Pb	4.60	98.65	178.08	44.10	6.72	225.25	21.58	161.32
Se	5.15	8.94	5.90	3.07	6.37	6.41	2.07	6.17
Sb	0.64	16.74	31.82	6.45	0.30	34.02	0.44	27.52
	82GRS-1026	82GRS-0168	82GRS-0088	82GRS-0284	82GRS-0056	82GRS-0297	84GRS-0235	82GRS-0366
$(La/Yb)_N$	0.81	0.67	0.91	0.64	4.35	8.61	0.58	0.66
$(La/Sm)_N$	0.94	0.80	1.00	0.78	2.97	3.14	0.68	0.84
$(Gd/Yb)_N$	0.94	0.87	1.04	0.90	1.04	1.88	0.97	0.80
$(La/Y)_N$	0.81	0.70	0.93	0.68	4.84	7.78	0.57	0.74
$(Th/Yb)_N$	0.96	0.95	0.98	0.95	0.98	1.42	1.05	0.87
$(Th/Y)_N$	0.96	0.99	1.01	1.01	1.09	1.28	1.04	0.97
$(Eu/Eu^*)_N$	1.01	1.00	0.96	0.93	0.94	0.95	1.00	0.80
AL_2O_3/TiO_2	19	18	14	19	33	16	14	10
Zr/Hf	32.80	36.76	34.18	34.60	40.74	40.26	38.91	38.16
La/Nb	1.59	1.42	1.48	1.44	2.95	4.92	0.60	0.61
Th/Nb	0.26	0.21	0.20	0.22	0.60	1.38	0.11	0.20
Th/La	0.17	0.15	0.13	0.16	0.20	0.28	0.18	0.34
Zr/Y	2.16	2.27	2.19	1.99	6.24	5.79	2.53	4.51
Ti/Zr	118	125	137	122	36	59	117	27
Ti/Sm	3022	3337	3282	2871	1397	1418	3638	1431
Pr/Nd	60.14	71.17	60.25	60.45	47.04	75.39	66.65	94.76
Ti/V	15.44	15.01	16.82	15.05	20.83	21.41	19.54	182.70
Sc/La	234	206	202	163	135	168	151	29
Nb/Nb^*	0.59	0.68	0.62	0.66	0.25	0.15	1.56	1.80
Zr/Zr^*	1.06	1.16	0.98	1.01	1.36	0.74	1.45	2.16
Hf/Hf^*	1.17	1.14	1.04	1.06	1.21	0.67	1.36	2.05
Ti/Ti^*	0.99	1.11	1.05	0.93	0.57	0.58	1.16	0.49
UTM Zone	15	15	15	15	15	15	15	15
Easting	607369	614736	611423	613572	608057	609671	653720	615657
Northing	5700410	5697418	5699601	5697579	5700733	5698420	5675560	5695987

	Meen-Dempster belt Felsic			Pickle Lake belt						
	82GRS-0412	84GRS-0205	84GRS-1244	PL-17A	PL-15	PL95-21A	PL95-21B	PL-16	PL95-20	PL-17B
SiO_2	74.93	72.84	67.08	62.33	53.25	54.60	54.80	56.43	54.21	52.83
TiO_2	0.21	0.49	1.31	0.63	1.53	1.36	1.44	1.35	1.30	1.47
Al_2O_3	14.52	16.42	13.65	16.71	13.01	12.15	12.67	12.25	12.46	13.26
Fe_2O_3	1.66	1.18	4.93	8.41	16.92	16.33	15.79	15.06	15.91	16.77
MnO	0.03	0.00	0.30	0.19	0.19	0.22	0.21	0.26	0.21	0.25
MgO	0.56	0.71	2.05	2.49	4.66	3.90	3.76	3.54	3.71	3.82
CaO	1.27	2.02	6.55	6.28	6.10	7.81	7.74	7.27	9.21	8.13
K_2O	1.46	1.44	0.49	2.17	0.60	1.13	0.25	0.78	0.27	0.30
Na_2O	5.32	4.78	3.33	0.59	3.57	2.33	3.17	2.90	2.55	2.99
P_2O_5	0.02	0.12	0.32	0.19	0.17	0.17	0.17	0.16	0.16	0.18
LOI	0.40	1.63	0.40	0.70	0.10	1.21	0.20	0.55	1.57	0.15
Mg#	43	57	48	39	38	34	34	34	34	33
Ti	1097	1772	5788	3277	9044	8140	9093	9635	7588	8423
P	113	529	1313	835	743	885	958	702	818	787
Cr	8	8	2	184	201	100	101	192	96	195
Co	4	7	35	22	52	50	55	57	50	54
Ni	3.7	6.4	5.9	50	21	25	27	24	24	22
Rb	41	45	5	108	21	56	1	39	3	3
Sr	275	483	150	450	135	432	106	149	493	285
Cs	1	3	1	5	1	2	0	2	0	0
Ba	768	525	103	298	199	511	29	480	29	55
Sc	2	3	35	15	34	46	49	32	43	35
V	16	29	45	120	367	387	425	315	379	359
Ta	0.81	0.22	0.48	0.48	0.37	0.34	0.38	0.33	0.32	0.39
Nb	6.15	3.35	6.93	7.08	6.85	5.34	6.15	5.65	5.32	6.21
Zr	131	101	110	122	125	113	114	112	105	122
Hf	3.70	2.49	2.85	3.34	3.14	3.22	2.88	2.99	2.78	3.65
Th	15.94	5.77	3.87	9.04	2.84	2.72	3.05	2.61	2.84	3.21
U	3.42	1.06	0.85	2.21	0.63	0.50	0.61	0.58	0.42	0.62
Y	6.44	3.59	31.76	19.16	30.04	22.68	25.53	25.96	23.69	29.90
La	16.79	24.72	18.02	32.17	12.14	14.57	14.47	13.99	15.27	14.84
Ce	28.57	49.70	36.82	64.48	27.78	31.36	31.72	29.96	31.13	31.38
Pr	2.92	5.62	4.68	7.01	3.34	3.60	3.57	3.59	3.59	3.88
Nd	10.07	19.94	19.55	26.87	14.32	16.76	15.68	15.36	15.87	15.98
Sm	1.89	2.86	4.79	4.72	3.91	3.76	3.84	3.66	3.81	4.01
Eu	0.47	0.71	1.32	1.29	1.26	1.12	1.28	0.98	1.36	1.36
Gd	1.53	1.71	5.01	4.08	4.41	4.34	4.57	4.23	4.40	4.55
Tb	0.21	0.15	0.85	0.49	0.72	0.70	0.73	0.66	0.69	0.76
Dy	1.08	0.74	5.52	3.32	5.06	4.56	4.70	4.29	4.30	5.13
Ho	0.22	0.11	1.22	0.64	1.04	0.96	1.02	0.89	0.97	1.01
Er	0.61	0.28	3.36	1.90	3.06	2.78	2.87	2.78	2.59	3.11
Tm	0.09	0.04	0.51	0.27	0.44	0.40	0.44	0.42	0.41	0.47
Yb	0.58	0.18	3.26	1.74	3.13	2.57	2.79	2.65	2.54	3.16
Lu	0.09	0.03	0.46	0.26	0.45	0.38	0.42	0.42	0.41	0.47
Cu	6	32	5	-	-	35	38	-	62	-
Zn	22	43	117	-	-	129	143	-	98	-
Mo	0.85	0.16	0.44	-	-	1.08	1.05	-	0.77	-
Ag	0.51	0.34	0.21	-	-	0.78	0.72	-	0.76	-
Tl	0.25	0.30	0.05	-	-	0.15	0.02	-	0.00	-
Pb	13.76	23.51	11.21	-	-	4.49	4.06	-	3.41	-
Sn	5.59	10.10	1.97	-	-	-	-	-	-	-
Sb	0.20	1.96	1.05	-	-	-	-	-	-	-
	82GRS-0412	84GRS-0205	84GRS-1244	PL-17A	PL-15	PL95-21A	PL95-21B	PL-16	PL95-20	PL-17B
(La/Yb)n	20.67	96.87	3.96	13.24	2.78	4.07	3.72	3.78	4.31	3.36
(La/Sm)n	5.75	5.59	2.43	4.40	2.00	2.50	2.44	2.47	2.59	2.39
(Gd/Yb)n	2.17	7.72	1.27	1.94	1.17	1.40	1.36	1.32	1.43	1.19
(La/Y)n	17.28	45.64	3.76	11.12	2.68	4.26	3.75	3.57	4.27	3.29
(Tb/Yb)n	1.65	3.79	1.19	1.29	1.05	1.23	1.19	1.14	1.24	1.09
(Tb/Y)n	1.38	1.78	1.13	1.08	1.01	1.29	1.20	1.07	1.22	1.07
(Eu/Eu*)n	0.82	0.91	0.81	0.88	0.92	0.84	0.93	0.76	1.01	0.97
AL_2O_3/TiO_2	79	54	12	30.58	8.63	8.87	8.32	7.63	9.87	9.41
Zr/Hf	35.31	40.40	38.62	36.35	39.68	35.16	39.60	37.45	37.79	33.44
La/Nb	2.73	7.37	2.60	4.54	1.77	2.73	2.35	2.48	2.87	2.39
Th/Nb	2.59	1.72	0.56	1.28	0.42	0.51	0.50	0.46	0.53	0.52
Th/La	0.95	0.23	0.21	0.28	0.23	0.19	0.21	0.19	0.19	0.22
Zr/Y	20.33	28.04	3.47	6.34	4.15	4.99	4.46	4.31	4.44	4.08
Ti/Zr	8	18	53	26.97	72.51	71.93	79.79	86.15	72.14	69.09
Ti/Sm	581	620	1208	694	2311	2164	2371	2633	1990	2103
P/Nd	11.24	26.54	67.18	31.08	51.84	52.83	61.11	45.70	51.53	49.22
Ti/V	67.09	61.86	128.46	27.40	24.64	21.02	21.40	30.64	20.05	23.49
Sc/La	27	110	75	59.14	74.82	120.93	116.10	75.05	105.75	74.53
Nb/Nb*	0.23	0.10	0.29	0.16	0.48	0.29	0.35	0.32	0.27	0.33
Zr/Zr*	2.08	0.92	0.79	0.75	1.15	0.99	1.02	1.03	0.94	1.05
Hf/Hf*	2.13	0.83	0.74	0.74	1.05	1.02	0.93	1.00	0.90	1.14
Ti/Ti*	0.26	0.32	0.47	0.30	0.86	0.80	0.86	0.97	0.73	0.78
UTM Zone	15	15	15	15	15	15	15	15	15	15
Easting	610117	638225	640565	6926500	693250	693299	693299	693300	693395	6926500
Northing	5698336	5677525	5676850	5668300	5686712	5686322	5686322	5686700	5686389	5668300

	Pickle Lake belt		Lake St. Joseph belt Tholeiites							
	PL95-19	PL95-17	DL87-8B	DL87-9B	DL87-15A	LSJ95-3	DL87-11B	DL87-15C	DL87-9A	WL87-10A
SiO_2	53.12	54.93	49.22	50.59	52.20	48.26	49.64	50.82	53.79	52.14
TiO_2	1.54	1.73	0.79	0.75	0.86	0.94	0.99	0.93	0.92	0.90
Al_2O_3	12.95	13.11	15.86	15.61	14.09	15.47	15.28	13.41	19.62	16.49
Fe_2O_3	17.98	17.91	12.05	11.14	12.95	14.25	13.13	14.15	9.67	13.73
MnO	0.22	0.22	0.19	0.20	0.19	0.19	0.22	0.22	0.13	0.17
MgO	3.85	2.79	8.63	6.70	7.19	7.83	7.21	6.51	3.87	4.65
CaO	6.54	4.91	11.02	13.01	11.39	10.38	12.00	12.05	7.75	9.49
K_2O	0.51	0.85	0.11	0.17	0.19	0.18	0.10	0.16	2.30	0.32
Na_2O	3.11	3.36	2.07	1.77	0.89	2.39	1.35	1.70	1.87	2.06
P_2O_5	0.18	0.19	0.06	0.06	0.06	0.19	0.07	0.06	0.07	0.06
LOI	0.10	0.20	1.21	2.93	1.73	0.40	0.91	3.41	1.32	0.71
Mg#	32	26	61	57	55	55	55	50	47	43
Ti	8829	10310	4451	5244	4827	5774	6935	5597	5487	5122
P	872	929	277	410	507	344	446	434	300	245
Cr	190	191	290	334	369	250	365	88	158	259
Co	51	49	52	72	55	38	67	54	62	47
Ni	21	3	124	145	60	102	168	46	133	92
Rb	24	46	2	7	7	2	1	4	67	9
Sr	183	237	219	146	95	300	174	160	201	218
Cs	4	42	0	0	1	0	0	0	3	1
Ba	84	670	15	254	48	41	17	60	434	38
Sc	57	52	42	56	53	47	51	51	41	52
V	444	199	243	362	364	248	342	361	289	335
Ta	0.40	0.45	0.14	0.13	0.17	0.15	0.19	0.18	0.19	0.16
Nb	6.54	7.71	2.68	1.75	2.37	2.67	3.20	2.52	3.09	2.75
Zr	116	123	49	42	47	65	59	52	67	51
Hf	3.23	3.48	1.50	1.26	1.43	1.96	1.62	1.56	1.78	1.45
Th	3.18	3.44	0.37	0.44	0.38	1.64	0.28	0.33	0.49	0.24
U	0.76	0.84	0.08	0.11	0.09	0.24	0.06	0.07	0.11	0.05
Y	29.32	25.82	17.72	19.14	17.44	19.35	22.61	18.83	14.99	23.53
La	18.01	9.80	3.40	2.56	2.82	4.40	2.90	2.85	3.87	2.95
Ce	36.56	18.18	9.00	6.30	7.02	12.07	8.31	7.11	9.94	8.01
Pr	4.00	2.08	1.28	0.93	1.13	1.66	1.32	1.21	1.37	1.20
Nd	18.55	10.30	6.16	4.92	6.05	8.65	7.10	6.33	6.75	5.98
Sm	4.52	3.16	1.93	1.76	2.05	2.76	2.45	2.37	2.01	1.96
Eu	1.37	1.17	0.74	0.66	0.71	0.94	0.90	0.83	0.71	0.92
Gd	5.06	4.22	2.53	2.64	2.69	3.21	3.29	2.86	2.44	2.83
Tb	0.82	0.73	0.44	0.48	0.48	0.55	0.53	0.50	0.43	0.50
Dy	5.28	4.81	2.92	3.49	3.35	3.51	3.77	3.52	2.96	3.75
Ho	1.11	1.03	0.64	0.78	0.74	0.71	0.84	0.80	0.63	0.84
Er	3.24	2.95	1.79	2.39	2.17	2.20	2.39	2.34	1.85	2.46
Tm	0.48	0.43	0.27	0.37	0.33	0.32	0.33	0.35	0.28	0.40
Yb	3.09	2.84	1.80	2.39	2.08	2.02	2.38	2.40	1.88	2.43
Lu	0.45	0.43	0.27	0.36	0.32	0.32	0.32	0.35	0.26	0.34
Cu	47	17	136	130	69	27	110	60	68	48
Zn	103	204	74	91	34	74	94	73	86	74
Mo	1.03	2.17	2.10	0.50	0.12	0.42	0.56	0.16	1.44	3.83
Ag	1.07	0.96	0.19	0.16	0.16	0.45	0.09	0.13	0.17	0.07
Tl	0.11	0.28	0.00	0.15	0.05	0.06	0.02	0.05	0.72	0.12
Pb	3.30	7.86	1.12	2.86	0.99	2.72	0.80	2.05	4.61	3.66
Se	-	-	0.52	0.44	0.44	-	0.75	1.23	0.63	0.98
Sb	-	-	0.20	0.15	0.41	-	0.25	0.57	0.02	0.07
	PL95-19	PL95-17	DL87-8B	DL87-9B	DL87-15A	LSJ95-3	DL87-11B	DL87-15C	DL87-9A	WL87-10A
(La/Yb)n	4.18	2.48	1.35	0.77	0.97	1.56	0.87	0.85	1.47	0.87
(La/Sm)n	2.57	2.01	1.14	0.94	0.89	1.03	0.76	0.78	1.25	0.97
(Gd/Yb)n	1.35	1.23	1.16	0.91	1.07	1.32	1.14	0.98	1.07	0.96
(La/Y)n	4.07	2.52	1.27	0.89	1.07	1.51	0.85	1.00	1.71	0.83
(Tb/Yb)n	1.20	1.17	1.10	0.92	1.05	1.24	1.02	0.94	1.03	0.94
(Tb/Y)n	1.17	1.18	1.03	1.06	1.15	1.19	0.99	1.11	1.19	0.90
(Eu/Eu*)n	0.87	0.98	1.02	0.93	0.93	0.97	0.97	0.97	0.98	1.19
AL_2O_3/TiO_2	8.77	7.63	21.00	17.7	17.19	15.8	13.0	15.58	21.0	19.0
Zr/Hf	36.08	35.38	32.94	33.3	32.61	33.0	36.1	33.58	37.4	35.0
La/Nb	2.75	1.27	1.27	1.46	1.19	1.64	0.91	1.13	1.25	1.07
Th/Nb	0.49	0.45	0.14	0.25	0.16	0.61	0.09	0.13	0.16	0.09
Th/La	0.18	0.35	0.11	0.17	0.13	0.37	0.10	0.12	0.13	0.08
Zr/Y	3.97	4.78	2.79	2.18	2.68	3.34	2.60	2.79	4.45	2.16
Ti/Zr	75.87	83.62	90.18	125	103.15	89	118	97.17	82	101
Ti/Sm	1952	3266	2301.78	2978	2359.72	2092	2828	2151.26	2734	2608
P/Nd	46.98	90.17	44.96	83	83.69	40	63	68.55	44	41
Ti/V	19.91	51.93	18.34	14	13.27	23	20	14.12	19	15
Sc/La	127.12	123.14	155.07	155	168.16	148	157	146.10	157	152
Nb/Nb*	0.27	0.54	0.78	0.63	0.78	0.62	1.18	0.83	0.76	0.94
Zr/Zr*	0.88	1.50	0.99	0.98	0.92	0.92	0.97	0.94	1.25	1.02
Hf/Hf*	0.88	1.53	1.09	1.07	1.02	1.01	0.98	1.01	1.22	1.06
Ti/Ti*	0.73	1.12	0.80	0.96	0.81	0.77	0.97	0.78	0.98	0.86
UTM Zone	15	15	16	16	16	15	16	16	16	16
Easting	693270	693056	304650	303000	301100	693709	306350	301100	303000	308300
Northing	5686237	5685489	5667400	5667450	5666550	5674089	5666400	5666550	5667450	5667850

Lake St. Joseph belt
Calc alkaline

	PL95-40	LSJ95-1	LSJ95-2	LSJ95-4	LSJ95-13a	LSJ95-13b	DL87-8A	DL87-11A	DL87-12A	DL87-12B	DL87-15B	WL87-10B
SiO_2	54.58	50.38	55.22	44.89	72.87	55.70	52.04	49.53	76.84	66.77	71.84	83.31
TiO_2	0.64	1.08	1.22	0.90	0.29	0.87	1.28	1.15	0.08	1.39	0.25	0.13
Al_2O_3	13.80	15.13	16.31	16.50	15.89	16.77	14.65	16.58	13.35	16.98	15.53	9.61
Fe_2O_3	6.43	13.59	9.58	14.86	0.65	12.71	11.88	15.56	3.16	12.17	1.93	2.15
MnO	0.09	0.19	0.27	0.28	0.01	0.18	0.18	0.24	0.10	0.19	0.03	0.12
MgO	9.63	6.79	4.01	8.53	0.31	2.53	7.77	4.11	1.45	2.73	0.81	0.51
CaO	9.94	9.59	8.50	12.40	2.43	6.31	9.91	11.16	1.16	2.20	2.58	1.44
K_2O	0.55	0.14	0.22	0.13	2.05	0.21	0.43	0.37	3.25	2.48	1.89	2.35
Na_2O	3.57	3.01	4.47	1.29	5.42	4.55	1.63	1.19	0.59	0.75	5.07	0.35
P_2O_5	0.17	0.09	0.19	0.11	0.09	0.15	0.23	0.12	0.02	0.34	0.07	0.02
LOI	0.55	0.45	0.40	0.86	1.42	0.30	0.81	0.55	1.68	0.50	1.47	1.01
Mg#	77	52	48	56	51	30	59	37	50	33	48	35
Ti	3991	6696	7710	5663	1803	4657	8778	8151	446	8064	1330	756
P	1672	458	713	390	319	613	1198	718	0	1431	433	84
Cr	448	232	190	294	18	4	290	380	4	3	39	7
Co	32	44	40	43	3	35	56	68	6	20	3	7
Ni	116	108	122	127	7	7	201	263	8	3	2	2
Rb	37	1	8	2	53	3	13	3	95	50	51	52
Sr	1655	343	308	317	424	407	420	275	255	128	368	52
Cs	18	0	1	2	1	0	1	0	3	3	2	3
Ba	1764	29	123	16	603	39	150	146	366	224	520	279
Sc	44	46	38	51	4	22	29	38	3	23	6	3
V	120	246	230	291	26	98	226	298	2	69	22	3
Ta	0.43	0.18	0.16	0.13	0.17	0.24	0.34	0.32	0.71	0.49	0.21	0.90
Nb	8.42	3.90	3.27	2.50	2.70	4.69	7.32	4.00	7.45	7.67	3.18	15.96
Zr	253	66	86	59	93	139	118	73	86	153	105	183
Hf	5.39	1.97	2.48	1.70	2.39	3.46	3.10	2.24	3.46	4.28	3.03	4.71
Th	36.51	1.63	2.95	1.30	4.14	4.72	2.84	2.17	7.59	3.82	3.29	7.14
U	6.36	0.59	0.66	0.29	0.86	0.64	0.64	0.37	1.80	0.53	1.04	2.17
Y	26.76	18.02	20.79	23.90	3.94	27.92	21.22	22.65	15.30	21.34	5.79	19.71
La	146.00	10.61	10.24	10.50	17.77	27.83	22.56	18.67	30.19	27.31	14.24	37.05
Ce	304.37	23.13	33.06	23.12	34.28	60.43	52.35	40.26	62.27	56.34	26.96	79.40
Pr	31.11	2.87	4.04	2.68	3.52	6.96	6.21	4.75	6.68	7.39	2.68	8.45
Nd	133.01	13.57	19.79	11.91	13.54	26.96	26.80	19.33	24.29	30.04	10.88	32.64
Sm	24.39	3.30	5.03	3.17	2.16	5.36	5.49	4.56	4.21	5.99	1.96	5.41
Eu	5.37	1.11	1.59	0.99	0.58	1.42	1.56	1.25	0.64	1.91	0.53	0.85
Gd	14.76	3.65	4.73	3.66	1.50	4.96	4.85	4.40	3.61	5.99	1.52	4.19
Tb	1.32	0.55	0.67	0.63	0.15	0.78	0.68	0.70	0.53	0.97	0.19	0.55
Dy	5.70	3.39	3.93	4.24	0.65	4.82	3.81	4.32	2.98	4.78	1.00	3.33
Ho	0.81	0.71	0.82	0.94	0.11	0.95	0.73	0.90	0.58	1.15	0.18	0.68
Er	1.88	1.92	2.15	2.65	0.26	2.73	2.02	2.36	1.71	2.72	0.49	2.07
Tm	0.21	0.28	0.30	0.40	0.04	0.42	0.30	0.35	0.23	0.42	0.08	0.33
Yb	1.18	1.82	1.80	2.62	0.24	2.68	1.76	2.15	1.66	3.14	0.44	2.32
Lu	0.17	0.28	0.28	0.41	0.03	0.39	0.24	0.31	0.23	0.42	0.06	0.34
Cu	8	97	47	54	5	25	93	35	2	6	5	16
Zn	96	92	100	75	16	110	182	128	50	49	45	26
Mo	1.16	0.51	0.27	0.47	0.87	1.01	2.43	1.12	1.25	0.19	0.81	6.74
Ag	0.00	0.43	0.40	0.30	0.18	0.31	0.34	0.15	0.23	0.43	1.08	0.41
Tl	0.23	0.08	0.13	0.05	0.44	0.02	0.26	0.03	0.65	0.97	0.40	0.26
Pb	15.87	3.07	5.62	3.01	8.53	6.19	6.27	3.36	10.09	5.24	9.75	5.99
Se	1.22	-	-	-	0.45	0.89	1.09	0.89	1.96	1.00	-	1.71
Sb	-	-	-	-	0.10	0.20	0.15	0.31	0.04	-	-	0.04

	PL95-40	LSJ95-1	LSJ95-2	LSJ95-4	LSJ95-13a	LSJ95-13b	DL87-8A	DL87-11A	DL87-12A	DL87-12B	DL87-15B	WL87-10B
(La/Yb)n	88.91	4.17	4.08	2.87	52.34	7.45	9.17	6.22	13.06	6.24	23.10	11.43
(La/Sm)n	3.87	2.08	1.31	2.14	5.31	3.36	2.65	2.65	4.63	2.94	4.69	4.42
(Gd/Yb)n	10.36	1.65	2.17	1.15	5.10	1.53	2.27	1.69	1.80	1.58	2.85	1.49
(La/Y)n	36.13	3.90	3.26	2.91	29.91	6.60	7.04	5.46	13.07	8.48	16.29	12.45
(Tb/Yb)n	5.08	1.37	1.70	1.08	2.84	1.33	1.74	1.49	1.45	1.41	1.94	1.07
(Tb/Y)n	2.07	1.28	1.36	1.10	1.62	1.18	1.34	1.30	1.45	1.92	1.37	1.16
(Eu/Eu*)n	0.80	0.97	0.98	0.88	0.93	0.83	0.91	0.84	0.49	0.96	0.90	0.52
AL_2O_3/TiO_2	20.5	13.3	12.6	17.2	67.2	21.3	9.8	12.0	177.8	12.4	68.6	76.3
Zr/Hf	47.0	33.3	34.9	34.4	38.8	40.1	38.3	32.5	24.9	35.7	34.7	38.8
La/Nb	17.35	2.72	3.13	4.21	6.59	5.93	3.08	4.67	4.05	3.56	4.48	2.32
Th/Nb	4.34	0.42	0.90	0.52	1.53	1.01	0.39	0.54	1.02	0.50	1.04	0.45
Th/La	0.25	0.15	0.29	0.12	0.23	0.17	0.13	0.12	0.25	0.14	0.23	0.19
Zr/Y	9.46	3.65	4.16	2.45	23.59	4.96	5.58	3.22	5.63	7.17	18.15	9.27
Ti/Zr	16	102	89	97	15	34	74	112	5	53	13	4
Ti/Sm	164	2029	1532	1788	649	869	1598	1789	106	1346	678	140
P/Nd	28	34	36	33	24	23	45	37	0	48	40	3
Ti/V	33	27	34	19	53	48	39	27	245	117	60	296
Sc/Lu	263	166	136	123	128	55	120	120	12	55	91	9
Nb/Nb*	0.04	0.30	0.38	0.20	0.11	0.14	0.28	0.17	0.19	0.22	0.16	0.34
Zr/Zr*	0.31	0.68	0.60	0.66	1.19	0.80	0.68	0.54	0.59	0.79	1.57	0.95
Hf/Hf*	0.24	0.74	0.62	0.70	1.11	0.72	0.64	0.60	0.86	0.80	1.64	0.89
Ti/Ti*	0.08	0.76	0.62	0.66	0.31	0.36	0.67	0.72	0.05	0.53	0.30	0.06
UTM Zone	15	15	15	15	15	15	16	16	16	16	16	16
Easting	694690	692477	693341	693857	693769	693769	304650	306350	306650	306650	301100	308300
Northing	5669729	5675582	5675451	5673466	5671949	5671949	5667400	5666400	5667600	5667600	5666550	5667850

IMAGE EVALUATION
TEST TARGET (QA-3)

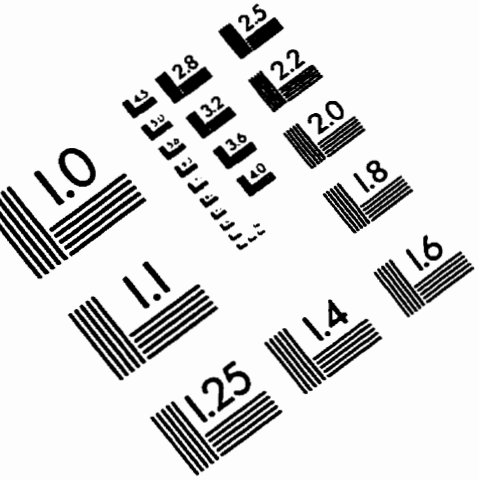

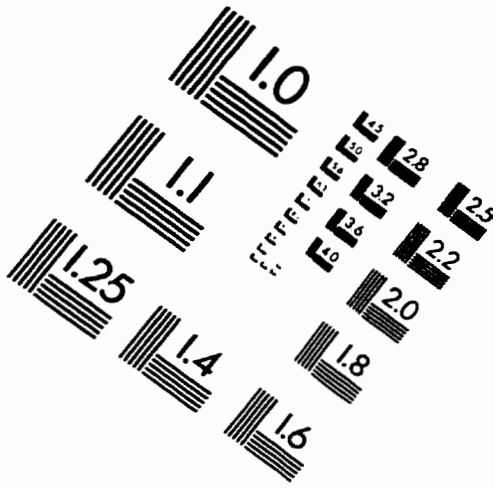

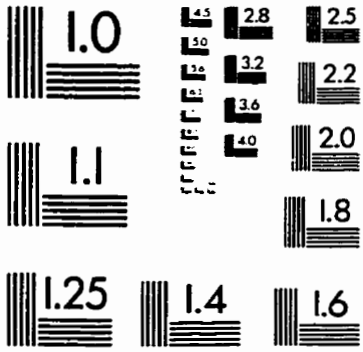

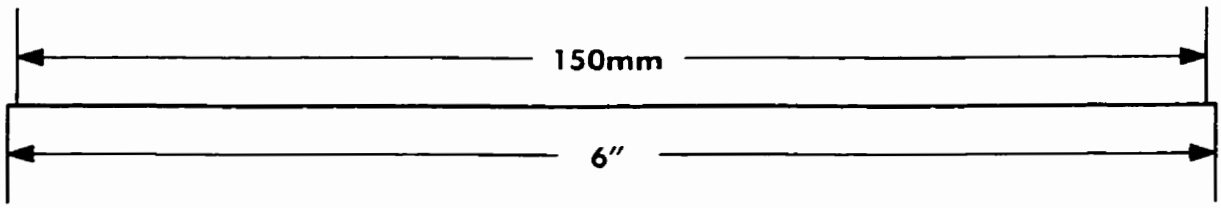

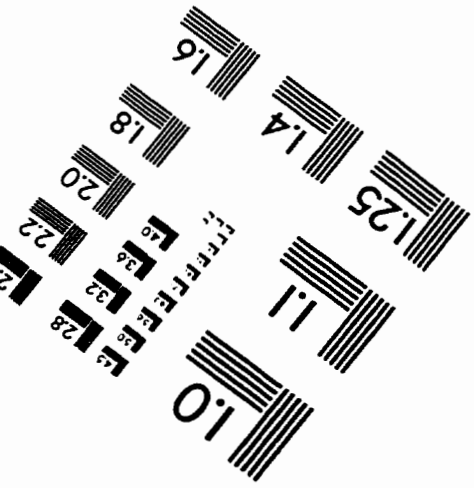

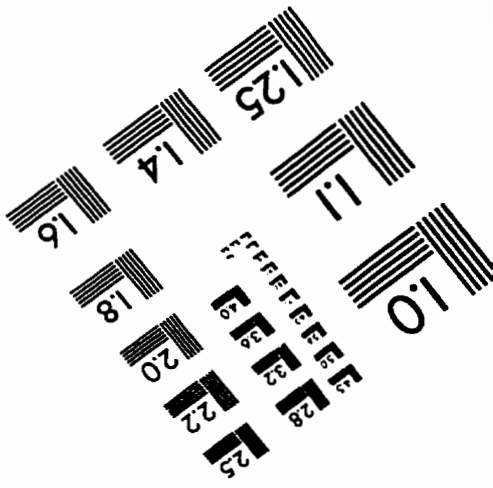

APPLIED IMAGE, Inc
1653 East Main Street
Rochester, NY 14609 USA
Phone: 716/482-0300
Fax: 716/288-5989

© 1993, Applied Image, Inc., All Rights Reserved